TOPICS IN CURRENT CHEMISTRY 296

Volume Editors W. Bielke · C. Erbacher

Nucleic Acid Transfection

Springer

296

Topics in Current Chemistry

Topics in Current Chemistry

Recently Published and Forthcoming Volumes

Nucleic Acid Transfection
Volume Editors: Bielke, W., Erbacher, C.
Vol. 296, 2010

Carbohydrates in Sustainable Development II
Volume Editors: Rauter, A.P., Vogel, P., Queneau, Y.
Vol. 295, 2010

Carbohydrates in Sustainable Development I
Volume Editors: Rauter, A.P., Vogel, P., Queneau, Y.
Vol. 294, 2010

Functional Metal-Organic Frameworks: Gas Storage, Separation and Catalysis
Volume Editor: Schröder, M.
Vol. 293, 2010

C-H Activation
Volume Editors: Yu, J.-Q., Shi, Z.
Vol. 292, 2010

Asymmetric Organocatalysis
Volume Editor: List, B.
Vol. 291, 2010

Ionic Liquids
Volume Editor: Kirchner, B.
Vol. 290, 2010

Orbitals in Chemistry
Volume Editor: Inagaki, S.
Vol. 289, 2009

Glycoscience and Microbial Adhesion
Volume Editors: Lindhorst, T.K., Oscarson, S.
Vol. 288, 2009

Templates in Chemistry III
Volume Editors: Broekmann, P., Dötz, K.-H., Schalley, C.A.
Vol. 287, 2009

Tubulin-Binding Agents: Synthetic, Structural and Mechanistic Insights
Volume Editor: Carlomagno, T.
Vol. 286, 2009

STM and AFM Studies on (Bio)molecular Systems: Unravelling the Nanoworld
Volume Editor: Samorì, P.
Vol. 285, 2008

Amplification of Chirality
Volume Editor: Soai, K.
Vol. 284, 2008

Anthracycline Chemistry and Biology II
Mode of Action, Clinical Aspects and New Drugs
Volume Editor: Krohn, K.
Vol. 283, 2008

Anthracycline Chemistry and Biology I
Biological Occurence and Biosynthesis, Synthesis and Chemistry
Volume Editor: Krohn, K.
Vol. 282, 2008

Photochemistry and Photophysics of Coordination Compounds II
Volume Editors: Balzani, V., Campagna, S.
Vol. 281, 2007

Photochemistry and Photophysics of Coordination Compounds I
Volume Editors: Balzani, V., Campagna, S.
Vol. 280, 2007

Metal Catalyzed Reductive C–C Bond Formation
A Departure from Preformed Organometallic Reagents
Volume Editor: Krische, M.J.
Vol. 279, 2007

Nucleic Acid Transfection

Volume Editors:
Wolfgang Bielke · Christoph Erbacher

With Contributions by

A. Ahmad · M.N. Bacon · K. Berg · M. Berstad · N.F. Bouxsein · C. Bräuchle · M. Bradley · M. Calderón · H.M. Evans · K.K. Ewert · W. Fischer · R. Haag · P. Hahn · I. Hedfors · A. Høgset · R. Koynova · C.S. McAllister · P.M. McLendon · L. Prasmickaite · T.M. Reineke · N. Ruthardt · C.R. Safinya · E.E. Salcher · C.E. Samuel · E. Scanlan · P.K. Selbo · A. Sizovs · S. Srinivasachari · B. Tenchov · A. Unciti-Broceta · E. Wagner · A. Weyergang · A. Zidovska

Springer

Editors
Dr. Wolfgang Bielke
QIAGEN GmbH
Qiagen Str. 1
40724 Hilden
Germany
wolfgang.bielke@qiagen.com

Dr. Christoph Erbacher
QIAGEN GmbH
Division Corporate Research
Qiagen Str. 1
40724 Hilden
Germany
Christoph.Erbacher@qiagen.com

ISSN 0340-1022 e-ISSN 1436-5049
ISBN 978-3-642-16429-3 e-ISBN 978-3-642-16430-9
DOI 10.1007/978-3-642-16430-9
Springer Heidelberg Dordrecht London New York

Library of Congress Control Number: 2010938948

Cover design: WMXDesign GmbH, Heidelberg, Germany

Printed on acid-free paper

Springer is part of Springer Science+Business Media (www.springer.com)

Volume Editors

Dr. Wolfgang Bielke

QIAGEN GmbH
Qiagen Str. 1
40724 Hilden
Germany
wolfgang.bielke@qiagen.com

Dr. Christoph Erbacher

QIAGEN GmbH
Division Corporate Research
Qiagen Str. 1
40724 Hilden
Germany
Christoph.Erbacher@qiagen.com

Editorial Board

Topics in Current Chemistry Also Available Electronically

Topics in Current Chemistry is included in Springer's eBook package *Chemistry and Materials Science*. If a library does not opt for the whole package the book series may be bought on a subscription basis. Also, all back volumes are available electronically.

For all customers who have a standing order to the print version of *Topics in Current Chemistry*, we offer free access to the electronic volumes of the Series published in the current year via SpringerLink.

If you do not have access, you can still view the table of contents of each volume and the abstract of each article by going to the SpringerLink homepage, clicking on "Chemistry and Materials Science," under Subject Collection, then "Book Series," under Content Type and finally by selecting *Topics in Current Chemistry*.

You will find information about the

– Editorial Board
– Aims and Scope
– Instructions for Authors
– Sample Contribution

at springer.com using the search function by typing in *Topics in Current Chemistry*.

Color figures are published in full color in the electronic version on SpringerLink.

Aims and Scope

The series *Topics in Current Chemistry* presents critical reviews of the present and future trends in modern chemical research. The scope includes all areas of chemical science, including the interfaces with related disciplines such as biology, medicine, and materials science.

The objective of each thematic volume is to give the non-specialist reader, whether at the university or in industry, a comprehensive overview of an area where new insights of interest to a larger scientific audience are emerging.

Thus each review within the volume critically surveys one aspect of that topic and places it within the context of the volume as a whole. The most significant developments of the last 5–10 years are presented, using selected examples to illustrate the principles discussed. A description of the laboratory procedures involved is often useful to the reader. The coverage is not exhaustive in data, but rather conceptual, concentrating on the methodological thinking that will allow the non-specialist reader to understand the information presented.

Discussion of possible future research directions in the area is welcome.

Review articles for the individual volumes are invited by the volume editors.

In references *Topics in Current Chemistry* is abbreviated *Top Curr Chem* and is cited as a journal.

Impact Factor 2009: 4.291; Section "Chemistry, Multidisciplinary": Rank 20 of 138

Preface

Transfection of macromolecules into various cell types or tissues, either in vitro or in vivo, has become an indispensable technique for most fields of biomedical research. Furthermore, future applications will likely lead to an increase in the importance of transfection technologies since, with the exception of using certain drugs, there is currently little alternative to transfection for gene-specific manipulation of cells. Typically, transfections are performed with various types of nucleic acids such as genetic expression constructs, siRNAs, and occasionally messenger RNAs. Although many physical and viral transfection methods have been developed for use in different applications, the majority of protocols use chemical transfection reagents.

In this volume, we have brought together articles from various experts in the chemical transfection reagent field. Topics covered include descriptions of the chemistry of chemical transfection compounds and details of the fundamental parameters that influence transfection efficiencies.

The article by *Hahn and Scanlan* gives a general overview of common transfection methods and presents a valuable entrance point to the field.

Students, but also advanced researchers, are advised to continue with the article by *Unciti-Broceta et al.*, which gives a comprehensive outline of the chemistry underlying liquid and solid synthesis of cationic lipids and dendrimers.

A summary and discussion of empirical data on relationships between cationic lipid molecular structure and transfection activity are provided by *Koynova and Tenchov* Structural features of cationic lipids are related to their interaction with biomembranes and the uptake efficiency of transfection complexes.

Several authors describe distinct classes of chemical transfection reagents. *Fischer et al.* summarize synthesis methods, features, and applications of hyperbranched polyamines as carriers for nucleic acids.

A review from *Sizovs et al.* discusses carbohydrate-based polymeric transfection reagents, turning special attention to their potential applications in preclinical models and for the treatment of diseases.

Ewert et al. present recent work on structural studies of cationic lipid/nucleic acid interaction, optimized for therapeutic nucleic acid delivery. Fundamental

physical and chemical parameters that influence the uptake of transfection complexes by a cell and that are important for the improvement of transfection efficiencies are discussed.

While several reviews collected in this volume describe the basic chemical composition of transfection reagent classes, *Salcher and Wagner* focus on the modification and functionalization of polymeric gene carriers to improve their transfection efficiencies for DNA or siRNA. Such modifications include the introduction of cell-specific ligands or pH-sensitive lytic residues.

An advanced, but promising example of improvement of gene delivery technologies is highlighted in the review from *Berg et al.* Photochemical internalization is described as a versatile tool to improve the release of cargo from endocytic vesicles during the course of transfection. To achieve this, cells or tissues are exposed to a photosensitizing dye together with the molecules to be delivered into the cell. After exposure to light with a suitable wavelength, ruption of endosomal membranes occurs and the contents of the vesicle are released into the cytosol. Several photosensitizers already approved for clinical studies are presented, and their applications are discussed.

Finally, *Ruthardt and Braeuchle* summarize recent findings, describing transfection pathways of non-viral gene carriers by single particle tracking approaches. This approach allows the detailed identification of potential hurdles for efficient nucleic acid delivery from a single cell viewpoint.

We, the volume editors, hope that this book will become a helpful resource for students, as well as for the advanced scientist, by providing a deeper understanding of the mechanisms and future promise of nucleic acid transfection for research and clinical applications. As of today, this exciting field is undoubtedly far from being comprehensively explored, and technological advances will provide even better transfection tools for basic and applied research as well as for the treatment of diseases.

Hilden, Germany, Summer 2010

Wolfgang Bielke
Christoph Erbacher

Contents

Top Curr Chem (2010) 296: 1–13
DOI: 10.1007/128_2010_71

Published online: 2 June 2010

Gene Delivery into Mammalian Cells: An Overview on Existing Approaches Employed *In Vitro* and *In Vivo*

Peter Hahn and Elizabeth Scanlan

Abstract Delivery of nucleic acids into cells is one of the central techniques underpinning molecular biology research and is also a critical process for *in vivo* applications such as gene therapy, vaccination, and drug development. Delivery of plasmid DNA enables expression of recombinant genes, while delivery of siRNA is used to downregulate gene expression. Over the last 40 years, multiple different methods of nucleic acid delivery have been developed. These include viral methods and non-viral methods, which can be further subdivided into mechanical, physical, and chemical methods. Here we describe the principal delivery methods, including their advantages, disadvantages, and suitability for particular applications.

Contents

P. Hahn (✉) and E. Scanlan
QIAGEN GmbH, Hilden, Germany
e-mail: peter.hahn@qiagen.com

1 Introduction

Gene delivery into eukaryotic cells is commonly performed for research purposes as well as in gene therapy procedures. Cellular membranes do not spontaneously take up ectopic nucleic acid because of the polar nature of the phospholipid bilayer [1] which functions as a natural barrier that prevents entry of most water-soluble molecules such as nucleic acids. In studies of gene or protein function and regulation, manipulation of the intracellular expression level is a fundamental approach. For this reason, multiple methods for delivery of nucleic acids through membranes using chemical, physical, or biological systems have been established in the last 40 years.

Predominantly, two main classes of nucleic acids are used in transfection experiments: plasmid DNA and short double-stranded RNA (such as chemically synthesized siRNA or miRNA). Both cargos differ significantly in two respects: length and function. siRNAs are short molecules of 19–21 nucleotides in length that exert their function in the cell cytoplasm, whereas plasmid DNAs are significantly larger molecules (typically 2–10 kilobases) that must be transferred into the nucleus of the target cells to enable expression of the encoded recombinant gene.

The goal of this chapter is to provide a general overview of the different kinds of technologies that have been developed and that are currently used for delivery of both plasmid DNA and short double-stranded RNA into eukaryotic cells *in vitro* and *in vivo*.

2 Recombinant Viruses or Virus-Like Particles for Nucleic Acid Delivery

2.1 Recombinant Viruses

Nonpathogenic attenuated viruses can be used for delivery of DNA molecules, especially plasmids, into cells [2]. The dominant application of this technique is the *in vivo* delivery of DNA. For therapeutic purposes, the gene of interest is integrated into the viral genome and the virus uses its innate infection mechanism to enter the cell and release the recombinant expression cassette in the cytoplasm of the infected cell. The gene is subsequently translocated into the nucleus, integrated into the genome of the host cell, and eventually expressed. Adenoviruses, adeno-associated viruses [3, 4], retroviruses [5, 6], lentiviruses [7], parvoviruses [8], and herpes simplex virus [9] are currently used or under investigation for their ability to transfer plasmid DNA. Certain tissues can potentially be infected with very high efficiency, including muscle, kidney, heart, ovary, and eye.

Despite the almost 100% efficient transfection rates that can be achieved using virus-mediated DNA delivery, there are a number of concerns over the therapeutic use of this method for DNA transfer in humans. One concern is the toxicity induced by the viral infection and the potential for the generation of a strong immune

response against viral capsid proteins, which often have a high immunogenic potential. Another drawback of this approach is the untargeted integration of therapeutic genes into the host genome by the virus. Since the exact location of insertion of the gene cannot be controlled, there is a significant risk of insertional mutagenesis that could inhibit the expression of a normal cellular gene or activate an oncogene, both of which could provoke deleterious consequences. Besides these drawbacks, many other factors limit the use of viral vectors for therapeutic applications. The expensive production procedure, the complexity of generating recombinant viruses, and the limited packaging capabilities of certain viral capsids, together with the need to work in a special laboratory environment, limit this approach almost exclusively to *in vivo* DNA delivery.

2.2 Virus-Like Particles

Virus-like particles (VLPs) represent an alternative approach to classical viral DNA transfer in which only the outer shell of the virus, the viral capsid, is used without any viral genetic information. One frequently used technique is the expression of recombinant viral capsid proteins. After isolation and purification of the proteins, empty viral particles can be reconstituted and stored at −80°C. The packaging of these empty viral capsids with plasmid DNA or siRNA can then take place during a chemical dissociation/reassociation process. For example, in the case of papilloma virus, the virion shells are composed of two types of proteins, L1 protein (the major capsid protein) and L2 protein (the minor capsid protein). L1, alone or together with L2, spontaneously self-assembles into virus-like particles [10]. Even though most available VLPs are currently predominantly used for vaccination because of the immunogenic potential of their viral capsid proteins, VLPs of a number of viruses have been used for gene delivery including human polyoma JC virus, murine polyomavirus, papillomaviruses, and AAV-based virus-like particles.

3 Non-Viral Nucleic Acid Delivery

3.1 Mechanical Methods

3.1.1 Microinjection

Microinjection involves the direct injection of nucleic acids into the nucleus or cytoplasm of target cells and is the simplest approach for gene delivery. Thin glass capillaries are used to inject nanoliters of nucleic acid solution into cells. One major drawback of this method is obviously the throughput; every single cell has to be manipulated individually. This limits the use of microinjection to applications in which individual cell manipulation is possible, such as genetic engineering of

embryos or manipulation of oozytes. Though relatively efficient, this method is slow and laborious, and therefore not suitable for research using large numbers of cells or for *in vivo* delivery. Recently, fully automated robotic systems have been used for microinjection, a development that could to some extent potentially widen this obvious bottleneck [11].

3.1.2 Particle Bombardment

Particle bombardment, which is also often referred to as ballistic particle delivery, can be used to deliver nucleic acid into many cells simultaneously. In this procedure, gold or tungsten micro particles are loaded with nucleic acid and accelerated to high velocity to enable them to pass through cellular membranes and plant cell walls. By the variation of the ballistic parameters (e.g., particle size or acceleration speed), it is possible to transfect successfully adherent cell cultures including plant cells [12]. This technology is widely used for genetic vaccination where local expression of the delivered DNA is sufficient to achieve effective immune response [13].

3.1.3 Single-Walled Carbon Nanotubes

Some reports have indicated that functionalized single-walled carbon nanotubes can be used to deliver various cargos, including plasmid DNA and siRNA, into mammalian cells [14, 15]. Single-walled carbon nanotubes (SWNTs) consist of a unidimensional layer of carbon-hexagons that form a tube. By addition of amino or carboxyl groups, these SWNTs can be functionalized to allow covalent or non-covalent binding of biomolecules such as proteins, peptides, or nucleic acids. SWNTs suitable for DNA oligonucleotide or siRNA delivery typically have a tube diameter in the range of 1–5 nm and a length of 50–200 nm. Using positively charged SWNTs, it was also possible to deliver siRNA successfully *in vivo* [16].

3.2 Physical Methods

3.2.1 Electroporation Techniques

Application of an electric field to lipid bilayers such as those found in cellular membranes causes short-term depolarization of the membrane and formation of pores and other structural changes [17]. These so-called electropores allow the uptake of hydrophilic macromolecules such as plasmid DNA, siRNA, or proteins that are otherwise unable to diffuse passively through this highly regulated barrier. The use of high-voltage electrical pulses to permeabilize cell membranes was first described as a tool to deliver DNA into mammalian cells in 1982 (Wong and Neumann 1982; Neumann et al. 1982). In cuvette-based methods, cells are

incubated between two planar electrodes in a buffer with low ionic strength containing the cargo intended for delivery. The pulse length, field strength, number of pulses, electroporation temperature, and cell number need to be optimized to achieve acceptable results. Unsurprisingly, due to the numerous factors that influence electroporation results, transfection efficiencies are highly variable among different studies. Approaches that combine highly optimized, cell line-specific electroporation protocols with dedicated and quality-controlled electroporation buffers, help to reduce the complexity of this method [18].

In addition, electroporation should ideally be carried out in a hypoosmolar buffer, which induces cell swelling [19]. However, for sensitive cell types even limited incubation in such hypoosmolar buffers can lead to apoptosis, so these cells should preferentially be treated in isoosmolar buffer systems.

3.2.2 Laser-Beam-Mediated DNA Delivery

Focused high-energy fields of laser light have successfully been used to permeabilize cellular membranes. In one report, high-intensity (10^{12} W cm^{-2}) near-infrared femtosecond-pulsed beams (800 nM wavelength) were tightly focused by using an objective with a high numerical aperture directed to a small (femtoliter volume) area of the cell membrane. This induced a single, site-specific, transient perforation which was used to shuttle plasmid DNA into the targeted cells. According to this report, the treatment left the cellular architecture completely untouched, the transfection rate was 100%, and virtually no detrimental effects such as cell death or reduced cell division rate were detected [20]. Even though this is a very elegant method to deliver ectopic nucleic acid into cells, its limitations are comparable to micromanipulation in that, as a labor-intense manual procedure, it can only be applied to the genetic manipulation of a small number of cells (e.g., for manipulation of stem cells, targeted gene therapy, and DNA vaccination).

Laser beams have also been used in an untargeted manner for delivery, by directing a grid of laser pulses into a cell culture well to permeabilize a statistically significant number of the plated cells. The advantages of such an untargeted approach are reduced operator time and the possibility to automate the procedure. On the other hand, such approaches use less focused laser beams (in the nanometer range) which do not maintain the untouched status of the treated cells. As a result, these cells may also show cytotoxicity or structural changes.

3.3 Chemical Methods

The best known transfection technique using chemicals is the calcium phosphate method. In this method, calcium chloride and sodium phosphate are mixed together with DNA. Calcium phosphate crystals are formed upon combination of the chemicals and these crystals bind to and precipitate the DNA onto the cells in a

culture dish (reviewed in [21]). Subsequently, the crystals are taken up by the cell together with the plasmid DNA by endocytosis.

This method is extremely sensitive to pH changes which can lead to inconsistent transfection efficiencies, especially when using homebrew transfection buffers. To some extent, this sensitivity can be limited by the use of commercially available kits containing chemicals and buffers that have undergone quality control procedures, ensuring better reproducibility of results and less lot-to-lot variation. Although the costs per transfection for this method are unrivaled, the attractiveness of calcium phosphate precipitation has declined over the past 15 years, partly due to the trickiness of the method itself, the limited transfection efficiencies, and the narrow cell spectrum for which it is suitable, and partly because more modern and efficient DNA delivery methods have emerged.

3.3.1 Lipid Formulations

Liposomes have emerged as one of the most versatile tools for the delivery of plasmid DNA and siRNA *in vitro*. Liposomes are vesicles that have an aqueous compartment enclosed by a phospholipid bilayer. If multiple bilayers of lipid are formed around the primary core in a concentric fashion, the complex assemblies that are generated are known as multilamellar vesicles (MLVs). MLVs can be formed by reconstituting thin lipid films in buffer [22]. Small unilamellar vesicles (SUVs) of specific size (100–500 nm) can be produced by extruding MLVs through polycarbonate membranes. SUVs (50–90 nm) can also be produced by sonication of MLVs or larger SUVs. Liposomes can be used as DNA delivery systems either by entrapping the nucleic acid inside the aqueous center or by complexing them to the phospholipid bilayer. Since the phospholipid composition in the liposome bilayers can be varied, the size, morphology, composition, and surface charge can be easily adapted. DNA that is complexed in liposomes seems to be protected against nucleases, which improves its biological stability [23].

Cationic Lipids

Cationic liposomal formulations have been used in numerous studies to deliver plasmid DNA constructs as well as siRNAs into a wide range of cell lines and primary cells *in vitro* [24]. Because of their nonimmunogenic nature and the ability to produce large amounts of these lipids, such systems are also very attractive for *in vivo* gene transfer. Although the transduction efficiency is in most cases significantly lower than that of viral delivery approaches, there is also a much lower risk of unintended side-effects such as genomic integration of the ectopic DNA. Low transfection efficiencies have been attributed to the heterogeneity and instability of cationic lipoplexes [25]. Dissimilarity in lipoplex size also adversely affects their quality control, scale-up, and long-term shelf stability. Another disadvantage to the *in vivo* use of cationic lipids is their rapid inactivation in the presence of serum

[26, 27]. It has been demonstrated that transient complexes formed between cationic liposomes and plasmid DNA prior to transfection were completely inactivated when experiments were performed in the presence of 2% fetal calf serum [26]. Similarly, Lipofectin-mediated transfection was inactivated by serum [27].

Cationic liposomal formulations generally consist of mixtures of cationic and zwitterionic lipids [24, 28]. Commonly used cationic lipids are 1,2-dioleoyl-3-trimethylammonium propane (DOTAP), *N*-(1-(2,3-dioleyloxy)propyl)-*N,N,N*-trimethylammonium chloride (DOTMA), 2,3-dioleoyloxy-*N*-(2-(sperminecarboxamido)ethyl)-*N,N*-dimethyl-1-propanaminium (DOSPA), dioctadecyl amido glycil spermine (DOGS), and 3,(*N*-(*N1,N*-dimethylethylenediamine)-carbamoyl) cholesterol (DC-chol) [29]. Commonly used zwitterionic lipids, also known as helper lipids, are DOPE and cholesterol [29]. The cationic lipids in the liposomal formulation serve as a nucleic acid complexation agent and, in the case of plasmid DNA, they also lead to condensation during lipoplex formation. The overall positive charge also permits association to the cellular membrane. The zwitterionic lipids help membrane perturbation and fusion. Proprietary formulations of cationic lipids such as Lipofectamine (Invitrogen, Carlsbad, CA), Effectene Transfection Reagent, and Attractene Transfection Reagent (both from Qiagen, Hilden, Germany) for plasmid DNA transfection or Lipofectamine RNAiMax (Invitrogen, Carlsbad, CA), and HiPerFect Transfection Reagent (Qiagen, Hilden, Germany) for siRNA transfection, are commercially available. Such reagents are virtually all intended for *in vitro* experimentation. Cytotoxic effects of cationic lipid formulations can be largely avoided by the establishment of sophisticated transfection protocols and the use of minimal amounts of transfecting agents.

The first human gene therapy trial using cationic liposomes was conducted in 1992 (Huang et al. 1999). The trial used 3ß(*N*-(*N′,N′*-dimethylaminoethane)-carbamoyl) cholesterol (DC-chol)/DOPE cationic liposomes to deliver the transgene of interest. Currently ∼13% of gene therapy trials in progress worldwide employ nonviral liposomal vectors for transgene delivery [30].

Despite the appreciable success of cationic lipids in gene transfer, toxicity is of great concern. There are several *in vivo* studies reporting cytotoxicity of cationic lipids upon administration [31, 32]. Cationic liposomes have also been shown to cause dose-dependent pulmonary toxicity in mice upon intratracheal instillation. The study demonstrated that cationic liposomes stimulated the production of reactive oxygen intermediates that have been previously implicated in pulmonary toxicity [31]. As mentioned, the transfection efficiencies of nonviral cationic liposomal vectors *in vivo* are significantly lower than those of viral vectors. These low transfection efficiencies have been attributed to the heterogeneity and instability of cationic lipoplexes [25]. Dissimilarity in lipoplex size also adversely affects their quality control, scale-up, and long-term shelf stability, issues that are pertinent to their pharmaceutical production. A further drawback in the use of cationic lipids is their rapid inactivation in the presence of serum [27]. However, although the drawbacks for *in vivo* use listed above are substantial, cationic lipids are by far the most frequently used transfection method for DNA or siRNA delivery *in vitro*. Here, potential serum inactivation is not an issue because the transfection

complexes are usually formed in the absence of serum. By choosing the optimal lipid formulation and optimizing experimental parameters, sufficiently high transfection efficiencies can be achieved in cell culture systems for both plasmid DNA and siRNA.

Anionic Lipids

As an alternative to cationic lipids, the potential of anionic lipids for DNA delivery has been investigated. Because of their negative charge, DNA or siRNA molecules are very inefficiently entrapped by anionic lipids alone. In the presence of cations such as K+, Na^+, or Ca^{2+}, the complex formation of such anionic lipids and nucleic acids can be enhanced. The resulting ternary complexes of DNA, anionic lipids, and divalent calcium ions have been reported to transfect mammalian cell lines efficiently [33]. Despite this, there has only been limited progress with these anionic lipid DNA delivery systems, a fact that may be attributed, in part, to the poor association between DNA molecules and anionic lipids, caused by electrostatic repulsion between these negatively charged species.

Specialized Lipid-Based Delivery Platforms

In addition to numerous cationic and anionic lipid derivatives, functionalized liposomal formulations have also been developed, predominantly for *in vivo* therapeutic gene delivery (Fattal et al. 2001; [34]; Hosokawa et al. 1997). Liposomes that contain targeting and functionalizing groups in their lipid bilayers can be tailor-made for a range of specialized DNA delivery options ([34]; Hosokawa et al. 1997). These strategies also offer potential for the development of sophisticated delivery platforms for DNA or siRNA drugs. Specialized liposomal delivery platforms include pH-sensitive liposomes, immunoliposomes, and stealth liposomes. Stealth liposomes are sterically stabilized liposomal formulations that include polyethylene glycol (PEG)-conjugated lipids. The lipids with PEG covalently attached can be included in the formulation at a desired ratio. Pegylation prevents the opsonization and recognition of the liposomal vesicles by the reticuloendothelial system. Consequently, stealth liposomes have long circulating times in the systemic circulation. They have been used in the delivery of oligonucleotides directed against the Ha-Ras oncogene in a primate model [35].

pH-sensitive liposomes can be generated by the inclusion of DOPE into liposomes composed of acidic lipids such as cholesterylhemisuccinate or oleic acid.[150] At neutral cellular pH 7, these lipids have the typical bilayer structure; however, upon endosomal compartmentalization they undergo protonation and collapse into a nonbilayer structure, thereby leading to the disruption and destabilization of the endosomal bilayer, which in turn helps in the rapid release of DNA into the cytoplasm [34]. Efficient gene delivery of beta-galactosidase and luciferase reporter plasmids has been achieved using pH-sensitive liposomes in a variety of mammalian cell lines [36].

Immunoliposomes are gene delivery systems that can be used for cell targeting by the incorporation of specific antibodies attached to lipid bilayers (Hosokawa et al. 1997). Immunoliposomes are therefore able to recognize specifically receptors and permit receptor-mediated endocytosis for the uptake of the lipoplex. Recently, immunoliposomes containing an antibody fragment against the human transferrin receptor were successfully used in targeted delivery of tumor-suppressing genes into tumors *in vivo* [37]. Tissue-specific gene delivery has also been successful *in vivo* in several tissues including brain cancer tissue [38].

3.3.2 Polymers

The first publications reporting the use of polymers for transfection of eukaryotic cells with nucleic acids appeared in the 1970s. Mayhew and Juliano reported increased binding and uptake of RNA by Ehrlich ascites tumor (EAT) cells after treatment with poly-L-lysine. Using radio-labeled RNA, they were able to demonstrate the uptake of the molecules only when the positively charged biopolymer was present. Cell electrophoresis showed a clear reduction in electrophoretic mobility of cells treated with poly-L-lysine. This was interpreted as a result of poly-L-lysine binding to the negatively charged cell surface, thus reducing the net charge and electrophoretic mobility [39].

A second polycation that has long been used for transfection of adherent cells with plasmid DNA is (dethylaminoethyl-) DEAE-dextran. As for many other polymers, no detailed information is available about the exact molecular mechanism of DEAE-dextran-mediated gene transfer. There is some evidence that the underlying mechanism is the enhanced endocytosis of nucleic acids that stick to cellular surface. Complex formation of DEAE-dextran and DNA prior to transfection seems to be unnecessary. In contrast, the sequential administration of DEAE-dextran and nucleic acid molecules appears to have a favorable effect on transfection efficiency, as reported by Holter and colleagues [40]. In addition, this modified procedure reduces the cytotoxic effects that usually occur using the conventional protocol of simultaneous administration of reagent and cargo.

A third class of polymers that can deliver large DNA molecules, including plasmid DNA, as well as small oligonucleotides such as siRNA, *in vitro* and *in vivo*, is polyethylenimines (PEIs). These synthetic polymers have a high cationic charge density and a protonable amino group at every third position of the molecule [41]. The underlying mechanism that enables the efficient transfer of nucleic acid into cells is the ability of PEIs to form transfection complexes containing highly condensed DNA that are efficiently taken up by the cells through endocytosis. The tight condensation of the DNA as well as the buffering capacity of PEI in cellular endosomes or lysosomes most likely protects the DNA from degradation. The cytotoxicity that is induced by PEI molecules seems to be closely related to the molecular weight of the respective polymer: high molecular weight PEIs (greater than 100 kDA) seem to form large aggregates of up to 2 μm on the cell surface which may then impair the normal function of the membrane and subsequently

induce necrosis of the cells. In a study done by Werth and colleagues, a 25-kDa PEI was found to optimal for DNA or siRNA delivery efficiency as well as for minimal cytotoxic effects. Other preparations of very low molecular weight were found to be almost completely ineffective as agents of nucleic acid delivery [42].

3.3.3 PAMAM Dendrimers

Polyamidoamine (PAMAM) dendrimers are non-linear polycationic cascade polymers that can bind plasmid DNA [43]. The interaction of activated PAMAM-dendrimers and plasmid DNA induces condensation of the nucleic acid. The compact transfection complexes can subsequently adhere to the cell surface and be taken up by endocytosis.

The core moiety of PAMAM dendrimers relevant for gene transfer consists of a multifunctional amine residue. Synthesis of these macromolecules is performed by repeated Michael addition of methylacrylate and the reaction of the product with ethylenamine, resulting in spherical molecules of well-defined size that have alternating amido and amine bonds and are built up by layers of shells [43]. The different shells are called generations. After generation four, steric factors cause PAMAM-dendrimers to be spherical. The net positive charge at physiological pH of these dendrimers is generated by the terminal amine groups. Generation six or seven PAMAM-dendrimers with a diameter between 6 and 10 nm are commonly used for gene transfer [44].

Newly synthesized PAMAM-dendrimers have a well-defined size and shape with only limited flexibility. Activation of the molecules, a process which induces hydrolytic cleavage of some amido bonds in the inner part and the removal of some branches of the dendrimers, enhances the flexibility. Such activation is a random process resulting in a mixed population of PAMAM-dendrimers that vary slightly in structure and molecular mass, whereas the size and shape of the activated molecules do not differ significantly from unactivated dendrimers. Even though both activated and non-activated dendrimers can form complexes with DNA by electrostatic interaction and are able to mediate transfer of the bound DNA into eukaryotic cells, the overall transfection efficiency of activated dendrimers is 2–3 times higher. This is most likely because the higher flexibility of these activated macromolecules enhances the endosomal release of the DNA [45]. Commercially available PAMAM dendrimers include SuperFect Transfection Reagent, and PolyFect Transfection Reagent (all from QIAGEN, Hilden, Germany).

4 Summary

Over the last four decades, there has been substantial progress in the development of dedicated, highly specialized delivery systems for nucleic acids *in vitro* as well as *in vivo*. Numerous different approaches addressing multiple established cell lines and primary cell cultures have been developed and refined. For most of the

chemical approaches mentioned in this chapter, the systems need to be adapted to the cargo to be delivered and there is no generic protocol or formulation that is equally well suited for both siRNA and plasmid DNA delivery. The alternative physical method of electroporation presents problems of cytotoxicity, though these may be partly solved by the development of more advanced systems. Nevertheless, certain cell types remain that are very difficult to address, especially with the techniques and tools available to the majority of research laboratories. Although virus-mediated gene or siRNA delivery has striking advantages including unrivalled transfection efficiencies, the labor-intensive production of recombinant viruses and the need for specialized lab safety equipment are just two of the many drawbacks of this approach for *in vitro* use.

For *in vivo* delivery of nucleic acid, several viral and nonviral delivery platforms have been developed in recent years. As is the case for *in vitro* applications, virus-mediated gene transfer is seen as the most efficient way to deliver nucleic acid into virtually any given cell type *in vivo*. Technical limitations, such as low packing capacity, can limit the success of this approach. However, the possibility of a severe immune response to viral capsid components or the risk of insertional mutagenesis are the greatest threats in the use of this approach for therapeutic applications. In contrast, nonviral delivery strategies appear to have less severe unintended side-effects, although the cellular uptake by target cells *in vivo* still is insufficient in most cases. The future development of highly specific tailor-made DNA and siRNA delivery systems will not only facilitate basic research by enabling researchers to study and manipulate biological processes in relevant *in vitro* models, but will also help to apply nucleic acid-based therapeutics that can help in providing individualized medicines for specific disease variations.

References

1. Singer SJ, Nicolson GL (1972) The fluid mosaic model of the structure of cell membranes. Science 175(23):720–731
2. Lotze MT, Kost TA (2002) Viruses as gene delivery vectors: application to gene function, target validation, and assay development. Cancer Gene Ther 9(8):692–699
3. Carter PJ, Samulski RJ (2000) Adeno-associated viral vectors as gene delivery vehicles. Int J Mol Med 6(1):17–27
4. Martin KR, Klein RL, Quigley HA (2002) Gene delivery to the eye using adeno-associated viral vectors. Methods 28(2):267–275
5. Zhang X, Godbey WT (2006) Viral vectors for gene delivery in tissue engineering. Adv Drug Deliv Rev 58(4):515–534
6. Devroe E, Silver PA (2002) Retrovirus-delivered siRNA. BMC Biotechnol 2:15
7. Cockrell AS, Kafri T (2007) Gene delivery by lentivirus vectors. Mol Biotechnol 36 (3):184–204
8. Blechacz B, Russell SJ (2004) Parvovirus vectors: use and optimisation in cancer gene therapy. Expert Rev Mol Med 6(16):1–24, Review
9. Marconi P, Argnani R, Berto E, Epstein AL, Manservigi R (2008) HSV as a vector in vaccine development and gene therapy. Hum Vaccin 4(2):91–105

10. Xu YF, Zhang YQ, Xu XM, Song GX (2006) Papillomavirus virus-like particles as vehicles for the delivery of epitopes or genes. Arch Virol 151(11):2133–2148, Epub 2006 Jun 22
11. Wang W, Liu X, Gelinas D, Ciruna B, Sun Y (2007) A fully automated robotic system for microinjection of Zebrafish embryos. PLoS ONE 2(9):e862
12. Butow RA, Fox TD (1990) Organelle transformation: shoot first, ask questions later. Trends Biochem Sci 15(12):465–468
13. Fynan EF, Webster RG, Fuller DH, Haynes JR, Santoro JC, Robinson HL (1993) DNA vaccines: protective immunizations by parenteral, mucosal, and gene-gun inoculations. Proc Natl Acad Sci USA 90:4146–4160
14. Kam NW, Liu Z, Dai H (2005) Functionalization of carbon nanotubes via cleavable disulfide bonds for efficient intracellular delivery of siRNA and potent gene silencing. J Am Chem Soc 127(36):12492–12493
15. Krajcik R, Jung A, Hirsch A, Neuhuber W, Zolk O (2008) Functionalization of carbon nanotubes enables non-covalent binding and intracellular delivery of small interfering RNA for efficient knock-down of genes. Biochem Biophys Res Commun 369(2):595–602
16. Liu Z, Chen K, Davis C, Sherlock S, Cao Q, Chen X, Dai H (2008) Drug delivery with carbon nanotubes for *in vivo* cancer treatment. Cancer Res 68(16):6652–6660
17. Tieleman DP (2004) The molecular basis of electroporation. BMC Biochem 5:10
18. Gresch O, Engel FB, Nesic D, Tran TT, England HM, Hickman ES, Körner I, Gan L, Chen S, Castro-Obregon S, Hammermann R, Wolf J, Müller-Hartmann H, Nix M, Siebenkotten G, Kraus G, Lun K (2004) New non-viral method for gene transfer into primary cells. Methods 33 (2):151–163
19. Golzio M, Mora MP, Raynaud C, Delteil C, Teissié J, Rols MP (1998) Control by osmotic pressure of voltage-induced permeabilization and gene transfer in mammalian cells. Biophys J 74(6):3015–3022
20. Tirlapur UK, König K (2002) Targeted transfection by femtosecond laser. Nature 418 (6895):290–291
21. Jordan M, Wurm F (2004) Transfection of adherent and suspended cells by calcium phosphate. Methods 33(2):136–143
22. Mayer LD, Tai LC, Bally MB, Mitilenes GN, Ginsberg RS, Cullis PR (1990) Characterization of liposomal systems containing doxorubicin entrapped in response to pH gradients. Biochim Biophys Acta 1025(2):143–151
23. Gregoriadis G, Saffie R, Hart SL (1996) High yield incorporation of plasmid DNA within liposomes: effect on DNA integrity and transfection efficiency. J Drug Target 3(6):469–475
24. Felgner JH, Kumar R, Sridhar CN et al (1994) Enhanced gene delivery and mechanism studies with a novel series of cationic lipid formulations. J Biol Chem 269(4):2550–2561
25. Lee H, Williams SK, Allison SD, Anchordoquy TJ (2001) Analysis of self-assembled cationic lipid-DNA gene carrier complexes using flow field-flow fractionation and light scattering. Anal Chem 73(4):837–843
26. Hofland HE, Shephard L, Sullivan SM (1996) Formation of stable cationic lipid/DNA complexes for gene transfer. Proc Natl Acad Sci U S A 93(14):7305–7309
27. Audouy S, Molema G, de Leij L, Hoekstra D (2000) Serum as a modulator of lipoplex-mediated gene transfection: dependence of amphiphile, cell type and complex stability. J Gene Med 2(6):465–476
28. Godbey WT, Mikos AG (2001) Recent progress in gene delivery using non-viral transfer complexes. J Control Release 72(1–3):115–125
29. Marshall J, Yew NS, Eastman SJ, Jiang C, Scheule RK, Cheng SH (1999) Cationic lipid-mediated gene delivery to the airways. In: Huang L, Hung M-C, Wagner E (eds) Nonviral vectors for gene therapy. Academic, San Diego, CA, pp 39–68
30. Merdan T, Kopecek J, Kissel T (2002) Prospects for cationic polymers in gene and oligonucleotide therapy against cancer. Adv Drug Deliv Rev 54(5):715–758
31. Dokka S, Toledo D, Shi X, Castranova V, Rojanasakul Y (2000) Oxygen radical-mediated pulmonary toxicity induced by some cationic liposomes. Pharm Res 17(5):521–525

32. Filion MC, Phillips NC (1997) Toxicity and immunomodulatory activity of liposomal vectors formulated with cationic lipids toward immune effector cells. Biochim Biophys Acta 1329 (2):345–356
33. Patil SD, Rhodes DG, Burgess DJ (2005) Biophysical characterization of anionic lipoplexes. Biochim Biophys Acta 1711(1):1–11
34. Venugopalan P, Jain S, Sankar S, Singh P, Rawat A, Vyas SP (2002) pH-sensitive liposomes: mechanism of triggered release to drug and gene delivery prospects. Pharmazie 57(10):659–671
35. Yu RZ, Geary RS, Leeds JM, Watanabe T, Fitchett JR, Matson JE, Mehta R, Hardee GR, Templin MV, Huang K, Newman MS, Quinn Y, Uster P, Zhu G, Working PK, Horner M, Nelson J, Levin AA (1999) Pharmacokinetics and tissue disposition in monkeys of an antisense oligonucleotide inhibitor of Ha-ras encapsulated in stealth liposomes. Pharm Res 16(8):1309–1315
36. Legendre JY, Szoka FC Jr (1992) Delivery of plasmid DNA into mammalian cell lines using pH-sensitive liposomes: comparison with cationic liposomes. Pharm Res 9(10):1235–1242
37. Xu L, Huang CC, Huang W, Tang WH, Rait A, Yin YZ, Cruz I, Xiang LM, Pirollo KF, Chang EH (2002) Systemic tumor-targeted gene delivery by anti-transferrin receptor scFv-immunoliposomes. Mol Cancer Ther 1(5):337–346
38. Shi N, Zhang Y, Zhu C, Boado RJ, Pardridge WM (2001) Brain-specific expression of an exogenous gene after i.v. administration. Proc Natl Acad Sci USA 98(22):12754–12759
39. Mayhew E, Juliano R (1973) Interaction of polynucleotides with cultured mammalian cells. II. Cell surface charge density and RNA uptake. Exp Cell Res 77(1):409–414
40. Holter W, Fordis CM, Howard BH (1989) Efficient gene transfer by sequential treatment of mammalian cells with DEAE-dextran and deoxyribonucleic acid. Exp Cell Res 184(2):546–551
41. Boussif O, Lezoualc'h F, Zanta MA, Mergny MD, Scherman D, Demeneix B, Behr JP (1995) A versatile vector for gene and oligonucleotide transfer into cells in culture and *in vivo*: polyethylenimine. Proc Natl Acad Sci U S A 92(16):7297–7301
42. Werth S, Urban-Klein B, Dai L, Höbel S, Grzelinski M, Bakowsky U, Czubayko F, Aigner A (2006) A low molecular weight fraction of polyethylenimine (PEI) displays increased transfection efficiency of DNA and siRNA in fresh or lyophilized complexes. J Control Release 112(2):257–270
43. Haensler J, Szoka FC Jr (1993) Polyamidoamine cascade polymers mediate efficient transfection of cells in culture. Bioconjug Chem 4(5):372–379
44. Dennig J, Duncan E (2002) Gene transfer into eukaryotic cells using activated polyamidoamine dendrimers. J Biotechnol 90(3–4):339–347
45. Tang MX, Redemann CT, Szoka FC Jr (1996) *In vitro* gene delivery by degraded polyamidoamine dendrimers. Bioconjug Chem 7(6):703–714

Top Curr Chem (2010) 296: 15–49
DOI: 10.1007/128_2010_65

Published online: 10 June 2010

Strategies for the Preparation of Synthetic Transfection Vectors

Asier Unciti-Broceta, Matthew N. Bacon, and Mark Bradley

Abstract In the late 1980s independent work by Felgner and Behr pioneered the use of cationic materials to complex and deliver nucleic acids into eukaryotic cells. Since this time, a vast number of synthetic transfection vectors, which are typically divided into two main "transfectors", have been developed namely: (1) cationic lipids and (2) polycationic polymers. In this chapter the main synthetic approaches used for the synthesis of these compounds will be reviewed with particular attention paid to: *cationic lipids* and *dendrimers*. This review is aimed primarily at the younger audience of doctoral students and non-specialist readers.

Keywords Cationic lipids · Cell delivery · Dendrimers · Gene therapy · Transfection

Contents

A. Unciti-Broceta (✉), M.N. Bacon and M. Bradley
School of Chemistry, University of Edinburgh, West Mains Road, Edinburgh EH9 3JJ, UK
e-mail: asier.ub@ed.ac.uk; mark.bradley@ed.ac.uk

Abbreviations

AIDS	Acquired immune deficiency syndrome
BAC	10,10′-*bis*[3-carboxypropyl]-9,9′-biacridinium dinitrate
BGTC	*Bis*guanidinium tren-cholesterol
Boc	*tert*-Butoxycarbonyl
CDAN	*N*1-Cholesteryloxycarbonyl-3,7-diazanonane-1,9-diamine
DCC	*N*,*N*′-Dicyclohexylcarbodiimide
DC-Chol	3β-([2-(Dimethylamino)ethyl]carbamate)cholest-5-en-3-ol
DIC	*N*,*N*′-Diisopropylcarbodiimide
DIPEA	Diisopropylethylamine
DMAP	*N*,*N*-Dimethylaminopyridine
DMF	Dimethylformamide
DMSO	Dimethylsulphoxide
DOGS	Dioctadylamidoglycylspermine, trifluoroacetic salt
DOPE	1,2-Dioleoyl-sn-glycero-3-phosphoethanolamine
DORI	*N*-[1-(2,3-Dioleoyloxy)propyl-*N*-[1-(2-hydroxy)ethyl]-*N*,*N*-dimethyl-ammonium iodide
DORIE	1,2-Dioleyloxypropyl-3-dimethylhydroxyethylammonium bromide
DOSPA	*N*,*N*-Dimethyl-*N*-[2-sperminecarboxamido)-ethyl]-2,3-bis(dioleyl oxy)-1-propanimium pentachloride
DOTMA	*N*-[1-(2,3-Dioleyloxy)propyl]-*N*,*N*,*N*-trimethylammonium chloride
Fmoc	Fluorenylmethoxycarbonyl
GS-1	Gemini Surfactant 1
HBTU	*O*-Benzotriazole-*N*,*N*,*N*′,*N*′-tetramethyl-uronium-hexafluoro-phosphate
HOBt	1-Hydroxybenzotriazole
NMP	*N*-Methylpyrrolidone
PAMAM	Polyamidoamine
Pbf	2,2,4,6,7-Pentamethyldihydrobenzofuran-5-sulphonyl
PEG	Poly(ethylene)glycol
PPI	Polypropyleneimine
PS	Polystyrene
Pyr	Pyridine
SAINT	Synthetic Amphiphiles INTerdisciplinary
siRNA	Small interfering RNA
TAMTAT	*N*-[*Tris*(3-(amino)propyl)methyl]tetraeicosanamide trihydrochloride
TFA	Trifluoroacetic acid
THF	Tetrahydrofuran
TIS	Triisopropyl silane
TMR	*N*,*N*,*N*′,*N*′-Tetramethylrhodamine

1 Introduction to Transfection

The delivery of nucleic acids into cells has widespread applications, ranging from therapeutic and advanced genetic engineering to basic biological research. Thus the introduction of DNA and RNA into cells is essential for the study of gene function and for the induction of phenotypic modifications [1–4], while, therapeutically, nucleic acids have the potential to target disorders at the genetic level (e.g. gene correction, gene silencing) [5, 6]. Gene therapy provides, in principle, a versatile approach for the treatment of both inherited syndromes (e.g. cystic fibrosis, muscular dystrophy, diabetes) and acquired diseases (e.g. flu, AIDS) [7–13], in essence, allowing the treatment of the origin of disease, not its symptoms. However, its application has not yet met the highly touted expectations [14]. This is due in part to the fact that cellular uptake of free nucleic acids is hindered by their charge and size, which has led to scientists seeking refuge in the use of biological mimicry to enable transfer into the cells, often with poor efficacy or toxicity. Since the applicability of this therapeutic option inevitably relies on the transport of genes and oligonucleotides into cells in vivo, research over the last few years has focused on the development of novel carriers and strategies to improve the efficacy and safety of this process.

2 Cellular Delivery

Delivery of nucleic acid can be divided into two main categories: (1) biochemical methods, which can be further subdivided into viral [15, 16] and synthetic vectors [5, 17, 18] and (2) physical methods [19, 20], which are predominantly restricted to in vitro applications and will not be the subject of this review. Whilst viruses are currently the most efficient transfection vectors, they suffer from a number of innate disadvantages (antigenicity, potential mutagenesis, limited size of cargo, etc) that jeopardises their use as potential therapeutic agents [21–24]. As such, much attention has focused on positively-charged lipids, polymers and dendrimers which have been shown to deliver DNA and siRNA into cells, and represent an attractive alternative to viral vectors, especially because of their low cost, biocompatibility and procedural simplicities [25]. Nevertheless, the transfection efficiency mediated by these non-viral gene delivery vectors needs much improvement, especially for in vivo application [26–28].

Cationic lipids and polymers (including dendrimers) deliver DNA and siRNA into cells via cargo compaction to give lipoplexes or polyplexes (or dendriplexes), respectively, of various sizes which are then taken up via non-specific endocytosis (see Fig. 1). Once these complexes have been endocytosed the cargo has to be released into the cytoplasm to avoid degradation by the lysosomes. This escape is based upon the ability of the carrier to disrupt endosomal integrity [29–33] and is a critical step in the process. Once in the cytoplasm, the genetic material needs to be

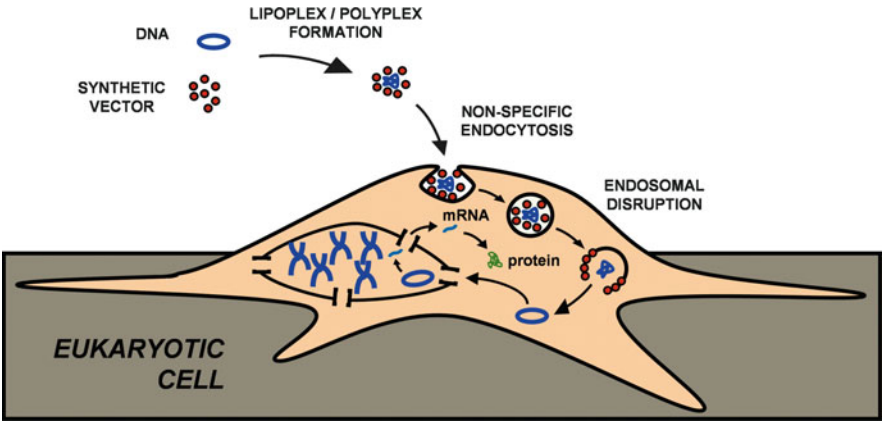

Fig. 1 DNA delivery using non-viral carriers

trafficked to the nucleus (DNA, see Fig. 1) or directly interferes at the post-transcriptional level (e.g. siRNA, miRNA) to perform its purpose. This complex multi-step process is influenced by numerous biochemical factors, being cell-cycle and cell-type dependent and, as recently demonstrated, highly affected by the extracellular microenvironment [34].

The structure of cationic lipids and polymers is readily amenable to chemical modification [35, 36] allowing the exploration of a virtually unlimited number of combinations and strategies at the mercy of chemists' creative abilities. Various reviews have been focused on cationic lipids, dendrimers and polymers in terms of their chemical structures and their transfection properties [36–41], in an attempt to shed some light on the chemical requirements necessary to mediate gene delivery. The focus of this chapter will be to explore these carriers from a synthetic perspective, with a description of the chemical strategies used for the preparation via synthetic organic chemistry (excluding polymer synthesis) of *cationic lipids* and *dendrimers*.

3 Cationic Lipids

3.1 Introduction

Since Felgner reported the first cationic lipid-based transfection reagent (DOTMA) [42], a range of positively-charged small molecules with amphiphilic properties have been described and their transfection abilities investigated [36–39, 41]. It is known that gene transfer relies upon the physicochemical characteristics of the lipoplexes (e.g. size, stability, overall charge, morphology, fluidity, degradability) [43–58], which are a function of numerous parameters (e.g. co-lipid, DNA/RNA

size, presence of serum, osmotic potential) and the molecular structure of the cationic lipid.

A cationic lipid has three fundamental constituent domains: (1) the hydrophobic part/s, (2) the cationic headgroup/s and (3) the linking moiety. Many structure-activity studies have tried to correlate structure (length, degree of saturation and type of lipid moieties, chemical nature of cationic headgroups and linking moieties, number of cationic headgroups, etc.) and gene transfer efficiency [59–67]. Despite this huge effort, cationic lipids have unrelated structural requirements and the transfection abilities of a cationic lipid are *a priori* difficult to predict. An experimental approach based on the systematic modification of the cationic lipid structural domains is thus the most advantageous to "devise" and investigate novel cationic lipid-based carriers.

3.2 Solution Synthesis of Cationic Lipids

Most cationic lipids described in the literature are synthesised by solution synthesis [36–39]. Depending upon the complexity of the structure, the synthetic routes vary from just one or two chemical steps, as in the case of DOTMA (**1**) and DC-Chol (**3**), to longer convergent synthesis, as for DOGS (**5**) (these three compounds being the earliest examples of cationic lipids prepared for transfection purposes [41, 68, 69]) (see Fig. 2).

3.2.1 Lipids: Types and Incorporation

Lipid moieties are usually integrated into the framework by alkylation or acylation reactions of amino and hydroxyl groups from the linking moiety. In solution approaches, this incorporation takes place at an early stage of the synthetic route (e.g. DOTMA (**1**) [42], DOTAP [70], DORI and DORIE [71], DC-Chol (**3**) [68], DOGS (**5**) [69]) (see Fig. 2).

Most cationic lipids are composed of either two lipophilic tails or a steroid moiety, typically based on cholesterol. The classic method for steroidyl incorporation involves the reaction of a steroidyloxycarbonyl halide (e.g. cholesteryloxycarbonyl chloride (**2**)) with primary amines from the linking moiety, a method used for the synthesis of most cholesterol-based cationic lipids including DC-Chol (**3**) [68, 72] (Fig. 2b) and BGTC (**7**) [73] (Fig. 3a).

Lipids employed in the synthesis of double-tailed cationic lipids are typically saturated or mono-unsaturated linear hydrocarbons of between 12 and 18 carbon atoms long, often derivatives of oleic (C18:1), stearic (C18:0), palmitic (C16:0) and myristic (C14:0) acids being the most widely investigated [36–39].

Lipid moieties up to 24 carbon atoms long have been used in the exploration of tridentate-cationic single-chained lipids giving remarkable transfection results [67] (see Fig. 3b).

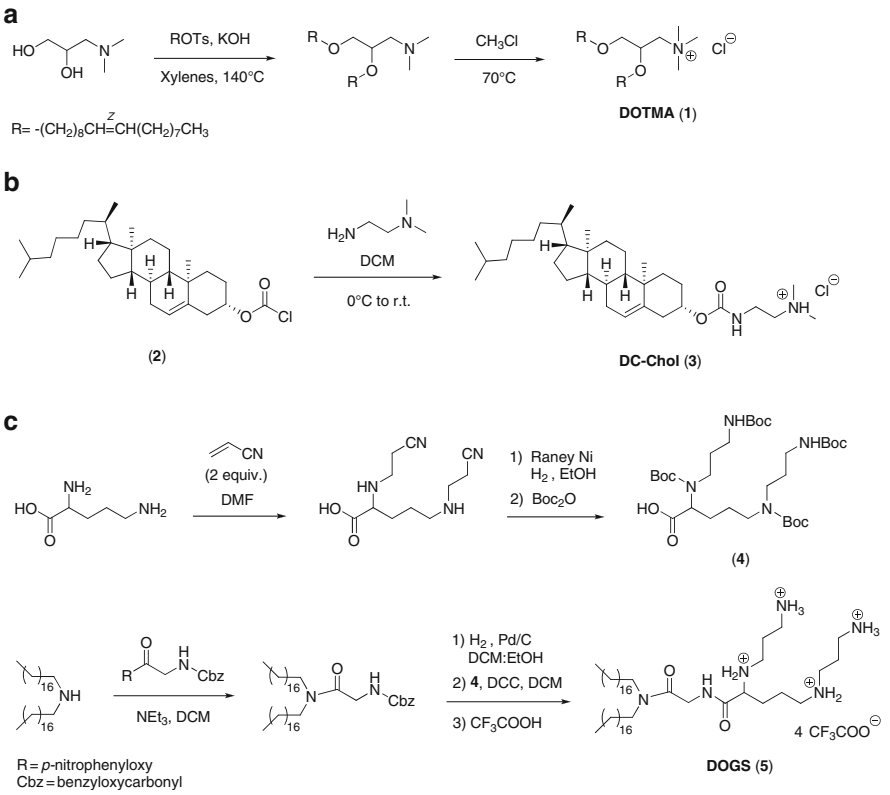

Fig. 2 Synthesis of (**a**) DOTMA, (**b**) DC-Chol, and (**c**) DOGS

3.2.2 Cationic Headgroups: Classes and Synthesis

Due to the difficulties in handling and purifying the positively-charged reagents, the cationic headgroups are preferentially formed in the last step of the synthesis. While various cationic headgroups have been investigated, nitrogen-based motifs (mainly guanidinium and ammonium groups) are the most widely used. Permanent positive charges are typically synthesised via quaternisation of tertiary amines (see Figs. 2a and 4) [41, 70, 75–82], with the counterion of the resulting quaternary ammonium salt being the corresponding leaving group of the alkylating reagent used.

Quaternary phosphonium and arsonium groups have been investigated by Clément as alternative positively-charged headgroups in the synthesis of cationic phosphonolipids [75, 76] (see Fig. 4) and lipophosphoramidates [83, 84].

Protonation of the ammonium groups are obtained from the treatment of primary, secondary and tertiary amines with inorganic acids. As the counterion may have a critical role on the stability and biocompatibility of the reagent [85], the selection of the inorganic acid or alkylating reagent used in the salt formation

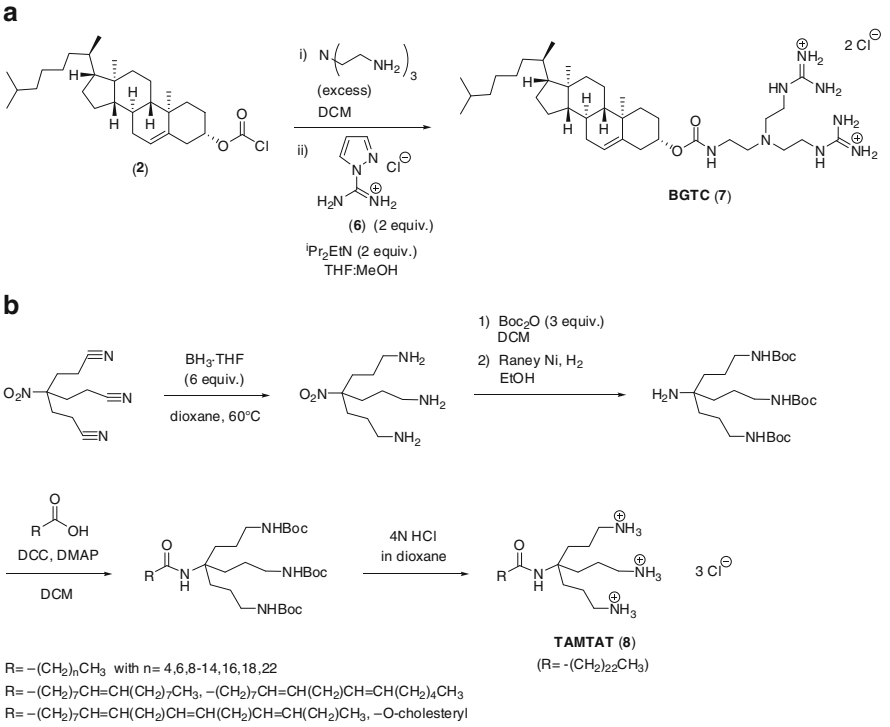

Fig. 3 Synthesis of BGTC and tripodal cationic lipids

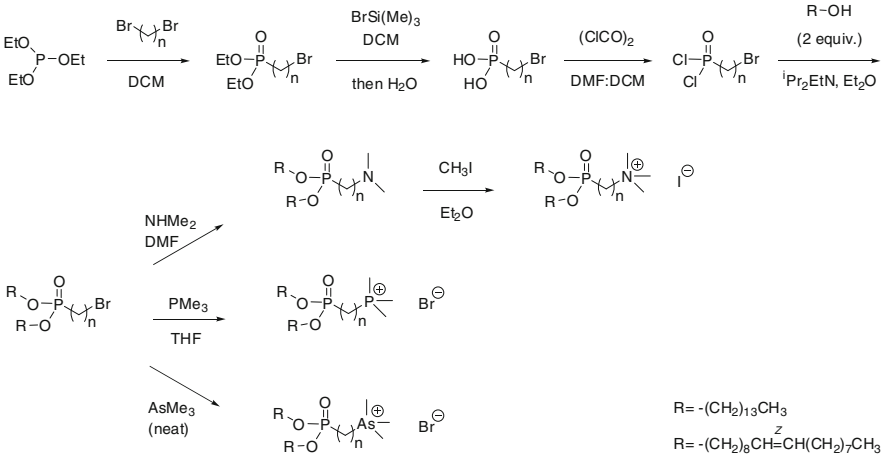

Fig. 4 Synthesis of cationic phosphonolipids

process may become critical. If the counterion complexed during this process is not satisfactory, an ion-exchange resin can easily be used to carryout the exchange [86].

Incorporation of natural polyamines such as spermidine and spermine into the lipid framework (e.g. DOGS (**5**) [69], DOSPA [87], CDAN [88], GL67 [89], MVL5 [90]) has been achieved by a number of convergent strategies (see Fig. 2a). The use of a polyamine as part of a cationic lipid incorporates protonation sites with different p*K*b values, as a way to buffer the endosome pH drop [91–93].

Guanidino-containing cationic lipids have been exploited in the synthesis of cationic lipid-based carriers [94–96] ever since Lehn described BGTC (**7**) [73, 97, 98] (see Fig. 3a). The guanidinium group is fully protonated at physiological pH (p*K*a $>$ 12) and behaves as a bidentate hydrogen-bond donor, which is thought to enhance the interaction with negative cell surface structures such as (heparin) sulphates and other proteoglycans [36, 99]. This group is traditionally incorporated by reaction of primary amines with protected or unprotected guanidinylation reagents such as 1*H*-pyrazole-1-carboxamidine, **6** (see Fig. 3a), or by assembling guanidino-containing moieties (e.g. arginines) [100, 101].

In most strategies applied to the production of cationic lipids bearing protonated primary or secondary amino and/or guanidino groups, these are protected throughout the synthesis with acid-labile protecting groups [67, 69, 82, 87–90, 102, 103]. In particular, the *tert*-butyloxycarbonyl group (Boc) is widely used for this purpose because its versatility (it can protect both primary and secondary amines) and, importantly, the volatile residues of cleavage (see syntheses of DOGS, **5**, and TAMTAT, **8**, respectively, in Figs. 2a and 3b, respectively).

3.2.3 Functional Linking Moieties

Gemini surfactants used in gene delivery [104, 105] are symmetric amphiphiles composed of two identical cationic lipid domains linked by a spacer. This class of chemicals have been widely investigated in transfection due to their remarkable surfactant properties and abilities to complex DNA [64, 91, 106–111]. Depending on their design, their synthesis may be carried out by assembling their constituent parts on a bi-functional spacer [109, 110] (see Fig. 5a) or synthesising the cationic lipid domain first and then linking two of these through a spacer at the end of the synthetic route [111] (see Fig. 5b).

Aryl groups have been used as rigid spacers between the lipophilic groups and the cationic moieties [84, 111, 112] (see Fig. 5b). Heteroaryl groups containing nitrogen (e.g. pyridine, imidazole, quinoline) have additionally been employed as headgroups of cationic lipids, in part because charge delocalisation is considered to diminish cellular toxicity [100, 113–125]. Among nitrogen-based heterocycles, quaternary pyridinium salts are the most widely used for the preparation of cationic lipids [118–125], being synthesised by quaternisation of the nitrogen atom [118–122] (see Fig. 6) or by reaction of primary amines with pyrylium salts [65, 123–125] (see Fig. 7), this last procedure generally offering better yields.

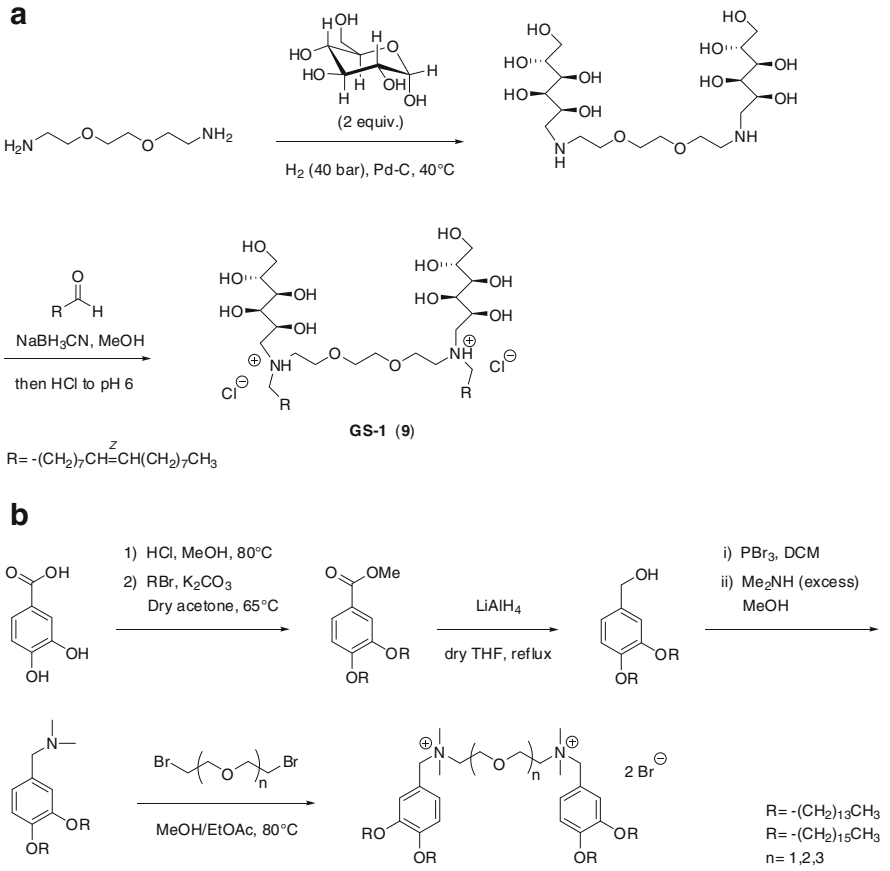

Fig. 5 Synthesis of gemini surfactants by a divergent assembly strategy

Attempting to improve transfection efficiency, the inclusion of enzyme, pH or redox susceptible chemical groups in the cationic lipid structure has been investigated [126–129] with, for example the synthesis of lipid moieties connected through ester bonds sensitive to intracellular esterases [64, 70, 71, 126].

An extensive structure-activity relationship study was carried out by Balaban [64] to identify structural parameters required for optimal transfection in different classes of gene transfer agents. To this end, they employed a strategy making use of the high reactivity of pyrylium salts toward primary amines, thus allowing access to over 60 pyridinium-based cationic lipids, including stimuli-sensitive lipids (containing either ester or disulphide groups), gemini surfactants, and oligomeric surfactants (see Fig. 7).

The introduction of redox-sensitive linkages, such as the disulphide group, has been used to prepare liposomes that are susceptible to the lower intracellular redox potential relative to the extracellular environment. Symmetrical disulphides are synthesised by oxidation of thiol-containing structures [64, 130, 131] (see Fig. 7),

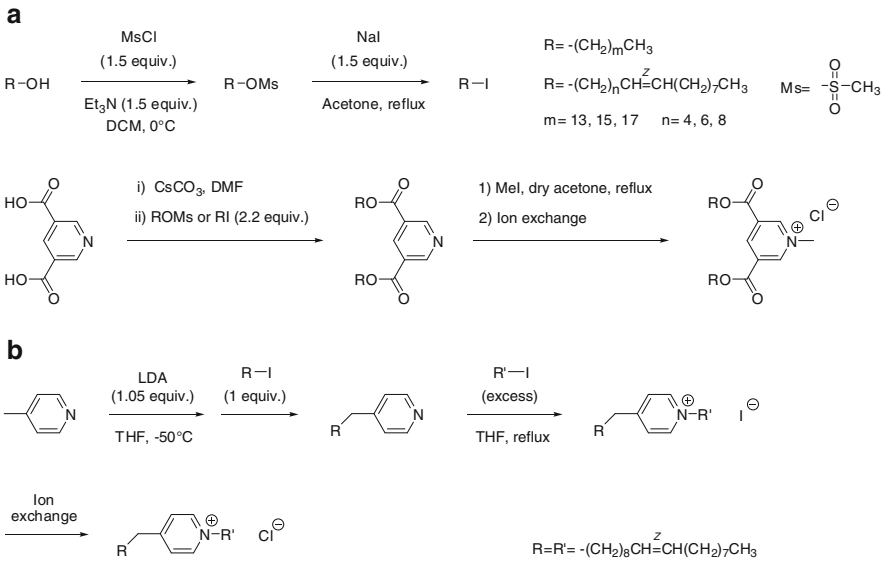

Fig. 6 Synthesis of (**a**) ester-containing SAINT lipids [120] and (**b**) sunfish cationic amphiphiles [121, 122]

while unsymmetrical disulphide bonds are assembled via cross-linking reaction mediated by activated symmetrical disulphide scaffolds such as 2,2-dipyridyl disulphide [132, 133].

Distinct classes of pH-sensitive linkages have been used to effect acid-catalysed phase transitions and thus improve transfection efficiency, with the use of ortho esters [134–136], vinyl ethers [137, 138], carbamates [139, 140], acylhydrazones [141], acetal [142, 143] and ketals [144] all applied. Nantz [134] synthesised the first ortho-ester-containing cationic lipid using a divergent approach (see Fig. 8). Ortho esters are highly sensitive to mild acid pH, thus making the resulting lipoplexes very sensitive to endosomal acidification. The key in the synthesis was the use of an oxetane scaffold with two hydroxymethyl moieties at position 3 (compound **11**), allowing the synthesis of acyloxymethyloxetane (**12**) and subsequent rearrangement to the ortho ester by treatment with catalytic BF_3 etherate [145]. Attachment of the ortho ester lipid (**13**) to the cationic lipid framework was achieved using oxyrane-mediated transesterification of the 2-bromoethyloxy moiety by aminoalkoxides [146].

Lehn synthesised guanidinium-based cationic steroids incorporating an acylhydrazone linker using the approach shown in Fig. 9 [141]. The synthesis was developed from a polyamine scaffold by guanidination of the primary amino groups and alkylation of the secondary amine with methyl chloroacetate to introduce the ester moiety required to form a hydrazide group by reaction with hydrazine monohydrate. Cationic steroid hydrazones were then prepared via an acetic acid catalysed reaction with cholestanones, which demonstrated high transfection efficiency and low toxicity in a variety of cell lines [141].

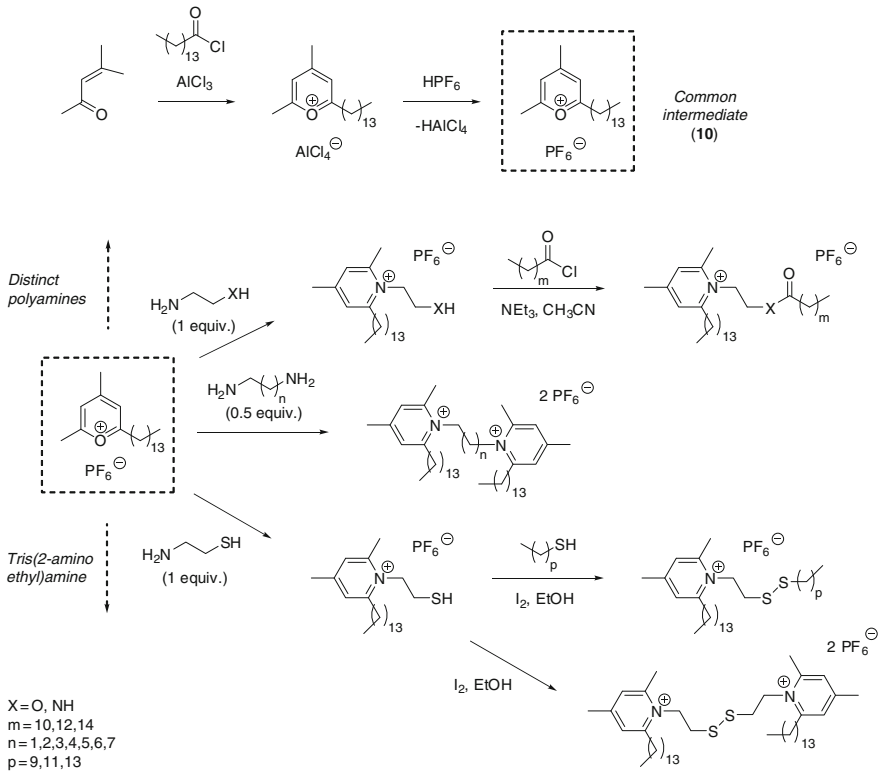

Fig. 7 Synthesis of pyridinium-based cationic lipids by a linear assembly strategy

3.3 Solid-Phase Synthesis of Cationic Lipids

A number of cationic lipids have been prepared using solid-phase methods [147–159]. Along with the well-known advantages that solid-phase chemistry provide (e.g. mass action, simple purification, compatibility with microwave synthesis [160, 161]), the main reason to use this approach is that it facilitates parallel synthesis of libraries of compounds, allowing potential structure activity relationships to be rapidly determined by the systematic modification of the cationic lipid structure per domain.

Each and every solid-phase strategy employed for the synthesis of cationic lipids has in common the use of acid-cleavable protecting groups and solid-phase linkers/resins. Solid-phase construction is usually initiated from the hydrophilic domain with headgroups and linking moieties successively incorporated into the construction, leaving the assembly of the lipid moieties for the latter stages of the synthesis, typically just before the cleavage.

Cationic lipids (lipitoids [147, 148]) were assembled on solid phase by Zuckermann using a submonomer approach, based on the sequential incorporation

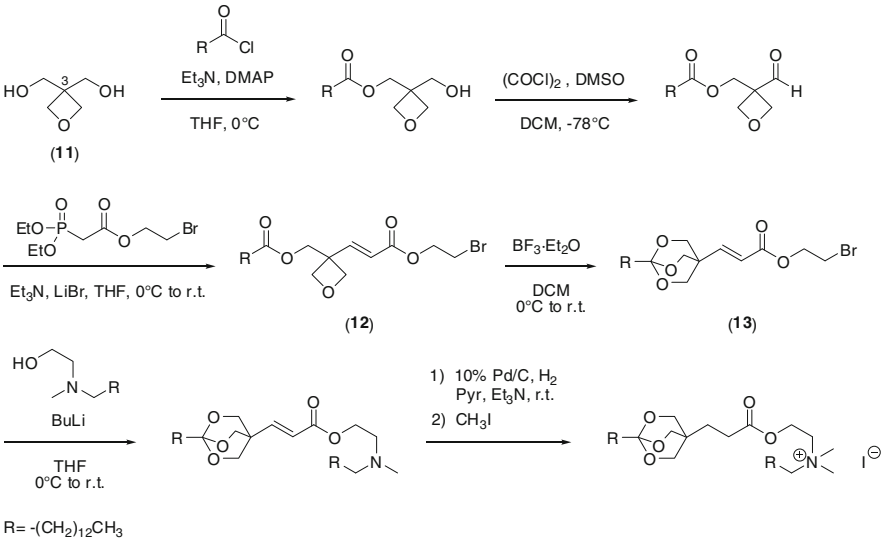

Fig. 8 Synthesis of ortho ester-containing cationic lipids

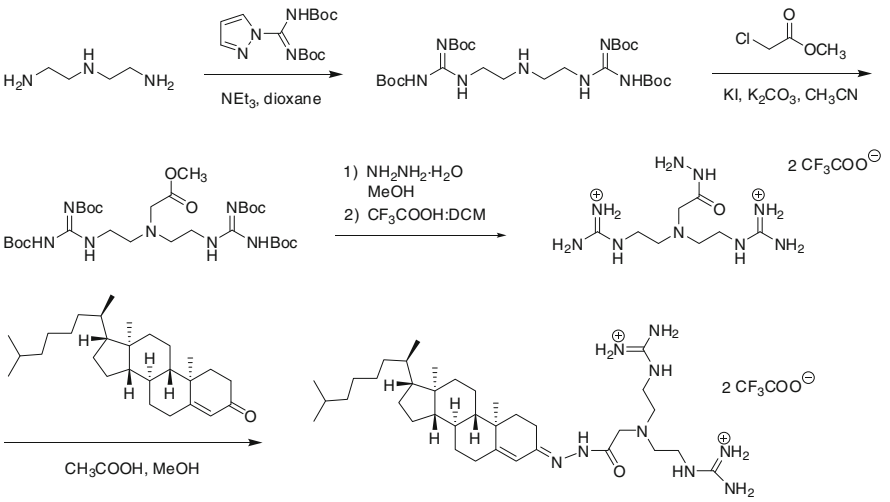

Fig. 9 Synthesis of·guanidinium-based cationic steroids incorporating an acylhydrazone linker [115]. Due to the chemical nature of the final reagent, lipid incorporation and salt formation steps are inverted in this synthetic approach

of bromoacetic acid and primary amines as building blocks (see Fig. 10a). Besides the use of readily-available starting materials, this strategy allowed a wide choice of functional groups to be introduced as side chains of the primary amines [147, 148].

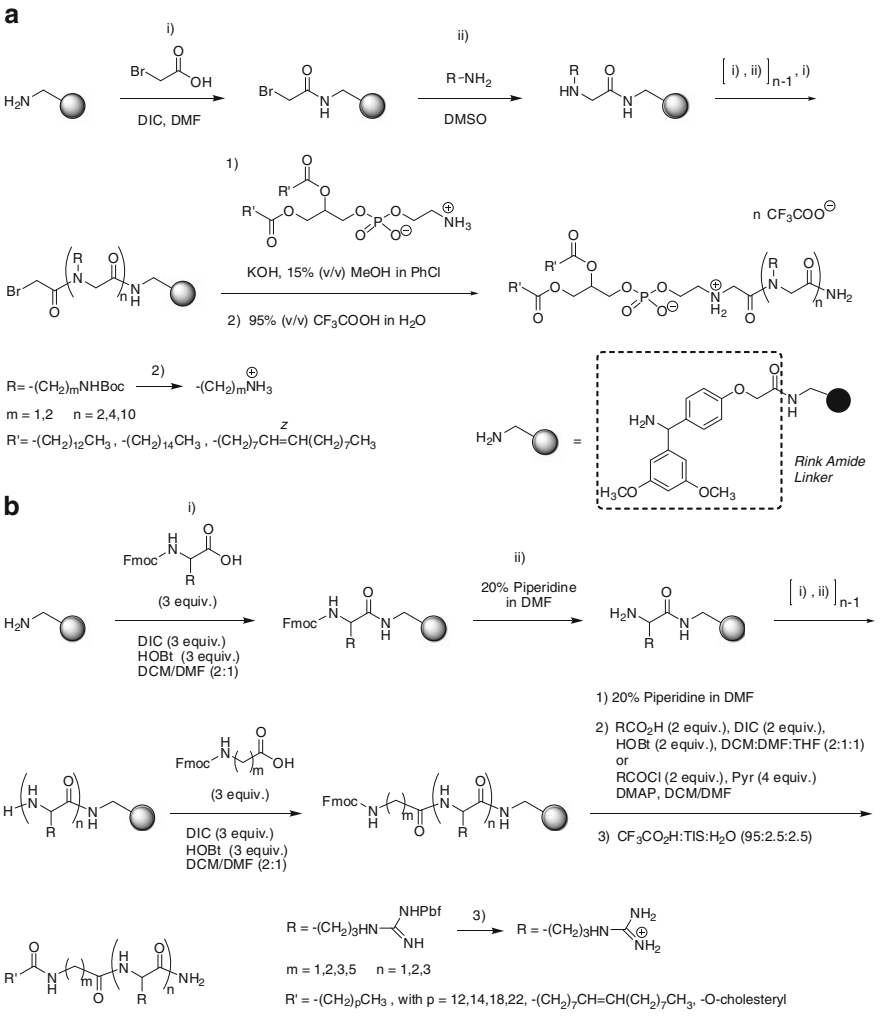

Fig. 10 Solid-phase synthesis of cationic lipids using submonomer (**a**) [147, 148] and monomer (**b**) [151, 152] linear assembly

Park [149, 150], Bradley [151, 152] and others [153] have assembled cationic lipids on the solid support using a linear strategy based on the assembly of protected building blocks (e.g. natural aminoacids). This "monomer" approach consists of a two-step deprotection-coupling sequence mediated by the use of building blocks which are protected with base-cleavable groups. This strategy was used for the synthesis of a library of arginine-containing lipid transfection agents on high-loading beads [151, 162]. Compounds were linked to various aliphatic tails or steroidal groups (see Fig. 10b), giving a total of 60 compounds which were screened from single beads. This approach was also applied for investigating the effect of

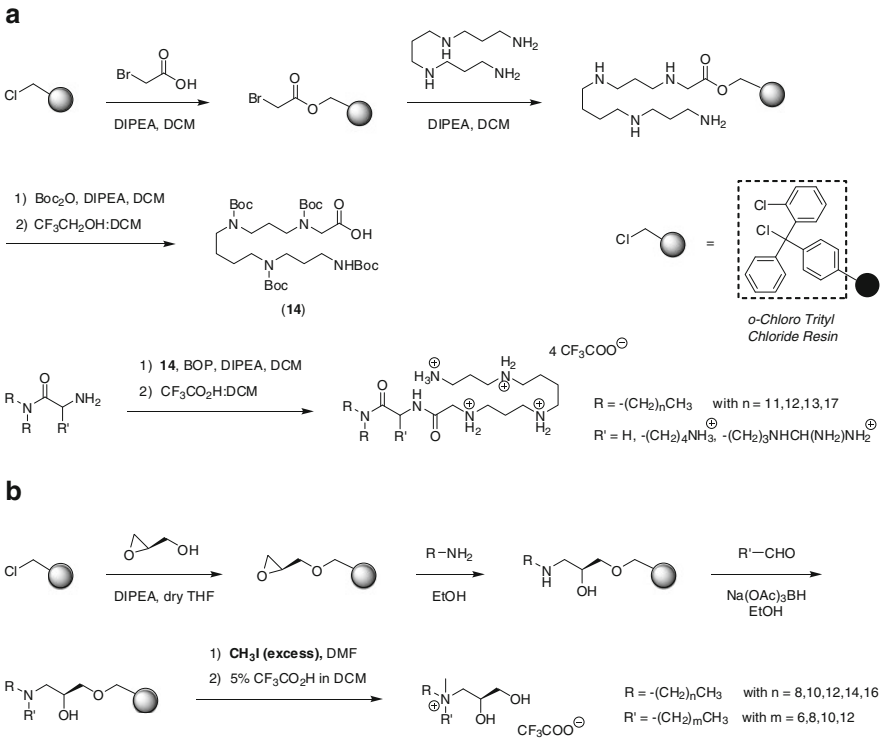

Fig. 11 (**a**) Convergent strategy for the synthesis of polyamine lipids [63, 154, 155]. (**b**) Solid-phase synthesis of quaternary ammonium double-tailed lipids [157]

very long-chain fatty tails (arachidyl (C20:0) and lignoceryl (C24:0)) in the transfection abilities of arginine-containing single-tailed lipids [152].

Byk applied solid-phase chemistry for the preparation of Boc-protected polyamines [154]. This synthetic method allowed easy access to unsymmetrically monofunctionalised polyamine building blocks of variable geometries. Using a convergent approach, these protected polyamines were used to prepare several libraries of cationic lipids (see Fig. 11a), allowing structure-activity relationship studies by introduction of lipids and linkers of variable length, and different polyamine geometries [63, 155]. Polyamine-containing cholesterol-based lipids (CDAN and analogues) were synthesised using a solid-phase strategy by Miller [156].

Massing described a synthesis of systematically modified cationic lipids by solid-phase chemistry starting with the immobilisation of (*R*)-2,3-epoxy-1-propanol on 4-methoxytrityl chloride resin [157]. Reaction of the epoxide with distinct long-chained amines was followed by reductive amination and tertiary amine quaternisation (see Fig. 11b). This interesting method allowed the solid-phase coupling of three different lipophilic moieties on an amino group and the synthesis

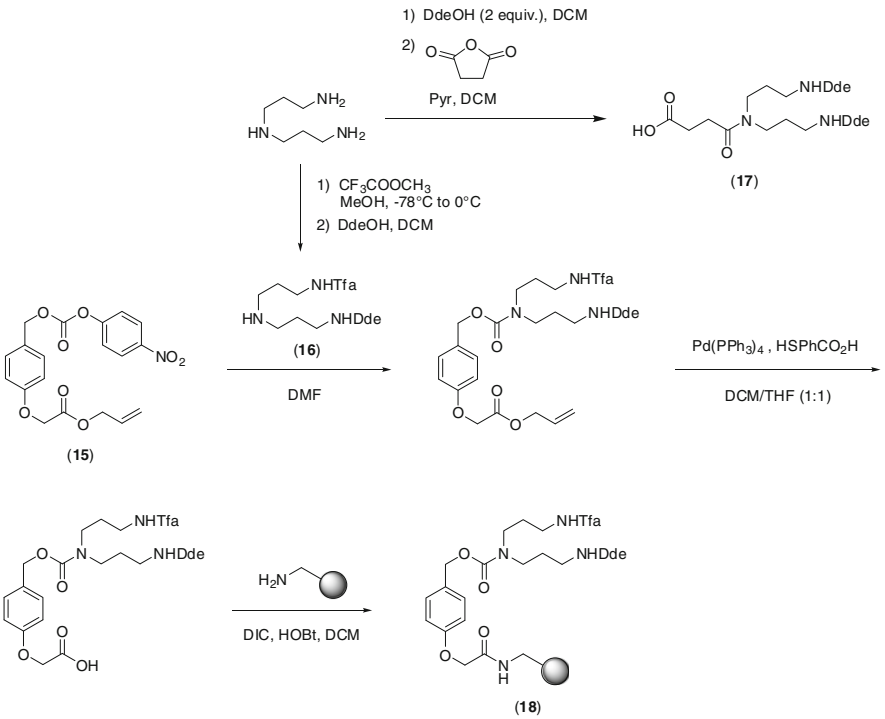

Fig. 12 Synthesis of orthogonally-protected polyamine-bound resin **18** [158]

of a new class of cationic lipids based on a 3-ammonium-1,2-dihydroxypropane moiety as the polar, cationic lipid part.

A divergent solid-phase approach for the synthesis of guanidino-containing cationic lipids was described by Bradley [158]. This synthesis was developed from orthogonally-protected polyamine-bound resin **18**, synthesised from orthogonally-protected polyamine scaffold **16**, coupled to acid-labile linker **15** (see Fig. 12). The blocking of the primary amino groups of polyamine **18** with two orthogonal protecting groups (Tfa and Dde) allowed the independent assembly of the cationic lipid by each terminal amino group, which was exploited to produce various cationic lipids (see Fig. 13).

This approach allowed the synthesis of three libraries of polyamine-based cationic lipids: mono-guanidino single-tailed lipids, mono-guanidino double-tailed lipids and bis-guanidino single-tailed lipids (see Fig. 13). A total of 89 cationic lipids were synthesised using diverse hydrophobic tails and structure-activity relationships determined for transfection ability. This combinatorial study demonstrated that bis-guanidino single-tailed lipids bearing a myristyl or oleyl moiety were the best transfection reagents, thus showing that double-chained lipids are not necessarily better gene carriers than their single-chained counterparts.

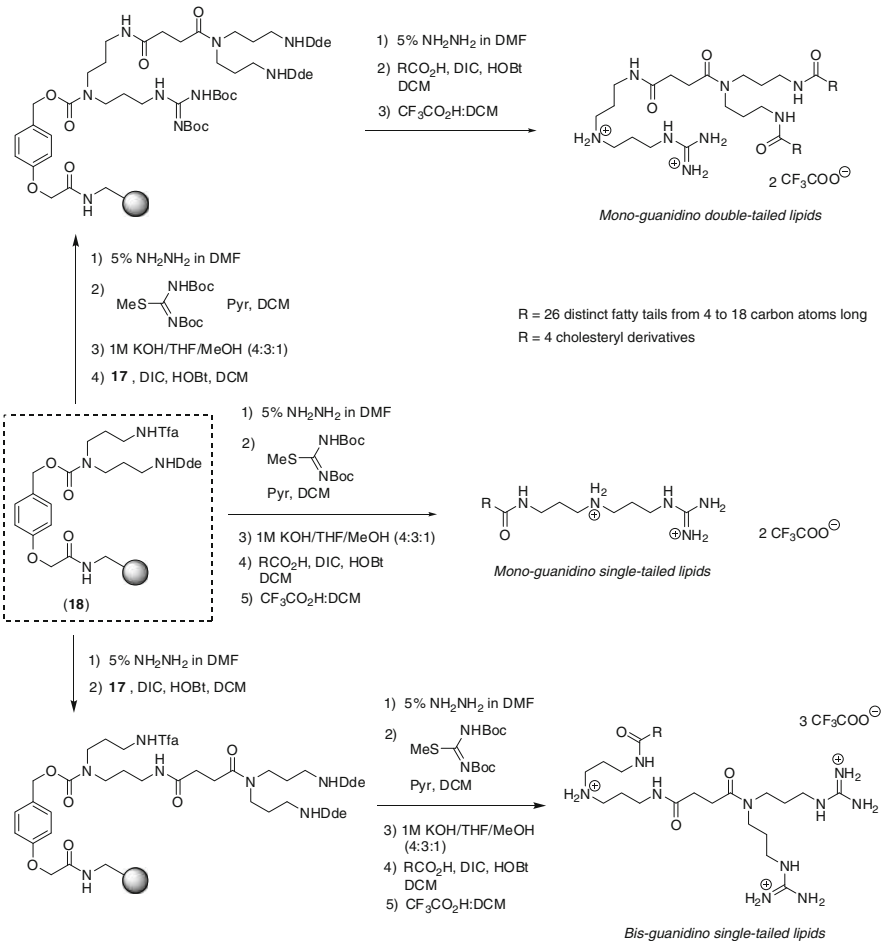

Fig. 13 Diversity-oriented synthesis of·guanidinium-based cationic lipids by divergent solid-phase assembly [158]

A combinatorial library of aminoglycerol-based monocationic lipids synthesised using a linear solid-phase approach was recently described by Yingyongnarongkul [159] (see Fig. 14).

4 Dendrimers

4.1 Introduction

Dendrimers (from the Greek "dendron": tree) are highly branched, monodisperse (ideally) polymers, based around a central core moiety, from which multiple wedge-shaped dendritic fragments or dendrons spread out [163, 164] (see Fig. 15).

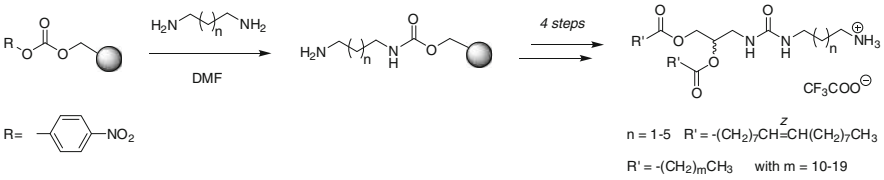

Fig. 14 Solid-phase synthesis of aminoglycerol-based monocationic lipids [159]

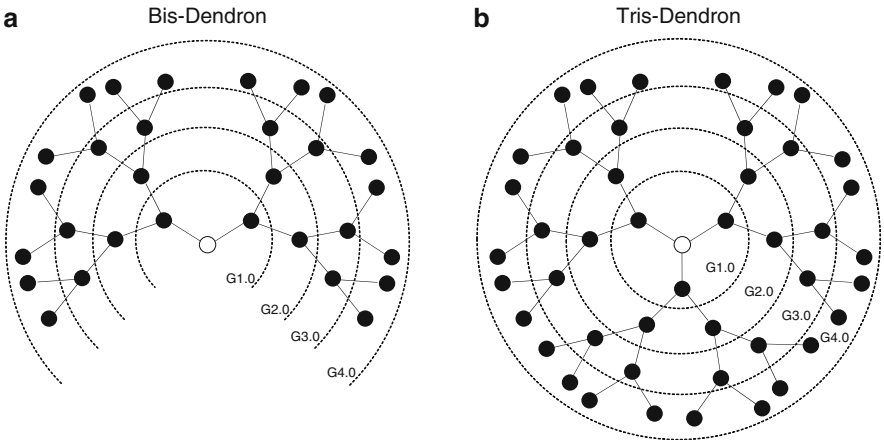

Fig. 15 Morphologies of bis and tris-dendron containing dendrimers. G1.0, G2.0, etc. represent rounds of synthesis that increase the number of groups on the surface

These structures are typically characterised as possessing a well-defined core, interior region layers, and a functionalised periphery, and begin to adopt a globular shape as the generation number increases (Gn). With each successive generation the number of end groups multiplies affording a high density of functional groups on the surface that strongly influences the properties of the dendrimer [165].

Dendrimers have great potential in biomedical applications, due to their low immunogenicity, relatively low toxicity, tuneable chemistry and ease of functionalisation [165–172]. Particularly promise has been demonstrated in the field of cellular delivery, and as such their ability to deliver biomaterials and both hydrophilic and hydrophobic drugs into eukaryotic cells has been, and is actively being, investigated [39, 167–169, 173–175]. Dendrimers of a polycationic nature have found application as DNA/siRNA delivery reagents, leading to the development of the commercially-available transfection reagent SuperFect [176].

Dendrimers are sequentially constructed using building blocks bearing several attachment sites and may be assembled following two substantially different strategies: *divergent* or *convergent assembly*. Divergent assembly consists of the sequential attachment of functionalised monomeric (or submonomeric) units onto a growing multi-branched scaffold (see Fig. 16) [177, 178], with each round of synthesis giving a higher generation dendrimer. In the convergent assembly

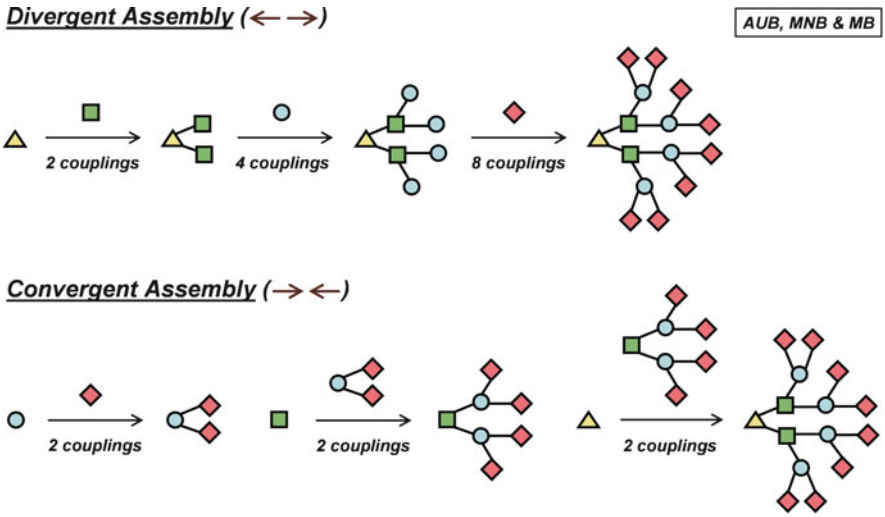

Fig. 16 Assembly approaches used for the construction of dendrimeric materials

approach growth initiates from what will eventually become the periphery of the dendrimer and progresses inward (see Fig. 16). The "dendrimer's branches" are then attached to the multi-functionalised core (the trunk of the dendrimer) to give the higher generation dendron. The convergent route differs from its divergent counterpart because in each round of synthesis the convergent synthesis typically involves a constant number of coupling reactions per molecule, independently from the generation being assembled, while the divergent approach exponentially increases the number of reactions in each generation.

To optimise the physico-chemical properties of a dendrimer (e.g. overall charge, buffering properties, solubility, biodegradability), it is crucial to design the appropriate monomer building blocks [165, 178]. The selection of the assembly strategy is also decisive for the optimal synthesis of the structure. In general convergent approaches are more suitable for the synthesis of very high-generation dendrimers but also much more complex and time-consuming than divergent strategies. Little research on polycationic dendrimers synthesised by convergent strategies has been described, while divergent strategies have been widely explored using both *solution* and *solid-phase* chemistry.

4.2 Solution Synthesis of Dendrimers

4.2.1 Polypropylenimine Dendrimers

Dendrimer chemistry began to emerge in the early 1980s, and like many discoveries it was a gradual evolution of the chemistry already available [174–178]. The first identifiable example of a true dendrimer was the divergent synthesis by Vögtle in

1978 of polypropylenimine (PPI) [179], utilising a double 1,4-addition of a primary amine containing core onto acrylonitrile followed by reduction of the nitrile (see Fig. 17a). The reduction step was initially problematic and significantly reduced the yield, preventing generations higher than three from being achieved [168].

The pioneering method used by Vögtle was optimised for large scale synthesis by the employment of a Raney-cobalt catalyst (see Fig. 17a). Using this optimised method, the yield of the nitrile reduction step could be drastically improved, allowing dendrimers up to G8 to be produced [180, 181]. It was expected that these larger dendrimers would be better transfection reagents; however, they have so far demonstrated poor ability and relatively high toxicity [182]. In contrast, G2-3 PPI dendrimers have been successfully used for transfection in vitro [182, 183].

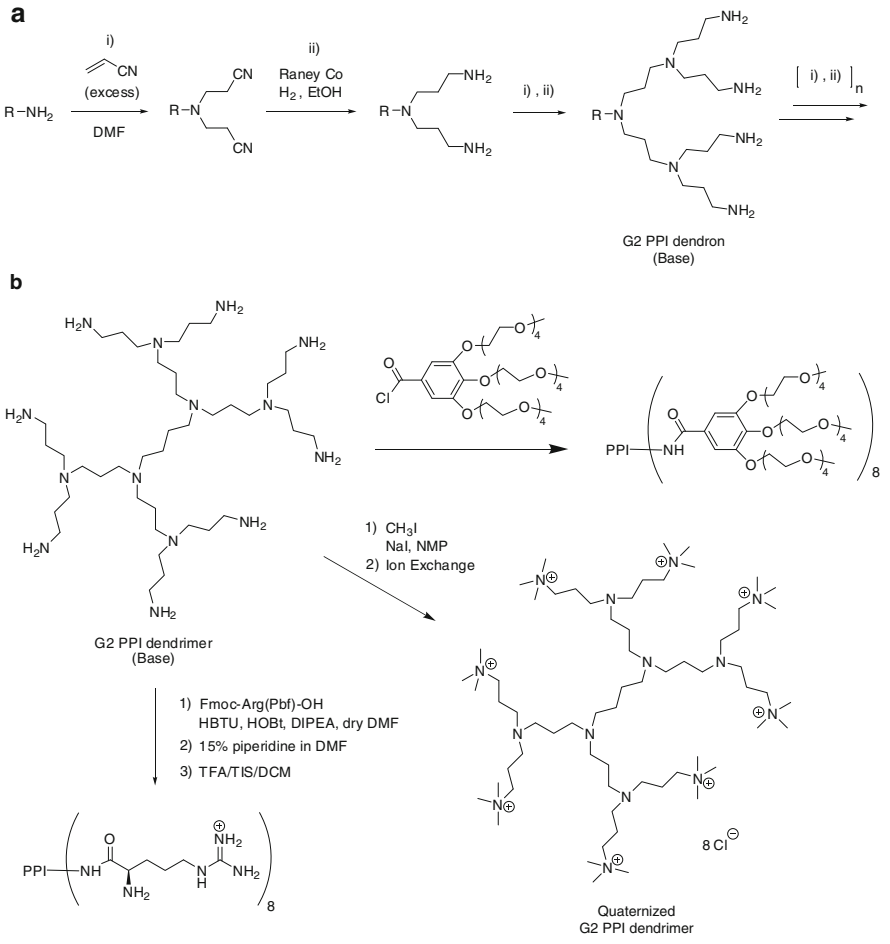

Fig. 17 (**a**) Optimised synthesis of PPI dendrimers. (**b**) Diverse functionalisation of G2 PPI dendrimers

Quaternisation of the terminal amines (see Fig. 17b) resulted in an improvement of the colloidal stability and biocompatibility profile of the dendriplexes, increasing delivery abilities both in vitro and in vivo [184]. Other studies described the in vitro transfection properties of a second generation dendrimer modified with glycol gallate (a PEG analogue) on its surface [185]. This was achieved by reacting glycol gallate acyl chloride with the free primary amines of the periphery of a second generation PPI dendrimer (Fig. 17b) [186]. Arginine-containing PPI dendrimers were also investigated by Park [187], being synthesised by the conjugation of arginine residues on the peripheral amino groups of the PPI dendrimers (Fig. 17b).

4.2.2 Polyamidoamine Dendrimers

Tomalia developed the polyamidoamine (PAMAM) dendrimers via the repetition of a simple two-step procedure: (1) 1,4-addition of a nucleophilic core (e.g. ammonia, ethylene diamine or tris(2-aminoethyl)amine) to methyl acrylate followed by amidation of the resulting ester with an amine functionality (e.g. ethylene diamine, propylene diamine) [188, 189] (see Fig. 18). PAMAM dendrimers could be synthesised as high as generation seven, due to the high yield of the synthetic procedure. From that point the steric considerations began to dominate, making the addition of any subsequent generations difficult [168].

The robust and simple chemistry used to prepare PAMAM dendrimers, coupled with its biocompatibility and high generation number achievable has lead to PAMAM becoming the most investigated dendrimer-based vector for gene transfer [168]. The first successful attempt at transfection using PAMAM dendrimers was described by Szoka [190]. Other studies conducted by Baker showed that high transfection efficiency was achieved using G5–G10 PAMAM, but the highest gene transfer efficiency varied with cell line [191]. Subsequent studies showed that when PAMAM dendrimers were treated with methanol or butanol and heated prior to complexation with DNA then rates of transfection increased significantly [173]. This is thought to be due to an increase in branch flexibility caused by the partial degradation, which allows the dendrimer to complex the DNA more tightly initially, and then swell more significantly in the endosome [173].

Much research has been carried out into the functionalisation of the primary amino groups on the surface of PAMAM dendrimers with a number of conjugates (e.g. aminoacids, sugars, lipids), leading to a variety of "decorated" PAMAM dendrimers with improved transfection abilities both in vitro and in vivo [192–201].

Verkman demonstrated the significant buffering capacity of PAMAM dendrimers by measuring endosome chloride concentration and pH changes over time in contrast to a non-buffering polymer (poly-lysine) [202]. Endosomal pH was investigated by fluorescence intensity variations of the fluorescein-conjugated poly-lysine and PAMAM dendrimer. Chloride endosomal concentration was determined by conjugating PAMAM to both chloride-sensitive (10,10′-bis[3-carboxypropyl]-9,9′-biacridinium dinitrate (BAC)) and insensitive fluorescent probes (tetramethylrhodamine (TMR)), and measuring the fluorescence ratio changes. This was achieved by first

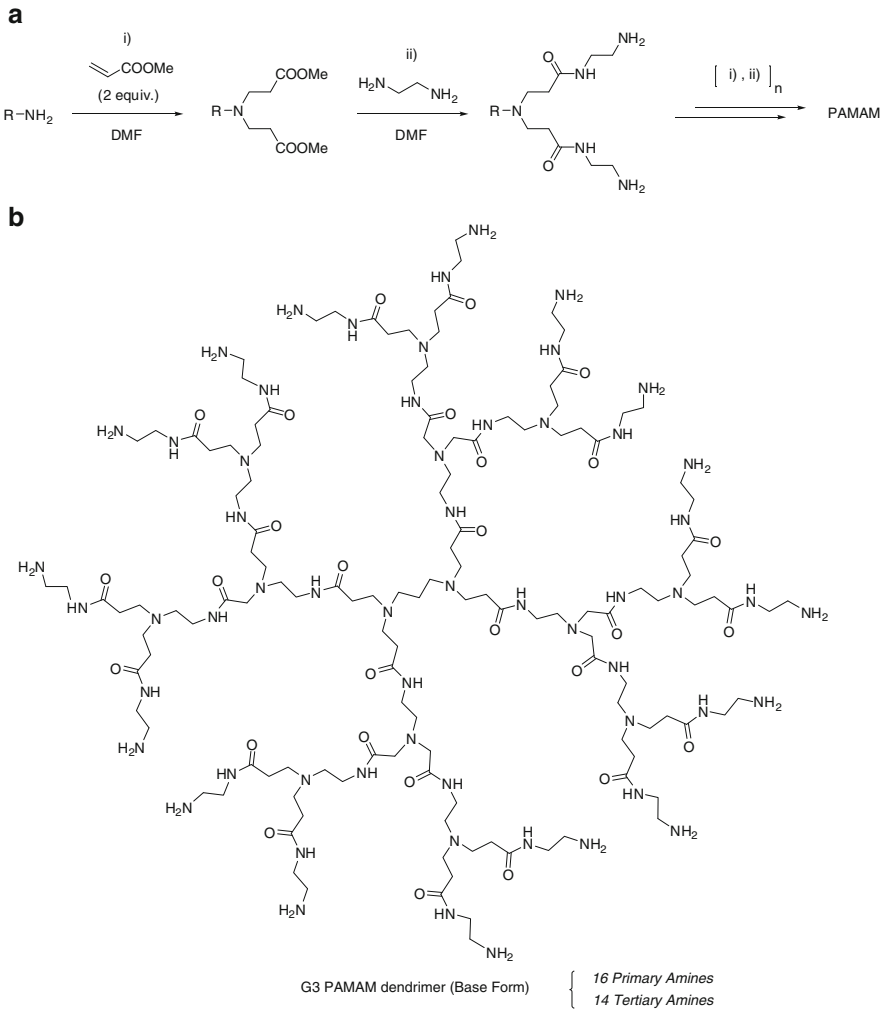

Fig. 18 (**a**) General synthesis of PAMAM dendrimers. (**b**) G3 PAMAM dendrimer

reacting PAMAM primary amino groups with the succinimidyl ester of tetramethylrhodamine followed by reaction with 2-iminothiolane (**19**) to generate thiol groups on the PAMAM-dendrimer surface, which were then reacted with BAC-labelled dextran conjugated to dithian-2-pyridyl [202] (see Fig. 19). Analysis demonstrated that, in the presence of PAMAM dendrimers, endosomal chloride accumulation increased significantly and the pH dropped slower in comparison with polylysine, indicating the occurrence of endosomal swelling/lysis and underscoring the relevance of the "proton sponge" theory [33] for PAMAM mediated gene delivery.

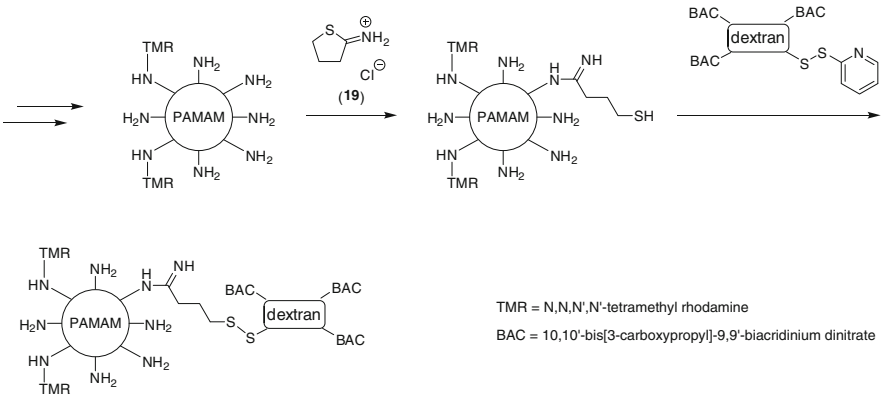

Fig. 19 A PAMAM dendrimer ratiometric sensor synthesised by conjugation of PAMAM dendrimers to a chloride-sensitive probe (BAC) and to a chloride-insensitive dye (TMR)

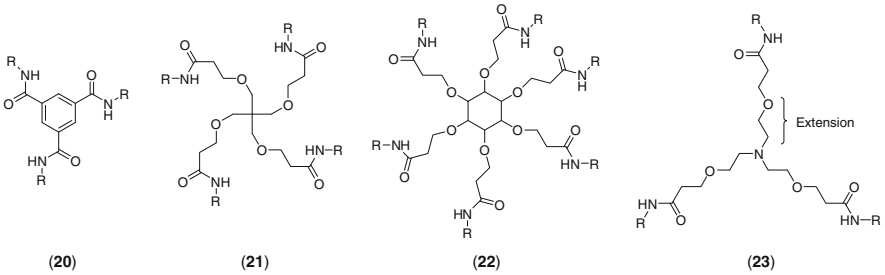

Fig. 20 Various core scaffolds used to prepare a number of PAMAM based dendrimers [203, 204]

To enhance the flexibility of the PAMAM structure, cores with different number of attachment sites have been synthesised. Zhang used trimesyl (**20**), pentaerythritol (**21**) and inositol (**22**) cores (see Fig. 20) to generate PAMAM dendrimers [203], with dendrimers constructed on the trimesyl scaffold demonstrating the best transfection abilities, probably due to increased flexibility and smaller dendrimer size [203]. Peng synthesised a series of PAMAM dendrimers where the distance between the amino core and the first branching units was extended via the insertion of an ethylene glycol unit [204] (molecule **23**, Fig. 20), which resulted in a drastic increment of siRNA delivery (determined by gene knockdown analysis) relative to the non-elongated PAMAM dendrimers.

Partially-convergent strategies have been applied for the synthesis of unsymmetrical PAMAM dendrimers by reaction of divergently-synthesised PAMAM dendrons either via a 1,3-dipolar cycloaddition reaction [205, 206] or through a poly(ethyleneglycol) (PEG) core [207]. In particular the PAMAM–PEG–PAMAM dendrimer showed high transfection efficiency, probably due to enhanced branch flexibility and DNA complexation [207]. Although a full convergent approach has

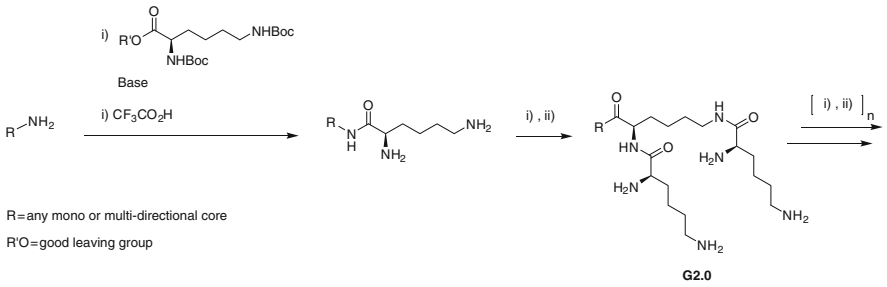

Fig. 21 Synthesis of poly(L-lysine) dendrimers

been used for the preparation of PAMAM dendrimers [208], this has not been employed in synthesising PAMAM-based transfection vectors.

4.2.3 Poly-(L-Lysine) Dendrimers

Poly(L-lysine) dendrimers were introduced by Denkewalter in 1981 [209]. Following a divergent strategy, poly(L-lysine) dendrons were synthesised from an amino-containing core by reaction with the *p*-nitrophenylester of Boc-L-Lys(Boc)-OH and subsequent acid-mediated deprotection. Repetitive coupling and deprotection procedure afforded the poly(L-lysine) dendrimers (see Fig. 21). Aoyagi developed the poly(L-lysine) approach to dendrimers using hexamethylenediamine as a core [210]. The synthesis followed standard Boc peptide chemistry, with Boc-L-Lys (Boc)-OH as the aminoacid monomer, and used HBTU, HOBt and DIPEA as coupling reagents. The sixth generation poly(L-lysine) dendrimers showed good ability to complex DNA and to transfect, while showing low toxicity.

Various modifications to the poly(L-lysine) dendrimer have been investigated to improve transfection efficiency, such as the replacement of terminal lysine residues with either arginine or histidine or modification of the core [211, 212].

4.2.4 Other Polycationic Dendrimers

In an effort to employ phosphorus-containing dendrimers for gene transfer, Meunier developed a class of ammonium-terminated polyaminophosphine dendrimers [213]. Synthesis of these compounds proceeded by the reaction of hexachlorocyclotriphosphazene with the sodium salt of 4-hydroxybenzaldehyde (see Fig. 22) [214]. This core, bearing six terminal aldehyde functions, was treated with dichlorophosphonomethylhydrazide to produce branches each with a terminal dichlorothiophosphine unit (G1 dendrimer). Treatment with the sodium salt of hydroxybenzaldehyde allowed production by iteration of new generations of dendrimers. Reaction of the corresponding dichlorothiophosphine-terminated

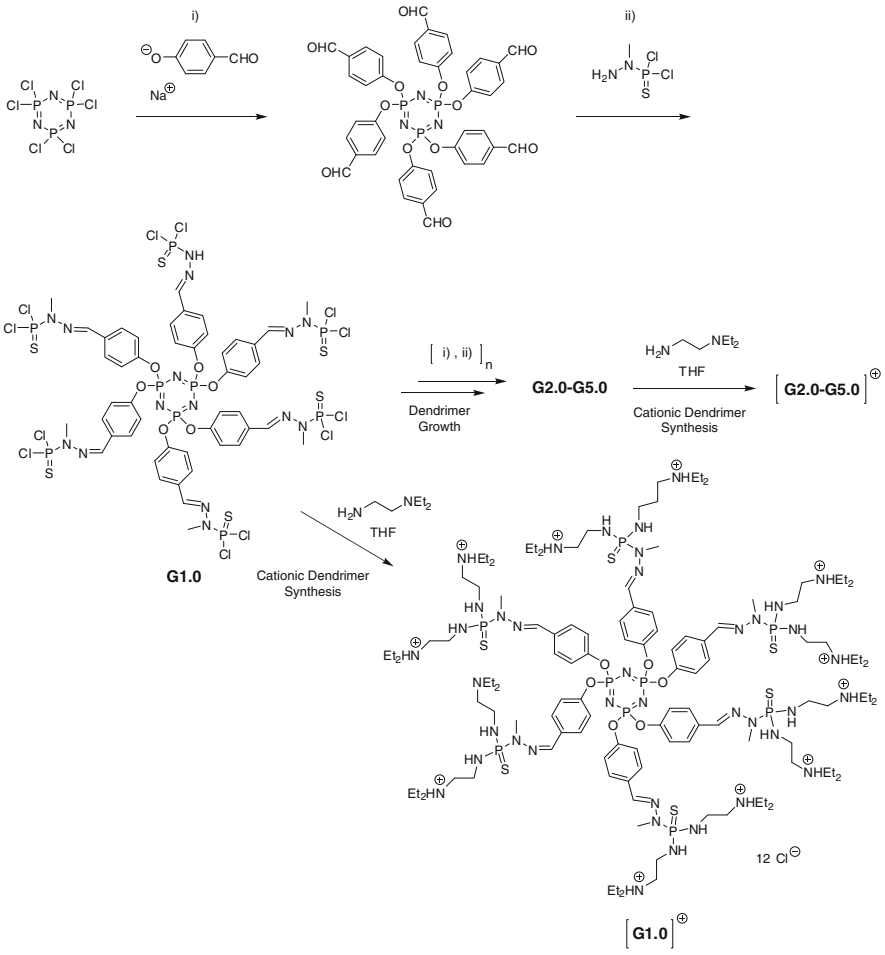

Fig. 22 Divergent synthesis of ammonium-terminated polyaminophosphine dendrimers [213]

dendrimer with *N*,*N*-diethylethylenediamine produced the cationic dendrimers, which showed significant gene transfer efficiency [213].

In recent years cationic dendritic structures such as carbosilane-based [215], triazine-based [216], polyester [217] and amphiphilic dendrimers [218] have been investigated for transfection purposes with promising results, thus offering novel alternatives to the exploration of dendrimer-based nucleic acid delivery.

4.3 Solid-Phase Synthesis of Dendrimers

Solution synthesis of dendrimers is often challenging, requiring long reaction times and non-trivial purification. In contrast, solid-phase methodology allows

the use of large excesses of reagents and microwave irradiation, thus enabling intricate reactions to be driven to completion. Besides, with the use of this methodology, purifications that would otherwise be very difficult simply become a matter of extensive washing of the resin [219]. For these reasons a number of research groups have explored this approach for the divergent synthesis of dendritic structures.

4.3.1 PAMAM Dendrimers on Solid-Support

Bradley described the first solid-phase synthesis of PAMAM dendrimers in 1997 [220]. To this end, phthaloyl-protected norspermidine was coupled to aminomethyl functionalised polystyrene-polyethylene-glycol resin ((PS-PEG)-NH_2) through an acid-labile linker (see Fig. 23). PAMAM dendrons were assembled by treating deprotected scaffold-bound resin **24** first with an excess of methyl acrylate

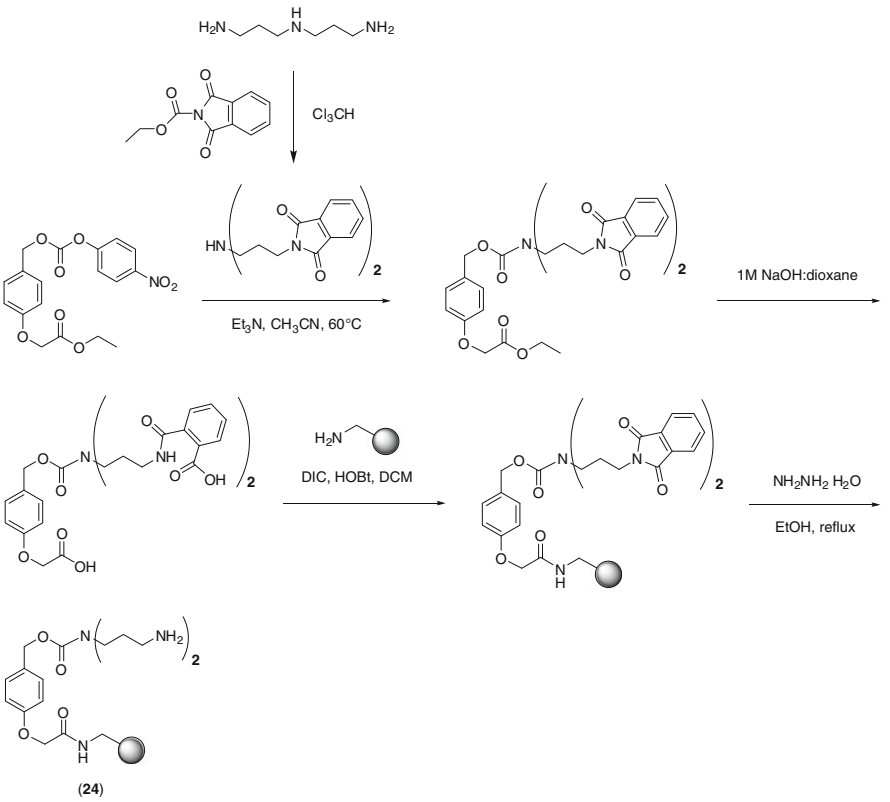

Fig. 23 The synthesis of polyamine-bound resin **24**

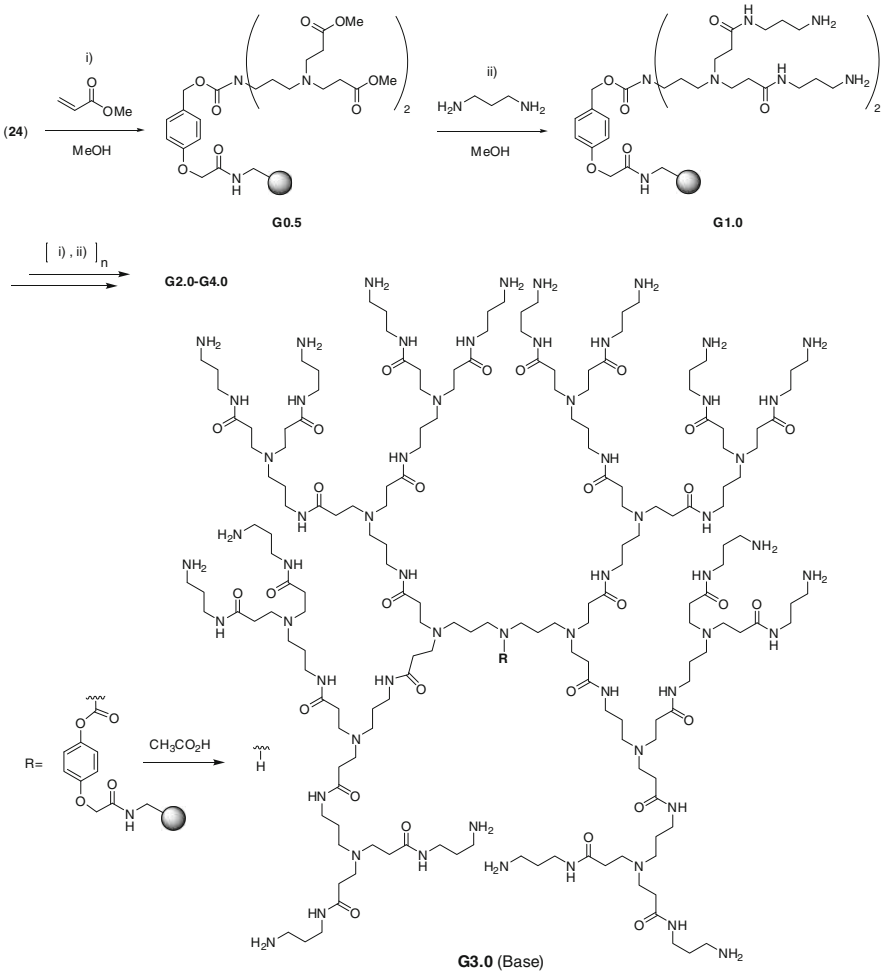

Fig. 24 Solid-phase synthesis of a G3 PAMAM dendrimer

(1,4-addition) and then by reaction of the methyl ester with 1,3-propanediamine (see Fig. 24). Sequential repetition of this two-step procedure afforded subsequent generations, with the cleavage being carried out under acid conditions (to cleave the linker). Despite the steric constraints imposed by the resin surrounding the reaction site, dendrimers with generations as high as five have been synthesised using this methodology, with high homogeneity and no irregularities in the structure.

PAMAM-bound resins can be functionalised with peptide sequences, being synthesised either separately and then coupled onto the resin immobilised PAMAM, or residue by residue on the dendrimer using standard Fmoc solid-phase peptide chemistry [221].

4.3.2 Peptide and Peptoid Dendrimers

The first polypeptide dendrimer synthesised on solid-phase was used as part of a multiple antigen peptide presentation system [222], and since this time researchers have synthesised this kind of dendrimer for a number of applications including transfection [223, 224]. The original solid-phase synthesis of an oligolysine dendrimer was based on a Boc-based synthetic strategy, starting from a β-alanyloxymethyl functionalised aminomethyl polystyrene resin. Dendrimer growth consisted of a two-step procedure: (1) coupling of pre-activated Boc-protected aminoacids and (2) subsequent acid-mediated deprotection [222], with final cleavage from the resin carried out using acetic anhydride and then a strong acid (HF). Peptide dendrimers synthesised using this method have found application in oligonucleotide delivery [223, 225].

Bradley developed a solid-phase synthesis of peptidomimetic dendrimers using the lysine-like peptoid monomer **25** [226] which led to G1–G3 dendrimers, bearing both primary and secondary amino groups on the periphery, with promising transfection abilities and no toxicity [227] (see Fig. 25).

Peptoid dendrimers were synthesised using an Fmoc solid-phase strategy using a Rink amide linker and an aminomethyl-polystyrene resin and microwave-mediated DIC/HOBt chemistry (Fig. 25). The use of microwave heating allowed each

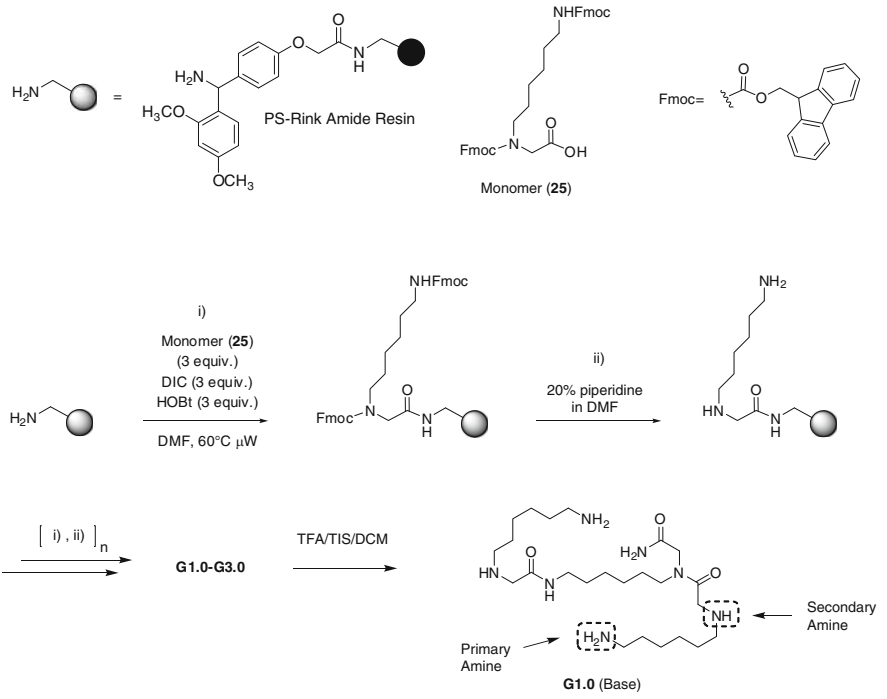

Fig. 25 Solid-phase synthesis of polycationic peptoid dendrimers

generation to be synthesised within half an hour (20 min for coupling, 10 min for deprotection), showing the great benefit that this tool brings to dendrimer synthesis [228, 229].

4.3.3 Polyamidourea Dendrimers

In order to investigate dendrimers of a different nature [230], Bradley described the synthesis and transfection efficiency of polyamidourea dendrimers synthesised from isocyanate-containing AB_3 monomers [231–234]. The use of this kind of tris-branched building block was addressed to enhance dendrimer synthesis by replacement of the 1,4-addition step typical of PAMAM synthesis and to a rapid increase in terminal functionality. The dendritic structures were synthesised using a divergent, microwave-assisted, solid-phase approach with the dendrimers assembled on polystyrene resin via an acid labile linker (see Fig. 26). In particular, a G3.0 polyamidourea bis-dendron with the peripheral amino groups conjugated to L-lysine residues demonstrated remarkable transfection abilities [234].

The synthesis of the dendrimers was initiated from acid-cleavable polyamine-bound resin **26** (prepared as described in Fig. 12), which was used as a core for

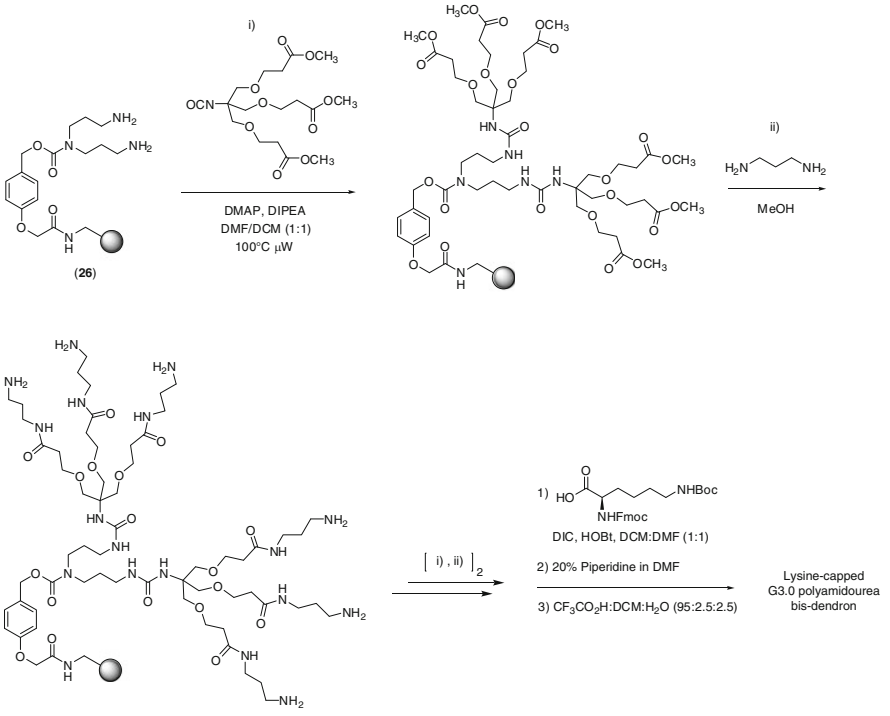

Fig. 26 Solid-phase synthesis of a lysine-capped G3.0 polyamidourea 1→3 C-branched bis-dendron

assembling the dendrons. The dendrimer was constructed (up to G3.0, 54 primary amines) by the sequential addition of the AB_3 isocyanate-type monomer under microwave irradiation, followed by the displacement of the methyl ester with propane-1,3-diamine (see Fig. 26). Coupling of the resulting G3.0 dendrimer-bound resin to lysine, deprotection and resin cleavage gave the final dendrimers with high purity, which showed remarkable transfection abilities in various mammalian cell lines, comparable or better than SuperFect.

5 Conclusions and Perspectives

The past decade has witnessed remarkable progress in the area of non-viral gene delivery. Many researchers now agree that, regardless of their efficiency, viral vectors will only be a temporary patch to restart the engine of the gene therapy field, while the real hope relies, yet again, on the ability of chemists to devise synthetic, highly-efficient materials with tuneable cell selectivity. Considering that humans have over 220 distinct cell types, ingenious approaches will indeed be needed.

New research ideas will profit from the results generated to date but future investigations need to address the barriers of biodegradability, selectivity and (if appropriate) intracellular trafficking to the nucleus, to name but a few. Decoration of cationic lipids and dendrimers with chemical groups recognised by membrane receptors and intracellular transporters is an approach widely investigated. However, results are still inconclusive and a deeper understanding of how viruses and natural biomaterials are trafficked within the cell is required. To this end, multidisciplinary collaborations along with the use of cutting-edge imaging techniques will be essential.

Acknowledgment We thank the MRC and BBSRC for funding.

References

1. Gaur RK, Rossi JJ (2009) Regulation of gene expression by small RNAs. CRC, Taylor & Francis, Boca Raton, p 431
2. Fu J-D, Jung Y, Chan CW, Li RA (2008) Stem Cells Dev 17:315
3. Okita K, Ichisaka T, Yamanaka S (2007) Nature 446:313
4. Takahashi K, Tanabe K, Ohnuki M, Narita M, Ichisaka T, Tomoda K, Yamanaka S (2007) Cell 131:861
5. Taira K, Kataoka K, Niidome T (eds) (2005) Non-viral gene therapy: gene design and delivery. Springer, Tokyo
6. Templeton NS (ed) (2008) Gene and cell therapy: therapeutic mechanisms and strategies. Marcel Dekker, New York
7. Conwell CC, Huang L (2005) In: Taira K, Kataoka K, Niidome T (eds) Non-viral gene therapy: gene design and delivery. Springer, Tokyo, p 3

8. Bainbridge JW, Smith AJ, Barker SS, Robbie S, Henderson R, Balaggan K, Viswanathan A, Holder GE, Stockman A, Tyler N, Petersen-Jones S, Bhattacharya SS, Thrasher AJ, Fitzke FW, Carter BJ, Rubin GS, Moore AT, Ali RR (2008) N Engl J Med 358:2231
9. Excoffon KJDA, Koerber JT, Dickey DD, Murtha M, Keshavjee S, Kaspar BK, Zabner J, Schaffer DV (2009) Proc Natl Acad Sci USA 106:3865
10. Mitsuyasu RT, Merigan TC, Carr A, Zack JA, Winters MA, Workman C, Block M, Lalezari J, Becker S, Thornton L, Akil B, Khanlou H, Finlayson R, McFarlane R, Smith DE, Garsia R, Ma D, Law M, Murray JM, Von Kalle C, Ely JA, Patino SM, Knop AE, Wong P, Todd AV, Haughton M, Furey C, Macpherson JL, Symonds GP, Evans LA, Pond SM, Cooper DA (2009) Nat Medicine 15:285
11. Tavazoie SF, Alarcón C, Oskarsson T, Padua D, Wang Q, Bos PD, Gerald WL, Massague J (2008) Nature 451:147
12. List of current clinical trials can be found at www.wiley.co.uk/genetherapy/clinical/
13. Yang F, Cho S-W, Son SM, Bogatyrev SR, Singh D, Green JJ, Mei Y, Park S, Bhang SH, Kim B-S, Langer R, Anderson DG (2010) Proc Natl Acad Sci USA 107:3317
14. Hoag H (2005) Nature 435:530
15. Machida CA (ed) (2002) Viral vectors for gene therapy: methods and protocols. Humana Press, Totowa
16. Young LS, Searle PF, Onion D, Mautner V (2006) J Pathol 208:299
17. Azzam T, Domb AJ (2004) Curr Drug Deliv 1:165
18. Ma H, Diamond SL (2001) Curr Pharm Biotechnol 2:1
19. Mehier-Humbert S, Guy RH (2005) Adv Drug Deliv Rev 57:733
20. Villemejane J, Mir LM (2009) Br J Pharmacol 157:207
21. Check E (2005) Nature 434:812
22. Scott DW (2006) Blood 108:2
23. Hacein-Bey-Abina S, von Kalle C, Schmidt M, Le Deist F, Wulffraat N, McIntyre E, Radford I, Villeval JL, Fraser CC, Cavazzana-Calvo M, Fischer A (2003) N Engl J Med 348:255
24. Woods NB, Bottero V, Schmidt M, von Kalle C, Verma IM (2006) Nature 440:1123
25. Li S, Huang L (2000) Gene Ther 7:31
26. Miller AD (2003) Curr Med Chem 10:1195
27. Dass CR (2004) J Mol Med 82:579
28. Wagner E (2004) Pharm Res 21:8
29. Walker GF, Fella C, Pelisek J, Fahrmeir J, Boeckle S, Ogris M, Wagner E (2005) Mol Ther 11:418
30. Koltover I, Salditt T, Radler JO, Safinya CR (1998) Science 281:78
31. van der Woude I, Visser HW, ter Beest MB, Wagenaar A, Ruiters MH, Engberts JB, Hoekstra D (1995) Biochim Biophys Acta 1240:34
32. Zuhorn IS, Bakowsky U, Polushkin E, Visser WH, Stuart MCA, Engberts JBFN, Hoekstra D (2005) Mol Ther 11:801
33. Behr J-P (1997) Chimia 51:34
34. Unciti-Broceta A, Díaz-Mochón JJ, Mizomoto H, Bradley M (2008) J Comb Chem 10:179
35. Niculescu-Duvaz D, Heyes J, Springer CJ (2003) Curr Med Chem 10:1233
36. Martin B, Sainlos M, Aissaoui A, Oudrhiri N, Hauchecorne M, Vigneron J-P, Lehn J-M, Lehn P (2005) Curr Pharm Des 11:375
37. Bhattacharya S, Bajaj A (2009) Chem Commun 31:4632
38. Guillot-Nieckowski M, Eisler S, Diederich F (2007) New J Chem 31:1111
39. Mintzer MA, Simanek EE (2009) Chem Rev 109:259
40. Hwang SJ, Davis ME (2001) Curr Opin Mol Ther 3:183
41. Hirko A, Tang F, Hughes JA (2003) Curr Med Chem 10:1185
42. Felgner PL, Gadek TR, Holm M, Roman R, Chan HW, Wenz M, Northrop JP, Ringold GM, Danielsen M (1987) Proc Natl Acad Sci USA 84:7413
43. Xu Y, Szoka FC Jr (1996) Biochemistry 35:5616

44. Zelphati O, Szoka FC Jr (1996) Proc Natl Acad Sci USA 93:11493
45. Lechardeur D, Verkman AS, Lukacs GL (2005) Adv Drug Deliv Rev 57:755
46. Nicolazzi C, Garinot M, Mignet N, Scherman D, Bessodes M (2003) Curr Med Chem 10:1263
47. Miller A (1998) Angew Chem 41:1768
48. Ewert K, Slack NL, Ahmad A, Evans HM, Lin AJ, Samuel CE, Safinya CR (2004) Curr Med Chem 11:133
49. Tranchant I, Thompson B, Nicolazzi C, Mignet N, Scherman D (2004) J Gene Med Suppl 1: S24
50. Smyth-Templeton N (2003) Curr Med Chem 10:1279
51. Zuhorn IS, Engberts JB, Hoekstra D (2007) Eur Biophys J 36:349
52. Tresset G (2009) PMC Biophys 2:3
53. Hoekstra D, Rejman J, Wasungu L, Shi F, Zuhorn I (2007) Biochem Soc Trans 35:68
54. Hofland HE, Shephard L, Sullivan SM (1996) Proc Natl Acad Sci USA 93:7305
55. Resina S, Prevot P, Thierry AR (2009) PLoS One 4:e6058
56. Ma B, Zhang S, Jiang H, Zhao B, Lv H (2007) J Control Release 123:184
57. Pedroso de Lima MC, Neves S, Filipe A, Düzgüneş N, Simões S (2003) Curr Med Chem 10:1221
58. Koynova R, Wang L, MacDonald RC (2006) Proc Natl Acad Sci USA 103:14373
59. Lv H, Zhang S, Wang B, Cui S, Yan J (2006) J Control Release 14:100
60. Niculescu-Duvaz D (2003) Heyes J. Springer C Curr Med Chem 10:1233
61. Montier T, Benvegnu T, Jaffrès PA, Yaouanc JJ, Lehn P (2008) Curr Gene Ther 8:296
62. Gardner RA, Belting M, Svensson K, Phanstiel O 4th (2007) J Med Chem 50:308
63. Byk G, Dubertret C, Escriou V, Frederic M, Jaslin G, Rangara R, Pitard B, Crouzet J, Wils P, Schwartz B, Scherman D (1998) J Med Chem 41:229
64. Bajaj A, Paul B, Kondaiah P, Bhattacharya S (2008) Bioconjug Chem 19:1283
65. Ilies MA, Seitz WA, Johnson BH, Ezell EL, Miller AL, Thompson EB, Balaban AT (2006) J Med Chem 49:3872
66. Karmali PP, Kumar VV, Chaudhuri A (2004) J Med Chem 47:2123
67. Unciti-Broceta A, Holder E, Jones LJ, Stevenson B, Turner AR, Porteous DJ, Boyd AC, Bradley M (2008) J Med Chem 51:4076
68. Gao X, Huang L (1991) Biochem Biophys Res Commun 79:280
69. Behr JP, Demeneix B, Loeffler JP, Perez-Mutul J (1989) Proc Natl Acad Sci USA 86:6982
70. Stamatatos L, Leventis R, Zuckermann MJ, Silvius JR (1988) Biochemistry 27:3917
71. Felgner JH, Kumar R, Sridhar CN, Wheeler CJ, Tsai YJ, Border R, Ramsey P, Martin M, Felgner PL (1994) J Biol Chem 269:2550
72. Islam RU, Hean J, van Otterlo WA, de Koning CB, Arbuthnot P (2009) Bioorg Med Chem Lett 19:100
73. Vigneron JP, Oudrhiri N, Fauquet M, Vergely L, Bradley JC, Basseville M, Lehn P, Lehn JM (1996) Proc Natl Acad Sci USA 93:9682
74. Lebreton S, Newcombe N, Bradley M (2002) Tetrahedron Lett 43:2475
75. Guénin E, Hervé AC, Floch VV, Loisel S, Yaouanc JJ, Clément JC, Férec C, Des Abbayes H (2000) Angew Chem Int Ed Engl 39:629
76. Floch V, Loisel S, Guenin E, Hervé AC, Clément JC, Yaouanc JJ, Des Abbayes H, Férec C (2000) J Med Chem 43:4617
77. Fletcher S, Ahmad A, Perouzel E, Heron A, Miller AD, Jorgensen MR (2006) J Med Chem 49:349
78. Mahidhar YV, Rajesh M, Chaudhuri A (2004) J Med Chem 47:3938
79. Bhattacharya S, Dileep PV (2004) Bioconjug Chem 15:508
80. Ghosh YK, Visweswariah SS, Bhattacharya S (2002) Bioconjug Chem 13:378
81. Mukherjee K, Bhattacharyya J, Sen J, Sistla R, Chaudhuri A (2008) J Med Chem 51:1967

82. Wheeler CJ, Felgner PL, Tsai YJ, Marshall J, Sukhu L, Doh SG, Hartikka J, Nietupski J, Manthorpe M, Nichols M, Plewe M, Liang X, Norman J, Smith A, Cheng SH (1996) Proc Natl Acad Sci USA 93:11454
83. Picquet E, Le Ny K, Delépine P, Montier T, Yaouanc JJ, Cartier D, Des Abbayes H, Férec C, Clément JC (2005) Bioconjug Chem 16:1051
84. Mével M, Montier T, Lamarche F, Delépine P, Le Gall T, Yaouanc JJ, Jaffrès PA, Cartier D, Lehn P, Clément JC (2007) Bioconjug Chem 18:1604
85. Paulekuhn GS, Dressman JB, Saal C (2007) J Med Chem 50:6665
86. Aberle AM, Bennett MJ, Malone RW, Nantz MH (1996) Biochim Biophys Acta 1299:281
87. Gebeyehu G, Jessee JA, Ciccarone VC, Hawley-Nelson P, Chytil A (1994) US Patent 5 (334):761
88. Cooper RG, Etheridge CJ, Stewart L, Marshall J, Rudginsky S, Cheng SH, Miller AD (1998) Chem Eur J 4:137
89. Lee ER, Marshall J, Siegel CS, Jiang C, Yew NS, Nichols MR, Nietupski JB, Ziegler RJ, Lane MB, Wang KX, Wan NC, Scheule RK, Harris DJ, Smith AE, Cheng SH (1996) Hum Gene Ther 7:1701
90. Ewert K, Ahmad A, Evans HM, Schmidt HW, Safinya CR (2002) J Med Chem 45:5023
91. Remy J-S, Sirlin C, Vierling P, Behr JP (1994) Bioconjug Chem 5:647
92. Ewert KK, Evans HM, Bouxsein NF, Safinya CR (2006) Bioconjug Chem 17:877
93. Ronsin G, Perrin C, Guédat P, Kremer A, Camilleri P, Kirby AJ (2001) Chem Commun 21:2234
94. Sen J, Chaudhuri A (2005) J Med Chem 48:812
95. Patel M, Vivien E, Hauchecorne M, Oudrhiri N, Ramasawmy R, Vigneron JP, Lehn P, Lehn JM (2001) Biochem Biophys Res Commun 281:536
96. Bajaj A, Mishra SK, Kondaiah P, Bhattacharya S (2008) Biochim Biophys Acta 1778:1222
97. Oudrhiri N, Vigneron JP, Peuchmaur M, Leclerc T, Lehn JM, Lehn P (1997) Proc Natl Acad Sci USA 94:1651
98. Luton D, Oudrhiri N, de Lagausie P, Aissaoui A, Hauchecorne M, Julia S, Oury JF, Aigrain Y, Peuchmaur M, Vigneron JP, Lehn JM, Lehn P (2004) J Gene Med 6:328
99. Rothbard JB, Jessop TC, Lewis RS, Murray BA, Wender PA (2004) J Am Chem Soc 126:9506
100. Heyes JA, Niculescu-Duvaz D, Cooper RG, Springer CJ (2002) J Med Chem 45:99
101. Sochanik A, Kaida I, Mitrus I, Rajca A, Szala S (2000) Cancer Gene Ther 7:513
102. Desigaux L, Sainlos M, Lambert O, Chevre R, Letrou-Bonneval E, Vigneron JP, Lehn P, Lehn JM, Pitard B (2007) Proc Natl Acad Sci USA 104:16534
103. Tang F, Hughes JA (1999) J Control Release 62:345
104. Kirby AJ, Camilleri P, Engberts JB, Feiters MC, Nolte RJ, Söderman O, Bergsma M, Bell PC, Fielden ML, García Rodríguez CL, Guédat P, Kremer A, McGregor C, Perrin C, Ronsin G, Van Eijk MC (2003) Angew Chem Int Ed 42:1448
105. Bombelli C, Giansanti L, Luciani P, Mancini G (2009) Curr Med Chem 16:171
106. Bajaj A, Kondaiah P, Bhattacharya S (2007) Bioconjug Chem 18:1537
107. Bajaj A, Kondiah P, Bhattacharya S (2007) J Med Chem 50:2432
108. Wasungu L, Scarzello M, van Dam G, Molema G, Wagenaar A, Engberts JB, Hoekstra D (2006) J Mol Med 84:774
109. Pestman JM, Terpstra KR, Stuart MCA, van Doren HA, Brisson A, Kellogg RM, Engberts JBFN (1997) Langmuir 13:6857
110. Johnsson M, Wagenaar A, Engberts JB (2003) J Am Chem Soc 125:757
111. Bajaj A, Kondaiah P, Bhattacharya S (2008) Biomacromolecules 9:991
112. Ewert KK, Evans HM, Zidovska A, Bouxsein NF, Ahmad A, Safinya CR (2006) J Am Chem Soc 128:3998
113. Solodin I, Brown CS, Bruno MS, Chow CY, Jang EH, Debs RJ, Heath TD (1995) Biochemistry 34:13537

114. Cheng J, Zeidan R, Mishra S, Liu A, Pun SH, Kulkarni RP, Jensen GS, Bellocq NC, Davis ME (2006) J Med Chem 49:6522
115. Kumar VV, Pichon C, Refregiers M, Guerin B, Midoux P, Chaudhuri A (2003) Gene Ther 10:1206
116. Singh RS, Goncalves C, Sandrin P, Pichon C, Midoux P, Chaudhuri A (2004) Chem Biol 11:713
117. Majeti BK, Karmali PP, Reddy BS, Chaudhuri A (2005) J Med Chem 48:3784
118. Sudholter EJR, Engberts JBFN, Hoekstra D (1979) J Am Chem Soc 102:2467
119. van der Woude I, Wagenaar A, Meekel AA, ter Beest MB, Ruiters MH, Engberts JB, Hoekstra D (1997) Proc Natl Acad Sci USA 94:1160
120. Pijper D, Bulten E, Smisterova J, Wagenaar A, Hoekstra D, Engberts JBFN, Hulst R (2003) Eur J Org Chem 22:4406
121. Hulst R, Muizebelt I, Oosting P, van der Pol C, Wagenaar A, Smisterová J, Bulten E, Driessen C, Hoekstra D, Engberts JBFN (2004) Eur J Org Chem 4:835
122. Scarzello M, Smisterová J, Wagenaar A, Stuart MC, Hoekstra D, Engberts JB, Hulst R (2005) J Am Chem Soc 127:10420
123. Ilies MA, Seitz WA, Caproiu MT, Wentz M, Garfield RE, Balaban AT (2003) Eur J Org Chem 14:2645
124. Ilies MA, Seitz WA, Ghiviriga I, Johnson BH, Miller A, Thompson EB, Balaban AT (2004) J Med Chem 47:3744
125. Zhu L, Lu Y, Miller DD, Mahato RI (2008) Bioconjug Chem 19:2499
126. Meers P (1999) Adv Drug Deliv Rev 53:265
127. Guo X, Szoka FC Jr (2003) Acc Chem Res 36:335
128. Wolff JA, Rozema DB (2008) Mol Ther 16:8
129. Oupický D, Diwadkar V (2003) Curr Opin Mol Ther 5:345
130. Tang FX, Hughes JA (1999) Bioconjugate Chem 10:791
131. Balakirev M, Schoehn G, Chroboczek J (2000) Chem Biol 7:813
132. Byk G, Wetzer B, Frederic M, Dubertret C, Pitard B, Jaslin G, Scherman D (2000) J Med Chem 43:4377
133. Huang Z, Li W, MacKay JA, Szoka FC Jr (2005) Mol Ther 11:409
134. Zhu J, Munn RJ, Nantz MH (2000) J Am Chem Soc 122:2645
135. Huang Z, Guo X, Li W, MacKay JA, Szoka FC Jr (2006) J Am Chem Soc 128:60
136. Chen H, Zhang H, McCallum CM, Szoka FC Jr, Guo X (2007) J Med Chem 50:4269
137. Boomer JA, Thompson DH, Sullivan SM (1997) Pharm Res 19:1292
138. Boomer JA, Qualls MM, Inerowicz HD, Haynes RH, Patri VS, Kim JM, Thompson DH (2009) Bioconjug Chem 20:47
139. Liu D, Hu J, Qiao W, Li Z, Zhang S, Cheng L (2005) Bioorg Med Chem Lett 15:3147
140. Savva M, Chen P, Aljaberi A, Selvi B, Spelios M (2005) Bioconjug Chem 16:1411
141. Aissaoui A, Martin B, Kan E, Oudrhiri N, Hauchecorne M, Vigneron JP, Lehn JM, Lehn P (2004) J Med Chem 47:5210
142. Knorr V, Allmendinger L, Walker GF, Paintner FF, Wagner E (2007) Bioconjug Chem 18:1218
143. Wong JB, Grosse S, Tabor AB, Hart SL, Hailes HC (2008) Mol Biosyst 4:532
144. Zhu M-Z, Wu Q-H, Zhang G, Ren T, Liu D, Guo Q-X (2002) Bull Chem Soc Jpn 75:2207
145. Corey EJ, Raju N (1983) Tetrahedron Lett 24:5571
146. Meth-Cohn O (1986) J Chem Soc Chem Commun 9:695
147. Murphy JE, Uno T, Hamer JD, Cohen FE, Dwarki V, Zuckermann RN (1998) Proc Natl Acad Sci USA 95:1517
148. Huang CY, Uno T, Murphy JE, Lee S, Hamer JD, Escobedo JA, Cohen FE, Radhakrishnan R, Dwarki V, Zuckermann RN (1998) Chem Biol 5:345
149. Choi JS, Lee EJ, Jang HS, Park JS (2000) J Biochem Mol Biol 33:476
150. Choi JS, Lee EJ, Jang HS, Park JS (2001) Bioconjug Chem 12:108
151. Yingyongnarongkul BE, Howarth M, Elliott T, Bradley M (2004) J Comb Chem 6:753
152. Liberska A, Unciti-Broceta A, Bradley M (2009) Org Biomol Chem 7:61

153. Kish PE, Tsume Y, Kijek P, Lanigan TM, Hilfinger JM, Roessler BJ (2007) Mol Pharm 4:95
154. Byk G, Frederic M, Scherman D (1997) Tetrahedron Lett 38:3219
155. Byk G, Soto J, Mattler C, Frederic M, Scherman D (1998) Biotechnol Bioeng 61:81
156. Oliver M, Jorgensen MR, Miller A (2004) Tetrahedron Lett 45:3105
157. Lenssen K, Jantscheff P, Von Kiedrowski G, Massing U (2002) Chembiochem 3:852, Combinatorial synthesis of new cationic lipids and high-throughput
158. Yingyongnarongkul BE, Howarth M, Elliott T, Bradley M (2004) Chemistry Eur J 10:463
159. Yingyongnarongkul BE, Radchatawedchakoon W, Krajarng A, Watanapokasin R, Suksamrarn A (2009) Bioorg Med Chem 17:176
160. Fara MA, Diaz-Mochon JJ, Bradley M (2006) Tetrahedron Lett 47:1011
161. Unciti-Broceta A, Diezmann F, Ou-Yang CY, Fara MA, Bradley M (2009) Bioorg Med Chem 17:959
162. Lebreton S, Newcombe N, Bradley M (2002) Tetrahedron Lett 43:2479
163. Fréchet JMJ, Tomalia DA (eds) (2001) Dendrimers and other dendritic polymers. Wiley, Chichester
164. Newkome GR, Moorefield CN, Vögtle F (eds) (2001) Dendrimers and dendrons. Concepts, synthesis and applications. Wiley-VCH, Weinheim
165. Grinstaff MW (2002) Chem Eur J 8:2839
166. Svenson S, Tomalia DA (2005) Adv Drug Deliv Rev 57:2106
167. Fréchet JMJ, Mackay JA, Cameron CL, Szoka FC (2005) Nature Biotech 23:1517
168. Eisler S, Diederich F, Guillot-Niecowski M (2007) New J Chem 31:1111
169. Grayson SM, Fréchet JM (2001) Chem Rev 101:3819
170. Smith DK (2003) Tetrahedron 59:3797
171. Kehat T, Goren K, Portnoy M (2007) New J Chem 31:1218
172. Antoni P, Nyström D, Hawker CJ, Hult A, Malkoch M (2007) Chem Commun 22:2249
173. Boas U, Heegaard PMH (2004) Chem Soc Rev 33:43
174. Medina SH, El-Sayed ME (2009) Chem Rev 109:3141
175. Zhou J, Wu J, Hafdi N, Behr JP, Erbacher P, Peng L (2006) Chem Comm 22:2362
176. Tang MX, Redemann CT, Szoka FC Jr (1996) Bioconj Chem 7:703
177. Newkome GR, Shreiner CD (2008) Polymer 49:1
178. Carlmark A, Hawker C, Hult A, Malkoch M (2009) Chem Soc Rev 38:352
179. Buhleier E, Wehner W, Vögtle F (1978) Synthesis 155
180. Mülhaupt R, Wörner C (1993) Angew Chem Int Ed 32:1306
181. Meijer EW, Brabander-van den Berg EMM (1993) Angew Chem Int Ed 32:1308
182. Zinselmeyer BH, Mackay SP, Schatzlein AG, Uchegbu LF (2002) Pharm Res 19:960
183. Hollins AJ, Benboubetra M, Omidi Y, Zinselmeyer BH, Schatzlein AG, Uchegbu IF, Akhtar S (2004) Pharm Res 21:458
184. Schatzlein AG, Zinselmeyer BH, Elouzi A, Dufes C, Chim YTA, Roberts CJ, Davies MC, Munro A, Gray AI, Uchegbu IF (2005) J Control Release 101:247
185. Tack F, Bakker A, Maes S, Dekeyser N, Bruining M, Elissen-Roman C, Janicot M, Brewster M, Janssen HM, De Waal BF, Fransen PM, Lou X, Meijer EW (2006) J Drug Target 14:69
186. Baars MWPL, Kleppinger R, Koch MHJ, Yeu SL, Meijer EW (2000) Angew Chem Int Ed 39:1285
187. Kim T-I, Baek JU, Bai CZ, Park JS (2007) Biomaterials 28:2061
188. Tomalia DA, Baker H, Dewald J, Hall M, Kallos G, Martin S, Roeck J, Ryder J, Smith P (1985) Polym J 17:117
189. Smith P, Ryder J, Roeck J, Martin J, Kallos G, Hall M, Dewald J, Baker H, Tomalia DA (1990) Angew Chem Int Ed 29:138
190. Haensler J, Szoka FC Jr (1993) Bioconj Chem 4:372
191. Kukowska-Latallo JF, Bielinska AU, Johnson J, Spindler R, Tomalia DA, Baker JR Jr (1996) Proc Natl Acad Sci USA 93:4897
192. Sig Choi J, Nam K, Park J, Kin JB, Lee JK, Park J (2004) J Control Release 99:445, Grafting with lysine arginene
193. Kono K, Akiyama H, Takahashi T, Takagishi T, Harada A (2005) Bioconj Chem 16:208
194. Takahashi T, Kono K, Itoh T, Emi N, Takagishi T (2003) Bioconj Chem 14:764

195. Takahashi T, Harada A, Emi N, Kono K (2005) Bioconj Chem 16:1160
196. Arima H, Wada K, Kihara F, Tsutsumi T, Hirayama F, Uekama K (2002) J Inclusion Phenom Macrocyclic Chem 44:361
197. Wada K, Arima H, Tsutsumi T, Chihara Y, Hattori K, Hirayama F, Uekama K (2005) J Control Release 104:397
198. Wada K, Arima H, Tsutsumi T, Hirayama F, Uekama K (2005) Biol Pharm Bull 28:500
199. Kihara F, Arima H, Tsutsumi T, Hirayama F, Uekama K (2002) Bioconj Chem 13:1211
200. Wood KC, Azarin SM, Arap W, Pasqualini R, Langer R, Hammond PT (2008) Bioconj Chem 19:403
201. Arima H, Kihara F, Hirayama F, Uekama K (2003) Bioconj Chem 12:476
202. Sonawane ND, Szoka FC Jr, Verkman AS (2003) J Biol Chem 278:44826
203. Leong KW, Mao HQ, Liu ZL, Zhuo RX, Huang SW, Wang XL, Zhang XQ (2005) Biomacromolecules 6:341
204. Wu J, Zhou J, Qu F, Bao P, Zhang Y, Peng L (2005) Chem Commun 3:313
205. Lee JW, Kim JH, Kim HJ, Han SC, Kim JH, Shin WS, Jin SH (2006) Macromolecules 39:2418, 9
206. Lee JW, Kim JH, Kim HJ, Han SC, Kim JH, Shin WS, Jin SH (2007) Bioconj Chem 18:57
207. Kim TI, Seo HJ, Choi JS, Jang HS, Baek JU, Kim K, Park JS (2004) Biomacromolecules 5:2487
208. Pittelkow M, Christensen JB (2005) Org Lett 7:1295
209. Lukasavage WJ, Kolc J, Dankewalter RG (1981) US Patent 4(289):872
210. Ohsaki M, Okuda T, Wada A, Hirayami T, Niidome T, Aoyagi H (2002) Bioconj Chem 13:510
211. Okuda T, Sugiyama A, Niidome T, Aoyagi H (2003) Biomaterials 25:537
212. Kaneshiro TL, Wang X, Lu ZR (2007) Mol Pharmaceutics 4:759
213. Loup C, Zanta MA, Caminade AM, Majoral JP, Meunier B (1999) Chem Eur J 5:3644
214. Galliot C, Prevote D, Caminade AM, Majoral JP (1995) J Am Chem Soc 117:5470
215. Bermejo JF, Ortega P, Chonco L, Eritja R, Samaniego R, Muellner M, de Jesus E, de la Mata JF, Flores JC, Gomez R, Munoz-Fernandez A (2007) Chem Eur J 13:483
216. Mintzer MA, Merkel OM, Kissel T, Simanek EE (2009) New J Chem 33:1918
217. Ma X, Tang J, Shen Y, Fan M, Tang H, Radosz M (2009) J Am Chem Soc 131:14795
218. Joester D, Losson M, Pugin R, Heinzelmann H, Walter E, Merkle HP, Diederich F (2003) Angew Chem Int Ed Engl 42:1486
219. Wells NJ, Basso A, Bradley M (1998) Biopolymers (Peptide Science) 47:381
220. Swali V, Wells NJ, Langley GJ, Bradley M (1997) J Org Chem 62:4902
221. Monaghan S, Griffith-Johnson D, Matthews I, Bradley M (2001) ARKIVOC Part 10, pp 46–53
222. Tam JP (1988) Proc. Natl Acad Sci USA 85:5409
223. Wimmer N, Marano RJ, RJ KPS, Rakoczy EP, Toth I (2002) Bioorg Med Chem Lett 12:2635
224. Choi JS, Joo DK, Kim CH, Kim K, Park JS (2000) J Am Chem Soc 122:474
225. Parekh HS, Marano RJ, Rakoczy EP, Blanchfield J, Toth I (2006) Bioorg Med Chem 14:4775
226. Peretto I, Sanchez-Martin RM, Wang X, Ellard J, Mittoo S, Bradley M (2003) Chem Commun 18:2312
227. Diaz-Mochon JJ, Fara MA, Sanchez-Martin RM, Bradley M (2007) Tet Lett 49:923
228. Chighine A, Sechi G, Bradley M (2007) Drug Discov Today 12:459
229. Kappe CO, Dallinger D (2009) Mol Diversity 13:71
230. Lebreton S, Monaghan S, Bradley M (2001) Aldrichimica Acta 34:75
231. Lebreton S, How SE, Buchholz M, Yingyongnarongkul BE, Bradley M (2003) Tetrahedron 59:3945
232. How SE, Yingyongnarongkul B, Fara MA, Diaz-Mochon JJ, Mittoo S, Bradley M (2004) Comb Chem HT Screen 7:423
233. Ternon M, Diaz-Mochon JJ, Belsom A, Bradley M (2004) Tetrahedron 60:8721
234. How SE, Unciti-Broceta A, Sánchez-Martín RM, Bradley M (2008) Org Biomol Chem 6:2266

Top Curr Chem (2010) 296: 51–93
DOI: 10.1007/128_2010_67

Published online: 2 June 2010

Cationic Lipids: Molecular Structure/ Transfection Activity Relationships and Interactions with Biomembranes

Rumiana Koynova and Boris Tenchov

Abstract Synthetic cationic lipids, which form complexes (lipoplexes) with polyanionic DNA, are presently the most widely used constituents of nonviral gene carriers. A large number of cationic amphiphiles have been synthesized and tested in transfection studies. However, due to the complexity of the transfection pathway, no general schemes have emerged for correlating the cationic lipid chemistry with their transfection efficacy and the approaches for optimizing their molecular structures are still largely empirical. Here we summarize data on the relationships between transfection activity and cationic lipid molecular structure and demonstrate that the transfection activity depends in a systematic way on the lipid hydrocarbon chain structure. A number of examples, including a large series of cationic phosphatidylcholine derivatives, show that optimum transfection is displayed by lipids with chain length of ~14 carbon atoms and that the transfection efficiency strongly increases with increase of chain unsaturation, specifically upon replacement of saturated with monounsaturated chains.

Keywords Cationic lipid, Lipoplex, Nucleic acid, Phase transition, Transfection

Contents

R. Koynova (✉)
Ohio State University College of Pharmacy, 517 Parks Hall, 500 W 12th Ave, Columbus, OH 43210, USA
Northwestern University, Evanston, IL, USA
e-mail: rkoynova@gmail.com

B. Tenchov
Ohio State University College of Pharmacy, 517 Parks Hall, 500 W 12th Ave, Colombus, OH 43210, USA; Bulgarian Academy of Sciences, Sofia, Bulgaria

1 Introduction

Progress in the understanding of cellular pathogenesis has made possible the therapeutic targeting of numerous genes involved in diseases [1]. Nucleic acids as drugs have become a reality and a number of disorders have been approached with gene therapy, including cystic fibrosis, hemophilia, immune deficiency, autosomal dominant disorders, many forms of cancer, HIV and other infectious diseases, inflammatory conditions, and intractable pain [2]. Since systemic circulation and cellular uptake of free DNA are hindered by nuclease degradation and by the size and negative charge of DNA, therapeutic procedures involving gene transfection and gene silencing require efficient delivery vectors in order to condense, protect, and chaperone the genetic material to the target cells. Two principal delivery vehicles include viral and nonviral vectors. Viral vectors are most effective [3, 4], but their application is limited by their immunogenicity and oncogenicity. Synthetic cationic lipids, which form complexes (lipoplexes) with polyanionic DNA, are presently the most widely used constituents of nonviral gene carriers [5–7]. However, a well known obstacle for the clinical applications of lipid-mediated gene delivery is its unsatisfactory efficiency for many cell types. Progress in enhancing the efficacy of lipid-assisted transfection has been impeded because its mechanism is still largely unknown and important stages in the process of intracellular delivery are not well understood [8–14].

Due to the complexity of the transfection pathway, no general schemes have evolved for correlating cationic lipid chemistry with transfection activity. A useful approach for designing and optimizing the cationic lipid vectors, as well as for

understanding the delivery mechanism, is based on systematic, but still largely empirical, modifications of their chemical structure and searching for correlations with its efficacy. Here we summarize data on reported relationships between transfection activity and cationic lipid molecular structure. Special attention is given to the structure of the lipid hydrocarbon moiety because recent reports have demonstrated its important role in transfection. On the basis of several examples of lipids with different hydrocarbon chains, including a large series of cationic phosphatidylcholine (PC) derivatives, we demonstrate that the transfection efficacy depends in a systematic way on the lipid hydrocarbon chain structure and closely correlates with the propensity for nonlamellar phase formation in cationic PC mixtures with membrane lipids.

2 Cationic Lipid Molecular Structure and Phase Behavior

The molecular architecture of cationic lipids used as nucleic acid carriers is similar to that of natural lipids, with the major difference being their cationic headgroup. These amphiphiles comprise a hydrophobic domain with two alkyl chains (monoalkyl cationic surfactants are scarcely used because of their high toxicity [15]) or a cholesterol moiety, a positively charged polar headgroup, and a linker functionality connecting the polar group with the hydrophobic moiety. Figure 1 exemplifies some common representatives of these components, and Figs. 2 and 3 illustrate structures of cationic lipids frequently used as vectors for gene delivery.

An attractive class of low toxicity, biodegradable cationic lipids has been derived from the natural PCs, in which the zwitterionic headgroup of the PC is converted into a cation by esterification of the phosphate group (Fig. 3) [16–18].

Most of the cationic lipids arrange into bilayers and readily form liposome dispersions in water [16]. At higher electrolyte concentrations, e.g., in physiological solutions, in which electrostatic repulsion is largely screened, and at higher lipid contents bringing the bilayers together, these lipids form well-correlated lamellar

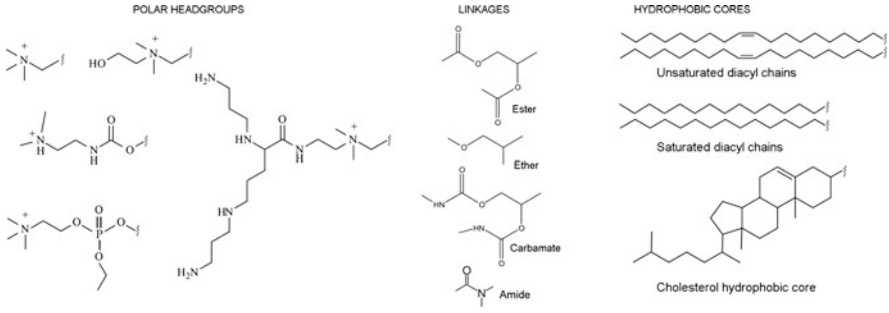

Fig. 1 Examples of cationic lipid structural components: polar headgroups, linkers, and hydrophobic moieties

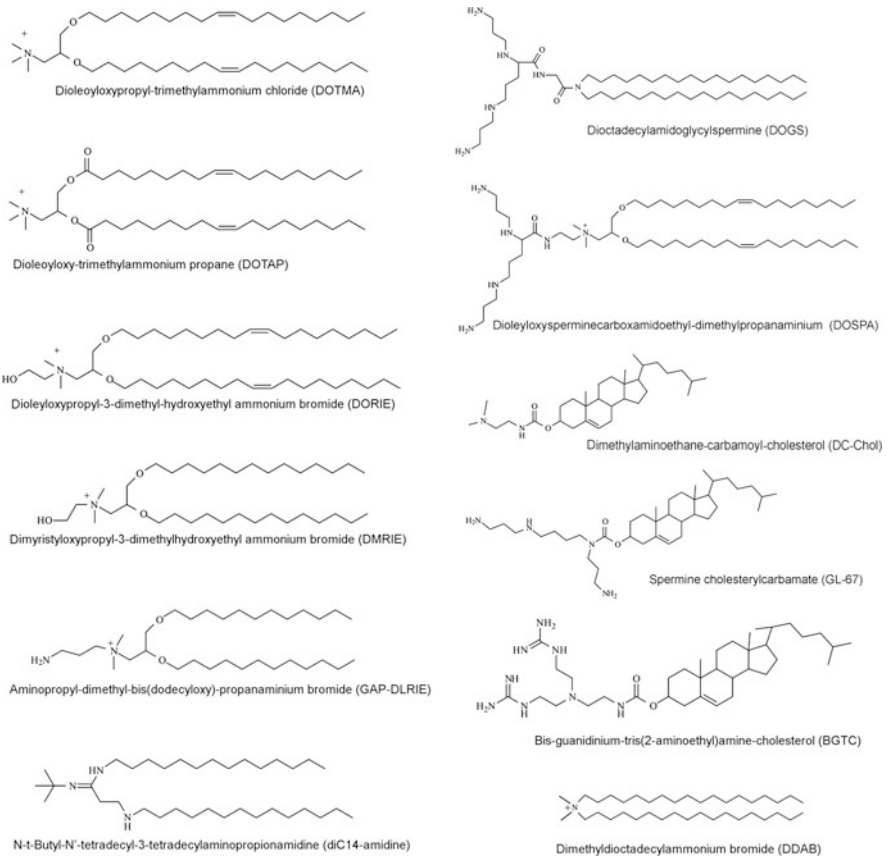

Fig. 2 Structures of commonly used cationic lipids

phases (Fig. 4a). Cationic lipids with saturated chains exhibit cooperative gel–liquid crystalline phase transitions [16, 19, 22, 23]. The gel–liquid crystal transition temperatures of the cationic PC derivatives are identical to those of their PC counterparts. However, their gel phases were found to be interdigitated, a likely result of electrostatic repulsion [19, 22, 23].

Certain cationic lipids are able to arrange into nonlamellar phases. For example, increasing the length of the R_3 chain in cationic PCs generally results in replacement of the lamellar L_α phase by nonlamellar phases [16]. A characteristic example of this behavior is given by a set of four dioleoyl PC derivatives with ethyl, propyl, hexyl, and octadecyl R_3 chains: the first two, diC18:1-EPC and diC18:1-C3PC, form L_α phase, diC18:1-C6PC forms cubic Pn3m phase, and diC18:1-C18PC forms inverted hexagonal phase in the whole temperature interval 0–90 °C [19–21, 24, 25] (Fig. 4). Several other PC derivatives were also found to form well-ordered nonlamellar phases, e.g., diC10-C14PC and diC22:1-EPC display irreversible lamellar–cubic Pn3m transitions on heating [20]; diC16:4me-C16PC forms

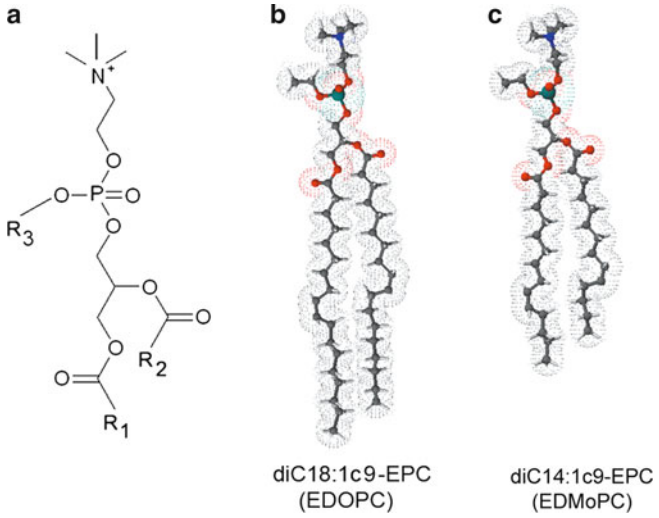

Fig. 3 (**a**) Structure of cationic phosphatidylcholines (PCs); (**b**) 1,2-Dioleoyl-*sn*-glycero-3-ethylphosphocholine (diC18:1-EPC; EDOPC), the best studied. (**c**) 1,2-Dimyristoleoyl-*sn*-glycero-3-ethylphosphocholine (diC14:1-EPC, EDMoPC), the most efficient representative of the cationic PCs

inverted hexagonal phases [21]. However, no correlations have been observed between cationic PC transfection activity and their ability to form nonlamellar phases [20, 26].

3 Molecular Structure: Transfection Activity Relationships

3.1 Lipid Headgroups

The headgroup of the cationic lipids typically comprises various amine derivatives such as primary, secondary, and tertiary amines (e.g., DOGS, DC-Chol), quaternary ammonium (e.g., DOTMA, DOTAP, DORIE, DMRIE), combinations of amines (e.g., DOSPA, GAP-DLRIE), and amidinium salts (e.g., diC14-amidine) (Fig. 2). Guanidine and imidazole groups [27] as well as pyridinium, piperizine, and amino acid headgroups (e.g., lysine, arginine, ornithine, and tryptophan) [28, 29] have also been utilized. Cationic lipids in which the cationic charge is carried by other elements from group 15 of the periodic table, such as phosphorus and arsenic instead of nitrogen, have also been developed [30].

Headgroups with multiple cationic charge, e.g., DOSPA, DOGS [31], are claimed to be more efficient than single-charged lipids such as DOTMA, DOTAP, DC-Chol, DMRIE [32]. This may be related to the greater ability of

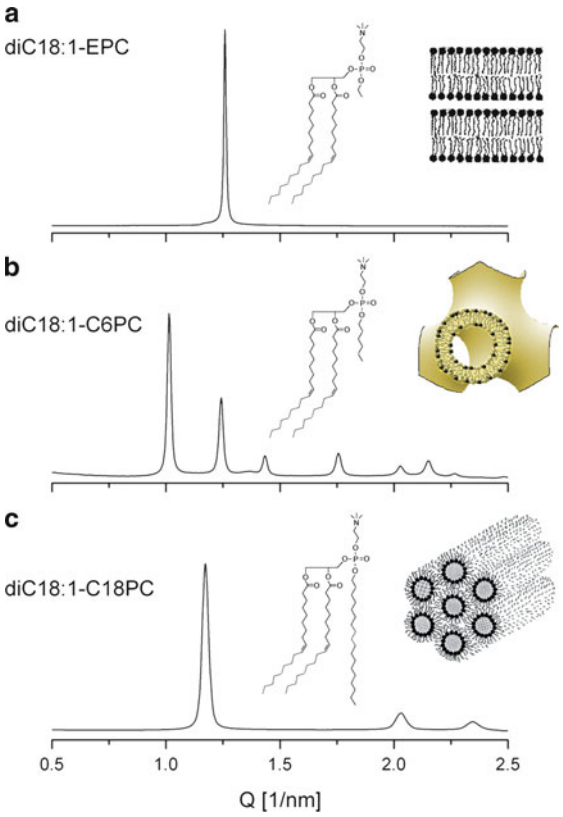

Fig. 4 Elongation of the R3 phosphate ester chain of the cationic PC results in nonlamellar phase formation. Small-angle X-ray diffraction patterns recorded at 20°C show (**a**) lamellar Lα; (**b**) cubic Pn3m; (**c**) inverted hexagonal H_{II} phases formed by dioleoyl cationic PCs with ethyl, hexyl and octadecyl R3 chains, respectively, diC18:1-EPC [19], diC18:1-C6PC [20] and diC18:1-C18PC [21]

the former to condense and protect DNA. However, increasing the number of positive charges may result in stronger DNA binding that would inhibit its subsequent intracellular release. In addition, multivalent cationic lipids are prone to formation of micelles typically contributing to increased toxicity [33]. Combinations of quaternary amine and polyamine enhance transfection activity. Indeed, the first cationic lipid containing these two functionalities, DOSPA, formulated with dioleoylphosphatidylethanolamine (DOPE) (Lipofectamine), was shown to exhibit superior efficiency; so does another representative of this group, GAP-DLRIE, containing one primary amine and a quaternary amine (Fig. 2), which has lower toxicity [34]. Replacing the methyl group in the quaternary ammonium lipid DOTMA with a hydroxyalkyl (ethyl, propyl, butyl, and pentyl) group also increases the transfection activity, with a maximum for the hydroxyethyl compound, DORIE (Fig. 5) [35].

Well-expressed correlations between headgroup structure and transfection activity have been found for cholesterol-based cationic derivatives. Polyamine derivatives with T-shaped structure exhibit considerably higher levels of transfection as compared to lipids with linear polyamine headgroups (Fig. 6) [36]. Varying

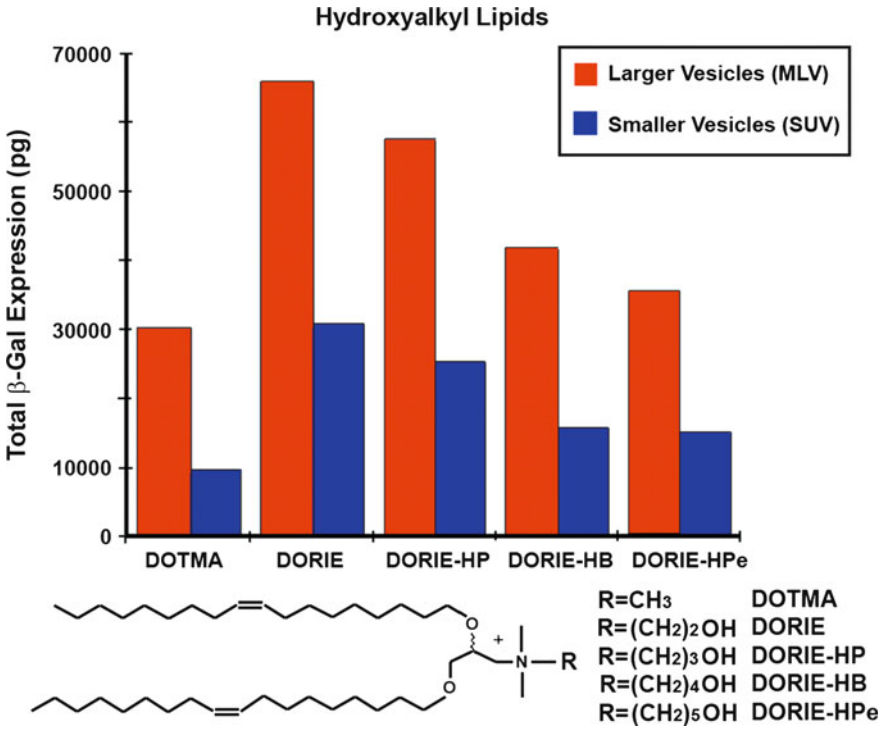

Fig. 5 Cationic lipids DORIE, DORIE-HP, DORIE-HB, DORIE-HPe, containing increasing numbers of methylene groups between the hydroxyl and amine moieties, and DOTMA, which lacks hydroxyl group, formulated with 50 mol% DOPE, and assayed for transfection (reproduced from [35]; copyright by the American Society for Biochemistry and Molecular Biology)

the amine group methylation in cholesterol derivatives showed that only the primary and secondary amines were able to mediate in vitro transfection in the absence of helper lipid. These results were consistent with fusion and cell internalization experiments, which showed that, although cell surface binding occurs for all of the cationic lipids, only the primary and secondary amine derivatives were able to gain entry into the cytosol [37] (Fig. 7).

A series of cholesterol-based ether linked derivatives with different headgroups exhibited considerable headgroup effect on the transfection activity in HeLa cells (Fig. 8) [38]. Chol–DMAP and Chol–PR were also found to show efficient transfection in the absence of the helper lipid DOPE, while the other cholesterol derivatives exhibited optimum transfection in a mixture with DOPE at molar ratio 1:1. The DNA binding was strongest with Chol-NMe_3 bearing trimethylammonium headgroup, whereas Chol–PR and Chol–PR+ were found to be the weakest in DNA binding [38].

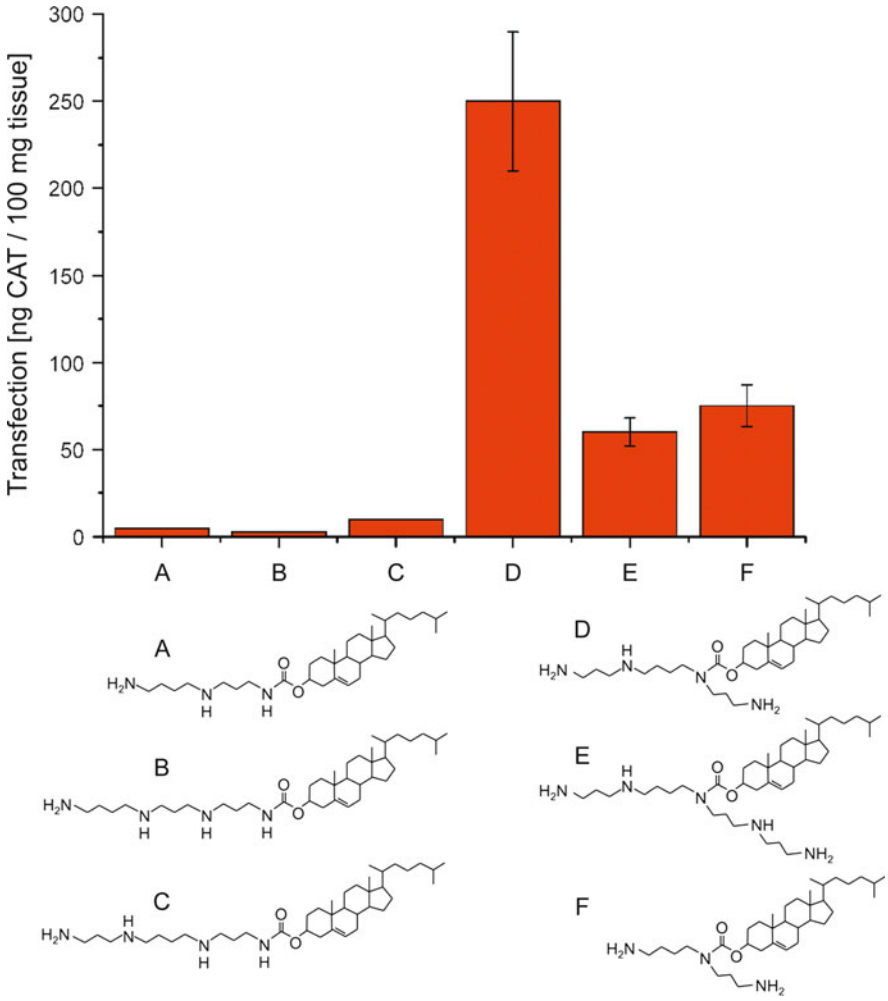

Fig. 6 Transfection activity of polyamine cholesterol cationic derivatives with linear (**a**–**c**) and T-shaped (**d**–**f**) structures. The activity of their mixtures with the helper lipid DOPE was measured in vivo as chloramphenicol acetyl transferase (CAT) expression in mouse lung [36]

3.2 Linkers

The linker group that bridges the cationic lipid headgroup with the hydrocarbon moiety controls the biodegradability of a cationic amphiphile. Most of the linker bonds are ether, ester, or amide bonds (Fig. 1). Compounds with ether links generally render better transfection efficiency. However, they are more stable and may cause higher toxicity, while cationic lipids with ester links such as DOTAP are more biodegradable and less cytotoxic in cultured cells [28, 39]. Noteworthy,

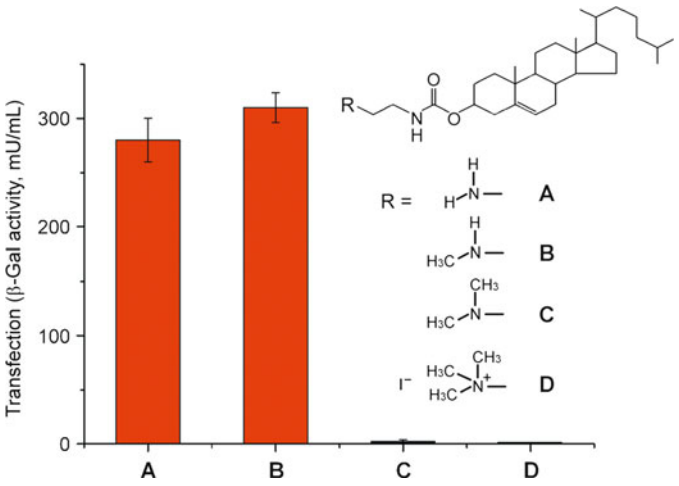

Fig. 7 Transfection of β-galactosidase by cholesterol-based amine derivatives at lipid/DNA ratio of 4:1 in mouse melanoma cells (B16F0) [37]

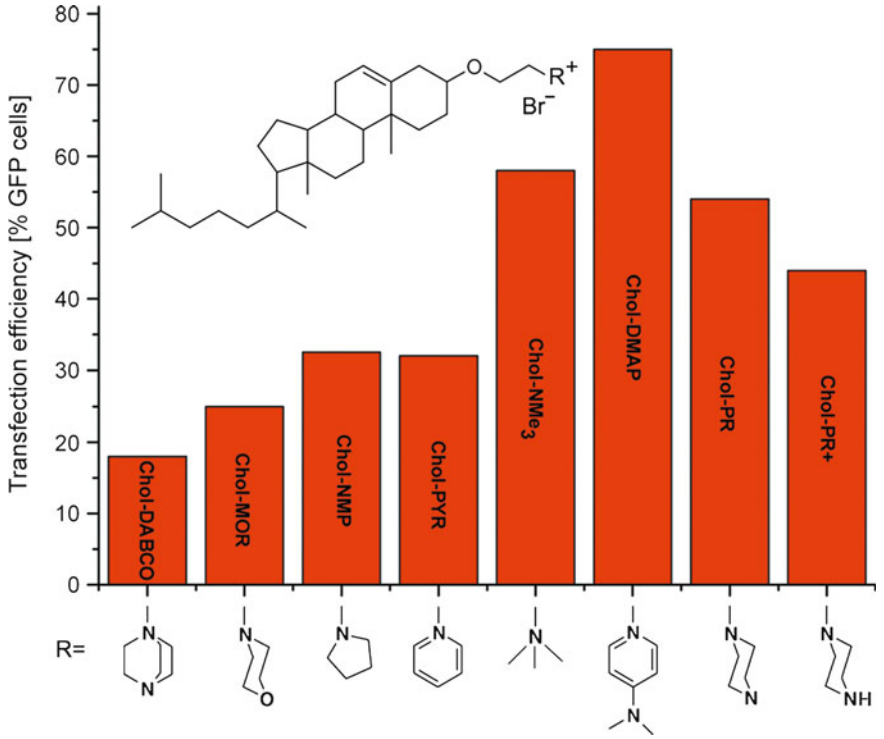

Fig. 8 Transfection of HeLa cells using cholesterol-based ether linked cationic lipids with different headgroups at N/P ratio 3:1, in the presence of 10% serum; the formulations were optimized for the helper lipid DOPE content [38]

cholesterol-based cationic lipids with ether links exhibit remarkably high in vitro gene transfer efficacies relative to their ester counterparts [40].

The length of the linker controls the lipid hydration and conformational flexibility [41]. Incorporating oxyethylene units between cholesterol moiety and the polar headgroup has been reported to increase hydration but decrease the transfection activity [42]. The effect of linker length is illustrated by a series of cationic lysine-based lipids with hydrocarbon spacers 0, 3, 5, and 7 carbon atoms long, or with a hydrophilic oxyethylene spacer (Fig. 9) [43]. Cationic lipids with hydrophobic spacers were able to fuse with biomembrane-mimicking bilayers. For example, 1,5-dihexadecyl-*N*-lysyl-*N*-heptyl-L-glutamate, having the longest 7 carbon atom spacer (Fig. 9, column 2c), exhibited the highest fusogenic potential among the lipids in Fig. 9, in correlation with its superior gene expression efficiency. By contrast, a hydrophilic oxyethylene chain spacer resulted in lower gene expression efficiency (Fig. 9, column 3).

An instructive quantitative structure–activity relationship (QSAR) analysis carried out on published data about a large set of cationic lipids, including both successful and unsuccessful compounds, permitted to delineation of a high-efficiency region

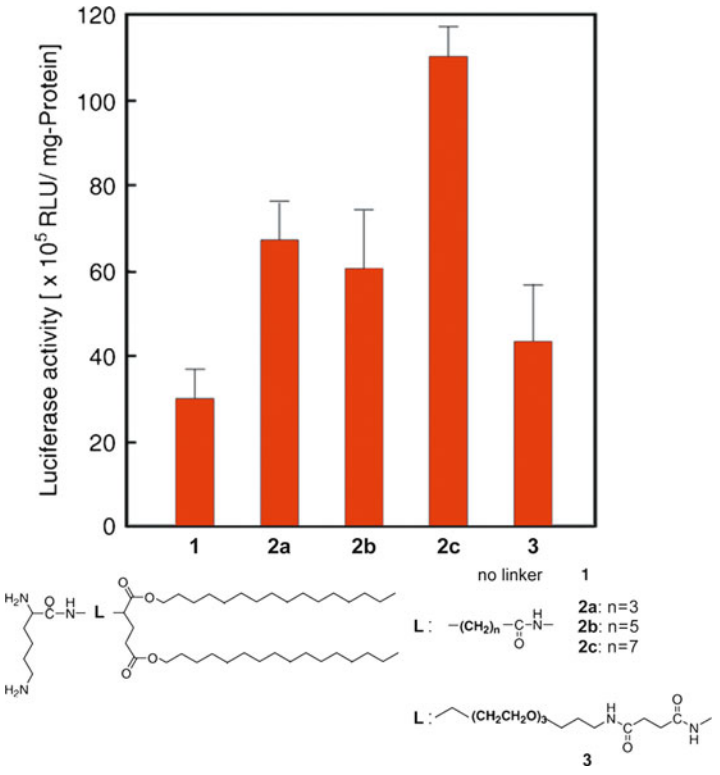

Fig. 9 Luciferase activity of pDNA-encapsulating liposomes composed of cationic lipids with linker groups of increasing length [43]

defined by molecular parameters such as amphiphilicity, lipophilicity, lipid partition between octanol and water, headgroup size and charge, etc [44]. It was found that the higher amphiphilicity values of C14-chain lipids with oxygen-containing –O–, $–CO_2–$ and –NHCO– linkers correlate with higher transfection efficiency relative to lipids with chains directly attached to the cationic nitrogens.

3.3 Hydrocarbon Chain Length and Saturation

In view of the important role of electrostatic interactions of the lipid headgroups with DNA, most of the efforts for improving the cationic lipids efficiency have been focused on synthesis of amphiphiles with new versions of positively charged polar groups. Less attention has been given to the role of the lipid hydrophobic domain. This appears to have been an unfortunate development because recent investigations suggest that the nonpolar portions determine in an important way the potency of the transfection agents. The great majority of cationic lipids currently in use are dioleoyl derivatives with two monounsaturated C18:1c9 hydrocarbon chains (e.g., DOTAP, DOSPA, DOTMA, DORIE, DOGS, EDOPC). However, studies on the effect of the hydrocarbon chains indicate that this choice of alkyl chains is not the most successful and that lipids with shorter chains usually display higher activity. In the following, we summarize the data, which correlate transfection efficiency with the lipid hydrocarbon chain structure.

Series of hydroxyethyl quaternary ammonium lipids with myristoyl (diC14:0, DMRIE), palmitoyl (diC16:0, DPRIE), stearoyl (diC18:0, DSRIE), and oleoyl (diC18:1c9, DORIE) chains studied by Felgner et al. [35] showed a clearly expressed inverse chain length–activity correlation. The lipid with the shortest dimyristoyl chains, DMRIE, exhibited superior activity with COS7 cells. Noteworthy, the unsaturated diC18:1 compound, DORIE, was considerably more effective than the saturated analog, DSRIE (Fig. 10). Studies on carbamate-linked cationic lipids also showed increasing transfection efficiency with decrease of the chain length (Fig. 11) [45]. Shorter hydrocarbon chains also favored fusion and the penetration of cationic liposomes through cell membranes, in correlation with their higher transfection potency.

The cationic PCs (Figs. 3 and 12) are an attractive cationic lipid class due to their biodegradability by lipolytic enzymes and remarkably low toxicities [16, 17]. At the same time, lipids of this type exhibit reasonably good transfection efficiencies. EDOPC, the best studied representative of cationic PCs (Fig. 3b), is similarly active in transfecting baby hamster kidney (BHK) cells as the widely used Lipofectamine [16]; some recently synthesized PC derivatives have over an order of magnitude higher efficiency than EDOPC [47]. Cationic PCs were also found to exhibit high-transfection activity, both in vitro and in vivo, in antitumor and anti-cystic fibrosis pharmaceuticals [48–54].

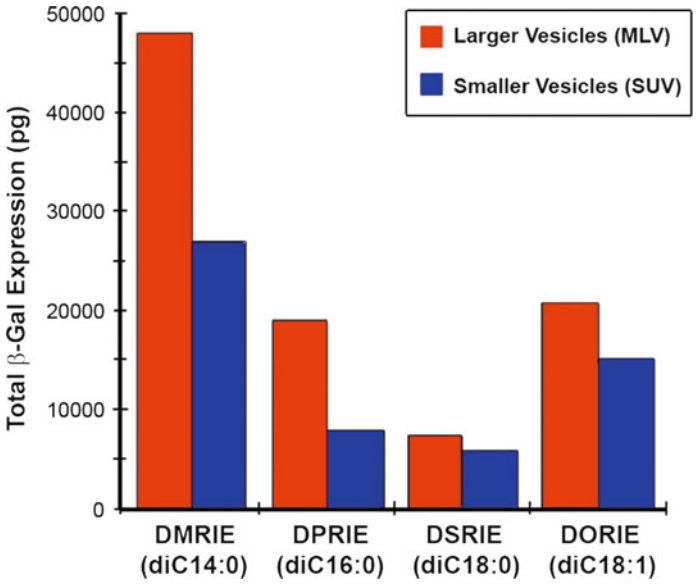

Fig. 10 Cationic lipids DMRIE, DPRIE, and DSRIE, containing saturated alkyl chains of increasing length (14, 16 and 18 carbon atoms, respectively), and DORIE, which contains monounsaturated C18:1 alkyl chains, formulated with 50 mol% DOPE, assayed for transfection activity by the β-galactosidase expressed in COS.7 cells transfected with pMVlacZ plasmid DNA (reproduced from [35]; copyright by the American Society for Biochemistry and Molecular Biology)

Among a large number of cationic PCs with different R_1, R_2, and R_3 hydrocarbon chains that have been synthesized and tested for transfection, of particular interest are several compounds displaying activities considerably exceeding the EDOPC activity. Their structures, together with the structures of the lipids with transfection activity similar to that of EDOPC, are given in Fig. 12. The transfection activity of the cationic PCs varies by over two orders of magnitude and strongly increases for lipids with total of two double bonds (one per chain) and 30 carbon atoms in the chains ($R_1 + R_2 + R_3$) (Fig. 13a). Maximum transfection, exceeding 10–12 times that of EDOPC, was observed for lipids having 14:1 myristoleoyl or myristelaidoyl chains [47]. The maximum is represented by three lipids, each comprising two 14:1 (myristoleoyl or myristelaidoyl) hydrocarbon chains: diC14:1c-EPC, diC14:1t-EPC and C14:1C2:0-C14:1PC (Fig. 12). Decreasing the unsaturation to 1 or to 0 double bonds per molecule and varying the chain length away from this maximum both result in drastic reduction of transfection activity (Fig. 13a) [26].

The transfection data summarized in Fig. 13 were obtained with primary human umbilical artery endothelial cells (HUAEC). Vascular endothelial cells, acting as an interface between circulating blood and tissues, are known to be involved in inflammatory processes, in atherosclerosis and angiogenesis, and represent a remarkable challenge as a gene therapy target. Their therapy with nonviral vectors

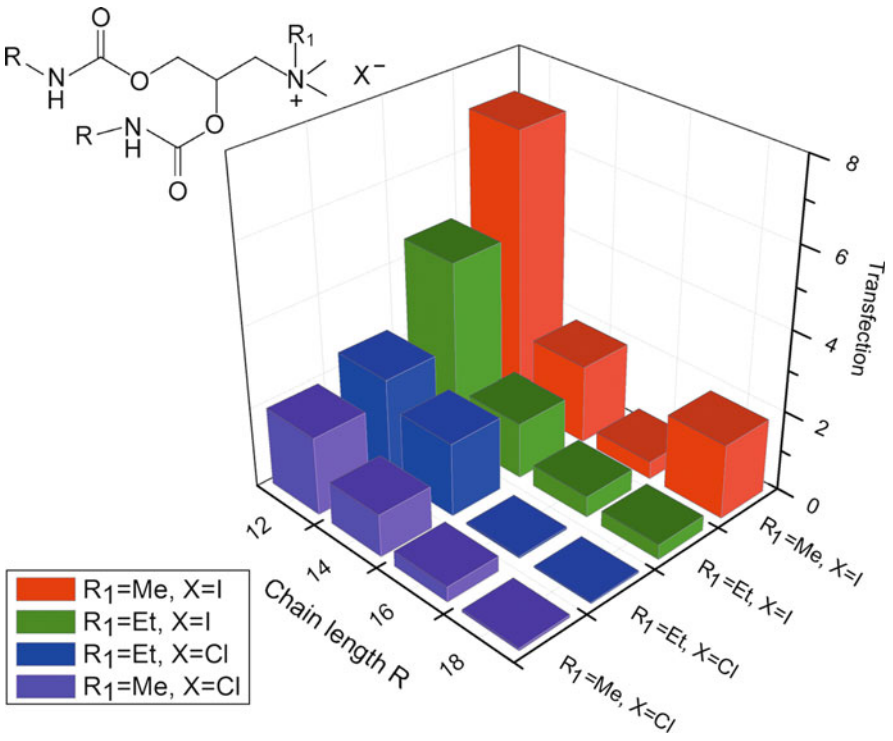

Fig. 11 Transfection efficiency of carbamate-linked quaternary ammonium transfection agents (up-left) with chlorine or iodine counterions/pGL3 plasmid DNA complexes in COS-7 cell line [45]

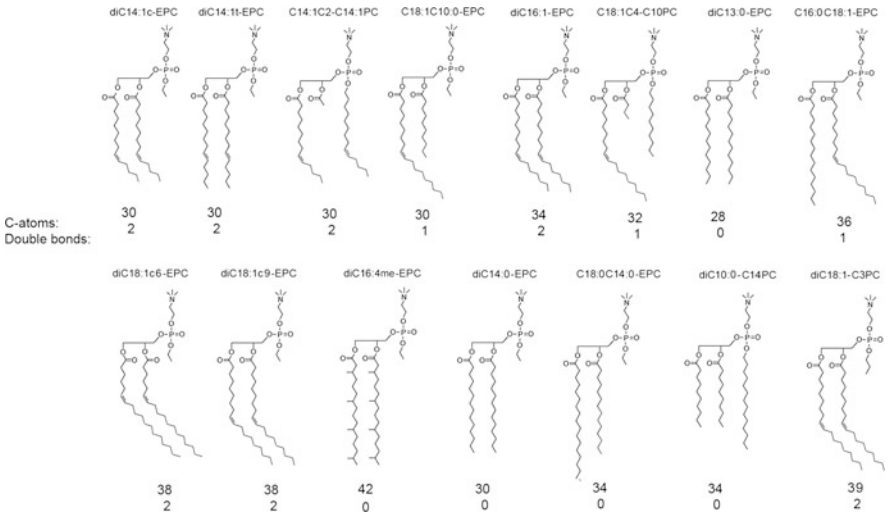

Fig. 12 Cationic PCs exhibiting highest transfection activity [46] (reproduced by permission of the Royal Society of Chemistry)

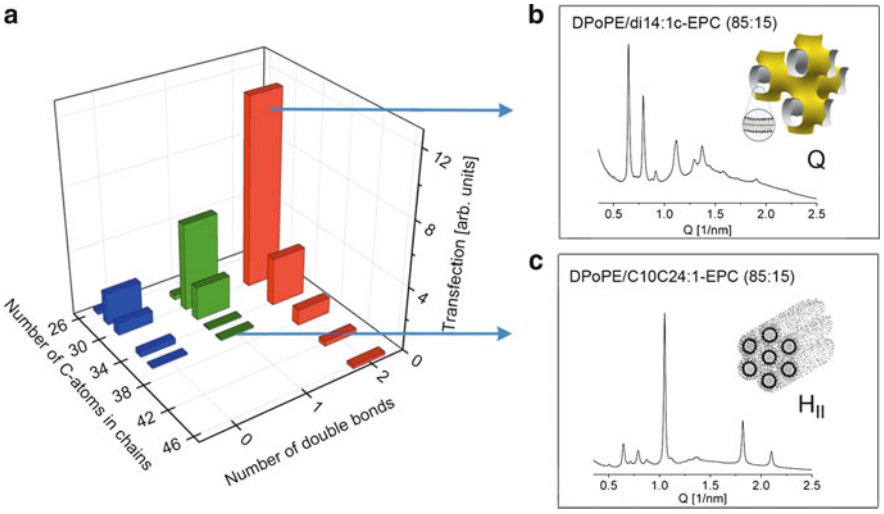

Fig. 13 Correlations between hydrocarbon chain structure, mixing behavior and transfection efficiency of the cationic PC derivatives. (**a**) Transfection activity plotted as a function of the total number of carbon atoms and double bonds in the lipid chains; (**b**) Cubic Pn3m phase formed in DPoPE mixture with a strong transfection agent, diC14:1c-EPC. (**c**) Hexagonal HII phase, coexisting with a small amount of cubic phase, in a mixture of DPoPE with a weak transfection agent, C10C24:1-EPC; (b) and (c) are representative for the effects of strong and weak transfection agents, respectively [47] (reproduced with permission from [26]; copyright (2009) American Chemical Society)

has been hampered because these cells are very difficult to transfect and the development of new, highly efficient carriers for their transfection is of considerable interest.

The effect of chain length on the transfection activity of double-chained 1,4-dihydropyridine (DHP) cationic derivatives (Fig. 14, inset) was examined with β-galactosidase gene into fibroblasts (CV1-P) and retinal pigment epithelial (D 4O7) cell lines in vitro [55]. Variation of the alkyl chain length at positions 3 and 5 of the 1,4-DHP ring showed that increasing the chain length from C12 to C18 results in gradually declining DNA condensation and transfection activity (Fig. 14), so that the compound with C18 chains was completely inactive [55].

Yingyongnarongkul et al. [56] studied a library of aminoglycerol–diamine conjugate-based cationic lipids with urea linkage between varying length of diamines and hydrophobic chains. Cationic lipids with short spacers and short hydrophobic chains delivered DNA into HEK293 cells more efficiently than those with longer ones (Fig. 15). Soltan et al. [39] studied *N*4,*N*9-diacyl spermines with didecanoyl, dilauroyl, dimyristoyl, dimyristoleoyl, dipalmitoyl, distearoyl, dioleoyl, and diretinoyl hydrophobic chains for their ability to deliver siRNA to primary skin cells and cervix carcinoma cells. The highest efficiency was found with the dimyristoyl (diC14:0) and dimyristoleoyl diC(14:1) compounds. However, the latter compounds were also found to exhibit toxicity.

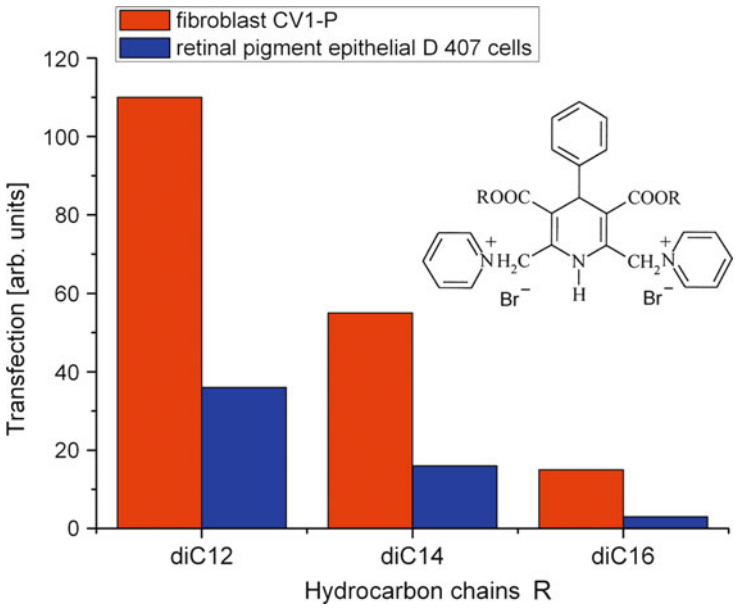

Fig. 14 Transfection activity of cationic double-chained 1,4-dihydropyridine derivatives with β-galactosidase gene into fibroblasts (CV1-P) and retinal pigment epithelial (D 4O7) cell lines (+/− charge ratio = 4) [55]

To summarize the data on chain length effects, we have represented the transfection activity as a function of the total number of carbon atoms in the lipid hydrocarbon chains (Fig. 16). It is evident from this figure that *transfection typically exhibits a maximum at an average chain length of about 14 carbon atoms*. These data indicate that the most frequently used cationic lipid derivatives with dioleoyl chains do not appear to be the most appropriate choice of carriers in transfection studies.

An amphiphilicity-partition coefficient diagram based on a QSAR analysis of a large set of cationic lipids with saturated chains also shows that compounds with two C14 chains provide the highest probability for superior efficiency [44].

In addition to the chain length, the hydrocarbon chain unsaturation also plays a very important role. This is clearly shown by the data on cationic PCs, which demonstrate drastic transfection increase with increase of the number of double bonds per lipid from 0 to 2 (Fig. 13a). Studies on double chained pyridinium compounds SAINT (Synthetic Amphiphile INTeraction) (Fig. 17, inset) have shown that, while elongation of the saturated alkyl chains from C16:0/C16:0 to C18:0/C18:0 resulted in a reduction by a factor of about two in the transfection efficiency, introduction of double bonds reversed this effect and resulted in very strong increase of the transfection efficiency (Fig. 17). When substituting only one of the saturated C18:0 alkyl chains for unsaturated C18:1 chain, the transfection efficiency increased by an order of magnitude, while the diunsaturated compound,

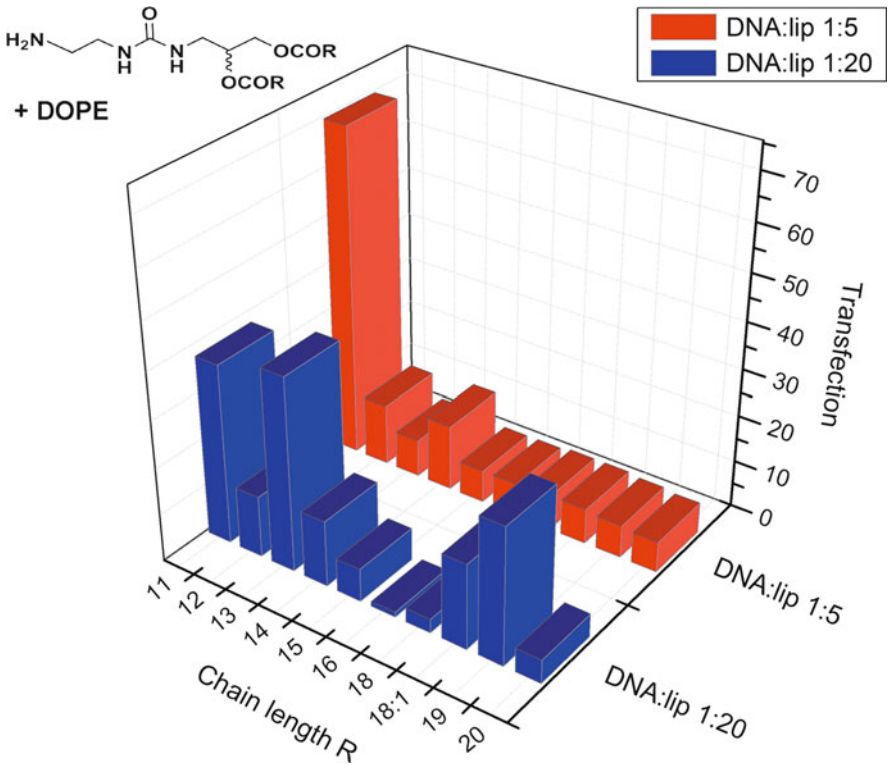

Fig. 15 Transfection activity of cationic aminoglycerol–diamine conjugate lipids (up-left) employing β-galactosidase (0.1 μg/well). The lipoplexes were used at DNA/lipids w/w ratios of 1:5 and 1:20. The transfection efficiencies of the lipids were compared to that of commercially available reagent, Effectene, which was calculated as 100% transfection efficiency [56]

C18:1/C18:1, was 10–30 times more efficient than the disaturated compound. Most importantly, the improved transfection efficiency was not accompanied by an increase in toxicity. The double bonds in the diunsaturated compound, C18:1/C18:1, was found to be 85% in *cis* orientation. To investigate the relevance of a *cis* vs a *trans* conformation, pure *trans* and *cis* C18:1/C18:1 isomers were compared and it was found that the *trans* isomer was more efficient in the transfection enhancement than the *cis* isomer (Fig. 17).

An interesting recent result demonstrating that pyridinium-based cationic lipids with *trans*-unsaturated hydrocarbon chains are more efficient than the *cis*-unsaturated analogs in transfecting CHO cells is shown in Fig. 18 [57].

The chain unsaturation effect was also studied for dimethylaminopropane (DMA) cationic lipids with 0–3 double bonds per chain [59]. The authors used a series of four lipids of the same alkyl chain length (diC18) modified with a systematic addition of double bonds, from 0 to 3 per chain: distearoyl (DSDMA), dioleoyl (DODMA, dilinoleyl (DLenDMA), and dilinolenoyl (DLinDMA). It was

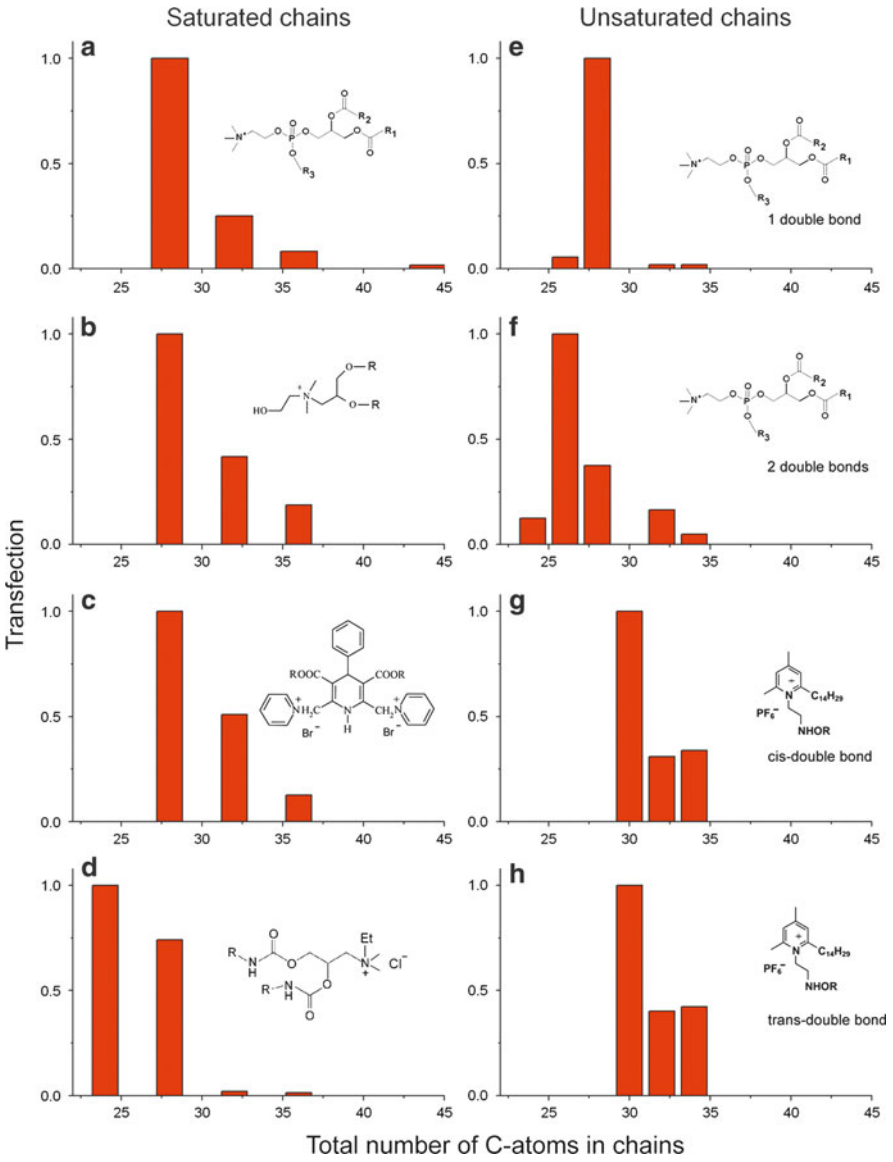

Fig. 16 Normalized transfection activity as a function of the hydrocarbon chain length (total number of carbon atoms) for the cationic lipids with structures given in the insets: cationic phosphatidylcholines with saturated (**a**) and unsaturated (**e**, **f**) chains [46]; hydroxyethyl quaternary ammonium lipids [35] (**b**); 1,4-dihydropyridine lipids [55] (**c**); carbamate-linked lipids [45] (**d**); pyridinium-based lipids with *cis*- (**g**) and *trans*-unsaturated (**h**) chains [57]

reported that the degree of saturation of cationic lipids affected lipid pK_a, fusogenicity, cellular uptake, and gene silencing ability when used to encapsulate and deliver small interfering RNA (siRNA). The observed luciferase expression was

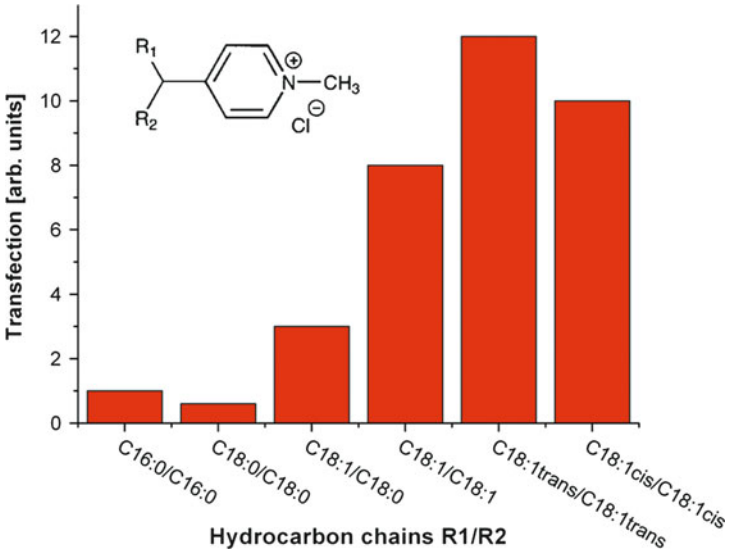

Fig. 17 Transfection activity of different amphiphiles formulated with DOPE (1:1), examined in COS-7 cells [58]

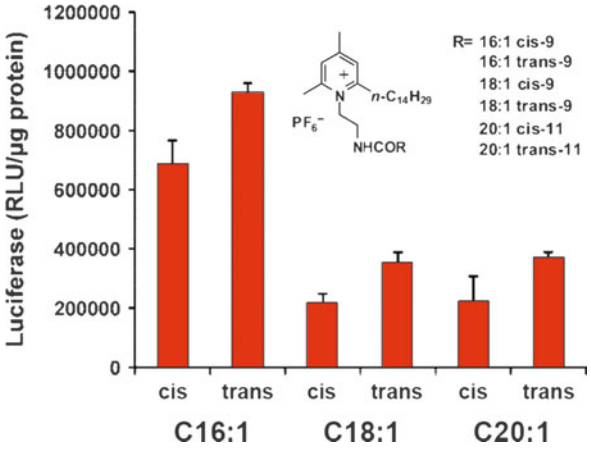

Fig. 18 Effects of cationic lipid *cis* and *trans* isomers on the transfection activity of luciferase gene in CHO cells (reproduced with permission from [57]; copyright (2008) American Chemical Society)

as follows: DLinDMA 21%; DLenDMA 32%; DODMA 54%; DSDMA 100% (no gene silencing). It was also suggested that endocytosis is not the rate-limiting step in gene silencing, and that events which have the greatest effect on the efficiency take place after the siRNA has been internalized by the cell.

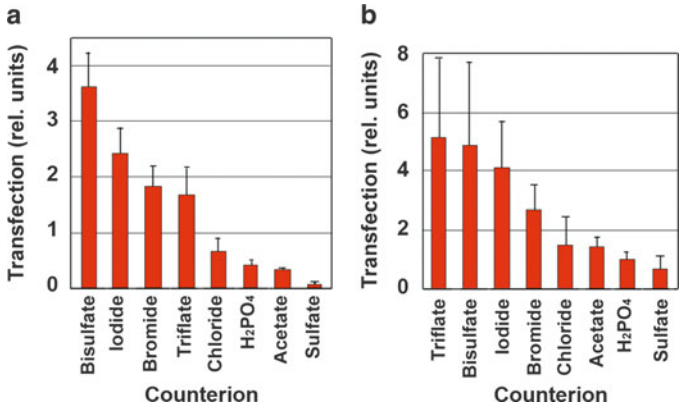

Fig. 19 Counterion effects on the transfection by DOTAP lipoplexes as estimated from luciferase expression of NIH3T3 cells (**a**) and Balb-C murine lung (**b**) [60]

3.4 Role of Counterions

Cationic lipids have been shown to present different transfection activity depending on the counterion. Lipids with iodine counterion have been shown to exhibit better transfection efficiency than those with chlorine anion [45]. A study on plasmid DNA transfection into NIH3T3 cells and mouse lung by using a set of DOTAP lipids with various counterions showed that transfection decreases in the following counterion order: bisulfate > iodide > bromide > chloride > dihydrogenphosphate > acetate > sulfate (Fig. 19) [60]. A similar activity trend was also found in vivo. Remarkably, this trend correlates with the counterion lyotropic ordering (Hofmeister series). However, since manifestations of the Hofmeister effect in lipid dispersions require rather high, molar concentrations of the chaotropic and kosmotropic anions [61], it is unclear what is the mechanism underlying the observed counterion ordering in lyotropic series with respect to their effect on transfection.

4 Structure and Properties of Lipoplexes

Cationic lipids interact electrostatically and form stable complexes (lipoplexes) with the polyanionic nucleic acids. The structure of most lipoplexes is a multilamellar sandwich in which lipid bilayers alternate with layers of DNA strands [16, 62–64] (Fig. 20). Although infrequent, nonlamellar structures have also been found. The free energy gain upon lipoplex formation was shown to be essentially of entropic nature resulting from the counterion release and macromolecule dehydration [65, 66].

Lipoplex formation taking place upon DNA mixing with cationic lipid vesicles proceeds in steps of substantially different kinetics: (1) adhesion of DNA to the

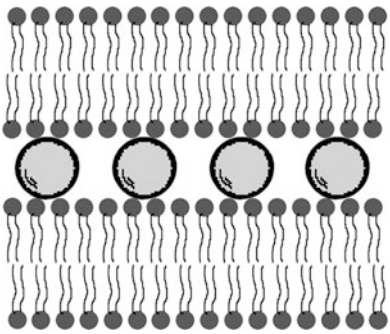

Fig. 20 Lamellar lipid/DNA lipoplex

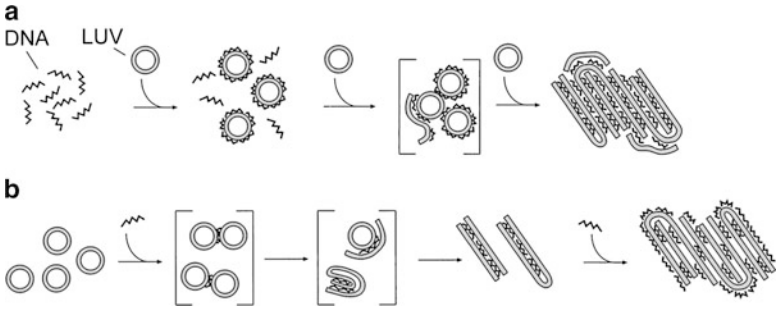

Fig. 21 Proposed mechanisms of lipoplex formation: (**a**) vesicle titration (DNA initially in excess) – DNA coats the vesicle surfaces as the latter are added to the DNA solution – with increase of the vesicle concentration, clusters of DNA-coated vesicles form and consequently rupture; (**b**) DNA titration (lipid initially in excess) – DNA encounters with bare membranes result in vesicle associations – vesicle–DNA–vesicle adhesion generates stresses, which lead to vesicle rupture, followed by continued aggregation and growth of the complex upon further addition of DNA. (reproduced with permission from [67]; copyright (2000) Biophysical Society)

vesicle surface; (2) vesicle rearrangement into a multilamellar lipoplex with additional DNA binding to newly exposed inner monolayers; (3) growth and coalescence of lipoplex particles, potentially leading to precipitation under certain conditions [67]. While the first step actually takes place as soon as lipid and DNA come into contact, the next two steps include slow rearrangement of the complex. The morphology of the lipid/DNA complexes, as well as the kinetics of their formation, have been reported to be protocol-dependent. The proposed different pathways of lipoplex formation upon DNA titration into a vesicle suspension or vice versa are illustrated in Fig. 21 [67]. Flow fluorometry studies discriminate two distinct morphologies in the lipoplex formation and growth with time: (1) coexistence of DNA-coated vesicles and multilamellar lipoplexes at shorter incubation times, and (2) highly fused multilamellar lipoplexes typically used in transfection studies [68].

4.1 Lipoplex Size and Surface Charge

Lipoplex parameters such as zeta potential and size (Fig. 22) have been reported to influence the transfection activity. The lipoplex zeta potential is critical for the interactions with the negative cell surfaces, and its value has been reported to affect transfection [71]. Thus, release of DNA is strongly suppressed for lipoplex formulations containing excess of DNA and bearing negative zeta potential, relative to those with positive zeta potential [46]. Lipoplexes bearing positive zeta potentials and larger (within limits) sizes are generally considered to be more efficient [67, 69, 72, 73].

Lipoplex size has a strong effect on transfection, especially *in vivo*, but the sizes that are most appropriate for efficient transfection are subject to some controversy. Early results indicated that the lipoplex sizes in the range 200–2,000 nm were strongly correlated with uptake and transfection efficiency, with bigger lipoplexes being generally more efficient [73]. However, later studies indicated that smaller (<200 nm) lipoplexes are more efficient [74]. Measurement of the endosomal uptake of fluorescent dextran beads of various sizes clarified that particles smaller than 200 nm were predominantly taken up by means of clathrin mediated endocytosis; with increasing the size, a shift to another mechanism occurred, so that particles larger than 500 nm were taken up predominantly by caveolae mediated pathways [75]. Later on, several publications addressed the pathway preferences of lipoplexes [76–78], but the issue remains controversial and presently it is not clear which of the endocytic pathways dominate in the lipoplex uptake. A confusing issue is the heterogeneity associated with the lipoplex sizes. Smaller lipoplexes, in

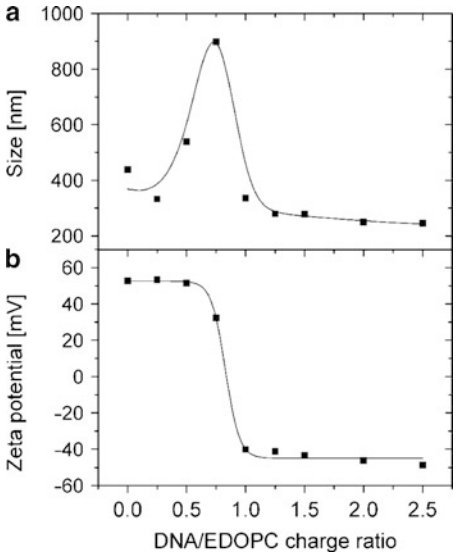

Fig. 22 Size (**a**) and zeta potential (**b**) of EDOPC/DNA lipoplexes at different lipid/DNA ratios [69]; as is known, lipoplex aggregation taking place at the isoelectric point results in lipoplex size growth [70]

the range of 100 nm, are considered more appropriate to enter narrow capillaries. Since lipid–DNA complexes are generally bigger, addition of nonlipidic condensing agents such as polyethyleneimine, polylysine, protamine sulfate, etc. before the addition of cationic lipids has recently become widely used practice for preparation of small, homogeneous lipoplexes [79, 80].

4.2 Lipoplex Phase Structures

Generally, lipids forming lamellar phase by themselves, form lamellar lipoplexes; in most of these cases, lipids forming H_{II} phase by themselves tend to form H_{II} phase lipoplexes. Notable exceptions to this rule are the lipids forming cubic phase. Their lipoplexes do not retain the cubic symmetry and form either lamellar or inverted hexagonal phase [20, 24]. The lamellar repeat period of the lipoplexes is typically ~1.5 nm higher than that of the pure lipid phases, as a result of DNA intercalation between the lipid bilayers. In addition to the sharp lamellar reflections, a low-intensity diffuse peak is also present in the diffraction patterns (Fig. 23a) [81]. This peak has been ascribed to the in-plane positional correlation of the DNA strands arranged between the lipid lamellae [19, 63, 64, 82]. Its position is dependent on the lipid–DNA ratio. The presence of DNA between the bilayers has been verified by the electron density profiles of the lipoplexes [16, 62–64] (Fig. 23b).

4.3 Gel Phase Lipoplexes with Columnar DNA Superlattice

DNA arranges into rectangular superlattice in the low-temperature gel phase of saturated cationic lipids [83, 84]. This is evidenced by two or three diffuse reflections in addition to the set of lamellar reflections; these are attributed to DNA ordering both within the layer and across the lipid bilayers, from one DNA layer to another. These reflections index on a centered rectangular lattice. Noteworthy, DNA does not affect the gel–liquid crystalline transition temperatures of the lipoplexes [16, 19, 84]. This transition is associated with loss of the DNA interlamellar correlation.

4.4 Inverted Hexagonal Phase Lipoplexes

Certain cationic lipids were found to form inverted hexagonal phase lipoplexes [21, 46, 85–87]. The H_{II} phase lipoplexes consist of DNA coated by lipid monolayers and arranged on a two-dimensional hexagonal lattice. This arrangement is identified by small-angle X-ray reflections in the ratio 1:3:4 (Fig. 24a). The lower intensity of the (11) and (20) lipoplex diffraction peaks relative to the H_{II} pattern

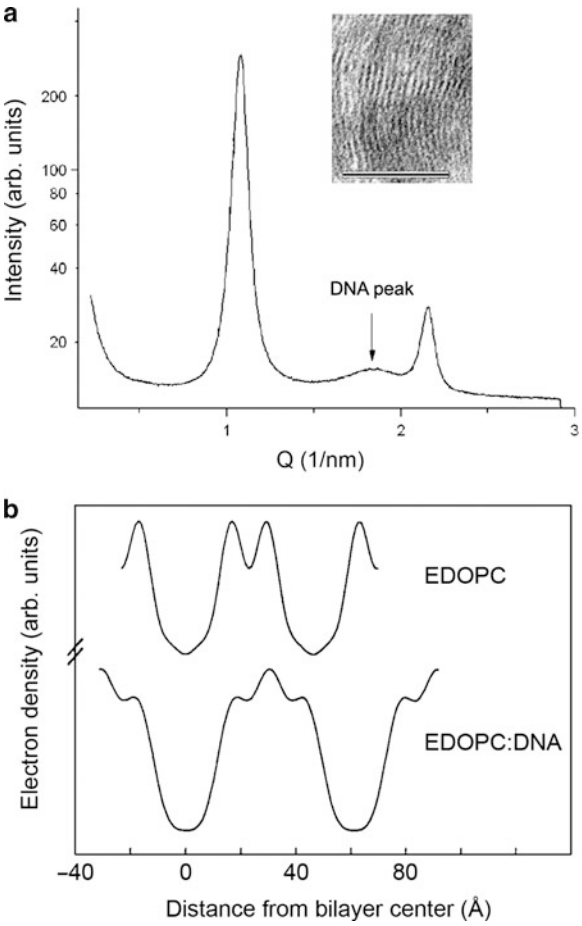

Fig. 23 (**a**) Small-angle X-ray diffraction profile of EDOPC lipoplexes at 4:1 lipid/DNA weight ratio (*arrow* points to the peak originating from DNA–DNA in-plane correlation); *inset*: thin-section electron microscopy image of EDOPC lipoplexes (reproduced with permission from [81]; copyright (2007) Elsevier). (**b**) Electron density profiles of the lipid bilayer in presence and in absence of DNA [16] (copyright (2000) Biophysical Society)

of the pure lipid is known to result from the higher electron density of DNA relative to water [88]. It is thus an indication of the presence of DNA in the core of the hexagonal phase cylinders [21]. A representative of the cationic PCs, which forms cubic phase by itself, was reported to form H_{II} phase lipoplexes (Fig. 24b) [20]. In some earlier studies, it has been suggested that hexagonal phase lipoplexes are more efficient in transfection than the lamellar lipoplexes [86, 87]. However, recently accumulated evidence shows rather low activities of hexagonal phase lipoplexes and a general lack of correlation between lipoplex phase structures and transfection activity for various experimental systems [20, 21, 24, 85, 89–93].

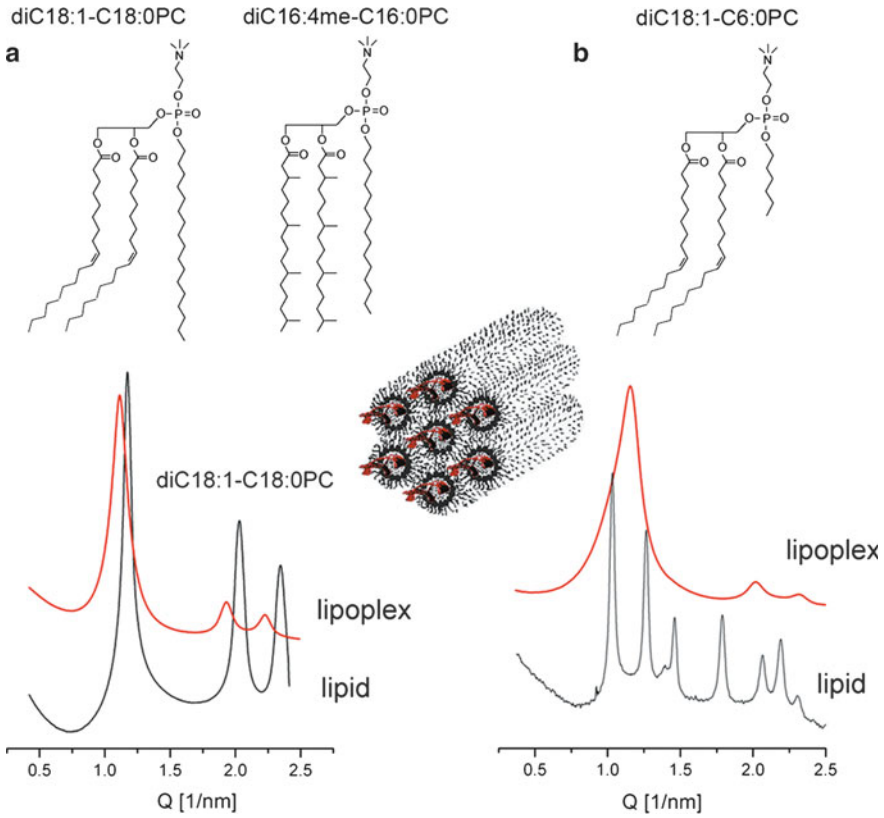

Fig. 24 Inverted hexagonal phase lipoplexes with cationic PCs forming HII phase (**a**) and cubic Pn3m phase (**b**). Lipid/DNA 4:1 w/w, 37 °C [46] (reproduced by permission of the Royal Society of Chemistry)

5 Mechanism of Nucleic Acid Release from Lipoplexes

According to current views, the basic events of lipid-assisted transfection include lipoplex binding and internalization by the cells, followed by DNA release and transport to the nucleus for transcription [94–96]. This process involves a number of obscure, poorly understood intermediate stages, e.g., lipoplex escape from the endosomes and intracellular disassembly. A key process in this sequence is the DNA unbinding from the lipoplex believed to be driven by cationic lipid charge neutralization upon mixing with the cellular anionic lipids. Indeed, in vitro addition of negatively charged liposomes to lipoplexes was shown to result in dissociation of DNA from the lipid [16, 97–100]. However, charge neutralization alone appears not to be sufficient to explain the different rates of DNA release measured with different types of anionic lipids [98]. The data in Fig. 25 show that both release

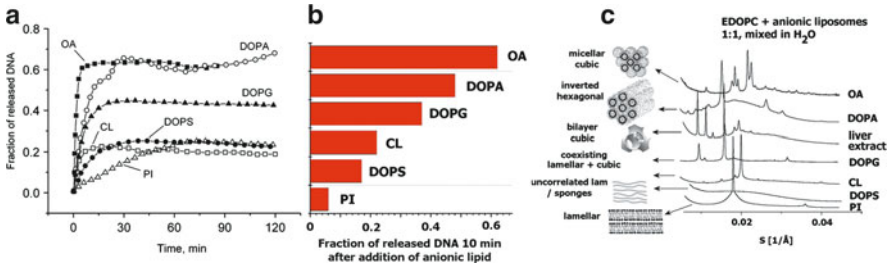

Fig. 25 (**a**) DNA release from EDOPC–DNA lipoplexes after addition of negatively charged lipid dispersion, as monitored by FRET (*OA*, oleic acid; *DOPA*, dioleoyl phosphatidic acid; *DOPG*, dioleoyl phosphatidylglycerol; *CL*, cardiolipin; *DOPS*, dioleoyl phosphatidylserine; *PI*, phosphatidylinositol). (**b**) Fraction of released DNA from EDOPC lipoplexes 10 min after addition of the respective anionic liposomes; (**c**) X-ray diffraction patterns of mixtures of EDOPC and anionic liposome dispersions; the respective structures are shown schematically on the left side (reproduced with permission from [98]; copyright (2004) Biophysical Society)

kinetics and saturation values are strongly modulated by the type of anionic lipid used. For example, in conditions of anionic lipid excess, DOPG and DOPA turn out to be two to three times more efficient than DOPS. Similar differences were also observed with other anionic lipids.

A remarkable insight into the origin of this behavior was provided by X-ray diffraction experiments, which showed that correlation exists between the releasing capacity of the anionic lipids and the mesomorphic structures that they form in mixtures with the cationic lipid [98]. Anionic lipids, which were more efficient in releasing DNA, induced nonlamellar phases of high negative curvatures; conversely, the less efficient anionic lipids did not significantly perturb the lamellar phase of the cationic lipid (Fig. 25). The sequence of the cationic/anionic lipid phases correlating with increasing DNA release may be described as lamellar–(disordered lamellar)–bilayer cubic–inverted hexagonal–inverted cubic phase. This sequence is identical to the general progression of inverted lyotropic liquid crystalline phases, corresponding to a succession of more negative spontaneous monolayer curvatures and can be induced in lipid dispersions, e.g., by heating [101, 102]. Induction of nonlamellar phases by anionic lipids may be expected to facilitate DNA release as it disrupts the multilayered lipoplex structure and destroys the lipid bilayer integrity. The anionic lipids thus appear to have a twofold effect: they compensate the surface charge and eliminate the electrostatically driven DNA binding to the membrane interface, and they also disrupt the lipoplex structure and facilitate DNA departure into the solution by inducing nonlamellar phases upon mixing with the lipoplex lipids.

Even though the individual lipid components form stable lamellar phases, formation of inverted nonlamellar phases in EDOPC mixtures with anionic lipids of the type found in cell membranes is certainly not surprising, taking into account a number of reports which demonstrate that a variety of cationic/anionic lipid

mixtures are unusually prone to nonlamellar phase formation [103–106]. Variations of the cationic/anionic lipid ratio were found to generate virtually the entire panoply of lipid arrays. For example, a regular progression was observed for mixtures of cardiolipin and EDOPC, which form inverted hexagonal phase H_{II} at net charge neutrality and bicontinuous cubic structures when one type of lipid is in excess [106]. Increasing the excess of cationic or anionic charge results in the appearance of bilayers with numerous irregular interlamellar contacts. Similarly, numerous contacts have been visualized by electron microscopy between lipoplexes and intracellular membranes [81], suggesting a process of layer-by-layer lipoplex disassembly. In considering the mechanism of DNA release, the lipoplex size should also be taken into account because lipoplexes with typical mean sizes of ~400–500 nm and lamellar repeat distances of ~5–6 nm comprise several tens of layers and it is obvious that extensive intermembrane interactions are required for their disassembly.

The process of lipoplex/membrane lipid mixing resulting in DNA release is most often discussed in terms of membrane fusion. However, it should be remembered that monomer exchange could produce similar intermixing, especially with charged lipids, which generally exhibit much higher solubility than the zwitterionic compounds. For example, the critical micelle concentration (CMC) values of the anionic diC10-PS and diC10-PG were reported to be ~20 and ~85 times higher, respectively, than the diC10-PC CMC of 5 μM [107]. Correspondingly, the partitioning of anionic monomer species into positively charged lipoplexes can be expected to proceed at rates that are orders of magnitude higher. On the same grounds, one can also expect higher CMC and faster monomer exchange for the cationic lipids. Indeed, the lipid exchange in codispersions of vesicles and lipoplexes with different lipid compositions was found to proceed at significantly higher rates for EDMPC and EDPPC in comparison to their zwitterionic counterparts DMPC and DPPC, respectively, and at significantly higher rate for the shorter-chain and presumably more soluble EDMPC than for EDPPC [108].

It still remains controversial as to what extent the escape from endosomes contributes to gene transfection [35, 76, 95, 109]. Moreover, considering the physical differences between siRNA and plasmid DNA (the size and charge of siRNA are much smaller) and their different sites of action (siRNA mediates its effect in the cytosol [110], while DNA requires entry into the nucleus in order to gain access to the transcriptional apparatus), it has yet to be determined whether endosomal escape plays a significant role in functional siRNA delivery by the various carrier systems. A recent study [111] showed that, although most of the cellular uptake of siRNA lipoplexes is via endocytic pathways, this mode of entry does not appear to contribute significantly to functional siRNA delivery. Instead, a minor but rapid pathway, probably mediated by direct fusion of siRNA lipoplexes with the plasma membrane, appears responsible for most of the observed siRNA-mediated target gene knockdown.

6 Correlation of Transfection Activity with Lamellar-to-Nonlamellar Phase Conversions in Cellular Lipids

Given the need for intermixing of membrane lipids with lipoplex lipids as an important step in the sequence of transfection events, a set of recent findings, discussed below, takes on particular significance. These findings demonstrate that transfection efficiency closely correlates both with the cationic PC chain structure (Fig. 13a) [26] and with its effect on the lamellar-to-nonlamellar phase progressions observed in membrane lipids upon mixing with cationic PCs (Fig. 13, 26, and 27).

The mechanism underlying the prominent chain effect on the transfection efficiency is of considerable interest. It is clearly not of electrostatic nature because the cationic PCs have identical surface charge groups and cannot be distinguished at the level of electrostatic interactions. Other factors that may conceivably play role in this effect can also be excluded from consideration on the basis of the evidence thus far accumulated. As mentioned above, most of the cationic PCs, among them all high-transfection lipids, display phase behavior, which is similar to that of their parent PCs, and form lamellar liquid crystalline phases stable up to high temperatures. The properties of these phases do not appear to display relationships with the lipid transfection activity (few lipids forming H_{II} or cubic phases by themselves are typified by rather low-transfection efficiency). Moreover, the lamellar cationic PCs form highly stable lamellar liquid crystalline lipoplexes, which do not display structural transitions or experience damage upon heating up to 100°C. This behavior gives no grounds to seek correlations of the variation in a broad range transfection activity with the properties of the cationic PCs lipoplexes per se, but rather focuses the attention on their interactions with the intracellular membrane structures. Following this line of reasoning, we studied a model system in which

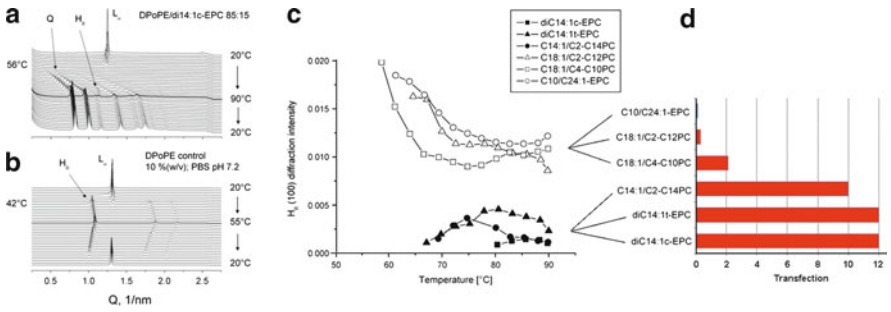

Fig. 26 Influence of a high-transfection cationic PC on the lamellar–nonlamellar phase transformation in lipids: (a) DPoPE/diC14:1c-EPC 85:15 mixture; (b) DPoPE control; diffraction patterns recorded every minute during heating and cooling scans at 3 and 5 °C/min, respectively; effect on the existence range and intensity of the HII phase in DPoPE (c) for high- and low-transfection cationic PCs (d). The HII phase diffraction intensity and temperature of appearance illustrate the extent of HII phase suppression by the high-efficiency agents and distinguish clearly the two kinds of strong and weak transfection agents (reproduced with permission from [47]; copyright (2007) Elsevier)

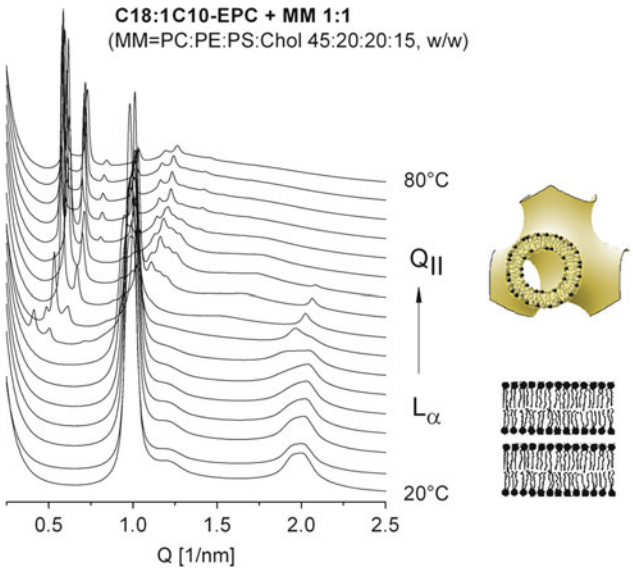

Fig. 27 Lamellar-cubic transition in membrane-mimicking lipid composition induced by mixing with C18:1C10-EPC, recorded by X-ray diffraction at heating scan rate of 1°C/min. (reproduced from [112]; copyright (2007) National Academy of Sciences, USA)

electrostatic cationic–anionic lipid interactions are not present: binary mixtures of the zwitterionic phospholipid dipalmitoleoyl phosphatidylethanolamine (DPoPE) with a set of high- and low-transfection cationic PCs [47]. DPoPE represents the most abundant class of nonlamellar-forming membrane lipids, the zwitterionic phosphatidylethanolamines (PEs), which are believed to be involved in lipidic fusion events. It exhibits lamellar–inverted hexagonal ($L_\alpha \rightarrow H_{II}$) phase transition at 42 °C (Fig. 26) [113]. The effects of the cationic PCs on this transition were found to correlate very well with their transfection efficiency. X-ray diffraction measurements showed that high-transfection agents eliminated the direct $L_\alpha \rightarrow H_{II}$ phase transition and promoted formation of an inverted cubic phase between the L_α and H_{II} phases, which replaced the H_{II} phase over a wide temperature range (Figs. 13b and 26a) [47]. In contrast, moderate and weak transfection agents retained the $L_\alpha \rightarrow H_{II}$ transition, but shifted to higher temperatures, and induced cubic phase formation at a later stage [47]. Thus, the hydrocarbon chain structures of cationic PCs exhibiting highest transfection appear to facilitate formation of inverted cubic phases in nonlamellar phase-forming lipid mixtures.

This behavior of the DPoPE/cationic PC mixtures is not surprising, because both the double bonds and hydrocarbon chain length variations are known to have considerable effect on the lamellar-to-nonlamellar transitions in lipids [113]. A specific structural characteristic of lipid arrays that exhibits distinct change around the chain length of 14 carbons is the formation of inverted bicontinuous cubic phases Q_{II}. The latter phases tend to form in diacyl or dialkyl phospholipids

and glycolipids that have chain lengths of C14 or shorter; the longer-chain lipids typically experience direct lamellar–inverted hexagonal L_α–H_{II} phase transitions [101, 102, 113]. The rationale underlying this behavior is that longer hydrocarbon chains can relieve packing frustration by filling the "voids" that otherwise exist between parallel adjacent cylinders, the consequence of which is that such lipids are able to form more easily the H_{II} phase [102]. In contrast, the shorter chains are unable to extend easily to fill voids, and therefore the inverse bicontinuous cubic phases, with lower packing frustration, dominate [114–116].

The effect of double bonds on both transfection and phase behavior is well illustrated by the pair C18:1/C10-EPC and C18:0/C10-EPC. These two lipids differ by one double bond only. However, the unsaturated lipid is over ten times more efficient as transfection agent than the saturated one [112]. The superior efficiency of C18:1/C10-EPC relative to C18:0/C10-EPC is also implied by the phases that evolve in membrane lipid formulations upon mixing with these two cationic lipids. A biomembrane-mimicking lipid formulation DOPC/DOPE/DOPS/Chol 45:20:20:15 remained lamellar in mixtures with C18:0/C10-EPC; in contrast, the more efficient C18:1/C10-EPC induced a lamellar–nonlamellar phase conversion in this mixture, which was taking place at physiological temperature (Fig. 27).

The relationship between the ability of the cationic lipids to induce a cubic phase and their transfection activity may be related to the molecular details of lipoplex fusion with cellular membranes. Representation of lipid membrane fusion with lamellar–nonlamellar (specifically, lamellar–cubic) phase transitions has long been a prominent feature in the literature, and has been well elaborated with respect to molecular mechanism and energetics [117, 118]. Simple geometric considerations also indicate that membrane fusion should proceed with formation of nonlamellar motifs and, in fact, a prospective nonlamellar membrane fusion intermediate structure has been experimentally observed [119]. Thus, the recorded disposition of the highly active transfection agents to induce cubic arrays in membrane lipids is an indication for their high fusogenicity, promoting in turn high-transfection activity. These results highlight the phase properties of the carrier lipid/cellular lipid mixtures as a decisive factor for transfection success.

7 Transfection Enhancement in Multicomponent Carrier Systems

The studies on the transfection activity of cationic lipids have led to the conclusion that simple binary cationic lipid/DNA complexes rarely exhibit satisfactory in vivo efficiency so as to be clinically viable. Their insufficient activity is supposedly related to the complexity of the delivery route, including multiple barriers. Thus, the cationic lipids essential for DNA condensation and protection require additional components to be efficient *in vivo*. That is why the present efforts for improving the efficiency are focused on the development of multicomponent carriers, such as

cationic lipid mixtures with neutral or zwitterionic helper lipids (colipids), with PEG lipids, with other cationic lipids, and with nonlipid compounds such as polymers (lipopolyplexes), peptides, etc.

7.1 Helper Lipids

Cationic lipids are often combined with neutral and zwitterionic lipids in formulations for gene therapy. The most frequent colipids are cholesterol, DOPE and dioleoylphosphatidylcholine (DOPC) (or other PCs) (Fig. 28). These neutral lipids may play a role in transfection by increasing the level of DNA protection against DNases or facilitating the destabilization of the endosomes [35, 103]. The optimum cationic lipid/helper lipid stoichiometry varies for the different cationic lipids, nucleic acids, and cells.

Due to its ability to form inverted hexagonal phase, DOPE is believed to impart fusogenicity to lipoplexes, thus facilitating fusion followed by destabilization of the endosomal membrane, lipoplex escape from the endosomes, and eventually the DNA release. Indeed, inclusion of DOPE into lipoplexes was shown to enhance considerably the transfection activity of some of the cationic lipid carriers [35, 120, 121]. For example, formulations of oxypropyl quaternary ammonium cationic lipids with 50 mol% DOPE have been reported to exhibit 2–5 times higher transfection activity in COS7 cells than formulations with pure cationic lipid (Fig. 29) [35]. Recently, a triple-bond dialkynoyl analog of DOPE has been

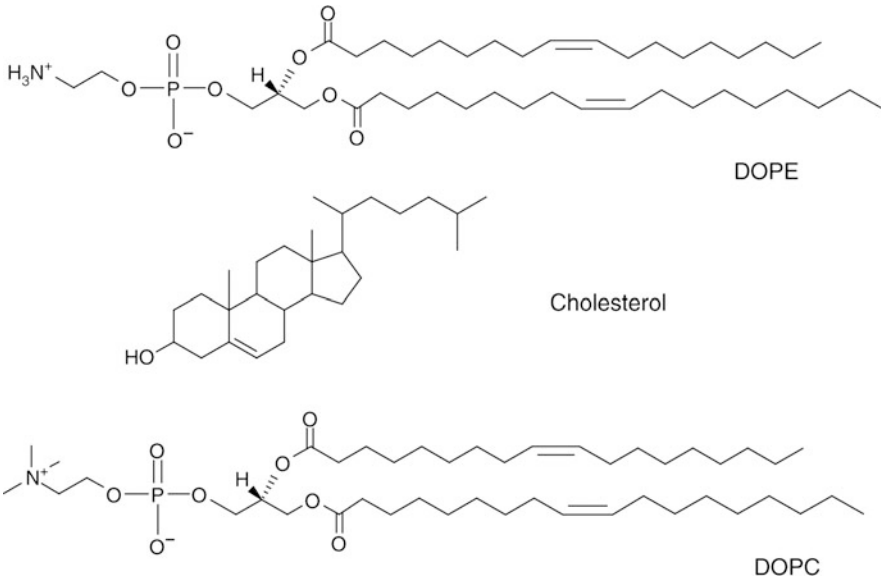

Fig. 28 Structures of the most common helper lipids

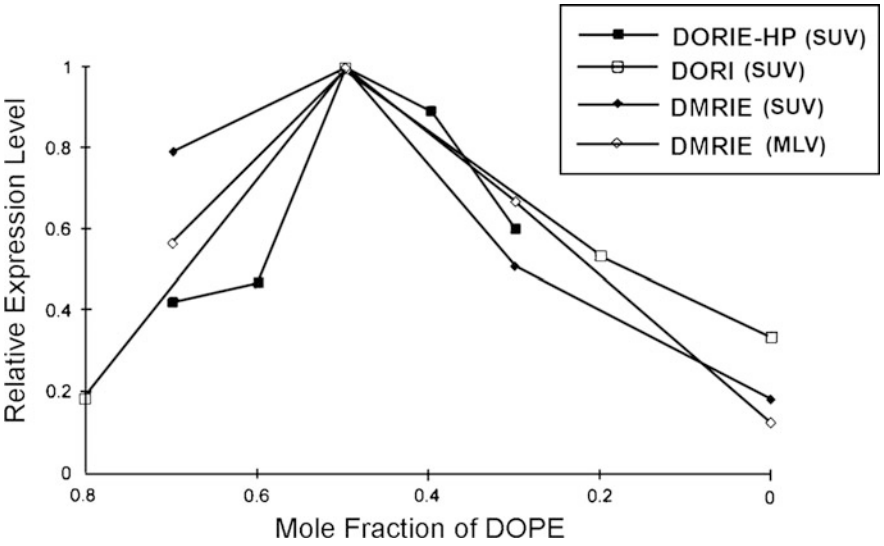

Fig. 29 Optimum mole fraction of 0.5 for the helper DOPE in cationic lipid transfection formulations (reproduced from [35]; copyright by the American Society for Biochemistry and Molecular Biology)

suggested as helper lipid, in an effort to reduce the mol fraction of cationic lipid in lipoplexes without impairing the overall transfection efficiency [122].

Cholesterol has also been employed as a colipid due to its ability to modify bilayer fluidity. Inclusion of cholesterol results in the formation of more stable but less efficient in vitro complexes than those containing DOPE. In contrast, addition of cholesterol results in very active complexes for in vivo administration [123–127].

DOPC and other PCs are also used as helper lipids, mainly for dilution of the membrane surface charge.

The helper effects of DOPE and cholesterol appear to be hydrocarbon chain-specific. This is demonstrated in studies of their mixtures with a series of alkyl acyl carnitine esters (alkyl 3-acyloxy-4-trimethylammonium butyrate chloride) tested with CV-1 cell culture (monkey fibroblast) [127]. The influence of the aliphatic chain length (n = 12–18) on transfection in vitro was determined using cationic liposomes prepared from these lipids and their mixtures with the helper lipids DOPE and cholesterol (Fig. 30). Both helper lipids provided for significant transfection enhancements in an apparently chain-specific manner, with the highest effects found for short-chain lipids with diC12:0 and diC14:0 chains in 1:1 mixtures with the respective helper lipid.

A chain-specific helper lipid effect can also be claimed for a series of trimethylammoniumpropane (TAP) cationic derivatives [128]. In the absence of helper lipids, the mixed-chain C12:0/C16:0 compound exhibited superior efficiency.

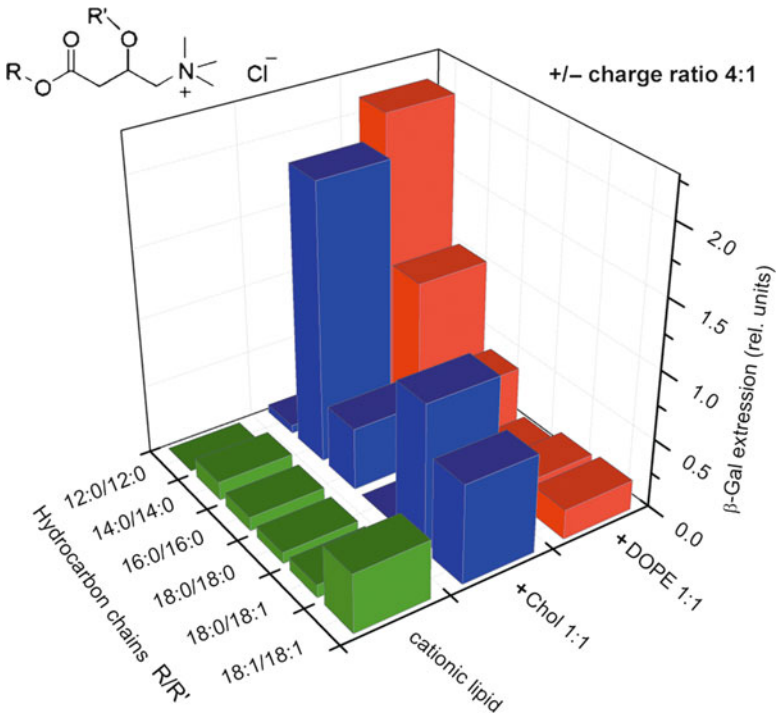

Fig. 30 Transfection activity of lipoplexes consisting of alkyl/acyl carnitine esters, alone and with helper lipid (DOPE or cholesterol), on β-galactosidase expression in CV-1 cell culture (monkey fibroblast); cationic lipid/DNA charge ratio 4:1 [127]

However, in 1:1 mixtures with cholesterol and DOPE, the diC14:0 and diC16:0 lipids were the top performers (Fig. 31).

7.2 PEG–Lipid Conjugates

Lipid moieties coupled to polyethylene glycol (PEG) have been used to increase the blood circulation time of lipoplexes (Fig. 32). The PEG–lipid conjugates such as DOPE–PEG, Chol–PEG, ceramides–PEG and their derivatives are then coformulated with the cationic lipid, helper lipid, and DNA. This results in coating the surface of the lipoplexes with PEG and preventing undesired association with plasma proteins or circulating cells (stealth liposomes). Recently, α-tocopheryl PEG-succinate (TPGS) was also used in gene delivery formulations because of its ability to confer not only a stealth property but also antioxidant and absorption enhancer properties [129].

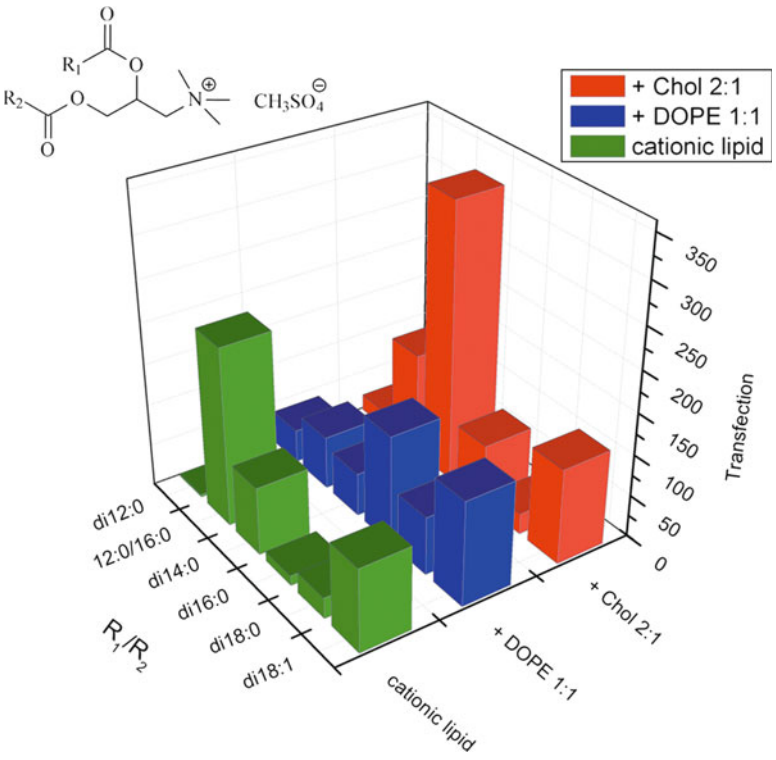

Fig. 31 Chain-specific effects of the helper lipids DOPE and cholesterol on the transfection activity of lipoplexes comprising TAP lipids with different hydrocarbon chains for COS-7 cells at cationic lipid/DNA charge ratio 2.5:1. Transfection activity was expressed as rel. units per μg of cellular protein [128]

7.3 Cationic Lipid Mixtures

Systematic transfection studies carried out on binary mixtures of cationic lipids have shown that, in general, the activities of the mixtures do not follow a superposition principle and several of them have been found to exhibit activities, which considerably exceed the activities of the individual lipids. On this basis, cationic lipid mixing has been suggested as an attractive strategy for fine tuning the lipoplex properties and enhancing their transfection potency [130]. Particularly strong synergy was observed with the combination of dilauroyl and dioleoyl ethylphosphatidylcholines (EDLPC/EDOPC). At the optimal EDLPC/EDOPC 60:40 composition, this mixture transfected more than 30-fold more efficiently than either component separately (Fig. 33) [131]. Both EDLPC/EDOPC dispersions and their lipoplexes formed lamellar arrays at all compositions and no correlations were found between structural parameters and transfection activity of these phases. However, upon mixing with anionic lipids, progressions of nonlamellar phases were formed, similar to those

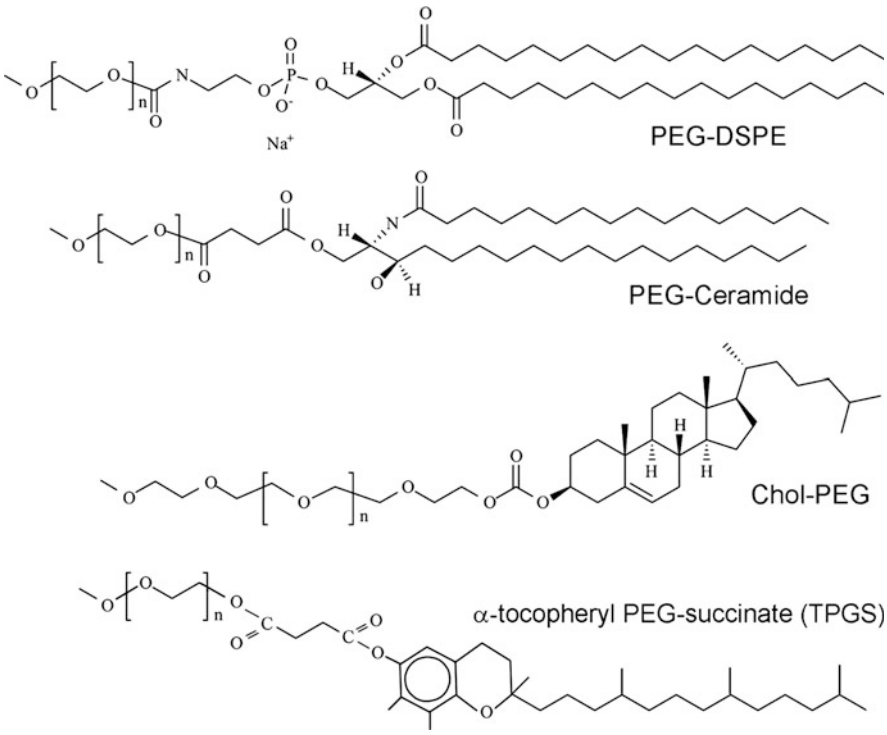

Fig. 32 Commonly used PEG–lipid conjugates

described above for anionic lipid mixtures with EDOPC, with curvatures well-correlated with the transfection activity of the EDLPC/EDOPC binaries. The composition with highest transfection, EDLPC/EDOPC 60:40, formed the inverted micellar cubic phase, Fd3m, in mixtures with cardiolipin, DOPG, and DOPS, while compositions of lower transfection formed nonlamellar phases of less negative curvatures such as inverted hexagonal or bilayer cubic.

Cationic lipid mixtures exhibiting solid–liquid crystalline phase transitions provide another example of mixtures displaying higher transfection activity than the separate components. By juxtaposing their temperature–composition phase diagrams with their transfection activity, it was found for all five mixtures studied that the compositions of maximum activity resided within the solid–liquid crystalline two-phase coexistence regions at physiological temperature [132]. The transfection efficacy of formulations exhibiting solid–liquid crystalline phase coexistence exceeded more than five times that of the gel (solid) phase formulations, and more than twice that of the liquid crystalline formulations. The EDMC/EDPPC and diC14DAB/diC18DAB mixtures in Fig. 34 exemplify this type of behavior [132]. Such a relationship between delivery activity and physical property can be rationalized based on known features of the lipid phase transitions; namely, accumulation of defects and increased disorder at the solid–liquid crystalline phase

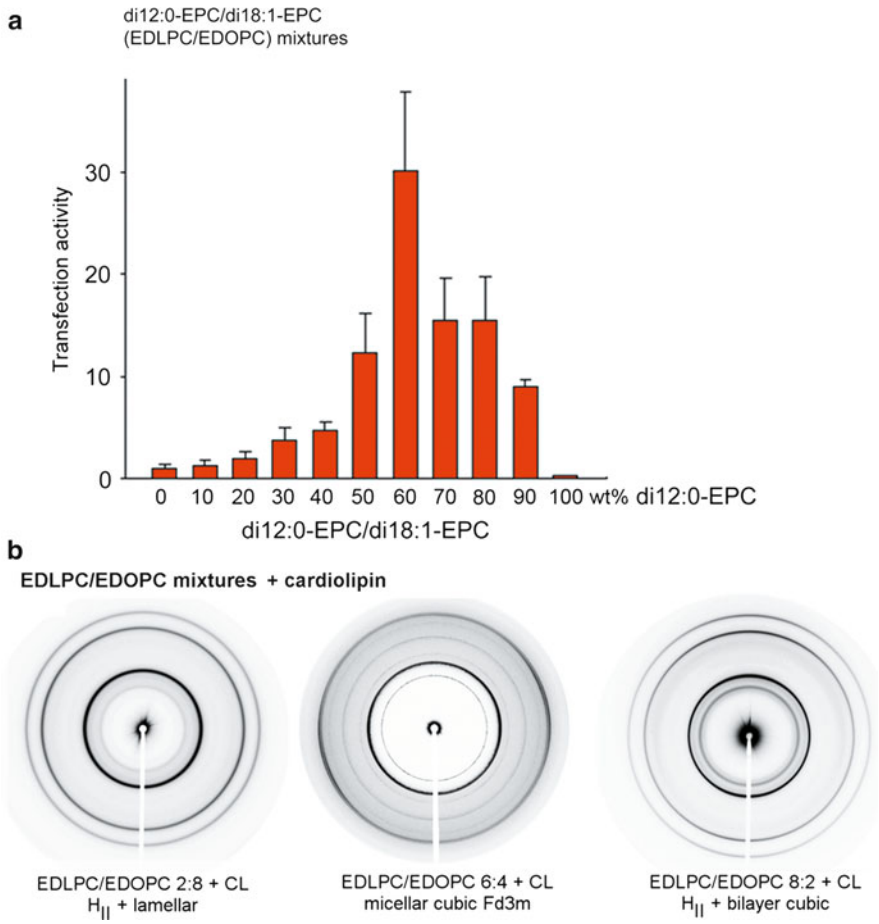

Fig. 33 (**a**) Transfection activity of EDLPC/EDOPC formulations. (**b**) Diffraction patterns of cardiolipin mixtures with EDLPC/EDOPC dispersions of different composition (reproduced with permission from [131]; copyright (2005) American Chemical Society)

boundaries could be responsible for the enhanced fusogenicity of the lipoplexes. This study shows that choosing carrier compositions such that their melting phase transition takes place at physiological temperature can significantly enhance their delivery efficacy.

7.4 Other Components

Addition of polyelectrolyte DNA-condensing agents such as polyethyleneimine, polylysine, protamine sulfate, etc., before the addition of cationic lipids has become a widely accepted practice in an effort to stabilize and optimize lipoplexes performance

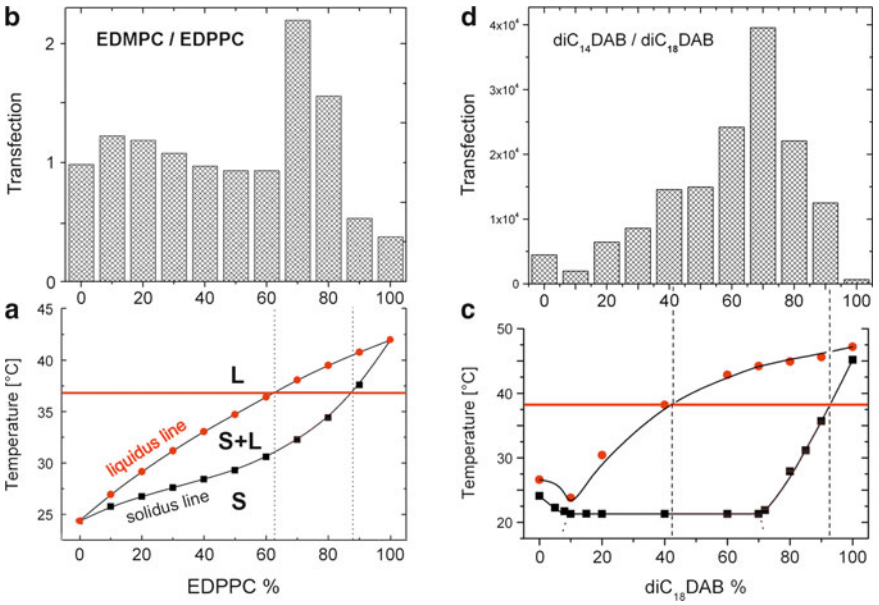

Fig. 34 Enhanced transfection in the gel–liquid crystal coexistence region. Phase diagrams of EDMPC/EDPPC (**a**) and diC14DAB/diC18DAB (**c**) mixtures. Transfection activities of the EDMPC/EDPPC (**b**) and diC14DAB/diC18DAB (**d**) formulations. (reproduced with permission from [132]; copyright (2007) American Chemical Society)

[79, 133]. Such complex particles are typically characterized with highly improved activity [80].

8 Conclusions

1. The transfection efficiency of cationic lipids displays a well-expressed dependence on the lipid hydrocarbon chain structure. Lipids with chain length of about 14 carbon atoms are generally the most effective.
2. Chain unsaturation strongly modifies transfection. Cationic lipids with monounsaturated chains exhibit much higher activity relative to their saturated counterparts. For example, maximum transfection with the cationic ethylphosphatidylcholines was found for the compounds with two monounsaturated 14:1 chains.
3. Compounds with *trans*-unsaturated chains are generally more efficient than compounds with *cis*-unsaturated chains.
4. Cationic PCs of high and low-transfection can be discriminated only on the basis of their interactions with membrane lipids. There appears to exist no correlation between lipoplex phase behavior and transfection activity. However, there is a distinct, well-expressed correlation between transfection activity and the way

cationic PCs modulate the nonlamellar phase conversions in membrane lipids. The hydrocarbon chain structures of high-transfection cationic PCs promote formation of inverted cubic phases replacing the H_{II} phase in membrane lipids. This may be considered as an indication that higher activity results from enhanced lipoplex fusion with cellular membranes.

5. Cellular anionic lipids have a twofold effect on DNA release from the lipoplexes. They compensate the cationic lipid surface charge and eliminate the electrostatically driven DNA binding to the membrane interface, and they also disrupt the lipoplex structure and facilitate DNA departure into the solution by inducing formation of nonlamellar phases upon mixing with the lipoplex lipids.

Acknowledgments The present work was supported by NSF grant EEC-0425626 and in part by NIH grant CA119341.

References

1. Venter JC, Adams MD, Myers EW et al (2001) The sequence of the human genome. Science 291:1304–1351
2. Flotte TR (2007) Gene therapy: the first two decades and the current state-of-the-art. J Cell Physiol 213:301–305
3. Giacca M (2007) Virus-mediated gene transfer to induce therapeutic angiogenesis: where do we stand? Int J Nanomedicine 2:527–540
4. Hendrie PC, Russell DW (2005) Gene targeting with viral vectors. Mol Ther 12:9–17
5. Felgner PL, Ringold GM (1989) Cationic liposome-mediated transfection. Nature 337:387–388
6. Gao X, Huang L (1991) A novel cationic liposome reagent for efficient transfection of mammalian cells. Biochem Biophys Res Commun 179:280–285
7. Leventis R, Silvius JR (1990) Interactions of mammalian cells with lipid dispersions containing novel metabolizable cationic amphiphiles. Biochim Biophys Acta 1023:124–132
8. Gaucheron J, Wong T, Wong EF et al (2002) Synthesis and properties of novel tetraalkyl cationic lipids. Bioconjug Chem 13:671–675
9. Ghosh YK, Visweswariah SS, Bhattacharya S (2002) Advantage of the ether linkage between the positive charge and the cholesteryl skeleton in cholesterol-based amphiphiles as vectors for gene delivery. Bioconjug Chem 13:378–384
10. Jaaskelainen I, Sternberg B, Monkkonen J et al (1998) Physicochemical and morphological properties of complexes made of cationic liposomes and oligonucleotides. Int J Pharm 167:191–203
11. Lobo BA, Vetro JA, Suich DM et al (2003) Structure/function analysis of peptoid/lipitoid: DNA complexes. J Pharm Sci 92:1905–1918
12. Niculescu-Duvaz D, Heyes J, Springer CJ (2003) Structure–activity relationship in cationic lipid mediated gene transfection. Curr Med Chem 10:1233–1261
13. Song YK, Liu F, Chu SY et al (1997) Characterization of cationic liposome-mediated gene transfer in vivo by intravenous administration. Human Gene Ther 8:1585–1594
14. Subramanian M, Holopainen JM, Paukku T et al (2000) Characterisation of three novel cationic lipids as liposomal complexes with DNA. Biochim Biophys Acta-Biomembranes 1466:289–305
15. Pinnaduwage P, Schmitt L, Huang L (1989) Use of a quaternary ammonium detergent in liposome mediated DNA transfection of mouse L-cells. Biochim Biophys Acta 985:33–37

16. MacDonald RC, Ashley GW, Shida MM et al (1999) Physical and biological properties of cationic triesters of phosphatidylcholine. Biophys J 77:2612–2629
17. MacDonald RC, Rakhmanova VA, Choi KL et al (1999) *O*-Ethylphosphatidylcholine: a metabolizable cationic phospholipid which is a serum-compatible DNA transfection agent. J Pharm Sci 88:896–904
18. Solodin I, Brown CS, Heath TD (1996) Synthesis of phosphotriester cationic phospholipids. Cationic lipids 2. Synlett 5:457–458
19. Koynova R, MacDonald RC (2003) Cationic *O*-ethylphosphatidylcholines and their lipoplexes: phase behavior aspects, structural organization and morphology. Biochim Biophys Acta-Biomembranes 1613:39–48
20. Koynova R, Wang L, MacDonald RC (2008) Cationic phospholipids forming cubic phases: lipoplex structure and transfection efficiency. Mol Pharm 5:739–744
21. Wang L, Koynova R, Parikh H et al (2006) Transfection activity of binary mixtures of cationic *O*-substituted phosphatidylcholine derivatives: the hydrophobic core strongly modulates their physical properties and DNA delivery efficacy. Biophys J 91:3692–3706
22. Lewis RNAH, Winter I, Kriechbaum M et al (2001) Studies of the structure and organization of cationic lipid bilayer membranes: calorimetric, spectroscopic, and x-ray diffraction studies of linear saturated P-O-ethyl phosphatidylcholines. Biophys J 80:1329–1342
23. Winter I, Pabst G, Rappolt M et al (2001) Refined structure of 1, 2-diacyl-P-O-ethylphosphatidylcholine bilayer membranes. Chem Phys Lipids 112:137–150
24. Rakhmanova VA, McIntosh TJ, MacDonald RC (2000) Effects of dioleoylphosphatidylethanolamine on the activity and structure of *O*-alkyl phosphatidylcholine-DNA transfection complexes. Cell Mol Biol Lett 5:51–65
25. Rosenzweig HS, Rakhmanova VA, McIntosh TJ et al (2000) *O*-Alkyl dioleoylphosphatidylcholinium compounds: the effect of varying alkyl chain length on their physical properties and in vitro DNA transfection activity. Bioconjug Chem 11:306–313
26. Koynova R, Tenchov B, Wang L et al (2009) Hydrophobic moiety of cationic lipids strongly modulates their transfection activity. Mol Pharm 6:951–958
27. Heyes JA, Niculescu-Duvaz D, Cooper RG et al (2002) Synthesis of novel cationic lipids: effect of structural modification on the efficiency of gene transfer. J Med Chem 45:99–114
28. Karmali PP, Chaudhuri A (2007) Cationic liposomes as non-viral carriers of gene medicines: resolved issues, open questions, and future promises. Med Res Rev 27:696–722
29. Karmali PP, Kumar VV, Chaudhuri A (2004) Design, syntheses and in vitro gene delivery efficacies of novel mono-, di- and trilysinated cationic lipids: a structure-activity investigation. J Med Chem 47:2123–2132
30. Floch V, Loisel S, Guenin E et al (2000) Cation substitution in cationic phosphonolipids: a new concept to improve transfection activity and decrease cellular toxicity. J Med Chem 43:4617–4628
31. Behr JP, Demeneix B, Loeffler JP et al (1989) Efficient gene-transfer into mammalian primary endocrine-cells with lipopolyamine-coated DNA. Proc Natl Acad Sci USA 86:6982–6986
32. Ferrari ME, Nguyen CM, Zelphati O et al (1998) Analytical methods for the characterization of cationic lipid nucleic acid complexes. Hum Gene Ther 9:341–351
33. de Lima MCP, Neves S, Filipe A et al (2003) Cationic liposomes for gene delivery: from biophysics to biological applications. Curr Med Chem 10:1221–1231
34. Wheeler CJ, Felgner PL, Tsai YJ et al (1996) A novel cationic lipid greatly enhances plasmid DNA delivery and expression in mouse lung. Proc Natl Acad Sci USA 93:11454–11459
35. Felgner JH, Kumar R, Sridhar CN et al (1994) Enhanced gene delivery and mechanism studies with a novel series of cationic lipid formulations. J Biol Chem 269:2550–2561
36. Lee ER, Marshall J, Siegel CS et al (1996) Detailed analysis of structures and formulations of cationic lipids for efficient gene transfer to the lung. Hum Gene Ther 7:1701–1717
37. Kearns MD, Donkor AM, Savva M (2008) Structure-transfection activity studies of nove cationic cholesterol-based amphiphiles. Mol Pharm 5:128–139

38. Bajaj A, Mishra SK, Kondaiah P et al (2008) Effect of the headgroup variation on the gene transfer properties of cholesterol based cationic lipids possessing ether linkage. Biochim Biophys Acta-Biomembranes 1778:1222–1236
39. Soltan MK, Ghonaim HM, El Sadek M et al (2009) Design and synthesis of N-4, N-9-disubstituted spermines for non-viral siRNA delivery – structure–activity relationship studies of transfection efficiency versus toxicity. Pharm Res 26:286–295
40. Ghosh YK, Visweswariah SS, Bhattacharya S (2000) Nature of linkage between the cationic headgroup and cholesteryl skeleton controls gene transfection efficiency. FEBS Lett 473:341–344
41. Rajesh M, Sen J, Srujan M et al (2007) Dramatic influence of the orientation of linker between hydrophilic and hydrophobic lipid moiety in liposomal gene delivery. J Am Chem Soc 129:11408–11420
42. Ghosh YK, Visweswariah SS, Bhattacharya S (2002) Advantage of the ether linkage between the positive charge and the cholesteryl skeleton in cholesterol-based amphiphiles as vectors for gene delivery. Bioconjug Chem 13:378–384
43. Obata Y, Saito S, Takeda N et al (2009) Plasmid DNA-encapsulating liposomes: effect of a spacer between the cationic head group and hydrophobic moieties of the lipids on gene expression efficiency. Biochim Biophys Acta-Biomembranes 1788:1148–1158
44. Horobin RW, Weissig V (2005) A QSAR-modeling perspective on cationic transfection lipids. 1. Predicting efficiency and understanding mechanisms. J Gene Med 7:1023–1034
45. Liu D, Qiao D, Li Z et al (2008) Structure–function relationship research of glycerol backbone-based cationic lipids for gene delivery. Chem Biol Drug Des 71:336–344
46. Koynova R, Tenchov B (2009) Cationic phospholipids – structure/transfection activity relationships. Soft Matter 5:3187–3200
47. Tenchov BG, Wang L, Koynova R et al (2008) Modulation of a membrane lipid lamellar–nonlamellar phase transition by cationic lipids: a measure for transfection efficiency. Biochim Biophys Acta-Biomembranes 1778:2405–2412
48. Das A, Niven R (2001) Use of perfluorocarbon (Fluorinert) to enhance reporter gene expression following intratracheal instillation into the lungs of Balb/c mice: implications for nebulized delivery of plasmids. J Pharm Sci 90:1336–1344
49. Faneca H, Cabrita AS, Simoes S et al (2007) Evaluation of the antitumoral effect mediated by IL-12 and HSV-tk genes when delivered by a novel lipid-based system. Biochim Biophys Acta-Biomembranes 1768:1093–1102
50. Faneca H, Faustino A, de Lima MCP (2008) Synergistic antitumoral effect of vinblastine and HSV-Tk/GCV gene therapy mediated by albumin-associated cationic liposomes. J Control Release 126:175–184
51. Faneca H, Simoes S, de Lima MCP (2004) Association of albumin or protamine to lipoplexes: enhancement of transfection and resistance to serum. J Gene Med 6:681–692
52. Gorman CM, Aikawa M, Fox B et al (1997) Efficient in vivo delivery of DNA to pulmonary cells using the novel lipid EDMPC. Gene Ther 4:983–992
53. McDonald RJ, Liggitt HD, Roche L et al (1998) Aerosol delivery of lipid: DNA complexes to lungs of rhesus monkeys. Pharm Res 15:671–679
54. Noone PG, Hohneker KW, Zhou ZQ et al (2000) Safety and biological efficacy of a lipid–CFTR complex for gene transfer in the nasal epithelium of adult patients with cystic fibrosis. Mol Ther 1:105–114
55. Hyvonen Z, Plotniece A, Riene I et al (2000) Novel cationic amphiphilic 1,4-dihydropyridine derivatives for DNA delivery. Biochim Biophys Acta-Biomembranes 1509:451–466
56. Yingyongnarongkul BE, Radchatawedchakoon W, Krajarng A et al (2009) High transfection efficiency and low toxicity cationic lipids with aminoglycerol-diamine conjugate. Bioorg Med Chem 17:176–188
57. Zhu L, Lu Y, Miller DD et al (2008) Structural and formulation factors influencing pyridinium lipid-based gene transfer. Bioconjug Chem 19:2499–2512

58. VanDerWoude I, Wagenaar A, Meekel AAP et al (1997) Novel pyridinium surfactants for efficient, nontoxic in vitro gene delivery. Proc Natl Acad Sci USA 94:1160–1165
59. Heyes J, Palmer L, Bremner K et al (2005) Cationic lipid saturation influences intracellular delivery of encapsulated nucleic acids. J Control Release 107:276–287
60. Aberle AM, Bennett MJ, Malone RW et al (1996) The counterion influence on cationic lipid-mediated transfection of plasmid DNA. Biochim Biophys Acta-Lipids Lipid Metabolism 1299:281–283
61. Koynova R, Brankov J, Tenchov B (1997) Modulation of lipid phase behavior by kosmotropic and chaotropic solutes – experiment and thermodynamic theory. Eur Biophys J Biophys Lett 25:261–274
62. Boukhnikachvili T, AguerreChariol O, Airiau M et al (1997) Structure of in-serum transfecting DNA-cationic lipid complexes. FEBS Lett 409:188–194
63. Lasic DD, Strey H, Stuart MCA et al (1997) The structure of DNA–liposome complexes. J Am Chem Soc 119:832–833
64. Radler JO, Koltover I, Salditt T et al (1997) Structure of DNA-cationic liposome complexes: DNA intercalation in multilamellar membranes in distinct interhelical packing regimes. Science 275:810–814
65. Bruinsma R (1998) Electrostatics of DNA cationic lipid complexes: isoelectric instability. Eur Phys J B 4:75–88
66. Hirsch-Lerner D, Barenholz Y (1999) Hydration of lipoplexes commonly used in gene delivery: follow-up by laurdan fluorescence changes and quantification by differential scanning calorimetry. Biochim Biophys Acta-Biomembranes 1461:47–57
67. Kennedy MT, Pozharski EV, Rakhmanova VA et al (2000) Factors governing the assembly of cationic phospholipid–DNA complexes. Biophys J 78:1620–1633
68. Pozharski EV, MacDonald RC (2007) Single lipoplex study of cationic lipoid-DNA, self-assembled complexes. Mol Pharm 4:962–974
69. Koynova R, MacDonald RC (2007) Natural lipid extracts and biomembrane-mimicking lipid compositions are disposed to form nonlamellar phases, and they release DNA from lipoplexes most efficiently. Biochim Biophys Acta-Biomembranes 1768:2373–2382
70. Zelphati O, Nguyen C, Ferrari M et al (1998) Stable and monodisperse lipoplex formulations for gene delivery. Gene Ther 5:1272–1282
71. Takeuchi K, Ishihara M, Kawaura C et al (1996) Effect of zeta potential of cationic liposomes containing cationic cholesterol derivatives on gene transfection. FEBS Lett 397:207–209
72. Almofti MR, Harashima H, Shinohara Y et al (2003) Lipoplex size determines lipofection efficiency with or without serum. Mol Membr Biol 20:35–43
73. Ross PC, Hui SW (1999) Lipoplex size is a major determinant of in vitro lipofection efficiency. Gene Ther 6:651–659
74. Zhang JS, Huang L (2003) Cationic liposome–protamine–DNA complexes for gene delivery. Methods Enzymol 373:332–342
75. Rejman J, Oberle V, Zuhorn IS et al (2004) Size-dependent internalization of particles via the pathways of clathrin-and caveolae-mediated endocytosis. Biochem J 377:159–169
76. Hoekstra D, Rejman J, Wasungu L et al (2007) Gene delivery by cationic lipids: in and out of an endosome. Biochem Soc Trans 35:68–71
77. Lechardeur D, Verkman AS, Lukacs GL (2005) Intracellular routing of plasmid DNA during non-viral gene transfer. Adv Drug Deliv Rev 57:755–767
78. Prasad TK, Rangaraj N, Rao NM (2005) Quantitative aspects of endocytic activity in lipid-mediated transfections. FEBS Lett 579:2635–2642
79. Elouahabi A, Ruysschaert JM (2005) Formation and intracellular trafficking of lipoplexes and polyplexes. Mol Ther 11:336–347
80. Tyagi P, Wu PC, Chancellor M et al (2006) Recent advances in intravesical drug/gene delivery. Mol Pharm 3:369–379

81. Koynova R, Tarahovsky Y, Wang L et al (2007) Lipoplex formulation of superior efficacy exhibits high surface activity and fusogenicity, and readily releases DNA. Biochim Biophys Acta-Biomembranes 1768:375–386
82. Salditt T, Koltover I, Radler JO et al (1997) Two-dimensional smectic ordering of linear DNA chains in self-assembled DNA–cationic liposome mixtures. Phys Rev Lett 79:2582–2585
83. Artzner F, Zantl R, Rapp G et al (1998) Observation of a rectangular columnar phase in condensed lamellar cationic lipid–DNA complexes. Phys Rev Lett 81:5015–5018
84. Koynova R, MacDonald RC (2004) Columnar DNA superlattices in lamellar *o*-ethylphosphatidylcholine lipoplexes: mechanism of the gel-liquid crystalline lipid phase transition. Nano Lett 4:1475–1479
85. Congiu A, Pozzi D, Esposito C et al (2004) Correlation between structure and transfection efficiency: a study of DC-Chol-DOPE/DNA complexes. Coll Surf B Biointerfaces 36:43–48
86. Koltover I, Salditt T, Radler JO et al (1998) An inverted hexagonal phase of cationic liposome–DNA complexes related to DNA release and delivery. Science 281:78–81
87. Smisterova J, Wagenaar A, Stuart MCA et al (2001) Molecular shape of the cationic lipid controls the structure of cationic lipid/dioleylphosphatidylethanolamine-DNA complexes and the efficiency of gene delivery. J Biol Chem 276:47615–47622
88. Francescangeli O, Pisani M, Stanic V et al (2004) Evidence of an inverted hexagonal phase in self-assembled phospholipid-DNA-metal complexes. Europhys Lett 67:669–675
89. Caracciolo G, Caminiti R (2005) Do DC-Chol/DOPE-DNA complexes really form an inverted hexagonal phase? Chem Phys Lett 411:327–332
90. Caracciolo G, Pozzi D, Caminiti R et al (2003) Structural characterization of a new lipid/DNA complex showing a selective transfection efficiency in ovarian cancer cells. Eur Phys J E 10:331–336
91. Lin AJ, Slack NL, Ahmad A et al (2003) Three-dimensional imaging of lipid gene-carriers: membrane charge density controls universal transfection behavior in lamellar cationic liposome–DNA complexes. Biophys J 84:3307–3316
92. Ross PC, Hensen ML, Supabphol R et al (1998) Multilamellar cationic liposomes are efficient vectors for in vitro gene transfer in serum. J Liposome Res 8:499–520
93. Simberg D, Danino D, Talmon Y et al (2003) Phase behavior, DNA ordering and size instability of cationic lipoplexes: relevance to optimal transfection activity. J Liposome Res 13:86–87
94. Legendre JY, Szoka FC (1992) Delivery of plasmid DNA into mammalian-cell lines using Ph-sensitive liposomes – comparison with cationic liposomes. Pharm Res 9:1235–1242
95. Zabner J, Fasbender AJ, Moninger T et al (1995) Cellular and molecular barriers to gene-transfer by a cationic lipid. J Biol Chem 270:18997–19007
96. Zhou XH, Huang L (1994) DNA transfection mediated by cationic liposomes containing lipopolylysine – characterization and mechanism of action. Biochim Biophys Acta-Biomembranes 1189:195–203
97. Ashley GW, Shida MM, Qiu R et al (1996) Phosphatidylcholinium compounds: a new class of cationic phospholipids with transfection activin and unusual physical properties (abstract). Biophys J 70:88-A
98. Tarahovsky YS, Koynova R, MacDonald RC (2004) DNA release from lipoplexes by anionic lipids: correlation with lipid mesomorphism, interfacial curvature, and membrane fusion. Biophys J 87:1054–1064
99. Xu YH, Szoka FC (1996) Mechanism of DNA release from cationic liposome/DNA complexes used in cell transfection. Biochemistry 35:5616–5623
100. Zelphati O, Szoka FC (1996) Mechanism of oligonucleotide release from cationic liposomes. Proc Natl Acad Sci USA 93:11493–11498
101. Koynova R, Tenchov B (2009) Phase transitions of lipids. In: Begley TP (ed) Wiley encyclopedia of chemical biology. Wiley, Hoboken, NJ, pp 601–615

102. Seddon JM, Templer RH (1995) Polymorphism of lipid–water systems. In: Lipowsky R, Sackmann E (eds) Handbook of biological physics. Elsevier Science, Amsterdam, pp 97–160
103. Hafez IM, Maurer N, Cullis PR (2001) On the mechanism whereby cationic lipids promote intracellular delivery of polynucleic acids. Gene Ther 8:1188–1196
104. Koynova R, MacDonald RC (2003) Mixtures of cationic lipid *O*-ethylphosphatidylcholine with membrane lipids and DNA: phase diagrams. Biophys J 85:2449–2465
105. Lewis RNAH, McElhaney RN (2000) Surface charge markedly attenuates the nonlamellar phase-forming propensities of lipid bilayer membranes: calorimetric and P-31-nuclear magnetic resonance studies of mixtures of cationic, anionic, and zwitterionic lipids. Biophys J 79:1455–1464
106. Tarahovsky YS, Arsenault AL, MacDonald RC et al (2000) Electrostatic control of phospholipid polymorphism. Biophys J 79:3193–3200
107. Kleinschmidt JH, Tamm LK (2002) Structural transitions in short-chain lipid assemblies studied by P-31-NMR spectroscopy. Biophys J 83:994–1003
108. Koynova R, MacDonald RC (2005) Lipid transfer between cationic vesicles and lipid-DNA lipoplexes. Effect of serum. Biochim Biophys Acta-Biomembranes 1714:63–70
109. Simoes S, Pires P, Duzgunes N et al (1999) Cationic liposomes as gene transfer vectors: barriers to successful application in gene therapy. Curr Opin Mol Ther 1:147–157
110. Sen GL, Blau HM (2005) Argonaute 2/RISC resides in sites of mammalian mRNA decay known as cytoplasmic bodies. Nat Cell Biol 7:633–636
111. Lu JJ, Langer R, Chen JZ (2009) A novel mechanism is involved in cationic lipid-mediated functional siRNA delivery. Mol Pharm 6:763–771
112. Koynova R, Wang L, MacDonald RC (2006) An intracellular lamellar – nonlamellar phase transition rationalizes the superior performance of some cationic lipid transfection agents. Proc Natl Acad Sci USA 103:14373–14378
113. Lipid Data Bank (2000) http://www.lipidat.ul.ie/
114. Anderson DM, Gruner SM, Leibler S (1988) Geometrical aspects of the frustration in the cubic phases of lyotropic liquid-crystals. Proc Natl Acad Sci USA 85:5364–5368
115. Shearman GC, Ces O, Templer RH et al (2006) Inverse lyotropic phases of lipids and membrane curvature. J Phys Condens Matter 18:S1105–S1124
116. Templer RH, Seddon JM, Duesing PM et al (1998) Modeling the phase behavior of the inverse hexagonal and inverse bicontinuous cubic phases in 2:1 fatty acid phosphatidylcholine mixtures. J Phys Chem B 102:7262–7271
117. Siegel DP (2005) Bicontinuous Liquid Crystals. In: Lynch ML, Spicer PT (eds) Bicontinuous liquid crystals. Taylor & Francis Group, CRC Press, Boca Raton, pp 59–98, Chap 4
118. Siegel DP, Epand RM (1997) The mechanism of lamellar-to-inverted hexagonal phase transitions in phosphatidylethanolamine: implications for membrane fusion mechanisms. Biophys J 73:3089–3111
119. Yang L, Huang HW (2002) Observation of a membrane fusion intermediate structure. Science 297:1877–1879
120. Farhood H, Serbina N, Huang L (1995) The role of dioleoyl phosphatidylethanolamine in cationic liposome-mediated gene-transfer. Biochim Biophys Acta-Biomembranes 1235:289–295
121. Zuhorn IS, Oberle V, Visser WH et al (2002) Phase behavior of cationic amphiphiles and their mixtures with helper lipid influences lipoplex shape, DNA translocation, and transfection efficiency. Biophys J 83:2096–2108
122. Fletcher S, Ahmad A, Price WS et al (2008) Biophysical properties of CDAN/DOPE-analogue lipoplexes account for enhanced gene delivery. Chembiochem 9:455–463
123. Hong KL, Zheng WW, Baker A et al (1997) Stabilization of cationic liposome–plasmid DNA complexes by polyamines and poly(ethylene glycol)-phospholipid conjugates for efficient in vivo gene delivery. FEBS Lett 400:233–237
124. Liu Y, Mounkes LC, Liggitt HD et al (1997) Factors influencing the efficiency of cationic liposome-mediated intravenous gene delivery. Nat Biotechnol 15:167–173

125. Smith JG, Wedeking T, Vernachio JH et al (1998) Characterization and in vivo testing of a heterogeneous cationic lipid–DNA formulation. Pharm Res 15:1356–1363
126. Sternberg B, Hong KL, Zheng WW et al (1998) Ultrastructural characterization of cationic liposome–DNA complexes showing enhanced stability in serum and high transfection activity in vivo. Biochim Biophys Acta-Biomembranes 1375:23–35
127. Wang JK, Guo X, Xu YH et al (1998) Synthesis and characterization of long chain alkyl acyl carnitine esters. Potentially biodegradable cationic lipids for use in gene delivery. J Med Chem 41:2207–2215
128. Regelin AE, Fankhaenel S, Gurtesch L et al (2000) Biophysical and lipofection studies of DOTAP analogs. Biochim Biophys Acta-Biomembranes 1464:151–164
129. Jiao J (2008) Polyoxyethylated nonionic surfactants and their applications in topical ocular drug delivery. Adv Drug Deliv Rev 60:1663–1673
130. Wang L, MacDonald RC (2004) New strategy for transfection: mixtures of medium-chain and long-chain cationic lipids synergistically enhance transfection. Gene Ther 11:1358–1362
131. Koynova R, Wang L, Tarahovsky Y et al (2005) Lipid phase control of DNA delivery. Bioconjug Chem 16:1335–1339
132. Koynova R, Wang L, MacDonald RC (2007) Synergy in lipofection by cationic lipid mixtures: superior activity at the gel–liquid crystalline phase transition. J Phys Chem B 111:7786–7795
133. Wagner E, Culmsee C, Boeckle S (2005) Targeting of polyplexes: toward synthetic virus vector systems. Adv Genet 53:333–354

Top Curr Chem (2010) 296: 95–129
DOI: 10.1007/128_2010_64

Published online: 10 June 2010

Hyperbranched Polyamines for Transfection

Wiebke Fischer, Marcelo Calderón, and Rainer Haag

Abstract The successful application of gene therapy through DNA transfection into the cell is still a great challenge in ongoing research. Hyperbranched polyamines are highly branched macromolecules, and have gained significant attention in the last two decades, due to their relative ease of preparation, their shape, and their multi-functionality.

This review deals with the syntheses of various hyperbranched polyamines that are prepared through a one-step polymerization process. Furthermore, we present the current status of polyamines as gene carriers and describe their versatility, and their properties such as structure-property dependency, gene transfection efficiency, and cytotoxicity profiles of hyperbranched polyamines.

Keywords Applications · Cytotoxicity profile · Gene delivery · Hyperbranched polyamines · Poly(amido amine) · Poly(amido ester) · Poly(ethylene imine) · Polyglycerol amines · Structure-property dependence · Synthesis · Transfection efficiency

Contents

W. Fischer, M. Calderón, and R. Haag (✉)
Institute of Chemistry and Biochemistry, Freie Universität Berlin, 14195 Berlin, Germany
e-mail: haag@chemie.fu-berlin.de

293T	Cell line
Å	Angström
A549	Cell line (carcinomic human alveolar basal epithelial cell)
AEPZ	1-(2-Aminoethyl) piperazine
AFM	Atomic force microscope
$AlCl_3$	Aluminum chloride
AMP	4-(Aminomethyl)piperidine
ATPase	Enzyme which catalyzes the degradation of adenosine triphosphate
B16F10	Cell line (murine melanoma cell)
BDDA	1,4-Butanediol diacrylate
bis-MPA	2,2-Bis-(methylol)propionic acid
bPEI-*g*-lPEG	Poly(ethyleneimine)-graft-poly(ethyleneglycol) copolymers
C2C12	Cell line (mouse myoblast cell)
C6	Rat glioma cell line
CBA	*N*,*N*′-Cystamine bisacrylamide
Cbz	Benzyl carbamate
CDC2	Cell line (cell division control protein 2)
$CHCl_3$	Chloroform
CHO-K1	Cell line (Chinese hamster ovary-K1)
COS-7	Cell line (African green monkey)
D	Dendritic unit
Da	Dalton
DB	Degree of branching
DEAPA	Diethylaminopropylamine
DETA	Diethylenetriamine
DMDPTA	*N*,*N*-Dimethylaminodipropylene-triamine
DNA	Deoxyribonucleic acid
dPG	Dendritic polyglycerols
DTT	Dithiothreitol
EGDA	Ethylene glycol diacrylate
EI	Ethylene imine
FA	Folic acid
G	Generation
g	Graft
GSH	Reduced glutathione
h	Hour
H_2	Hydrogen
HDDA	1,6-Hexanediol diacrylate
HEEI	*N*-(2-Hydroxyethyl) ethylene imine
HEK 293	Cell line (human embryonic kidney 293 cells)
HeLa	Cell line (Henrietta Lacks, immortal cell line)
HepG2	Cell line (human hepatocellular carcinoma)
HMBA	*N*,*N*′-Hexamethylene bisacrylamide

HMW	High molecular weight
HPAMAM	Hyperbranched PAMAM
HPB	Hyperbranched polymer
IC	Inhibitory concentration
kDa	Kilo Dalton
L	Linear unit
$LiAlH_4$	Lithium aluminum hydride
LMW	Low molecular weight
MA	Methyl acrylate
MAPK2	Cell line (mitogen-activated kinase 2)
MDD-MB-231	Cell line (breast cancer cells)
MEDA	*N*-Methylethylenediamine
MeOH	Methanol
Mn	Number average molecular weight
MTT	3-(4,5-Dimethylthiazol-2-yl)-2,5-diphenyltetrazolium bromide
MW	Molecular weight
MWD	Molecular weight distribution (Mw/Mn)
N/P ratio	Ratio of nitrogen versus phosphate
N2a	Cell line (Mouse neuroblastoma cells)
NIH/3T3	Cell line (House embryonic fibroblast)
NMR	Nuclear magnetic resonance
OH	Hydroxyl groups
PAMAM	Poly(amido amine)
Pd	Palladium
PD	Polydispersity
PEG	Poly(ethylene glycol)
pEGFP-C1	Plasmid (encodes a red-shifted variant of wild-type GFP)
PEG-PEI	PEGylated poly(ethylene imine)
PEI	Poly(ethylene imine)
PG	Polyglycerol
pGL3-Luc	Luciferase reporter vector
PG-PEHA	Polyglycerol pentaethylenhexamine carbamate
PG-Q-n	PG functionalized with quaternary amines
PG-T-n	PG functionalized with tertiary amines
PHE	Phenylalanine
PPI	Poly(propyl imine)
RHB	Reducible hyperbranched polymer
RNA	Ribonucleic acid
ROP	Ring opening polymerization
SCID	Severe combined immunodeficiency
SEC	Size exclusion chromatography
SIM MC 7721	Cell line (human normal hep-atocyte cells)
siRNA	Small interfering RNA
T	Terminal unit

TEM	Transmission electron microscopy
THF	Tetrahydrofuran
TMPTA	Trimethylol-propane triacrylate
XTT	Cell proliferation kit

1 Polyamines in Gene Delivery

In the last 20 years, gene therapy has drawn a lot of attention due to its potential for treating chronic diseases and genetic disorders, as well as an alternative method to traditional chemotherapy for cancer management [1–3]. Research has focused on designing an efficient and safe delivery system that transfects therapeutic genes to cells to allow them to produce their own therapeutic proteins in case of delivery of DNA, or to silence certain proteins in case of delivery of siRNA [4]. The goal is the development of systems which compact and protect gene fragments, simultaneously achieving a high transfection efficiency, prolonged gene expression/silencing, and low toxicity [5].

Recent research indicates that genes condensation is a prerequisite for transport through the cell membrane for gene therapy applications [6]. In principle, two basic carrier systems, viral and non-viral transfection agents for the delivery of oligonucleotides in target cells, are under development [7–9]. Viral gene therapy has a high efficacy, but is plagued by serious safety risks, production and manufacturing challenges, and other limitations like cargo space development [8]. In contrast, non-viral gene delivery usually requires condensation with positively charged cationic lipid or polymer based systems to enable binding of polyanionic complexes to plasma membrane and further internalization by the cells.

Non-viral gene delivery is frequently regarded as a potentially safer alternative to viral gene delivery. Although it addresses these challenges, it is often less effective and many polycations show high in vitro toxicity [10, 11]. A large variety of cationic compounds, including cationic lipids and cationic polymers, were shown to be able to compact and deliver nucleic acids into the cell efficiently and were therefore the best studied compounds [10, 12–17]. The interaction between a single protonated amine and the phosphate backbone of DNA is relatively weak and competes with salt binding under biological conditions. Therefore polyamines are used to achieve high gene affinity [18] with better gene transfer efficiency. The electrostatic interaction of polyamines with genes causes localized bending of the structure, which results in the collapse of the genes into rods, spheres, and toroids [19]. Furthermore, polycations induce membrane destabilization at acidic pH between protonated amines and the negatively charged membrane [20]. It has already been reported that the small size (less than 250 nm) of the compact gene/polymer complex is an optimal structural feature for an efficient endocytosis process and consequent gene transfer [21–23].

In general, polyamines have been reported to mediate an endosomal escape of polyplexes by the "proton sponge" effect [24–26], which is based on the fact that polyamines can buffer the endosomal vesicle. These so-called "proton-sponge" polymers contain a large number of secondary amines and exhibit pK_a values between physiological and lysosomal pH. After endocytosis the endosome is acidified by the ATPase enzyme that actively transports protons from the cytosol into the vesicle to reach pH 5–6. Nearly every third atom of these polymers is an amino nitrogen which can be protonated, and therefore these polymers undergo large changes in protonation during endocytic trafficking. The accumulation of protons in the vesicle must be balanced by an influx of counter ions. The increased ion concentration ultimately causes osmotic swelling and rupture of the endosome membranes, which releases the polyplexes into the cytosol [27–29]. The "proton sponge" effect results in a faster release of the DNA and thereby degradation of the nucleotide chain can be avoided. The general mechanism of polyamine mediated gene transfection is illustrated in Fig. 1.

From the structural point of view, polyamines used for gene transfection vary widely in their structures, which range between linear [24, 29–35], branched [12, 30, 32], hyperbranched, and perfect branched dendrimers [36]. In this chapter we present a general overview of the research reported so far using dendritic polyamines in gene delivery applications. Particular focus is made on hyperbranched

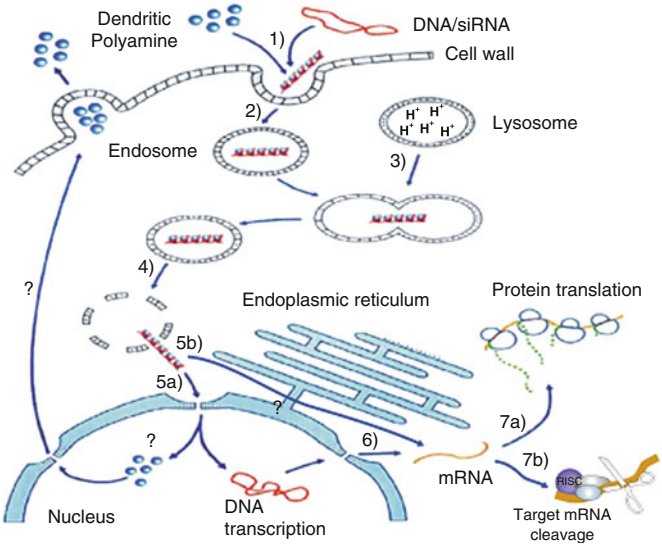

Fig. 1 Proposed mechanism of gene transfection [117]. (1) Formation of the DNA/polymer complex (polyplex), (2) endocytosis of the polyplex, (3) fusion of endosome and lysosome, (4) release of the polyplex into the cytosol, (5a) incorporation of the polyplex into the nucleus, (5b) release of the siRNA into the cytosol, (6) transcription of the DNA into mRNA followed by release of the polyamine back into the cytosol, (7a) translation of mRNA, and (7b) mRNA degradation. The metabolism of the polyamine is still unclear. Reproduced with permission from [117]. Copyright 2002 Elsevier

polymers, which emerged recently as powerful gene vectors for further development for in vitro and in vivo applications.

2 Development of Dendritic Architectures

In general, three major macromolecular classes, namely linear, cross-linked, and branched architectures, are produced by statistical polymerization processes. Therefore their architectures are not structurally-controlled as in many biological systems [37]. However, the discovery of dendrimers has changed this paradigm.

Since the pioneering work of Vögtle [38], Tomalia [39, 40], and Newkome [41], in constructing three-dimensional perfectly branched macromolecules by repetitive growth of building units, interest in dendritic polymers has increased at an amazing rate. The concept opened the opportunity to produce structure-controlled molecules and study of these polymers has expanded to all areas including theory, synthesis, characterization, properties, and investigations of potential applications. Furthermore, a new class, dendritic architectures (VI), has been introduced.

In the beginning, the term "dendrimer", which was established by Tomalia in 1985 [42, 43], described all types of dendritic polymers. Later a distinction based on the relative degree of structural control present in the architecture was drawn. Nowadays, many other types of dendritic architectures are known, even if most of them, however, have not yet been widely investigated and fully characterized. The term "dendritic polymer" involves four substructures (Fig. 2), namely dendrimers themselves, dendrons, random hyperbranched polymers, and dendrigraft polymers [44, 45].

Dendrimers and dendrons are almost perfectly monodispersed, three-dimensional macromolecules, with a well-defined tree-like globular structure and a high density of functional groups [44–46]. Their size, shape, and reactivity are determined by generations [$=G_x$] and chemical composition of the core, their degree of branching, and their surface functionalities (end groups) (Fig. 3) [44].

The globular structure of the dendritic polymers and the missing entanglement results in low viscosity in solution [47]. In addition to improved solubility, the presence of large number of functional terminal groups unlike that of linear polymers,

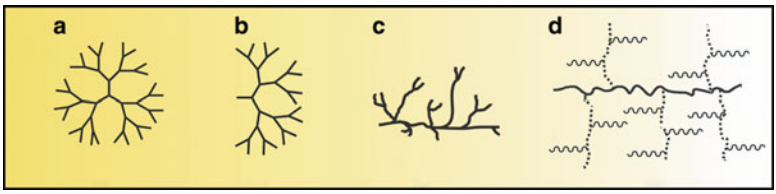

Fig. 2 Structurally controlled polymers: (**a**) dendrimer, (**b**) dendron, (**c**) random hyperbranched, and (**d**) dendrigrafts. The metabolism of the polyamine is still unclear. Reproduced with permission from [37]. Copyright 2001 Elsevier

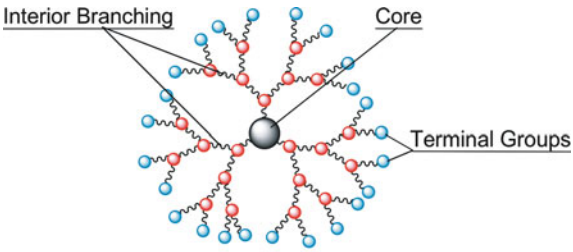

Fig. 3 General structure of dendrimers

makes dendrimers attractive in various fields, e.g., in the fields of medicine [48–57] and host-guest chemistry [58–72].

These features of these materials spurred the scientific community to utilize them in biomedical applications [49]. In particular, the synergy between their multivalency and size on the nanoscale enables a chemical "smartness" along their molecular scaffold that achieves environmentally sensitive modalities. These functional materials are expected to revolutionize the existing therapeutic practice. Dendritic molecules, such as polyamidoamine, polylysine, polyester, polyglycerol (PG), and triazine dendrimers, have been introduced for biomedical applications to amplify or multiply molecularly pathopharmacological effects [73].

3 Dendritic Polyamines: Structural Requirements for Efficient Gene Binding

In 1991, Luger et al. revealed by X-ray analysis the crystal structure of a natural DNA-histone complex. The X-ray structure shows in atomic detail how the histone protein octamer is assembled and how the base pairs of DNA are organized into a superhelix around it [74]. Since then this protein structure with cationic amino acids on the surface has acted as a model for the rational design of dendritic polymer-based gene vectors to mimic the globular shape of the natural histone complex [75–77].

Perhaps the most studied macromolecule of the dendritic family is poly(amidoamine) (PAMAM) [39, 40, 78, 79]. PAMAM dendrimers consist of an alkyl-diamine core, typically ethylenediamine or ammonia, and tertiary amine branches. Haensler and Szoka reported the first gene transfer studies performed with PAMAM and their high level of transfection in a wide variety of cells in culture with low cytotoxicity. By using a systematic series of perfectly branched commercially available PAMAM dendrimers (G = 2–10), they could show that dendrimer-mediated transfection is a function of dendrimer to DNA ratio and the diameter of the polymer. The spherical diameter of sixth generation PAMAM (68 Å) was found to be especially optimal for mediating transfection [80]. Further studies have also shown that not only the size and the generation but also the density of amino groups on the dendrimer surface

influences gene delivery efficiency [54, 81]. Increasing the number and charge density of the amines typically improves transfection efficiency. However, the increased charge density is generally accompanied by high cytotoxicity, which is a problem when designing new vectors for gene delivery [82–84]. Gebhart et al. reported the concentration- and generation-dependent toxicity behavior of PAMAM and confirmed that the high density of cationic amines would damage the cellular membranes [85]. However, a prerequisite for gene transfection is the formation of DNA/dendrimer supramolecular assemblies that ensure charged groups remain available on the surface of the complex for interaction with the cell [84]. Various alternatives have been investigated in an effort to improve PAMAM/DNA dendriplex formation with respect to cytotoxicity, complex formation, cell binding, release, and targeting.

Further studies of Szoka et al. could not reproduce the high transfection levels previously reported. In fact, stringently synthesized and purified PAMAM was found to be 100-fold less active than partially degraded PAMAM [84, 86]. The transfection activity of PAMAM improved dramatically after random degradation by heat treatment in *n*-butanol/H_2O with the result that such degraded structures were named "activated" (Fig. 4). The transfection efficiency of activated dendrimers was two to three orders of magnitude higher than that of intact PAMAM dendrimers [86]. A comparison of the resulting DNA complexes formed by each polymer, whether intact or activated, shows that both form compact DNA structures of nearly the same size. This finding leads one to conclude that the key for optimal transfection activity is correlated to the polymer flexibility.

Hyperbranched polymers represent a compromise between the perfect structures of dendrimers and the partially degraded architecture of activated PAMAMs. In this way such polymeric architectures are the structural prerequisites implicated in the design of an efficient gene vector. Hyperbranched polymers are highly branched molecules, composed of dendritic (D), linear (L), and terminal units (T) (Fig. 5).

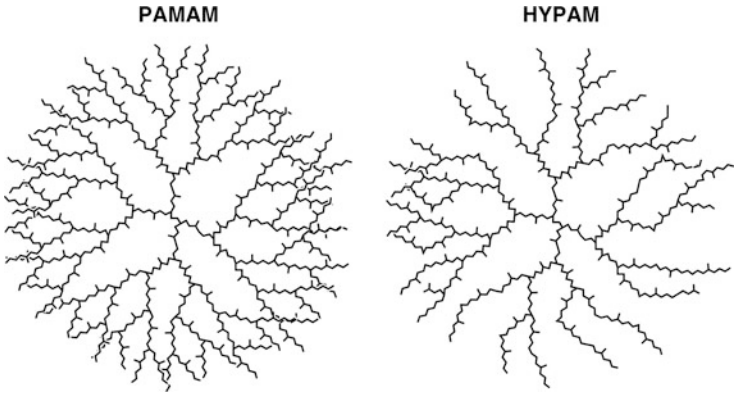

Fig. 4 Perfect PAMAM dendrimer and hyperbranched polymer (HYPAM). Reproduced with permission from [117]. Copyright 2002 Elsevier

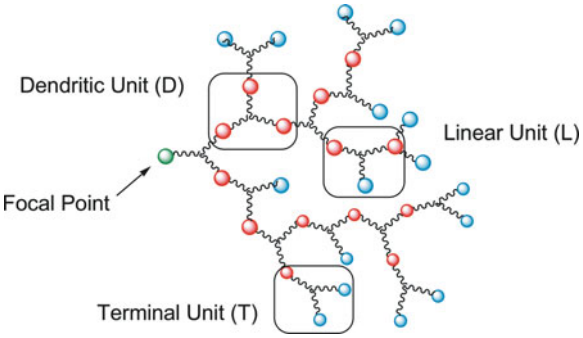

Fig. 5 Schematic structure of hyperbranched polymer with dendritic (D), linear (L) and teminal (T) units

Instead of the step-wise and tedious procedures used for synthesis of perfect dendrimers, hyperbranched polymers are prepared in a one-step synthetic strategy [87].

Due to their similar physicochemical properties like low viscosity, good solubility, and multi-functionality, dendrimers and hyperbranched polymers are referred to as dendritic polymers in the literature [45, 88], and they can be indistinctly used for many applications [89–91]. They exhibit a similar tree-like like structure which is more flexible than dendrimers due to lower degree of branching (DB). The common polymerization reactions to assess hyperbranched polymers are classified into three categories: step-growth polycondensation of AB_x monomers, self-condensing vinyl polymerization of AB monomers, and multibranching ring-opening polymerization of latent AB_x monomers.

In 1992, Suzuki et al. reported palladium catalyzed, ring-opening polymerization (ROP) of a cyclic carbamate. The polymerization was proposed to be an in situ multibranching process.

The molecular weight of the polymers is controlled by the initiator/monomer ratio. The first hyperbranched polymer obtained via ROP is poly(ethylene imine) (PEI) (Scheme 1).

Proceeding from these highly defined architectures, further functionalization of the terminal amino groups was investigated to convert hyperbranched PEI into fully branched dendritic polymers, PAMAM or PPI [38, 92–94].

Our group described a simple access to well-defined hyperbranched polyamines from hyperbranched PEI with different molecular weights, narrow molecular weight distributions, and an adjustable degree of branching [91]. According to this protocol fully branched analogs of polypropyleneimine (PPI) and polyamidoamine (PAMAM) dendrimers can be derived from hyperbranched PEI (M_w = 5,000, and 25,000 g mol^{-1}) in a two-step synthetic process (Scheme 2).

Furthermore, we studied the influence of the molecular weight and degree of branching on transfection efficiency and cell toxicity, which is supposed to have influence, as initially analyzed in several adherent cell lines (NIH/3T3, CHO-K1, COS-7, and HeLa), with unfunctionalized poly(ethylene imine)s [91, 95, 96]

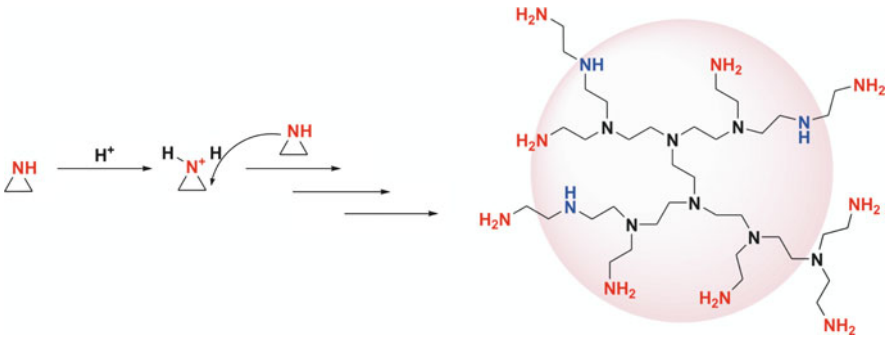

Scheme 1 Synthesis of hyperbranched poly(ethylene imine) (PEI) via acid catalyzed ring-opening polymerization of aziridine. Each color represents a different branching unit: *blue* for linear units (L), *black* for dendritic units (D), *red* for terminal units (T). PEI has a degree of branching (DB) of 62–73%, the depicted structure represents only a small idealized fragment. Reproduced with permission from [91]

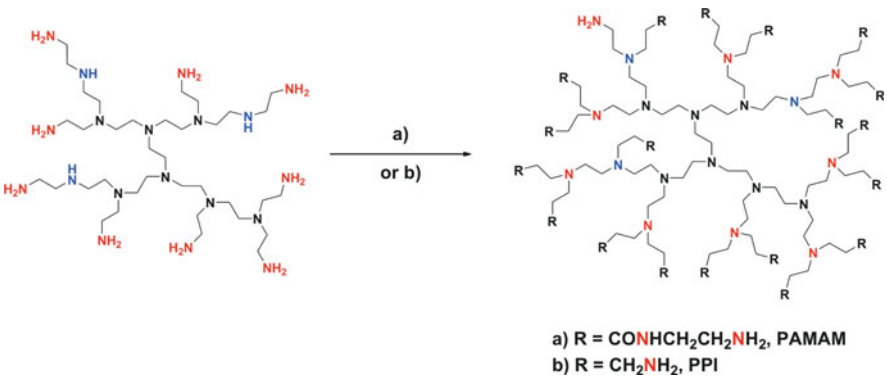

Scheme 2 Synthesis pathway of hyperbranched polyamines, PEI/PAMAM and PEI/PPI based on hyperbranched PEI: (**a**) PEI/PAMAM: (1) CH_2=CHCOOMe, THF, 25°C, 4 days, (2) CH_2=CHOOMe, 25°C, 8 days, and finally (3) $H_2NCH_2CH_2NH_2$, 50°C, 8 days, THF; (**b**) PEI/PPI: (1) CH_2=CHCN in water, 25°C, 2 days and (2) $LiAlH_4/AlCl_3$ in THF, 25°C, 1 day. Reproduced with permission from [91]. Copyright 2004 Wiley

(Fig. 6). The highest efficiencies were observed for polymers whose PEI cores had molecular weights between 15 and 60 kDa. Along with increasing core size the cytotoxicity also increased. The DNA transfection efficiency, however, depended on the investigated cell line.

Our group reported that the degree of branching influenced both linear and fully branched polymer in terms of low transfection efficiency, whereas two polymers with a lower degree of branching (DB $\sim$ 60%) achieved the best transfection results. The higher the degree of branching, the lower the flexibility which consequently resulted in significantly lower gene transfection efficiency [91]. On the

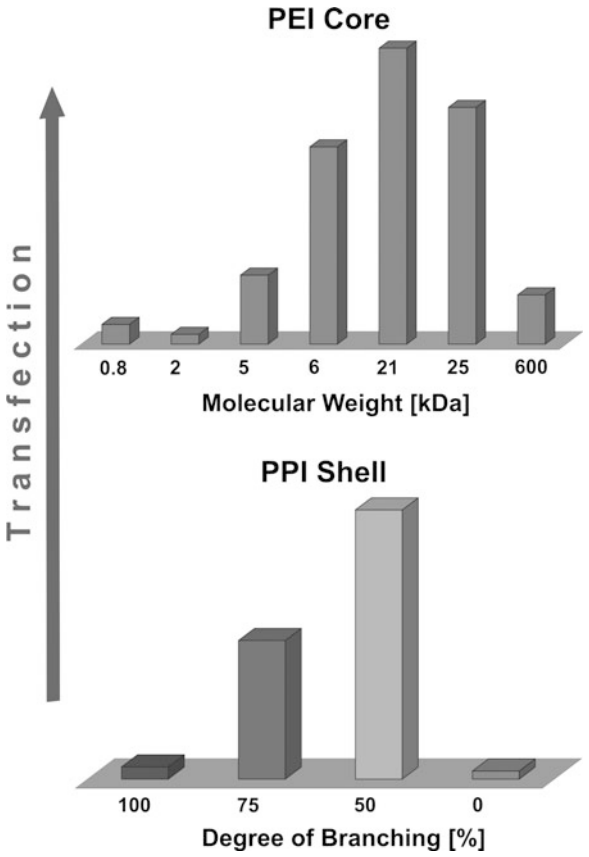

Fig. 6 Transfection efficiencies of several PEIs and transfection efficiencies of $PEI_{25}PPI$ with different degrees of branching

other hand linear PEI of the same molecular weight resulted in very low transfection efficiencies.

4 Hyperbranched Polyamines in Gene Delivery Applications

As shown by the studies described above on PAMAM and PEI systems, the flexibility of the dendritic architecture plays an important role in the efficient gene binding and subsequent transfection. To this end, hyperbranched polymers appear to be optimal candidates for the intracellular delivery of therapeutically important oligonucleotides.

In the following sections a detailed analysis of the different hyperbranched scaffolds commonly used in gene delivery is described. Several examples are

presented showing the different structural modifications explored to tailor the properties of the polyamines toward the development of an optimal gene vector, e.g., (1) end-capping with short chains or organic molecules, (2) terminal grafting via living polymerization, (3) growing hyperbranched polymers on the surface, or grafting from/onto the surface, (4) hypergrafting to obtain hyperbranched polymers with a linear macromolecular core, and (5) blending or crosslinking.

4.1 Hyperbranched Poly(Ethylene Imine)

Hyperbranched poly(ethylene imine) (PEI) is the commercially available prototypical hyperbranched polymer, which has been produced for almost 50 years on a ton scale by BASF (Lupasol®) [97, 98]. Typically, PEI is synthesized via an acid catalyzed ring-opening polymerization process of aziridine (ethylene imine) at 90–100°C in water or organic solvents. In general, the linear amino nitrogen units (Scheme 1) showed a higher reactivity than the terminal amino groups (Scheme 1), which leads to a faster reaction of the linear units with an aziridine monomer. Therefore the degree of branching is higher (62–73%) than theoretical 50%. Moreover, PEI can be obtained with narrow molecular weight distributions (MWD, typically below 2.0) [97] and molecular weights (M_n) up to 10,000 g mol^{-1}. This corresponds to the typically used PEI 25 kDa (with PD of about 2.5). Even higher molecular weight PEIs are accessible via crosslinking with bifunctional compounds such as 1,2-dichloroethane.

Hyperbranched PEIs have found application in many different technical fields, e.g., as crosslinkers (in coatings), in the paper industry (as additives) [99], and for water treatment due to their ability to form strong complexes with metal ions [100, 101].

Due to its unique transfection efficiencies, PEI is often considered as the gold standard. A variety of PEI derivatives have already been tested and numerous physical characterizations of PEI/DNA complexes including size, shape, surface charge, and concentrations for their gene transfer efficiency have been performed. Most of them focused on both the degree of branching and the influence of molecular weight on transfection efficiency. The first studies in this direction using PEI were reported by Behr et al. in 1995 [29].

A systematic structural analysis was performed by Kissel et al. to elucidate the effects of molecular weight and degree of branching on the efficiency of PEI for intracellular delivery of genes. In 1999 the group reported the synthesis of low molecular weight poly(ethyleneimine) (LMW–PEI) and compared its transfection properties and cytotoxicity profile to commercially available high molecular weight PEI (800 kDa, HMW–PEI) [102]. They also observed that the LMW–PEI showed a lower degree of branching that had a relatively low in vitro cytotoxicity profile and 100-fold higher expression of luciferase in 3T3 cells than HMW–PEI. The authors postulated that the higher transfection efficacy of the low MW analogs was caused by the lower cytotoxicity and the formation of stable nano-sized particles capable of

being endocytozed. Furthermore, they reported the synthesis of LMW–PEI with a degree of branching of 50% which resulted in an improved gene vector in comparison to commercially available PEI of MW 25 kDa. The excellent properties are believed to be the result of both, the lower molecular weight and the reduced degree of branching [103].

In another approach, the influence of the degree of branching on gene transfection was determined using novel polymers based on poly[(ethylene imine)-*co*-*N*-(2-hydroxyethyl-ethylene imine)]. These polymers were synthesized by copolymerization of aziridine and *N*-(2-hydroxyethyl)-aziridine, a reagent which allowed a systematic manipulation of the degree of branching. Polymers with a higher ethylene imine (EI) content and therefore higher branching resulted in greater transfection efficiency than polymers with more *N*-(2-hydroxyethyl) ethylene imine (HEEI) content. The increased transfection efficiency could be correlated with improved capability of DNA binding and condensation due to a higher content of primary and secondary amines, which led to the formation of smaller sized complexes. The structure-efficiency correlation in efficiency was in good agreement with the higher pK_a values of the polymers.

A common strategy used to improve stability and solubility of polyplexes is the attachment of poly(ethylene glycol) (PEG) units to the hyperbranched polyamine. Pegylation of polymers is a promising method to render water solubility, minimize immunogenicity, and increase blood circulation half-life of the resulting nanocarriers which mimic the structure of so-called "stealth" liposomes [104]. Again, Kissel and co-workers reported the synthesis of two series of poly(ethyleneimine)-graft-poly(ethylene glycol) copolymers and their performance on DNA complexation [105]. In the first series, different grafting degrees of PEG chains (MW 5 kDa) were performed onto PEI with MW 25 kDa, while in the second series, the molecular weight of PEG was also varied (550 Da to 20 kDa) to elucidate the influence of copolymer block structure on DNA condensation (Fig. 7). Atomic force microscopy (AFM) measurements of the first series of compounds showed the effect of the PEG shell density on the size and shape of the polyplexes formed with DNA. By varying the degree of PEG substitution a reduction in the diameter from 142 to 60 nm was found. Furthermore, PEI/DNA-complexes lost their spherical shape via rodlike particles to ill-defined shape structures with increasing amount of substituents. Another trend was observed in AFM for the second series: With decreasing MW of PEG the complexes gradually lost their compact and spherical shape. Surface charge measurements demonstrated that copolymers with many short PEG blocks formed large and diffused complexes of high positive surface charge, whereas a few, long PEG blocks self-assembled to small and compact condensates of low surface charge. By further analysis of the PEG length and density effect on the transfection efficiency in vitro, it was found that DNA is most effectively transfected when a high density of relatively short (550 Da) PEG chains are grafted onto PEI [106]. Interestingly, siRNA gene silencing was more effective when a low density of longer (5 kDa) PEG chains were conjugated to PEI.

To overcome the high toxicity of PEI and the relatively low transfection efficiency of the pegylated PEI systems (PEG–PEI), several examples were

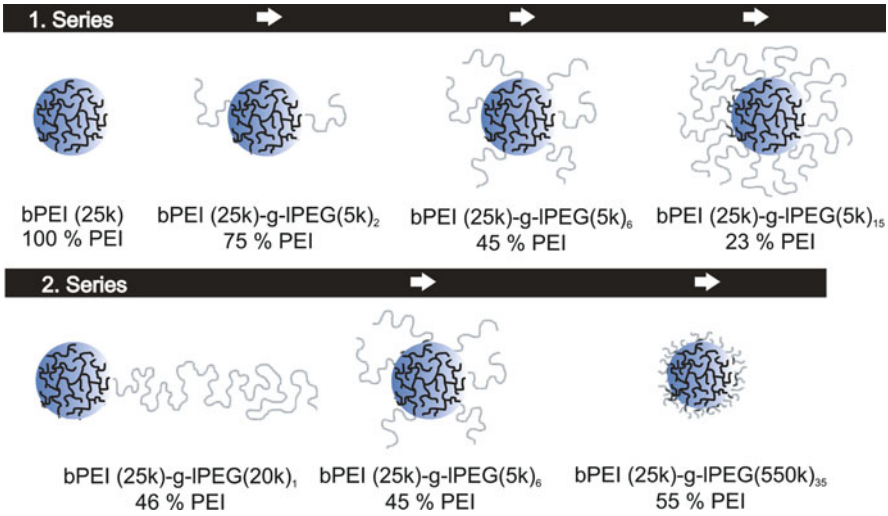

Fig. 7 Structures of the bPEI-*g*-lPEG copolymers. The *black part* of the structure represents the cationic branched PEI, and the *gray part* represents the nonionic linear PEG blocks. Reproduced with permission from [105]. Copyright 2002 ACS

reported using targeting moieties which promoted an enhanced cellular uptake. Peng et al. investigated linking folate (FA) as cell specific target molecules on the PEG surface of PEI-PEG (25 kDa) [107]. FA is a well-known targeting ligand for anti-cancer agents, because its target receptor is often over-expressed in many cancer cells [108]. The above-mentioned PEG-PEI/DNA polyplexes could be obtained with sufficient gene delivery efficiency by controlling the grafting density, molecular weight, and linkage bond between PEI and PEG [106]. Peng et al. used a biodegradable succinate linkage to conjugate PEG to PEI. After study of the in vitro properties of the polymer, it turned out that the novel PEG–PEIs not only reduced the toxicity compared to PEI by sevenfold but also increased the transgene expression level. It was found that FA–PEG–PEI reached the highest transfection efficiency by administering an N/P ratio of about 15 in 293T and C6 glioma cells. The results showed that the presence of FA–PEG is a promising carrier for folate receptor-bearing tumor cells.

The degradation of gene delivery polymers in vivo is of high significance for efficient therapeutic delivery because the appropriate degradation of the polymer into low molecular weight breakdown products enables the reduction of cytotoxicity by reducing cumulative cellular exposure time and an easy elimination by excretion pathways in vivo [23, 109, 110]. It has been reported that biodegradable cationic polymers are nontoxic and condense DNA into compact particles that can transfect mammalian cells. Furthermore, the degradation of drug carriers can also be used to control the release of the DNA inside the cell [109–112]. Pack et al. developed a flexible, biodegradable, hyperbranched system based on PEI [113]. The polymers were obtained by addition of amino groups on a PEI core (800 Da) to

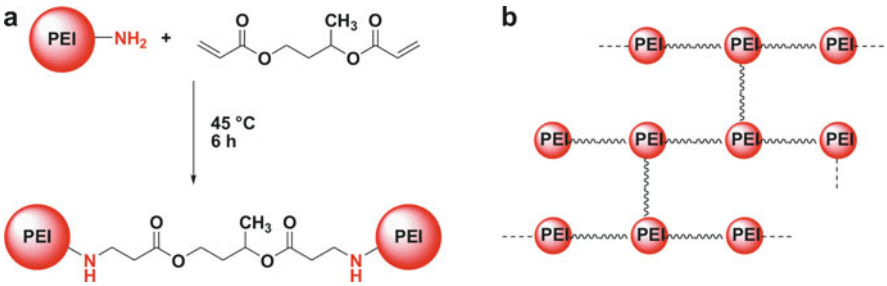

Scheme 3 Synthesis of degradable PEI derivatives in bulk: (**a**) 800-Da PEI is reacted with diacrylates (1,3-butanediol diacrylate shown) to generate the ester-cross-linked polymers; (**b**) the acrylate groups can react with either primary or secondary amines, resulting in a highly branched structure. Reproduced with permission from [126] Copyright 2003 ACS

two diacrylates (1,3-butanediol diacrylate and 1,6-hexanediol diacrylate) with three- and six-carbon spacers, respectively (Scheme 3). Two polymers with MW of 14 kDa and 30 kDa were prepared. The polymers showed high affinity towards plasmid DNA in ethidium bromide exclusion studies, and formed aggregates of 30–80 nm diameter. Cell transfection studies were evaluated by luciferase enzyme activity in murine myoblasts (MDA-MB-231) and in human breast carcinoma (C2C12) cells, showing that both polymers (14 kDa, and 30 kDa) mediated luciferase expression. In the case of transfection studies with 14 kDa polymer (1), the luciferase levels had a twofold greater yield in C2C12 cells and a ninefold greater yield in MDA-MB-231 compared to PEI 25 kDa mediated increment of luciferase level. On the other hand, the 30 kDa polymer (2) resulted in 6-fold greater luciferase levels in C2C12 cells and 16-fold greater in MDA-MB-231. The cytotoxicity of 14 and 30 kDa polymer was assayed using XTT assay and showed a significantly reduced toxicity compared to 25 kDa PEI. MDA-MB-231 cells showed resistance to all three polymers. In C2C12 cells, the 30 kDa polymer was more effective in gene transfer than the 14 kDa variant. By administering 15 μg/mL, the later reduced the metabolic activity of the cells twice as much as the former. The authors concluded that low molecular weight PEI cross linked with diacrylates exhibited lower toxicity and were more than one order of magnitude more efficient gene transfering agents than commercially available 25 kDa PEI.

4.2 Hyperbranched PAMAM

Poly(amido amine) (PAMAM) dendrimers are the most common class of dendritic macromolecules and, due to their ease of synthesis and commercial availability, they have been the most utilized dendrimer-based vectors for gene transfer [1, 37, 84]. PAMAM dendrimers consist of an alkyl-diamine core with tertiary amine

branches, which exert endosome buffering effects and primary amino groups which participate in DNA binding due to their pK_a values [114, 115].

Besides generation number and degree of flexibility, hyperbranched PAMAM can be synthesized with different chemical properties [37, 43, 56, 58, 80, 114, 116]. The biotechnology company QIAGEN offers two commercially available hyperbranched PAMAM dendrimers: Superfect® and Polyfect® as in vitro transfections agents, which have been successfully used in many laboratories.

Since the initial work of Haensler and Szoka in 1993 [1], PAMAM seemed to be perfect candidates for gene delivery due to their capability of DNA binding, high level of transfection, and their good tolerability in a wide variety of cells in culture [80]. In addition, PAMAM is often referred to as an "artificial protein" [37], due to that fact that higher generation dendrimers have diameters similar to that of the natural histone core of chromatin (68 Å). In fact, Haensler and Szoka obtained maximal transfection of luciferase by applying a diameter of 68 Å. Larger diameters resulted in increased toxicity, and reduced transfection efficiency [80] which led the authors to conclude that dendrimer mediated transfection is dependent upon both the dendrimer/DNA ratio and the diameter.

Several groups have reported the use of hyperbranched PAMAM as gene carriers [86, 87, 116–120]. As mentioned earlier in the introductory section, Szoka and coworkers have shown that partially activated PAMAM showed better transfection efficiency than its "Perfect" analog [86]. The randomly degraded "activated" architectures suggested that the transfection efficacy is dependent upon flexibility and positive charge, and is independent of the molecular weight. Both structures, PAMAM dendrimers and hyperbranched PAMAM, were able to form compact structures of the same size and morphology.

Denning et al. reviewed the gene transfer into eukaryotic cells using hyperbranched PAMAM as gene vector [117]. The hyperbranched architectures showed a higher degree of flexibility and only a slight difference in structure and molecular mass compared to PAMAM dendrimers. After polyplex formation, DNA was highly condensed and therefore protected from degradation by endosomal nucleases. The transfection efficiency proved to be two to three orders of magnitude higher than for intact dendrimers, and to be influenced by the dendrimer generation and "activation" time. As expected, shorter activation/degradation times yielded polymers with less flexibility and lower transfection efficiency. Transfection experiments evaluated by β-galactosidase reporter gene assay in mouse fibrioplastic NIH/3T3 cells using activated PAMAM dendrimers of different generations showed that generation six dendrimers exhibited the highest transfection efficiency (Fig. 8a). Furthermore, the transfection efficiency was evaluated regarding it as a function of activation time (in hours). It was observed that the transfection efficiency increased until reaching an optimal activation time (t_3 in Fig. 8b) and decreased after further activation. Transfection efficiency decreased with longer activation times up to almost negligible transfection efficiencies.

Although hyperbranched PAMAM are tolerated in many cell lines in vitro, their in vivo applications are still limited due to a significant toxicity. In an attempt to overcome this limitation, Xu et al. recently reported the synthesis and evaluation of

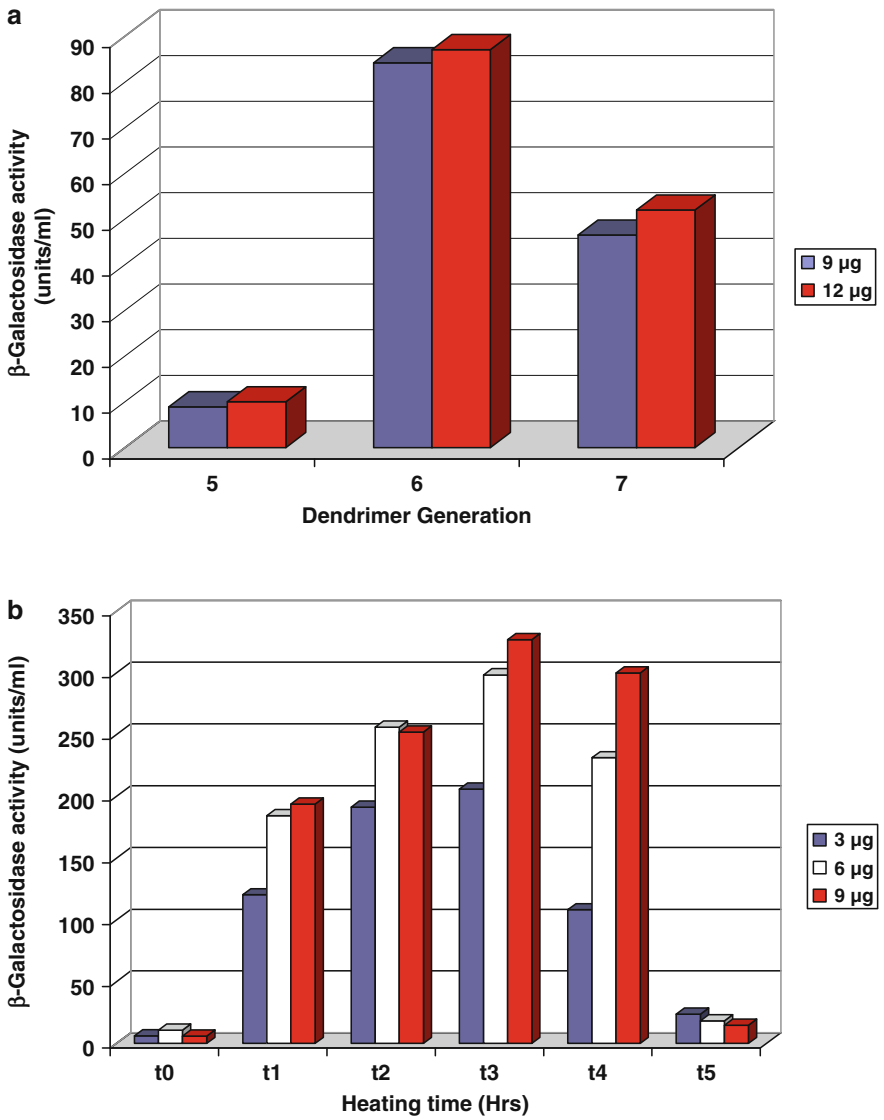

Fig. 8 (**a**) Influence of dendrimer generation on transfection efficiency. (**b**) Influence of dendrimer activation on transfection efficiency. The *different bar colors* represent different amounts of transfection agent used. Reproduced with permission from [117]. Copyright 2002 Elsevier

phenylalanine (PHE)-modified hyperbranched PAMAM (HPAMAM) as promising gene carriers [116]. HPAMAM were synthesized by a one-pot polymerization of methyl acrylate (MA) and diethylenetriamine (DETA). Various loading degrees of phenylalanine were then achieved by conjugation to the terminal amino groups as shown in Fig. 9 (HPAMAM-PHE30, -PHE45, and -PHE60). As PHE conjugation to

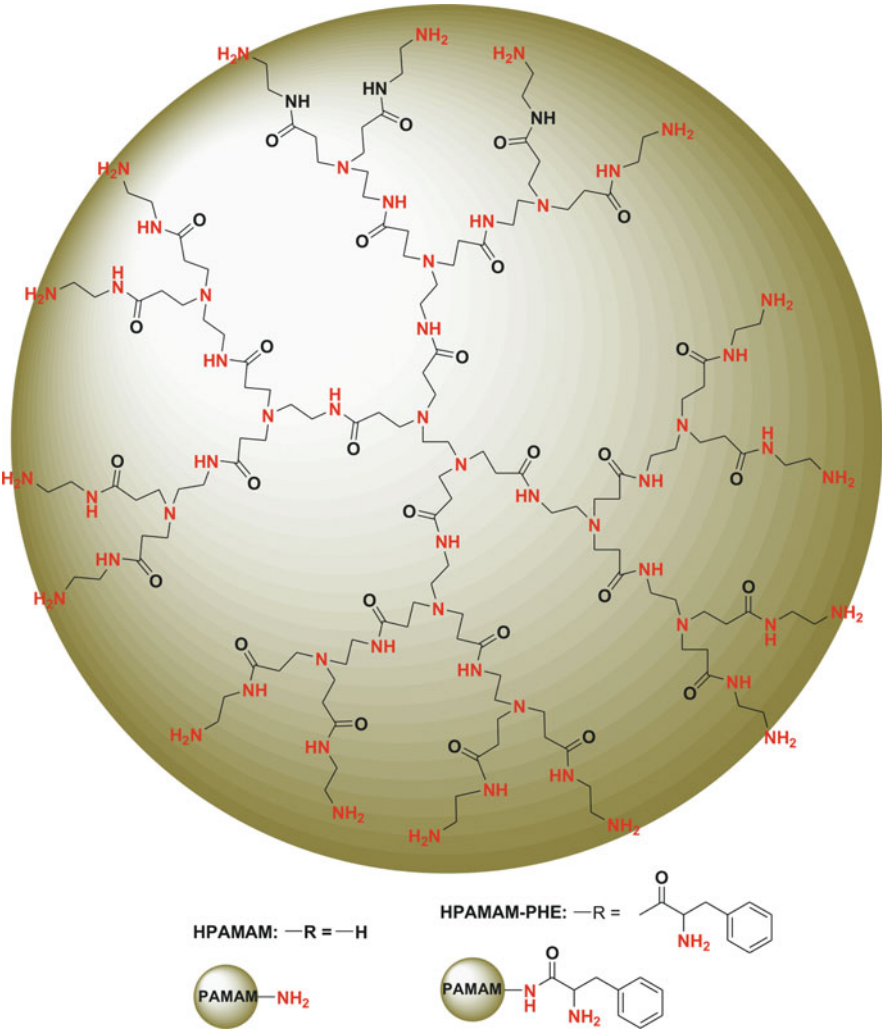

Fig. 9 Chemical structures of hyperbranched poly(amido amine) (HPAMAM) and HPAMAM modified with phenylalanine (HPAMAM-PHE). Adapted with permission from [116]. Copyright 2010 ACS

HPAMAM decreased the surface charge densities, more polymers were needed to condense the DNA. All HPAMAM-PHE/DNA complexes showed condensed structures with average sizes around 50–300 nm. The HPAMAM-PHEs obtained were quite effective in transfection, as shown in SMMC-7721, human hepatoma SMMC-7721 cells, and in COS-7, African green monkey kidney cells, using luciferase reporter gene assay. The highest transfection activity was obtained using HPAMAM-PHE60, the polymer with the highest PHE surface modification. The efficiency was almost one order of magnitude higher in comparison to PEI

(25 kDa). The reason for the effective transfection was probably due to the formed hydrophobic environment in the periphery, which led to reduced protonation of α-amino groups. The cytotoxic profile assessed by MTT assay showed that all HPAMAM-PHE only had marginal cytotoxicities. Further studies of Xu et al. showed that larger molecular weight of HPAMAMs affected the DNA complexation properties and increased the transfection efficiencies.

In a smart approach of Oupicky et al. the reducing intracellular environment was exploited to trigger the release of DNA upon reduction of a reductive labile PAMAM architecture. The sharp difference in redox potential (100–1,000 fold) existing between the reducing intracellular space and the oxidizing extracellular space is a potential stimuli for the triggered release of therapeutics agents. Therefore Oupicky et al. prepared a complete series of reducible hyperbranched PAMAMs (RHB), which were synthesized by Michael addition copolymerization of *N*,*N*-dimethylaminodipropylene-triamine (DMDPTA) with either *N*,*N*′-hexamethylene bisacrylamide (HMBA) or *N*,*N*′-cystamine bisacrylamide (CBA) (Fig. 10) [118]. A library of compounds with different co-monomer ratios was built, with special emphasis given to the preparation of RHB with different disulfide loadings. All prepared RHB were able to condense and compact DNA. Disulfide bonds can easily be reduced in intracellular environments and mediated by thiol/disulfide exchange reactions with small redox molecules like glutathione (GSH). The glutathione pathway which controls the intracellular redox potential [121] is significantly involved in such stimuli-sensitive mechanisms. In this approach, when the polyplexes were treated with dithiothreitol (DTT) to mimic the intracellular environment, DNA was released. The triggered release profile improved with the increasing amount of disulfide moieties within the RHB structure.

Transfection activity was measured in B16F10 mouse melanoma cells. The transfection efficiency of all RHB/DNA complexes was 3–30 times higher compared to PEI (25 kDa) polyplexes. Investigation on transfection activity on the

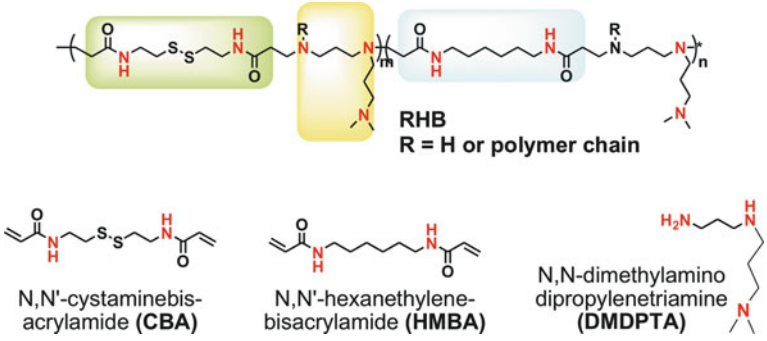

Fig. 10 Reducible hyperbranched poly(amido amine)s (RHB), obtained by copolymerization of *N*,*N*-dimethylaminodipropylene-triamine (DMDPTA) and two bisacrylamide monomers *N*,*N*′-hexamethylene bisacrylamide (HMBA) or *N*,*N*′-cystamine bisacrylamide (CBA). Adapted with permission from [118] Copyright 2009 ACS

effect of chloroquine showed that presence of disulfide bonds in RHBs affects intracellular trafficking of their DNA complexes. The transfection activity of RHB-100, -75, and -50 (the numbers reflect the amount of CBA content in the polymer) polyplexes increased three- to sixfold, whereas RHB-0 polyplexes showed a negligible increase. The cytotoxicity profile of RHBs was found to be related to their reducible nature and to decrease with increasing amounts of disulfide bonds. The transfection activities of all RHB/DNA polyplexes were up to 30 times higher compared to the control experiments using PEI/DNA complexes.

4.3 Hyperbranched Poly(Amino Ester)s

Several approaches to reduce the cytotoxicity of gene carriers have been performed including an introduction of biodegradable poly(amino ester)s, which received much interest in biomedical and biomaterial areas as a platform for gene and drug delivery systems [122, 123]. Generally, polyplexes based on these polymers showed comparable in vitro transfection activity, lower cytotoxicity, and shorter in vivo circulation times compared to non-degradable polycations [124]. Therefore they are suitable for repeated administration in therapy of chronic diseases because of the lack of accumulation in the target organs [125].

Poly(amino ester)s are degradable by hydrolysis of backbone ester bonds and contain tertiary amines to facilitate DNA binding [124].

Different hyperbranched poly(amino ester)s have been reported, which can be prepared from commercially available starting materials, without solvents, catalysts, or complex protecting group strategies [124]. They offer great variety in size and degrees of branching and could easily be engineered to possess amine pK_a values spanning the range of physiologically relevant pH [122].

One of the first investigations with hyperbranched poly(amino ester)s as gene mediators was reported by Park et al. in 2001 [126]. The synthesis of the poly(amino ester) was carried out by reacting an AB_2 monomer, bearing one hydroxyl group, two methyl ester groups, and one tertiary amine group with a PAMAM dendrimer of generation 0.5 as a core moiety (Scheme 4). The surface was functionalized with amine groups by transesterification of the methyl esters with *N*-cbz–ethanol amine. The poly(amino ester) was obtained after deprotection. The transfection efficiency that was evaluated by luciferase gene expression assay in human embryonic kidney cells (HEL 293) was comparable to PAMAM and PEI. The cytotoxicity of the poly (ester amine) was only minimal, and compared to PAMAM and PEI much lower accordingly to MTT assay.

Leong et al. evaluated a hyperbranched poly(amino ester) synthesized in a novel A_3+2BB'B"approach by Michael addition polymerization of trimethylol-propane triacrylate (TMPTA) (A_3-type monomer, triacrylate), with a double molar of 1-(2-aminoethyl) piperazine (AEPZ) (BB'B"-type monomer, trifunctional amine) (Fig. 11) [127]. To check its DNA condensation behavior and cytotoxicity, the poly(TMPTA1-AEPZ2) obtained was protonated. Due to the protonation ability of

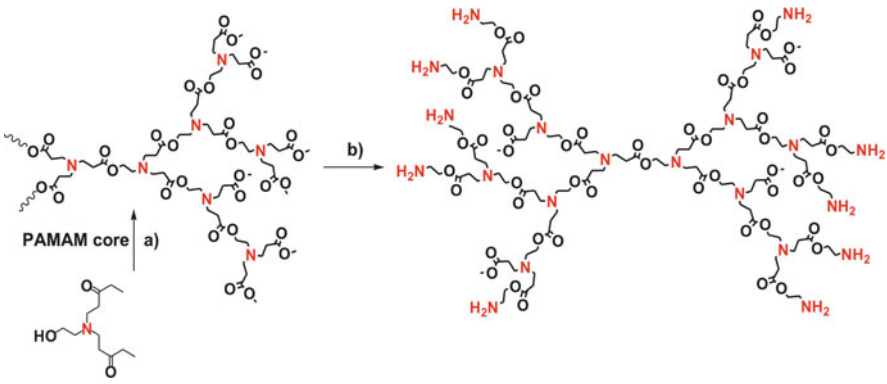

Scheme 4 Synthesis of hyperbranched poly(amino ester). (**a**) Bulk polymerization under reduced pressure at 140°C; (**b**) (1) bulk polymerization under reduced pressure at 140°C and (2) H_2, 10% Pd/C, MeOH, $CHCl_3$, room temperature. Adapted with permission from [126]. Copyright 2001 ACS

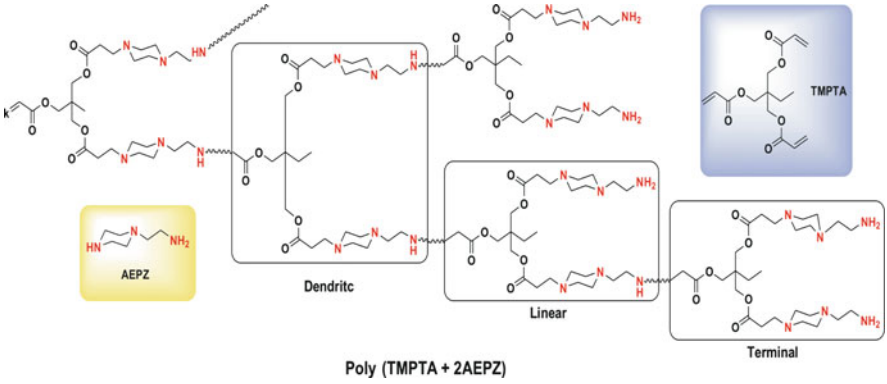

Fig. 11 Structure of biodegradable, hyperbranched poly(amino ester) poly(TMPTA+ 2AEPZ) obtained by Michael addition polymerization of trimethylol-propane triacrylate (TMPTA) and 1-(2-aminoethyl) piperazine (AEPZ). Adapted with permission from [127]. Copyright 2005 ACS

primary, secondary, and tertiary amines in the polymer, poly(TMPTA1-AEPZ2) could show a good interaction with the DNA backbone and the formation of a neutral polyplex was achieved. Depending on cell line used (COS-7 and HEK 293), the complexes formed reached value efficiencies up to 70% of the control experiments employing PEI (25 kDa). The results are summarized in Fig. 12. The cytotoxicity assay showed 60% higher cell viability at a concentration of 500 μg/mL, compared to PEI at the same concentration. In conclusion, this concept opened a way to synthesize hyperbranched poly(amino ester) with tertiary and terminal amino groups that are easily tunable to different types of amines through adopting different A_3-type, and BB'B"-type monomers.

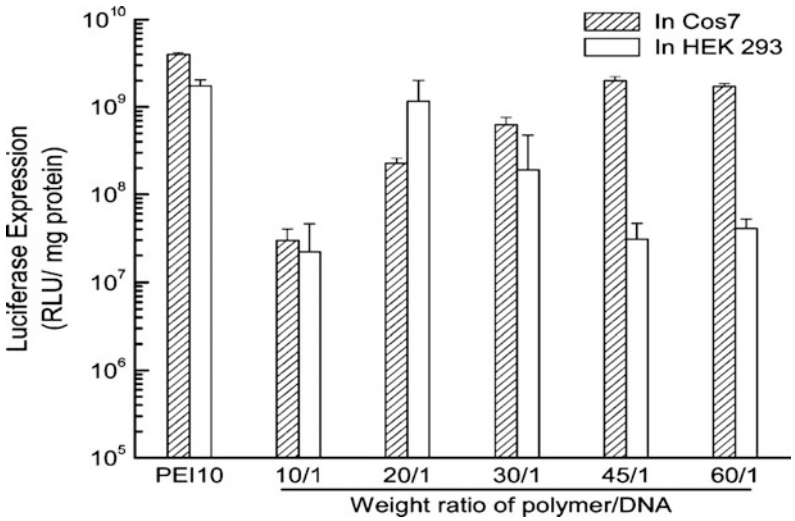

Fig. 12 Transfection efficiency of the complexes of protonated poly(TMPTA1-AEPZ2)/DNA (pCMV-Luc) complexes in COS-7 and HEK 293 cells compared to that of PEI (25 kDa). The transfection efficiency of PEI (25 K) was obtained under an optimal N/P ratio of 10:1. Values were presented as mean ± standard deviation ($n = 4$). Reproduced with permission from [127]. Copyright 2005 ACS

Zhong et al. synthesized a versatile family of hyperbranched poly(amino ester)s, which contain primary, secondary, and tertiary amino groups in their structures. The polymers were obtained in high yields through a "Michael type" conjugate addition of diacrylate (ethylene glycol diacrylate (EGDA), 1,4-butanediol diacrylate (BDDA), and 1,6-hexanediol diacrylate (HDDA)) monomers with trifunctional amines (*N*-methylethylenediamine (MEDA), 1-(2-aminoethyl)piperazine (AEPZ), and 4-(aminomethyl)piperidine (AMP)) [124]. Transfection measurements clearly indicated that the capability to complex and transfect DNA depends on the polymer structure. Three out of nine synthesized polymers, p(HDDA-AEPZ), p(HDDA-AMP), and p(BDDA-AMP), allowed effective condensation of the negatively charged DNA to nano sized particles (Fig. 13). By comparison with conventional cationic polymers like PEI (25 kDa) and poly(lysine) (PLL), a reduced cytotoxicity was observed and determined by XTT assay.

Cho et al. investigated the synthesis of hyperbranched poly(amine ester)s based on poloxamer diacrylate and low molecular weight branched PEI as crosslinker [23]. The poly(amino ester)s prepared through Michael addition (Scheme 5) showed degradability and great ability to condense DNA. The sizes of the DNA/polymers (polyplex) formed were below 150 nm under physiological conditions, which showed the potential of these poly(amino ester)s for intracellular uptake [21–23]. It was found that the polymers showed lower cytotoxicity than with PEI (25 K) in different cell lines (A549, HepG2, and 293T). The authors postulated that the high cell viability was a result of the combination of degradability of the polymer and the

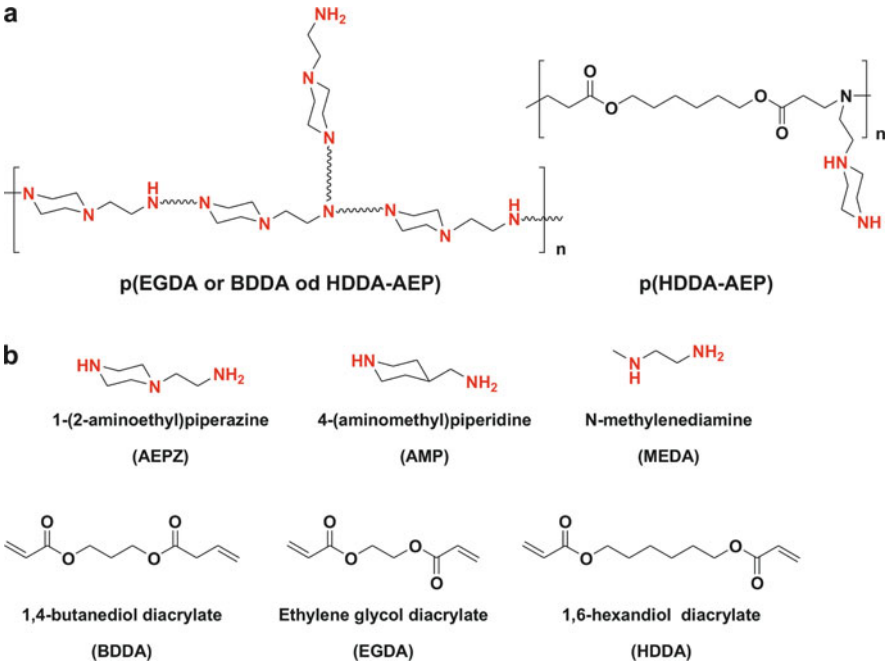

Fig. 13 (**a**) Possible structures of hyperbranched polymer (p(X-Y)) from the conjugate addition of X (diacrylate) and Y (trifunctional amines). (**b**) Structures of diacrylates and trifunctional amine monomers used for the synthesis: 4-(aminomethyl)piperidine) (AMP), *N*-methylethylenediamine (MEDA), 1-(2-aminoethyl)piperazine (AEPZ), ethylene glycol diacrylate (EGDA), 1,4-butanediol diacrylate (BDDA), and 1,6-hexanediol diacrylate (HDDA). Adapted with permission from [124]. Copyright 2005 Elsevier

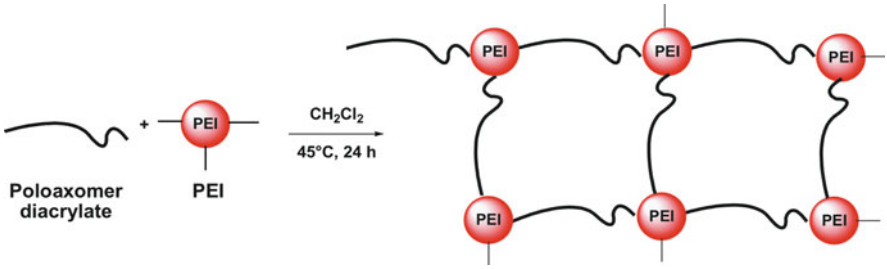

Scheme 5 Synthetic scheme of hyperbranched polyester amines from Michael addition reaction of poloxamer diacrylate and low molecular weight branched PEI, adapted with kind permission of Prof. Cho [23]. Copyright 2007 Wiley

low toxicity profile of the building blocks. Furthermore, the transfection efficiency was investigated by applying the luciferase assay in vitro. Surprisingly, the efficiency depended not only on the cell lines used, but also upon the composition of

poloxamer in the poly(amine ester). A systematic analysis allowed the conclusion that 10 mol% of poloxamer seems to be an optimal composition for the polymer as far as the luciferase expression is concerned. Therefore, these poly(amino ester)s showed much higher transfection efficacy in all three used cell lines compared with PEI (25 K) and PEI (1.8 K). In a further development, Cho et al. recently reported an alternative hyperbranched poly(amino ester)s (PEA)s based on biodegradable and biocompatible polycaprolactone (PCL) and polyethylenimine (PEI) [128].

Kissel et al. investigated amine-modified hyperbranched polyesters by introducing tertiary amines on polymers based on 2,2-bis-(methylol)propionic acid (bis-MPA) (Boltorn H®, a commercially available hyperbranched polymer (HBP)) [110]. By using carbonyldiimidazole chemistry the terminal hydroxyl (–OH) groups from Boltorn were esterified with increasing equivalents (9, 19, 35, 48, and 60) of diethylaminopropylamine (DEAPA) (Scheme 6). These polymers, which only contain ester bonds and terminal carbamate linkages, showed degradability, very low toxicity, and an ability to transfect cells. The different degrees of amine substitution allowed a systematic investigation of the influence of amine density on degradation rate and transfection efficiency. The transfection profile, which was tested in A549 cells (human alveolar epithelial cell line), showed that the hyperbranched polymers with only 9 or 19 amines displayed weak transfection efficiency, whereas an increase of the amine density to 35, 48, and 60 enhanced the transfection efficiency 20 fold.

The authors postulated that the enhanced transfection efficiency is due to the higher zeta potential of the higher substituted polyesters, which resulted in an enhanced uptake and increased DNA complexation efficiency. Furthermore, all HBP-DEAPA polymers were tested concerning their cytotoxicity using an MTT assay. All polymers showed such a low cytotoxicity that IC50 values could not be detected at concentrations relevant for transfection.

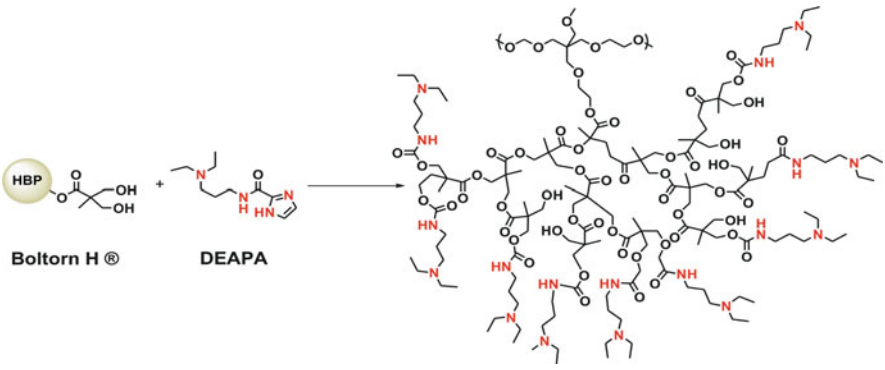

Scheme 6 Synthetic scheme of HBP-DEAPA through coupling of the activated DEAPA to hyperbranched polymer (Botoron H). Adapted with permission from [110]. Copyright 2009 Elsevier

4.4 Hyperbranched Polyglycerol

Dendritic polyglycerols (dPG)s are structurally defined macromolecular scaffolds, have an aliphatic polyether backbone, and possess multiple hydroxyl end groups. Since dPGs are synthesized in a controlled manner to obtain definite molecular weight and narrow polydispersity, they have been evaluated for variety of applications [49, 129, 130]. Multiple approaches to design different dPG architectures have been reported that offer a great variety in the degree of branching, size, surface topology, and chemical properties in general. Along with the synthesis of hyperbranched PG, fabrication routes to perfect dendrimers, dendrons, microgels, and hydrogels have also been reported over the last decade.

Due to their highly biocompatible nature, dendritic PGs have a broad range of potential applications in medicine and pharmacology. The versatility of the polyglycerol scaffolds for application in the biomedical field has recently been reviewed [131], and a number of examples were described, therein, e.g., smart and stimuli-responsive delivery and release of bioactive molecules, enhanced solubilization of hydrophobic compounds, surface-modification and regenerative therapy, as well as transport of active agents across biological barriers (cell-membranes, tumor tissue, etc.).

Several studies have demonstrated the biocompatibility of dendritic PGs and their potential safe profile for in vitro and in vivo applications. In preliminary cell culture experiments, hyperbranched PG with a molecular weight of 5 kDa showed absolutely no toxicity on the cellular level [130]. Brooks et al. reported several studies including a comprehensive analysis of PGs as a function of MW distribution and compositions [132–135]. Both linear and hyperbranched PGs were reported to have a similar or even better biocompatibility profile than PEG with MW ranging from 4.2 to 670 kDa. *In vivo* studies conducted on mice revealed no sign of toxicity after i.v. injection of the dose up to 1 g/kg. For a period of 28 days no sign of weight disturbances or untoward effects were observed. Although the biocompatibility of polymers in general is a function of molecular weight, no MW dependant toxicity was found up to 540 kDa for dendritic PG architectures. Currently, hyperbranched PG candidates are seriously being considered as delivery enhancers for many bioactive agents. This could substantially increase the internalization of active components, specifically into targeted cells, enhancing the therapeutic benefits and decreasing the adverse side effects [136–138]. Recently we demonstrated that post-modified hyperbranched polyglycerol presents sufficiently low zeta potentials, lower interactions with serum albumin, enhanced cellular uptake, and higher cellular viability on human hematopoietic cell line U-937, to be considered a promising candidate for a systematic delivery of therapeutic agents [139].

Several amine functionalized hyperbranched PGs have been reported as potential gene delivery systems after a proper surface group functionalization. In comparison to other dendritic structures, these scaffolds have the added advantage of being open, flexible, and possessing a polyether backbone which keeps the toxicity profile low. Different systems have been studied by post-modification of the hydroxyl groups

from the polyglycerol structure with amine bearing compounds. The post-modification approach for the preparation of hyperbranched polyglycerols based on core-shell architectures allowed an easy control of the transfection/toxicity ratio by tuning the surface chemistry. It was proved that it is possible, by fine-tuning the nitrogen containing shell, to obtain better transfection/toxicity ratios in vitro.

Kizhakkedathu and coworkers [132] presented a complete study of blood compatibility and DNA binding of PG decorated with PEG chains and tris(2-aminoethyl)amine (Mn 116 kDa, Fig. 14). The scaffolds with different degrees of amine quaternization proved to be highly blood compatible as seen by their insignificant effect on hemolysis, erythrocyte aggregation, complement activation, platelet activation, and coagulation. In comparison to a standard branched PEI (MW 25 kDa), a much lower cytotoxicity of the PG derivatives was observed in mouse neuro-2a (N2a) cell line. At a concentration of 400 mg/mL, only 3% of cells survived in the presence of PEI, whereas cell survival was 81% in the presence of PG-PEG-amine. Although cytotoxicity increases with an increase in the percentage of quaternization, 36% cell viability was still observed in the presence of PG-PEG-amine-100, where all the nitrogen atoms are quarternized. Regarding the DNA binding profile, a high affinity in the nanomolar range was found at low levels of quaternization,

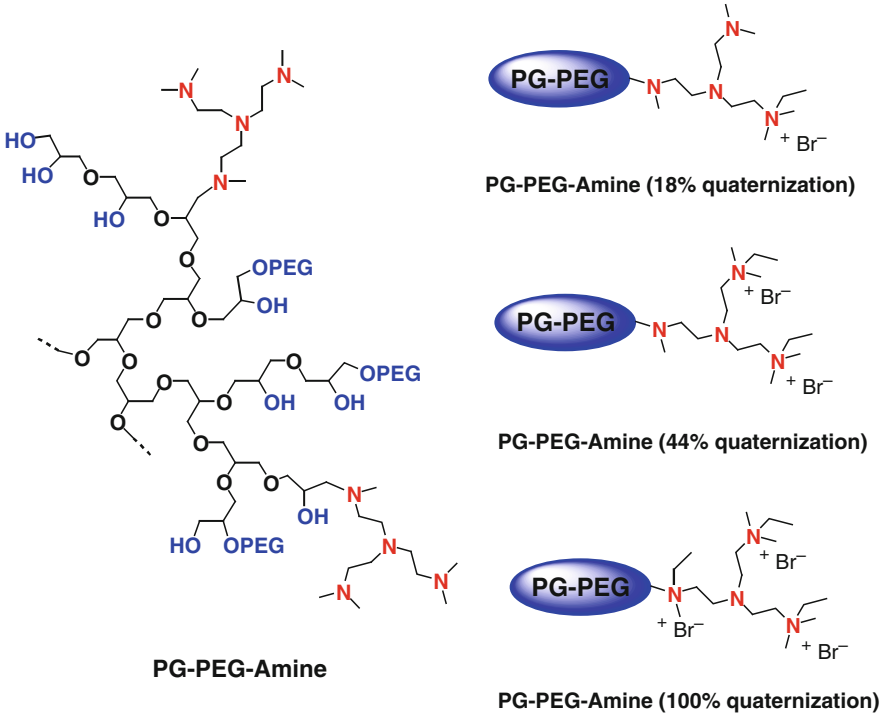

Fig. 14 PG architecture decorated with PEG chains and tris(2-aminoethyl)amine with different degrees of quaternization. Reproduced with permission from [129]. Copyright 2006 Elsevier

comparable to the binding affinities of cationic multivalent dendrimers with much lower biocompatibility [140]. The PG-PEG-amine derivates were able to condense DNA to highly compact, stable, water soluble nanoparticles in the range of 60–80 nm. Gel electrophoresis studies showed that they form electroneutral complexes with DNA around N/P ratio 1, irrespective of the percentage of quaternization.

In a different approach, hyperbranched PG with MW 5 kDa was partially functionalized with quaternary and tertiary ammonium groups with different loading degrees [141]. Partial functionalization of the hyperbranched polyether polyols with 4, 8, and 12 quaternary (6, 11, and 17% molar coverage) or 4 and 21 tertiary ammonium groups (6 and 31% molar coverage) was achieved (Fig. 15). All the polymers showed interaction with DNA and formed neutral polyplexes. The transfection efficiency, which was quantitatively evaluated by luciferase reporter gene assay in human kidney cells, showed that only the quaternized polymers exhibited transfection efficiency, while the introduction of the tertiary amino group on polyglycerol did not improve the transfection of the ineffective parent polymer. The cytotoxicity of the quaternary active derivates (PG-Q-n) was marginal even at high concentrations (90% cell viability was registered for PG-Q-2 and PG-Q-3 at 200 μg/mL which corresponds to the highest weight ratio of 100 employed in the transfection experiments) and it was much lower than PEI (MW 25 kDa) accordingly to the MTT assay. In an attempt to correlate the results obtained from the physicochemical characterization of the PG-Q-n and PG-T-n/pDNA polyplexes, the authors concluded that large compact polyplexes with a slightly positive charge obtained with the quaternized derivates could act as efficient transfection agents. On the other hand, polyplexes with low transfection efficiency formed loose aggregates.

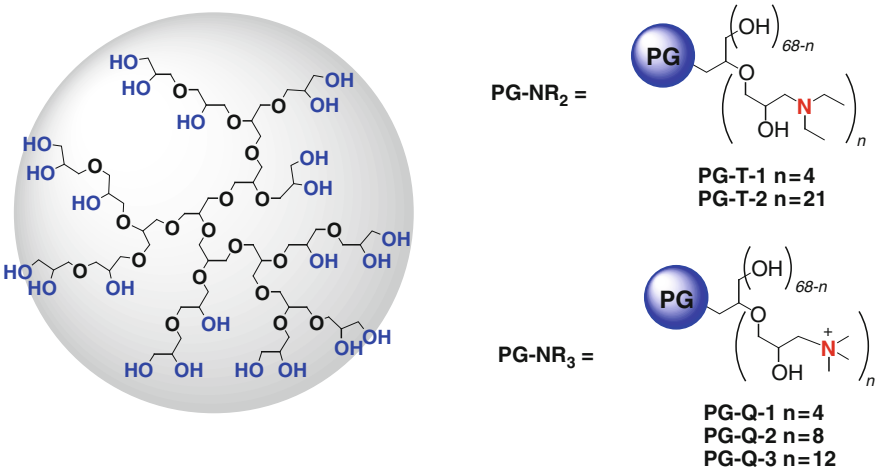

Fig. 15 Hyperbranched PG partially functionalized with quaternary and tertiary ammonium groups with different loading degrees. Reproduced with permission from [130]. Copyright 2008 Elsevier

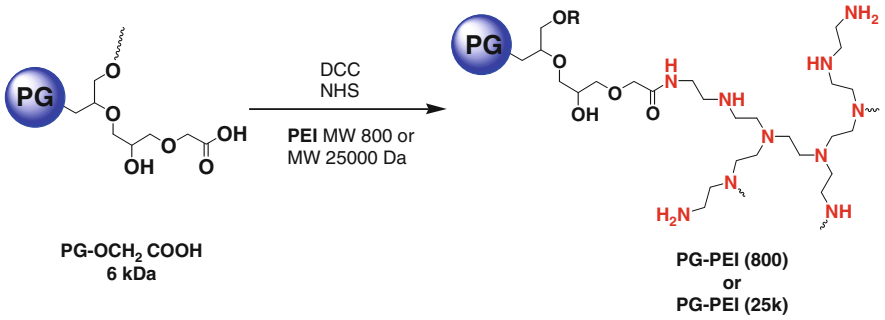

Scheme 7 Synthetic pathway followed for the synthesis of PG–PEI gene vectors. Reproduced with permission from [131]. Copyright 2010 Elsevier

In an attempt to synthesize high molecular weight transfection agents, hyperbranched polyglycerol of MW 6 kDa was used as a linking unit between branched PEI molecules with MW of 800 Da or 25 kDa [142]. The grafting of the PEI units to the hyperbranched polyglycerol cores (Scheme 7) yielded products with narrow polydispersities and molecular weights ranging from 100 to 180 kDa. NMR and SEC analysis showed that each hyperbranched polymer contains several PG cores, with a weight composition ranging from 10% to 20%.

Through agarose gel electrophoresis retardation assay, TEM, and particulate size analysis, PG–PEI (25 k) and PG–PEI (800) were demonstrated to have a capability for DNA binding. The activity of PG6–PEIs to mediate transfection of reporter plasmids pEGFP-C1 and pGL3-Luc was evaluated on 293T and HeLa cell lines. PG6–PEI25k and PG6–PEI800 showed enhanced levels in transgene expression and decreased cytotoxicities compared to PEI25k and PEI800, respectively.

In a recent investigation, our group synthesized novel enzyme-labile core-shell architectures based on hyperbranched polyglycerol (MW 5 kDa) with oligoamine shells [143]. In the core-shell system obtained, the aminated moieties (spermine, spermidine, or pentaethylenehexamine as shown in Fig. 16) were connected to the polyglycerol through a carbazate bond, known to be enzymatic and pH-cleavable. These dendritic polyamine compounds were clearly multivalent in gene complexation as shown by an ethidium bromide displacement assay. The affinity of the individual amine bearing moieties increased significantly after their attachment onto the PG scaffold.

Preliminary cytotoxicity studies showed that the dendritic nanocarriers exhibited a safe profile at the required concentrations for gene transfection. To determine the in vitro activity of the core-shell architectures, the knockdown efficiency of siRNA-polyplexes was studied in cell cultures and compared to HiPerFect® (a benchmark compound used commonly in gene transfection applications) in HeLaS3 cells with siRNAs directed against different mRNAs and leading to expression reduction of the proteins Lamin, CDC2, and MAPK2 (Fig. 17). Amongst the analyzed compounds, the structure bearing pentaethylenehexamine chains (PG-PEHA in Fig. 16) showed comparable silencing efficiency to HiPerFect.

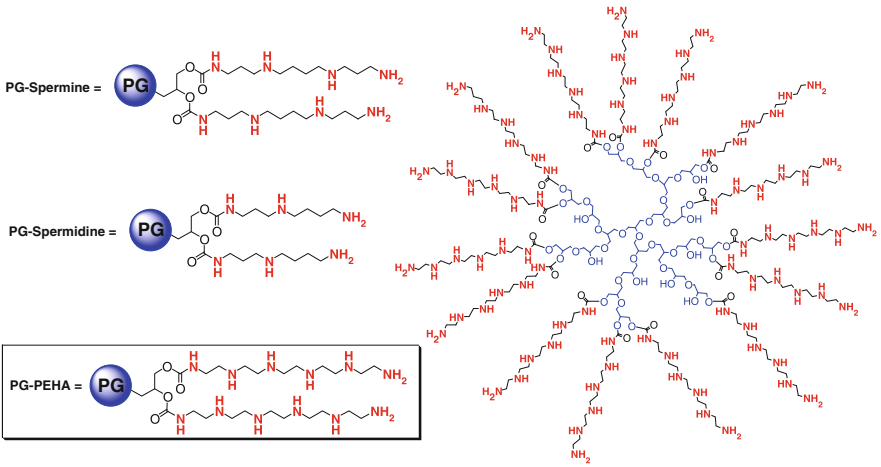

Fig. 16 Abbreviation of the depicted structures of polyglyceryl spermine carbamate (PG-spermine), polyglycerol spermidine carbamate (PG-spermidine), and polyglycerol pentaethylenehexamine (PG-PEHA) and the full structure of PG-PEHA (the depicted structure is a small idealized fragment of the actual polymer)

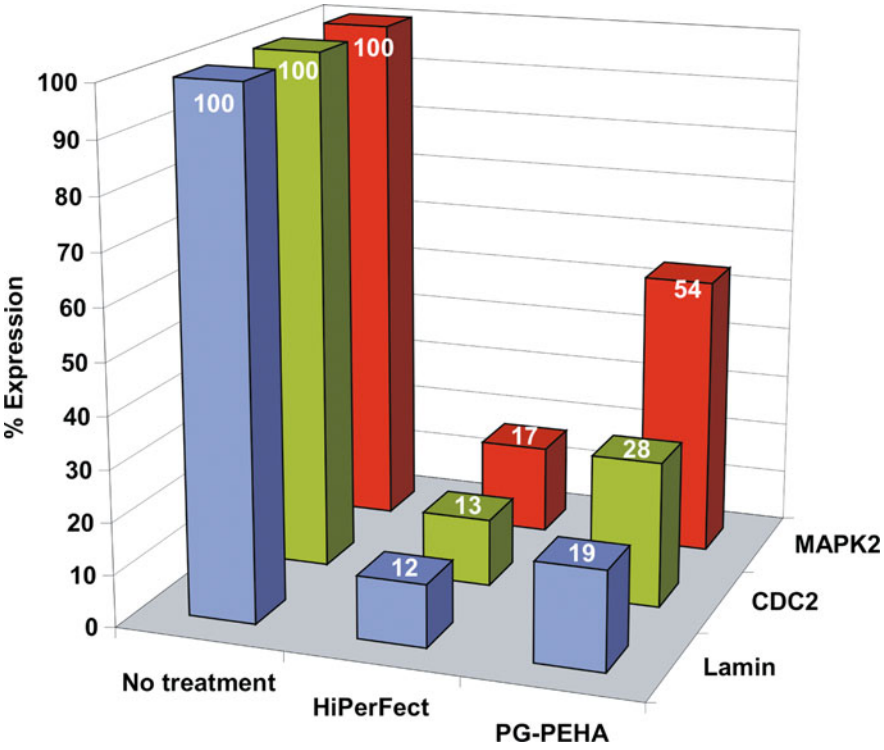

Fig. 17 Transfection efficiencies of PG-PEHA compared with HiPerFect in HeLaS3 cells. siRNAs directed against, Lamin, CDC2, and MAPK2 were used. The expression of the protein without any treatment was set as 100%

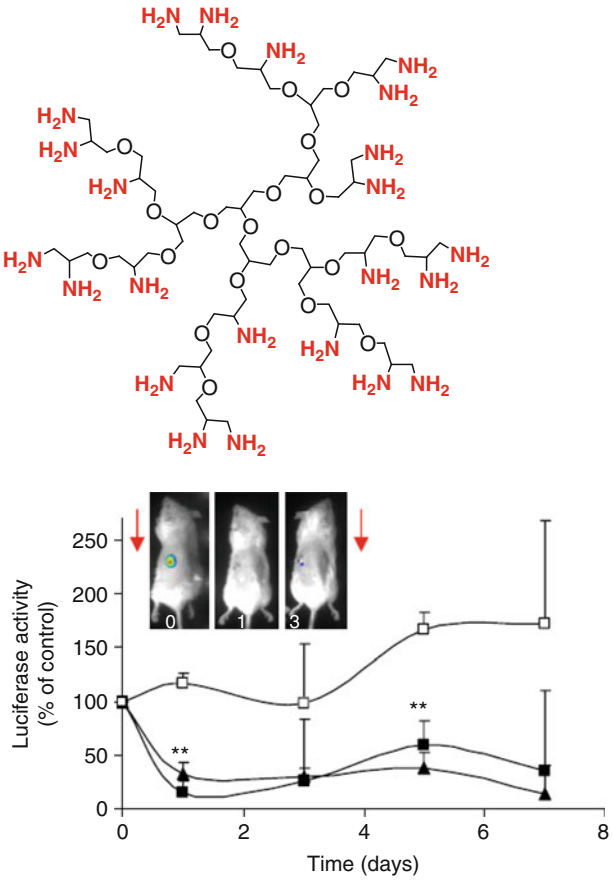

Fig. 18 Idealized fragment of polyglycerolamine (*left*) and SCID mice bearing U87-Luc tumors treated with 10 mg/kg PG-NH_2, complexed with 2.5 mg/kg luciferase siRNA (*filled squares*), 20 mg/kg PG-NH_2, complexed with 5 mg/kg luciferase siRNA (*triangles*), or saline as control (*open squares*)

We recently synthesized hyperbranched polyglycerolamine (PG-NH2) with average MW of 10 kDa (Fig. 18) in an attempt to explore the effects of post-modification of hyperbranched polyglycerol with primary amines in the favorable 1,2-orientation [144]. In a previous study, the polyglycerolamine architecture, which consists of primary amine groups spread all around the polyglycerol structure, has showed promising properties as a prospective system for gene delivery, namely high charge with a relative low cytotoxicity, and an optimal charge/pH behavior so far as the buffering capacity is concerned [139]. Of all the polyglycerol systems analyzed for gene transfection, the hyperbranched polyglycerolamine showed the highest affinity towards DNA fragments, according to the ethidium bromide displacement assay. Complexation of PG-NH_2 with siRNA neutralized the charge and condensed the

supramolecular structures 3–5 nm in size. The polymer was able to complex siRNA yielding slightly positive charged globular polyplexes with heights up of up to 3 nm. The knockdown efficiency of the siRNA-polyplex was comparable to HiPerFect for the proteins Lamin, CDC2, and MAPK2 in HeLAS3 cells. In a comparison of silencing efficiency and cytotoxicity with PEI derivates, the polyglycerolamine architecture showed a better toxicity profile at concentrations relevant for its activity. It was found that the siRNA polyplex it was internalized into glioblastoma cells within 24 h by endosome-lysosome mediated system.

More interestingly, siRNA-PG-amine polyplex was administered intratumorally or intravenously to tumor-bearing mice, resulting in a major silencing effect and no apparent toxicity (Fig. 18). High levels of fluorescently-labeled siRNA were detected in the tumor and not in other healthy organs examined. These findings indicate that PG-NH_2 is an outstanding candidate for in vivo tumor-directed systemic delivery of siRNA.

5 Conclusion

The problems associated with viral gene transfection, such as immune response and limited selectivity, show that the search for non-viral alternatives remains a critical challenge. Nonviral gene delivery carriers, including cationic polymers and lipids, have been studied as alternatives to viral carriers because of their lower cytotoxicity, non-immunogenicity, more convenient handling, and better gene delivery. Among them, dendritic polymers have been utilized and examined in biomedical fields for drug and gene delivery systems because of lower toxicity and particular physicochemical properties than traditional cationic polymers.

The search for an efficient and non-toxic gene transfection vector has led to the design and synthesis of a great variety of macromolecular scaffolds. An extensive analysis of the key features for the efficient and safe delivery of genes in vivo and in vitro has led to the conclusion that hyperbranched polymers are potential candidates for further development. In this chapter we have presented a detailed analysis of the different hyperbranched polymer scaffolds commonly used in gene delivery applications. Several structural modifications toward the development of an optimal gene vector have been analyzed.

The main future directions that can be foreseen given the current progress in structural sophistication is the formation of multi-purpose targeting for genes based on hyperbranched nanocarriers that are capable of carrying out several functions, in particular the targeted delivery of bioactive gene fragments to the site of action. However, there is still a need for in vivo proof of the concept of the potential of such multifunctional systems.

References

1. Mintzer MA, Simanek EE (2009) Chem Rev 109:259
2. Park TG, Jeong JH, Kim SW (2006) Adv Drug Deliv Rev 58:467
3. Yang ZR, Wang HF, Zhao J, Peng YY, Wang J, Guinn BA, Huang LQ (2007) Cancer Gene Ther 14:599
4. Schaffer DV, Lauffenburger DA (1998) J Biol Chem 273:28004
5. Merdan T, Kopecek J, Kissel T (2002) Adv Drug Deliv Rev 54:715
6. Wang JY, Casero RA, Jr. (2006) Polyamine Cell Signaling Physiology, Pharmacology, and Cancer Research. Humana Press Inc., Totowa, NJ
7. Verma IM, Somia N (1997) Nature 389:239
8. Luo D, Saltzman WM (2000) Nat Biotechnol 18:33
9. Li S, Huang L (2000) Gene Ther 7:31
10. Pack DW, Hoffman AS, Pun S, Stayton PS (2005) Nat Rev Drug Discov 4:581
11. Green JJ, Zugates GT, Tedford NC, Huang Y-H, Griffith LG, Lauffenburger DA, Sawicki JA, Langer R, Anderson DG (2007) Adv Mater 19:2836
12. Itaka K, Kanayama N, Nishiyama N, Jang WD, Yamasaki Y, Nakamura K, Kawaguchi H, Kataoka K (2004) J Am Chem Soc 126:13612
13. Minakuchi Y, Takeshita F, Kosaka N, Sasaki H, Yamamoto Y, Kouno M, Honma K, Nagahara S, Hanai K, Sano A, Kato T, Terada M, Ochiya T (2004) Nucleic Acids Res 32: e109
14. Khalil IA, Kogure K, Akita H, Harashima H (2006) Pharmacol Rev 58:32
15. Carmichael GG (2002) Nature 418:379
16. Karmali PP, Chaudhuri A (2007) Med Res Rev 27:696
17. Martin B, Sainlos M, Aissaoui A, Oudrhiri N, Hauchecorne M, Vigneron JP, Lehn JM, Lehn P (2005) Curr Pharm Des 11:375
18. Vijayanathan V, Thomas T, Shirahata A, Thomas TJ (2001) Biochemistry 40:13644
19. Wilson RW, Bloomfield VA (1979) Biochemistry 18:2192
20. Yessine M-A, Lafleur M, Meier C, Petereit H-U, Leroux J-C (2003) Biochim Biophys Acta Biomembr 1613:28
21. Guy J, Drabek D, Antoniou M (1995) Mol Biotechnol 3:237
22. Seymour LW (1992) Crit Rev Ther Drug Carrier Syst 9:135
23. Kim TH, Cooka SE, Arote RB, Cho M-H, Nah JW, Choi YJ, Cho CS (2007) Macromol Biosci 7:611
24. Brissault B, Kichler A, Guis C, Leborgne C, Danos O, Cheradame H (2003) Bioconjug Chem 14:581
25. Sonawane ND, Szoka FC Jr, Verkman AS (2003) J Biol Chem 278:44826
26. Behr JP (1997) Chimica 51:34
27. Thomas TJ, Bloomfield VA (1983) Biopolymers 22:1097
28. Wolff JA, Rozema DB (2008) Mol Ther 16:8
29. Boussif O, Lezoualc'h F, Zanta MA, Mergny MD, Scherman D, Demeneix B, Behr JP (1995) Proc Natl Acad Sci USA 92:7297
30. Dunlap DD, Maggi A, Soria MR, Monaco L (1997) Nucleic Acids Res 25:3095
31. Kichler A, Leborgne C, Coeytaux E, Danos O (2001) J Gene Med 3:135
32. Wightman L, Kircheis R, Rossler V, Carotta S, Ruzicka R, Kursa M, Wagner E (2001) J Gene Med 3:362
33. Kabanov AV, Kabanov VA (1995) Bioconjug Chem 6:7
34. Hartmann L, Häfele S, Peschka-Süss R, Antonietti M, Börner Hans G (2008) Chem Eur J 14:2025
35. Fischer W, Brissault B, Prévost S, Kopaczynska M, Andreou I, Janosch A, Gradzielski M, Haag R (2010) Macromol Biosci accepted
36. Akinc A, Anderson DG, Lynn DM, Langer R (2003) Bioconjug Chem 14:979

37. Esfand R, Tomalia DA (2001) Drug Discov Today 6:427
38. Buhleier E, Wehner W, Vögtle F (1978) Synthesis 155
39. Tomalia DA, Baker H, Dewald J, Hall M, Kallos G, Martin S, Roeck J, Ryder J, Smith P (1985) Polymer Journal 17:117
40. Tomalia DA, Baker E, Dewald J, Hall M, Kallos G, Martin S, Roeck J, Ryder J, Smith P (1986) Macromolecules 19:2466
41. Newkome GR, Yao Z, Baker GR, Gupta VK (1985) J Org Chem 50:2003
42. Fischer M, Vögtle F (1999) Angew Chem Int Ed 38:884
43. Bosman AW, Janssen HM, Meijer EW (1999) Chem Rev 99:1665
44. Frechet JMJ, Tomalia DA (2001) Dendrimers and other dendritic polymers. Wiley, Chichester, p 155
45. Newkome GR, Moorefield CN, Vögtle F (2001) Dendrimers and dendrons: concepts, syntheses, applictions. Wiley-VCH, Weinheim
46. Frechet JM (1994) Science 263:1710
47. Uppuluri S, Keinath SE, Tomalia DA, Dvornic PR (1998) Macromolecules 31:4498
48. Krause W, Hackmann-Schlichter N, Maier FK, Müller R (2000) Top Curr Chem 210:261
49. Stiriba SE, Frey H, Haag R (2002) Angew Chem Int Ed Engl 41:1329
50. Barth RF, Adams DM, Soloway AH, Alam F, Darby MV (1994) Bioconjug Chem 5:58
51. Chen CZ, Beck-Tan NC, Dhurjati P, van Dyk TK, LaRossa RA, Cooper SL (2000) Biomacromolecules 1:473
52. Kojima C, Kono K, Maruyama K, Takagishi T (2000) Bioconjug Chem 11:910
53. Nishiyama N, Stapert HR, Zhang GD, Takasu D, Jiang DL, Nagano T, Aida T, Kataoka K (2003) Bioconjug Chem 14:58
54. Malik N, Wiwattanapatapee R, Klopsch R, Lorenz K, Frey H, Weener JW, Meijer EW, Paulus W, Duncan R (2000) J Control Release 65:133
55. Wiener EC, Brechbiel MW, Brothers H, Magin RL, Gansow OA, Tomalia DA, Lauterbur PC (1994) Magn Reson Med 31:1
56. Chen CZ, Cooper SL (2000) Adv Mater 12:843
57. Lünig U (2000) Nachr Chem 48:134
58. Jansen JF, de Brabander-van den Berg EM, Meijer EW (1994) Science 266:1226
59. Baars MW, Kleppinger R, Koch MH, Yeu SL, Meijer EW (2000) Angew Chem Int Ed Engl 39:1285
60. Stephan H, Spies H, Johannsen B, Kauffmann C, Vögtle F (2000) Org Lett 2:2343
61. Kleij AW, van de Coevering R, Klein Gebbink RJ, Noordman AM, Spek AL, van Koten G (2001) Chemistry 7:181
62. Teobaldi G, Zerbetto F (2003) J Am Chem Soc 125:7388
63. Naylor AM, Goddard WA III, Kiefer GE, Tomalia DA (1989) J Am Chem Soc 111:2339
64. Kim YH, Webster OW (1990) J Am Chem Soc 112:4593
65. Stevelmans S, van Hest JCM, Jansen JFGA, van Boxtel DAFJ, de Brabander-van den Berg EMM, Meijer EW (1996) J Am Chem Soc 7398
66. Chechik V, Zhao M, Crooks RM (1999) J Am Chem Soc 121:4910
67. Pistolis G, Malliaris A, Tsiourvas D, Paleos CM (1999) Chem Eur J 5:1440
68. Schmitzer A, Perez E, Rico-Lattes I, Lattes A, Rosca S (1999) Langmuir 15:4397
69. Chen S, Yu Q, Li L, Boozer CL, Homola J, Yee SS, Jiang S (2002) J Am Chem Soc 124:3395
70. Kojima C, Haba Y, Fukui T, Kono K, Takagishi T (2003) Macromolecules 36:2183
71. Sideratou Z, Tsiourvas D, Paleos CM (2000) Langmuir 16:1766
72. Ghosh SK, Kawaguchi S, Jinbo Y, Izumi Y, Yamaguchi K, Taniguchi T, Nagai K, Koyama K (2003) Macromolecules 36:9162
73. Gillies ER, Fréchet JMJ (2005) Drug Discovery Today 10:35
74. Luger K, Mader AW, Richmond RK, Sargent DF, Richmond TJ (1997) Nature 389:251
75. Joester D, Losson M, Pugin R, Heinzelmann H, Walter E, Merkle HP, Diederich F (2003) Angew Chem Int Ed Engl 42:1486
76. Uyemura M, Aida T (2002) J Am Chem Soc 124:11392

77. Hecht S, Fréchet JMJ (2001) Angew Chem Int Edit 40:74
78. Tomalia DA, Dewald JR (1985) U.S. Patent 4 507 466
79. Tomalia DA, Dewald JR (1986) U.S. Patent 4 568 737
80. Haensler J, Szoka FC Jr (1993) Bioconjug Chem 4:372
81. Vlasov GP, Korol'kov VI, Pankova GA, Tarasenko I, Baranov AN, Glazkov PB, Kiselev AV, Ostapenko OV, Lesina EA, Baranov VS (2004) Bioorg Khim 30:15
82. Service RF (2003) Science 300:243
83. Nel A, Xia T, Madler L, Li N (2006) Science 311:622
84. Guillot-Nieckowski M, Joester D, Stohr M, Losson M, Adrian M, Wagner B, Kansy M, Heinzelmann H, Pugin R, Diederich F, Gallani JL (2007) Langmuir 23:737
85. Gebhart CL, Kabanov AV (2001) J Control Release 73:401
86. Tang MX, Redemann CT, Szoka FC Jr (1996) Bioconjug Chem 7:703
87. Jikei M, Kakimoto M (2001) Prog Polym Sci 26:1233
88. Lyulin AV, Adolf DB, Davies GR (2001) Macromolecules 34:3783
89. Roller S, Zhou H, Haag R (2005) Mol Divers 9:305
90. Haag R, Sunder A, Hebel A, Roller S (2002) J Comb Chem 4:112
91. Krämer M, Stumbé JF, Grimm G, Kaufmann B, Krüger U, Weber M, Haag R (2004) Chembiochem 5:1081
92. Wörner C, Mülhaupt R (1993) Angew Chem 105:1367
93. De Brabander-Van Den Berg M, Meijer EW (1993) Angew Chem Int Ed 32:1308
94. Moors R, Vögtle F (1993) Chem Ber 126:2133
95. Fischer D, von Harpe A, Kunath K, Petersen H, Li Y, Kissel T (2002) Bioconjug Chem 13:1124
96. von Harpe A, Petersen H, Li Y, Kissel T (2000) J Control Release 69:309
97. Dick CR, Ham GE (1970) J Macromol Sci A Pure Appl Chem 4:1301
98. Dick CR, Potter JL, Coker WP (1971) US Patent 3 565 941
99. Horn D, Linhart F (1991) In: Roberts JC (ed) Paper chemistry. Blackie, London, p 44
100. Frey H, Haag R, Buschow KHJ, Robert WC, Merton CF, Bernard I, Edward JK, Subhash M, Patrick V (2001) Encyclopedia of materials: science and technology. Elsevier, Oxford, p 3998
101. Kobayashi S, Hiroishi K, Tokunoh M, Saegusa T (1987) Macromolecules 20:1496
102. Fischer D, Bieber T, Youxin L, Elsässer H-P, Kissel T (1999) Pharm Res 16:1273
103. Kunath K, von Harpe A, Fischer D, Petersen H, Bickel U, Voigt K, Kissel T (2003) J Control Release 89:113
104. Allen TM, Cullis PR (2004) Science 303:1818
105. Petersen H, Fechner PM, Martin AL, Kunath K, Stolnik S, Roberts CJ, Fischer D, Davies MC, Kissel T (2002) Bioconjug Chem 13:845
106. Mao S, Neu M, Germershaus O, Merkel O, Sitterberg J, Bakowsky U, Kissel T (2006) Bioconjug Chem 17:1209
107. Liang B, He M-L, Chan C-y, Chen Y-c, Li X-P, Li Y, Zheng D, Lin MC, Kung H-F, Shuai X-T, Peng Y (2009) Biomaterials 30:4014
108. Baker JR Jr (2009) Hematology 2009:708
109. Putnam D, Langer R (1999) Macromolecules 32:3658
110. Reul R, Nguyen J, Kissel T (2009) Biomaterials 30:5815
111. Lim YB, Han SO, Kong HU, Lee Y, Park JS, Jeong B, Kim SW (2000) Pharm Res 17:811
112. Lim Y, Choi YH, Park JS (1999) J Am Chem Soc 121:5633
113. Forrest ML, Koerber JT, Pack DW (2003) Bioconjug Chem 14:934
114. Lee JH, Lim YB, Choi JS, Lee Y, Kim TI, Kim HJ, Yoon JK, Kim K, Park JS (2003) Bioconjug Chem 14:1214
115. Luo D, Haverstick K, Belcheva N, Han E, Saltzman WM (2002) Macromolecules 35:3456
116. Wang X, He Y, Wu J, Gao C, Xu Y (2009) Biomacromolecules 11:245
117. Dennig J, Duncan E (2002) Rev Mol Biotechnol 90:339
118. Chen J, Wu C, Oupicky D (2009) Biomacromolecules 10:2921

119. Inoue Y, Kurihara R, Tsuchida A, Hasegawa M, Nagashima T, Mori T, Niidome T, Katayama Y, Okitsu O (2008) J Control Release 126:59
120. Voit B (2000) J Polym Sci A Polym Chem 38:2505
121. Meister A, Anderson ME (1983) Annu Rev Biochem 52:711
122. Lynn DM, Langer R (2000) J Am Chem Soc 122:10761
123. Li X, Su Y, Chen Q, Lin Y, Tong Y, Li Y (2005) Biomacromolecules 6:3181
124. Zhong Z, Song Y, Engbersen JF, Lok MC, Hennink WE, Feijen J (2005) J Control Release 109:317
125. Luten J, van Nostrum CF, De Smedt SC, Hennink WE (2008) J Control Release 126:97
126. Lim Y-b, Kim S-M, Lee Y, Lee W-k, Yang T-g, Lee M-j, Suh H, Park J-s (2001) J Am Chem Soc 123:2460
127. Wu D, Liu Y, Jiang X, Chen L, He C, Goh SH, Leong KW (2005) Biomacromolecules 6:3166
128. Arote RB, Lee E-S, Jiang H-L, Kim Y-K, Choi Y-J, Cho M-H, Cho C-S (2009) Bioconjug Chem 20:2231
129. Haag R, Kratz F (2006) Angew Chem Int Ed Engl 45:1198
130. Frey H, Haag R (2002) J Biotechnol 90:257
131. Calderón M, Quadir MA, Sharma SK, Haag R Advanced Materials 22:190
132. Kainthan RK, Gnanamani M, Ganguli M, Ghosh T, Brooks DE, Maiti S, Kizhakkedathu JN (2006) Biomaterials 27:5377
133. Kainthan RK, Hester SR, Levin E, Devine DV, Brooks DE (2007) Biomaterials 28:4581
134. Kainthan RK, Brooks DE (2007) Biomaterials 28:4779
135. Kainthan RK, Mugabe C, Burt HM, Brooks DE (2008) Biomacromolecules 9:886
136. Xu S, Luo Y, Graeser R, Warnecke A, Kratz F, Hauff P, Licha K, Haag R (2009) Bioorg Med Chem Lett 19:1030
137. Calderón M, Graeser R, Kratz F, Haag R (2009) Bioorg Med Chem Lett 19:3725
138. Kolhe P, Khandare J, Pillai O, Kannan S, Lieh-Lai M, Kannan R (2004) Pharm Res 21:2185
139. Khandare J, Mohr A, Calderón M, Welker P, Licha K, Haag R Biomaterials 31:4268
140. Ganguli M, Jayachandran KN, Maiti S (2004) J Am Chem Soc 126:26
141. Tziveleka LA, Psarra AM, Tsiourvas D, Paleos CM (2008) Int J Pharm 356:314
142. Zhang L, Hu C-H, Cheng S-X, Zhuo R-X (2009) Colloids and Surfaces B: Biointerfaces 76:427
143. Fischer W, Calderón M, Schulz A, Andreou I, Weber W, Haag R submitted
144. Ofek P, Fischer W, Calderon M, Haag R, Satchi-Fainaro R FASEB J.: fj.09

Top Curr Chem (2010) 296: 131–190
DOI: 10.1007/128_2010_68

Published online: 11 June 2010

Carbohydrate Polymers for Nonviral Nucleic Acid Delivery

Antons Sizovs*, Patrick M. McLendon*, Sathya Srinivasachari, and Theresa M. Reineke

Abstract Carbohydrates have been investigated and developed as delivery vehicles for shuttling nucleic acids into cells. In this review, we present the state of the art in carbohydrate-based polymeric vehicles for nucleic acid delivery, with the focus on the recent successes in preclinical models, both *in vitro* and *in vivo*. Polymeric scaffolds based on the natural polysaccharides chitosan, hyaluronan, pullulan, dextran, and schizophyllan each have unique properties and potential for modification, and these results are discussed with the focus on facile synthetic routes and favorable performance in biological systems. Many of these carbohydrates have been used to develop alternative types of biomaterials for nucleic acid delivery to typical polyplexes, and these novel materials are discussed. Also presented are polymeric vehicles that incorporate copolymerized carbohydrates into polymer backbones based on polyethylenimine and polylysine and their effect on transfection and biocompatibility. Unique scaffolds, such as clusters and polymers based on cyclodextrin (CD), are also discussed, with the focus on recent successes *in vivo* and in the clinic. These results are presented with the emphasis on the role of carbohydrate and charge on transfection. Use of carbohydrates as molecular recognition ligands for cell-type specific delivery is also briefly

*both authors contributed equally to this review.

A. Sizovs and T.M. Reineke (✉)
Department of Chemistry, Macromolecules and Interfaces Institute, Virginia Polytechnic Institute and State University, Blacksburg, VA24060, USA
e-mail: treineke@vt.edu

S. Srinivasachari
Department of Chemistry, University of Cincinnati, Cincinnati, OH 45229, USA
Institute for Stem Cell Biology and Regenerative Medicine, Bangalore, India

P.M. McLendon
Department of Chemistry, Macromolecules and Interfaces Institute, Virginia Polytechnic Institute and State University, Blacksburg, VA24060, USA
Department of Molecular Cardiovascular Biology, Cincinnati Children's Hospital Medical Center, Cincinnati, OH 45228, USA

reviewed. We contend that carbohydrates have contributed significantly to progress in the field of *non-viral* DNA delivery, and these new discoveries are impactful for developing new vehicles and materials for treatment of human disease.

Keywords Carbohydrate · DNA · Nucleic acid delivery · polysaccharide · Transfection

Contents

Abbreviations

APC	Antigen-presenting cell
apoB	Apolipoprotein B
ASF	Asialofetuin
ASGP	Asialoglycoprotein receptor
AS-ODN	Antisense oligodeoxynucleotide
CD	Cyclodextrin
CDI	1,1'-Carbonyldiimidazole
CDP	Cyclodextrin-containing polycations
CPP	Cell penetrating peptide
DCC	*N,N'*-Dicyclohexylcarbodiimide
DDMC	2-Diethyl-aminoethyl–dextran–methyl methacrylate graft copolymer
DEAE	2-Diethyl-aminoethyl
DMEM	Dulbecco's Modified Eagle Medium
EDC	1-Ethyl-3-(3-dimethyl amino)propyl carbodiimide
EtiBr	Ethidium bromide
HA	Hyaluronic acid
IL	Interleukin
N4C3	Tripropylenetetramine
NHS	*N*-Hydroxysuccinimide

NPC	Non-parenchymal
PAMAM	Polyamidoamine
PBS	Phosphate buffered saline
PC	Parenchymal
PDGF	Platelet-derived growth factor
PEG	Poly(ethylene glycol)
PEI	Polyethylenimine
PGP	PEGylated glycopeptide
PLGA	Poly(lactide-*co*-glycolide)
PLL	Poly-L-lysine
PO-DNA	Phosphodiester-DNA
poly(A)	Polyadenine
poly(C)	Polycytosine
poly(dA)	Polydeoxyadenine
poly(dT)	Polydeoxythymine
PS-DNA	Phosphorothioate-DNA
PVP	Poly(vinylpyrrolidone)
R8	Octaarginine
RGD	Arginine-glycine-aspartic acid
SMC	Smooth muscle cell
SPG	Schizophyllan
TNF	Tumor necrosis factor

1 Introduction

Nucleic acids have broad potential for use in human therapeutics. The completion of the Human Genome Project has brought the promise of nucleic acid-based drugs to treat a myriad of acquired and inherited human diseases, including HIV, cancer, cystic fibrosis, rheumatoid arthritis, asthma, cardiovascular disease, and neurodegenerative disorders [1–3]. As nucleic acids are large, charged molecules and susceptible to enzymatic degradation, a delivery vehicle is required to condense the polynucleotide into a compact structure which protects it from degradation and facilitates its cellular internalization. Past and present delivery vehicle technology has been centered about the genetically-engineered virus as a means of nucleic acid delivery. Viral vectors have demonstrated successful gene transfer *in vivo* due to their innate cellular internalization and gene transduction capabilities, and many viral vectors have progressed into the clinic [4, 5]. However, the widespread applicability of viral vehicles is tempered by the potential to elicit unpredictable immune responses and their relative difficulty of manufacture [6, 7]. The potential clinical pitfalls of viral-based nucleic acid delivery have spurred a broad research focus devoted to developing non-viral delivery systems that allows similar gene transduction capacities but have reduced potential for toxicity.

Synthetic materials for nucleic acid condensation can offer marked improvement over viral delivery. Materials can be designed for high nucleic acid loading capacity, cell-specific targeting through chemical conjugation of molecular recognition elements, and biocompatibility, and are better suited to scale up for mass production. These materials are typically cationic, and may contain primary, secondary, and tertiary amines that can be protonated at physiological pH, which is necessary for electrostatic binding with the negatively-charged phosphate groups on the DNA backbone. This cooperative binding event and polycation charge neutralization facilitates compaction of the polymer nucleic acid complexes into small colloidal nanoparticles (termed polyplexes) [8, 9]. Structures such as branched and linear polyethylenimine (PEI) [9–11], poly-L-lysine (PLL) [12–14], spermine [15, 16], and polyamidoamine (PAMAM) [5, 17–19] can bind nucleic acids quite well and have been developed for DNA delivery with varied success. A fine, detailed review of non-viral delivery has been published recently [20]. However, these charge-dense polycations have demonstrated toxicity [4, 8, 21]; thus, design of a nontoxic analog is key to development of a suitable vehicle for human therapy.

Using carbohydrates in nucleic acid delivery is an obvious choice for improving toxicity. Carbohydrates are naturally-available unique scaffolds that have been exploited by synthetic chemists for materials design. Structural features, such as the presence of an anomeric carbon, multiple hydroxyl groups, cyclic structures, and chirality are advantageous for designing biomacromolecules [22–25]. In addition, carbohydrates are readily available, renewable resources; inexpensive materials for introducing hydrophilicity and biocompatibility into polymeric systems. These facets have led to their use in developing novel sustainable materials for biomedical applications [26, 27].

Glycopolymers have broadened the scope of nucleic acid delivery research, as many novel saccharide-based materials have been developed and analyzed for favorable nucleic acid delivery and toxicity profiles. This review provides critical perspective on the progress and favorable results of carbohydrate-based vehicles in nucleic acid delivery. We have focused on glycopolymeric delivery systems, including those derived from pure carbohydrates (chitosan, hyaluronan, pullulan, schizophyllan, dextran, and cyclodextrin) as well as carbohydrate comonomers incorporated into a polymer backbone. Carbohydrates have also been used as molecular recognition elements for targeting receptor-mediated endocytosis and have been conjugated as pendent groups for recognition by cell-surface lectins. Polymers incorporating carbohydrate-mediated targeting will be discussed; however, a full discussion of their use in targeting is beyond the scope of this review.

2 Natural Polysaccharides as Nucleic Acid Delivery Scaffolds

Polysaccharides are complex carbohydrates possessing high structural diversity. They are composed of several monosaccharide units joined together through glycosidic bonds. Typically, polysaccharides are isolated from a natural source,

prepared via ring-opening polymerization of anhydro sugars or synthesized by enzymatic polymerization, which provides stereo-control over the polysaccharides synthesized, even at high molecular weight [28]. The natural polysaccharides, such as dextran [29], schizophyllan [30], chitosan [31], hyaluronan [32], and pullulan [33] have all been studied as nucleic acid carriers, and the following section highlights significant recent findings with these polysaccharides.

2.1 Dextran

Dextrans are biodegradable homopolymers of glucose with predominantly α-(1→6) linkages with some branching via α-(1→3) linkage which vary depending on the source of dextran. They are synthesized from sucrose by the action of bacteria, such as *Streptococcus mutans* or *Leuconostoc mesenteroides*. The first report of polycation-mediated DNA complexation was published in 1965 on 2-diethyl-aminoethyl (DEAE)-dextran, synthesized from diethyleaminoethyl chloride and dextran [34]. This study was an important milestone in this area because it was the first published example of a non-viral polysaccharide nucleic acid carrier. These vehicles continue to be investigated. The cationic nature of DEAE-dextran enables it to complex effectively with nucleic acids of various types and sizes [29].

About three decades after these first studies, Mack and coworkers [35] used DEAE-dextran to transfect primary cultured human macrophages. Macrophages play a pivotal role in regulating immune response and gene expression and, hence, transfection experiments performed in this study were both interesting and challenging, as macrophages are difficult to transfect. Reproducible luciferase expression was observed with DEAE-dextran, as opposed to with liposome delivery or electroporation. The addition of 100 or 400-μM concentrations of chloroquine also was not seen to enhance gene expression, suggesting that DEAE-dextran particles were not sequestered in endosomes. However, the presence of serum in the transfection medium reduced transgene expression by 60%.

Onishi et al. [36] grafted DEAE-dextran with methyl methacrylate (DDMC), with the hypothesis that methyl methacrylate graft chains could protect the complex from degradation by dextranases present in the cytoplasm, resulting in increased transfection efficiency and decreased cytotoxicity. Transfection experiments were completed in human embryonic kidney (HEK293) cells in serum-containing media. The results showed a fivefold increase in transgene expression with DDMC polyplexes compared with DEAE-dextran polyplexes, supporting the authors' hypothesis. In addition, the cytotoxicity was shown to be reduced by DDMC grafting during these experiments.

Cationic dextrans (40 kDa) were synthesized by Azzam et al. through conjugation with a variety of oligoamines, including spermine and spermidine [37, 38]. An ethidium bromide exclusion assay (qualitative assay for binding affinity) revealed that the dextran-spermine conjugates bound DNA more strongly than other oligoamine derivatives. Transfection efficiency experiments in NIH3T3 and HEK293 cells showed high gene expression in serum-free media, similar to the positive

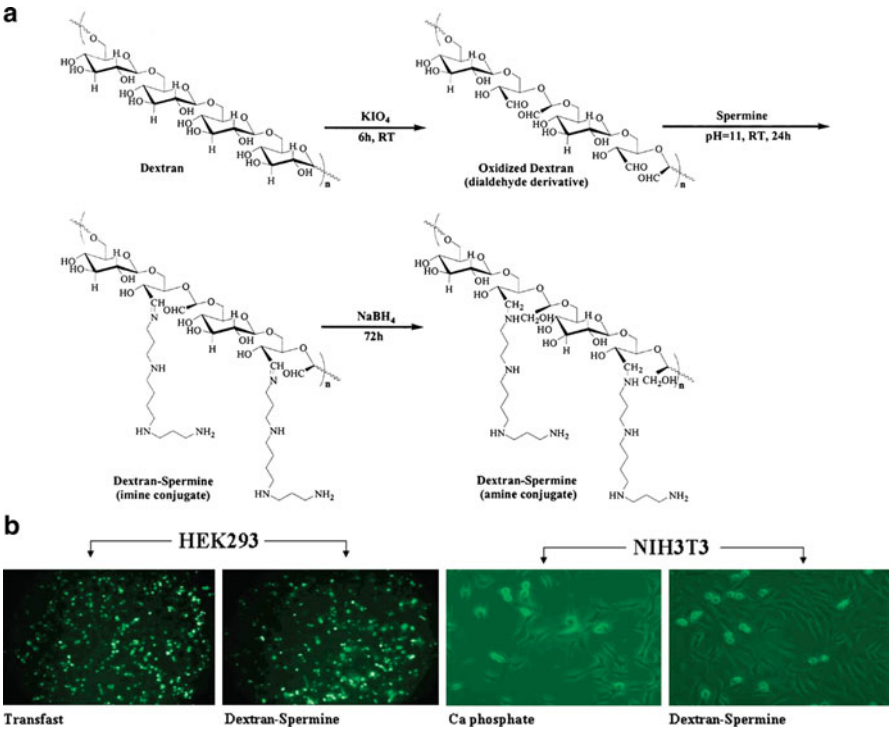

Fig. 1 (**a**) Synthesis of dextran-spermine conjugates. (**b**) Fluorescence micrographs of dextran-spermine compared to common transfection reagents in HEK293 and NIH3T3 cells. Adapted with permission from [38]. © 2002 American Chemical Society

controls Transfast and DOTAP/Chol (1/1), and much enhanced from calcium phosphate (Fig. 1). The most efficacious vehicles were 6–8 kDa in molecular weight, with a spermine content of 2 μmol/mg and 25–30% branching. Unfortunately, a reduction in gene expression was noted with a similar experiment in serum-containing media. To improve the transfection in serum, Hosseinkhani et al. [39] synthesized a poly(ethylene glycol) (PEG)-containing dextran-spermine conjugate (G7TA141) and three dextran-based spermine conjugates (G7TA103, G7TA107, and G7TA141). When NIH3T3 cells were transfected with these PEGylated vectors in NIH3T3 cells in serum-containing media, they showed higher luciferase expression than their nonPEGylated counterparts, with maximum gene expression observed at a polycation:DNA weight ratio of 5:1. Intramuscular injection of PEGylated G7TA141 in mice at a 5:1 weight ratio (polyplexes dosed at a pDNA dose of 50 μg/mouse) revealed a higher level of transgene (β-galactosidase) expression in mouse muscle than naked pDNA or pDNA complexed with the non-PEGylated analog. Gene expression in the liver was monitored for mice dosed with complexes prepared with dextran-spermine conjugates modified with different levels of PEG conjugation. The results indicated the highest level of β-galactosidase expression in the liver resulted from the 5% PEGylated complexes noted

2 days post-injection. These results demonstrated that delivery in serum-containing media can be improved through PEGylation strategies and elicit favorable results in animal models.

Further *in vivo* studies with dextran-spermine conjugates have been explored recently by Eliyahu et al. [40, 41]. The efficacy of local and systemic delivery in mice was assessed through intramuscular (i.m.) and intranasal (i.n.) injections, respectively. Efficacy, measured by X-gal expression in paraffin-embedded tissue sections, was observed primarily in lung tissue (bronchial epithelial cells, pneumocytes, and alveoli), fibrocytes in the skeletal muscle, and hepatocytes. X-gal expression was higher in each organ when pDNA was delivered by the cationic dextran compared to pDNA only. In comparison, lipoplex (DOTAP/cholesterol lipoplexes) injections resulted in expression only at the site of injection, with distant sites such as liver not being transfected, an observation that did not change with increased lipoplex dosing. Upon histopathological assessment of toxicity, mild inflammation and necrosis were observed in the skeletal muscle, but no toxic effects were seen locally in the lung or liver tissue when pDNA was delivered by dextrans. Systemic toxicity was also low, as injections of polyplex or free polymer showed little effect on organ weight, white blood cell and platelet counts, and serum transaminase levels [41]. PEGylation of spermine-dextran conjugates and decrease in spermine content resulted in lower transgene expression. Systemic transfection of PEGylated dextrans was not dose dependent, since increasing the dose from 6 to 40 μg DNA did not increase transgene expression. This series of initial studies demonstrate the promise of DEAE-dextran as a non-viral delivery vehicle; it remains a promising delivery platform.

Additional recent work has focused on developing dextrans into functional hydrogels for effective delivery of nucleic acids. Singh et al. developed hydrogels containing crosslinked dextran vinyl sulfone and tetra-functional PEG thiols encapsulating siRNA/pDNA-loaded microparticles and dendritic cell chemoattractants for the dual delivery of chemokines and nucleic acids [42]. The chemoattractants were encapsulated in degradable microspheres composed of poly(lactide-*co*-glycolide) (PLGA); the siRNA is also encapsulated in PLGA and functionalized with PEI before addition of pDNA. Hydrogels were crosslinked in situ via Michael-type addition reactions, and the dextran vinyl sulfone and PEG components were mixed to form hydrogels. The stoichiometry of the components was varied to control the crosslinking density, which can impact the release rate of the microparticles. These materials were nontoxic in multiple cell lines *in vitro* and exhibited slow release of chemokine from 30% dextran/10% PEG hydrogels. These hydrogels released 70% of encapsulated chemokine after 72 h, indicating that sustained drug release is possible. In primary antigen-presenting cells (APCs), chemokine-induced dendritic cell migration was observed, as well as siRNA-induced knockdown of IL-3. These promising results show that dextran can be used in functional material design for sustained release of drugs and nucleic acids.

Other promising work describing DNA delivery with dextrans has been published recently from the Fréchet laboratory [43]. Acetal-derivatized dextran was solvent evaporated to form dextran nanoparticles which are cleavable under acidic pH [44]. Exploiting the reducing chain ends present on the carbohydrate particles,

the authors used alkoxyamine-terminated poly(arginine), commonly referred to as a cell penetrating peptide (CPP) for its purported ability to penetrate cell membranes transiently, to introduce CPP onto the dextran particles through formation of oxime linkages. Using CPP-derivatized dextran particles (containing 20% poly(β-amino ester) polymer) encapsulating a pDNA encoding luciferase, they attained a 60-fold increase in luciferase expression in HeLa cells compared to unmodified particles [43]. These results demonstrate the broad applicability and the future use of dextran in nucleic acid delivery.

2.2 *Schizophyllan*

Schizophyllans (SPGs) are naturally-occurring water soluble polysaccharides that are produced by the fungus *Schizophyllan commune*. SPG belongs to the family of β-(1→3) glucans, and it has one branch through β-(1→6)-D-glucosyl linkage per three glucose units (Fig. 2). The safety of these materials has been well demonstrated, as they have been used as adjuvants for over two decades in drug formulations and in treatment of gynecological cancer [46, 47].

In water, SPG exists as a thermodynamically stable triple-helix (Fig. 2) held together by hydrogen bonds. Under special conditions these hydrogen bonds can be broken; for further discussion, it is important to know that, in DMSO, schizophyllan dissociates and exists as a single randomly-coiled chain, but it will re-associate into triple helices upon dilution with water.

The Sakurai lab has reported that SPG can form complexes with polycytosine (poly (C)) and polyadenine (poly(A)) [48]. Shortly thereafter, they reported that polydeoxyadenine (poly(dA)) and polydeoxythymine (poly(dT)) can form such complexes

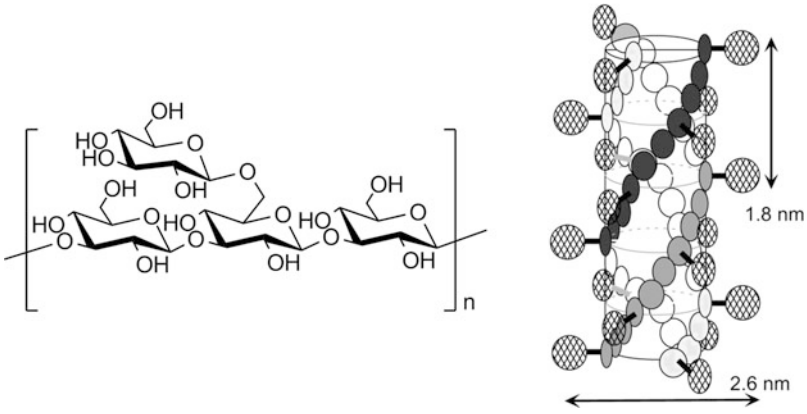

Fig. 2 Structure of schizophyllan repeat unit and a schematic representation of the triple helix formed in aqueous solution. Figure adapted with permission from [45]. © 2003 Elsevier

with SPG as well [49]. It was also noted that none of these homopolynucleotides form supramolecular structures on their own and, instead, exist in solutions as single chains, thus not self-assembling via hydrogen bond formation. This seems to be a necessary requirement, as other homopolynucleotides (e.g., polyuracil) which form intermolecular and/or intramolecular bonds in solution do not form complexes with SPG. The structure of SPG–polynucleotide complexes is not yet completely clear. Sakurai proposed, based on circular dichroism studies, the SPG–polynucleotide complex is a hetero-triplex similar to the original SPG-triplex, with one of the schizophyllan chains being replaced by one homopolynucleotide chain [49]. Additionally, the complex will form only with single-stranded SPG. Both of these statements were recently challenged [50], as it was shown that SPG–poly(C) complex can be formed with triplex-SPGs that have been previously denatured and renatured, and these complexes have identical melting temperatures to ones that are formed with a single-stranded SPGs. This newer approach allows one to prepare SPG–polynucleotide polyplexes in more physiologically relevant conditions – since no use of DMSO is required – but complex stoichiometry will likely be different.

Since schizophyllan can form complexes only with single stranded *homo*polynucleotides, this polynucleotide fragment must be incorporated into DNA/RNA that is used for delivery. Nonetheless, it was demonstrated that such polynucleotides can be efficiently complexed with SPG and be protected from degradation by nucleases within the complex [51], as well as act as an antisense inhibitor of a complementary mRNA in cell-free media [52]. It was concluded that, in order to retain its silencing function, the single stranded antisense oligodeoxynucleotide (AS-ODN) must have stronger affinity toward target mRNA than SPG. This effect was confirmed by Koumoto et al. who demonstrated that the presence of the ss-homopolynucleotide complementary to the one complexed inside SPG·DNA and SPG·RNA polyplex is sufficient to induce release of the cargo [53].

For the complexation of double-stranded DNA, a more elaborate polynucleotide morphology has been designed via the introduction of homopolynucleotide sequences on the ends for SPG binding [54]. Poly(dA) 80-mer was introduced at both ends of DNA, forming loops which provide protection from degradation by endonucleases, an approach adopted from viruses.

It is possible to avoid incorporation of homopolynucleotide by using ternary complexes between polynucleotide, SPG, and polycation. It was recently demonstrated that such ternary complexes can be prepared with PEI and cationic cellulose (quaternized nitrogen is a charged functional group in cationic cellulose) [55]. However, this kind of approach is a step away from the non-cationic nature of schizophyllan-based delivery systems and will not be discussed here.

Soon after the discovery of the ability of SPG to complex homopolynucleotides, it was demonstrated that schizophyllan complexes with poly(A) or poly(C) will dissociate at pH 4–6 [45]. This property is important as SPG polyplexes could potentially release their polynucleotide cargo in the acidic pH environment of endosomes and/or lysosomes. However, since these polyplexes possess a net negative charge and lack targeting groups, they are inefficient in terms of cellular internalization.

In initial attempts to improve SPG as a nucleic acid delivery vehicle, lactose and mannose were incorporated in schizophyllan by chemical modification of branching glucose units [51, 56]. The chemical modification is chemoselective to the branched glucose units on the main polymer backbone, such that the polymer backbone remains intact. Oxidation by periodate ion requires hydroxyl groups to be vicinal, and that is why the oxidation of schizophyllan main chain is avoided. Aldehydes formed in this step are good handles to be used in further modification, which, as we shall see further, mostly involve reductive amination. Furthermore, these modifications do not interfere with the ability of SPG to form triple-helices and polyplexes. Mannose- and lactose-modified SPGs were demonstrated to protect homopolynucleotides poly(C) and poly(dA) from degradation, and these targeted polyplexes were able to bind to corresponding lectins. It is not clear if similar protection and recognition by receptors can be achieved in the case of AS-ODNs, since data for such experiments was not presented, but *in vitro* studies demonstrated that lactose-functionalized SPG deliver antisense oligonucleotide to HepG2 cells. Phosphorothioate AS-ODN that would suppress mRNA of *c-myb*, a proto oncogene that causes cancer when overexpressed, was used. The antisense effect was 10% higher for SPG-mediated delivery and 40% higher for lactose-SPG-mediated delivery compared to naked AS-ODN at 30 μg/mL; it was 10% and 45% higher, respectively, at 60 μg/mL. The delivery efficiency was decreased for lactose-SPG-mediated delivery, but not for SPG-mediated delivery, in the presence of galactose; however, a large concentration of galactose – 20 mM – was used to demonstrate the specificity.

An analogous strategy was used for grafting SPG with folic acid (FA) and, as in the previously-described study, SPG–FA was used for the delivery of phosphorothioate AS-ODN that would suppress *c-myb* [47]. This time it was noted that after grafting the weight-averaged molecular weight of SPG was decreased from 150 to 90 kDa. The degree of grafting was estimated to be 9% and grafted folic acid could be recognized by folate binding proteins. *In vitro* experiments showed that SPG–FA complexes can efficiently deliver AS-ODN to KB cells, causing 45% decrease in cell viability, and that delivery efficiency is dependent on the concentration of free folic acid in the media. Importantly, it was demonstrated that scrambled AS-ODN delivered by the same SPG–FA vehicle does not suppress cell growth, proving that cell growth suppression is mediated by the antisense ODN and not a nonspecific effect of the delivery vehicle.

Following initial work on SPGs, Matsumoto et al. [57], in an attempt to improve cellular internalization, modified SPGs with octaarginine (R8), spermine, arginine-glycine-aspartic acid tripeptide (RGD), or single amino acids (Arg and Ser). The SPG modification was done using the route described above and was in a 0.5–24.7 mol% range. Antisense delivery experiments were conducted in A375 melanoma cells and the HL-60 leukemia cell line. A 60% decrease in cell growth was observed with AS-ODN complexes formed with R8-SPG, and a 56% decrease in cell growth was revealed with RGD-SPG complexes at a concentration of 12.5 μg/mL in A375 cells. It should be noted that the antisense activity was minimal while using the positive control, Lipofectamine, or SPGs modified with spermine,

arginine, or serine. When the same experiment was performed using the sense sequence (S-*c-myb*), Lipofectamine and spermine-modified SPGs were highly cytotoxic compared to naked S-*c-myb*, but the rest of the modified SPG-systems showed the level of toxicity similar to naked S-*c-myb*. An analogous trend was observed when the experiments were performed in HL-60 cells. Thus, the authors demonstrated that octaarginine- or RGD-modified SPGs elicited a more potent antisense effect (likely derived from increased internalization) than Lipofectamine and negligible toxicity comparable to unmodified SPG, thereby providing new insight into schizophyllans as nucleic acid carriers. It is important to note here that, although schizophyllan was modified with cationic (at physiological pH) functionalities, the *N*/*P* ratio used for polyplex formulation was less than one. The polyplex ζ-potential was not reported, but authors expect it to be negative based on the *N*/*P* ratio and stress that modified SPG is principally different and advantageous compared to polycationic polynucleotide carriers.

Work on the modification of SPG and delivery of AS-ODN to A375 cells was continued with introduction of amino-modified PEG (5 kDa) through previously-described reductive amination [58]. The degree of modification used in this study was 10.1% (The PEGylation strategy was suggested in order to promote fusion of polyplexes with the cell membrane – as opposed to endocytic cellular internalization; this approach is very unusual because PEG is typically used to shield vehicle charge, preventing aggregation in serum and nonspecific associations). Cell culture studies show that inhibition of endocytosis leads to a decreased antisense effect, which suggests that internalization occurs through an endocytic route, rather than by vesicle fusion. Using nigericin, a chemical inhibitor that blocks transport from endosomes to lysosomes, the antisense-mediated decrease in cell growth was preserved for PEG-SPG/AS-ODN but nearly completely abrogated for RGD-SPG/AS-ODN. The authors suggest that this result confirms endosomal escape of PEG-SPA/AS-ODNs prior to transport to the lysosome. Instead, this result could be indicative that the incorporation of PEG on the delivery vehicle affects the internalization route. These polyplexes may also enter the cell through an alternative pathway which does not traffic to lysosomes, in which case nigericin would have no effect. This is evidenced with the RGD-modified polyplex, for which nigericin-sensitive trafficking appears to be essential for efficient function. More studies are needed to elucidate the effect of PEG on polyplex trafficking.

PEG modification of SPG was attempted together with galactose modification [59]. Galactose-terminated PEGs of different lengths were introduced into SPG by reductive amination. *In vitro* studies conducted in serum-containing medium with HepG2 cells demonstrated that, among tested PEG lengths (0.2, 0.6, 2, and 6 kDa) used for SPG modification, the longest one (6 kDa) was the most efficient in reducing cell growth through delivery of AS-ODN. This 10 mol% Gal-PEG-modified SPG delivery vehicle was more efficient in reducing cell growth than 8.7 mol% galactose-modified SPG (Gal8.7-SPG), naked AS-ODN, and SPGs modified by glucose-terminated PEGs. Importantly, there was no difference in the antisense effect in A375 cells (which do not express galactose receptors) when SPGs modified by glucose- and galactose-terminated PEG-SPGs were compared. However,

both of these delivery vectors caused a significant (up to 65%) decrease in cell viability; this toxicity is potentially problematic for systemic delivery applications. In addition, this work demonstrates the propensity for internalization of complexes made with galactose-modified PEG-SPGs by cells other than hepatocytes.

Mizu and coworkers [60] utilized the same SPG modification strategy with spermine, R8, RGD, or cholesterol to deliver unmethylated, CpG motif-containing single stranded oligo DNA with $(dA)_{40}$ tail at the 3′ end into murine macrophage-like cells (J774.A1) to enhance cytokine secretion. Consistent with the study described above, the degree of functionalization was kept low: 0.5 mol% and 6.9 mol% in the cases of R8 and cholesterol, respectively. CpG DNA has been shown to be an effective adjuvant in various vaccines to treat numerous diseases [61]. Previous studies have shown that complexation of phosphorothioate AS-ODNs with modified SPGs reduces their non-specific interactions with proteins and increases their cellular uptake. In this study, the secretion of three different cytokines (IL-6, IL-12, and TNF-α) was assessed. A five- to tenfold increase in cytokine secretion was observed for the modified SPG complexed with CpG DNA over naked CpG DNA. The SPGs modified with octaarginine were found to have the highest efficacy, followed by RGD- and cholesterol-modified SPGs. However, only 20–40% enhancement in cytokine secretion was found when CpG DNA complexed with unmodified SPG was used.

This work with antigen-presenting cells was continued using phosphodiester (PO)-DNA instead of phosphorothioate (PS)-DNA to avoid "unexpected biological responses" [62]. For many antisense oligonucleotides, the phosphodiester bond is replaced by phosphorothioate, which reduces nuclease susceptibility, presumably by introducing chirality [63]. *In vitro* experiments with mouse primary spleen cells revealed an interleukin (IL) expression trend similar to those described by Mizu et al. [60]. R8-modified SPG elicited the highest expression of IL-6 and IL-12 at both 25 μg/mL and 50 μg/mL DNA concentrations, while spermine-modified SPG yielded a slightly lower response. When PO-DNA was used, four- to sixfold higher DNA concentrations were needed to induce IL secretion comparable to PS-DNA, a finding attributed to lower PO-DNA stability toward nuclease degradation. While further development of SPG vehicles for PO-DNA delivery is needed, the ability to deliver DNA to primary cells by SPG vehicles is a substantial achievement. Follow-up *in vivo* experiments in mice showed a significant increase in IL-12 secretion when SPG was used for delivery, as compared to naked DNA. Unfortunately it was not mentioned whether PS-DNA or PO-DNA was used, but the ability to deliver DNA *in vivo* was demonstrated.

SPG modifications to create cationic vehicles by grafting amines (ethanolamine, spermine, spermidine, and tripropylenetetramine (N4C3)) onto the SPG backbone have also been attempted [46]. *In vitro* experiments in COS-1 cells revealed that, among amines used for SPG grafting, N4C3-modified SPG was the most efficient in transfection, a result related to its high amine density. Thus 34 kDa SPG containing 41 mol% grafting with N4C3 was fivefold more efficient in transfection (at *N*/*P* 10) than PEI (25 kDa); however, it was also the most toxic vehicle – 40% more toxic than PEI. Toxicity followed the same trend as the transfection efficiency,

suggesting that the more charge-dense polymers were also the most toxic. The molecular weight of glucan has a role as well, and 80-kDa SPG was the most efficient (among 12-, 34-, 80-, and 150-kDa tested), while 12- and 150-kDa were the least efficient. To reduce toxicity, PEG was introduced via amide linkage with succinimide-activated, carbonyl-terminated PEG. Both 2 and 5-kDa PEG-SPG derivatives showed 100% cell viability, but transfection efficiency was also reduced, becoming similar to PEI. Finally, it was demonstrated that SPG vectors have long-term transfection, with detectable intracellular plasmid DNA over 30 days post-transfection. This sustained DNA residence was speculated to be the result of *slow* non-enzymatic hydrolysis of the SPG backbone.

Studies utilizing SPG as a nucleic acid carrier have been performed over the last decade and highlight the potential applicability of SPG for nucleic acid delivery applications. The unique ability to form complexes with polynucleotides via hydrogen bonding – without electrostatic interactions – has great promise, since cytotoxicity mediated by positive charge density can thereby be avoided. Moreover, branched glucose units offer attractive and facile modification sites due to selective modification by oxidation or reductive amination; this leaves the main chain intact, preserving the ability to condense polynucleotides. The SPG backbone cannot be cleaved enzymatically in mammals due to the lack of appropriate enzymes, making schizophyllan a good candidate for slow-release delivery vehicle development. Further research on the efficiency and versatility of this polymer will reveal the future of schizophyllan as a non-viral nucleic acid carrier.

2.3 Hyaluronan

Hyaluronan, also called hyaluronic acid (HA), is a glycosaminoglycan, a major component of the extracellular matrix. It is composed of *N*-acetyl-D-glucosamine and D-glucuronic acid (Fig. 3) [64]. It has been extensively used in biomedical applications due to its biodegradability as well as lubricating, shock-absorbing, and non-immunogenic properties [65]. As can be seen from the structure, hyaluronic acid has several sites for chemical modifications. Functionalization via the carboxyl group is used most often in gene delivery applications, because there is only one carboxyl group per repeat unit (as opposed to multiple hydroxyl groups). Such modification also removes the negative charge, which is beneficial for the

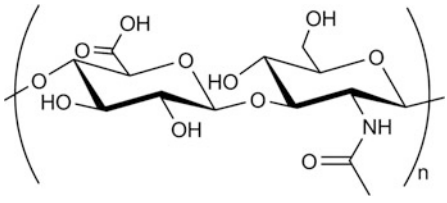

Fig. 3 Structure of hyaluronan

complexation of negatively-charged polynucleotides. As discussed later in this chapter, the carboxyl group can be activated toward nucleophiles in aqueous solution.

In 2003, Kim and coworkers [65] formulated pDNA encoding platelet-derived growth factor (PDGF) with HA and studied *in vitro* transfection efficiency in COS-1 cells (Fig. 4). In this study, solutions containing various amounts of pDNA were mixed with HA solution, flash-frozen and lyophilized, yielding DNA-HA matrices. These matrices were then placed in a DMF/H_2O solution of adipic dihydrazide and 1-ethyl-3-(3-dimethyl amino)propyl carbodiimide (EDC), a conventional water-soluble, carboxyl-activating agent. An HCl solution was subsequently added to lower the pH. By allowing these mixtures to incubate for various amounts of time, DNA-HA matrices with different degrees of crosslinking could be obtained. It should be pointed out here that the DNA is physically entrapped in a pre-formed, mesh-like HA matrix. While relatively uncommon for nucleic acid delivery, this approach is common for the delivery of small molecule therapeutics.

The pDNA release kinetics from the matrices in the presence of the enzyme hyaluronidase (at concentrations that were intended to resemble serum conditions) were shown to be dependent on the pDNA loading and the degree of HA crosslinking. It was observed that pDNA release is faster from the matrices with lesser degrees of crosslinking, and it was suggested that matrices with higher extents of crosslinking could potentially be used for slow release applications.

One such application could be delivery of Has2-pDNA, a plasmid that codes for hyaluronan synthase 2 [66]. This enzyme facilitates the synthesis of larger HA molecules and can prevent post-surgical peritoneal adhesions. In one study, DNA-HA films were prepared using previously-described chemistry; however, lyophilization was replaced with air-drying under sterile conditions and an isopropanol/H_2O mixture was used instead of DMF/H_2O. The release kinetics of DNA were similar to that from the HA film described previously, but release did not occur until after 7 days. The reason for this delay was not completely clear; the authors suggest that a possible way to overcome the delay is to use a crosslinked DNA-HA film sandwiched between two non-crosslinked DNA-HA films. Non-crosslinked film

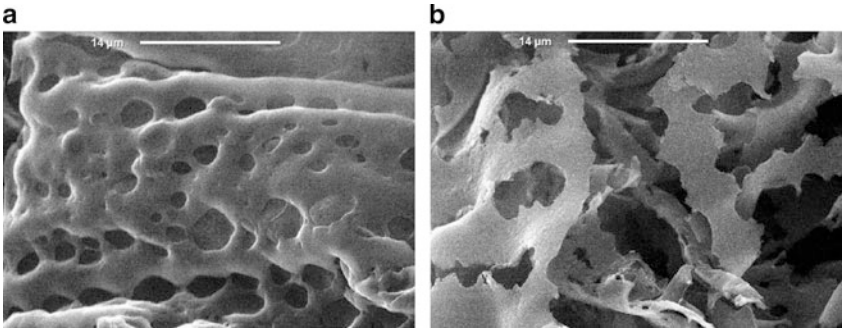

Fig. 4 SEM images of DNA-HA matrices: (**a**) before and (**b**) after incubation in hyaluronidase solution (10 units/ml) for 7 days. Figure adapted with permission from [65]. © 2003 Elsevier

would be expected to undergo rapid hydrolysis, thus serving as a source of HA during the initial period.

As an extension of the HA film approach, Yun and coworkers [32] synthesized hyaluronan microspheres using the chemistry described above, but the synthesis was completed in emulsion in one step, yielding 5- to 20-μm microspheres. These microspheres were found to be biodegradable and released three times more pDNA when incubated with hyaluronidase in PBS (phosphate buffered saline) solution (vs enzyme-free PBS). As in the case of films, DNA release from the microspheres was dependent on the DNA loading. DNA-HA microspheres were not directly used for transfection; instead, DNA obtained from release experiments was used in transfection of Chinese hamster ovary (CHO) cells using Lipofectamine. The relative levels of transfection over time had the same trend as DNA release from the DNA-HA microspheres and confirmed that released DNA is bioactive.

The transfection capabilities of the HA microspheres were investigated *in vivo* by injecting the microspheres containing pDNA (encoding β-galactosidase) in rat hind limb muscles [67]. Three weeks post-injection, animals were sacrificed and RT-PCR showed detectable pDNA, indicating that DNA-HA microspheres are suitable for slow DNA release *in vivo*. In addition, the humanized monoclonal antibody that recognizes E- and P-selectin in modified CHO cells and human umbilical vein endothelial cells (HUVECs) were conjugated to HA microspheres. Antibody-conjugated HA microspheres showed very specific binding to cells expressing E- and P-selectin, demonstrating a great potential for development of site-selective HA delivery vectors [67].

Recently, other approaches and modifications of HA for gene delivery applications have been investigated. Among the most interesting ones are mixed chitosan-hyaluronan based gene delivery systems [68–70] and PEG-HA photocrosslinked hydrogels [71]. HA has also been used to improve the biocompatibility of branched PEI via covalent conjugation [72].

A more sophisticated system was reported recently in which HA is modified with spermine and a lipophilic amine containing a long hydrocarbon chain. This system was shown to be efficient in siRNA complexation, has a very low critical micelle concentration (40–140 mg/L, depending on the length of lipophilic amine chain), and forms cationic micelles with 125–555 nm diameter [73].

2.4 Pullulan

Pullulan is a neutral, water-soluble polysaccharide synthesized from starch by the fungus *Aureobasidium pullulans*. It is composed of maltotriose units, in which the three glucose units of the maltotriose are linked via α-(1→4) glycosidic linkages and consecutive maltotriose units are linked by a α-(1→6) glycosidic unit (Fig. 5) [74]. The versatility of pullulan has encouraged its usage in a variety of applications, including use as decorative materials in baking, coatings, capsules, and also in soft-chew candies [74, 75]. Perhaps the most significant work has been done with

Fig. 5 Structure of pullulan

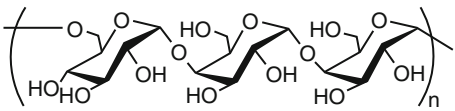

pullulan nanoparticles as drug carriers, where water-insoluble drug molecules [76], vitamins [77], or cholesterol [78] have been encapsulated in the hydrophobic pullulan interior and used in treating a variety of diseases. However, it was not until 2004 that pullulan was used to design biomaterials that could be used to deliver nucleic acid therapeutics.

In 2002 Hosseinkhani et al. synthesized and evaluated several pullulan derivatives for gene delivery *in vivo* [79]. This work will not be discussed here in detail, since no *in vitro* transfection experiments were conducted; however, this study presents an interesting approach to delivery vehicle design. Pullulan was grafted with diethylene triamine pentaacetic acid (using a corresponding anhydride and DMAP(4-(dimethylamino)pyridine)) and with diethylenetriamine and triethylenetetramine (using 1,1'-carbonyldiimidazole (CDI)). After purification, pullulan derivative solutions were mixed with pDNA solutions. This was followed by addition of Zn^{2+} ions, which were chelated by delivery vectors to allow tighter DNA encapsulation. These complexes showed enhanced gene expression in liver parenchymal cells which lasted for over 14 days.

In their further studies, the Tabata lab have synthesized pullulans grafted with spermine, using the same approach – CDI-mediated coupling [80]. This grafting procedure calls for 15 equivalents of spermine per hydroxyl group (or 69 equivalents of spermine per primary hydroxyl group) of pullulan, yielding pullulan with 12.3% spermine introduction. After the purification, modified pullulan was used for transfection of human bladder cancer (T24) cells. This study revealed that pullulan-*g*-spermine polyplexes enter the cell through clathrin- and caveolae-mediated endocytosis with involvement of sugar-recognition receptors. The transfection efficiency evaluated by reporter gene expression was tenfold better than Lipofectamine. Moreover, it is mentioned that, according to the authors' unpublished data, similar enhancement in transfection is observed for Caki-1, ACHN, PC3, LNCaP, HepG2, UMUC-3, EJ, and primary isolated rat bone marrow stromal cells.

Their next study investigated the influence of pullulan molecular weight and the amount of spermine grafting on transfection [81]. Among three tested molecular weights (22.8, 47.3, and 112 kDa), pullulan with an intermediate molecular weight (47.3 kDa) was the most efficient in transfecting HepG2 cells. The optimal amount of grafted spermine for transfection varied for different molecular weight pullulans, and this amount decreased with increasing pullulan molecular weight. However, the optimal molar ratio of polymer to DNA was similar (close to 100) for all three tested molecular weights. Receptor-mediated endocytosis was suggested because transfection inhibition was observed upon pretreatment of cells with asialofetuin, a competitive inhibitor for the asialoglycoprotein receptor on hepatocytes.

Gupta and coworkers have formulated pullulan hydrogel nanoparticles as a pDNA delivery carrier [33]. The *in vitro* delivery efficacy and cytotoxicity of this approach were determined by β-gal expression and MTT assay, respectively, in HEK293 and COS-7 cells. In this study, water-soluble materials such as pDNA could be encapsulated within the hydrophilic core of these hydrogels and thus transported into the cells. The extent of pDNA protection from nuclease degradation was tested using gel electrophoresis. The results indicated that the pullulan nanoparticles were effective in protecting pDNA against DNase degradation. The cell viability in COS-7 and HEK293 cells determined using an MTT assay indicated that pullulan was relatively nontoxic; however, the cell viability decreased to about 80% (COS-7 cells) and 70% (HEK293 cells) with an increase in dosage to about 20 mg/mL. The cellular uptake mechanism of these nanoparticles was studied using SEM and fluorescent staining of cytoskeleton components in primary human fibroblast (hTERT-bJ1) cells, which revealed that the nanoparticles entered the cells via an endocytic pathway. Following this, transfection was performed in serum-containing media to mimic *in vivo* conditions in both COS-7 and HEK293 cell lines. The results indicated maximum expression at pullulan concentration of 250 μg/mL. However, the transfection decreased with an increase in polymer concentration, which could be related to the cytotoxicity revealed in the MTT assay. The delivery efficacy was cell-type dependent, with COS-7 cells having higher gene expression than HEK293 cells. The pullulan-containing nanoparticles yielded comparable β-galactosidase expression to Lipofectamine. This was the first study demonstrating the utility of pullulan as a DNA delivery carrier, and these results have been significant in motivating further development of pullulan-based non-viral vectors.

Consequently, San Juan and coworkers chemically cross-linked DEAE-pullulan and synthesized a cationic, 3D pullulan matrix that could be loaded with pDNA (pSEAP) and function as a delivery vehicle (Fig. 6) [82]. *In vitro* transfection and

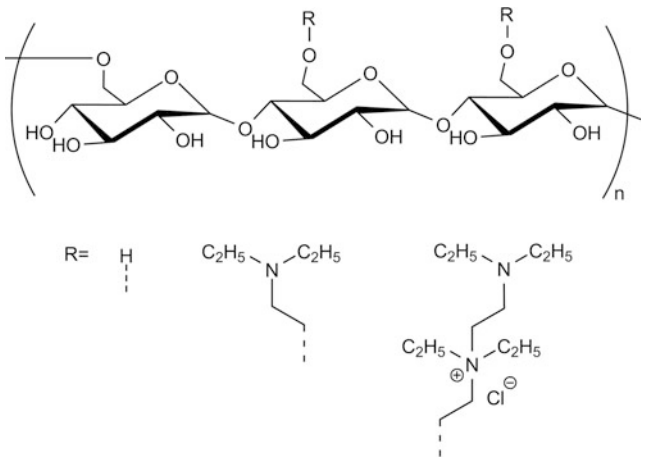

Fig. 6 Structure of DEAE-pullulan

cytotoxicity experiments were performed in vascular smooth muscle cells (SMCs). In this study, pullulan was first grafted with *N*,*N*-diethylamine groups yielding cationic DEAE-pullulan and then chemically crosslinked using $POCl_3$ to form a 3D matrix in the form of a hydrogel disc. All the experiments were performed with both cationic DEAE-pullulan and the crosslinked DEAE-pullulan matrix. The extent of DEAE-pullulan/pDNA binding was studied via dye exclusion assay using PicoGreen. The results indicated that neutral pullulan did not bind pDNA, as no fluorescence quenching was observed. However, fluorescence intensity decreased sharply with DEAE-pullulan, indicating pDNA binding with the cationic molecule (and PicoGreen exclusion). The cell viability determined via the MTT assay indicated no significant toxicity when the SMCs were treated with either pSEAP/pullulan or pSEAP/DEAE–pullulan. The delivery efficacy in media containing serum was 150-fold higher using DEAE-pullulan than for naked pSEAP or a pSEAP/neutral pullulan mixture. The pSEAP extracted from the DEAE–pullulan matrix was found to be protected from nuclease degradation when compared with neutral pullulan, as indicated by gel electrophoresis. Furthermore, the DEAE-pullulan matrix has been shown to be nontoxic to SMCs, as revealed via MTT assay. Significant delivery efficacy was noted using DEAE–pullulan matrix at 6 days after initial transfection (when compared to pSEAP only). The nontoxicity and biodegradability of these 3D pullulan hydrogels will be useful towards their development as efficient non-viral DNA carriers for implantable devices to facilitate controlled release from surfaces.

The research performed by several groups on pullulans has demonstrated their potential as nucleic acid delivery vehicles. Although most of the pullulan-based delivery systems yielded low toxicity, some modifications of the backbone or introduction of substituents resulted in higher toxicity. Such modifications are unavoidable because the parent structure is incapable of efficient delivery and lacks target specificity.

2.5 Chitosan

Chitosan is the most widely studied polymeric vehicle for nucleic acid delivery, and the remainder of this section is devoted to its use and development as a delivery vehicle. Chitosan is a polysaccharide composed of glucosamine and *N*-acetyl glucosamine units bonded via β(1→4) glycosidic bonds (Fig. 7a). The intense study of chitosan stems from its low cost, low toxicity, biodegradability, and the presence of primary and secondary hydroxyls and primary amines – functional groups that can be readily used for modifications via a range of well-established reactions. Amino groups in chitosan have a pKa value of ∼6.5, making chitosan positively-charged in neutral and acidic solutions. Chitosan has been found to complex with a variety of polyanions, such as indomethacin [83], sodium hyaluronate [84], pectin, and acacia polysaccharides [85], via electrostatic interactions. This concept has been explored extensively to complex chitosan with therapeutic

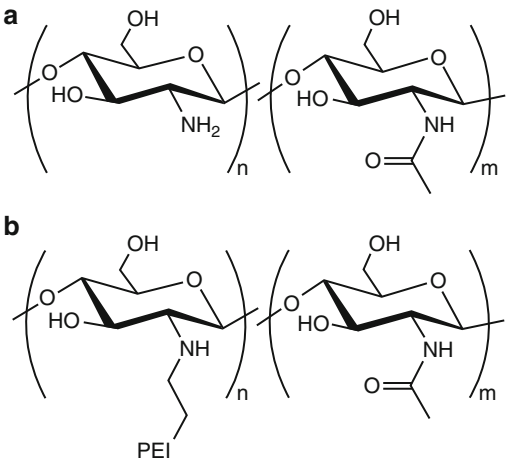

Fig. 7 (**a**) Structure of chitosans. (**b**) Structure of chitosan-graft-PEI

nucleic acids [31, 86]. The first study describing the formation of chitosan/nucleic acid nanoparticles for gene delivery was reported by Mumper and coworkers in 1995 [87].

Chitosan is produced by basic hydrolysis of chitin [88–90]. Chitin is a natural polysaccharide, found widely in fungi and various arthropods, like spiders, insects and crustaceans (shrimp, crabs, lobsters, etc.). In its native state, chitin is a long polymer (molecular weight of 1–10 MDa), insoluble in water and organic solvents. It is made of *N*-acetyl-2-amino-2-deoxyglucose units linked via β(1→4) glycosidic bonds. Because chitin is semicrystalline and water-insoluble, its hydrolysis is heterogeneous, possibly leading to the formation of localized blocks of *N*-acetyl-2-amino-2-deoxyglucose units [91]. The influence of these blocks on polyplex formation and transfection is not well documented. In general, the deacetylation degree of commercially-available chitosan is ∼80%, but methods affording complete 100% deacetylation have been reported [92]. Notably, by fractionating chitosan via semi-preparative SEC, it was possible to reveal heterogeneity in molecular weights. In the case of the low-molecular-weight fractions of chitosan obtained via degradation with nitrous acid, a deacetylation degree dependence on molecular weight has been shown [93]. Methods for characterization of the deacetylation degree and molecular weight of chitosan and their influence on properties directly related to transfection efficiency, such as biodegradability, mucoadhesion, endothelium permeation enhancement and others, have been extensively reviewed, and the authors suggest using chitosan of ∼10 kDa with deacetylation degree ≤80% for gene delivery applications [90].

Chitosan is generally considered nontoxic, with the rare reported toxicity explained by Köping–Höggård et al. as a result of impurities [94]. In their study conducted with ultrapure chitosan, transfection efficiency of 293 cells was shown to be dependent on the polyplex stability, which in turn was dependent on the deacetylation degree of chitosan. A deacetylation degree of at least 65% was

found to be required to give efficient transfection. Variations in the molecular weight of chitosan within the range of 31–170 kDa, however, were shown to have no significant effect on polyplex stability and transfection results. *In vivo* experiments in mice showed that ultrapure chitosan is less efficient in gene delivery to the lung than PEI, but comparable to lipid-based delivery vehicles.

Kiang et al. [95] synthesized chitosans with different deacetylation degrees via acylation of high-deacetylation degree chitosan with acetic anhydride. Cell culture studies with HEK293, HeLa and SW756 cell lines revealed that the transfection efficiency is dependent on both the deacetylation degree and the molecular weight, with chitosan having the highest deacetylation degree being the most efficient. This was attributed to a greater polyplex stability afforded by the high-deacetylation degree chitosan in serum-containing media. However, for intramuscular injection of polyplexes in mice, high-deacetylation degree chitosan was the least efficient, likely due to slower release of the cargo. This study illustrates the potential differences between *in vitro* and *in vivo* transfection efficiencies [95].

Similar *in vitro* results were obtained in a study by Huang et al. [96]. High-deacetylation degree chitosans were also more efficient in protecting DNA from degradation. Transfection of A549 cells with pDNA was made to be more efficient by increasing the deacetylation degree of chitosan. These results showed good correlation between ζ-potential, cellular uptake, and transfection efficiency, suggesting the electrostatic interactions between the nanoparticle and the cell membrane mediate cellular uptake and lead to gene expression [96]. Similar effects were observed with siRNA gene silencing experiments, as polyplex stability and delivery efficiency were generally higher for high-molecular-weight chitosans with higher deacetylation degrees in H1299 human lung carcinoma cells [97].

As discussed in the aforementioned studies, deacetylation degree plays a crucial role in transfection, with the desirable value being in the range of 65–80%. Polyplexes prepared with chitosans having lower amine density, do not protect the cargo from degradation by enzymes, and are not stable in serum. The influence of chitosan molecular weight is less well understood. As previously described, variations in chitosan molecular weight within the range of 31–170 kDa did not affect transfection of 293 cells. However, in an earlier study by MacLaughlin and coworkers [88], it was discovered that a decrease in molecular weight of chitosan from 540 to 7 kDa caused a concomitant decrease in complex size, from 500 to 100 nm. The ability to modify polyplex size can influence the mechanism of endocytosis [98], which likely affects the intracellular fate of the polyplex. In serum-containing media, pDNA delivered with 540-kDa chitosan leads to higher transgene expression than other molecular weight chitosans. In general, it can be speculated that longer chains of high-molecular-weight chitosan are able to form more stable polyplexes with DNA but are less efficient in releasing the cargo than low-molecular-weight chitosans.

The size of the polyplex depends not only on the chemical structure of chitosan but also on the ratio between chitosan and DNA used for polyplex formulation, the concentrations of polymers, and formulation technique. This is commonly described in terms of "*N*/*P* ratio," the ratio of protonatable polymer amines to

phosphate groups in the nucleic acid. Increasing *N*/*P* ratios typically lead to formation of polyplexes with more positive surface charge, which is evident from ζ-potential measurements. High ζ-potential may seem desirable because it should increase interactions with the negatively-charged cell surface and, hence, lead to higher cellular uptake and transfection. However, high charge density usually results in cytotoxicity, likely caused by the disruption of the cellular membrane [99]. It was shown by Erbacher et al. [100] that *N*/*P* ratios greater than 2 are necessary for formation of polyplexes with chitosan (70 kDa was used in this study) having positive ζ-potential. The optimal *N*/*P* ratio is specific to each polymer and is usually based on polyplex stability, polyplex ζ-potential, and the ability of the polymer to protect cargo from degradation.

As previously discussed, the protection of pDNA against degrading enzymes is a critical parameter for a non-viral carrier. Such ability is needed for the polyplex to protect the nucleic acid for an extended period of time in the blood while the polyplex circulates and distributes. Research conducted in 1999 by Richardson and coworkers [101] to study the ability of chitosan to protect against DNase degradation revealed that incubation of polyplexes prepared at *N*/*P* ratio of 3/1 in the presence of DNase I (8 U, 1 h incubation) protected pDNA from degradation. Other studies of chitosans as gene delivery vehicles confirm that the *N*/*P* ratio has to be at least 3/1 to 5/1 in order to provide a sufficient protective effect against DNases.

Shortly after Mumper and coworkers published their original work with chitosan, Murata et al. synthesized quaternary chitosan using MeI in *N*-methylpyrrolidone (it was also further derivatized by incorporation of galactose) [102, 103]. Since then, quaternization of chitosan has become a primary strategy in the development of chitosan nucleic acid delivery systems. Quaternization introduces pH-independent charges into the polymer backbone and increases the charge density. The efficiency of the quaternization approach was elegantly demonstrated by Thanou and coworkers [104]. They investigated the transfection efficiency and cytotoxicity of quaternized chitosan oligomers (<20 monomer units) in COS-1 and Caco-2 cells. The results demonstrated higher transfection, in both serum-free and serum-containing media, for polyplexes prepared with quaternized chitosan than with unmodified chitosan polyplexes. The increase in transfection was especially significant in COS-1 cells. The efficacy was dependent on the weight ratio of the DNA/chitosan-oligomer polyplexes. The optimal weight ratio for transfection of COS-1 cells in serum-free media was 1:14. MTT assays revealed that the quaternized chitosan remained nontoxic, comparable to unmodified chitosan, in both cell lines.

Kean and coworkers investigated the difference in transfection efficiencies of oligomeric (3–6 kDa) and polymeric (∼100 kDa) quaternized chitosans, using monkey kidney fibroblasts (COS-7) and epithelial breast cancer cells (MCF-7) [105]. Both oligomeric and polymeric chitosan at optimized degrees of quaternization (44% for oligomeric chitosan, 57% and 93% for polymeric chitosan) transfected MCF-7 cells more efficiently than PEI as measured by luciferase assay. In the case of COS-7 cells, however, only oligomeric chitosan with 44% quaternization showed transfection comparable to, but not exceeding that of, PEI. Importantly, chitosans showing the highest transfection efficiency showed moderate

cytotoxicity, with the polymeric chitosan exhibiting higher toxicity than its oligomeric counterpart.

Attempts to improve transfection of chitosan-based vectors by grafting PEI onto a chitosan backbone have been reported. The goal of such efforts is improvement of the buffering capacity and charge density of chitosan while preserving its low inherent cytotoxicity. One of the first attempts to utilize PEI buffering properties in chitosan based gene delivery systems was made by Kim et al. [106]. PEI was physically added to (not chemically grafted on) chitosan/DNA polyplexes; addition of PEI to water-soluble chitosan/DNA polyplexes increased their transfection efficiency in HeLa, A549, and 293 T cells. Furthermore, a synergistic effect between water-soluble chitosan and PEI was demonstrated in the transfection of 293 T cells. This approach was also efficient in the case of a targeted delivery system – galactosylated chitosan. Addition of moderate amounts (1–2 μg) of PEI to galactosylated chitosan/DNA polyplexes increased the transfection efficiency in HepG2 cells while retaining receptor-mediated cellular internalization. However, addition of a greater amount of PEI (5 μg) decreased cell specificity and, in this case, the transfection efficiency of HepG2 cells by galactosylated chitosan/DNA was not different from that of nongalactosylated water-soluble chitosan/DNA polyplexes.

Taking the idea a step further, Wong and coworkers [107] have grafted low molecular weight PEI ($M_n = 0.206$ kDa) on water-soluble chitosan ($M_n = 3.4$ kDa) via cationic polymerization of aziridine, with chitosan amino groups functioning either as initiators or terminators of polymerization (Fig. 7b). It should be noted that such an approach can lead to formation of free, non-bound oligoethyleneamines. However, dialysis performed after polymerization likely removes this side product. The effect of PEI grafting was studied in HeLa, HepG2, and primary hepatocytes. Chitosan-*g*-PEI complexed pDNA at an N/P ratio of 2.5, but the maximum transfection efficiency in serum-free media was achieved at $N/P = 40$ for all three tested cell lines. At this N/P ratio, transfection efficiency was similar to PEI (25 kDa) at $N/P = 10$. The cell viability, assessed via the MTT assay, was reported only for free polymers in HeLa cells and revealed, interestingly, that chitosan-*g*-PEI had a sevenfold higher LD_{50} than PEI. Chitosan-*g*-PEI transfection was investigated *in vivo* by administration of polyplexes into the common bile duct in rats for liver delivery. Delivery with chitosan-*g*-PEI at $N/P = 10$ was 141-fold greater than that of naked DNA, 58-fold greater than PEI (25 kDa), and 3-fold greater than unmodified chitosan.

Following their successful tandem use of water soluble chitosan/galactosylated chitosan and PEI for the polyplex formulation, Cho et al. chemically grafted PEI onto chitosan [108, 109]. The grafting was accomplished by partial oxidation of 100 kDa chitosan with periodate followed by reductive amination using 1.8-kDa PEI (Fig. 8). Periodate is widely known to be used in oxidation of vicinal diols, presumably via a five-member intermediate. However, as noted by Vold et al., IO_4^- oxidative cleavage of 1,2-aminoalcohols is also known [110] and can be successfully used for oxidative cleavage of the C2–C3 bond within the glucosamine unit in

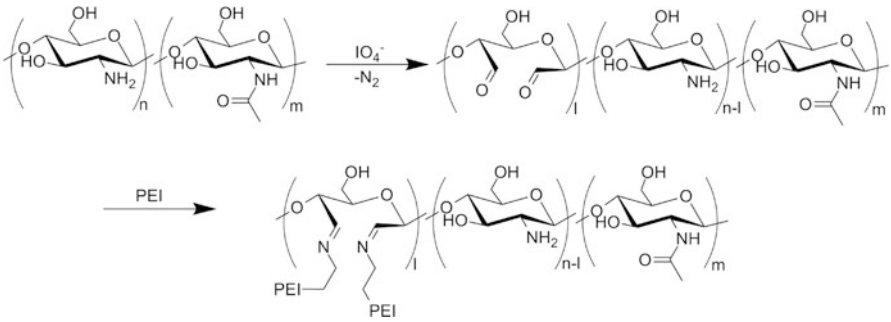

Fig. 8 Synthesis of chitosan-graft-PEI. Figure reproduced with permission from [109]. © 2007 Elsevier

chitosan [111]. Thus, it is necessary to exercise careful control of reaction conditions to avoid overoxidation and depolymerization of chitosan.

Synthesized chitosan-*g*-PEI was evaluated by transfection in HeLa, HepG2, and 293 T cells. In this case, chitosan-*g*-PEI was found to complex pDNA stably, with an average polyplex size of 250 nm, and protected pDNA from nuclease degradation. The cytotoxicity of these polymers was much lower than that of PEI (25-kDa) in all three cell lines. Similar to the aforementioned study by Wong et al., the transfection efficiency for this grafted system in serum-free media was higher than unmodified PEI (25-kDa) at $N/P = 35$ ($N/P = 10$ was used in the study by Wong et al.). Furthermore, high luciferase expression, similar to that of Lipofectamine, was noted in 293 T cells using chitosan-*g*-PEI. Interestingly, transgene expression in serum-containing media with chitosan-*g*-PEI was only slightly decreased in comparison to PEI and Lipofectamine.

To explore further the potential of chitosan-*g*-PEI vectors, Jiang et al. have synthesized galactosylated chitosan-*g*-PEI [112] and galactosylated poly(ethylene glycol)-chitosan-*g*-PEI (Gal-PEG-chitosan-*g*-PEI) [113], with the latter prepared by linking galactose-terminated PEG carboxylic acid to chitosan-*g*-PEI via amide bond. Incorporation of PEG is a standard approach to improve the polyplex colloidal stability and prevent undesirable electrostatic interactions with negatively-charged components of plasma and cellular membranes. This approach was successful in this case as well, showing that Gal-PEG-chitosan-*g*-PEI was less efficient in transfection of HepG2 and HeLa cells than chitosan-*g*-PEI due to reduced electrostatic interactions. But, more importantly, Gal-PEG-chitosan-*g*-PEI was better in transfecting HepG2 cells than non-targeted PEG-chitosan-*g*-PEI, whereas in HeLa cells their transfection efficiency was similar. These results show that cell-specific targeting can be achieved for chitosan-*g*-PEI vectors.

Recently, new ways to graft PEI on chitosan have emerged. Lu et al. have used a maleic acid anhydride reaction with the amino groups of chitosan, followed by the Michael-type addition of PEI [114]. Lou and coworkers used ethylene glycol diglycidyl ether to link PEI with chitosan through hydroxyl and amino groups of chitosan [115]. Wu et al. have used alkylation of primary hydroxyl groups of chitosan with chloroacetic acid, followed by purification, activation of carboxyl

groups with *N*,*N*'-dicyclohexylcarbodiimide (DCC) and *N*-hydroxysuccinimide (NHS), and subsequent coupling with PEI through amide bond formation [116]. It is not clear how self-coupling of chitosan was avoided in this approach, however.

PEI grafting on chitosan is becoming a popular approach for modification of chitosan for gene delivery applications. In recent years several efforts to develop chitosan-*g*-PEI delivery vectors have been published. These include incorporation of mannose [117] and folic acid [118] derivatives for targeted delivery and application of chitosan-*g*-PEI for the delivery of siRNA [119].

A means by which the buffering capacity of chitosan delivery vehicles can be improved without significantly increasing their cationic character is to graft the chitosan backbone with imidazole. Imidazole contains a protonatable nitrogen having a pKa of 6.15; thus, imidazole may facilitate endosomal rupture through the proton-sponge mechanism. For this reason, imidazole has been used widely in nucleic acid delivery vectors, and these materials have been discussed elsewhere [120–122].

Kim et al. decorated the chitosan backbone with imidazole groups by coupling of urocanic acid to chitosan through EDC/NHS condensation (Fig. 9) [123]. Urocanic acid-modified water-soluble chitosan (50 kDa) was evaluated for transfection efficiency using 293 T, HeLa, and MCF-7 cells. The modified chitosans were found to bind pDNA and also protected from DNase degradation at charge (*N*/*P*) ratios between 5 and 30. The transfection performed in 293 T cells yielded greater transgene expression for urocanic acid-modified chitosan than the unmodified analog, and the efficacy also tended to increase with greater extents of grafting, demonstrating the role of imidazole groups for transfection of 293 T cells. However, no significant enhancement in gene expression was evident when the same experiment was performed in HeLa and MCF-7 cells, thereby indicating that the transfection is highly cell-type dependent. This delivery vehicle was later also used for *in vivo* studies for aerosol delivery of nucleic acids to the lung, which led to tumor suppression in this model [124, 125].

Thiols are typically incorporated into polymers for gene delivery to take advantage of the reducing environment of the cytoplasm. Thiols can be mildly oxidized to produce disulfide (S–S) bonds for delivery vehicle crosslinking,

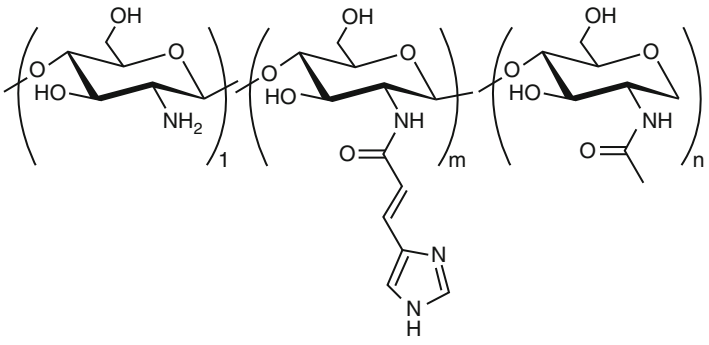

Fig. 9 Structure of urocanic acid-modified chitosan

providing protection for the cargo from degradative enzymes and preventing premature nucleic acid release. In the cytosol, the S–S bond can be reduced (primarily due to high concentrations of glutathione), causing changes in polyplex organization that result in release of carried nucleic acid. More information on disulfide usage in polymeric gene delivery systems, disulfide bond synthesis, and mechanism of action can be found in a recent review by Bauhuber et al. [126].

Thiolated chitosans [127] (Fig. 10) have been used for the development of an oral gene delivery vehicle [128]. The synthesis was accomplished in aqueous media using 2-iminothiolane and low-molecular-weight chitosan. Thiolated chitosan complexed pDNA into 125-nm polyplexes with a positive ζ-potential and was able to protect pDNA in artificial intestinal fluids at multiple physiologically-relevant salt concentrations. These complexes were stable at pH = 1.2. Under reducing conditions, thiolated chitosan releases 50% of its pDNA cargo in ~3.5 h, whereas in non-reducing conditions only ~7% of pDNA is released at this time point. Moderate transfection of Caco-2 cells was observed with thiolated chitosan, but it was higher than both controls – naked pDNA and (unmodified) chitosan/pDNA. Based on the stability to artificial intestinal fluids and low pH, as well as low cytotoxicity, it was concluded that thiolated chitosans are candidates to be studied further as oral gene delivery vectors.

In another study from the same lab [129], thiolated chitosan (12 kDa) was synthesized by conjugation of chitosan with thioglycolic acid. The thiolated chitosan/DNA nanoparticles were more resistant to DNase degradation at pH 4.0 and 5.0 than naked DNA and complexes formed with unmodified chitosan. MTT assays performed at pH 5.0 in Caco-2 cells indicated that the nanoparticles formed using unmodified chitosan and non-crosslinked thiolated chitosan were nontoxic. Crosslinked chitosan at pH 5.0 and both, non-crosslinked and crosslinked thiolated chitosans at pH 4.0, were slightly toxic, with cell viability 80–90% of untreated cells. The transfection experiments performed in Caco-2 cells revealed that both non-crosslinked and crosslinked thiolated chitosan yielded higher transgene expression levels than their unmodified analog in this cell model. In addition, thiolated chitosan/DNA nanoparticles formulated at pH 4.0 exhibited fivefold higher efficiency than unmodified chitosan.

Chitosan has also been grafted with saccharide-based ligands as molecular recognition elements to promote receptor-mediated endocytosis for cell specific

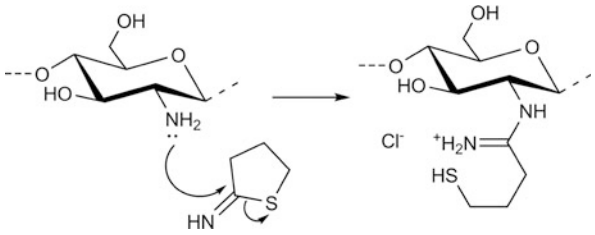

Fig. 10 Synthesis of thiolated chitosan. Figure reproduced with permission from [127]. © 2004 Elsevier

delivery *in vivo*. Extensive research has been completed by various groups in developing chitosan-based delivery vectors that have been conjugated to saccharides for target-specific delivery. The remainder of this section focuses on targeting cell surface lectins with carbohydrates grafted onto a chitosan backbone.

Nearly a decade ago, Murata et al. [102] synthesized quaternary chitosan polymers grafted with galactosyl residues along the side chain (Fig. 11a) and utilized them to transfect HepG2 cells (which express the asialoglycoprotein receptor (ASGPr), for which galactose is a ligand) in serum-free media. The β-galactosidase expression observed in HepG2 cells revealed that the gene expression tended to be higher for galactosylated trimethylchitosan than the non-galactosylated polymer. It was also found that increased amounts of galactose substitution yielded higher transfection efficiency, suggesting a multivalent effect for efficient uptake. Furthermore, the cytotoxic effects of these galactosylated chitosans were similar to those of DEAE-dextran.

In a similar study, Park and coworkers [131] synthesized chitosan-based vectors in which the chitosans were conjugated to lactobionic acid, which contains galactose residues. These structures were then grafted with either dextrans ($M_n = 5.9$ kDa) (GCD), polyethylene glycol ($M_n = 5.0$ kDa) (GCP), or poly-(vinylpyrrolidone) (GCPVP) to enhance polyplex stability (prevent aggregation). In the first study, galactosyl chitosan ($M_n = 4.0$ kDa) was conjugated with dextran and examined for delivery efficacy in Chang liver cells (express ASGPr) and HeLa cells (non-ASGPr-expressing). As expected, the dextran conjugation was found to stabilize the polyplexes from aggregation and yielded higher gene expression in Chang liver cells than in HeLa cells. In a related study by the same group, similar results were obtained when galactosyl chitosan ($M_n = 7.0$ kDa) was conjugated with PEG

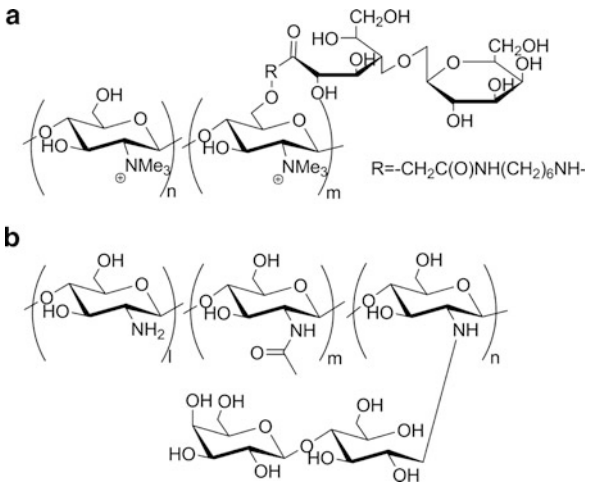

Fig. 11 (**a**) Structure of galactosylated chitosan. Figure reproduced with permission from [102]. © 1996 Elsevier. (**b**) Structure of lactose conjugated chitosan. Figure reproduced with permission from [134]. © 2006 American Chemical Society

[132]. Polyplexes formed with this polymer were used to transfect in HeLa, CT-26, and HepG2 cells, and the results were compared to those from the previous study. It was found that these PEGylated analogs had comparable stability to the dextran-mediated vectors and were found to protect pDNA from nuclease degradation. The transfection experiments indicated the vehicle had negligible cytotoxicity and that GCP/pDNA yielded transgene (green fluorescent protein) expression in HepG2 cells, but not in HeLa and CT-26 cells, thereby suggesting that the transfection occurs through ASGPr. In a more recent study by the same group, galactosyl chitosan (10 kDa and 50 kDa) were grafted with poly(vinylpyrrolidone) (PVP) using radical polymerization and similarly studied as a hepatocyte-targeting vehicle [130, 133]. PVP has been found to have similar properties to PEG; however, the PVP-modified polyplexes were found to have longer retention time in the blood than the PEG-modified systems.

All of the aforementioned studies demonstrate that chitosan grafted with polycations can be effectively used for hepatocyte-specific delivery applications. In addition, incorporation of flexible hydrophilic groups in the polymer structure provides a steric barrier that prevents aggregation and reduces interactions of the complexes with plasma proteins and phagocytes, thereby increasing the circulation time of these complexes in the plasma and facilitating complexes reaching target cells. However, the syntheses of these grafted systems are slightly more tedious and difficult to manufacture on an industrial scale; in addition, they often result in a highly polydisperse polymer mixture with high batch to batch differences in conjugation efficiency.

Similar results to galactosyl chitosan were seen when lactose-conjugated chitosan (53-kDa) conjugates (lac-chitosan) were synthesized (Fig. 11b) by Hashimoto et al. [134] and used to transfect HepG2 cells. In this study, conjugates were prepared for which the amines along the chitosan backbone were either 8% or 33% functionalized with lactose. Both were found to bind and compact pDNA into ~140-nm polyplexes at $N/P \geq 3$ (ζ-potential $= +43$ mV). Unlike polyplexes prepared with nonlactosylated chitosan, these lac-chitosan-containing polyplexes were stable from aggregation and adsorption after 1 h incubation with bovine serum albumin (polyplexes remained ~150 nm in diameter), thereby indicating that the lactose modification on chitosan results in serum stability. The 8% lac-chitosan/pDNA complexes revealed transfection efficiency in COS-7 cells similar to those made with the unmodified analog, whereas polyplexes formulated with the 33% lac-chitosan/DNA had about a twofold lower transfection efficiency than unmodified chitosan/DNA complex. However, in HepG2 cells, a 16-fold enhancement in transgene (luciferase) expression was observed when 8% lac-chitosan/DNA was used for transfection, suggesting receptor-mediated delivery leads to higher gene expression. In both cell lines, Lipofectamine showed much higher gene expression when compared to the conjugated and non-conjugated chitosans.

Inspired by earlier work on galactose-conjugated chitosans, Hashimoto and coworkers [135] synthesized mannose-grafted chitosan (53-kDa) conjugates (man-chitosan) to deliver pDNA in mouse peritoneal macrophages that express the mannose receptor. Here, man-chitosan containing either 5% or 21%

modification were synthesized, and mixing with pDNA resulted in formation of ~300-nm polyplexes. Both complexes formed with the man-chitosan derivatives were found to exhibit increased transfection in macrophages compared to pDNA/chitosan polyplexes and yielded comparable transfection to man-PEI/DNA polyplexes in macrophages. When a control experiment was performed in COS-7 cells, the transgene expression of pDNA/5% man-chitosan polyplexes was the same as that of pDNA/chitosan; however, the transfection efficiency of pDNA/chitosan was four times higher than pDNA/21% man-chitosan. The cell viability in experiments in macrophages also revealed negligible cytotoxicity of the man-chitosan polyplexes, which contrasted with the toxicity observed for man-PEI/pDNA complexes. Even though all the above experiments have been promising and have shown effective transfection and target-specificity, particularly with hepatocytes, most of these *in vitro* experiments have been performed only in serum-free media. The future of this area depends on performing these experiments in media containing serum, which are a better simulation of *in vivo* conditions. Also, *in vivo* data in this field are minimal and more are needed to advance this area toward the clinic. These extensive studies using chitosan have shown that this polysaccharide is indeed very useful for delivering therapeutic DNA into cells and the structure affords nearly limitless potential for chemical modification. However, their transfection efficiencies being lower than other non-viral analogs and viral-vehicles needs to be overcome by chemical and structural modifications. Much further work on this delivery platform is ongoing.

3 Carbohydrate Copolymers

Saccharide copolymers are recently emerging biomaterials with high applicability as nucleic acid delivery vehicles. To date, the structures created can generally be categorized as AABB step-growth type polymers consisting of two different monomers, where one monomer facilitates nucleic acid binding and the other (carbohydrate) monomer imparts biocompatibility. Previous results have shown that saccharide groups contribute to reduction of the cytotoxicity of non-viral vehicles. For example, when relatively toxic polymers, such as PEI, are grafted with carbohydrates, the cytotoxicity is generally decreased (e.g., [136]). For this reason, carbohydrate moieties have been incorporated in the polymer backbone using a variety of synthetic organic reactions, such as polycondensation, cycloaddition, or ring-opening polymerization. The structure of monomers used and synthetic methodologies have been found to influence various parameters, such as solubility, degree of polymerization, branching, and tacticity of the polymers. Furthermore, as with previously-presented systems, the studies in this section also demonstrate that subtle changes in the chemical and structural characteristics of these polycations have a significant effect on the cellular uptake, gene expression, and cell viability. This section describes novel polymers that have been synthesized with a variety of monosaccharides [21, 137], disaccharides [138–140], or cyclic oligosaccharides [141], and their efficacy as *non-viral* nucleic acid delivery vehicles.

3.1 Monosaccharide-Based Copolymers

The introduction of carbohydrates in polymeric structures could temper the cytotoxicity observed with these vehicles. Two commonly studied polymeric vectors – poly-L-lysine (PLL), a polypeptide consisting of repeating lysine residues, and polyethylenimine (PEI), composed of repeating ethylenediamine units – have shown the ability to deliver DNA for gene expression at a high level *in vitro* and *in vivo* [10, 13, 142]. Significant cytotoxicity, likely due to their high charge density and possible membrane-disrupting effects, limits the potential clinical utility of these vehicles. Reduction of the charge density by incorporation of carbohydrates could yield transfection efficiencies greater than those of polysaccharide-based vehicles and afford increased biocompatibility, thus resulting in an improved delivery system. In the first study using this strategy, published by Reineke and coworkers in 2004, dimethyl glucarate was polymerized with diethylenetriamine, triethylenetetramine, tetraethylenepentamine, and pentaethylenehexamine to derive polymers containing 1-4 secondary amines in the polymer repeat unit [137]. These polymers were able to self-assemble with DNA into polyplexes. When transfected into BHK-21 cells, pDNA complexes containing these polymers showed high levels of transgene expression with considerably lower toxicity than PEI. In fact, the analog with four secondary amines, dubbed D4, showed transgene expression comparable to PEI. A similar study was published afterwards by Guan et al. in 2005, using a similar strategy; however, the incorporated charge centers were L-lysines [145]. An acid chloride derivative of galactose was polymerized with oligolysines to develop three polymers with varied amounts of primary amines and spacing between the primary amine and the polymer backbone. These polymers also showed enhanced biocompatibility vs PLL and gene expression was comparable to PLL at low molar concentrations. These polymers did not elicit an immune response when administered to rats via intravenous or subcutaneous injection [145]. These first two studies showed that interrupting the charge density of PEI and PLL is advantageous for achieving low toxicity *in vitro* and *in vivo* without sacrificing delivery efficacy.

These favorable results led Reineke and colleagues to expand their initial study using three different carbohydrates to study the effects that hydroxyl number and stereochemistry, as well as amine stoichiometry, have on biological activity. A library of 16 polycations was developed, containing alternating monosaccharides and amine units along the main polymeric backbone, and were termed poly(glycoamidoamine)s (PGAAs) (Fig. 12) [21, 137]. These polymers contain one of four different carbohydrate comonomers: a mixture of dimethyl-D-glucarate, methyl-D-glucarate 1,4-lactone, and methyl-D-glucarate 6,3-lactone (D), dimethyl-*meso*-galactarate (G), D-mannaro-1,4:6,3-dilactone (M), or dimethyl-L-tartrate (T). These comonomers were polymerized with the same series of oligoamine comonomers as the first study (diethylenetriamine (1), triethylenetetramine (2), tetraethylenepentamine (3), or pentaethylenehexamine (4)) via step-growth polymerization to generate a series of polymers (D1–D4, G1–G4, M1–M4, T1–T4) with degrees of polymerization (n) around 11–14. These initial structures were found to bind and

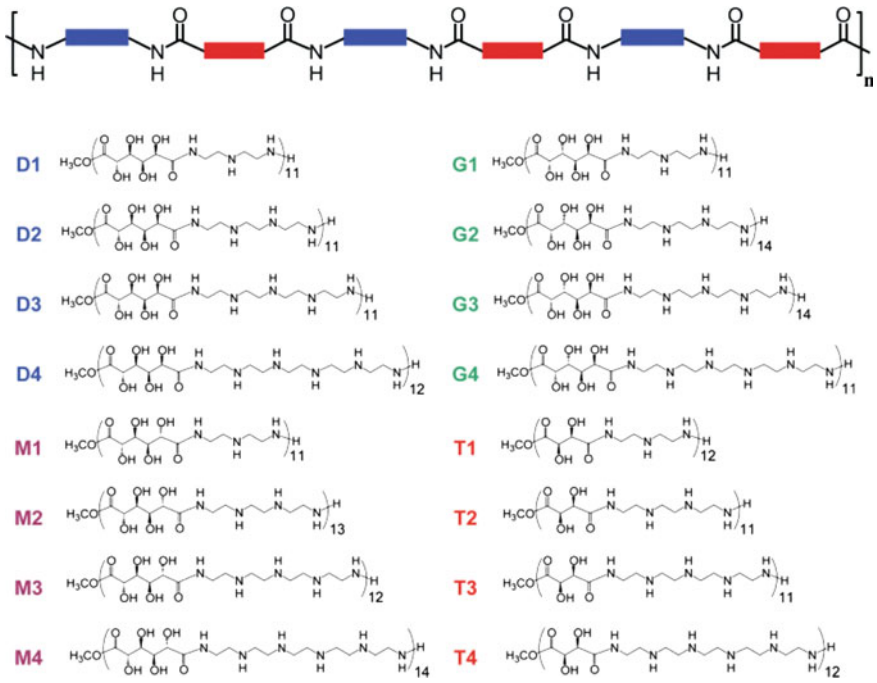

Fig. 12 Generalized block diagram of PGAA design structure and structures of the 16-polymer library of PGAAs. These polymers allow the direct comparison of changes in amine stoichiometry, as well as hydroxyl number and stereochemistry, on biological properties. Figure adapted with permission from [186]. © 2006 John Wiley & Sons, Inc

compact pDNA into cationic polyplexes, and increasing the amine number generally led to more efficient DNA binding and smaller polyplex size.

This library of cationic glycopolymers was screened for cell viability and transgene expression, and the results were compared to chitosan and PEI to assess the improvements achieved over these vehicles (Fig. 13). To ensure widespread utility, these vehicles were tested in four different cell lines to mimic a wide range of mammalian cell types: BHK-21, HeLa, HepG2, and H9c2(2-1) [21, 144, 146]. High levels of transgene expression was observed in all cell lines; the polymers containing four secondary amines yielded the highest transfection levels (Fig. 13). At the *N*/*P* ratio of maximum expression, the luciferase expression efficiency of these vehicles was comparable (within an order of magnitude) to that of PEI and significantly enhanced over chitosan. These results also showed very low toxicity that was comparable to chitosan and significantly lower than PEI. The highest transgene efficiency was observed for G4 and T4, which bind DNA the strongest among the series, and were shown to protect pDNA from degradation by nucleases. Further study in cardiomyoblast (H9c2(2-1)) cells revealed that, despite a significant polyplex size increase in salt and serum, high levels of gene expression were also observed, which were related to high levels of polyplex cellular internalization.

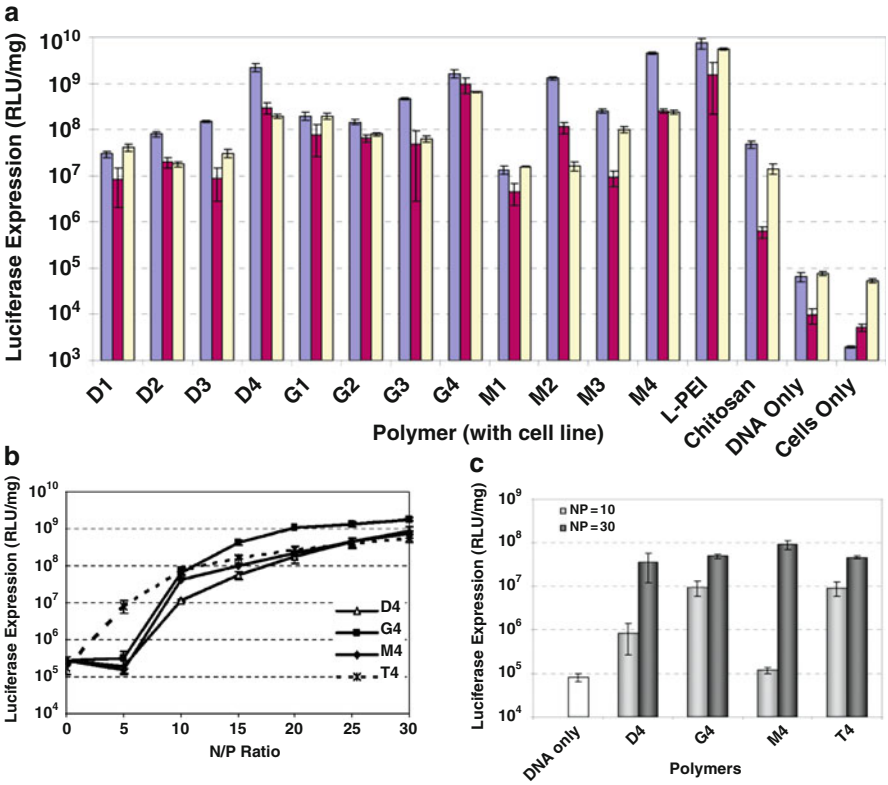

Fig. 13 Transgene expression efficiency of PGAA polymers in multiple mammalian cell types. (**a**) G, D, and M polyplexes shown high levels of transfection in multiple cell types. PGAAs with four secondary amines/repeat unit in H9c2 cells in (**b**) serum-free and (***c***) serum-containing media. Figures adapted with permissions from [21] and [146]. © 2005 and 2006 American Chemical Society

Using polyplexes containing FITC-labeled pDNA, the cellular internalization of PGAA polyplexes was assessed in serum-free and serum-containing media. The data show high levels of uptake, with nearly every cell analyzed containing DNA-associated fluorescence under both conditions. These data illustrate the high efficiency by which PGAA polyplexes can enter cells.

These promising results have led to systematic study on the effects of polymer structure on DNA binding and bioactivity. These further studies probe many aspects of polymer structure to determine the structural elements that lead to efficient delivery. DNA binding of PGAAs occurs through a combination of electrostatics and hydrogen bonding, a direct result of carbohydrate incorporation into the polymer [147]. The close-range hydrogen bonding interactions likely afford greater polyplex stability such that the DNA can remain packaged while inside the cell. Using similar techniques as described above, Lee et al. investigated the effect of increasing the number of secondary amines in the polymer backbone from four to

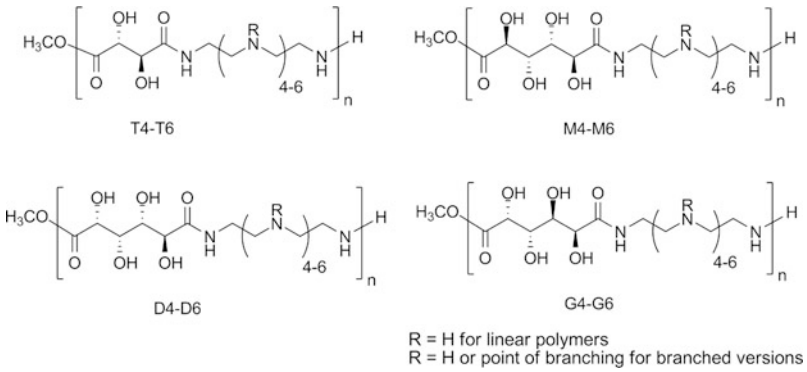

Fig. 14 Structures of linear PGAAs

five and six (Fig. 14), as well as the effect of polymer branching, on delivery efficacy and toxicity [148]. The linear and branched polymers yielded polyplexes of generally larger size than those with four secondary amines, but the galactarate and tartrate series with five and six secondary amines did not significantly swell or aggregate in serum-containing media, suggesting the higher secondary amine numbers prevent increasing size in serum. However, these modifications did not result in much enhancement of cellular uptake, as polyplex internalization was mostly unaffected (in some cases it was lower or a little higher and this depended on the cell type). Similar results were observed for transgene expression, as transfection. However, these modifications did have a significant effect on cell viability, as the linear polymers with five and six secondary amines displayed increased toxicity over the series with four secondary amines in the polymer repeat unit. This study confirmed that four secondary amines in the polymer repeat unit yields the highest internalization and transgene expression, and these analogs are the focus of further structure-bioactivity studies.

Polymer buffering capacity can have a significant effect on the cellular uptake and gene expression in mammalian cells, as polymer charge likely plays a key role in cell surface binding and either escape or trafficking out of the endosomal/lysosomal path. Liu et al. used titration experiments to calculate the buffering capacity of the D-glucaroamidoamine (D1–D4) and L-tartaroamidoamine (T1–T4), which allows a direct measure of the percentage of amines that can be protonated during endosome acidification [149]. The results of these experiments allow a direct comparison of polymer buffering capacity with cellular internalization and transgene expression. Two new polymers were created by polymerizing the dimethyl-D-glucarate (this is a mixture with lactone derivatives) or dimethyl-L-tartrate with spermine (yielding DS and TS, respectively) to incorporate butylene groups between neighboring secondary amines, thereby increasing the amine spacing. Interestingly, buffering capacity decreased with increasing amine number; however, the delivery efficacy and gene expression increased with increase in amine number. This argues against the proton sponge mechanism of endosomal

escape, as this hypothesis states that a higher buffering capacity should promote greater endosomal escape and should lead to increased gene expression. However, when comparing differences in amine spacing, the polymers containing the spermine groups (DS and TS) yielded a substantial decrease in buffering capacity compared to the original PGAAs with ethylene spacing. This suggests that proximal amines (ethylene spacer) have a lower charged state at pH 7.5 due to electrostatic suppression of protonation from neighboring charged amines. However, when comparing the gene expression results, DS and TS had higher gene expression than their PGAA analogs with two ethylene amines (D2 and T2) but the analogs with four amines (D4 and T4) still remained the most efficient delivery systems. Polymers with increased amine spacers also exhibited much higher toxicity, suggesting the charge spacing and charge density plays a significant role in biocompatibility. Buffering capacity also appears to influence the transfection of polymers having the same amine stoichiometry but different carbohydrates, as D4 possesses lower buffering capacity than T4, resulting in higher transgene expression with T4. Increasing cellular uptake was observed with higher amine number, which suggests higher amine density promotes multivalent interactions with the cell surface proteoglycans, facilitating higher uptake. Indeed, cellular uptake was found to be a major contributing factor to efficient transgene expression. This study proves that ethylene spacers between amines lead to more biocompatible gene expression and reveals a complex role of polymer buffering capacity that does not directly correlate with high delivery efficiency and gene expression.

Recent results in the Reineke lab reveal that the PGAAs are biodegradable under physiological conditions, and that removal of the carbohydrate or the oligoethyleneamine groups leads to a polymer that does not degrade under physiological conditions [150]. This points toward a synergistic effect in the presence of both the carbohydrates and ethyleneamine groups in polymer degradation. However, the transgene expression efficiency suffers when non-degradable polymer analogs are used as the delivery vehicle, suggesting that polymer degradation facilitates pDNA release and availability for transcription. This feature can possibly be exploited to develop novel nanodevices for sustained release of nucleic acids. Using dip-coating, the biodegradable polymer T4 and pDNA were deposited in a layer-by-layer assembly on a quartz slide (Fig. 15) [151]. Layer thickness of these devices could be assessed by ellipsometry and monitored by measurement of DNA absorbance. These materials resulted in slow, sustained release of pDNA over time which could be easily delivered into cells for gene expression by another suitable vehicle added separately. The amount of pDNA that was internalized by cells increased with time, consistent with slow release of pDNA. Interestingly, despite more released DNA at the earlier time points, gene expression remained constant, which is likely a function of the pathway of internalization/trafficking of DNA such that only a portion of the internalized DNA reaches the nucleus. This type of study demonstrates the wide utility of these polymers for sustained release. The favorable bioactivity can be further developed for use as a therapeutic delivery vehicle or in novel scaffolds and nanodevices in biomedical applications.

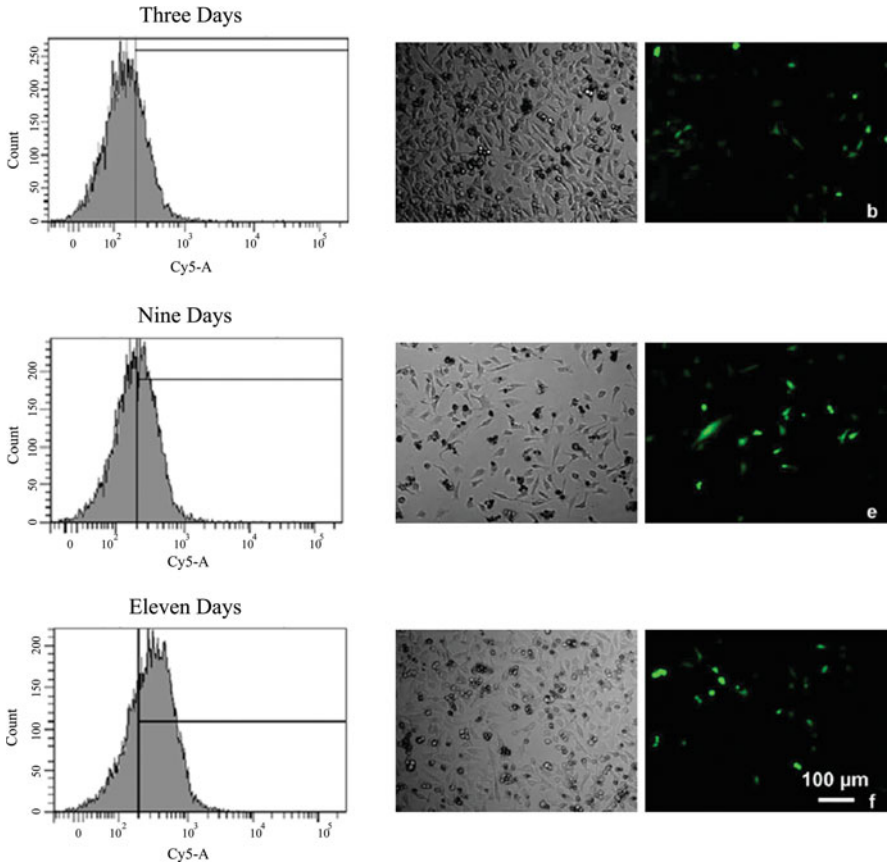

Fig. 15 Internalization and gene expression of pDNA released from a multilayer assembly. Release of pDNA occurs upon degradation of T4 polyamide. Notable increase in fluorescence intensity over time is observed in the flow histograms. Gene expression (measured by intracellular GFP fluorescence) does not increase at the same rate as DNA uptake. Figure adapted with permission from [151]. © 2009 Elsevier

3.2 Disaccharide-Containing Polymers

Disaccharides can have similar utility to monosaccharides in DNA delivery polymers. Trehalose, a disaccharide composed of two glucose units linked via an α-(1→1) glycosidic bond, has been shown to have cryo- and lyo-protective properties, attributed to an unusually large hydration volume [152]. As a function of these properties, trehalose has been shown to prevent aggregation and fusion of proteins and lipids [153]. Logically, incorporation of these features into a polymer backbone could afford similar characteristics to a DNA delivery system and may prevent aggregation of polyplexes in physiological serum concentrations and ionic

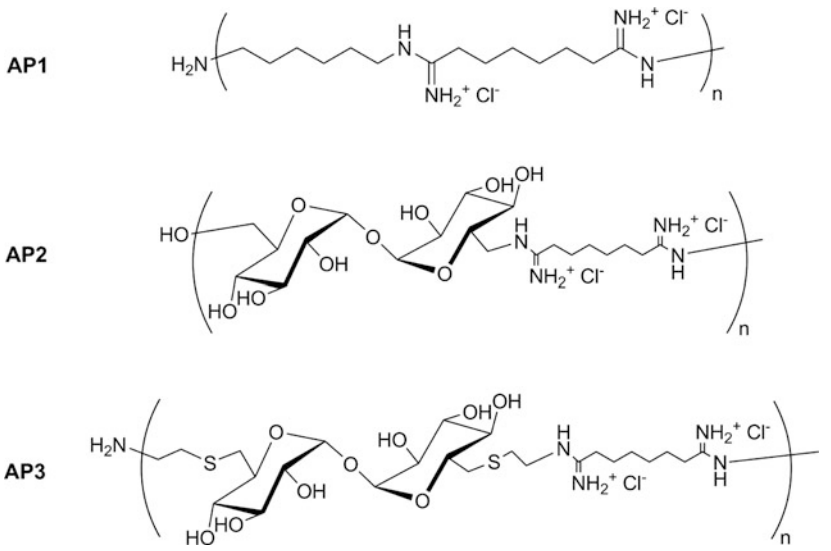

Fig. 16 Structures of trehalose-containing copolymers. Figure adapted with permission from [138]. © 2003 American Chemical Society

strengths. In a pioneering study, Reineke and Davis [138] synthesized a series of polymers via condensation polymerization of amine-functionalized D-trehalose monomers with amidine-based comonomers (AP2 and AP3) (Fig. 16). Based on previous studies [141], six methylene units were used as spacers between the amidine units; however, the distance between the amidine groups and the carbohydrate units was modified to understand further the polymer structure-bioactivity relationships. These polymers self-assemble with pDNA into cationic nanostructures around 80 nm in diameter. The delivery efficiency, in terms of transgene expression and toxicity, in BHK-21 cells *in vitro* was determined under serum-free conditions to preliminarily assess the bioactivity of these polymers, compared to an analogous structure (AP1) in which the carbohydrate group was replaced with a butylene spacer. Trehalose-based polymers (AP2 and AP3) exhibited improved biocompatibility compared to the non-carbohydrate analog (AP1), which exhibited significant toxicity at low charge (N/P) ratios (including only 20% cell survival at $N/P = 5$). Toxicity appears to be a function of spacer distance between the amidine and the carbohydrate moieties, with AP2 maintaining ~40% lower toxicity than AP3 at charge ratios greater than 10. The transfection experiments in BHK-21 cells indicated that AP3 yielded an order of magnitude higher luciferase expression at $N/P = 5$ when compared to AP2. At the same charge ratio, the trehalose containing polymers AP2 and AP3 have two and three orders of magnitude higher luciferase expression, respectively, than AP1. These favorable results confirm the benefit of incorporating trehalose into a polymer structure for gene delivery.

Based on these initial results, new trehalose-based vehicles were developed and their efficacy assessed under physiological conditions, as these previous studies

[138] have been performed under serum-free conditions. Previous work has shown that polyplexes can aggregate *in vivo* and are rapidly cleared from the bloodstream, such that extended circulation times are not achieved [8, 154]. Successful results previously described by Liu et al. [21, 146] and Reineke and Davis [138] prompted Srinivasachari et al. to synthesize a series of trehalose-containing polymers by systematically increasing the amine number (1–4) in the polymer structure, as well as to develop longer polymers to determine whether polymer length plays a role in formation of stable complexes with pDNA [140].

A series of trehalose-based polymers (Tr1–Tr3) with 1,2,3-triazole linkages were synthesized via the "click reaction" of acetylated-diazido trehalose and a series of dialkyne-oligoethyleneamines (1–3) (Fig. 17). Gel electrophoresis revealed that the polymers bind pDNA stably at $N/P = 2$, with TEM revealing the polyplexes to have either spherical or rod-like morphologies with diameters around 50–125 nm. Dynamic light scattering measurements demonstrated an increase in polyplex size upon incubation in serum-free media (Opti-MEM), suggesting swelling or aggregation of the particles. This effect appeared suppressed in serum-containing media; polyplex resistance to size increases improved with increasing amine stoichiometry. Cellular internalization, transgene expression efficiency, and cell viability were assessed *in vitro* in HeLa cells under both serum-free and serum-containing experimental conditions [140, 155]. When the HeLa cells were transfected with complexes containing FITC-labeled pDNA in Opti-MEM ($N/P = 7$), the cellular uptake profile showed that Tr1 and Tr3 were the most effective vehicles, transfecting a higher percentage of cells (>99%) than Tr2 or the positive control, jetPEI. However, in serum-containing media – Dulbecco's Modified Eagle Medium (DMEM), 99% of cells internalized complexes containing Tr3, more than for Tr1 (76%) or Tr2 (35%) and similar to jetPEI. This could be attributed to the increased stability of Tr3-containing polyplexes from aggregation in the presence of serum proteins. The transfection efficiency results in serum-free and serum-containing media indicated increased bioactivity of Tr3, which yielded higher transgene (luciferase) levels than Tr1 and Tr3. In serum-free media, luciferase expression from Tr2 was comparable to Tr3, whereas in serum-containing media, Tr3 induced one and two orders of magnitude higher gene expression than Tr1 and Tr2, respectively; these results correlated with the enhanced stability of Tr3 in DMEM. The trehalose-based polymers exhibit low (<20%) toxicity in serum-containing media at $N/P = 7$, markedly lower than control polymer jetPEI. These results suggest that incorporation of trehalose imparts favorable biological properties. In line with previous polymers, favorable biological activity improves with

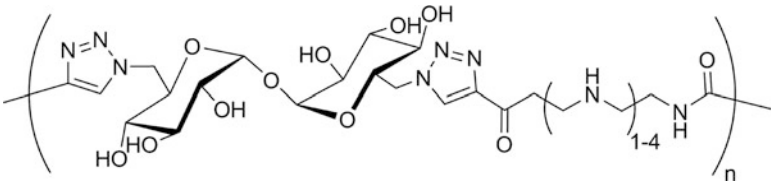

Fig. 17 Structures of trehalose click polymers

increasing amine stoichiometry across the polymer series, reaffirming that subtle changes in the polymer structures can measurably influence bioactivity.

To test these theories directly, trehalose-based polymers with four oligoethyleneamine units in the polymer chain were developed. The degree of polymerization of these analogs was varied to assess the influence of polymer length on biological properties [155]. Binding of pDNA and polyplex stability improved as a function of increasing degrees of polymerization in both Opti-MEM and DMEM. The polymers with greater amine stoichiometry have been shown to promote tight DNA binding and favorable polyplex stability due to a combination of electrostatic and hydrogen bonding interactions with the pDNA, with hydrogen bonding likely occurring between secondary amines and/or triazole nitrogens and the guanine/thymine nucleobases (Fig. 18) [156]. In contrast to Tr4, Tr1 did not show evidence of interaction with DNA structure elements, and the interaction appears to be more electrostatic in nature with lower amine stoichiometry. Due to higher amount of secondary amine and triazole groups in the longer Tr4 polymers, binding cooperativity plays a large role in increasing pDNA binding and stability with the increase in degree of polymerization. Indeed, the increase in both the electrostatic and the hydrogen bonding potential of the polymer increases cooperativity.

Cytotoxicity was shown to increase with increasing polymer length under serum-free conditions, but the polyplexes were nontoxic in serum in HeLa and H9c2(2-1) cells (Fig. 19). Cellular internalization under both conditions increased with increasing polymer degree of polymerization, as did transgene expression in serum-free media. However, increasing degree of polymerization did not influence transgene expression in serum, as all analogs had similar transgene expression in serum at $N/P = 7$. Furthermore, all Tr4 analogs were internalized to a higher degree and were less toxic than jetPEI in both serum-free and serum-containing media and, in HeLa cells, higher levels of transgene expression was observed for Tr4. This effect was cell-type dependent, as transgene expression was slightly lower in cardiomyocytes compared to PEI [155]. These results suggest that the stability of these polymers from aggregation in serum-containing media is an important property and may be advantageous in developing these materials towards various *in vivo* applications.

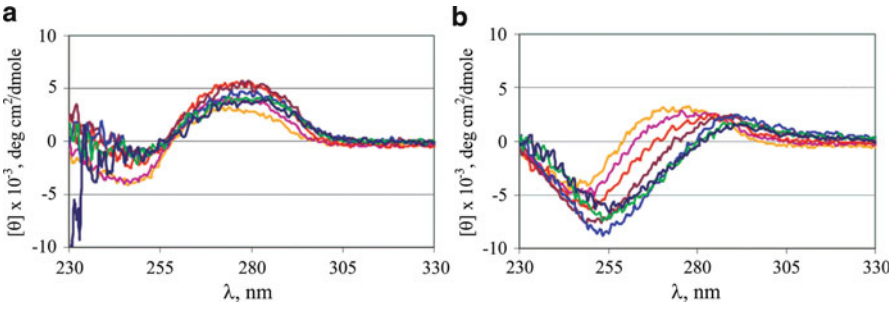

Fig. 18 Circular dichroism spectra comparing (**a**) Tr1 and (**b**) Tr4. Titration of pDNA with Tr1 results in minimal change in molar ellipticity representative of B-form DNA. Tr4 elicits a shift in ellipticity to a modified B-form, suggesting interaction with DNA base pairs by the polymer. Figure adapted with permission from [156]. © 2008 American Chemical Society

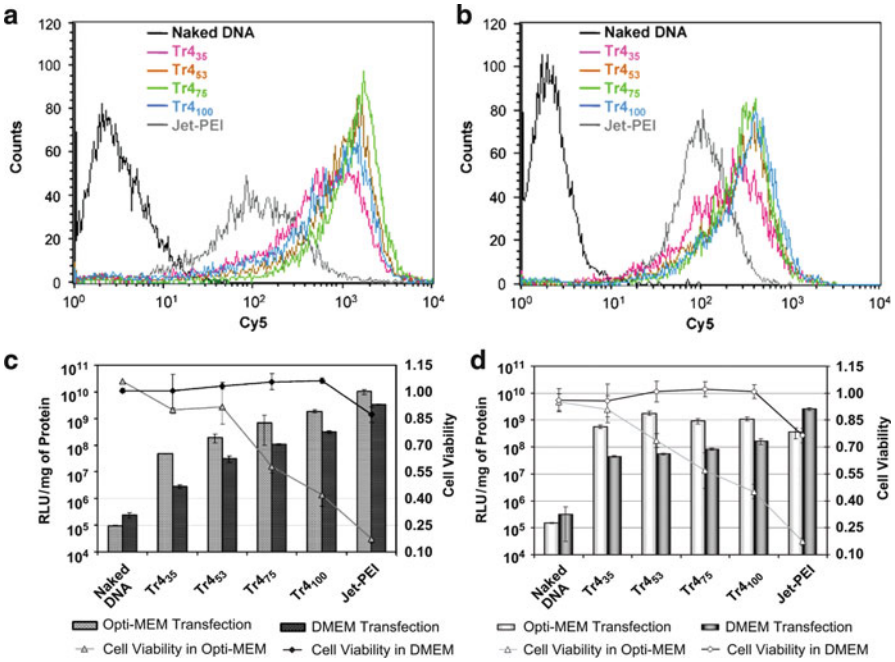

Fig. 19 Cellular internalization, transgene expression, and relative cell viability of Tr4. Cellular uptake in (**a**) serum-free and (**b**) serum-containing media. Transgene expression and cell viability in (**c**) HeLa and (**d**) H9c2(2-1) cells. Figure adapted with permission from [155]. © 2007 American Chemical Society

3.3 Polycationic Cyclodextrin Polymers

Cyclodextrins (CDs) have been popular in developing supramolecular polycations for DNA delivery. Of particular utility is the ability to modify selectively the primary and secondary hydroxyl groups, which has enabled synthesis of a wide variety of biomaterials [157–161]. In contrast to other carbohydrates, CDs contain a hydrophobic interior cavity which has been shown to form inclusion complexes with hydrophobic molecules. CDs have been extensively used in a variety of biomedical applications, and numerous drug molecules have been included in the interior of CDs and utilized towards target-specific delivery [162–167]. Such applications have used CDs as an adjuvant to complex and increase the bioavailability of hydrophobic drugs, an approach used particularly in delivery of inhaled drugs [168]. This hydrophobic "cup" opens up the potential to conjugate functional groups to a hydrophobic molecule for serum stability or cell-specific targeting, such that the hydrophobic molecule is bound within the CD core, and conjugates a pendant molecule for delivery enhancement. This section will describe some notable DNA delivery scaffolds based on CDs, as well as describe recent work

with targeted β-CD polymers in clinical and pre-clinical studies for treatment against cancer.

Star polymeric scaffolds based on α-CD have been developed by Yang et al. They were prepared by conjugation of mono-, penta-, nano-, and tetradeca-ethyleneamine units to hydroxyl groups on carbon 6 of glucose moieties using 1,1'-carbonyldiimidazole, such that pendant amine-containing arms stretch from the CD [169]. Since difunctional oligoamines were used, large excess was needed to minimize intra- and intermolecular crosslinking, the purification required precipitation and size exclusion chromatography. The number of oligoamine arms per CD was calculated using ^{1}H-NMR and it varied from 3.4 to 6.8. Unfortunately no attempt was made to explain how the number of oligoamine arms could exceed six. M_w, M_n and polydispersity index of synthesized macromolecules was not reported. These star polymers have been found to compact pDNA stably into spherical cationic nanoparticles ranging between 100 and 200 nm at $N/P \geq 8$. These polymers show significant, dose-dependent toxicity in HEK293 and COS-7 cells; this toxicity and resulting transgene expression both increased with increasing oligoethyleneamine content. The transgene expression was comparable in both serum-free and serum-containing media, suggesting that serum does not interfere with polyplex structure. Transgene expression profiles were cell type-dependent, with star polymers exhibiting transgene expression similar to PEI in HEK293 cells but significantly less in COS-7 cells [169]. While the transgene expression profiles in serum are encouraging, high toxicity will likely limit the future utility of these materials.

Cryan and coworkers [170] synthesized a series of polycations by modifying the 6-position of each glucose moiety within the CD structure with a variety of functional groups, such as pyridylamino (AP), alkylimidazole (IM), methoxyethylamino (ME), or primary amine (AM). Ethidium bromide (EtiBr) exclusion experiments indicated that the pDNA binding affinity of these polycationic CDs was wholly dependent on the substituents present in the branching arms. These studies further showed that AP- and AM-modified CDs had higher pDNA binding than ME-CD. These three analogs displayed significantly higher EtiBr exclusion than the IM-CD, a result which could be attributed to increasing hydrophobicity of the IM group. Overall, the N/P ratio required for pDNA binding was quite high (optimal N/P for transfections was 200), necessitating a high concentration of polymer for efficient pDNA compaction. Transgene expression experiments in serum-free conditions revealed high levels of transgene (luciferase) expression compared to uncomplexed pDNA, with AM-substituted CD leading to the highest expression. Addition of chloroquine, used to disrupt endosomal membranes, yielded 10- to 400-fold enhancement in luciferase expression for modified CDs compared to the untreated polymers, suggesting sequestration in endosomal compartments inhibits transfection. In serum, AM-CD showed comparable transgene expression to the cationic lipid, DOTAP. The modified CDs were cytotoxic in a concentration-dependent manner, and were quite toxic at high N/P (the cell viability was around 70% at N/P 200), suggesting limited potential for development as gene delivery agents.

Gonzalez and coworkers synthesized a series of polyamidine-CD polymers via AABB-type condensation of diamino-CD or di(2-aminoethanethio)-CD monomers

with difunctionalized-amidine comonomers (six methylene groups between the amidine units). These materials were used to study the effect of spacer length between the charge center and the carbohydrate moiety on pDNA binding and gene expression in BHK-21 and CHO-K1 cells under both serum-free and serum-rich conditions [171]. The polymers had a degree of polymerization around 6 that was determined using gel permeation chromatography. Binding studies revealed that a longer spacer between the CDs and the charge center was required for pDNA condensation, likely due to steric constraints with shorter linkers. Using the longer spacers, stable nanoparticles of 150–180 nm at $N/P = 10$ were attained. Transfection experiments resulted in similar transgene expression as branched PEI (25 kDa) and slightly higher expression than PLL, SuperFect, and Lipofectamine in both cell lines under serum-free conditions. When similar experiments were performed in serum-containing media, a 10% decrease in gene expression was observed for all the polyplexes. The cell viability assay demonstrated that the CD-containing polymers were less toxic than commercial vectors under both conditions.

In a similar study, Hwang et al. [141] studied the effect of spacing between the amidine groups on pDNA binding ability and gene expression by systematic modifications to the number of methylene groups (from 4 to 10) in between the amidine units (Fig. 20). The polymers (β-CDPs) contained four to five repeat units and compacted pDNA into nanoparticles of 12–150 nm in diameter. This study also

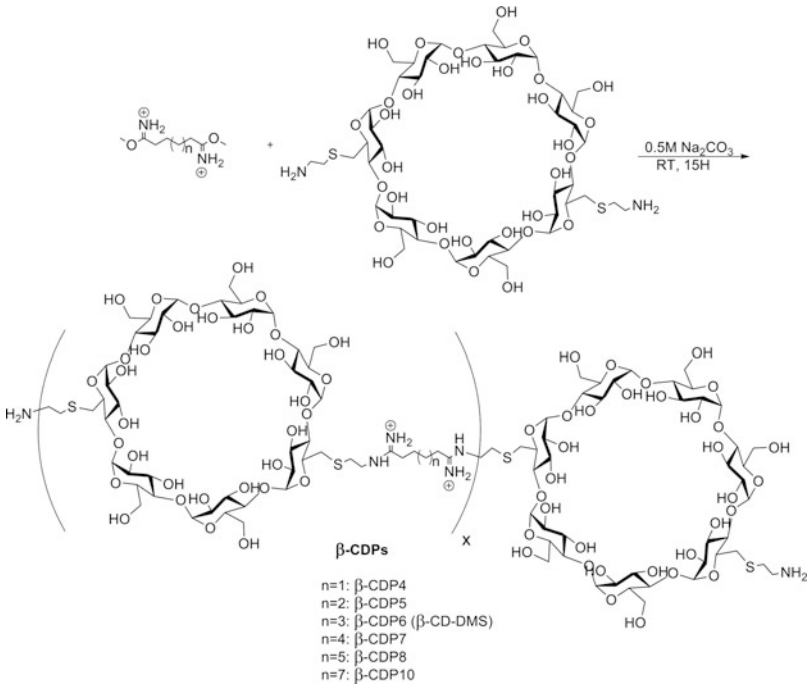

Fig. 20 Synthesis of β-CD-based polymer. Reproduced with permission from [141]. © 2001 American Chemical Society

showed that polymers with four, five, and ten methylene units formed slightly larger particles than the other β-CDPs. The DNase protection ability of these polymers revealed that polymers containing four, six, eight, and ten methylene units protected pDNA against nuclease degradation, while analogs possessing five and seven methylene units offered only partial protection. These results could possibly be due to an effect of odd vs. even methylene spacing on pDNA binding and/or stability. Transfection experiments in BHK-21 cells showed β-CDP6 (6 methylene spacing) yielded higher transgene (luciferase) expression than the other β-CDPs. In addition, nearly 20% reduction in luciferase gene expression was observed when the cells were transfected with β-CDP5 (5 methylene spacing), thereby demonstrating that an optimal spacer length between the amidine units is important for maximal delivery. The cytotoxicity assay at $N/P = 50$ showed that β-CDP8 and β-CDP7 afforded almost 100% cell viability. However, all the other β-CDPs were found to be toxic, which was also evident via MTT assay. Thus, these experiments demonstrate that an optimal spacing between the amidine units is significant for increased transfection efficiency and decreased cytotoxicity.

Srinivasachari et al. designed a novel series of macromolecule vehicles using a β-CD core, where the 6-position of the glucose units has been grafted with pendant oligoethyleneamine groups of specified length (where the secondary amine stoichiometry varied from 0 to 4) [172]. To avoid formation of under-substituted impurities, the core and the branching units were conjugated via a 1,2,3-trizole linkage utilizing the high-yielding 1,3-dipolar cycloaddition, termed the "click reaction". These completely monodisperse β-CD "click clusters" bind and compact pDNA at $N/P > 2$ into spherical nanoparticles with a diameter around 80–130 nm. Structures with two, three, or four secondary amines in the oligoethyleneamine arms protected pDNA from nuclease degradation when incubated in serum at 37°C for up to 48 h. These macromolecules were able to deliver efficiently Cy5-labeled pDNA into HeLa and H9c2(2-1) cells, and the internalization was comparable to transfection reagents jetPEI and SuperFect with dramatically lower toxicity. Transgene expression in both cell lines increased with increasing secondary amine content, and the analogs with three and four secondary amines showed similar (within an order-of-magnitude) transgene expression as jetPEI and SuperFect.

These promising initial results on the click cluster vehicles were succeeded by analogous studies to incorporate β-CD into a polymeric scaffold for gene delivery [173]. In this case, the β-CD was di-functionalized with azide groups and polymerized with dialkyne-functionalized oligoethylenamines to derive linear β-CD polymers containing between one and four secondary amines per repeat unit (Cd1–Cd4; Fig. 21). Based upon earlier favorable results with similar systems [21, 140, 146, 155], several different molecular weights of Cd4 (contains four secondary amines in the repeat unit), were synthesized to examine the effect of variation in the polymer length. Incorporation of β-CD into this polymer showed similar DNA binding and polyplex size and cationic surface profiles as were seen previously for the β-CD click clusters. CD-containing polymers showed significant enhancement in cellular uptake over jetPEI in HeLa cells, with Cd2, Cd3, and Cd4 internalized significantly better that Cd1. With polymer vehicle Cd4, molecular weight did not appear to affect

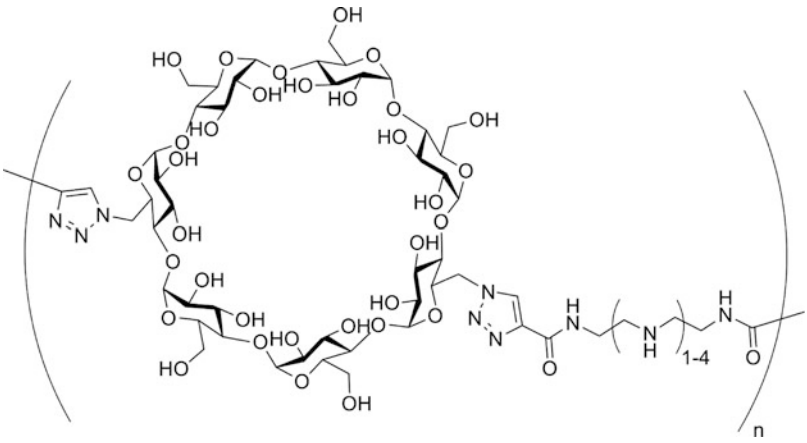

Fig. 21 Structure of β-CD "click" polymers. Figure reproduced with permission from [173]. © 2009 American Chemical Society

internalization significantly, as similar high levels of polyplex internalization was observed for all lengths. In general, high levels of transgene expression were observed with these polymers, and the highest expression was observed with Cd3, slightly higher than Cd4, and both had similar profiles to Jet-PEI. The authors attribute the high delivery of Cd3 to a more flexible, randomly-coiled structure. This assessment is sensible, as lack of polymer rigidity could be important in DNA release, or accessibility of RNA polymerases, depending on how the polymer:DNA polyplex traffics within the cell. Interestingly, despite much more favorable uptake profiles compared to jetPEI, similar transgene expression was observed. This may be due to differences in trafficking mechanisms and rates, which may lead PEI to the nucleus in a more efficient manner. However, if nuclear delivery is not exclusive, this may afford a unique opportunity to deliver siRNA in high levels to the cytosol, an advantageous result for gene knockdown via RNA interference as a therapeutic strategy.

Oligonucleotide delivery with β-CD for targeted cancer therapeutics has been explored extensively by the group of Mark Davis, and the remainder of this section is focused on the groundbreaking *in vivo* results attained by this laboratory. Previous work in this lab has extensively exploited the hydrophobic interior cavity of β-CD for inclusion of hydrophobic molecules conjugated to targeting groups [175], and this technology will be discussed in greater detail in the next section. In many of these studies, a β-CD polycation end-capped with imidazole groups was used as the delivery vehicle, and the human transferrin protein was used as a targeting ligand due to upregulation of transferrin receptors on tumor cells (Fig. 22). Pun et al. used these targeted β-CD-containing polycations to deliver fluorescently-labeled DNAzymes targeted to the *c-myc* proto-oncogene – to which tumor cells have been shown to require for proliferation – in tumor-bearing mice [176]. Using whole-body imaging techniques, Cy3-labeled DNAzymes were seen associating with the actin cytoskeleton. The highest levels of sustained fluorescence

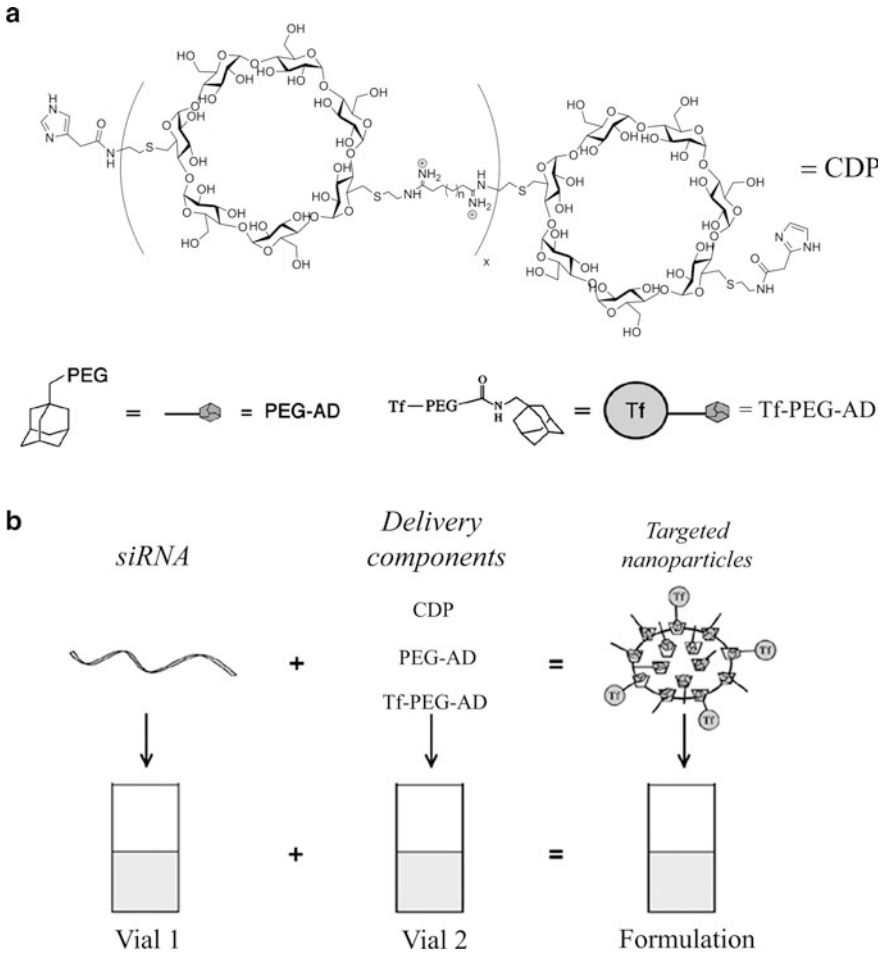

Fig. 22 (**a**) Structure of β-cyclodextrin-containing polycations (CDP)s and (**b**) formulation of siRNA-containing targeted nanoparticles formed with CDP. Figure reprinted with permission from [177]. © 2007 National Academy of Sciences, U.S.A

were observed when polyplexes were administered via intravenous bolus injection (compared to intraperitoneal injection, for which uptake of particles by tumor tissue was low). Unmodified DNAzyme was observed in cryosectioned tumor, liver, and kidneys 8 h post-injection but was not observed after 24 h, suggesting clearance from the body within this time frame. However, DNAzymes delivered in β-CD polyplexes were sustained in the tissues after 24 h, suggesting that the PEG groups afford prolonged circulation time that allows tumor delivery over extended time [176]. These experiments show that targeted delivery of oligonucleotides can be achieved *in vivo* by β-CD-containing polycations.

In a mouse model of Ewing's sarcoma, Hu-Lieskovan et al. used these β-CD-containing vehicles to deliver siRNA against the *EWS-FLI1* gene expressed

in this disease model [174]. Ewing's sarcoma (TC71) cells were modified to express stably luciferase and injected into immunocompromised mice to attain a disseminated tumor model, which was verified by bioluminescence imaging and MRI. Mice were dosed twice weekly with transferrin-targeted β-CD polycations complexing siRNA against *EWS-FLI1* (siEFBP2), with treatment beginning the same day as injection of tumor cells. Delivery of naked siEFBP2 and targeted polyplexes containing control (non-*EWS-FLI1*-targeting; siCON1) siRNA did not decrease tumor size compared to control mice, and untargeted siEFBP2 polyplexes showed delayed tumor formation. However, targeted polyplexes containing siEFBP2 reduced tumor growth to 20% of that of control mice, indicating that targeted delivery of siRNA to transferrin-overexpressing tumor cells prevented the tumorigenicity of injected Ewing's sarcoma cells. Substantial tumor reduction was observed during the course of the experiment (Fig. 23a). Importantly, these repeated

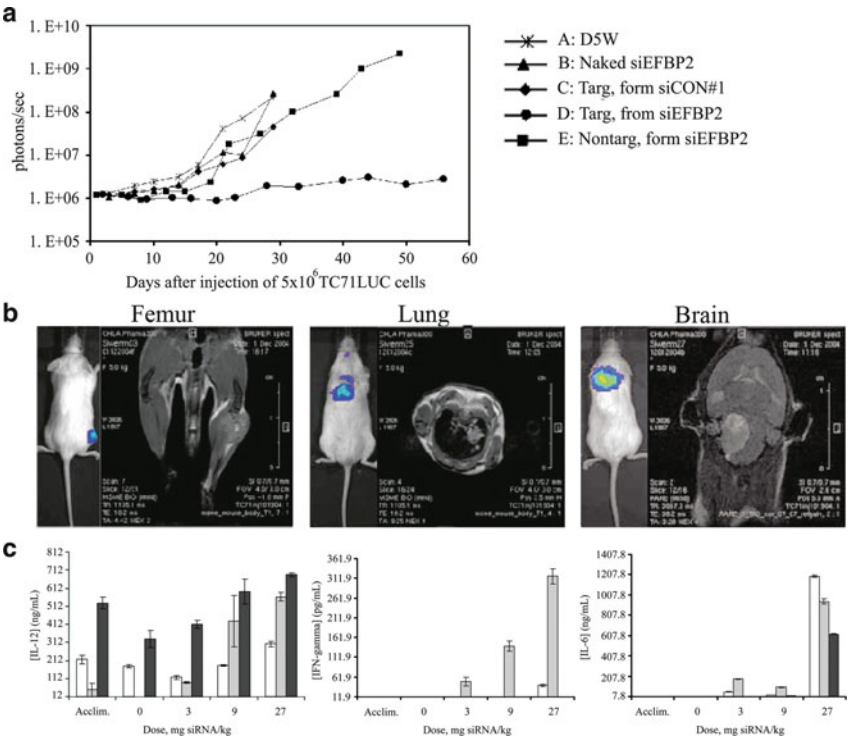

Fig. 23 *In vivo* performance of targeted cyclodextrin polycations. (**a**) Growth curves for engrafted tumors. The median integrated tumor bioluminescent signal (photons/s) for each treatment group (n = 8–10) is plotted vs time after cell injection (days). (**b**) MRI confirmation of tumor engraftment. (**c**) Dose-dependent effects on cytokine production in non-human primates. Only very high dosage led to significant increases in cytokines. (**a**, **b**) reprinted with permission from [174], figures 3 and 5. © 2005 American Association for Cancer Research. (c) reprinted with permission from [177]. © 2007 National Academy of Sciences, U.S.A

treatments did not lead to increased cytokine levels or induce tissue damage, suggesting toxic and immune responses by the animals were minimal. These results show that targeted, systemic delivery of siRNA can treat disseminated cancers with carbohydrate-based *non-viral* gene delivery in a sequence-specific manner.

These promising results have led to further studies *in vivo* to assess gene knockdown efficacy of vehicles targeted to cancer cells. Heidel et al. used escalating doses of β-CD-siRNA nanoparticles delivered intravenously in monkeys (Fig. 23b). These are fundamental studies, as determination of dose-dependent tolerance levels is crucial for minimization of drug-induced toxicity and/or other untoward side effects. Escalating doses of 3, 9, and 27 mg/kg (with respect to the siRNA component) were administered 3 days apart, followed by a washout period of 11–12 days prior to a final dosing of 3 mg/kg. Serum chemistry and immune effects were measured 6 h post-injection. The lower doses of nanoparticle (3 and 9 mg/kg) were well tolerated and did not lead to significant increases in hematological factors (i.e., coagulation factors) or pro-inflammatory cytokines (Fig. 23c). At the highest dose (27 mg/kg), increases in creatinine and blood urea nitrogen were observed, indicative of acute renal toxicity. Coagulation factors were unaffected by the high dosage, but increases in pro-inflammatory cytokines IL-6 and IFN-γ, indicative of a helper T cell response, were observed shortly after injection of high doses of siRNA. Interestingly, increasing levels of TNF-α were not observed, providing convincing evidence that systemic inflammation is not occurring. Unfortunately, longer term measurements of these cytokines were not reported, so it is unclear whether these effects are transient or chronic. Exposure of the animals to high dosage of siRNA-containing nanoparticles did not lead to high titer antibody formation, suggesting that repeated doses of nanoparticles over time would be well-tolerated by the animals and would not lead to ineffective dosing due to an immune (neutralizing antibody) response. Importantly, high levels of nanoparticles were detected in the blood 5 min post-injection, verifying circulation of nanoparticles and avoiding rapid clearance from the bloodstream [177]. This elegant study confirms the safety of these nanoparticle siRNA delivery systems and suggests that repeating high dosage treatment could be well tolerated in patients. These promising vehicles have shown that high delivery and treatment efficacy can be attained with *non-viral* nucleic acid delivery, and are among the first carbohydrate-based vehicles to advance to human clinical trials. These preliminary studies have been reviewed recently [178] and provide a bright outlook to the future of the field.

4 Targeted Gene Delivery with Carbohydrates

As described earlier, carbohydrates have been used extensively in their native forms and as components of novel polymeric structures to transfer exogenous nucleic acids into cells. In addition, carbohydrates have also been conjugated to polymeric delivery systems as targeting moieties. While an extensive amount of work has been completed and continues to be published utilizing various carbohydrate

structures for targeting, a full review of this area is beyond the scope of this review. As an example of the promise of this extensive research, we briefly review the use of β-D-galactose and β-D-galactosamine cell-specific targeting of polyplexes to hepatocytes, which are commonly studied targeting ligands in this research field. Hepatocytes overexpress the asialoglycoprotein receptor (ASGPr), a lectin that specifically recognizes the β-D-galactose and β-D-galactosamine carbohydrates. Conjugating these sugars as pendant groups on polymeric vehicles has been used extensively to achieve hepatocyte-specific targeting *in vitro* and *in vivo*. The following section briefly describes recently-published work to facilitate hepatocyte-selective delivery of DNA.

Early work by Zanta et al. describes galactosylated PEI (lactose was used in a reductive amination with PEI) as a liver-specific delivery system, which maintained tight DNA binding at low *N*/*P* ratios [179]. These galactosylated polyplexes were able to transfect NIH 3T3, a non-hepatocyte cell line, indicating incomplete specificity for ASGPr. However, the transgene expression efficiency was less than that observed for unmodified PEI, which can be interpreted as being due to a lack of cell-surface affinity from low levels of ASGPr. By contrast, murine (BNL CL.2) and human (HepG2) hepatocytes showed higher transgene expression from galactosylated PEI than unmodified PEI at low *N*/*P*. At high *N*/*P*, unmodified PEI demonstrated higher transgene expression, which may be artificially high due to increased toxicity. Incubation of cells with a competitive binding inhibitor to ASGPr, asialofetuin (ASF), led to a decrease in transgene expression, signifying receptor-mediated uptake [179]. A later study by Pun and Davis described the development of a hepatocyte-specific DNA delivery system using β-CD-containing polymers. In this approach, galactosamine was installed at the PEG end of galactose-PEG-tetrapeptide-adamantane via amide bond and this macromolecule was used to create a targeted vehicle by taking advantage of the ability of adamantane to form inclusion complexes with the hydrophobic core of β-CD [175]. Specific delivery to HepG2 cells was partially successful, as inhibition of targeted polyplex internalization was inhibited by ASF. However, as before, significant internalization was still observed for targeted polyplexes inhibited with ASF – this was seen for untargeted polyplexes as well. These studies demonstrate that galactosylation of polymeric vehicles can possibly provide receptor-specific uptake *in vitro*, but non-specific delivery is still observed. In addition, transgene expression is used to assess receptor-specific uptake, but this is a downstream event from receptor-mediated internalization. It was clear from these studies that more work was needed to achieve exclusive delivery to hepatocytes and better research tools were needed to assess receptor-mediated internalization.

Further studies have attempted to optimize the amount of galactose conjugation with the specific delivery efficiency. The mole percentage of galactose on PEI was modified by varying the amount of lactose used in reductive amination reaction, to assess the effect of galactose concentration on transfection [180]. Increasing the mol % galactose up to 31.1% did not affect binding of PEI analogs to DNA. However, polyplex size grew with increasing galactose, and this was accompanied by a decrease in zeta potential, which became nearly neutral at high (31.1%) galactose

concentration. Increasing galactose has a favorable effect on cell viability – improvement in biocompatibility was directly proportional to percent galactose, which corresponded to lower membrane-damaging effects as evidenced by LDH release. However, receptor-specific delivery was not achieved, as unmodified PEI showed higher levels of luciferase expression than galactosylated analogs. Polyplex size and charge clearly played a role in delivery, as larger, more neutral particles showed lower transgene expression than smaller, cationic polyplexes. A similar study by Ren et al. observed the effect of increasing the number of galactose molecules from one to three on a dendritic structure [26]. Less transgene (luciferase) expression was seen in HepG2 cells than in a non-hepatocyte cell line (BL-6 cells), indicating that hepatocyte specificity is not observed. However, increasing luciferase expression was observed as a function of the number of conjugated galactose molecules, as highest luciferase expression was observed for the tri-galactosylated compounds at low concentration. These results suggest that increasing the number of galactose groups may improve targeting based on a multivalent effect.

A potential problem with assessing receptor-mediated delivery may indeed be use of an *in vitro* system. HepG2 cells are hepatocellular carcinoma cells, so receptor expression may be more varied than a typical liver cell, and the rapid growth of malignant cells may help to internalize polyplexes non-specifically. Therefore, Nishikawa et al. monitored targeted DNA delivery *in vivo* to determine pharmacokinetic and biodistribution profiles with poly-L-ornithine-based polymers conjugated with galactose [181]. The conjugation was done using 2-imino-2-methoxyethyl-thio-β-D-galactopyranoside. Conjugation of galactose did not impact the polyplex size, so polyplexes formulated with [^{32}P] DNA were injected intravenously into mice. As these materials are not serum-stabilized in any way, rapid clearance of polyplexes occurred, as the half-life was 8.2 min or less. However, the majority of radioactivity and luciferase expression was observed in the liver (with respect to other organs monitored – lungs, kidneys, spleen, heart), and the delivery to the liver increased with time. More significantly, when parenchymal (hepatocytes) and non-parenchymal (Kupffer, non-hepatocytes) liver cells were separated by collagenase perfusion, much higher radioactivity and luciferase expression was seen in the parenchymal cells than the non-parenchymal cells, suggesting hepatocyte-specific delivery was preferred over non-specific delivery. Some non-specific delivery was still observed – particularly to the lungs – but these are generally promising results that suggest that, in an animal model, hepatocyte specificity can be achieved.

The previously-published work in the fields of hepatocyte-targeted nucleic acid delivery and serum stabilization can be combined to develop smart delivery vehicles that contain structural elements for overcoming cellular barriers. In an elegant study, Chen et al. described the design and synthesis of PEGylated glycopeptides containing a cysteine-terminated triantennary glycopeptide (Fig. 24), PEGylated peptide, and melittin to form polymers through formation of disulfide bonds under oxidative conditions [182].

These polymers have been designed to achieve serum stability and sustained circulation with the PEGylated peptide, specific targeting to hepatocytes with

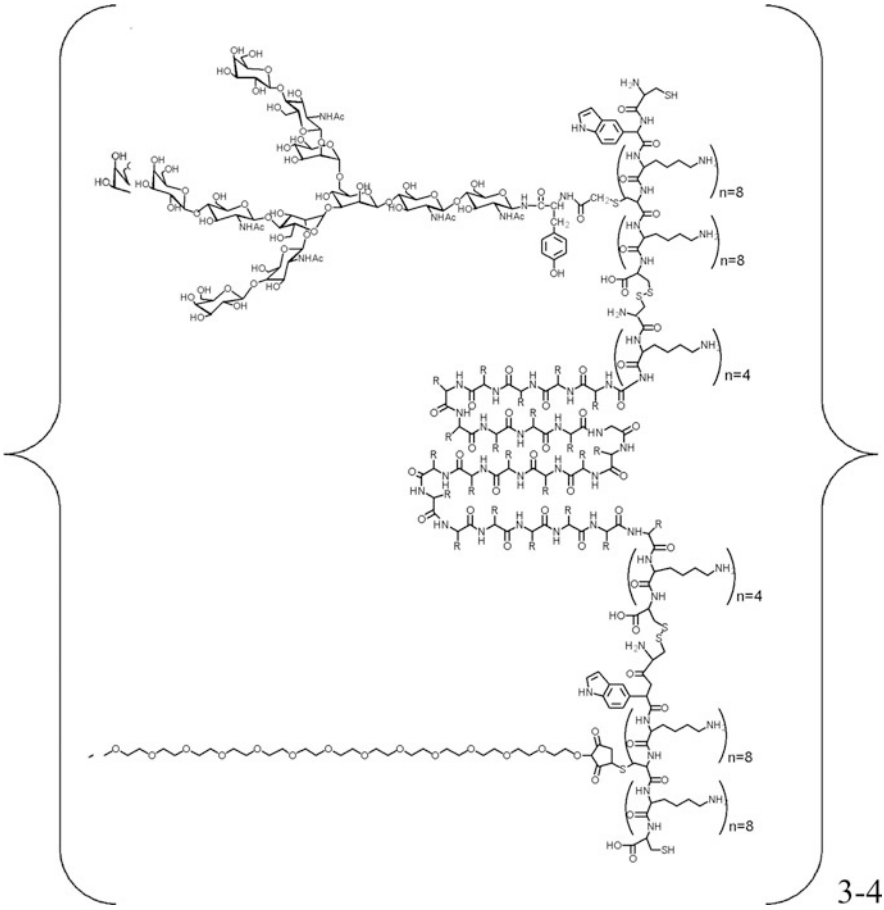

Fig. 24 Structure of PEGylated glycopeptide. Figure reproduced with permission from [182]. © 2007 American Chemical Society

galactosylated peptide, and increased cellular internalization and endosomal disruption with the fusogenic peptide monomer (melittin). Under the reducing conditions of the cell, the disulfide bonds can be reduced to sulfhydryl groups, degrading the polymer and releasing the pDNA. They developed five PEGylated glycopeptides (PGPs) with increasing melittin concentrations from 0% (PGP1) to 73% (PGP5), as well as a control polymer, PGP3*, that did not contain galactose for targeting. The specific delivery of DNA to hepatocytes was monitored in a murine model (Fig. 25). Polyplexes were administered intravenously by injection into the tail vein, which was followed by hydrodynamic stimulation via saline injection 5 min later to promote high levels of cellular uptake. Polymeric delivery of DNA was retained in the body twice as long as uncomplexed DNA, having a half-life of

structure	monomer composition[a] (mol %)	measured composition[b] (mol %)	molecular weight (PLL)[c], (PEO)[d]	particle size[e]	zeta potential[f]	$t_{1/2}$[g] hr	PC/NPC[h]
PGP 1	0:90:10	0:91.7:8.3	106 kDa, 50 kDa	221 8	+0.5	1.1	60:40
PGP 2	10:80:10	12.8:82.5:4.7	109 kDa, 51 kDa	210 13	+5	1.2	59:41
PGP 3	20:70:10	24.4:70.3:5.3	99 kDa, 47 kDa	227 11	+6	1.2	65:35
PGP 4	40:50:10	44.8:46.4:8.8	83 kDa, 46 kDa	232 1	+6	1.3	60:40
PGP 5	70:20:10	73.2:19.8:7.0	35 kDa, 21 kDa	295 7	+5	1.1	63:37
PGP 3*i	20:70:10	12.6:80.9:6.5	99 kDa, 47 kDa	227 11	+6	1.0	38:62

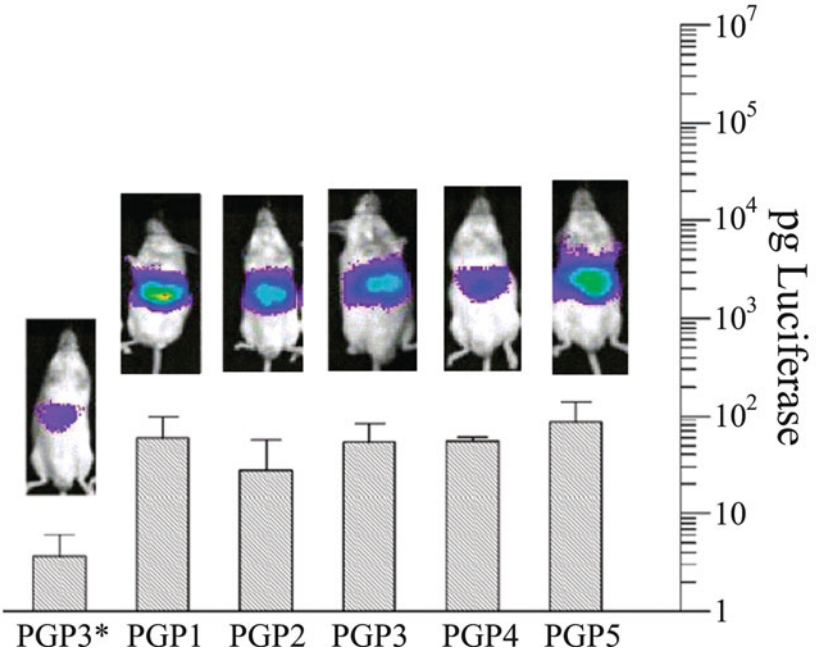

Fig. 25 Characterization and luciferase expression of PGP DNA condensates in vivo. These results show that luciferase expression is dependent on galactose incorporation but independent of amount of melittin. (**a**) Represents the input mol ratio of Cys-terminated melittin, PEG-peptide, and glycopeptide. (**b**) Represents the measured mol ratio of Cys-terminated melittin, PEG-peptide, and glycopeptide for each purified PGP. (**c**) Values are the calculated MW based on polylysine standards. (**d**) Values are the calculated MW based on PEG standards. (**e**) The mean particle size determined at a stoichiometry of 0.3 nmol of PGP per mg of DNA. The value represents the mean diameter (nm) based on unimodal analysis. (**f**) The zeta potential of PGP DNA condensates at a stoichiometry of 0.3 nmol of PGP per mg of DNA. (**g**) The metabolic half-life of PGP 125I-DNA in triplicate mice. The results are derived from Fig. 6. (**h**) The PC/NPC ratio of DNA-targeted liver. (**i**) Represents a control PGP 3 in which galactose has been removed. Figure adapted with permission from [182]. © 2007 American Chemical Society

1 h. Hepatocyte-specific targeting was assessed by the ratio of DNA in parenchymal vs non-parenchymal liver cells, and the galactosylated polymers led to 50% higher delivery to parenchymal cells than to non-parenchymal cells. A control of non-galactosylated polymer showed 50% higher uptake in non-parenchymal cells vs parenchymal cells. Luciferase expression was measured 24 h post-injection, and

significantly higher luciferase expression was observed in the galactosylated analogs (Fig. 25). These results suggest that hepatocyte-favored delivery leading to transgene expression of DNA can be achieved through rational therapeutic design.

Targeted delivery of siRNA has also been achieved using rationally-designed polymeric vehicles using galactose as a hepatocyte-targeting group. Rozema et al. describe a polymeric system, dubbed Dynamic PolyConjugates, to attach *N*-acetylgalactosamine, PEG, and siRNA to a polymeric backbone for hepatocyte-targeting, charge shielding for serum stability, and gene knockdown, respectively [183]. The PEG was conjugated through an acid-labile maleamate linkage for release of PEG in endosomal compartments that can expose polymer amines for endosome

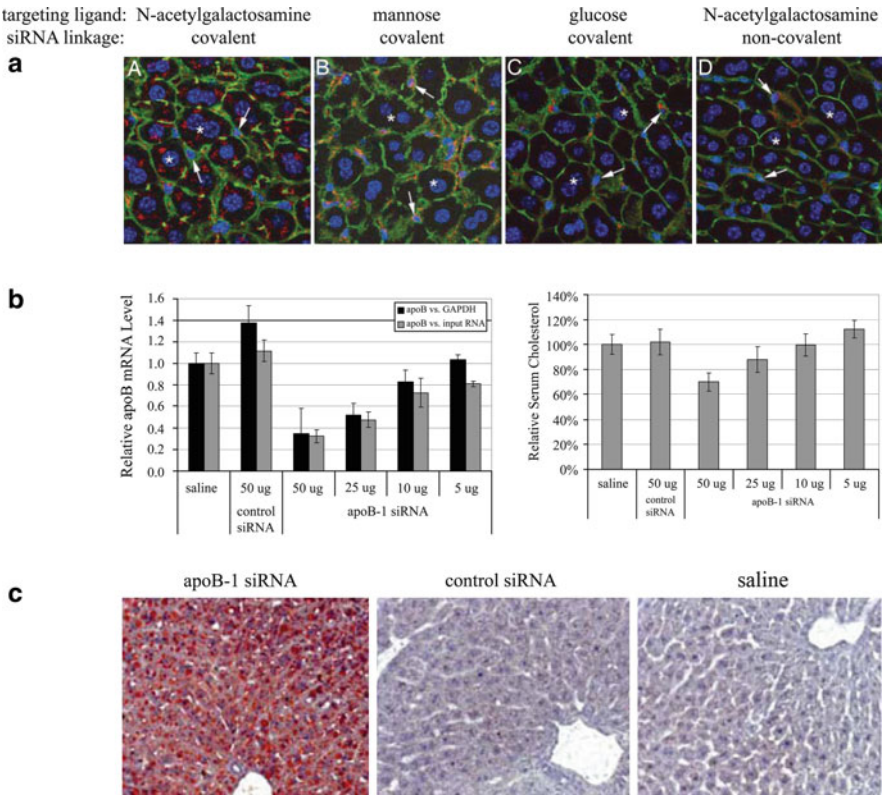

Fig. 26 Specific delivery of siRNA to hepatocytes with Dynamic PolyConjugates. (**a**) Confocal micrographs indicate specific intracellular delivery of oligonucleotides by targeting hepatocytes with *N*-acetylgalactosamine, as Cy3-labeled oligonucleotide (red) is seen within mouse hepatocytes, compared to when mannose and glucose are used as targeting moieties and Cy3 oligonucleotides are seen in the pericellular regions. (**b**) RT-qPCR shows dose-dependent decrease in apoB mRNA, corresponding to (**c**) decreasing serum cholesterol levels. (**d**) Increased hepatic lipid content (stained with oil red) relative to control siRNA and saline injections confirm knockdown of apoB-mediated cholesterol transport from the liver. Figure adapted with permission from [183].

disruption, and the siRNA was attached through a disulfide linkage which is cleaved under the reducing conditions of the cytoplasm. Using an siRNA targeted against the mRNA for apolipoprotein B (apoB), a gene expressed by hepatocytes, they were able to achieve 80% knockdown of apoB in mouse primary hepatocytes compared to 60–70% knockdown for a commercially-available transfection reagent, *Trans*IT-siQuest. Mice injected intravenously with *N*-acetylgalactosylated oligonucleotide polyconjugates showed intracellular delivery of Cy3-oligonucleotide to hepatocytes, compared to no intracellular delivery when the targeting group was mannose or glucose (Fig. 26a). Mice injected with apoB siRNA-containing polyconjugates (Fig. 26b, c) showed dose-dependent knockdown of apoB mRNA two-days post-injection, as well as corresponding decreases in serum cholesterol. Hepatic lipid content was visualized by oil red staining of tissue sections, and mice treated with apoB siRNA showed increased lipid content corresponding in decreasing cholesterol transport from the tissue by apoB (Fig. 26d). These results confirm the liver-specific delivery of siRNA with polymers conjugated to *N*-acetylgalactosamine.

The results discussed in this section present a brief sampling of the literature focused on hepatocyte-specific delivery with carbohydrate-based targeting ligands. This section focused on galactose for targeting the ASGPr on hepatocytes, but other carbohydrates have also been studied for cell-specific targeting, including lactose for targeting the airway epithelia and mannose for targeting cells of the immune system [143, 184, 185]. While a detailed review of this subfield is beyond the scope of this chapter, work in this area is ongoing and continues to develop polymeric systems for specific delivery of nucleic acids through lectin-mediated targeting.

5 Outlook

More than a decade of intense research has been devoted to developing carbohydrate-based polymers as nucleic acid carriers for the treatment of disease. This review has outlined the progression and successes attained by carbohydrate-based vehicles. As described herein, carbohydrates allow biocompatible transfection of nucleic acids into mammalian cells, enable chemical modification for delivery enhancement, and can be used as targeting moieties for achieving receptor-specific delivery. Indeed, the last few years have yielded substantial progress in the development of carbohydrates as delivery vehicles, including tumor-specific delivery of siRNA for human therapeutics, specific delivery of pDNA to hepatocytes, and development of rationally-designed vehicles designed to promote efficient delivery by systematically bypassing extracellular and intracellular barriers. These promising studies prove that the past years of research have led to valuable information about how DNA delivery vehicles are processed by the cell, and this knowledge is actively applied to develop new, functional materials designed for use in humans. While this prospect has yet to be achieved, the progress in the field is evident and carbohydrate-based nucleic acid delivery vehicles will remain at the

forefront of *non-viral* delivery research. Future studies in this area will continue to develop cutting-edge reagents for delivery of nucleic acids, and progress more promising vehicles towards the clinic for eventual treatment of devastating human disease.

Acknowledgments We apologize to our many colleagues whose elegant work we were unable to discuss directly in this review. The authors acknowledge NIH New Innovator Award. T.M.R. is a fellow of the Alfred P. Sloan Research Foundation and a recipient of the Camille Dreyfus Teacher-Scholar Award.

References

1. Pickler RH, Munro CL (1995) Gene therapy for inherited disorders. J Pediatr Nurs 10:40–47
2. Anderson WF (1992) Human gene therapy. Science 256:803–813
3. Mulligan RC (1993) The basic science of gene therapy. Science 260:926–932
4. Wiethoff CM, Middaugh CR (2003) Barriers to nonviral gene delivery. J Pharm Sci 92 (2):203–217
5. Braun CS, Vetro JA, Tomalia DA et al (2005) Structure/function relationships of polyamidoamine/DNA dendrimers as gene delivery vehicles. J Pharm Sci 94(2):423–436
6. Behr J-P (1993) Synthetic gene-transfer vectors. Acc Chem Res 26:274–279
7. Luo D, Saltzman WM (2000) Synthetic DNA delivery systems. Nat Biotechnol 18:33–37
8. Davis ME (2002) Non-viral gene delivery systems. Curr Opin Biotechnol 13(2):128–131
9. Kircheis R, Wagner E (2000) Polycation/DNA complex for *in vivo* gene delivery. Gene Ther Regul 1:95–114
10. Godbey WT, Wu KK, Mikos AG (1999) Poly(ethylenimine) and its role in gene delivery. J Control Release 60(2–3):149–160
11. Godbey WT, Wu KK, Mikos AG (1999) Size matters: molecular weight affects the efficiency of poly(ethylenimine) as a gene delivery vehicle. J Biomed Mater Res B 45 (3):268–275
12. Mannisto M, Vanderkerken S, Toncheva V et al (2002) Structure-activity relationships of poly(L-lysines): effects of pegylation and molecular shape on physicochemical and biological properties in gene delivery. J Control Release 83(1):169–182
13. Kim SW (2007) Polylysine copolymers for gene delivery. Gene Transfer 461–471
14. Kwoh DY, Coffin CC, Lollo CP et al (1999) Stabilization of poly-L-lysine/DNA polyplexes for *in vivo* gene delivery to the liver. Biochim Biophys Acta 1444(2):171–190
15. Smith DK (2006) Dendritic supermolecules–towards controllable nanomaterials. Chem Commun 1:34–44
16. Eliyahu H, Siani S, Azzam T et al (2006) Relationships between chemical composition, physical properties and transfection efficiency of polysaccharide–spermine conjugates. Biomaterials 27:1646–1655
17. Hong S, Bielinska AU, Mecke A et al (2004) Interaction of poly(amidoamine) dendrimers with supported lipid bilayers and cells: hole formation and the relation to transport. Bioconjug Chem 15(4):774–782
18. Kraemer M (2004) Dendritic polyamines: simple access to new materials with defined treelike structures for application in nonviral gene delivery. ChemBioChem 5(8):1081
19. Svenson S, Tomalia DA (2005) Dendrimers in biomedical applications – reflections on the field. Adv Drug Deliv Rev 57(15):2106–2129
20. Mintzer MA, Simanek EE (2009) Nonviral vectors for gene delivery. Chem Rev 109:259–303

21. Liu Y, Reineke TM (2005) Hydroxyl stereochemistry and amine number within poly(glycoamidoamine)s affect intracellular DNA delivery. J Am Chem Soc 127(9):3004–3015
22. Velter I, La Ferla B, Nicotra F (2006) Carbohydrate-based molecular scaffolding. J Carbohydr Chem 25:97–138
23. Varma AJ, Kennedy JF, Galgali P (2004) Synthetic polymers functionalized by carbohydrates: a review. Carbohydr Polym 56:429–445
24. Yudovin-Farber I, Domb AJ (2007) Cationic polysaccharides for gene delivery. Mat Sci Eng 27:595–598
25. Miyata T, Nakamae K (1997) Polymers with pendant saccharides – 'glycopolymers'. Trends Polym Sci 5(6):198–205
26. Ren T, Zhang G, Liu D (2001) Synthesis of galactosyl compounds for targeted gene delivery. Bioorg Med Chem 9(11):2969–2978
27. Lundquist JJ, Toone EJ (2002) The cluster glycoside effect. Chem Rev 102(2):555–578
28. Ladmiral V, Melia E, Haddleton DM (2004) Synthetic glycopolymers: an overview. Eur Polym J 40:431–449
29. Mehvar R (2000) Dextrans for targeted and sustained delivery of therapeutic and imaging agents. J Control Release 69:1–25
30. Sakurai K, Uezu K, Numata M et al (2005) b-1,3-Glucan polysaccharides as novel one-dimensional hosts for DNA/RNA, conjugated polymers and nanoparticles. Chem Commun 35:4383–4398
31. Borchard G (2001) Chitosans for gene delivery. Adv Drug Deliv Rev 52(2):145–150
32. Yun YH, Goetz DJ, Yellen P et al (2004) Hyaluronan microspheres for sustained gene delivery and site-specific targeting. Biomaterials 25(1):147–157
33. Gupta M, Gupta AK (2004) Hydrogel pullulan nanoparticles encapsulating pBUDLacZ plasmid as an efficient gene delivery carrier. J Control Release 99(1):157–166
34. Vaheri A, Pagano JS (1965) Infectious poliovirus RNA: a sensitive method of assay. Virology 27(3):434–436
35. Mack KD, Wei R, Elbagarri A et al (1998) A novel method for DEAE-dextran mediated transfection of adherent primary cultured human macrophages. J Immunol Methods 211:79–86
36. Onishi Y, Eshita Y, Murashita A et al (2005) Synthesis and characterization of 2-diethylaminoethyl-dextran-methyl methacrylate graft copolymer for nonviral gene delivery vector. J Appl Polym Sci 98:9–14
37. Azzam T, Eliyahu H, Makocitzki A et al (2003) Dextran-spermine conjugate: an efficient vector for gene delivery. Macromol Symp 195:247–261
38. Azzam T, Raskin A, Makovitzki A et al (2002) Cationic polysaccharides for gene delivery. Macromolecules 35(27):9947–9953
39. Hosseinkhani H, Azzam T, Tabata Y et al (2004) Dextran–spermine polycation: an efficient nonviral vector for *in vitro* and *in vivo* gene transfection. Gene Ther 11:194–203
40. Eliyahu H, Joseph A, Schillemans JP et al (2007) Characterization and *in vivo* performance of dextran-spermine polyplexes and DOTAP/cholesterol lipoplexes administered locally and systemically. Biomaterials 28(14):2339–2349
41. Eliyahu H, Joseph A, Azzam T et al (2006) Dextran-spermine-based polyplexes – evaluation of transgene expression and of local and systemic toxicity in mice. Biomaterials 27 (8):1636–1645
42. Singh A, Suri S, Roy K (2009) In-situ crosslinking hydrogels for combinatorial delivery of chemokines and siRNA-DNA carrying microparticles to dendritic cells. Biomaterials 30 (28):5187–5200
43. Beaudette TT, Cohen JA, Bachelder EM et al (2009) Chemoselective ligation in the functionalization of polysaccharide-based particles. J Am Chem Soc 131(30):10360–10361
44. Bachelder EM, Beaudette TT, Broaders KE et al (2008) Acetal-derivatized dextran: an acid-responsive biodegradable material for therapeutic applications. J Am Chem Soc 130 (32):10494–10495

45. Sakurai K, Iguchi R, Mizu M et al (2003) Polysaccharide-polynucleotide complexes. Part 7. Hydrogen-ion and salt concentration dependence of complexation between schizophyllan and single-stranded homo RNAs. Bioorg Chem 31(3):216–226
46. Nagasaki T, Hojo M, Uno A et al (2004) Long-term expression with a cationic polymer derived from a natural polysaccharide: schizophyllan. Bioconjug Chem 15:249–259
47. Hasegawa T, Fujisawa T, Haraguchi S et al (2005) Schizophyllan–folate conjugate as a new non-cytotoxic and cancer-targeted antisense carrier. Bioorg Med Chem Lett 15(2):327–330
48. Sakurai K, Shinkai S (2000) Molecular recognition of adenine, cytosine, and uracil in a single-strand RNA by a natural polysaccharide: schizophyllan. J Am Chem Soc 122:4520–4521
49. Sakurai K, Mizu M, Shinkai S (2001) Polysaccharide-polynucleotide complexes. 2. Complementary polynucleotide mimic behavior of a natural polysaccharide: schizophyllan in the macromolecular comple with a single strand RNA: poly(C). Biomacromolecules 2:641–650
50. Sletmoen M, Naess SN, Stokke BT (2009) Structure and stability of polynucleotide-(1, 3)-[beta]-D-glucan complexes. Carbohydr Polym 76(3):389–399
51. Hasegawa T, Umeda M, Matsumoto T et al (2004) Lactose-appended schizophyllan is a potential candidate as a hepatocyte-targeted antisense carrier. Chem Commun 4:382–383
52. Mizu M, Koumoto K, Anada T et al (2004) Antisense oligonucleotides bound in the polysaccharide complex and the enhanced antisense effect due to the low hydrolysis. Biomaterials 25:3117–3123
53. Koumoto K, Mizu M, Sakurai K et al (2004) Polysaccharide/polynucleotide complexes. Part 6. Chem Biodivers 1(3):520–529
54. Anada T, Karinaga R, Koumoto K et al (2005) Linear double-stranded DNA that mimics an infective tail of virus genome to enhance transfection. J Control Release 108(2–3):529–539
55. Takeda Y, Shimada N, Kaneko K et al (2007) Ternary complex consisting of DNA, polycation, and a natural polysaccharide of schizophyllan to induce cellular uptake by antigen presenting cells. Biomacromolecules 8(4):1178–1186
56. Hasegawa T, Fujisawa T, Numata M et al (2004) Schizophyllans carrying oligosaccharide appendages as potential candidates for cell-targeted antisense carrier. Org Biomol Chem 2 (21):3091–3098
57. Matsumoto T, Numata M, Anada T et al (2004) Chemically modified polysaccharide schizophyllan for antisense oligonucleotides delivery to enhance the cellular uptake efficiency. Biochem Biophys Acta 1670:91–104
58. Karinaga R, Koumoto K, Mizu M et al (2005) PEG-appended beta-(1–>3)-D-glucan schizophyllan to deliver antisense-oligonucleotides with avoiding lysosomal degradation. Biomaterials 26(23):4866–4873
59. Karinaga R, Anada T, Minari J et al (2006) Galactose-PEG dual conjugation of beta-(1–>3)-D-glucan schizophyllan for antisense oligonucleotides delivery to enhance the cellular uptake. Biomaterials 27(8):1626–1635
60. Mizu M, Koumoto K, Anada T et al (2004) A polysaccharide carrier for immunostimulatory CpG DNA to enhance cytokine secretion. J Am Chem Soc 126(27):8372–8373
61. Klinman DM, Klaschik S, Sato T et al (2009) CpG oligonucleotides as adjuvants for vaccines targeting infectious diseases. Adv Drug Deliv Rev 61(3):248–255
62. Shimada N, Coban C, Takeda Y et al (2007) A polysaccharide carrier to effectively deliver native phosphodiester CpG DNA to antigen-presenting cells. Bioconjug Chem 18(4):1280–1286
63. Dias N, Stein CA (2002) Antisense oligonucleotides: basic concepts and mechanisms. Mol Cancer Ther 1(5):347–355
64. Pouyani T, Prestwich GD (1994) Functionalized derivatives of hyaluronic acid oligosaccharides: drug carriers and novel biomaterials. Bioconjug Chem 5(4):339–347
65. Kim A, Checkla DM, Dehazya P et al (2003) Characterization of DNA-hyaluronan matrix for sustained gene transfer. J Control Release 90:81–95
66. Kim AP, Yellen P, Yun YH et al (2005) Delivery of a vector encoding mouse hyaluronan synthase 2 via a crosslinked hyaluronan film. Biomaterials 26:1585–1593

67. Yun YH, Chen W (2005) Microspheres formulated from native hyaluronan for applications in gene therapy. In: Mansoor MA (ed) Polymeric gene delivery: principles and applications, CRC Press LLC, USA, pp 475–486
68. de la Fuente M, Seijo B, Alonso MJ (2008) Bioadhesive hyaluronan-chitosan nanoparticles can transport genes across the ocular mucosa and transfect ocular tissue. Gene Ther 15 (9):668–676
69. de la Fuente M, Seijo B, Alonso MJ (2008) Design of novel polysaccharidic nanostructures for gene delivery. Nanotechnology 19(7):075105/1–075105/9
70. Duceppe N, Tabrizian M (2009) Factors influencing the transfection efficiency of ultra low molecular weight chitosan/hyaluronic acid nanoparticles. Biomaterials 30(13):2625–2631
71. Wieland JA, Houchin-Ray TL, Shea LD (2007) Non-viral vector delivery from poly(ethylene glycol)-hyaluronic acid hydrogels. J Control Release 120(3):233–241
72. Saraf A, Hacker MC, Sitharaman B et al (2008) Synthesis and conformational evaluation of a novel gene delivery vector for human mesenchymal stem cells. Biomacromolecules 9 (3):818–827
73. Shen Y, Li Q, Tu J et al (2009) Synthesis and characterization of low molecular weight hyaluronic acid-based cationic micelles for efficient siRNA delivery. Carbohydr Polym 77 (1):95–104
74. Bruneel D, Schacht E (1995) End group modification of pullulan. Polymer 36:169–172
75. Kaneo Y, Tanaka T, Nakano T et al (2001) Evidence for receptor-mediated hepatic uptake of pullulan in rats. J Control Release 70:365–373
76. Nabi IR, Le PU (2003) Caveolae/raft-dependent endocytosis. J Cell Biol 161(4):673–677
77. Na K, Lee ES, Bae YH (2003) Self-assembled nanoparticles of hydrophobically-modified polysaccharide bearing vitamin H as a targeted anti-cancer drug delivery system. Eur J Pharm Biopharm 18(2):165–173
78. Akiyoshi K, Kobayashi S, Shichibe S et al (1998) Self-assembled hydrogel nanoparticle of cholesterol-bearing pullulan as a carrier of protein drugs: complexation and stabilization of insulin. J Control Release 54(3):313–320
79. Hosseinkhani H, Aoyama T, Ogawa O et al (2002) Liver targeting of plasmid DNA by pullulan conjugation based on metal coordination. J Control Release 83(2):287–302
80. Kanatani I, Ikai T, Okazaki A et al (2006) Efficient gene transfer by pullulan-spermine occurs through both clathrin- and raft/caveolae-dependent mechanisms. J Control Release 116(1):75–82
81. Jo J, Ikai T, Okazaki A, Nagane K, Yamamoto M, Hirano Y, Tabata Y (2007) Expression profile of plasmid DNA obtained using spermine derivatives of pullulan with different molecular weights. J Biomater Sci Polym Ed 18(7):883–899
82. San Juan A, Hlawaty H, Chaubet F et al (2007) Cationized pullulan 3D matrices as new materials for gene transfer. J Biomed Mater Res A 82A(2):354–362
83. Imai T, Shiraishi S, Saito H et al (1991) Interaction of indomethacin with low molecular weight chitosan, and improvements of some pharmacuetical properties of indomethacin by low molecular weight chitosans. Int J Pharm 67:11–20
84. Takayama K, Hirata M, Machida Y et al (1990) Effect of interpolymer complex formation on bioadhesive property and drug release phenomenon of compressed tablet consisting of chitosan and sodium hyaluronate. Chem Pharm Bull 38:1993–1997
85. Meshali MM, Gabr KE (1993) Effect of interpolymer complex formation of chitosan with pectin or acacia on the release behavior of chlorpromazine HCl. Int J Pharm 89:177–181
86. Mao H-Q (2001) Chitosan-DNA nanoparticles as gene carriers: synthesis, characterization and transfection efficiency. J Control Release 70(3):399–421
87. Mumper R, Wang JJ, Claspell JM et al (1995) Novel polymeric condensing carriers for gene delivery. Proc Intl Sym Control Release Bioact Mater 22:178–179
88. MacLaughlin FC, Mumper RJ, Wang J et al (1998) Chitosan and depolymerized chitosan oligomers as condensing carriers for *in vivo* plasmid delivery. J Control Release 56:259–272

89. Dodane V, Vilivalam VD (1998) Pharmaceutical applications of chitosan. Pharm Sci Technol Today 1(6):246–253
90. Aranaz I, Mengibar M, Harris R et al (2009) Functional characterization of chitin and chitosan. Curr Chem Biol 3:203–230
91. Aiba S-i (1991) Studies on chitosan: 3. Evidence for the presence of random and block copolymer structures in partially N-acetylated chitosans. Int J Biol Macromol 13(1):40–44
92. Mima S, Miya M, Iwamoto R et al (1983) Highly deacetylated chitosan and its properties. J Appl Polym Sci 28(6):1909–1917
93. Nguyen S, Hisiger S, Jolicoeur M et al (2009) Fractionation and characterization of chitosan by analytical SEC and 1H NMR after semi-preparative SEC. Carbohydr Polym 75(4):636–645
94. Köping-Höggård M, Tubulekas I, Guan H, Edwards K, Nilsson M, Vårum KM, Artursson P (2001) Chitosan as a nonviral gene delivery system. Structure–property relationships and characteristics compared with polyethylenimine *in vitro* and after lung administration *in vivo*. Gene Ther 8:1108–1121
95. Kiang T, Wen J, Lim HW et al (2004) The effect of the degree of chitosan deacetylation on the efficiency of gene transfection. Biomaterials 25:5293–5301
96. Huang M, Fong C-W, Khor E et al (2005) Transfection efficiency of chitosan vectors: effect of polymer molecular weight and degree of deacetylation. J Control Release 106(3):391–406
97. Liu X, Howard KA, Dong M et al (2007) The influence of polymeric properties on chitosan/siRNA nanoparticle formulation and gene silencing. Biomaterials 28(6):1280–1288
98. Rejman J, Oberle V, Zuhorn IS et al (2004) Size-dependent internalization of particles via the pathways of clathrin- and caveolae-mediated endocytosis. Biochem J 377(1):159–169
99. Choksakulnimitr S, Masuda S, Tokuda H et al (1995) *In vitro* cytotoxicity of macromolecules in different cell culture systems. J Control Release 34(3):233–241
100. Erbacher P, Zou S, Bettinger T et al (1998) Chitosan-based vector/DNA complexes for gene delivery: biophysical characteristics and transfection ability. Pharm Res 15(9):1332–1339
101. Richardson SCW, Kolbe HVJ, Duncan R (1999) Potential of low molecular mass chitosan as a DNA delivery system: biocompatibility, body distribution and ability to complex and protect DNA. Int J Pharm 178(2):231–243
102. Murata J, Ohya Y, Ouchi T (1996) Possibility of application of quaternary chitosan having pendant galactose residues as gene delivery tool. Carbohydr Polym 29(1):69–74
103. Murata J, Ohya Y, Ouchi T (1997) Design of quaternary chitosan conjugate having antennary galactose residues as a gene delivery tool. Carbohydr Polym 32(2):105–109
104. Thanou M, Florea BI, Geldof M et al (2002) Quaternized chitosan oligomers as novel gene delivery vectors in epithelial cell lines. Biomaterials 23:153–159
105. Kean T, Roth S, Thanou M (2005) Trimethylated chitosans as non-viral gene delivery vectors: cytotoxicity and transfection efficiency. J Control Release 103:643–653
106. Kim TH, Kim SI, Akaike T et al (2005) Synergistic effect of poly(ethylenimine) on the transfection efficiency of galactosylated chitosan/DNA complexes. J Control Release 105(3):354–366
107. Wong K, Sun G, Zhang X et al (2006) PEI-*g*-chitosan, a novel gene delivery system with transfection efficiency comparable to polyethylenimine *in vitro* and after liver administration *in vivo*. Bioconjug Chem 17:152–158
108. Jiang H-L, Kim Y-K, Arote R et al (2007) Chitosan-graft-polyethylenimine as a gene carrier. J Control Release 117:273–280
109. Kim T-H, Jiang H-L, Jere D et al (2007) Chemical modification of chitosan as a gene carrier *in vitro* and *in vivo*. Prog Polym Sci 32(7):726–753
110. Nicolet BH, Shinn LA (1939) The action of periodic acid on α-amino alcohols. J Am Chem Soc 61(6):1615
111. Vold IMN, Christensen BE (2005) Periodate oxidation of chitosans with different chemical compositions. Carbohydr Res 340(4):679–684
112. Jiang H, Kwon J, Kim Y et al (2007) Galactosylated chitosan-graft-polyethylenimine as a gene carrier for hepatocyte targeting. Gene Ther 14(19):1389–1398

113. Jiang H-L, Kwon J-T, Kim E-M et al (2008) Galactosylated poly(ethylene glycol)-chitosan-graft-polyethylenimine as a gene carrier for hepatocyte-targeting. J Control Release 131 (2):150–157
114. Lu B, Xu X-D, Zhang X-Z et al (2008) Low molecular weight polyethylenimine grafted N-maleated chitosan for gene delivery: properties and *in vitro* transfection studies. Biomacromolecules 9(10):2594–2600
115. Lou Y-L, Peng Y-S, Chen B-H et al (2009) Poly(ethylene imine)-*g*-chitosan using EX-810 as a spacer for nonviral gene delivery vectors. J Biomed Mater Res A 88A(4):1058–1068
116. Wu Y, Liu C, Zhao X et al (2008) A new biodegradable polymer: PEGylated chitosan-*g*-PEI possessing a hydroxyl group at the PEG end. J Polym Res 15(3):181–185
117. Jiang H-L, Kim Y-K, Arote R et al (2009) Mannosylated chitosan-graft-polyethylenimine as a gene carrier for Raw 264.7 cell targeting. Int J Pharm 375(1-2):133–139
118. Jiang H-L, Xu C-X, Kim Y-K et al (2009) The suppression of lung tumorigenesis by aerosol-delivered folate-chitosan-graft-polyethylenimine/Akt1 shRNA complexes through the Akt signaling pathway. Biomaterials 30(29):5844–5852
119. Jere D, Jiang H-L, Kim Y-K et al (2009) Chitosan-graft-polyethylenimine for Akt1 siRNA delivery to lung cancer cells. Int J Pharm 378(1–2):194–200
120. Pack DW, Putnam D, Langer R (2000) Design of imidazole-containing endosomolytic biopolymers for gene delivery. Biotechnol Bioeng 67(2):217–223
121. Muzzarelli RAA, Mattioli-Belmonte M, Tietz C et al (1994) Stimulatory effect on bone formation exerted by a modified chitosan. Biomaterials 15(13):1075–1081
122. Midoux P, Monsigny M (1999) Efficient gene transfer by histidylated polylysine/pDNA complexes. Bioconjug Chem 10(3):406–411
123. Kim TH, Ihm JE, Choi YJ et al (2003) Efficient gene delivery by urocanic acid-modified chitosan. J Control Release 93(3):389–402
124. Jin H, Kim T, Hwang S et al (2006) Aerosol delivery of urocanic acid–modified chitosan/programmed cell death 4 complex regulated apoptosis, cell cycle, and angiogenesis in lungs of K-ras null mice. Mol Cancer Ther 5(4):1041
125. Jin H, Xu CX, Kim HW et al (2008) Urocanic acid-modified chitosan-mediated PTEN delivery via aerosol suppressed lung tumorigenesis in K-rasLA1 mice. Cancer Gene Ther 15(5):275–283
126. Bauhuber S, Hozsa C, Breunig M et al (2009) Delivery of nucleic acids via disulfide-based carrier systems. Adv Mater 21(32–33):3286–3306
127. Bernkop-Schnürch A, Hornof M, Guggi D (2004) Thiolated chitosans. Eur J Pharm Biopharm 57(1):9–17
128. Schmitz T, Bravo-Osuna I, Vauthier C et al (2007) Development and *in vitro* evaluation of a thiomer-based nanoparticulate gene delivery system. Biomaterials 28(3):524–531
129. Martien R, Loretz B, Thaler M et al (2007) Chitosan–thioglycolic acid conjugate: an alternative carrier for oral nonviral gene delivery? J Biomed Mater Res A 82A(1):1–9
130. Park IK, Ihm JE, Park YH et al (2003) Galactosylated chitosan (GC)-graft-poly(vinyl pyrrolidone) (PVP) as hepatocyte-targeting DNA carrier. Preparation and physicochemical characterization of GC-graft-PVP/DNA complex (1). J Control Release 86:349–359
131. Park YK, Park YH, Shin BA et al (2000) Galactosylated chitosan-graft-dextran as hepatocyte-targeting DNA carrier. J Control Release 69(1):97–108
132. Park IK, Kim TH, Park YH et al (2001) Galactosylated chitosan-*graft*-poly(ethylene glycol) as hepatocyte-targeting DNA carrier. J Control Release 76:349–362
133. Park IK, Ihm JE, Park YH et al (2003) Galactosylated chitosan (GC)-graft-poly(vinyl pyrrolidone) (PVP) as hepatocyte-targeting DNA carrier: *In vivo* transfection. Arch Pharm Res 27 (12):1284–1289
134. Hashimoto M, Morimoto M, Saimoto H et al (2006) Lactosylated chitosan for DNA delivery into hepatocytes: the effect of lactosylation on the physicochemical properties and intracellular trafficking of pDNA/chitosan complexes. Bioconjug Chem 17(2):309–316

135. Hashimoto M, Morimoto M, Saimoto H et al (2006) Gene transfer by DNA/mannosylated chitosan complexes into mouse peritoneal macrophages. Biotechnol Lett 28(11):815–821
136. Forrest ML, Gabrielson N, Pack DW (2005) Cyclodextrin-polyethylenimine conjugates for targeted *in vitro* gene delivery. Biotechnol Bioeng 89(4):416–423
137. Liu Y, Wenning L, Lynch M et al (2004) New poly(D-glucaramidoamine)s induce DNA nanoparticle formation and efficient gene delivery into mammalian cells. J Am Chem Soc 126(24):7422–7423
138. Reineke TM, Davis ME (2003) Structural effects of carbohydrate-containing polycations on gene delivery. 1. Carbohydrate size and its distance from charge centers. Bioconjug Chem 14 (1):247–254
139. Reineke TM, Davis ME (2003) Structural effects of carbohydrate-containing polycations on gene delivery. 2. Charge center type. Bioconjug Chem 14(1):255–261
140. Srinivasachari S, Liu Y, Zhang G et al (2006) Trehalose click polymers inhibit nanoparticle aggregation and promote pDNA delivery in serum. J Am Chem Soc 128(25):8176–8184
141. Hwang SJ, Bellocq NC, Davis ME (2001) Effects of structure of beta-cyclodextrin-containing polymers on gene delivery. Bioconjug Chem 12(2):280–290
142. Boussif O, Lezoualc'h F, Zanta MA, Mergny MD, Scherman D, Demeneix B, Behr JP (1995) A versatile vector for gene and oligonuceotide transfer into cells in culture and *in vivo*: polyethylenimine. Proc Natl Acad Sci USA 92:7297–7301
143. Grosse S, Aron Y, Honore I, Thevenot G, Danel C, Roche A-C, Monsigny M, Fajac I (2004) Lactosylated polyethylenimine for gene transfer into airway epithelial cells: role of the sugar moiety in cell delivery and intracellular trafficking of the complexes. J Gene Med 2004 (6):345–356
144. Liu Y, Wenning L, Lynch M et al (2006) Gene delivery with novel poly(L-tartaramidoamine) s. In: Svenson S (ed) Polymeric drug delivery, volume I: particulate drug carriers. American Chemical Society, Washington DC, pp 217–227
145. Metzke M, O'Connor N, Maiti S et al (2005) Saccharide–peptide hybrid copolymers as biomaterials. Angew Chem Int Ed 44:6529–6533
146. Liu Y, Reineke TM (2006) Poly(glycoamidoamine)s for gene delivery: stability of polyplexes and efficacy with cardiomyoblast cells. Bioconjug Chem 17(1):101–108
147. Prevette LE, Kodger TE, Reineke TM et al (2007) Deciphering the role of hydrogen bonding in enhancing pDNA-polycation interactions. Langmuir 23(19):9773–9784
148. Lee C-C, Liu Y, Reineke TM (2008) General structure-activity relationship for poly(glycoamidoamine)s: the effect of amine density on cytotoxicity and DNA delivery efficiency. Bioconjug Chem 19(2):428–440
149. Liu Y, Reineke TM (2007) Poly(glycoamidoamine)s for gene delivery. structural effects on cellular internalization, buffering capacity, and gene expression. Bioconjug Chem 18(1):19–30
150. Liu Y, Reineke TM (2010) Degradation of poly(glycoamidoamine) DNA delivery vehicles: polyamide hydrolysis at physiological conditions promotes DNA release. Biomacromolecules 11(2):316–325
151. Taori VP, Liu Y, Reineke TM (2009) DNA delivery *in vitro* via surface release from multilayer assemblies with poly(glycoamidoamine)s. Acta Biomater 5(3):925–933
152. Paiva C, Panek A (1996) Biotechnological applications of the disaccharide trehalose. Biotechnol Annu Rev 2:293
153. Lins RD, Pereira CS, Hünenberger PH (2004) Trehalose-protein interaction in aqueous solution. Proteins 55(1):177–186
154. Wagner E (2004) Pharm Res 21:8–14
155. Srinivasachari S, Liu Y, Prevette LE et al (2007) Effects of trehalose click polymer length on pDNA complex stability and delivery efficacy. Biomaterials 28:2885–2898
156. Prevette LE, Lynch ML, Kizjakina K et al (2008) Correlation of amine number and pDNA binding mechanism for trehalose-based polycations. Langmuir 24(15):8090–8101

157. Ortiz-Mellet C, Benito JM, Garcia Fernandez JM et al (1998) Cyclodextrin-scaffolded glycoclusters. Chem Eur J 4(12):2523–2531
158. Perez-Balderas F, Ortega-Munoz M, Morales-Sanfrutos J et al (2003) Multivalent neoglycoconjugates by regiospecific cycloaddition of alkynes and azides using organic-soluble copper catalysts. Org Lett 5(11):1951–1954
159. Garcia-Lopez JJ, Hernandez-Mateo F, Isac-Garcia J et al (1999) Synthesis of per-glycosylated **beta**-cyclodextrins having enhanced lectin binding affinity. J Org Chem 64(2):522–531
160. Gadella A, Defaye J (1991) Selective halogenation at primary postions of cyclomaltooligosaccharides and a synthesis of per-3,6-anhydro cyclomaltooligosaccharides. Angew Chem Int Ed 30:78–80
161. Andre S, Kaltner H, Furuike T et al (2004) Persubstituted cyclodextrin-based glycoclusters as inhibitors of protein-carbohydrate recognition using purified plant and mammalian lectins and wild-type and lectin-gene-transfected tumor cells as targets. Bioconjug Chem 15(1):87–98
162. Bellocq NC, Pun SH, Jensen GS et al (2003) Transferrin-containing, cyclodextrin polymer-based particles for tumor-targeted gene delivery. Bioconjug Chem 14(6):1122–1132
163. Davis ME, Bellocq NC (2001) Cyclodextrin-containing polymers for gene delivery. J Incl Phenom Macro Chem 44:17–22
164. Croyle MA, Roessler BJ, Hsu C-P et al (1998) Beta-cyclodextrins enhance adenoviral-mediated gene delivery to the intestine. Pharm Res 15(9):1349–1355
165. Boger J, Corcoran RJ, Lehn J-M (1978) Cyclodextrin chemistry. Selective modification of all primary hydroxyl groups of alpha- and beta-cyclodextrins. Helv Chim Acta 61:2190–2218
166. Mocanu G, Vizitiu D, Carpov A (2001) Cyclodextrin polymers. J Bioact Compat Polym 16:315–328
167. Zhao Q, Temsamani J, Agrawal S (1995) Use of cyclodextrin and its derivatives as carriers for oligonucleotide delivery. Antisense Res Dev 5(3):185–192
168. Salem LB, Bosquillon C, Dailey LA et al (2009) Sparing methylation of [beta]-cyclodextrin mitigates cytotoxicity and permeability induction in respiratory epithelial cell layers *in vitro*. J Control Release 136(2):110–116
169. Yang C, Li H, Goh SH et al (2007) Cationic star polymers consisting of [alpha]-cyclodextrin core and oligoethylenimine arms as nonviral gene delivery vectors. Biomaterials 28 (21):3245–3254
170. Cryan S-A (2004) Cell transfection with polycationic cyclodextrin vectors. Eur J Pharm Sci 21(5):625–633
171. Gonzalez H, Hwang SJ, Davis ME (1999) New class of polymers for the delivery of macromolecular therapeutics. Bioconjug Chem 10(6):1068–1074
172. Srinivasachari S, Fichter KM, Reineke TM (2008) Polycationic β-cyclodextrin "click clusters": monodisperse and versatile scaffolds for nucleic acid delivery. J Am Chem Soc 130:4618–4627
173. Srinivasachari S, Reineke TM (2009) Versatile supramolecular pDNA vehicles via "click polymerization" of [beta]-cyclodextrin with oligoethyleneamines. Biomaterials 30 (5):928–938
174. Hu-Lieskovan S, Heidel JD, Bartlett DW, Davis ME, Triche TJ (2005) Sequence-specific knockdown of EWS-EFI1 by targeted, nonviral delivery of small interfering RNA inhibits tumor growth in a murine model of metastatic Ewing's sarcoma. Cancer Res 65:8984–8992
175. Pun SH, Davis ME (2002) Development of a nonviral gene delivery vehicle for systemic application. Bioconjug Chem 13:630–639
176. Pun SH, Tack F, Bellocq NC, Cheng J, Grubbs BH, Jensen GS, Davis ME, Brewster M, Janicot M, Janssens B, Floren W, Bakker A (2004) Targeted delivery of RNA-cleaving DNA enzyme (DNAzyme) to tumor tissue by transferrin-modifed, cyclodextrin-based particles. Cancer Biol Ther 3(7):641–650

177. Heidel JD, Yu ZP, Liu JYC et al (2007) Administration in non-human primates of escalating intravenous doses of targeted nanoparticles containing ribonucleotide reductase subunit M2 siRNA. Proc Natl Acad Sci USA 104(14):5715–5721
178. Davis ME (2009) The first targeted delivery of siRNA in humans via a self-assembling, cyclodextrin polymer-based nanoparticle: from concept to clinic. Mol Pharm 6(3):659–668
179. Zanta M-A, Boussif O, Adib A, Behr J-P (1997) *In vitro* gene delivery to hepatocytes with galactosylated polyethylenimine. Bioconjug Chem 8:839–844
180. Kunath K, von Harpe A, Fischer D et al (2003) Galactose-PEI-DNA complexes for targeted gene delivery: degree of substitution affects complex size and transfection efficiency. J Control Rel 88(1):159–172
181. Nishikawa M, Yamauchi M, Morimoto K et al (2000) Hepatocyte-targeted *in vivo* gene expression by intravenous injection of plasmid DNA complexed with synthetic multi-functional gene delivery system. Gene Ther 7(7):548–555
182. Chen C-p, Kim J-s, Liu D et al (2007) Synthetic PEGylated glycoproteins and their utility in gene delivery. Bioconjug Chem 18(2):371–378
183. Rozema DB, Lewis DL, Wakefield DH et al (2007) Dynamic polyconjugates for targeted *in vivo* delivery of siRNA to hepatocytes. Proc Natl Acad Sci USA 104(32):12982–12987
184. Weiss SI, Sieverling N, Niclasen M et al (2006) Uronic acids functionalized polyethyleneimine (PEI)-polyethyleneglycol (PEG)-graft-copolymers as novel synthetic gene carriers. Biomaterials 27(10):2302–2312
185. Diebold SS, Kursa M, Wagner E, Cotten M, Zenke M (1999) Mannose polyethylenimine conjugates for targeted DNA delivery into dendritic cells. J Biol Chem 274:19087–19094
186. Reineke TM (2006) Poly(glycoamidoamine)s: cationic glycopolymers for DNA delivery. J Polym Sci A Polym Chem 44(24):6895–6908

Top Curr Chem (2010) 296: 191–226
DOI: 10.1007/128_2010_70

Published online: 8 June 2010

Cationic Liposome–Nucleic Acid Complexes for Gene Delivery and Silencing: Pathways and Mechanisms for Plasmid DNA and siRNA

Kai K. Ewert, Alexandra Zidovska, Ayesha Ahmad, Nathan F. Bouxsein, Heather M. Evans, Christopher S. McAllister, Charles E. Samuel, and Cyrus R. Safinya

Abstract Motivated by the promises of gene therapy, there is great interest in developing non-viral lipid-based vectors for therapeutic applications due to their low immunogenicity, low toxicity, ease of production, and the potential of transferring large pieces of DNA into cells. In fact, cationic liposome (CL) based vectors are among the prevalent synthetic carriers of nucleic acids (NAs) currently used in gene therapy clinical trials worldwide. These vectors are studied both for gene delivery with CL–DNA complexes and gene silencing with CL–siRNA (short interfering RNA) complexes. However, their transfection efficiencies and silencing efficiencies remain low compared to those of engineered viral vectors. This reflects the currently poor understanding of transfection-related mechanisms at the molecular and self-assembled levels, including a lack of knowledge about interactions between membranes and double stranded NAs and between CL–NA complexes and cellular components. In this review we describe our recent efforts to improve the mechanistic understanding of transfection by CL–NA complexes, which will help

K.K. Ewert, A. Zidovska, A. Ahmad, N.F. Bouxsein, H.M. Evans, and C.R. Safinya (✉)
Physics, Materials & Molecular, Cellular and Developmental Biology Department, University of California at Santa Barbara, Santa Barbara, CA 93106, USA
e-mail: safinya@mrl.ucsb.edu

A. Zidovska
Department of Systems Biology, Harvard Medical School, Boston, MA, USA

A. Ahmad
Dynavax Technologies, Berkeley, CA, USA

H.M. Evans
National Nanotechnology Coordination Office, Washington, DC, USA

C.S. McAllister and C.E. Samuel
Molecular, Cellular and Developmental Biology Department & Biomolecular Science and Engineering Program, University of California at Santa Barbara, Santa Barbara, CA 93106, USA

C.S. McAllister
Department of Medicine, University of California, San Diego, CA, USA

to design optimal lipid-based carriers of DNA and siRNA for therapeutic gene delivery and gene silencing.

Keywords Cholesterol · Gene delivery · Multivalent cationic lipid · siRNA · Small angle X-ray scattering

Contents

Abbreviations

Chol	Cholesterol
CL	Cationic liposome
DL	Lipid with dendritic headgroup
DOPC	1,2-Dioleoyl-*sn*-glycero-3-phosphatidylcholine
DOPE	1,2-Dioleoyl-*sn*-glycero-3-phosphatidylethanolamine
DOTAP	1,2-Dioleoyl-3-trimethylammonium-propane
FF	Firefly

MEF	Mouse embryonic fibroblast
MVL	Multivalent lipid
NA	Nucleic acid
NL	Neutral lipid
PEG	Poly(ethylene glycol)
RL	Renilla
RNAi	RNA interference
SE	Silencing efficiency
siRNA	Short interfering RNA
TE	Transfection efficiency
UVL	Univalent lipid
XRD	X-ray diffraction

1 Introduction

In this chapter, we provide an overview of our recent efforts to develop a fundamental science base for the design and preparation of optimal lipid-based carriers of DNA and siRNA for gene therapy and gene silencing. We employ synthesis of custom multivalent lipids, synchrotron X-ray diffraction (XRD) techniques, optical and cryo-electron microscopy, as well as biological assays in order to correlate the structures, chemical, and biophysical properties of cationic liposome (CL)–NA complexes to their biological activity and to clarify the interactions between CL–NA complexes and cellular components. Earlier work has been reviewed elsewhere [1–7] and will not be covered exhaustively here.

1.1 Motivation

Gene therapy – addressing disease at the level of the genetic cause, typically with nucleic acid (NA) "drugs" – holds great promise for future medical applications. In fact, numerous clinical trials are currently ongoing, targeting cancers, inherited diseases, and many other disorders with this novel medical approach [8, 9, 10]. Concurrently, substantial research efforts are directed towards developing and fundamentally understanding NA carriers (vectors). These include engineered viruses as well as synthetic vectors, where the negatively charged NA is complexed with cationic liposomes [2, 4, 11–15] or cationic polyelectrolytes [16–18]. Synthetic (non-viral) vectors have garnered much interest due to their low immunogenicity and their ability to transfer very large DNA pieces into cells (which is not feasible with viral vectors) [19]. To improve their efficiencies by rational design, significant ongoing research efforts are aimed at elucidating the mechanisms of action of non-viral vectors intended for therapeutic applications. Cationic lipid-based vectors are studied both for gene delivery (as CL–DNA complexes) and gene silencing

(as CL–siRNA complexes). Their transfection efficiency (TE: a measure of the expression of an exogenous gene that is transferred) and silencing efficiency (SE: a measure of specific post-transcriptional silencing of the gene targeted by the transferred siRNA), however, remain low compared to viral vectors. Understanding the pathways and mechanisms governing the interaction of CL–NA complexes and cells is crucial to make lipid-mediated gene delivery therapeutically viable. The complexity of the transfection process – from initial attachment of a CL–NA complex to the plasma membrane to internalization of the complex via endocytosis, its release from the endosome followed by the dissociation of the lipids from the NA and (in the case of DNA transfection), finally the transport of the NA into the nucleus followed by successful gene expression – suggests that an interplay of many critically important parameters needs to be considered in order to achieve successful NA delivery.

1.2 Gene Delivery Barriers and CL–DNA Complex Properties

The many barriers to successful gene delivery range from serum stability to endosomal release and delivery to the nucleus [20]. Physico-chemical parameters of CL–DNA complexes often strongly affect their ability to overcome these barriers. Two examples of key parameters which impact the TE of CL–DNA complexes are the membrane charge density (σ_M, average charge per unit area of the membrane) of the cationic lipid membranes and the cationic lipid to DNA charge ratio, ρ_{chg} [4, 7, 21]. These parameters are directly affected by complex composition, since the membrane charge density is defined by the ratio and nature of cationic and neutral lipid in the membrane. Another important parameter is the nanoscopic internal structure of the complexes, which is affected by the choice of lipids and complex composition.

1.3 Structures of CL–DNA Complexes

CL–DNA complexes form spontaneously when solutions of cationic liposomes (typically containing both a cationic lipid and a neutral "helper" lipid) are combined. We have discovered several distinct nanoscale structures of CL–DNA complexes by synchrotron X-ray diffraction, three of which are schematically shown in Fig. 1. These are the prevalent lamellar phase with DNA sandwiched between cationic membranes (L_α^C) [22], the inverted hexagonal phase with DNA encapsulated within inverse lipid tubes (H_{II}^C) [23], and the more recently discovered H_I^C phase with hexagonally arranged rod-like micelles surrounded by DNA chains forming a continuous substructure with honeycomb symmetry [24]. Both the neutral lipid and the cationic lipid can drive the formation of specific structures of CL–DNA complexes. The inverse cone shape of DOPE favors formation of the

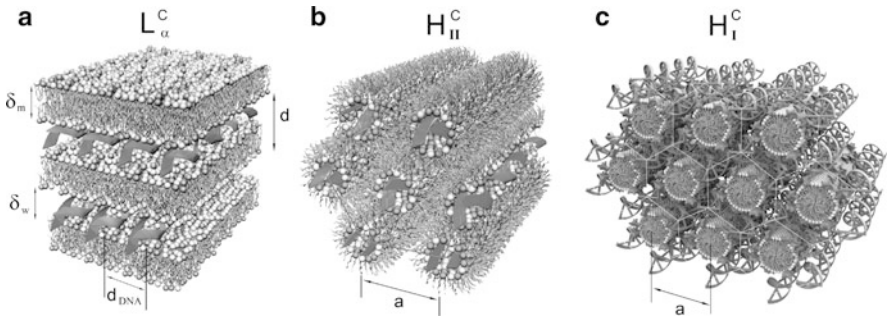

Fig. 1 Mixing DNA and cationic liposomes results in the spontaneous formation of CL–DNA complexes with equilibrium self-assembled structures. The schematics show the local (nanoscale) interior structure of CL–DNA complexes as derived from synchrotron X-ray diffraction data. (**a**) The lamellar L_α^C phase of CL–DNA complexes with alternating lipid bilayers and DNA monolayers [22]. (**b**) The inverted hexagonal H_{II}^C phase of CL–DNA complexes, comprised of DNA inserted within inverse lipid tubules, which are arranged on a hexagonal lattice [23]. (**c**) The more recently discovered hexagonal H_I^C phase of CL–DNA complexes, where a cationic lipid with a large dendritic headgroup leads to the formation of rod-like lipid micelles arranged on a hexagonal lattice with DNA inserted within the interstices with honeycomb symmetry [24]. Reprinted in part from [23] and [24] with permission. L_a^C and H_{II}^C phase images Copyright 1998 American Association for the Advancement of Science. H_I^C phase image Copyright 2006 American Chemical Society

H_{II}^C phase, while the formation of micelles in the H_I^C phase is driven by a highly charged (16+), cone-shaped multivalent cationic lipid.

1.4 The Effect of CL–DNA Complex Structure on Transfection Mechanism and Efficiency

The internal structure of the complexes can directly determine the mechanism of transfection [4, 23, 25]. We have found that for L_α^C CL–DNA complexes, the membrane charge density (σ_M) is a predictive parameter for transfection efficiency [21] (see Sect. 2), i.e., the data for monovalent and multivalent cationic lipids are described by a simple bell-curve. In contrast, for inverted hexagonal H_{II}^C CL–DNA complexes, TE is independent of σ_M, suggesting a distinctly different mechanism of transfection. Consistent with the TE data, confocal microscopy revealed distinctly different CL–DNA complex pathways and interactions with cells, which depended on both the structure (H_{II}^C vs L_α^C) and, for L_α^C complexes, on σ_M [25]. Thus, the mechanism of transfection by CL–DNA complexes is dependent both on their structure and, for a given structure, on chemical and physical parameters of the complexes.

For lamellar CL–DNA complexes, endosomal escape via activated fusion limits TE and strongly depends on σ_M, whereas the inverted hexagonal phase promotes

fusion of the CL–DNA complex membranes with cellular membranes independent of σ_M (see Fig. 3). For H_{II}^C CL–DNA complexes, a model was proposed that recognizes the importance of the outer (water-facing) layer of positive curvature around the inverted hexagonal CL–DNA complex [25]. The lipids in the outer layer have a negative spontaneous curvature and thus are energetically frustrated, which favors fusion of the complexes' membranes with extra-cellular and endosomal membranes encountered along the gene transfer pathway.

2 A Universal Curve for Transfection Efficiency Versus Membrane Charge Density

In this section, we describe some of our efforts focused on clarifying the role of the membrane charge density (σ_M) as a key chemical parameter for transfection by L_α^C CL–DNA complexes. In a previous study, we had tentatively identified σ_M as a universal parameter for transfection by lamellar complexes [25]. However, that study was limited by the range of charge densities accessible with commercially available lipids.

To study the dependence of TE on σ_M more thoroughly and to evaluate a broad range of higher charge densities, we synthesized a series of new multivalent lipids (MVLs) with headgroup valencies ranging from +2 to +5 which allowed systematic variation of headgroup size and charge [21, 26]. Figure 2 shows the chemical structures of the lipids DOTAP, DOPC, DOPE, and MVL5. DOTAP is a commercially available, commonly used univalent lipid (UVL). X-ray diffraction showed that the new MVLs form CL–DNA complexes that exhibit the lamellar L_α^C phase (Fig. 1a). Figure 3 shows TE results for complexes transfecting mouse fibroblast cells at various MVL/DOPC ratios [21]. Also included are data for the monovalent lipid DOTAP mixed with DOPC, as a control system. The complexes were prepared at the optimum cationic lipid/DNA charge ratio $\rho_{chg} = 2.8$, and the amount of DNA and cationic lipid per sample was kept constant. Thus, only the amount of neutral lipid varies between data points.

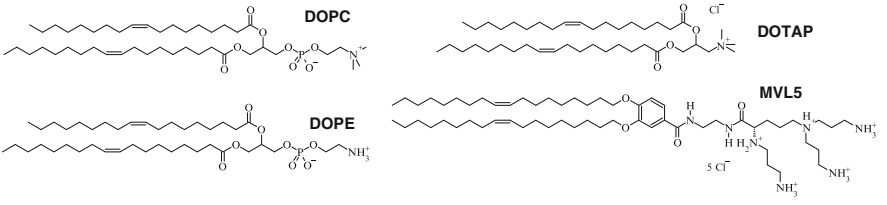

Fig. 2 Chemical structures of the zwitterionic neutral lipids DOPC (1,2-dioleoyl-*sn*-glycero-3-phosphatidylcholine) and DOPE (1,2-dioleoyl-*sn*-glycero-3-phosphatidylethanolamine) and the cationic lipids DOTAP (1,2-dioleoyl-3-trimethylammonium-propane, a UVL) and MVL5 (a custom-synthesized MVL)

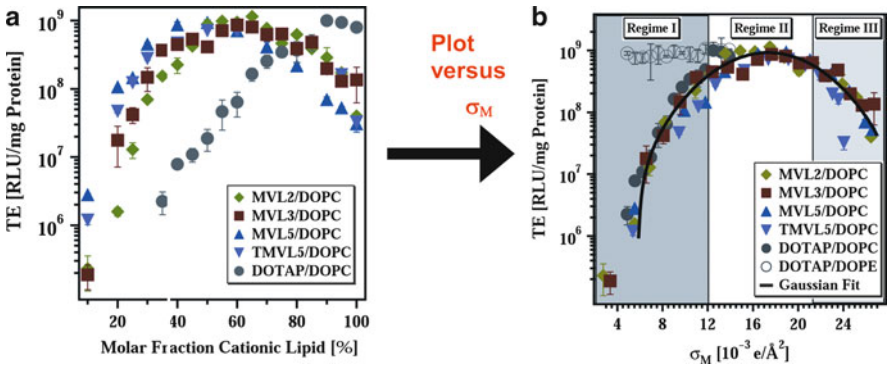

Fig. 3 (**a**) Transfection efficiency (TE) as a function of mol% DOPC for DNA complexes prepared with MVL2 (*diamonds*), MVL3 (*squares*), MVL5 (*triangles*), TMVL5 (*inverted-triangles*), and DOTAP (*open circles*). All data was taken at $\rho_{chg} = 2.8$. (**b**) The same TE data plotted against the membrane charge density, σ_M shows that TE of the lamellar L_α^C complexes describes a universal, bell-shaped curve as a function of σ_M (the *solid line* is a Gaussian fit to the data). Data for DOTAP/DOPE complexes (*open circles*, H_{II}^C phase) deviate from the universal curve, indicative of a distinctly different transfection mechanism for the inverted hexagonal phase. Three regimes of transfection efficiency are labeled. Reproduced with permission from [21]. Copyright 2005 John Wiley & Sons Limited

Figure 3a shows the TE data as a function of the mole fraction of cationic lipid. For all cationic lipids, a maximum in TE as a function of lipid composition is observed: at 65 mol% for MVL2, 70 mol% for MVL3, 50 mol% for MVL5, 55 mol% for TMVL5, and 90 mol% for DOTAP. The optimal molar ratio results in a TE that is close to three decades higher than that of the lowest transfecting complexes in these systems, and each data set fits a skewed bell-shaped curve. Figure 3b shows the data of Fig. 3a plotted vs the membrane charge density, σ_M ($\sigma_M = [1-\Phi_{nl}/(\Phi_{nl} + r\Phi_{cl})]\sigma_{cl}$), where $r = A_{cl}/A_{nl}$ is the ratio of the headgroup areas of the cationic and the neutral lipid; $\sigma_{cl} = eZ/A_{cl}$ is the charge density of the cationic lipid with valence Z (measured experimentally [21]), and Φ_{nl} and Φ_{cl} are the mole fractions of the neutral and cationic lipids, respectively. We used $A_{nl} = 72$ Å^2, $r_{DOTAP} = 1$, $r_{MVL2} = 1.05 \pm 0.05$, $r_{MVL3} = 1.30 \pm 0.05$, $r_{MVL5} = 2.3 \pm 0.1$, $r_{TMVL5} = 2.5 \pm 0.1$, $Z_{DOTAP} = 1$, $Z_{MVL2} = 2.0 \pm 0.1$, $Z_{MVL3} = 2.5 \pm 0.1$, $Z_{MVL5} = Z_{TMVL5} = 4.5 \pm 0.1$. The resulting solid curve going through the data describes a Gaussian $TE = TE_0 + A \exp-[(\sigma_M-\sigma_0)/w]^2$, with optimal charge density $\sigma_0 = 17.0 \pm 0.1 \times 10^{-3}$ e/Å^2, $TE_0 = -(2.4 \pm 0.4) \times 10^7$ RLU/mg protein, $A = 9.4 \pm 0.6 \times 10^8$ RLU/mg protein, and $w = 5.8 \pm 0.5 \times 10^{-3}$ e/Å^2.

Remarkably, all the data points for cationic lipids with different valence merge onto a single bell-shaped curve. This identifies σ_M, rather than the charge of the lipid, as a universal parameter for transfection by lamellar L_α^C CL–DNA complexes (i.e. a predictor of transfection efficiency). The bell curve of Fig. 3b identifies three distinct regimes related to interactions between complexes and cells: at low σ_M (Regime I), TE increases with increasing σ_M; at intermediate σ_M (Regime II),

TE exhibits saturated behavior; and unexpectedly, at high σ_M (Regime III), TE *decreases* with increasing σ_M [21].

The TE data, combined with our confocal microscopy data for low and high TE L_α^C complexes interacting with cells [25], suggests a model of cellular uptake of L_α^C complexes depicted schematically in Fig. 4 [21]. The initial attachment of CL–DNA complexes to cells is mediated by electrostatics (Fig. 4a) and followed by cellular uptake via endocytosis (Fig. 4b). At low $\sigma_M < \sigma_M^*$ (Regime I, Fig. 3b), transfection is limited by endosomal escape (Fig. 4c, d). As σ_M increases towards an optimal value $\sigma_M \approx \sigma_M^*$ (near the boundary between Regimes I and II shown in Fig. 3b), TE increases exponentially with σ_M over three orders of magnitude as the complexes are able to overcome this barrier by fusing with the endosomal membrane and releasing smaller complexes into the cytoplasm (Fig. 4e, f). In the regime of high $\sigma_M > \sigma_M^*$ (Regime III, Fig. 3b), accessible to us for the first time with the custom synthesized multivalent cationic lipids [21, 26], complexes are able to escape the endosome, yet they exhibit a decreasing level of efficiency as σ_M further increases, presumably due to the DNA's inability to dissociate from the highly charged membranes of complexes in the cytosol (Fig. 4e, g). The optimal TE in Regime II reflects the compromise between opposing requirements (Fig. 4f): escape from endosomes requires high σ_M, but dissociation of complexes in the cytoplasm requires low σ_M. Future optimization of TE requires decoupling of these requirements. The following two sections show how specific neutral or cationic lipid components are able to force deviations from the universal curve.

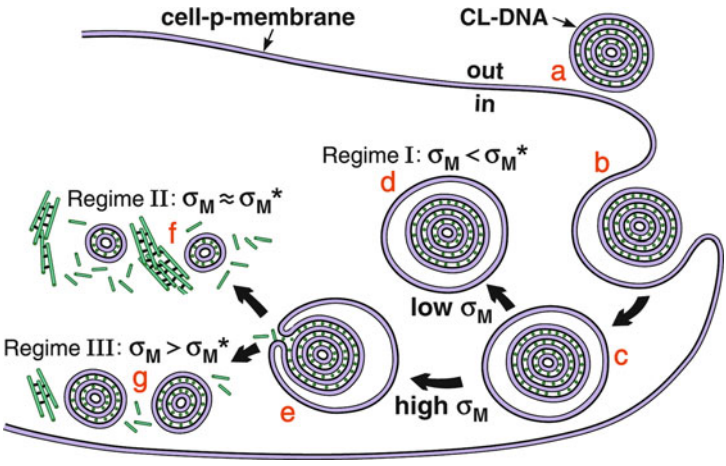

Fig. 4 Model of cellular uptake of L_α^C complexes. Complexes adhere to cells due to electrostatics (**a**) and enter through endocytosis (**b**, **c**). Low σ_M complexes remain trapped in the endosome (**d**). High σ_M complexes escape the endosome (**e**) where released DNA may form aggregates with cationic biomolecules (**f**) or the complexes are less able to dissociate and less DNA is available (**g**). Reproduced with permission from [21]. Copyright 2005 John Wiley & Sons Limited

3 The Role of Cholesterol and Structurally Related Molecules in Enhancing Transfection by CL–DNA Complexes

Motivated by its important role in gene delivery, we have studied the effect of cholesterol (chol) and several analogs on the transfection efficiency of lamellar CL–DNA complexes *in vitro* [27]. As evident from the results on DOPC/DOTAP and DOPE/DOTAP vectors, the nature of the neutral lipid component is an important parameter that is worth further exploration. Conveniently, a number of neutral lipids are commercially available. In addition, modifying the neutral lipid component has the potential to improve TE in a regime (at low σ_M) where DNA dissociation from the complex in the cytosol is not yet a barrier to transfection.

Several reports in the literature state that DOPE, while successfully used for *in vitro* gene delivery, is a poor helper lipid for *in vivo* applications [28–32]. Instead, for reasons that are not understood, lipid mixtures for successful transfection *in vivo* seem to require cholesterol [33]. In fact, an equimolar mixture of cholesterol and DOTAP is widely used for *in vivo* experiments and clinical trials. Cholesterol has also been included in liposomes along with cationic DOTAP and fusogenic DOPE to form a potent mixture used to study the treatment of ovarian cancer by delivery of the p53 tumor suppressor gene [34, 35].

We recently discovered an unexpectedly large enhancement in TE of poorly transfecting lamellar CL–DNA complexes upon incorporation of cholesterol. To elucidate the cause of this enhancement, we studied the effect of added cholesterol and structurally related molecules in the low membrane charge density regime (low Φ_{DOTAP}) of the DOTAP/DOPC–DNA system. In addition to cholesterol, we investigated sterols (ergosterol, the plant version of cholesterol, and β-estradiol, an estrogen), other steroids (progesterone, a progestin hormone, and dihydroisoandrosterone, a testosterone precursor), and ergocalciferol (which derives from a sterol precursor by opening of a central ring) [27]. Thus, we were able to correlate the biophysical properties of membranes, inter-membrane interactions and changes in TE to structural properties of the steroid molecules. While keeping the membrane charge (i.e., the lipid/DNA charge ratio and the molar fraction of DOTAP) constant, we gradually replaced DOPC molecules by cholesterol or its analogs. TE of low-transfecting DOTAP/DOPC–DNA complexes ($\Phi_{\mathrm{DOTAP}} = 0.3$) increases by a factor of ten with the inclusion of only 15 mol% cholesterol, and further inclusion of cholesterol continues to increase TE exponentially.

3.1 Structure and Membrane Charge Density of CL–DNA Complexes Containing Cholesterol and Analogs

X-ray diffraction showed that DOTAP/DOPC–DNA complexes containing added cholesterol or structurally related molecules form a single lamellar phase. The only exception is ergocalciferol, where two lamellar phases coexist for $\Phi_{\mathrm{ergocalciferol}} \geq 0.2$.

At $\Phi_{\text{chol}} \geq 0.4$, phase coexistence of CL–DNA complexes and cholesterol monohydrate crystals is observed, which means that the lipid composition (and most notably of Φ_{DOTAP}) in the complex differs from that of the lipid mixture used for preparation of the complexes. This is in agreement with previous reports in the literature, which also observe membrane saturation with cholesterol at about 40 mol % [36, 37]. The phase behavior of DOTAP/DOPC–DNA complexes containing cholesterol analogs is similar: they exhibit membrane saturation at high analog content, coexisting with phase-separated cholesterol analog for $\Phi_{\text{ergosterol}} \geq 0.4$, $\Phi_{\text{ergocalciferol}} \geq 0.4$, and for $\Phi_{\text{steroid}} \geq 0.3$ in the case of β-estradiol, progesterone, and dihydroisoandrosterone.

Thus, the structural features of β-estradiol, progesterone and dihydroisoandrosterone, i.e., absence of an alkyl tail and the presence of a second polar group (see Fig. 6), seem to favor membrane saturation at lower molar fractions of steroid compared to cholesterol. In addition, XRD shows that the lamellar repeat distance d (see Fig. 1a, $d = \delta_w + \delta_m$) of complexes containing these steroids is about 5 Å shorter than that of corresponding complexes containing cholesterol or ergosterol. This suggests a different packing of these groups of molecules within the lipid bilayer.

At the isoelectric point, the membrane charge density of the lipid bilayer in lamellar complexes can be calculated from the observed DNA spacing d_{DNA} (see Fig. 1a), because the negative charge of DNA has to neutralize the positive charge on the adjacent lipid bilayers [22, 38, 39]. A simple geometrical calculation, taking the lamellar geometry of the CL–DNA complex into account, yields [39]

$$\sigma_M = e/(d_{\text{DNA}} \times 3.4\,\text{Å}), \tag{1}$$

where e is the elementary charge and 3.4 Å corresponds to the bare distance between two charges along a DNA molecule.

As expected, due to the small headgroup area of cholesterol ($A_{\text{chol}} = 40$ Å^2, while $A_{\text{DOPC}} = 72$ Å^2) [40, 41], the membrane charge density of DOTAP/DOPC/Chol–DNA complexes increases with cholesterol content. Exchanging DOPC for cholesterol reduces the total membrane area while the membrane charge, given by $\Phi_{\text{DOTAP}} = 0.3$, remains constant; thus σ_M increases. A particularly strong increase in σ_M occurs for $\Phi_{\text{chol}} \geq 0.4$, where part of the cholesterol is not incorporated in the complex. This results in an increased Φ_{DOTAP} and thus σ_M.

3.2 *Transfection Efficiency of CL–DNA Complexes Containing Cholesterol and Analogs*

Figure 5a shows the transfection efficiency of (lamellar) DOTAP/DOPC–DNA complexes (circles) as a function of Φ_{DOTAP}. TE increases over several orders of magnitude with the molar fraction of cationic DOTAP. Also evident from this plot

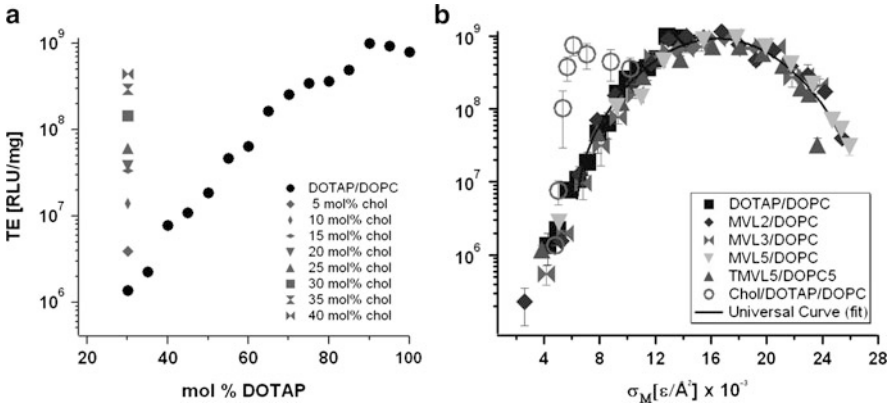

Fig. 5 (**a**) TE of DNA complexes of binary DOTAP/DOPC lipid mixtures (*black circles*). Their TE increases over several orders of magnitude with increasing molar fraction of monovalent DOTAP (Φ_{DOTAP}). *Gray symbols* represent TE of DNA complexes of ternary DOTAP/DOPC/Chol lipid mixtures with constant $\Phi_{\mathrm{DOTAP}} = 0.3$. *Different symbol shapes* correspond to different Φ_{chol} (cf. legend). (**b**) The TE of the DNA complexes of ternary DOTAP/DOPC/Chol lipid mixtures (*empty circles*) plotted against σ_M significantly deviates from the universal bell shaped curve observed for binary systems [21]. Reprinted with permission from [27]. Copyright 2009 American Chemical Society

is the dramatic increase in TE upon partially replacing DOPC with cholesterol at $\Phi_{\mathrm{DOTAP}} = 30\%$ (symbols of different shapes correspond to different Φ_{chol}; see legend). TE increases by a factor of ten with the addition of only 15 mol% cholesterol, and further addition of cholesterol continues to increase TE exponentially. Of note, the amount of DOTAP and DNA is constant for all data points.

3.2.1 Transfection Efficiency and Membrane Charge Density

Using the experimentally obtained values of σ_M calculated using (1), Fig. 5b plots TE of DOTAP/DOPC/Chol–DNA complexes (empty circles) as a function of membrane charge density, together with the universal curve and the TE data used for its derivation [21].

TE of the DOTAP/DOPC/Chol–DNA complexes strongly deviates from the universal bell-shaped curve observed for binary systems. The TE of cholesterol-containing complexes increases more rapidly with increasing cholesterol content than the increase in membrane charge density predicts for $0 < \Phi_{\mathrm{chol}} \leq 0.4$. No further TE increase is seen for $\Phi_{\mathrm{chol}} > 0.4$ (where the membrane is saturated with cholesterol: $\Phi_{\mathrm{chol,\ membrane}} = 0.4 = \mathrm{const.}$).

3.2.2 The Effect of Cholesterol Analogs

Figure 6a shows the TEs of DOTAP/DOPC–DNA complexes containing the structural analogs of cholesterol. Two distinct trends can be observed. The data for

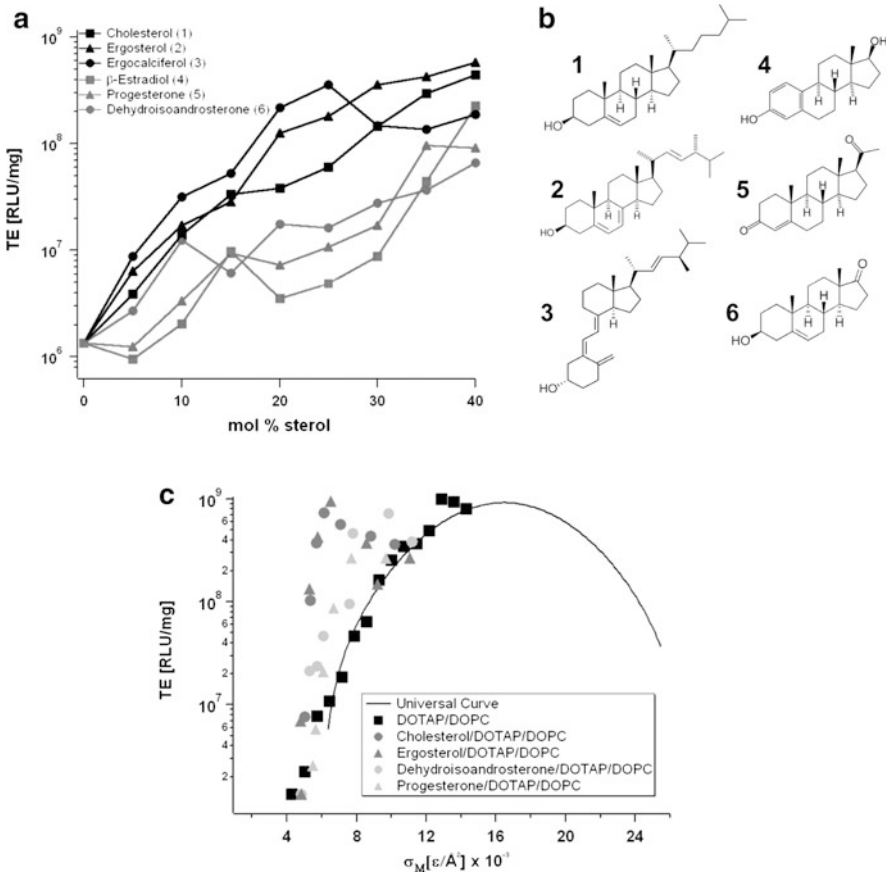

Fig. 6 (**a**) TEs of DOTAP/DOPC/steroid–DNA complexes. The TE data for ergosterol 2 and ergocalciferol 3 follows a similar dependence on the steroid content in the membrane as that of cholesterol 1: TE rapidly increases with Φ_{steroid}. In contrast, addition of β-estradiol 4, progesterone 5, and dehydroisoandrosterone 6 only modestly enhances TE until high steroid contents (35 mol% and higher) are reached, where phase separation occurs and TE suddenly increases to values comparable with TE of cholesterol-containing complexes. The major structural differences between these two groups of molecules are the absence of the terminal alkyl chain and the presence of a second polar moiety in case of 4–6. (**b**) Chemical structure of the investigated steroid molecules. (**c**) TEs of DOTAP/DOPC/steroid–DNA complexes plotted as a function of experimentally obtained σ_M. The data for cholesterol (*dark circles*) and ergosterol (*dark triangles*) deviate significantly from the universal TE curve (*black solid line*), whereas the TE data for progesterone (*gray triangles*) and dehydroisoandrosterone (*gray circles*) nearly follow the universal behavior. Reprinted with permission from [27]. Copyright 2009 American Chemical Society

ergosterol and ergocalciferol are similar to that of cholesterol: TE rapidly increases with the increasing molar fraction of steroid, dramatically improving TE. In contrast, when β-estradiol, progesterone, and dihydroisoandrosterone are incorporated into CL–DNA complexes, TE rises less rapidly until membrane saturation occurs at high

steroid contents (35 mol% and higher). At this point, TE suddenly increases to values comparable with those obtained for cholesterol. The major structural differences between the two groups of molecules are the absence of the short alkyl chain attached to the hydrophobic core and the presence of a second polar moiety in its place in case of β-estradiol, progesterone, and dihydroisoandrosterone (see the chemical structures in Fig. 6b).

Figure 6c shows the TEs of the DOTAP/DOPC/steroid–DNA complexes plotted as a function of σ_M. The membrane charge densities were obtained from X-ray diffraction data using (1). The data for cholesterol (dark circles) and ergosterol (dark triangles) deviate significantly from the universal TE curve (black solid line), whereas the TE data for progesterone (gray triangles) and dehydroisoandrosterone (gray circles) nearly follow the universal behavior.

3.2.3 Reduced Hydration-Repulsion Causes Enhanced Transfection Efficiency

The results described above show that adding cholesterol and certain analogs increases TE more than the resulting increase in membrane charge density would predict. Previous work has demonstrated that CL–DNA complexes at low σ_M transfect poorly due to inefficient endosomal escape (which involves fusion) [21, 25]. Thus, our findings suggest that cholesterol and certain analogs facilitate fusion of the membranes of the complex and the endosome, independent of their effect on σ_M. A possible explanation for this is the overall reduction of the hydration repulsion layer of the membrane.

As two lipid membrane surfaces approach each other, short-range hydration and steric repulsions set in at distances between 1 and 3 nm and exponentially increase with decay lengths between 0.08 and 0.64 nm for the range of lipids and surfactants that have been studied to date [42]. Hydration repulsion forces result from the presence of water molecules strongly bound to hydrophilic membrane lipids, because of the energy required to dehydrate the lipids as the membranes approach each other [42]. The term steric repulsion refers to excluded volume effects, which include the effects of thermal height fluctuations of the lipid membranes. The adhesion energy for oppositely charged membranes (at given positive and negative charge densities) will be optimized as the hydration/steric repulsive forces are decreased, allowing the membranes to approach more closely. For oppositely charged membranes, increased adhesion will facilitate fusion [42, 43], which is favored by electrostatics. That is, membranes comprised of cationic/anionic lipids (after fusion) have a lower electrostatic energy compared to two approaching membranes with cationic and anionic lipids in different membranes (before fusion). Furthermore, the entropy of mixing is increased when oppositely charged membranes fuse.

It is known that the hydration repulsion layer of cholesterol is much smaller than that of DOPC [42, 44]. Therefore, exchanging DOPC for cholesterol enhances fusion [42]. For CL–DNA complexes, this enhanced fusion of the membranes of

the complex with the endosomal membrane facilitates endosomal release and increases TE. Ergosterol and ergocalciferol show the same effect. On the other hand, CL–DNA complexes containing progesterone, estradiol, and dehydroisoandrosterone show different behavior, even though they likely reduce the average hydration repulsion layer of the membrane in the same way as cholesterol. A possible explanation for this phenomenon is that these steroid molecules also enhance the repulsion of the membranes because of increased protrusion forces. Progesterone, estradiol, and dehydroisoandrosterone possess two polar groups, one at each end of the polycyclic framework, which dictate a positioning of the molecules close to the water interface (due to their increased hydrophilicity). The resulting protrusion forces appear to cancel the benefits of the reduced hydration repulsion layer with respect to the activated fusion with the endosomal membrane.

To test the hypothesis that the reduction of the hydration repulsion layer by cholesterol is responsible for the enhancement of TE, we have performed transfection experiments with DNA complexes of a ternary mixture of DOTAP, DOPC and PC-cholesterol (cholesteryl–phosphatidylcholine), a cholesterol derivative in which the hydroxyl group of cholesterol has been replaced by a phosphatidylcholine group. The chemical structure of PC-cholesterol is shown in Fig. 7b. The headgroups of PC-cholesterol and DOPC are essentially identical, thus having a similar (if not identical) hydration repulsion layer. Figure 7a compares the TE of lamellar DNA-complexes of DOTAP/DOPC/Chol (black squares) and DOTAP/DOPC/PC-cholesterol lipid mixtures (gray bowties), again at constant $\Phi_{\mathrm{DOTAP}} = 0.3$. The data show the large increase in transfection efficiency by $\approx$ two decades as DOPC lipids

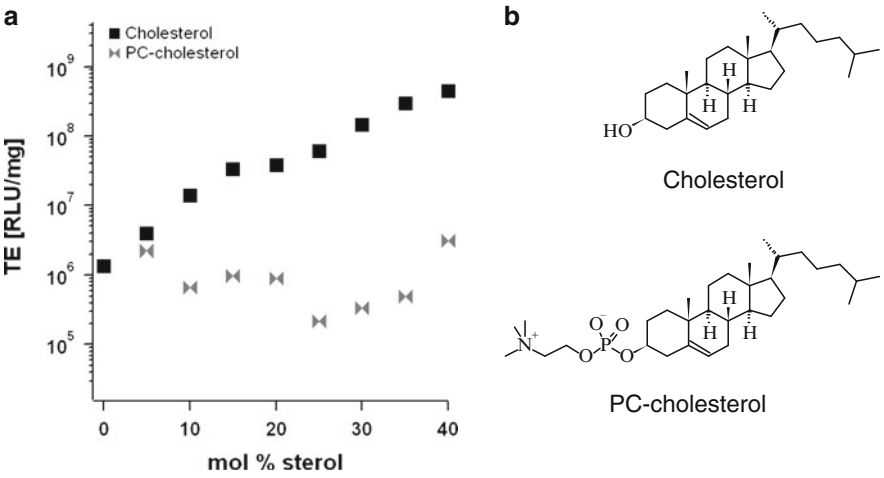

Fig. 7 (**a**) A comparison of the TE of DOTAP/DOPC/Chol–DNA complexes (*black squares*) and DOTAP/DOPC/PC-cholesterol–DNA complexes (*gray bowties*). The replacement of DOPC with PC-cholesterol, which has a similarly hydrated headgroup, fails to increase TE. (**b**) The chemical structures of cholesterol and PC-cholesterol. Reprinted with permission from [27]. Copyright 2009 American Chemical Society

are replaced by cholesterol (black squares). In contrast, no increase in TE is observed if instead DOPC is replaced by cholesterol-PC (gray bowties). This is strong evidence that the reduction of the hydration repulsion layer is, indeed, crucial for the TE enhancement.

In summary, our findings suggest that cholesterol and certain analogs are a highly valuable neutral lipid component ("helper lipid") for CL–DNA complexes because they facilitate endosomal escape by reducing the repulsive hydration and protrusion forces. They are thus able to lower the kinetic barrier for fusion of the cationic membranes of CL–DNA complexes with the anionic membrane of the endosome and increase TE, in addition to their beneficial effect on σ_M.

4 Highly Charged Multivalent Cationic Lipids with Dendritic Headgroups Promote Novel Structures and Mechanisms

The cationic lipids exhibiting universal behavior in our earlier studies (see Sect. 2) ranged in their headgroup valency from 2+ to 5+ [21]. The corresponding upper limit of σ_M, for membranes of pure pentavalent MVL5, was 27.17×10^{-3} e/Å^2. To study the transfection behavior of CL–DNA complexes at even higher membrane charge densities σ_M, we synthesized a series of highly charged lipids with dendritic headgroups (DLs) and studied their DNA complexes [24, 45, 46].

4.1 Synthesis of DLs

Dendrimers are monodisperse, highly branched spherical molecules [47]. They are typically assembled by adding AB_2 building blocks to a central core, thus yielding sequential "generations" of increasing size and endgroup number. Employing a building block approach for lipid design and synthesis, we have prepared a series of multivalent DLs based on ornithine as the AB_2 building block [24, 45]. Figure 8 shows the chemical structures, molecular models and valencies at full protonation for the studied DLs. Branching ornithine groups (highlighted by rectangles) double the number of end groups with cationic charges in each generation. Using both zeta potential measurements and an ethidium bromide displacement assay [24, 45, 48], the charges of the lipid headgroups effective in DNA complexation were determined as 4.0 ± 0.2 for MVLG2, 7.9 ± 0.3 for MVLG3, 8.0 ± 0.1 for MVLBisG1, and 14.6 ± 0.4 for MVLBisG2 independent of Φ_{DOPC}. Thus, the headgroup charges of the DLs are very close to their charge at full protonation. To date, only very few other lipids with a similar number of charges in the headgroup have been reported [49]. Mixing of these lipids with neutral DOPC results in liposomes having σ_M of up to 40×10^{-3} e/Å^2.

The synthesis of the branched core of the lipid headgroups [24, 45] proceeds in the same manner as that of multiple antigenic peptides (MAPs) [50, 51] or polyethylene glycol-dendritic oligo-lysine block copolymers [52]. It starts from ornithine

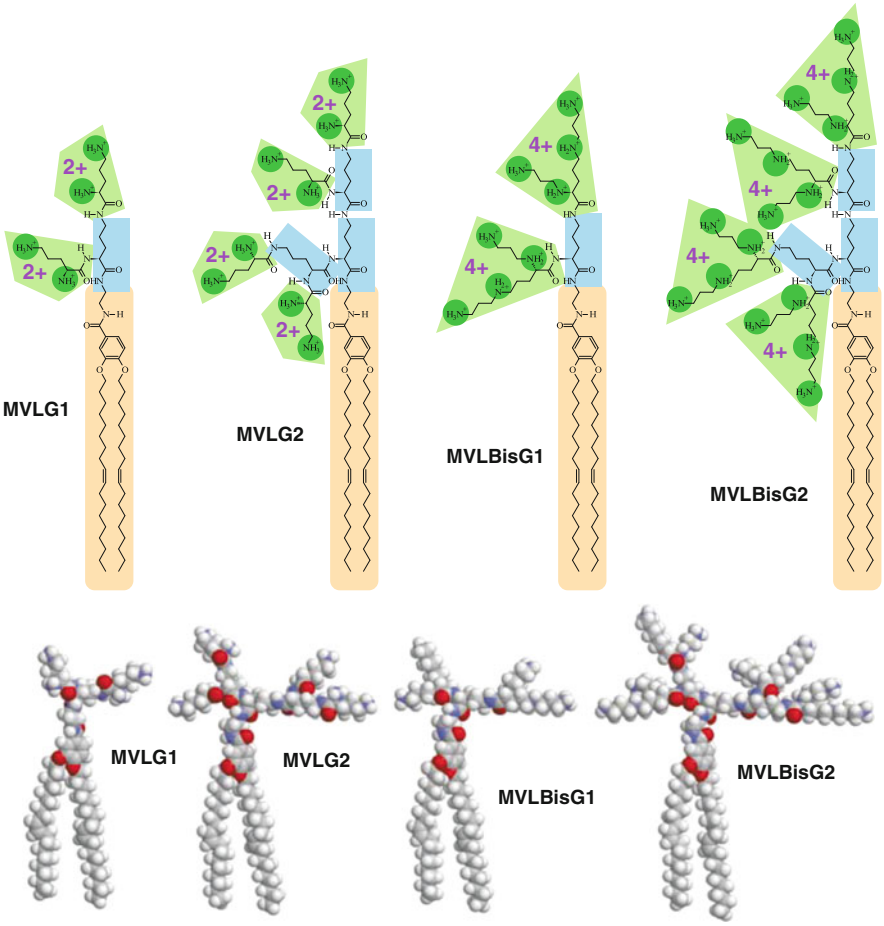

Fig. 8 Chemical structures, maximum charge, and molecular models of the DLs MVLG2, MVLG3, MVLBisG1, and MVLBisG2. Branching ornithine spacer groups (highlighted by *rectangles*) double the number of end groups in each generation. The lipid tails are underlaid with a *rounded rectangle*, and the cationic end groups (carboxyspermine (4+) or ornithine (2+)) and their charged moieties are also *highlighted*

methyl ester, which is acylated with Boc-protected ornithine. After deprotection of the amino groups, this process is repeated to increase the headgroup generation. By aminolysis of the methyl ester of the headgroup building block with an excess of ethylene diamine, a spacer with a distal amino group is introduced in a single step. In the synthesis of the headgroup moieties of MVLBisG1 and MVLBisG2, the final acylation is performed using Boc-protected carboxyspermine, which yields four charges after deprotection. This building block was prepared starting from ornithine through Michael-addition of acrylonitrile, followed by reduction of the cyano-groups using Raney nickel [53–55] and Boc-protection of the resulting amino groups

[26]. To finish the synthesis of the DLs, the headgroup-spacer moiety is coupled with our lipid building block [56]. The product is purified extensively and finally deprotected using TFA.

4.2 Novel Structures of DL/DOPC–DNA Complexes

MVLG2(4+)/DOPC–DNA self-assemblies exhibit the lamellar L_α^C phase for all Φ_{DOPC}. XRD indicates a very tight packing of DNA molecules within MVLG2/DOPC–DNA complexes even at low σ_M. This is consistent with previous findings for the multivalent lipids MVL3(3+) and MVL5(5+) by Farago et al. who attributed the tight packing found even at low σ_M to a unique DNA locking mechanism involving the multivalent headgroups [57].

MVLBisG2(16+) bears the largest headgroup of the studied DLs, the size of which results in a conical molecular shape, favoring positive spontaneous membrane curvature. When mixed with cylindrically shaped DOPC, MVLBisG2 exhibits a rich phase diagram [58]. Cryo-TEM revealed that micelles coexist with vesicles at $0.5 \leq \Phi_{MVLBisG2} < 0.75$. At $\Phi_{MVLBisG2} \geq 0.75$, the MVLBisG2/DOPC lipid mixture forms only micelles.

X-ray diffraction of MVLBisG2/DOPC–DNA complexes reveals the lamellar L_α^C phase for $\Phi_{MVLBisG2} < 0.2$. In a narrow interval around $\Phi_{MVLBisG2} \approx 0.25$, the novel hexagonal CL–DNA complex phase (H_I^C, see also Fig. 1c) is found [24], with coexistence of the two phases at $\Phi_{MVLBisG2} = 0.2$. At $\Phi_{MVLBisG2} = 0.4$, a phase transition to a distorted hexagonal lattice occurs, persisting up to $\Phi_{MVLBisG2} = 1$. This phase is characterized by broad diffraction peaks with the ratio of peak positions $q_2/q_1 = 1.6$. Similarly, the phase transition from lamellar to hexagonal can be clearly identified by the change in q_2/q_1 from 2 to 1.7. The phase transition from the hexagonal phase to the distorted hexagonal phase coincides with the appearance of micelles in the MVLBisG2/DOPC lipid mixture at $\Phi_{MVLBisG2} \approx 0.5$, suggesting a direct impact of the presence of micelles on the assembly of MVLBisG2/DOPC–DNA complexes. At higher $\Phi_{MVLBisG2}$ ($0.6 \leq \Phi_{MVLBisG2} \leq 1$), XRD experiments further revealed a coexisting phase of tightly packed DNA bundles [46].

Figure 9 shows schematic depictions of the two newly discovered structures described above. A cross section of a distorted hexagonal lattice is shown in Fig. 9a, displaying lipid micelles of an elliptical cross section and DNA molecules localized in the interstitial space. The distortion of the lattice is likely caused by the asymmetry in the micellar shape. X-ray diffraction data shows that the distortion increases with $\Phi_{MVLBisG2}$.

Figure 9b shows a schematic of the DNA bundle phase observed at $\Phi_{MVLBisG2} > 0.5$. The bundling phase requires the presence of salt (as found in the cell culture medium used for all our experiments) and is formed by the interplay of the salt-induced screening of the electrostatic interactions and the depletion–attraction [59, 60] caused by the lipid micelles. While depletion–attraction has previously been reported for like-charged or neutral objects, the screening of the electrostatic interactions also

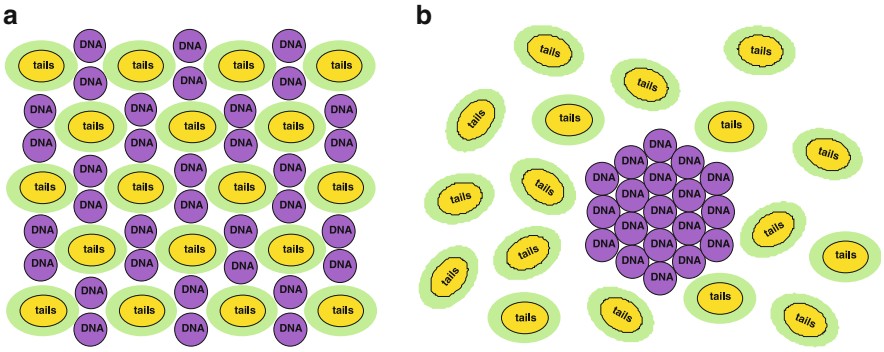

Fig. 9 (**a**) Schematics of the molecular structure of DL/DOPC–DNA complexes assembled in slightly disordered H_I^C. (**b**) DNA bundles surrounded by a cloud of micelles. The depletion–attraction force caused by micelles and the screening of the electrostatic interaction in the system enables the formation of the DNA bundles. Reprinted with permission from [46]. Copyright 2009 American Chemical Society

enables this effect to be observed between DNA and the oppositely charged lipid micelles, for which the electrostatic interactions are attractive. The presence of salt not only facilitates bundling of DNA by reducing the electrostatic repulsion between DNA molecules. It also reduces the electrostatic attraction between positively charged micelles and negatively charged DNA (Fig. 9a) to a level where it is less than the entropy gained by the micelles upon confining the DNA into bundles (Fig. 9b).

As expected from their intermediate headgroup size and charge, MVLG3(8+) and MVLBisG1(8+) form DL/DOPC–DNA complexes which occupy a middle ground in their phase behavior. Figure 10a, b shows X-ray diffraction data for MVLG3/DOPC–DNA complexes and MVLBisG1/DOPC–DNA complexes, respectively, at three different compositions: $\Phi_{DL} = 0.2$, 0.4, and 1. DL/DOPC–DNA complexes of both lipids form a lamellar L_α^C phase for $\Phi_{DL} \leq 0.5$. Figure 10c,d shows plots of the ratios of the peak positions q_2/q_1 and q_3/q_1 vs Φ_{DL} which signify the nature of the self-assembly. For the lamellar phase, $q_2 = 2q_1$ and $q_3 = 3q_1$, which is clearly satisfied for $\Phi_{DL} \leq 0.5$. For $0.5 < \Phi_{DL} < 0.8$, the ratio between the first and the second order peaks q_2/q_1 is 1.7 (3), while $q_2/q_1 = 1.6$ for $\Phi_{DL} \geq 0.8$. This suggests a sequence of phases similar to that observed for MVLBisG2/DOPC–DNA complexes, from L_α^C to H_I^C to a distorted hexagonal phase. An indication of a DNA bundle phase is only seen for $\Phi_{MVLG3} = 1$ (a characteristic DNA bundle peak at $q = 0.241$ Å^{-1}).

4.3 *Transfection Efficiency of DL/DOPC–DNA Complexes*

We have mapped the transfection efficiency of DL/DOPC–DNA complexes as a function of molar fraction of DL (Φ_{DL}) and the cationic lipid/DNA charge ratio (ρ_{chg}). As observed for DOTAP and multivalent lipids with valencies up to +5, TE

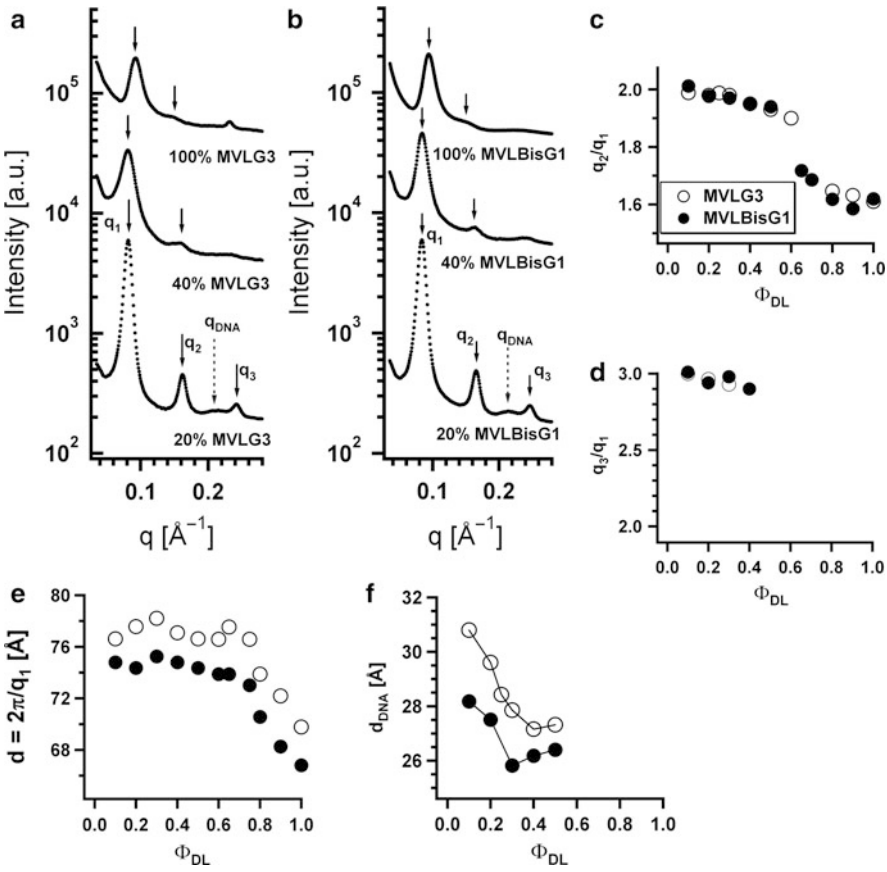

Fig. 10 X-ray diffraction data for (**a**) MVLG3/DOPC–DNA complexes and (**b**) MVLBisG1/DOPC–DNA complexes at $\Phi_{DL} = 0.2$, 0.4, and 1. (**c**) Ratio of the first and second order diffraction peaks, $q2/q1$, and (**d**) ratio of the first and third order diffraction peaks, $q3/q1$, plotted as a function of Φ_{DL}. (**e**) The spacing $d = 2\pi/q_1$ as a function of Φ_{DL}. (**f**) Plot of d_{DNA} as a function of increasing Φ_{DL} in lamellar complexes. Reprinted with permission from [46]. Copyright 2009 American Chemical Society

at the optimal Φ_{DL} increases with ρ_{chg} up to a saturation value. Interestingly, this value is higher for the DLs ($\rho_{chg} \approx 4.5$) than for previously investigated lipids ($\rho_{chg} \approx 3$) [45].

The TE data of DL/DOPC–DNA complexes at $\rho_{chg} = 4.5$ and $\rho_{chg} = 8$ as a function of σ_M are plotted in Fig. 11. Also shown are fits representing the universal TE curves at those values of ρ_{chg} (black solid lines) [21, 46]. TE of MVLG2(4+)/DOPC–DNA complexes exhibits the previously observed dependence on σ_M and closely follows the universal curve. However, the data for both MVLBisG1/DOPC–DNA complexes as well as MVLBisG2/DOPC–DNA complexes deviate strongly from the universal TE curve for $\sigma_M \geq 18 \times 10^{-3}$ e/Å^2, which is close to the

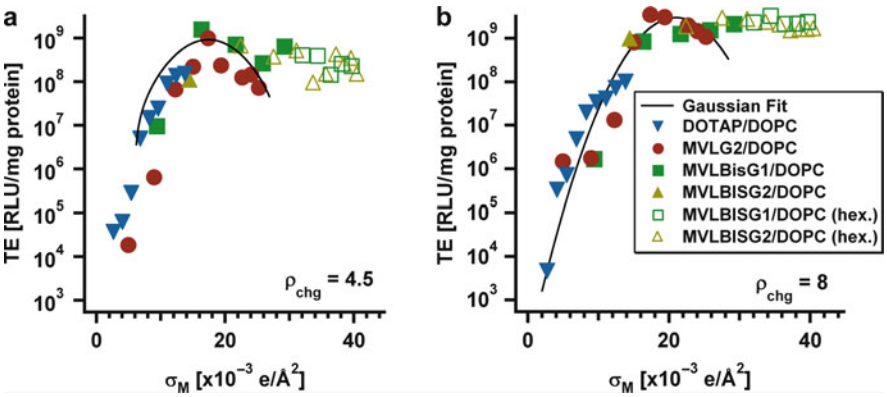

Fig. 11 TE of DL/DOPC–DNA complexes containing MVLG2, MVLBisG1 or MVLBisG2 plotted as a function of σ_M for two different values of ρ_{chg}. (**a**) TE at $\rho_{chg} = 4.5$ and (**b**) TE at $\rho_{chg} = 8$. The *solid line* represents the universal TE curve [21]. The *solid symbols* mark data for DL/DOPC–DNA complexes in the lamellar phase, while *empty symbols* correspond to DL/DOPC–DNA complexes in hexagonal phases. Reprinted with permission from [46]. Copyright 2009 American Chemical Society

maximum of the universal TE curve. Instead of dropping, TE of these complexes remains high beyond this value of σ_M. This behavior is reminiscent of the TE of DOTAP/DOPE–DNA complexes, which is independent of σ_M, albeit at low membrane charge densities. DOTAP/DOPE–DNA complexes exhibit the inverted hexagonal phase at *low* σ_M, and their constant, high TE reflects their different mechanism of action (see also Sect. 1) [25].

4.3.1 Correlations Between Structure and TE of DL/DOPC–DNA Complexes

As evident from Fig. 11, where different symbols are used to distinguish TE data for lamellar (filled symbols) and non-lamellar phases (open symbols), DL/DOPC–DNA complexes in the L_α^C phase closely follow the universal behavior. These are MVLG2/DOPC–DNA complexes at all Φ_{DL} and DNA complexes of the other DLs at low Φ_{DL}. In contrast, TE of the H_I^C phase and the new distorted hexagonal and DNA bundle phases is not only high but independent of Φ_{DL} and thus σ_M. The appearance of non-lamellar phases therefore coincides with the deviation from the universal TE curve, suggesting a different mechanism of action for the different structures of DNA complexes.

The non-lamellar DL/DOPC–DNA complexes exhibit enhanced TE (over lamellar complexes of the same σ_M) in the σ_M regime where release of DNA from the complex is thought to be limiting TE. The structure of the H_I^C complexes gives a clue as to its possible role in the transfection mechanism and high TE. In contrast to the L_α^C phase, both the H_I^C phase and the distorted hexagonal phase exhibit a continuous sub-structure of DNA within the complexes. The DNA bundle phase

observed with MVLBisG2 even seems to allow the delivery of a lipid-free subphase of DNA. The existence of a continuous DNA substructure likely facilitates release of DNA, because all DNA is accessible as soon as a part of it is exposed to the cell interior. Interestingly, the TE of these complexes does not exceed that of the optimized lamellar complexes, which may hint at the presence of another barrier for complexes of high σ_M.

4.3.2 MVLBisG2 Efficiently Transfects MEFs, a Hard-to-Transfect Cell Line

Another important discovery was made when comparing MVLBisG2 and DOTAP in a number of different cell lines. As shown in Fig. 12, complexes of MVLBisG2 efficiently transfect a variety of mouse and human cells in culture [24]. Their TE reaches or surpasses that of optimized complexes prepared from commercially available DOTAP. Most importantly, complexes containing MVLBisG2 are significantly more transfectant over the entire composition range in mouse embryonic fibroblasts (MEFs). MEFs are important as feeder cells for embryonic stem cells and are a cell line that is empirically known to be hard to transfect.

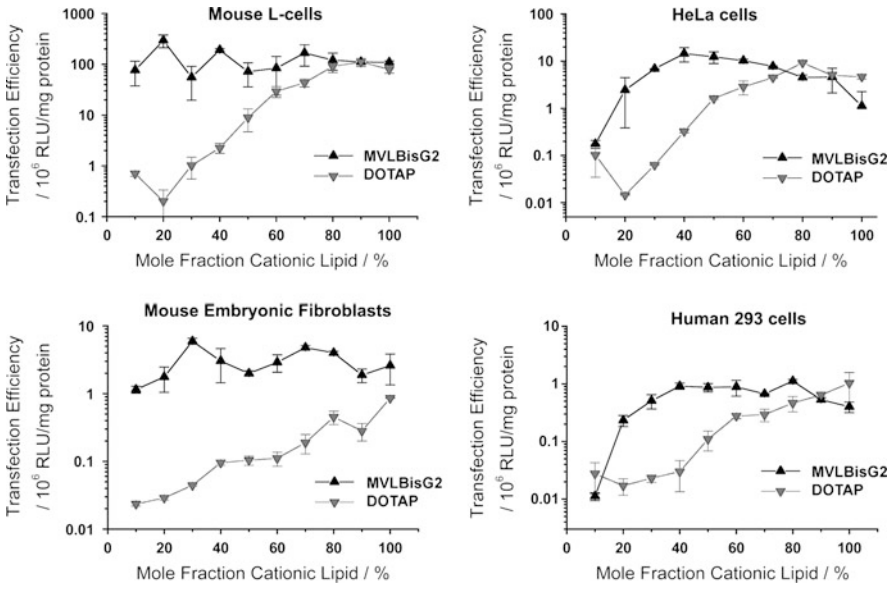

Fig. 12 Transfection efficiencies for DOTAP/DOPC and MVLBisG2/DOPC complexes in four different cell lines, plotted against the mole fraction of cationic lipid. The data points were obtained at a constant ρ_{chg} (7 for HeLa cells, 4.5 for all others), corresponding to a constant amount of DNA applied to the cells for each data point in a plot. Remarkably, MVLBisG2 complexes are significantly more transfectant in mouse embryonic fibroblasts, a cell line empirically know to be hard to transfect and of large practical importance as feeder cells for embryonic stem cells. Reprinted with permission from [24]. Copyright 2006 American Chemical Society

5 CL–siRNA Complexes for Gene Silencing

A novel direction in CL-based nucleic acid delivery research worldwide, including our laboratory, has arisen out of the recent major discovery of RNA interference (RNAi) as an evolutionary conserved post-transcriptional gene-silencing pathway, in the nematode worm *Caenorhabditis elegans* in 1998 [61], in plants [62, 63], and in filamentous fungi [64, 65]. The finding that short interfering RNA (siRNA) (19–27 bp strands of dsRNA, with 2*nt* 3′−overhangs) leads to sequence specific gene silencing via RNAi when introduced into mammalian cells [66, 67], without evoking the interferon pathway [68, 69], has led to a surge in research activity aiming to utilize the pathway more broadly in functional genomics studies [70, 71] and therapeutic applications [72–76]. The specificity of the RNAi machinery has been demonstrated by its ability to discriminate between mRNA targets with only one base pair difference [72]. Thus, in principle, siRNAs may be designed that selectively knock down the expression of any given gene product for which the sequence of the gene is known.

The therapeutic applications of RNAi are currently being explored, with potential targets including cancers and viral infections [74–78]. However, the utility of RNAi is limited by the efficiency and toxicity of the available siRNA delivery vehicles. To improve cationic lipid-based vectors, it is important to gain a better understanding of the relationship between the chemical-physical parameters and the biological, gene silencing activity of cationic liposome–siRNA (CL–siRNA) complexes. Understanding the mechanism of action of CL–siRNA complexes *in vitro* will allow optimization of lipid carriers for siRNA molecules, thereby making them a viable alternative to virus-based delivery methods which avoid their safety, immunogenicity, and production issues associated with these.

When investigating CL–siRNA complexes with the objective of optimizing their silencing efficiency (SE), it is of particular interest to reveal similarities and important differences with the process of optimizing transfection efficiency of CL–DNA complexes, which involves delivery of long dsDNA. Two key differences from the outset are the fact that siRNA complexes transport a much shorter cargo, and that they only need to deliver it to the cytoplasm, where the RNAi machinery is located. The shorter length of the siRNA duplex is expected to result in a weaker electrostatic stabilization of the complexes with CLs, and may, for some membrane compositions, lead to different structures.

We have found that efficient delivery of siRNAs to cells in culture requires a molar charge ratio (ρ_{chg}, cationic lipid/nucleic acid) nearly an order of magnitude larger than that optimal for CL–DNA complexes. This larger ρ_{chg} needed for efficient silencing results in a larger amount of cationic lipid per cell. Thus, toxicity becomes an important issue to consider in some composition regimes. This implies that cationic multivalent lipids (MVLs) should be better vectors compared to univalent lipids, because a smaller number of MVLs is required for a given ρ_{chg} of the complex. We have compared the silencing efficiency and toxicity of CL–siRNA

complexes in mammalian cells, using monovalent DOTAP and custom synthesized pentavalent MVL5 [21, 26] as cationic lipids [79].

MVL5(5+) exhibits superior silencing efficiency over a large range in the composition and ρ_{chg} phase diagram compared to monovalent DOTAP and was significantly less toxic. In fact, MVL5-based vectors achieved near-complete, specific silencing, a result that could not be attained using DOTAP-based vectors. In addition, the experiments showed that DOPE is not a viable neutral lipid for siRNA delivery due to its toxicity.

5.1 Structures of CL–siRNA Complexes

DOTAP/DOPC–siRNA complexes exhibit the lamellar (L_α^{siRNA}) structure at $0 < \Phi_{DOPC} < 0.9$ (mole fraction of DOPC) at $\rho_{chg} = 10$ (Fig. 13a). The L_α^{siRNA} structure is similar to the L_α^C structure shown in Fig. 1a, with the layer of DNA replaced by a layer of siRNA. An XRD scan displaying the [00L] layering peaks is shown in Fig. 13b. Figure 13c shows an XRD pattern of lamellar MVL5/DOPC–siRNA complexes at $\Phi_{DOPC} = 0.6$ and $\rho_{chg} = 10$. The lamellar structure was observed for all $\Phi_{DOPC} > 0.3$. For $\Phi_{DOPC} \leq 0.3$ a distinct, new phase was observed, the structure of which remains to be determined. This is in contrast to MVL5/DOPC–DNA complexes, which exhibit the lamellar structure for all values of $\Phi_{DOPC} > 0.1$ [21]. An important observation is the absence of NA–NA correlation peaks that are typically seen with CL–DNA complexes [22] in the DOTAP/DOPC–siRNA complexes. The short length of siRNA molecules disfavors 2D nematic liquid crystal ordering of siRNA rods (with orientational order). However, broad correlation peaks are observed for MVL5/DOPC–siRNA complexes. XRD

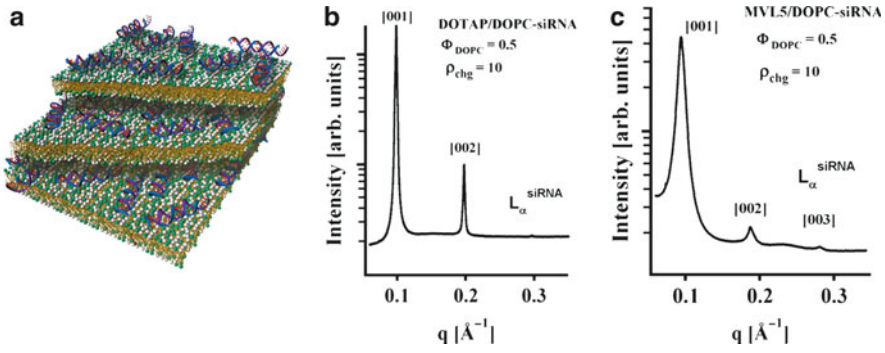

Fig. 13 (**a**) Schematic of a lamellar (L_α^{siRNA}) DOTAP/DOPC–siRNA complex. Partial bilayers have been removed, exposing 19 bp siRNAs in the isotropic phase. (**b**, **c**) Synchrotron X-ray data of CL–siRNA complexes reveal lamellar (L_α^{siRNA}) patterns for DOTAP/DOPC–siRNA complexes (**b**) and MVL5 DOPC complexes (**c**). Note the broad siRNA–siRNA correlation peak in (**c**), between q_{002} and q_{003}. Reprinted with permission from [79]. Copyright 2007 American Chemical Society

showed that DOTAP/DOPE–siRNA complexes exhibit the lamellar structure for $\Phi_{\mathrm{DOPE}} < 0.4$ and the inverted hexagonal structure ($H_{\mathrm{II}}^{\mathrm{siRNA}}$) for $\Phi_{\mathrm{DOPE}} > 0.6$, with a coexistence region in between [79]. The $H_{\mathrm{II}}^{\mathrm{siRNA}}$ structure is similar to the $\mathrm{H_{II}^{C}}$ structure shown in Fig. 1b, with siRNA inserted in the inverse tubular micelles.

5.2 Gene Silencing Activities of CL–siRNA Complexes

In order to quantify and compare effectively the gene silencing activity of CL–siRNA complexes, we measured the effect of lipid composition and ρ_{chg} on both the target gene knockdown and non-specific gene silencing (with the latter correlating to cytotoxicity). We prepared CL–siRNA complexes with monovalent (DOTAP) or pentavalent (MVL5) cationic lipid [26] combined with one of two commonly used neutral lipids (NLs), DOPC or DOPE. The delivered siRNA targeted the firefly luciferase mRNA and consisted of a 21 bp long siRNA. Varying the neutral lipid enabled us to elucidate its contribution to structure and SE for the CL–siRNA complexes.

To enable meaningful comparisons of gene silencing efficiencies, we developed a dual luciferase assay which allows us to distinguish the contributions from specific and non-specific gene silencing for a given vector. Mouse L-cells were first co-transfected with plasmids encoding the Firefly (FF) and Renilla (RL) luciferases. The cells were then either transfected with CL–siRNA complexes (at a given Φ_{NL} and ρ_{chg}) with siRNA targeting the mRNA for FF luciferase, or used as controls. A dual luciferase assay was used to measure the expression of FF (denoted $\mathrm{FF}(\Phi_{\mathrm{NL}},\rho_{\mathrm{chg}})$) and RL (denoted $\mathrm{RL}(\Phi_{\mathrm{NL}},\rho_{\mathrm{chg}})$) luciferase genes. For each measurement of FF and RL, expression levels were also measured in corresponding control cells (on volumes containing the same number of cells), yielding the controls $\mathrm{FF_{cont}}$ and $\mathrm{RL_{cont}}$. Thus, by measuring $\mathrm{FF}(\Phi_{\mathrm{NL}},\rho_{\mathrm{chg}})$, $\mathrm{FF_{cont}}$, $\mathrm{RL}(\Phi_{\mathrm{NL}},\rho_{\mathrm{chg}})$, and $\mathrm{RL_{cont}}$, one readily obtains the total normalized target gene knockdown $K_T = 1 - \mathrm{FF}(\Phi_{\mathrm{NL}},\rho_{\mathrm{chg}})/\mathrm{FF_{cont}}$ and the normalized non-specific gene knockdown $K_{\mathrm{NS}} = 1 - \mathrm{RL}(\Phi_{\mathrm{NL}},\rho_{\mathrm{chg}})/\mathrm{RL_{cont}}$.

The total knockdown K_T includes silencing resulting from two separate contributions: one due to sequence-specific silencing of the target FF by the siRNA, and another from the non-specific suppression of protein production. The non-specific knockdown K_{NS} measures this sequence-independent global suppression protein production by CL–siRNA complexes due to cytotoxicity, and is determined by measuring the silencing of the off-target RL gene in cells transfected with CL–siRNA complexes containing siRNA which targets the distinctly different FF luciferase mRNA. As outlined in more detail in Sect. 5.3, cytotoxicity and thus K_{NS} appears to be dominated by the cationic liposome component. Optimal gene silencing would correspond to K_T approaching 1 and K_{NS} approaching zero, where silencing is both complete and sequence-specific.

Figure 14 (left to right) shows plots of the total knockdown K_T and non-specific knockdown K_{NS} as a function of ρ_{chg} at $\Phi_{\mathrm{NL}} = 0.4$ for MVL5/DOPC–siRNA, DOTAP/DOPC–siRNA, and DOTAP/DOPE–siRNA complexes, respectively.

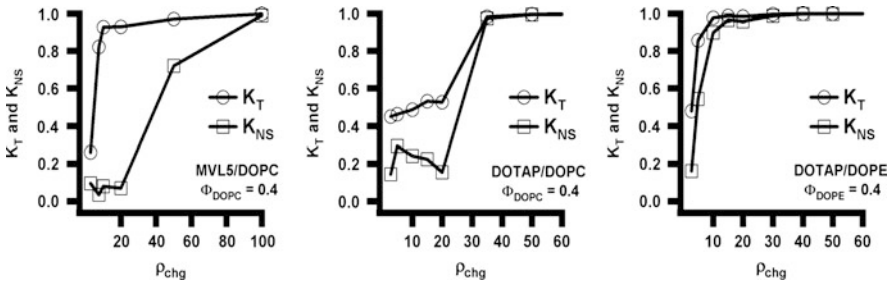

Fig. 14 Total (K_T, *open circles*) and non-specific (K_{NS}, *open squares*) gene knockdown vs cationic lipid/siRNA molar charge ratio (ρ_{chg}) at $\Phi_{NL} = 0.4$ for MVL5/DOPC–siRNA (*left*), DOTAP/DOPC–siRNA (*middle*), and DOTAP/DOPE–siRNA (*right*) complexes targeting FF luciferase mRNA in transfected L-cells. Reprinted with permission from [79]. Copyright 2007 American Chemical Society

Similar behavior was observed at $\Phi_{NL} = 0.1$. The data show that, for the lamellar MVL5/DOPC–siRNA complexes, the non-specific knockdown remains nearly constant and low with $K_{NS} < 0.1$ for $2.8 \leq \rho_{chg} \leq 20$, while K_T exhibits a rapid non-linear growth to $K_T \approx 0.9$ (for ρ_{chg} between 10 and 15), indicative of significant sequence-specific gene silencing (Fig. 14, left). In contrast, such a region of relatively high K_T and low K_{NS} was not observed for the lamellar phases of monovalent DOTAP/DOPC–siRNA complexes at $\Phi_{NL} = 0.4$ (or $\Phi_{NL} = 0.1$), where K_T increased slowly from 0.4 to 0.55 with $K_{NS} \approx 0.2$ (Fig. 14, middle). Furthermore, for DOTAP/DOPE–siRNA complexes (for which XRD indicates coexistence of the lamellar and inverted hexagonal structure), substantial non-specific knockdown K_{NS} (related to cell toxicity) is observed even at low $\rho_{chg} \approx 5$ (Fig. 14, right). This data is in striking contrast to DOTAP/DOPE–DNA inverted hexagonal complexes, which exhibit high TE in cell culture with low toxicity [25], albeit at lower ρ_{chg}.

Figure 15a shows total gene knockdown (K_T) data comparing the silencing efficiency of MVL5/DOPC–siRNA and DOTAP/DOPC–siRNA complexes at $\rho_{chg} = 15$ (i.e., in the regime where the non-specific knockdown shown in Fig. 14 is relatively low) as a function of Φ_{NL}. Complexes containing pentavalent MLV5 show high silencing efficiency over a broad range with $K_T \approx 0.9$ for $0 < \Phi_{NL} < 0.5$. In contrast, K_T of DOTAP-containing complexes remains relatively low and drops from 0.6 to ≈0.5 in the same range.

For a comparison at a charge ratio typically employed in DNA transfection, Fig. 15b shows the total gene knockdown for MVL5/DOPC–siRNA, DOTAP/DOPC–siRNA, and DOTAP/DOPE–siRNA complexes at $\rho_{chg} = 2.8$, which exhibits optimal transfection efficiency for DOTAP containing CL–DNA complexes with very low cell toxicity [21, 25]. At this lower charge ratio, CL–siRNA complexes are generally inefficient at gene silencing. While the silencing efficiency of MVL5/DOPC–siRNA complexes greatly increases as ρ_{chg} approaches 10, there was only a modest increase for the DOTAP containing complexes (Fig. 14).

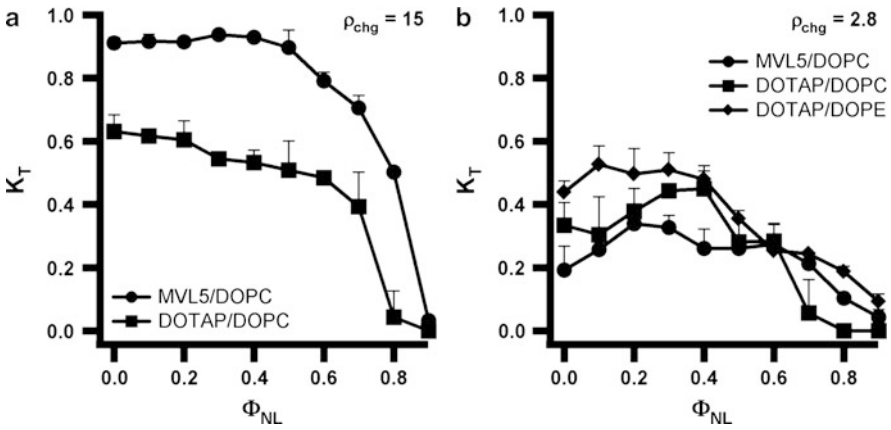

Fig. 15 Total gene knockdown (K_T) with siRNA complexes targeting the luciferase mRNA in transfected mouse L-cells as a function of mole fraction of neutral lipid Φ_{NL} at $\rho_{chg} = 15$ (**a**) and $\rho_{chg} = 2.8$ (**b**). Reprinted with permission from [79]. Copyright 2007 American Chemical Society

5.3 Cytotoxicity of CL–siRNA Complexes and Liposomes

Cytotoxicity data for CL–siRNA complexes (MVL5/DOPC–siRNA, DOTAP/DOPC–siRNA, DOTAP/DOPE–siRNA) as a function of Φ_{NL} are shown in Fig. 16. The filled triangles ($\rho_{chg} = 10$) and filled circles ($\rho_{chg} = 50$) represent toxicity data for cells incubated with complexes. Also plotted are the toxicities measured when cells were incubated with corresponding equivalent amounts of cationic liposomes *without siRNA* (open triangles and open circles). At $\rho_{chg} = 10$, only the DOTAP/DOPE–siRNA complexes and DOTAP/DOPE liposomes showed toxicity. For these systems, the toxicity exhibits a marked broad peak as a function of Φ_{DOPE}. This is in contrast to the DOTAP/DOPC–siRNA and MVL5/DOPC–siRNA complexes and the corresponding liposomes, where toxicity is low for all Φ_{DOPC}. For $\rho_{chg} = 50$, siRNA complexes and CLs showed significant toxicity for all lipid combinations. Thus, the toxicity data correlate well with the measured non-specific knockdown values K_{NS} (Fig. 14) and confirm the use of K_{NS} as an indicator for cell viability. Because the degree of cytotoxicity is qualitatively similar for cells incubated with either CL–siRNA complexes or cationic liposomes alone, its origin appears to be the lipid component of the complex.

In summary, the data on total knockdown K_T, non-specific knockdown K_{NS}, and cell cytotoxicity show that MVL5/DOPC–siRNA complexes have a significantly higher silencing efficiency (with $K_T \approx 0.9$ and $K_{NS} < 0.1$) and lower cell toxicity over a broader range of ρ_{chg} and Φ_{NL} than monovalent DOTAP/DOPC–siRNA complexes, with the latter not showing a regime with K_T approaching 1 at low K_{NS} [79]. This means that MVL5/DOPC–siRNA complexes are the only viable siRNA vector out of those tested, since a high total silencing simply amounts to a global suppression of protein production if K_{NS} is also high, as in the case of DOTAP vectors.

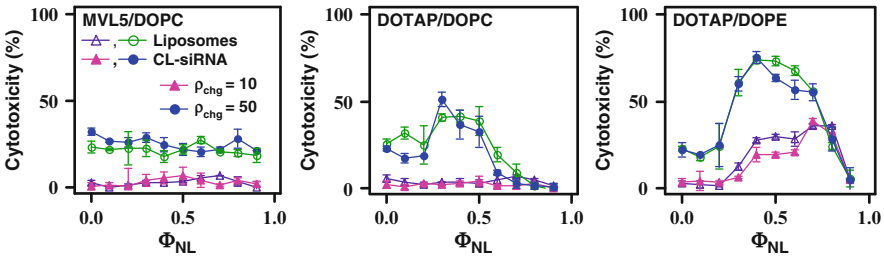

Fig. 16 Cytotoxicity of CL–siRNA complexes (MVL5/DOPC–siRNA, DOTAP/DOPC–siRNA, DOTAP/DOPE–siRNA) targeting the FF luciferase mRNA in mouse L-cells and the corresponding cationic liposomes (without siRNA) as a function of Φ_{NL} (mole fraction of neutral lipid). The *filled triangles* ($\rho_{chg} = 10$) and *filled circles* ($\rho_{chg} = 50$) represent toxicity data for cells incubated with complexes. Also plotted are the toxicities measured when cells were incubated with corresponding equivalent amounts of cationic liposomes *without siRNA* (*open triangles* ($\rho_{chg} = 10$) and *open circles* ($\rho_{chg} = 50$)). Cytotoxicity was measured by quantifying the amount of released lactate dehydrogenase from cells with damaged membranes. Reprinted with permission from [79]. Copyright 2007 American Chemical Society

6 Similarities and Differences in the Performance of Multivalent Lipids and Univalent Lipids

Since the synthetic effort required to prepare the lipid is generally greater for MVLs than for UVLs, with a view towards applications it is prudent to compare the overall performance of UVLs and MVLs, in particular considering the results shown in Sect. 2. Our work shows that while optimized formulations of MVLs and UVLs perform similarly in some cases, there are two important applications in which MVLs are far superior.

6.1 Systems Where MVLs and UVLs Have Comparable Performance

As we have elaborated in Sects. 2 and 4.3, the TE of lamellar DNA complexes of MVLs and UVLs shows universal behavior when plotted against the membrane charge density, implying that optimized complexes of MVLs and UVLs transfect equally well. Importantly, the fact that the universal curve is bell-shaped (where TE is plotted logarithmically) implies that optimization of the lipid composition is crucial for objectively comparing lipid performance. Interestingly, while complexes in the H_I^C and H_{II}^C phase do not follow this universal curve, their TE no more than equals that of optimized lamellar complexes.

6.2 *Systems Where MVLs Are Superior to UVLs*

We have identified two scenarios of high relevance in nucleic acid delivery for which MVLs are clearly superior to UVLs. These are plasmid delivery to hard to transfect cell lines and gene silencing with siRNA. In these applications, MVLs yield results that simply cannot be achieved by UVLs. As described in Sect. 4.3.2, a very highly charged MVL (MVLBisG2, 16+) has proven to be superior to the UVL DOTAP in MEFs, a hard to transfect cell line. We attribute this superiority of MVLBisG2 to its ability to induce the recently discovered hexagonal H_I^C structure, which is not found with UVLs. This unexpected finding is a very significant result, since hard to transfect cell lines are one of the most important current topics of basic research on DNA delivery. The second highly relevant difference between UVLs and MVLs is seen in the delivery of siRNA, where our studies show that MVLs are far superior (see Sect. 5.2). MVL5-based vectors showed near-complete and specific silencing, a result that could not be obtained with UVL vectors. MVLs permit using the large lipid/siRNA charge ratios required for high specific gene silencing without significant lipid-induced toxicity.

7 Future Directions

The ultimate goal of non-viral vector development is to rationally design and optimize vectors that are viable for *in vivo* applications. Non-viral vectors that can be successful at a task as complex as the delivery of nucleic acids *in vivo* will likely be sophisticated multi-component systems. En route to such systems, lipids specifically designed to lower or overcome known barriers to nucleic acid delivery will allow detailed investigations on the relevance of these barriers, ultimately leading to improved and "virus-like" lipid vectors. If these strategies are successful, they will benefit the development of more efficient non-viral vectors for research and therapeutic applications. At the very least, the improved understanding of barriers to successful delivery gained from this work will point the way to further improvement. Insights obtained on intracellular barriers and toxicity issues are relevant for both *in vitro* and *in vivo* applications since both share these barriers. Targeted vectors, which make use of cell specific attachment and internalization capabilities, will benefit not only *in vivo* applications but also *in vitro* work with hard to transfect cell lines. The same is true for lipids that facilitate endosomal escape, which may serve to recover efficiency that is lost by sterical stabilization.

Many of the known barriers to transfection may be addressed by custom synthesized lipids. For example, easily biodegradable cationic lipids should (1) enhance TE of CL–DNA complexes in the high membrane charge density regime, where dissociation and release of DNA from the cationic lipid membrane of the complex in the cytoplasm appears to be a barrier to TE, and (2) reduce toxicity in gene silencing applications with CL–siRNA complexes.

In addition, for CL–siRNA complexes, further exploration of the relationships between cationic lipid valence, complex stability, silencing efficiency, and cytotoxicity with a series of multivalent lipids such as the MVLS or DLs is a logical next step.

7.1 Non-Viral Vectors for In Vivo Gene Delivery

In vivo transfection by CL–DNA complexes poses a number of additional requirements when compared with transfection *in vitro*. This most notably shows in the fact that formulations which are optimal for transfection *in vitro* are not the best or even suitable for *in vivo* applications [29, 80, 81]. Addition of large amounts of serum to the transfection medium has a similar effect.

While the causes of this phenomenon are still the subject of active research, it is clear that CL–DNA complexes for systemic administration need to be stable in the circulatory system long enough to reach at least the target organ. Sterical stabilization by PEGylation, i.e., addition of PEG-lipids (PEG = poly(ethylene glycol)), can achieve this goal by preventing the attachment of opsonins and by limiting the activation of the complement system [82]. PEGylation also confers colloidal stability, high solubility, and a small, well-defined, size to CL–DNA complexes [83–85]. A stable, consistent particle size of about 100 nm diameter, as achieved by PEGylation, is most advantageous for cancer therapy *in vivo*, being too large for fast renal excretion and too small for rapid clearance by the reticuloendothelial system (RES) [85]. Particles of this size have the added advantage that they accumulate in tumors and sites of inflammation – the so-called enhanced permeation and retention (EPR) effect [86].

However, complexes that have been stabilized against aggregation and degradation by PEGylation exhibit much lower TE than their unshielded counterparts [83, 85, 87, 88]. PEGylation reduces the ability of CL–DNA complexes to attach to cells via electrostatic interactions and inhibits escape from the endosomes. These properties need to be regained by adding lipids that perform specific functions. Thus, to counter the undesired effects of a PEG coating, PEG-lipids with targeting ligands and degradable PEG-lipids, which shed their PEG chains after endocytosis, may prove valuable.

To regain efficient cell attachment capabilities, the PEGylated complex must be decorated with ligands that bind to receptors on the surface of the target cells. Fortuitously for *in vivo* applications, screening of the charge-mediated attraction between CL–DNA complexes and sulfated cell surface proteoglycans by the PEG shell offers the opportunity to replace this unspecific attraction with specific, ligand mediated interactions. Thus, PEGylation indirectly enables targeting which allows for delivery to a specific cell or tissue type after systemic injection. Of the many potential targeting ligands, peptides are of particular interest. Recently, *in vivo* phage display methods have revealed a system of "vascular zip codes" which vary not only from tissue to tissue but also from healthy to diseased tissue [89–91].

Similar to cell attachment, endosomal escape of simple lamellar complexes is a process driven by electrostatics [21, 25, 83] (see Sect. 2) and therefore inhibited by PEGylation. A strategy to recover efficient endosomal escape is to prepare PEG-lipids in which the PEG chains are attached via bonds that are quickly cleaved as the endosomal pH is lowered in the course of maturation. This practically converts the shielded complex back into an unshielded complex. Several acid-labile moieties have been investigated for similar purposes, e.g., hydrazones [92], vinyl ethers [93] and orthoesters [87, 94].

7.2 Novel Liposome Structures: Block Liposomes

The landmark discovery of liposomes by A. D. Bangham in the early 1970s [95] sparked intense interest in them by the scientific community. Because of their similarities to biological membranes, they are used in model studies of cell–cell interactions as well as interactions between membranes of eucaryotic organelles. Furthermore, their ability to stably encapsulate liquid solutions has enabled their

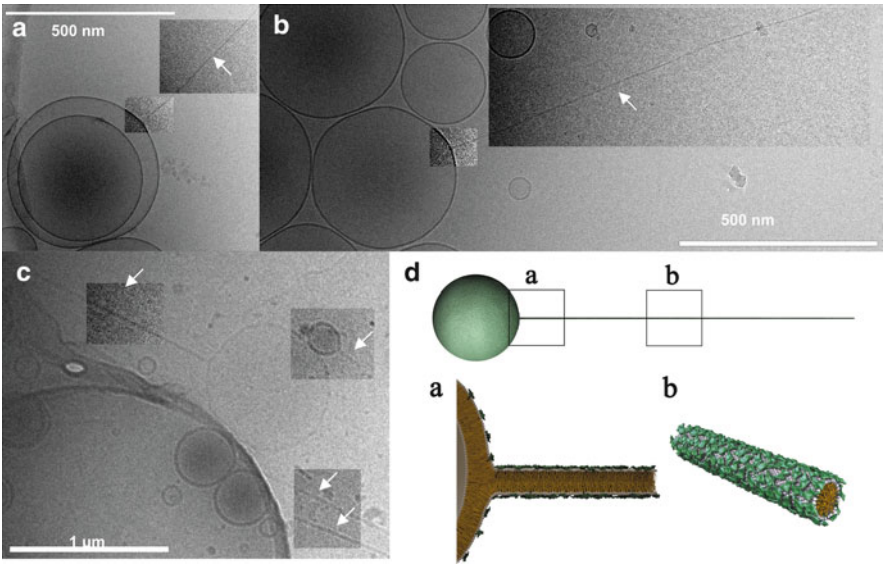

Fig. 17 (**a–d**) Cryo-TEM images of diblock (*sphere-rod*) liposomes comprised of liquid-phase lipid nanorods (*white arrows*) connected to spherical vesicles. The lipid nanorods are stiff cylindrical micelles with an aspect ratio ≈1000. Their diameter equals the thickness of a lipid bilayer (≈4 nm) and their length reaches up to several micrometers, with a persistence length on the order of millimeters. (**c**) An inset of B, demonstrating the thickness of the nanorod: *white arrow heads* point out a thickness of ≈4 nm (approximate bilayer thickness, identical for the spherical vesicle and the nanorods). (**d**) Schematic of a MVLBisG2/DOPC sphere-rod diblock liposome. Reprinted with permission from [58]. Copyright 2008 American Chemical Society

use as chemical carriers, and liposomes will continue to have a major impact in the medical field as drug and gene delivery systems.

Using optical microscopy and cryo-TEM, we have recently discovered block liposomes, which are liposomes consisting of connected, but distinctly shaped, nanoscale liposome blocks: spheres or pears connected to tubes or rods [58, 96, 97]. The key to this discovery is the curvature stabilizing ability of our new, highly charged DL MVLBisG2 (see Sect. 4) [24].

Figure 17a–d shows cryo-TEM images of diblock (sphere-rod) liposomes, which consist of micellar nanorods (arrows) attached to spherical vesicles. Their diameter equals the thickness of the bilayer (≈4 nm) and their lengths can reach up to several micrometers. A lower magnification image (Fig. 17c) shows a collection of these novel block liposomes with different spherical vesicle sizes. Figure 17d shows a schematic depiction of this remarkable liposome structure. The large charge and persistence lengths of the rods provide ideal conditions for templating of nanostructures (e.g., wires or needles).

Two asymmetric triblock (pear–tube–pear) liposomes (with vesicles of differing size capping the nanotube) are shown in Fig. 18a. The high-magnification inset shows that the tubular section has an inner lumen diameter of ≈10 nm (Fig. 18b). A diblock

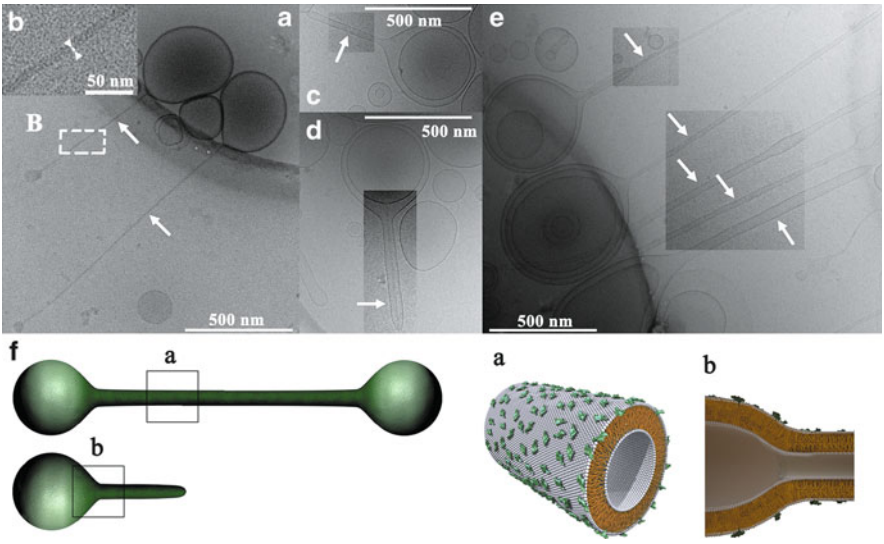

Fig. 18 (**a–f**) Cryo-TEM images of triblock (pear–tube–pear) and diblock (pear–tube) liposomes comprised of liquid-phase lipid nanotube segments capped by spherical vesicle. The tubule blocks (*arrows*) are the first examples of liquid-phase (chain-melted) tubes with diameter on the nanometer scale (between 10 and 50 nm). (**a**) Triblock liposomes (pear–tube–pear). (**b**) An *inset* of panel A, disclosing the hollow tubular structure (*white arrowheads* and *white bar* point out the bilayer thickness of 4 nm). (**c**) A diblock (pear-tube) liposome. (**d**) One block liposome encapsulated within another one. (**e**) A group of block liposomes. (**f**) Schematics of the MVLBisG2/DOPC tri- and diblock liposomes, manifesting the symmetry breaking between outer and inner monolayer. Reprinted with permission from [58]. Copyright 2008 American Chemical Society

(pear–tube) liposome with inner diameter of ≈50 nm is seen in Fig. 2c. Figure 18e shows a diblock liposome (lower arrow) and several block liposomes (second, third, and fourth arrows from bottom), which are either di- or triblocks. Schematic depictions of block liposomes containing tubular sections are shown in Fig. 18f. These lipid nanotubes and nanorods may find applications in biotechnology and drug/gene delivery. Importantly, their membranes are in the liquid (chain-melted) phase, which is mandatory for the functional incorporation of membrane proteins.

New theory will be required to describe the phase diagram of block liposomes. In particular, theories have to break new ground in explaining why nanorods and nanotubes stay attached to spherical vesicles. All current theories of lipid self-assemblies (based on Helfrich's theory of membranes [98]), in contrast, predict spherical, tubular, and micellar shaped liposomes but only as separate objects. In our experiments, not a single instance of an isolated rod- or tube-shaped liposome (i.e., not connected to a sphere- or pear-shaped vesicle) was found.

Acknowledgments KKE, AZ, AA, NFB, HME, and CRS were supported primarily by NIH GM-59288-11 and in part, by DOE-BES grant DE-FG02-06ER46314 (lipid microstructure) and NSF-DMR 0803103 (lipid phase behavior). CSM and CES were supported by NIH AI-12520 and AI-20611. Cryo-TEM experiments were conducted at the National Resource for Automated Molecular Microscopy which is supported by the National Institutes of Health though the National Center for Research Resources' P41 program (RR17573). The X-ray diffraction work was carried out at the Stanford Synchrotron Radiation Laboratory which is supported by the Department of Energy.

References

1. Safinya CR, Koltover I (1999) Self assembled structures of lipid–DNA nonviral gene delivery systems from synchrotron X-ray diffraction. In: Huang L, Hung M-C, Wagner E (eds) Non-viral vectors for gene therapy. Academic, San Diego
2. Ewert KK, Slack NL, Ahmad A, Evans HM, Lin A, Samuel CE, Safinya CR (2004) Cationic lipid–DNA complexes for gene therapy: understanding the relationship between complex structures and gene delivery pathways at the molecular level. Curr Med Chem 11:1241–1253
3. Ewert K, Evans H, Ahmad A, Slack L, Lin A, Martin-Herranz A, Safinya CR (2005) Lipoplex structures and their distinct cellular pathways. In: Huang L, Hung M-C, Wagner E (eds) Non-viral vectors for gene therapy, 2nd edn. Part I (Advances in genetics 53). Elsevier, San Diego
4. Ewert K, Ahmad A, Evans H, Safinya CR (2005) Cationic lipid–DNA complexes for non-viral gene therapy: relating supramolecular structures to cellular pathways. Expert Opin Biol Ther 5:33–53
5. Safinya CR, Ewert KK, Ahmad A, Evans HM, Raviv U, Needleman DJ, Lin AJ, Slack NL, George CX, Samuel CE (2006) Cationic liposome–DNA complexes: from liquid crystal science to gene delivery applications. Phil Transact Royal Soc A 364:2573–2596
6. Ewert KK, Samuel CE, Safinya CR (2008) Lipid–DNA interactions: structure-function studies of nanomaterials for gene delivery. In: Dias R, Lindman B (eds) Interaction of DNA with surfactant and polymers. Blackwell, Boston, MA
7. Ewert KK, Ahmad A, Bouxsein NF, Evans HM, Safinya CR (2008) Non-viral gene delivery with cationic liposome–DNA complexes. In: Le Doux J (ed) Gene therapy protocols, 3rd edn. Humana, Totowa, NJ
8. Edelstein ML, Abedi MR, Wixon J, Edelstein RM (2004) Gene therapy clinical trials worldwide 1989–2004 – an overview. J Gene Med 6:597–602

9. Edelstein ML, Abedi MR, Wixon JJ (2007) Gene therapy clinical trials worldwide to 2007: an update. Gene Med 9:833–842
10. The journal of gene medicine clinical trial site. http://www.wiley.co.uk/genetherapy/clinical Accessed 5 Nov 2009
11. Huang L, Hung M-C, Wagner E (eds) (1999) Nonviral vectors for gene therapy. Academic, San Diego, pp 91–117
12. Huang L, Hung M-C, Wagner E (2005) Non-viral vectors for gene therapy, 2nd edn, Advances in genetics. Elsevier, San Diego
13. Mahato RI, Kim SW (eds) (2002) Pharmaceutical perspectives of nucleic acid-based therapeutics. Taylor & Francis, London and New York
14. Chesnoy S, Huang L (2000) Structure and function of lipid–DNA complexes for gene delivery. Annu Rev Biophys Biomol Struct 29:27–47
15. Byk G, Dubertret C, Escriou V, Frederic M, Jaslin G, Rangara R, Pitard B, Crouzet J, Wils P, Schartz B, Scherman D (1998) Synthesis, activity, and structure-activity relationship studies of novel cationic lipids for DNA transfer. J Med Chem 41:224–235
16. Boussif O, Lezoualc'h F, Zanta MA, Mergny MD, Scherman D, Demeniex B, Behr J-P (1995) A versatile vector for gene and oligonucleotide transfer into cells in culture and *in vivo*: polyethylenimine. Proc Natl Acad Sci USA 92:7297–7301
17. Haensler J, Szoka FC (1993) Polyamidoamine cascade polymers mediate efficient transfection of cells in culture. Bioconjug Chem 4:372–379
18. Tang MX, Redemann CT, Szoka FC Jr (1996) In vitro gene delivery by degraded polyamidoamine dendrimers. Bioconjug Chem 7:703–714
19. Thomas CE, Ehrhardt A, Kay MA (2003) Progress and problems with the use of viral vectors for gene therapy. Nat Rev Genet 4:346–358
20. Tranchant I, Thompson B, Nicolazzi C, Mignet N, Scherman D (2004) Physicochemical optimisation of plasmid delivery with cationic lipids. J Gene Med 6:S24–S35
21. Ahmad A, Evans HM, Ewert K, George CX, Samuel CE, Safinya CR (2005) New multivalent lipids reveal bell-curve for transfection versus membrane charge density: nonviral lipid–DNA complexes for gene delivery. J Gene Med 7:739–748
22. Rädler JO, Koltover I, Salditt T, Safinya CR (1997) Structure of DNA-cationic liposome complexes: DNA intercalation in multilamellar membranes in distinct interhelical packing regimes. Science 275:810–814
23. Koltover I, Salditt T, Rädler JO, Safinya CR (1998) An inverted hexagonal phase of cationic liposome–DNA complexes related to DNA release and delivery. Science 281:78–81
24. Ewert KK, Evans HM, Zidovska A, Bouxsein NF, Ahmad A, Safinya CR (2006) A columnar phase of dendritic lipid-based cationic liposome–DNA complexes for gene delivery: hexagonally ordered cylindrical micelles embedded in a DNA honeycomb lattice. J Am Chem Soc 128:3998–4006
25. Lin AJ, Slack NL, Ahmad A, George CX, Samuel CE, Safinya CR (2003) Three-dimensional imaging of lipid gene-carriers: membrane charge density controls universal transfection behavior in lamellar cationic liposome–DNA complexes. Biophys J 84:3307–3316
26. Ewert K, Ahmad A, Evans HM, Schmidt H-W, Safinya CR (2002) Efficient synthesis and cell-transfection properties of a new multivalent cationic lipid for non-viral gene delivery. J Med Chem 45:5023–5029
27. Zidovska A, Evans HM, Ahmad A, Ewert KK, Safinya CR (2009) The role of cholesterol and structurally related molecules in enhancing transfection by cationic liposome–DNA complexes. J Phys Chem 113:5208–5216
28. Song YK, Liu F, Chu S, Liu D (1997) Characterization of cationic liposome-mediated gene transfer *in vivo* by intravenous administration. Hum Gene Ther 8:1585–1594
29. Liu Y, Mounkes LC, Liggitt HD, Brown CS, Solodin I, Heath TD, Debs RJ (1997) Factors influencing the efficiency of cationic liposome-mediated intravenous gene delivery. Nat Biotechnol 15:167–173

30. Audouy S, Molema G, de Leij L, Hoekstra D (2000) Serum as a modulator of lipoplex-mediated gene transfection: dependence of amphiphile, cell type and complex stability. J Gene Med 2:465–476
31. Crook K, Stevenson BJ, Dubouchet M, Poreous DJ (1998) Inclusion of cholesterol in DOTAP transfection complexes increases the delivery of DNA to cells *in vitro* in the presence of serum. Gene Ther 5:137–143
32. Li S, Tseng WC, Stolz DB, Wu SP, Watkins SC, Huang L (1999) Dynamic changes in the characteristics of cationic lipidic vectors after exposure to mouse serum: implications for intravenous lipofection. Gene Ther 6:585–594
33. Ilies MA, Johnson BH, Makori F, Miller A, Seitz WA, Thompson EB, Balaban AT (2005) Pyridinium cationic lipids in gene delivery: an *in vitro* and *in vivo* comparison of transfection efficiency versus a tetraalkylammonium congener. Arch Biochem Biophys 435:217–226
34. Kim CK, Haider KH, Choi SH, Choi EJ, Ahn WS, Kim YB (2002) Nonviral vector for efficient gene transfer to human ovarian adenocarcinoma cells. Gynecol Oncol 84:85–93
35. Kim CK, Choi EJ, Choi SH, Park JS, Haider KH, Ahn WS (2003) Enhanced p53 gene transfer to human ovarian cancer cells using the cationic nonviral vector, DDC. Gynecol Oncol 90:265–272
36. Epand RM, Hughes DW, Sayer BG, Borochov N, Bach D, Wachtel E (2003) Novel properties of cholesterol-dioleoylphosphatidylcholine mixtures. Biochim Biophys Acta Biomembr 1616:196–208
37. Huang JY, Buboltz JT, Feigenson GW (1999) Maximum solubility of cholesterol in phosphatidylcholine and phosphatidylethanolamine bilayers. Biochim Biophys Acta Biomembr 1417:89–100
38. Koltover I, Salditt T, Safinya CR (1999) Phase diagram, stability, and overcharging of lamellar cationic lipid–DNA self-assembled complexes. Biophys J 77:915–924
39. Rädler JO, Koltover I, Jamieson A, Salditt T, Safinya CR (1998) Structure and interfacial aspects of self-assembled cationic lipid–DNA gene carrier complexes. Langmuir 14:4272–4283
40. Slotte JP, Jungner M, Vilcheze C, Bittman R (1994) Effect of sterol side-chain structure on sterol-phosphatidylcholine interactions in monolayers and small unilamellar vesicles. Biochim Biophys Acta Biomembr 1190:435–443
41. Tristram-Nagle S, Petrache HI, Nagle JF (1998) Structure and interactions of fully hydrated dioleoylphosphatidylcholine bilayers. Biophys J 75:917–925
42. Israelachvili JN (1992) Intermolecular and surface forces, 2nd edn. Academic, London
43. Hed G, Safran SA (2004) Attractive instability of oppositely charged membranes induced by charge density fluctuations. Phys Rev Lett 93:138101(1–4)
44. Petrache HI, Harries D, Parsegian VA (2004) Alteration of lipid membrane rigidity by cholesterol and its metabolic precursors. Macromol Symp 219:39–50
45. Ewert KK, Evans HM, Zidovska A, Bouxsein NF, Ahmad A, Safinya CR (2006) Dendritic cationic lipids with highly charged headgroups for efficient gene delivery. Bioconjug Chem 17:877–888
46. Zidovska A, Evans HM, Ewert KK, Quispe J, Carragher B, Potter CS, Safinya CR (2009) Liquid crystalline phases of dendritic lipid–DNA self-assemblies: lamellar, hexagonal and DNA bundles. J Phys Chem B 113:3694–3703
47. Bosman AW, Janssen HM, Meijer EW (1999) About dendrimers: structure, physical properties, and applications. Chem Rev 99:1665–1688
48. Boger DL, Fink BE, Brunette SR, Tse WC, Hedrick MP (2001) A simple, high-resolution method for establishing DNA binding affinity and sequence selectivity. J Am Chem Soc 123:5878–5891
49. Takahashi T, Harada A, Emi N, Kono K (2005) Preparation of efficient gene carriers using a polyamidoamine dendron-bearing lipid: improvement of serum resistance. Bioconjug Chem 16:1160–1165
50. Veprek P, Jezek J (1999) Peptide and glycopeptide dendrimers. Part I. J Pept Sci 5:5–23
51. Veprek P, Jezek J (1999) Peptide and glycopeptide dendrimers. Part II. J Pept Sci 5:203–220

52. Choi JS, Lee EJ, Choi YH, Jeong YJ, Park JS (1999) Poly(ethylene glycol)-block-poly (L-lysine) dendrimer: novel linear polymer/dendrimer block copolymer forming a spherical water-soluble polyionic complex with DNA. Bioconjug Chem 10:62–65
53. Brabender-van den Berg EMMD, Meijer EW (1993) Poly(propylene imine) dendrimers–large-scale synthesis by heterogeneously catalyzed hydrogenations. Angew Chem Int Ed Engl 32:1308–1311
54. Wörner C, Mülhaupt R (1993) Polynitrile-functional and polyamine-functional poly(trimethylene imine) dendrimers. Angew Chem Int Ed Engl 32:1306–1308
55. Behr J-P (1989) Photohydrolysis of DNA by polyaminobenzenediazonium salt. Chem Commun 101:101–103
56. Schulze U, Schmidt HW, Safinya CR (1999) Synthesis of novel cationic poly(ethylene glycol) containing lipids. Bioconjug Chem 10:548–552
57. Farago O, Ewert KK, Ahmad A, Evans HM, Grønbech-Jensen N, Safinya CR (2008) Transitions between distinct compaction regimes in complexes of multivalent cationic lipids and DNA. Biophys J 95:836–846
58. Zidovska A, Ewert KK, Quispe J, Carragher B, Potter CS, Safinya CR (2009) Block liposomes from curvature-stabilizing lipids: connected nanotubes, –rods or –spheres. Langmuir 25:2979–2985
59. Vroege GJ, Lekkerkerker HNW (1992) Phase transitions in lyotropic colloidal and polymer liquid crystals. Rep Prog Phys 55:1241–1309
60. Vasilevskaya VV, Khokhlov AR, Matsuzawa Y, Yoshikawa K (1995) Collapse of single DNA molecule in poly(ethylene glycol) solutions. J Chem Phys 102:6595–6602
61. Fire A, Xu SQ, Montgomery MK, Kostas SA, Driver SE, Mello CC (1998) Potent and specific genetic interference by double-stranded RNA in *Caenorhabditis elegans*. Nature 391:806–811
62. Napoli CA, Lemieux C, Jorgensen R (1990) Introduction of a chimeric chalcone synthase gene into petunia results in reversible co-suppression of homologous genes in trans. Plant Cell 2:279–289
63. Jorgensen RA, Cluster PD, English J, Que Q, Napoli CA (1996) Chalcone synthase cosuppression phenotypes in petunia flowers: comparison of sense vs antisense constructs and single-copy vs complex T-DNA sequences. Plant Mol Biol 31:957–973
64. Cogoni C, Macino G (2000) Post-transcriptional gene silencing across kingdoms. Curr Opin Genet Dev 10:638–643
65. Hammond SM, Caudy AA, Hannon GJ (2001) Post-transcriptional gene silencing by double-stranded RNA. Nat Rev Genet 2:110–119
66. Elbashir SM, Harborth J, Lendeckel W, Yalcin A, Weber K, Tuschl T (2001) Duplexes of 21-nucleotide RNAs mediate RNA interference in cultured mammalian cells. Nature 411:494–498
67. Caplen NJ, Parrish S, Imani F, Fire A, Morgan RA (2001) Specific inhibition of gene expression by small double-stranded RNAs in invertebrate and vertebrate systems. Proc Natl Acad Sci USA 98:9742–9747
68. Samuel CE (2004) Knockdown by RNAi—proceed with caution. Nat Biotechnol 22:280–282
69. McAllister CS, Samuel CE (2009) The RNA-activated protein kinase enhances the induction of interferon-beta and apoptosis mediated by cytoplasmic RNA sensors. J Biol Chem 284:1644–1651
70. McManus MT, Sharp PA (2002) Gene silencing in mammals by small interfering RNAs. Nat Rev Genet 3:737–747
71. Elbashir SM, Harborth J, Weber K, Tuschl T (2002) Analysis of gene function in somatic mammalian cells using small interfering RNAs. Methods 26:199–213
72. Martinez LA, Naguibneva I, Lehrmann H, Vervisch A, Tchenio T, Lozano G, Harel-Bellan A (2002) Synthetic small inhibiting RNAs: efficient tools to inactivate oncogenic mutations and restore p53 pathways. Proc Natl Acad Sci USA 99:14849–14854
73. Hannon GJ, Rossi JJ (2004) Unlocking the potential of the human genome with RNA interference. Nature 431:371–378
74. Karagiannis TC, El-Osta A (2005) RNA interference and potential therapeutic applications of short interfering RNAs. Cancer Gene Ther 12:787–795
75. Sioud M (2004) Therapeutic siRNAs. Trends Pharmacol Sci 25:22–28

76. Caplen NJ (2003) RNAi as a gene therapy approach. Expert Opin Biol Ther 3:575–586
77. Spagnou S, Miller AD, Keller M (2004) Lipidic carriers of siRNA: differences in the formulation, cellular uptake, and delivery with plasmid DNA. Biochemistry 43:13348–13356
78. Yin JY, Ma ZY, Selliah N, Shivers DK, Cron RQ, Finkel TH (2006) Effective gene suppression using small interfering RNA in hard-to-transfect human T cells. J Immunol Meth 312:1–11
79. Bouxsein NF, McAllister CS, Ewert KK, Samuel CE, Safinya CR (2007) Structure and gene silencing activities of monovalent and pentavalent cationic lipid vectors complexed with siRNA. Biochemistry 46:4785–4792
80. Faneca H, Simoes S, Pedroso de Lima MC (2004) Association of albumin or protamine to lipoplexes: enhancement of transfection and resistance to serum. J Gene Med 6:681–692
81. Yang J-P, Huang L (1997) Overcoming the inhibitory effect of serum on lipofection by increasing the charge ratio of cationic liposome to DNA. Gene Ther 4:950–960
82. Plank C, Mechtler K, Szoka FC, Wagner E (1996) Activation of the complement system by synthetic DNA complexes: a potential barrier for intravenous gene delivery. Hum Gene Ther 7:1437–1446
83. Martin-Herranz A, Ahmad A, Evans HM, Ewert K, Schulze U, Safinya CR (2004) Surface functionalized cationic lipid–DNA complexes for gene delivery: PEGylated lamellar complexes exhibit distinct DNA–DNA interaction regimes. Biophys J 86:1160–1168
84. Hong K, Zheng W, Baker A, Papahadjopoulos D (1997) Stabilization of cationic liposome-plasmid DNA complexes by polyamines and poly(ethylene glycol)-phospholipid conjugates for efficient *in vivo* gene delivery. FEBS Lett 400:233–237
85. Kostarelos K, Miller AD (2005) Synthetic, self-assembly ABCD nanoparticles; a structural paradigm for viable synthetic non-viral vectors. Chem Soc Rev 34:970–994
86. Maeda H, Greish K, Fang J (2006) The EPR effect and polymeric drugs: a paradigm shift for cancer chemotherapy in the 21st century. Adv Polym Sci 193:103–121
87. Choi JS, MacKay A, Szoka FC Jr (2003) Low-pH-sensitive PEG-stabilized plasmid-lipid nanoparticles: preparation and characterization. Bioconjug Chem 14:420–429
88. Wheeler JJ, Palmer L, Ossanlou M, MacLachlan I, Graham RW, Zhang YP, Hope MJ, Scherrer P, Cullis PR (1999) Stabilized plasmid-lipid particles: construction and characterization. Gene Ther 6:271–281
89. Ruoslahti E, Duza T, Zhang L (2005) Vascular homing peptides with cell-penetrating properties. Curr Pharm Des 11:3655–3660
90. Ruoslahti E (2004) Vascular zip codes in angiogenesis and metastasis. Biochem Soc Trans 32:397–402
91. Laakkonen P, Åkerman ME, Biliran H, Yang M, Ferrer F, Karpanen T, Hoffman RM, Ruoslahti E (2004) Antitumor activity of a homing peptide that targets tumor lymphatics and tumor cells. Proc Natl Acad USA 101:9381–9386
92. Walker GF, Fella C, Pelisek J, Fahrmeir J, Boeckle S, Ogris M, Wagner E (2005) Toward synthetic viruses: endosomal pH-triggered deshielding of targeted polyplexes greatly enhances gene transfer *in vitro* and *in vivo*. Mol Ther 11:418–425
93. Boomer JA, Thompson DH (1999) Synthesis of acid-labile diplasmenyl lipids for drug and gene delivery applications. Chem Phys Lipids 99:145–153
94. Zhu J, Munn RJ, Nantz MH (2000) Self-cleaving ortho ester lipids: a new class of pH-vulnerable amphiphiles. J Am Chem Soc 122:2645–2646
95. Bangham AD, Hill MW, Miller NGA (1973) Preparation and use of liposomes as models of biological membranes. Methods Membr Biol 1:1–68
96. Zidovska A, Ewert KK, Quispe J, Carragher B, Potter CS, Safinya CR (2009) The effect of salt and pH on block liposomes studied by cryogenic transmission electron microscopy. Biochim Biophys Acta Biomembr 1788:1869–1876
97. Zidovska A, Ewert KK, Quispe J, Carragher B, Potter CS, Safinya CR (2009) Block liposomes: vesicles of charged lipids with distinctly shaped nanoscale sphere-, pear-, tube-, or rod-segments. Meth Enzymol 465:111–128
98. Helfrich W (1973) Elastic properties of lipid bilayers – theory and possible experiments. Z Naturforsch C 28:693–703

Top Curr Chem (2010) 296: 227–249
DOI: 10.1007/128_2010_69

Published online: 11 June 2010

Chemically Programmed Polymers for Targeted DNA and siRNA Transfection

Eveline Edith Salcher and Ernst Wagner

Abstract Plasmid DNA and siRNA have a large potential for use as therapeutic nucleic acids in medicine. The way to the target cell and its proper compartment is full of obstacles. Polymeric carriers help to overcome the encountered barriers. Cationic polymers can interact with the nucleic acid in a nondamaging way but still require optimization with regard to transfer efficiency and biocompatibility. Aiming at virus-like features, as viruses are the most efficient natural gene carriers, the design of bioresponsive polymers shows promising results regarding DNA and siRNA delivery. By specific chemical modifications dynamic structures are created, programmed to respond towards changing demands on the delivery pathway by cleavage of labile bonds or conformational changes, thus enhancing biocompatible gene delivery.

Keywords Bioresponsive · Cationic polymers · Chemical programming · DNA · siRNA

Contents

E.E. Salcher and E. Wagner (✉)
Department of Pharmacy, Pharmaceutical Biotechnology, Center for System-Based Drug Research, Ludwig-Maximilians University, Butenandtstraße 5-13, 81377 Munich, Germany
Center for Nanoscience (CeNS), Ludwig-Maximilians University, Butenandtstraße 5-13, 81377 Munich, Germany
e-mail: ernst.wagner@cup.uni-muenchen.de

1 Introduction

Gene therapy is a great hope in the fight against a variety of genetic-based disorders such as various cancer forms and congenital diseases. The concept includes systemic or local delivery of therapeutic nucleic acids such as DNA which can induce gene expression or short interfering RNA (siRNA) which mediates gene silencing. The therapeutic efficiency of the nucleic acids mentioned has already been experienced [1–7] but still encounters several drawbacks.

In order to be able to induce a therapeutic effect, these nucleic acids have to reach the target tissue and be internalized into target cells. Systemically delivered, both pure DNA and siRNA are unable to overcome the bloodstream passage due to enzymatic degradation. Passing the cell membrane is another obstacle on the way to the target cell compartment, neither DNA nor siRNA being able to cross this barrier freely by themselves: their relatively large size prevents passive diffusion and the electrostatic repulsion between the negatively charged nucleic acid phosphate backbone and the anionic cell membrane also inhibits internalization. Therefore, the nucleic acid needs an efficient carrier with the ability to condense it to an appropriate small particle size, to protect it during blood circulation without inducing unspecific interactions with blood components and to mediate cellular uptake without damaging the cell membrane. After internalization, the carrier has not completed its task; it has to help the nucleic acid to escape the acidic endosome, as it would be degraded during endosomal maturation into lysosomes. Finally, the carrier has to release the undamaged DNA or siRNA in or near the desired target cell compartment.

The target cell compartments are different though for DNA and siRNA. Delivered DNA must penetrate into the nucleus where it induces gene expression; thus it can provide a missing gene or lead to the expression of other therapeutic genes. In contrast, the smaller sized siRNA (21–23 nucleotides) acts in the cytosol. Once there, it is integrated into the multiprotein complex RNA induced silencing complex (RISC) [8], mediating cleavage of complementary target messenger RNA which encodes for a specific protein. Therefore, RNA interference (RNAi) leads to highly sequence-specific and efficient posttranscriptional gene silencing of target genes. This feature and the possibility of synthetic production and modification of siRNA is the reason why RNAi has been rapidly brought into focus as a therapeutic agent since its discovery by Fire et al. 11 years ago.

Obviously there are several challenges a gene carrier encounters during the transfection pathway and it is also a challenge for scientists to find the most efficient

and biocompatible 'smart' molecule that exhibits the ability to overcome changing environmental requirements.

Nature has already created the ideal gene carrier, namely viruses. Viruses are, due to their nanosized flexible structure, able to respond to differing conditions between extra- and intracellular compartments like enzymes, pH, and redox potential. They can dynamically change their conformation on environmental demand, securely leading the genetic material to its biological site of action. Viruses have already been used for therapeutic nucleic acid delivery but clinical application is limited by safety issues such as, e.g., host immune responses, capability of mutagenic integration, and high production costs [9]. Therefore, nonviral gene delivery systems have received much attention during the last few decades as they are able to circumvent some of the disadvantages associated with viral vectors, e.g., by displaying higher biocompatibility and feasibility for large-scale production. Unfortunately, they still cannot achieve comparable transfection efficiency.

However, a promising approach towards overcoming these obstacles is the design of nonviral gene carriers using bioresponsive dynamic viral features as a model. Nonadaptable synthetic cationic polymer-based systems, e.g., such as branched and linear poly(ethylenimine) (PEI), poly(lysine) (PLL), dendritic poly(amido amine) (PAMAM), and poly(propylenimine) (PPI) can interact with the nucleic acid in a nondamaging reversible manner, either by electrostatic interaction or by reversible covalent coupling, forming so called "polyplexes" [10–13]. The correlation between transfection efficiency and cytotoxicity has been shown to be unsatisfactory though, i.e., effective transfection agents also displayed undesired cytotoxic effects. The advantage of cationic polymers is that these can be chemically designed and produced which leaves room for further specific modifications directed to creating nonimmunogenic, bioresponsive and dynamically acting molecules [14–16].

This review focuses on chemically programmed polymers for DNA and siRNA delivery. More precisely, it will give an overview on chemical modifications making polymeric gene carriers more dynamic and enabling them to respond to microenvironmental changes in a controlled manner. Modifications such as introduction of targeting ligands enable specific target cell recognition. Regarding endosomal polyplex escape, incorporation of lytic residues responding to pH-decrease in the endosome is possible. Chemical integration of hydrolyzable, acid-sensitive or reducible bonds allow polymer degradation, thus preventing cytotoxicity and enabling cargo release or facilitating reversible conjugation to shielding moieties like poly(ethylene glycol) (PEG) for further transfection activity. Furthermore, an overview on polymers responding to artificial physical triggers such as light or heat will also be given.

2 Cell Targeting

The strategy for nanosized ($\leq\sim$200 nm) polyplexes to reach the tumor site after systemic *in vivo* delivery called "passive targeting" takes advantage of the enhanced permeability and retention (EPR) effect [17]. This phenomenon implies

polymer accumulation in tumor tissue due to its leaky vasculature and deficient lymphatic clearance [18]. Subsequent cellular uptake of passively targeted polymers takes place via endocytosis due to charge-mediated interactions of cationic polyplex with negatively charged proteoglycans on the cell surface [19]. To make accumulation possible though, polyplexes have to avoid fast elimination from the bloodstream: cationic polymers undergo ionic and hydrophobic interactions with serum proteins and are exposed to fast clearance after phagocytosis by cells of the reticulo-endothelial system (RES). It has been shown that systemically introduced hydrophilic particles in general can overcome these obstacles [20, 21]. Therefore, hydrophilic molecules such as the polymer PEG have been chemically attached to cationic polymers in order to elongate blood circulation time and thus enable the polyplexes and related nanoparticles to accumulate in tumor tissue.

In addition to passive targeting, "active targeting" can be exploited by targeting ligands which specifically bind to receptors expressed on cell surfaces (Fig. 1). For example, tumor cells show an overexpression of a series of specific receptors. Introduction of such specific ligands into polymers leads to selective recognition of target cells and polyplex internalization by receptor-mediated endocytosis. This strategy was introduced for DNA polyplex delivery over 20 years ago by George and Catherine Wu, who conjugated the hepatocyte target moiety asialoorosomucoid (ASOR) to PLL and complexed it with DNA [22].

There are numerous possibilities for selecting cell-receptor specific moieties; the bandwidth ranges from natural ligands, antireceptor antibodies, antibody fragments, and peptides to completely synthetic ligands; detailed specifications concerning ligand-receptor pairs can be found in [23–26]. Some of these are very specific, e.g., asialoglycoprotein directed to liver hepatocytes only.

In contrast to very specific ligands, the iron transporter transferrin (Tf) can be used as a target moiety for the Tf receptor in various tumor cells, as the iron

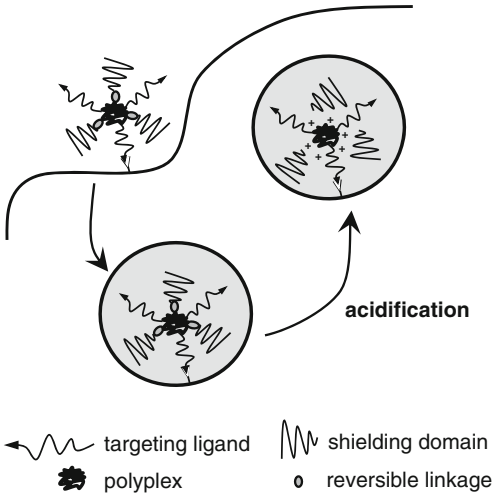

Fig. 1 Targeting and reversible shielding. Incorporation of targeting ligands enhances cellular uptake due to receptor-mediated endocytosis. Reversibly attached shielding moieties protect the polyplex during blood passage; the pH-sensitive bonds are cleaved in the endosome upon acidification, setting free the positively charged polymer for further activity

required is increased greatly due to their fast growth. Tietze et al. conjugated Tf-PEG to the oligoethylenimine-based polymer OEI-HD as a carrier for systemic siRNA delivery with the Ras-related nuclear protein Ran as a knock-out target. In a mouse neuroblastoma (Neuro2A) tumor Ran luciferase reporter gene expression was over 80% silenced, apoptosis was induced and tumor growth was reduced [27].

Another targeting ligand, the epidermal growth factor (EGF), is addressed to the EGF receptor, which is overexpressed in a variety of cancers. EGF conjugation to polymers not only takes advantage of receptor-mediated internalization but also considerably accelerates intracellular uptake of polyplexes [28]. PEI–PEG conjugates for siRNA and DNA delivery were also coupled to folic acid as a targeting moiety, a vitamin essential for nucleotide synthesis, showing considerably enhanced transfection in folate receptor overexpressing cells [29, 30].

RGD, the arginine–glycine–asparagine sequence of several extracellular matrix proteins like fibronectin, binds selectively to integrin receptors expressed on activated vascular endothelial cells in tumors and has often been used in tumor targeted gene delivery [31]. Oba et al. modified a micelle forming acetal-PEG-PLL with a cyclic RGD peptide c(RGDfK) for selective $\alpha_v\beta_3$ and $\alpha_v\beta_5$ integrin recognition via a thiazolidine ring formation. The synthesized block copolymer showed a distinct increase in pDNA transfection efficiency compared to nontargeted polyplex micelles in HeLa cells [32].

CNGRC, a cyclic pentapeptide containing the NGR (asparagines–glycine–arginine) sequence selectively recognizes aminopeptidase N/CD13 in tumor vasculature. Cristiano and colleagues modified CNGRC with phenyl(di)boronic acid for self-assembly with salicylhydroxamic acid modified PEI and also coupled a nuclear localization signal (NLS) motif and/or a DNA nuclear targeting signal (DNTS). This system displayed a considerable increase in gene expression compared to the polyplex lacking the CNGRC sequence [33].

A further peptide targeting moiety is the 7-mer peptide MQLPLAT with high affinity to fibroblast growth factor 2 (FGF2). MQLPLAT was coupled by Rao et al. to PEI/pDNA polyplexes via a PEG spacer either before (premodified) or after (postmodified) PEI/pDNA complexation. Interestingly, only the postmodified polyplexes showed enhanced transfection, presumably because in the premodified version MQLPLAT is buried within the polyplex and not accessible enough to the FGF receptor [34].

3 Bioresponsive Polyplex Shielding and Endosomal Escape

3.1 Reversible Polyplex Shielding

Systemic delivery of cationic polyplexes is a challenging strategy in gene therapy. Polyplexes carrying a positive net charge due to condensation of nucleic acid by polymers such as PEI, oligo(ethylene imine; OEI), or PLL encounter several

drawbacks on their way to the target tissue, such as interaction with blood and extracellular components and therefore rapid clearance from the blood stream [35], unspecific interactions with nontarget cells, formation of aggregates at physiological salt concentrations [36] and resultant cytotoxic effects. Chemical incorporation of hydrophilic moieties like the widely used PEG for electrostatic shielding offers a way to overcome these problems. PEGylation shows not only an elongated blood circulation time but also better water solubility and reduced cytotoxicity [37]. Transfection efficiency, however, is also reduced [38, 39], due to limited interaction of the shielded positive polymer charges with the negatively charged cell membrane. Besides that, PEG shielding hampers intracellular release of DNA and siRNA out of endosomal vesicles. This theory is confirmed by decreased transfection efficiency with stably PEGylated polyplexes compared to non-PEGylated polyplexes [40–42]. Including targeting ligands in PEGylated polyplexes is one way to enhance transfection efficiency as cellular uptake is improved due to receptor-mediated endocytosis [38, 43–48]. An additional possibility is to increase the cytosolic release of DNA or siRNA by chemically programmed PEG-polymer linkages to be pH-sensitive and thus cleavable in the endosome (Fig. 1). In this way the cationic charges of the polyplex are exposed at the polyplex surface for endosomal membrane destabilization, and hence release from the endosome, further enhancing transfection activity. Acid labile polymer-PEG linkages such as acetals [49, 50], acetone-bis-(*N*-maleimidoethyl)ketal linkers [51], ortho esters [52], and hydrazones [53, 54] were introduced and transfection tests have confirmed the increased nucleic acid activity compared to stable PEG conjugations.

Fella et al., for example, synthesized acid-cleavable polyethylene glycol aldehyde-carboxypyridylhydrazone, *N*-hydroxysuccinimide esters (PEG–HZN–NHS) by reacting succinimidyl hydraziniumnicotinate with mPEG-butyraldehyde (20 kDa) and applied these to bioreversible surface shielding of DNA polyplexes. The degradation profile was tested by zeta potential measurements and FCS (fluorescence correlation spectroscopy), showing that the pH-sensitive linkage remained stable over 4 h incubation at pH 7.4 and 37°C and was completely cleaved at pH 5 after 2 h. DNA transfection experiments with EGF containing polyplexes targeted to EGF-receptor overexpressing hepatoma HUH7 cells showed a 16-fold enhanced transfection efficiency compared to the stably linked counterparts [55].

Oishi et al. coupled lactosylated PEG to siRNA via an acid labile β-thiopropionate bond, followed by complexation with poly(L-lysine) into polyion complex micelles. The complex was internalized by receptor-mediated endocytosis into hepatoma cells and the gene silencing effect of RNAi was considerably enhanced compared to the free conjugate, demonstrating the effect of pH-sensitive PEGylation [56].

Reducible disulfide bonds for PEG conjugation were used by Takae and colleagues in order to improve transfection efficiency of PEG-based polyplex micelles. The gene vector was designed as a block catiomer, the polycation segment containing poly(aspartamide) with a flanking *N*-(2-aminoethyl)-2-aminoethyl group, p[Asp(DET)], as a buffering residue enhancing endosomal escape. PEG was attached to

this cationic segment via a disulfide bond, PEG-SS-p[Asp(DET)], sensitive to reductive endosomal cleavage as confirmed by confocal laser scanning microscopy (CLSM) imaging. However, the PEG-chains were only partly cleaved in the endosome, so that transfection efficiency was improved only compared to the stable PEGylated polycation and not compared to the non-PEGylated structure [57].

3.2 Activation of Endosomolytic Agents

Once internalized, the essential step for the polyplex is to escape rapidly the endosomal vesicle in order to release the nucleic acid in the cytosol and prevent its lysosomal degradation. As the endosomal and lysosomal pH presents values between 4.5 and 6.5 and therefore differs from the neutral pH of 7.4 in other biological compartments [58], some polycations containing protonable residues like PEI facilitate this step by the proton sponge effect [59, 60]. As not all cationic polymers display this attribute, another effective method for enhanced endosomal polyplex release is incorporation of specific endosomal membrane disrupting or pore-forming domains, such as lytic lipid moieties or endosomolytic peptides.

Melittin, for example, a peptide from bee venom consisting of 26 amino acids, is able to enhance transfection efficiency of polycations [61–65] by damaging interactions with the endosomal membrane [66]. The disadvantage, though, is that its high lytic activity is not only limited to acidic pH but that interaction with cell membranes can also occur at neutral pH, thus causing cytotoxic side effects before internalization. This knowledge reveals the opportunity of specific modifications of the lytic agent, designing dynamic endosomolytic agents responsive to the changing biological microenvironment. Rozema et al. covalently acylated the amine groups on melittin with 2-propionic-3-methylmaleic anhydride, anticipating lytic activity at neutral physiological pH. The created pH-sensitive amide bond is then cleaved upon protonation of the carboxylic group in the acidic endosomal environment, achieving selective activation of melittin and with it lower cytotoxicity [67]. Based on previous work, more recently Meyer et al. modified the amines of melittin with dimethylmaleic anhydride (DMMAn) and covalently coupled it to PEI and PLL, respectively, for siRNA delivery. The endosomolytic agent was inactive at neutral physiological pH and regained its activity upon acidification by cleavage of the protecting groups. siRNA polyplexes of unmodified PEI or PLL showed no knockdown effect, whereas coupling to acid-responsive melittin greatly enhanced luciferase gene silencing and reduced toxicity [68]. Similar findings were made with analogous PLL conjugates containing covalently coupled siRNA [69] (Fig. 2a).

Another strategy for shifting the lytic activity of melittin to acidic pH without using masking groups was shown by Boeckle et al. Positively charged domains which are important for the lytic activity were replaced by glutamic acid and histidine residues, these enabling the modified melittin to regain its activity upon protonation at acidic pH. This chemical modification greatly improved the

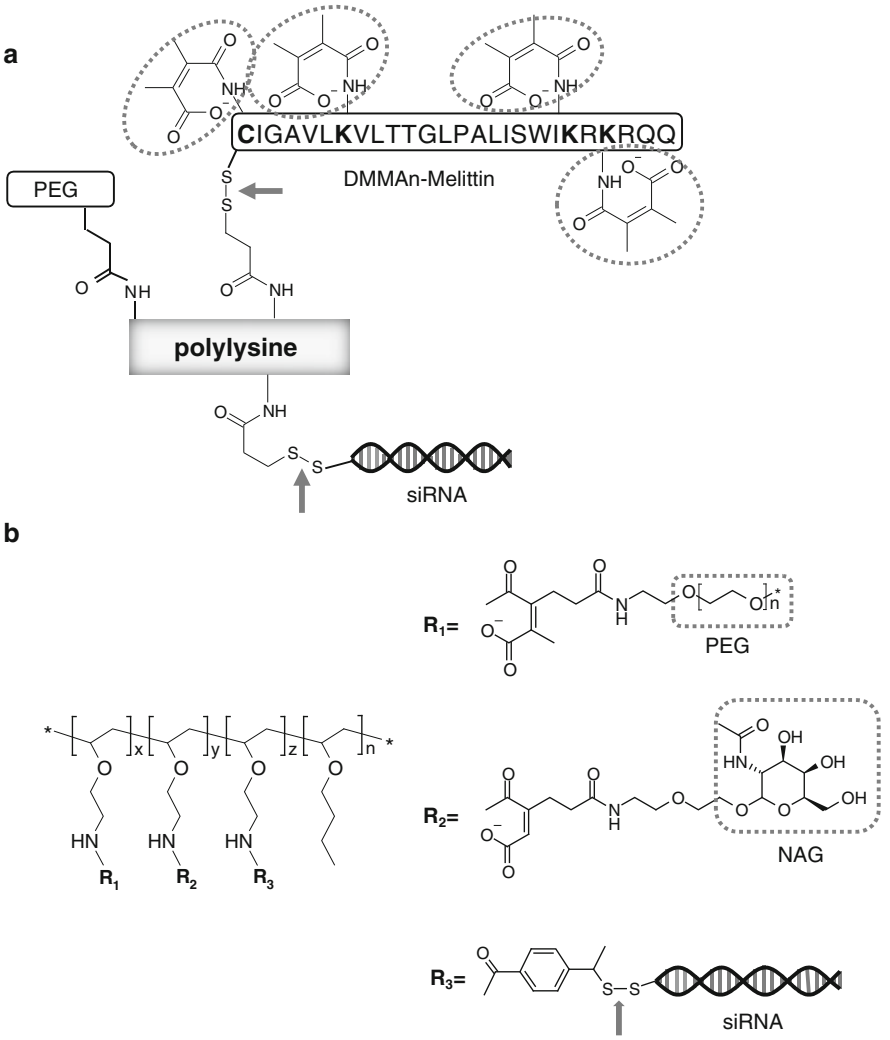

Fig. 2 Masked endosomolytic agents for pH-triggered endosomal escape. The polymers designed by Meyer et al. [69] (**a**) and Rozema et al. [71] (**b**) contain endosomolytic compounds whose lytic potential is activated by endosomal cleavage of masking groups coupled by acid-sensitive linkages. Furthermore, disulfide bonds are embedded which release the nucleic acid after endosomal escape by cleavage in the reducing cytosolic environment

lytic activity of C-terminally linked PEI conjugates at the endosomal pH of 5 and showed higher transfection efficiency than conjugates with unmodified melittin [70].

Besides melittin, Rozema and colleagues took advantage of the lytic activity of poly(vinyl ether) composed of butyl and amino vinyl ethers (PBAVE). They designed "Dynamic PolyConjugates" by developing an elegant strategy for

reversible chemical modification of the endosomolytic agent. PBAVE amine groups responsible for its lytic activity were masked by coupling to maleic anhydride modified with PEG and hepatocyte targeting moiety *N*-acetylgalactosamine (NAG). Cleavage of the acid labile maleamate bonds was triggered by pH-decrease in the endosome, unmasking PBAVE and thus setting free its lytic potential. These dynamic polyconjugates displayed effective and well tolerated *in vitro* and *in vivo* siRNA delivery [71] (Fig. 2b).

Saito and colleagues used the reducing endosomal environment as a trigger for the sulfhydryl-activated pore-forming protein Listeriolysin O (LLO) from *Listeria monocytogenes*. The unique cysteine 484 of LLO was coupled to the polycationic peptide protamine (PN) as a pDNA complexing residue via a reversible disulfide bond. In this conformation the molecule displayed no pore-forming activity, regaining it though upon reduction in the endosome. As shown in several cell culture experiments by means of luciferase marker gene expression, this nontoxic construct enhanced transfection efficiency [72].

4 Programmed Biodegradation and Nucleic Acid Release

4.1 Polymer Biodegradation Due to Hydrolyzable and Acid-Sensitive Linkages

The ability of introducing genes efficiently into cells with preferably no toxicity is a challenge in programmed carrier design. Several polymer characteristics like the at first glance conflicting necessity to condensate initially the nucleic acid in a stable complex and afterwards release it intracellularly, polyplex particle size and charge, polymer molecular weight, and low toxic side effects have to be considered and united at their optimum in one molecule. PEI with a high molecular weight (HMW) of 22–25 kDa, for example, displays some of these properties and has therefore been commonly used for efficient DNA delivery *in vitro* and *in vivo* [59, 73] but unfortunately it displays serious toxic effects [74, 75]. Being non-biodegradable also limits its repeated systemic application as a gene carrier. In contrast, the shorter counterpart OEI with a molecular weight of 800 Da shows insignificant toxicity but poor transfection results due to the restricted ability of forming stable polyplexes. A strategy towards uniting appropriate molecular weight, adequate nucleic acid condensation and cytosolic release for efficient transfection with low toxicity is the design of biodegradable vectors. These are composed of low molecular weight (LMW) monomers linked via degradable bonds resulting in an HMW polymer. Triggered by environmental conditions, these polymers are thus chemically programmed to degrade into their LMW nontoxic decomposition products.

Various efficient polymers bearing hydrolyzable ester bonds, which degrade in a time dependent manner, have been designed. The linkages connect monomers either integrated in the polymer backbone or as cross-linking agents. Such

bioresponsive polymers include poly(4-hydroxy-L-proline) (PHP), poly(α-(4-aminobutyl)-L-glycolic acid), and poly(L-lactide-*co*-L-lysine) [76–78].

Furthermore, a widely used class of degradable polymers based on acrylate esters are polyamino esters (PAE). These are both efficient gene carriers with an advantageous degradation profile and low cytotoxicity and also easy to synthesize [79, 80] by conjugate addition of either primary or bis(secondary amine)s to different diacrylate esters [81–87].

This synthetic strategy was used, for example, for the modification of LMW PEI [64, 82, 88–91]. Kloeckner et al. cross-linked OEI800 with hexanediol diacrylate (HD) at 20°C and at 60°C, respectively, resulting in the ester-based, fast-degrading, low temperature LT-OEI-HD with a MW of 8.7 kDa and slower degrading high-temperature HT-OEI-HD with a MW of 26.6 kDa containing predominantly amide bonds. Compared to each other in respect of DNA transfection efficiency and toxicity, LT-OEI-HD, although needing higher C/P ratios for gene delivery, maintains higher cell viability than HT-OEI-HD [82].

The aforementioned OEI-HD polymers, although efficient and biocompatible, have a spot of concern which is the heterogeneity in molecular weight as a result of synthesis procedure. An approach towards better defined hydrolyzable molecules is based on a hyperbranched polymer with pseudodendritic structure as shown by Russ et al. Out of a small library of molecules, which were built with OEI800 as a core, three different dioldiacrylates as hydrolyzable linkers and four different oligoamines as surface modifications, one polymer, namely HD O consisting of OEI core, hexane-1.6-dioldiacrylate linker, and OEI as a surface modification, showed the best DNA transfection results with low cytotoxicity *in vitro* and *in vivo* compared to "golden standards" linear and branched PEI [92] (Fig. 3a).

PAE are not only easy and fast to synthesize; they also offer structural diversity, so that this polymer class is viable for high-throughput combinatorial chemistry. Dramatically shortened synthesis and screening cycles make gaining information on structure/activity relationships possible. Based on a 2350-compound PAE library developed by Langer and co-workers [93], Green et al. screened the most promising vectors for DNA transfection concerning efficiency and cytotoxicity in human primary endothelial cells, identifying one top gene carrier [81]. They also showed that PAE in general as gene vector class are very efficacious but also that similar structures can differ in functionality, depending on the site and length of the carbon chain. Thomas et al., Lynn et al., and Kloeckner et al. also generated smaller libraries of biodegradable ester-linked polymers based on amine-acrylate reaction [83, 94, 95]. Efficacious and hardly toxic hyperbranched [85] and network-type PAEs [87, 96, 97] for DNA delivery also entered the field of gene delivery.

Polycations programmed on degradation triggered by pH-decrease in the acidic endosomal environment were designed for both DNA and siRNA delivery including acid-sensitive linkages like acetals, ketals [98], and imines [99]. Knorr et al. cross-linked OEI800 units with an acetone ketal-containing linker (MK) and a both acid-sensitive and hydrolyzable *p*-methoxy-benzaldehyde acetal diacrylate ester (BAA), respectively, resulting in larger acid-hydrolyzable polymers. Both polymers showed very fast degradation at pH 5 and a much slower degradation at

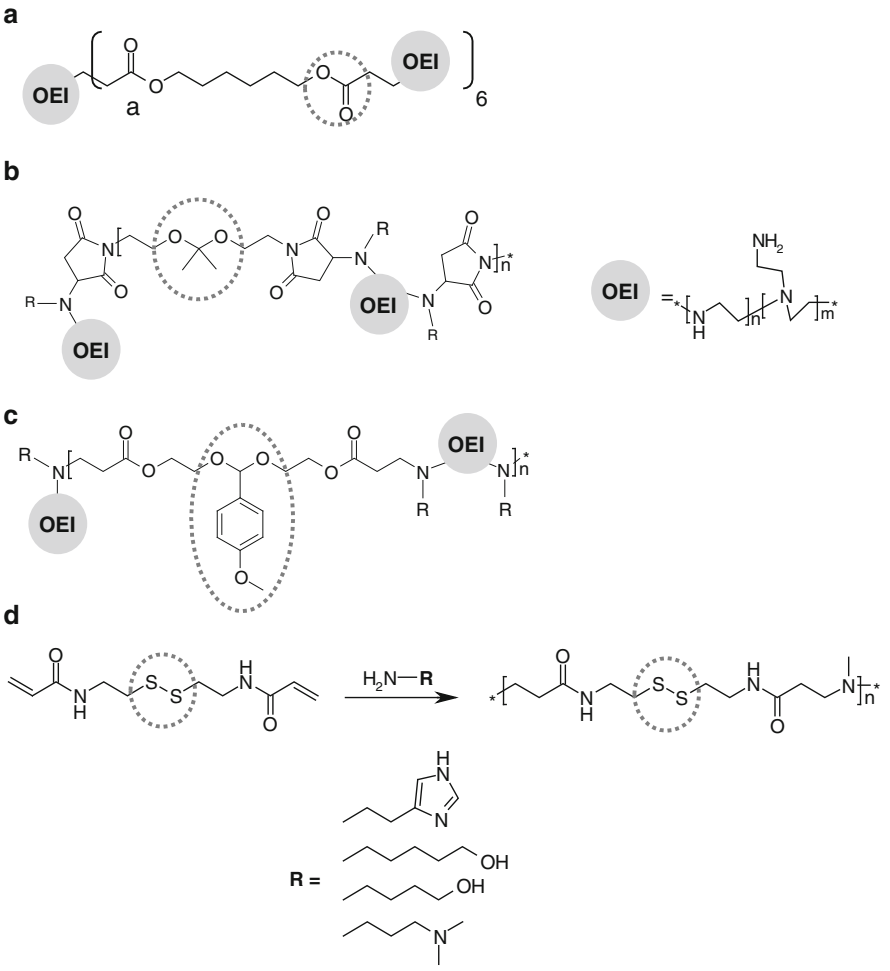

Fig. 3 Hydrolyzable, acid-sensitive and reducible bonds. Efficient and biocompatible high molecular weight polymers are created by reversible linkage of small molecular weight compounds. Thus, programmed biodegradation due to, for example, hydrolyzable ester bonds [92] (**a**), acid-sensitive ketal (**b**) or acetal linkages (**c**) [98] is possible. The reducing cytosolic environment can also be taken advantage of in order to create biodegradable polymers by introduction of disulfide bonds as shown in (**d**) [105, 106]

physiological pH 7.4. These carriers showed distinct advantages regarding toxicity in comparison to their acid-stable counterparts and mediated DNA transfer much more efficiently than OEI800 alone [98] (Fig. 3b, c).

Shim and Kwon coupled acid-responsive amino ketal branches to secondary amines of 25 kDa linear PEI, thus showing distinct eGFP silencing at N/P (polymer nitrogen to siRNA phosphate) ratios of 100 and low toxicity compared to

unmodified PEI. They also showed enhanced cytoplasmic release of siRNA from the polyplex compared once again to unmodified PEI [100].

The degradable polymer OEI-HD, based on OEI monomers cross-linked with beta-propionamide, was successfully used for siRNA transfection of murine neuroblastoma cells *in vitro* and *in vivo* [27].

4.2 Polymer Biodegradation Due to Reducible Disulfide Bonds

Another approach to efficient gene delivery with biodegradable cationic polymers takes advantage of the redox difference between oxidizing extracellular and reducing intracellular environment. Chemically incorporated disulfide linkages into polymeric compounds therefore remain relatively stable during blood circulation and can then be cleaved in the cytosol by the reducing agent glutathione (GSH), the most abundantly occurring thiol-source in mammalian cells [72].

Similar to hydrolysable ester-linked polymers, cationic carriers with integrated disulfide bonds can break down into their smaller molecular weight compounds and therefore release the nucleic acid in the cytosol with lower cytotoxicity than larger nondegradable carriers [101–103]. Lin and colleagues synthesized linear polyamido amines (PAA) by coupling 1-(2-aminoethyl)piperazine to disulfide containing cystaminebisacrylamide in a Michael addition reaction. These polymers improved DNA transfection with at the same time low toxicity compared to PEI 25 kDa [104]. The group continued their work on this topic, variously modifying these reducible structures by introduction of histidine and hydroxyl functionalities in the side chain [105], by design of random and block copolymers with histidine and tertiary amine-terminated side chains [106] (Fig. 3d) and by attaching oligoamine side chains to the reducible PAA backbone [107] for further improvement of transfection efficiency and cell viability.

Furthermore, cationic groups that help enclose the nucleic acid electrostatically can be attached to a polymer backbone by disulfide linkages which are then degraded in the cytosol [108]. Condensation of the nucleic acid and stabilization of the polyplex can also be accomplished by introducing reduction-sensitive cross-linking agents [109] or thiol-modified polycations where the free thiol groups crosslink by oxidation into disulfide bonds after electrostatic interaction of the polycation with the DNA or siRNA, respectively, thus stabilizing the polyplex [110–112]. The cross-linking can also be performed before complexation with the nucleic acid. Peng et al. introduced thiol groups to PEI of different MWs varying the thiolation degree and induced oxidation by dimethylsulfoxide (DMSO) before complexation with DNA. The transfection efficiency was the best for the PEI with the lowest MW and moderate thiolation degree, thus being dependent on disulfide density and polymer molecular weight [111].

Various carriers containing reducible disulfide bonds have also already been investigated for siRNA delivery [113]. This class of polymers seem to be a promising approach as programmed cytosolic carrier decomposition and siRNA

release is crucial for loading of the nucleic acid onto the RISC complex for further silencing activity [102, 114, 115]. Wan and colleagues delivered VEGF-targeted siRNA into cells by means of the reducible polymer poly(TETA/CBA) consisting of triethylenetetramine coupled to disulfide containing cystamine bis-acrylamide. In vitro transfection studies showed higher gene silencing effects compared to linear PEI/siRNA complex [115].

As the polyplexes formed with siRNA by electrostatic interaction are not expected to remain always stable in serum and extracellular matrix [116] and as synthetic siRNA production allows specific modifications, the reversible covalent coupling to a carrier opens the possibility to circumvent this obstacle. Meyer et al. conjugated thiol-modified siRNA via a reducible disulfide bond to a dynamic carrier consisting of the cation PLL, the hydrophilic PEG, and the endosomolytic peptide melittin masked by pH-responsive DMMAn groups. This polyplex has proved to be both highly biocompatible, as it did not elicit cytotoxicity or hemolysis at physiological neutral pH, and an efficient gene carrier comparable to electrostatically packed siRNA [117]. In order to prevent loss of cargo and to achieve programmed nucleic acid release into the cytosol at the same time, Rozema et al. also attached the siRNA by disulfide linkage to their Dynamic Poly Conjugates. [71].

5 Sequence-Defined Polymers Allow Synthetically Controlled Functionality

Chemical programming of polymers has proven to be a crucial tool in mimicking virus-like features. Thus, alterations in polymer structure and conformation can be correlated to transfection efficiency and cytotoxicity. It has to be considered that the better polymer structure is defined, the more detailed study of structure–activity relationships is possible. First approaches towards better defined polymer structure with narrow molecular weight distribution have been made by PAE and pseudo-dendrimer synthesis already discussed in Sect. 4.1.

Dendrimers form a class of molecules with defined architecture. They are characterized by a relatively low polydispersity due to the synthetic process, whereas stepwise synthesis can be performed by two different methods, divergent or convergent. The divergent strategy starts with a core to which branches are attached whereas the convergent starts with dendrimeric fragments, subsequently attaching to the core [118–120]. Cationic dendrimers like commercially available PAMAM and PPI have already been investigated as gene carriers [121, 122]. These studies, however, show that there is still improvement needed concerning transfection efficiency and cytotoxicity. As the synthetic process makes it possible to change the surface character of the dendrimer by introducing specific residues for enhanced gene transfection, several modified PAMAM [123–126] and PPI [127–131] dendrimers were investigated for DNA and siRNA transfection.

One step further, namely to monomeric sequence-defined polymeric vehicles, leads to the synthetic strategy based on standard peptide solid phase chemistry.

Hartmann et al. designed linear peptidomimetic polymers with PAA as a structural pattern. Dicarboxylates and diamines were stepwise coupled in an alternating manner; by exact introduction of functionalities in the linear PAA chain, such as polypeptide and poly(ethylene oxide; PEO), a single component block copolymer was generated, thus proving the versatility of the method [132]. PEO modified PAAs were studied in a subsequent work concerning dsDNA complexation and condensation qualities, resulting in clearly defined non-cytotoxic polyplexes [133]. Solid phase synthesis was also used for the design of a variety of efficient *in vitro* and *in vivo* siRNA branched carriers containing lysine and histidine residues [134, 135]. Wang et al. created a small library of reversibly polymerizable surfactants using combinatorial solid phase synthetic strategy. These vectors contain a protonable amino head group, two cysteine residues, and two lipophilic tails, exhibiting pH-sensitive membrane disruption potential. By means of the facilitated endosomal escape, the surfactants mediated efficient *in vitro* luciferase silencing, comparable with the effectivity of cationic lipids [136].

6 Polymers Responsive to Artificial Stimuli

6.1 Thermosensitive Polymers

Efficient gene delivery can also be mediated by chemically programmed polymers responding to artificial physical stimuli like heat. Depending on the stimulus, they have the ability to alter their conformation in so far as transfection enhancing effects are initiated.

Thermoresponsive structures gain or lose the ability to condense the nucleic acid by change of conformation depending on an artificially triggered temperature shift. Macroscopically perceptible polymer precipitation occurs at a specific phase transition temperature, also called the lower critical solution temperature (LCST) [137, 138]. More precisely, above the LCST the polymer collapses into a hydrophobic, tightly coiled conformation due to weakened polymer/water hydrogen bonds, displaying the ability to condense the nucleic acid. Kept below this temperature, responsive polymers show a relaxed, hydrophilic, extended chain conformation, thus allowing the polyplex to dissociate [139]. A widely used temperature-sensitive polymer is poly-*N*-isopropylacrylamide (pNIPAM) [140–145]. Its LCST of 32–33°C is close to physiological temperature but can be shifted by incorporation of hydrophobic or hydrophilic groups [138, 146]. It is also known that pNIPAM is able to destabilize liposomal membranes above its LCST [147] so that this feature can be taken advantage of regarding endosomal escape of polyplexes. Zintchenko et al. synthesized a hyperthermia-activated polymeric gene carrier responding at clinically relevant temperatures. The block copolymeric carrier consists of one PEI block conjugated to a block of statistical copolymer pNIPAM and different

hydrophilic acrylamide or vinylpyrrolidone monomers synthesized by radical copolymerization. Depending on the amount of the hydrophilic moieties, the LCST can be adjusted between 37 and 42°C. These molecules were shown to aggregate under hyperthermic conditions, i.e., heating from 37 to 42°C, in this way enhancing the DNA transfection efficiency [144]. Griffiths et al. quantified the temperature dependent conformational changes and the interaction between pNIPAM-*graft*-PEI copolymers by using small-angle neutron scattering (SANS) and pulse-gradient spin-echo NMR (PGSE-NMR). Various pNIPAM chain lengths were grafted and it was demonstrated that longer chain pNIPAM-*g*-PEI collapse more clearly and undergo attractive interpolymer interactions, unlike short chain copolymers [140].

6.2 *Photochemically Enhanced Transfection*

Light can also be an artificial stimulus for enhanced DNA and siRNA transfection. The group around Høgset described 10 years ago a new method that enhances gene or drug delivery by inducing endosomal release based on photosensitizing molecules which are localized in the endosomal membrane: "photochemical internalization" (PCI) [148]. They demonstrated the disruption of endosomal membranes by reactive oxygen species generated by light activated coincubated photosensitizers (PS) such as porphyrin and phthalocyanine derivatives. This smart strategy was used for controlled and targeted release of endosomally enclosed complexes into the cytosol, thus considerably enhancing nucleic acid delivery with polyplexes [149, 150] and PEG-shielded, receptor-targeted systems [64, 151, 152]. In some applications, however, the PSs applied as separate molecules showed significant phototoxicity due to possible interactions of the PSs with the plasma membrane and cytoplasmic organelles after endosomal escape, inducing cell death. In order to overcome this drawback and to provide for the essential endosomal colocalization of PS and gene carrier, Nishiyama et al. combined pDNA-loaded PEG–PLL block copolymers with dendrimer phthalocyanine (DP)-loaded micelles, forming polyion complex micelles through electrostatic interaction. In vitro transfection studies showed a highly enhanced transgene expression and low cytotoxicity. This achievement is supposed to be based on the endosomal colocalization of the two compounds, so that the photochemical induced membrane disruption ability of the DPc-micelle leads to endosomal escape of the pDNA carrier [153]. The same group also designed a pDNA/cationic peptide complex enveloped in DP-micelles for successful and site-directed *in vivo* light-induced transfection after subconjunctival injection in rat eye, also maintaining cell viability [154].

By means of PCI enhanced siRNA delivery was shown for the first time by Oliveira et al. They demonstrated a tenfold increased knockdown efficiency of the EGF receptor due to improved endosomal release by the activated PS meso-tetraphenylporphine, which was, however, not integrated in the polyplex [155].

7 Conclusion and Prospects

DNA and siRNA, respectively, cannot, on their own, overcome the biological obstacles associated with systemic delivery. Therefore, efficient carrier molecules have to protect the nucleic acid and support its delivery into cells. Among others, cationic polymers have been investigated and developed over decades as gene delivery vectors, showing promising progression towards high transfection efficiency and low cytotoxicity. The unbeaten particles in matters of transfection efficiency are viral vectors; development of polymer structure aims at virus-like features such as the potential of adaptation to changing microenvironmental conditions, but with better biocompatibility [14, 156]. Therefore, it has become evident that intelligent design of dynamically acting molecules is a crucial tool in nonviral gene delivery. Well-considered chemical polymer programming makes the carriers flexible and responsive to environmental challenges encountered on their way to, when systemically delivered, and in the target tissue, or to artificial physical stimuli, e.g., light or heat, leading to enhanced transfection ability and maintained cell viability. Chemical programming involves conjugation to targeting ligands, reversible attachment of shielding domains and pH-sensitive membrane-active agents or modification with biodegradable bonds. Also, as siRNA therapeutics is rapidly gaining importance, it has to be considered that vehicles optimized for DNA delivery are not always adequate for siRNA as well.

Structure–activity relationship studies are thus essential for adequate polymer design. Random polymers are hardly viable for such correlations, as, due to their polydispersity, the biological effect cannot be tracked back to one certain compound. Development of sequence-defined, monodisperse molecules, exhibiting a large potential for structural diversity, offers the possibility for controlled introduction of functionalities and, by means of similarly improving biological analytics, precise *in vitro* and *in vivo* impact investigation. Moreover, when thinking of bringing such compounds to human therapeutic application, defined structures facilitate large scale GMP production.

Therefore, improved chemical synthesis strategies for the design of tailored polymeric gene vectors and more information on transfection mechanisms will be needed for the optimization of DNA and siRNA vehicles.

References

1. Hannon GJ, Rossi JJ (2004) Unlocking the potential of the human genome with RNA interference. Nature 431:371–378
2. Sioud M (2004) Therapeutic siRNAs. Trends Pharmacol Sci 25:22–28
3. Behlke MA (2006) Progress towards *in vivo* use of siRNAs. Mol Ther 13:644–670
4. Aigner A (2006) Gene silencing through RNA interference (RNAi) *in vivo*: strategies based on the direct application of siRNAs. J Biotechnol 124:12–25

5. Meyer M, Wagner E (2006) Recent developments in the application of plasmid DNA-based vectors and small interfering RNA therapeutics for cancer. Hum Gene Ther 17:1062–1076
6. Blow N (2007) Small RNAs: delivering the future. Nature 450:1117–1120
7. de Fougerolles AR (2008) Delivery vehicles for small interfering RNA *in vivo*. Hum Gene Ther 19:125–132
8. Sen GL, Blau HM (2005) Argonaute 2/RISC resides in sites of mammalian mRNA decay known as cytoplasmic bodies. Nat Cell Biol 7:633–636
9. Boeckle S, Wagner E (2006) Optimizing targeted gene delivery: chemical modification of viral vectors and synthesis of artificial virus vector systems. AAPS J 8:E731–E742
10. Pack DW, Hoffman AS, Pun S et al (2005) Design and development of polymers for gene delivery. Nat Rev Drug Discov 4:581–593
11. Park TG, Jeong JH, Kim SW (2006) Current status of polymeric gene delivery systems. Adv Drug Deliv Rev 58:467–486
12. Wagner E, Kloeckner J (2006) Gene delivery using polymer therapeutics. Adv Polym Sci 192:135–173
13. Tiera MJ, Winnik FO, Fernandes JC (2006) Synthetic and natural polycations for gene therapy: state of the art and new perspectives. Curr Gene Ther 6:59–71
14. Wagner E (2004) Strategies to improve DNA polyplexes for *in vivo* gene transfer: will "artificial viruses" be the answer? Pharm Res 21:8–14
15. Wagner E (2007) Programmed drug delivery: nanosystems for tumor targeting. Expert Opin Biol Ther 7:587–593
16. Wolff JA, Rozema DB (2008) Breaking the bonds: non-viral vectors become chemically dynamic. Mol Ther 16:8–15
17. Noguchi Y, Wu J, Duncan R et al (1998) Early phase tumor accumulation of macromolecules: a great difference in clearance rate between tumor and normal tissues. Jpn J Cancer Res 89:307–314
18. Maeda H (2001) The enhanced permeability and retention (EPR) effect in tumor vasculature: the key role of tumor-selective macromolecular drug targeting. Adv Enzyme Regul 41:189–207
19. Mislick KA, Baldeschwieler JD (1996) Evidence for the role of proteoglycans in cation-mediated gene transfer. Proc Natl Acad Sci USA 93:12349–12354
20. Brigger I, Dubernet C, Couvreur P (2002) Nanoparticles in cancer therapy and diagnosis. Adv Drug Deliv Rev 54:631–651
21. Allen TM, Cullis PR (2004) Drug delivery systems: entering the mainstream. Science 303:1818–1822
22. Wu GY, Wu CH (1987) Receptor-mediated *in vitro* gene transformation by a soluble DNA carrier system. J Biol Chem 262:4429–4432
23. Wagner E, Ogris M, Zauner W (1998) Polylysine-based transfection systems utilizing receptor-mediated delivery. Adv Drug Deliv Rev 30:97–113
24. Schaffer DV, Lauffenburger DA (2000) Targeted synthetic gene delivery vectors. Curr Opin Mol Ther 2:155–161
25. Wickham TJ (2003) Ligand-directed targeting of genes to the site of disease. Nat Med 9: 135–139
26. Wagner E, Culmsee C, Boeckle S (2005) Targeting of polyplexes: toward synthetic virus vector systems. Adv Genet 53:333–354
27. Tietze N, Pelisek J, Philipp A et al (2008) Induction of apoptosis in murine neuroblastoma by systemic delivery of transferrin-shielded siRNA polyplexes for downregulation of Ran. Oligonucleotides 18:161–174
28. de Bruin K, Ruthardt N, von Gersdorff K et al (2007) Cellular dynamics of EGF receptor-targeted synthetic viruses. Mol Ther 15:1297–1305
29. Kim SH, Mok H, Jeong JH et al (2006) Comparative evaluation of target-specific GFP gene silencing efficiencies for antisense ODN, synthetic siRNA, and siRNA plasmid complexed with PEI–PEG–FOL conjugate. Bioconjug Chem 17:241–244

30. Liang B, He ML, Xiao ZP et al (2008) Synthesis and characterization of folate-PEG-grafted-hyperbranched-PEI for tumor-targeted gene delivery. Biochem Biophys Res Commun 367:874–880
31. Ikeda Y, Taira K (2006) Ligand-targeted delivery of therapeutic siRNA. Pharm Res 23:1631–1640
32. Oba M, Fukushima S, Kanayama N et al (2007) Cyclic RGD peptide-conjugated polyplex micelles as a targetable gene delivery system directed to cells possessing alphavbeta3 and alphavbeta5 integrins. Bioconjug Chem 18:1415–1423
33. Moffatt S, Wiehle S, Cristiano RJ (2006) A multifunctional PEI-based cationic polyplex for enhanced systemic p53-mediated gene therapy. Gene Ther 13:1512–1523
34. Rao GA, Tsai R, Roura D et al (2008) Evaluation of the transfection property of a peptide ligand for the fibroblast growth factor receptor as part of PEGylated polyethylenimine polyplex. J Drug Target 16:79–89
35. Dash PR, Read ML, Barrett LB et al (1999) Factors affecting blood clearance and *in vivo* distribution of polyelectrolyte complexes for gene delivery. Gene Ther 6:643–650
36. Ogris M, Steinlein P, Kursa M et al (1998) The size of DNA/transferrin-PEI complexes is an important factor for gene expression in cultured cells. Gene Ther 5:1425–1433
37. Lee M, Kim SW (2005) Polyethylene glycol-conjugated copolymers for plasmid DNA delivery. Pharm Res 22:1–10
38. Erbacher P, Bettinger T, Belguise-Valladier P et al (1999) Transfection and physical properties of various saccharide, poly(ethylene glycol), and antibody-derivatized polyethylenimines (PEI). J Gene Med 1:210–222
39. Oupicky D, Ogris M, Howard KA et al (2002) Importance of lateral and steric stabilization of polyelectrolyte gene delivery vectors for extended systemic circulation. Mol Ther 5:463–472
40. Kursa M, Walker GF, Roessler V et al (2003) Novel shielded transferrin–polyethylene glycol–polyethylenimine/DNA complexes for systemic tumor-targeted gene transfer. Bioconjug Chem 14:222–231
41. Brissault B, Kichler A, Leborgne C et al (2006) Synthesis, characterization, and gene transfer application of poly(ethylene glycol-b-ethylenimine) with high molar mass polyamine block. Biomacromolecules 7:2863–2870
42. Meyer M, Wagner E (2006) pH-responsive shielding of non-viral gene vectors. Expert Opin Drug Deliv 3:563–571
43. Ogris M, Brunner S, Schuller S et al (1999) PEGylated DNA/transferrin-PEI complexes: reduced interaction with blood components, extended circulation in blood and potential for systemic gene delivery. Gene Ther 6:595–605
44. Ogris M, Walker G, Blessing T et al (2003) Tumor-targeted gene therapy: strategies for the preparation of ligand–polyethylene glycol–polyethylenimine/DNA complexes. J Control Release 91:173–181
45. Wolschek MF, Thallinger C, Kursa M et al (2002) Specific systemic nonviral gene delivery to human hepatocellular carcinoma xenografts in SCID mice. Hepatology 36:1106–1114
46. Kim WJ, Yockman JW, Lee M et al (2005) Soluble Flt-1 gene delivery using PEI-g-PEG-RGD conjugate for anti-angiogenesis. J Control Release 106:224–234
47. Moffatt S, Papasakelariou C, Wiehle S et al (2006) Successful *in vivo* tumor targeting of prostate-specific membrane antigen with a highly efficient J591/PEI/DNA molecular conjugate. Gene Ther 13:761–772
48. Moffatt S, Wiehle S, Cristiano RJ (2005) Tumor-specific gene delivery mediated by a novel peptide–polyethylenimine–DNA polyplex targeting aminopeptidase N/CD13. Hum Gene Ther 16:57–67
49. Knorr V, Allmendinger L, Walker GF et al (2007) An acetal-based PEGylation reagent for pH-sensitive shielding of DNA polyplexes. Bioconjug Chem 18:1218–1225
50. Murthy N, Campbell J, Fausto N et al (2003) Design and synthesis of pH-responsive polymeric carriers that target uptake and enhance the intracellular delivery of oligonucleotides. J Control Release 89:365–374

51. Knorr V, Ogris M, Wagner E (2008) An acid sensitive ketal-based polyethylene glycol–oligoethylenimine copolymer mediates improved transfection efficiency at reduced toxicity. Pharm Res 25:2937–2945
52. Lin S, Du F, Wang Y et al (2008) An acid-labile block copolymer of PDMAEMA and PEG as potential carrier for intelligent gene delivery systems. Biomacromolecules 9:109–115
53. Walker GF, Fella C, Pelisek J et al (2005) Toward synthetic viruses: endosomal pH-triggered deshielding of targeted polyplexes greatly enhances gene transfer *in vitro* and *in vivo*. Mol Ther 11:418–425
54. Xiong MP, Bae Y, Fukushima S et al (2007) pH-responsive multi-PEGylated dual cationic nanoparticles enable charge modulations for safe gene delivery. ChemMedChem 2:1321–1327
55. Fella C, Walker GF, Ogris M et al (2008) Amine-reactive pyridylhydrazone-based PEG reagents for pH-reversible PEI polyplex shielding. Eur J Pharm Sci 34:309–320
56. Oishi M, Nagasaki Y, Itaka K et al (2005) Lactosylated poly(ethylene glycol)–siRNA conjugate through acid-labile beta-thiopropionate linkage to construct pH-sensitive polyion complex micelles achieving enhanced gene silencing in hepatoma cells. J Am Chem Soc 127:1624–1625
57. Takae S, Miyata K, Oba M et al (2008) PEG-detachable polyplex micelles based on disulfide-linked block catiomers as bioresponsive nonviral gene vectors. J Am Chem Soc 130:6001–6009
58. Mellman I (1996) Endocytosis and molecular sorting. Annu Rev Cell Dev Biol 12:575–625
59. Boussif O, Lezoualc'h F, Zanta MA et al (1995) A versatile vector for gene and oligonucleotide transfer into cells in culture and *in vivo*: polyethylenimine. Proc Natl Acad Sci USA 92:7297–7301
60. Akinc A, Thomas M, Klibanov AM et al (2005) Exploring polyethylenimine-mediated DNA transfection and the proton sponge hypothesis. J Gene Med 7:657–663
61. Boeckle S, Wagner E, Ogris M (2005) C- versus N-terminally linked melittin–polyethylenimine conjugates: the site of linkage strongly influences activity of DNA polyplexes. J Gene Med 7:1335–1347
62. Ogris M, Carlisle RC, Bettinger T et al (2001) Melittin enables efficient vesicular escape and enhanced nuclear access of nonviral gene delivery vectors. J Biol Chem 276:47550–47555
63. Shir A, Ogris M, Wagner E et al (2006) EGF receptor-targeted synthetic double-stranded RNA eliminates glioblastoma, breast cancer, and adenocarcinoma tumors in mice. PLoS Med 3:e6
64. Kloeckner J, Boeckle S, Persson D et al (2006) DNA polyplexes based on degradable oligoethylenimine-derivatives: combination with EGF receptor targeting and endosomal release functions. J Control Release 116:115–122
65. Bettinger T, Carlisle RC, Read ML et al (2001) Peptide-mediated RNA delivery: a novel approach for enhanced transfection of primary and post-mitotic cells. Nucleic Acids Res 29:3882–3891
66. Dempsey CE (1990) The actions of melittin on membranes. Biochim Biophys Acta 1031:143–161
67. Rozema DB, Ekena K, Lewis DL et al (2003) Endosomolysis by masking of a membrane-active agent (EMMA) for cytoplasmic release of macromolecules. Bioconjug Chem 14:51–57
68. Meyer M, Philipp A, Oskuee R et al (2008) Breathing life into polycations: functionalization with pH-responsive endosomolytic peptides and polyethylene glycol enables siRNA delivery. J Am Chem Soc 130:3272–3273
69. Meyer M, Dohmen C, Philipp A et al. (2009) Synthesis and biological evaluation of a bioresponsive and endosomolytic siRNA-polymer conjugate. Mol Pharm 6:752–762
70. Boeckle S, Fahrmeir J, Roedl W et al (2006) Melittin analogs with high lytic activity at endosomal pH enhance transfection with purified targeted PEI polyplexes. J Control Release 112:240–248

71. Rozema DB, Lewis DL, Wakefield DH et al (2007) Dynamic polyconjugates for targeted *in vivo* delivery of siRNA to hepatocytes. Proc Natl Acad Sci USA 104:12982–12987
72. Saito G, Swanson JA, Lee KD (2003) Drug delivery strategy utilizing conjugation via reversible disulfide linkages: role and site of cellular reducing activities. Adv Drug Deliv Rev 55:199–215
73. Zou SM, Erbacher P, Remy JS et al (2000) Systemic linear polyethylenimine (L-PEI)-mediated gene delivery in the mouse. J Gene Med 2:128–134
74. Moghimi SM, Symonds P, Murray JC et al (2005) A two-stage poly(ethylenimine)-mediated cytotoxicity: implications for gene transfer/therapy. Mol Ther 11:990–995
75. Chollet P, Favrot MC, Hurbin A et al (2002) Side-effects of a systemic injection of linear polyethylenimine–DNA complexes. J Gene Med 4:84–91
76. Li Z, Huang L (2004) Sustained delivery and expression of plasmid DNA based on biodegradable polyester, poly(D,L-lactide-co-4-hydroxy-l-proline). J Control Release 98: 437–446
77. Lim Y, Choi YH, Park J (1999) A self-destroying polycationic polymer: biodegradable poly (4-hydroxy-L-proline ester). J Am Chem Soc 121:5633–5639
78. Lim YB, Han SO, Kong HU et al (2000) Biodegradable polyester, poly[alpha-(4-aminobutyl)-L-glycolic acid], as a non-toxic gene carrier. Pharm Res 17:811–816
79. Wong SY, Pelet JM, Putnam D (2007) Polymer systems for gene delivery – past, present, future. Prog Polym Sci 32:799–837
80. Green JJ, Zugates GT, Langer R et al (2009) Poly(beta-amino esters): procedures for synthesis and gene delivery. Methods Mol Biol 480:53–63
81. Green JJ, Shi J, Chiu E et al (2006) Biodegradable polymeric vectors for gene delivery to human endothelial cells. Bioconjug Chem 17:1162–1169
82. Kloeckner J, Bruzzano S, Ogris M et al (2006) Gene carriers based on hexanediol diacrylate linked oligoethylenimine: effect of chemical structure of polymer on biological properties. Bioconjug Chem 17:1339–1345
83. Thomas M, Lu JJ, Zhang C et al (2007) Identification of novel superior polycationic vectors for gene delivery by high-throughput synthesis and screening of a combinatorial library. Pharm Res 24:1564–1571
84. Lynn DM, Langer R (2000) Degradable poly(-amino esters): synthesis, characterization, and self-assembly with plasmid DNA. J Am Chem Soc 122:10761–10768
85. Zhong Z, Song Y, Engbersen JF et al (2005) A versatile family of degradable non-viral gene carriers based on hyperbranched poly(ester amine)s. J Control Release 109:317–329
86. Arote R, Kim TH, Kim YK et al (2007) A biodegradable poly(ester amine) based on polycaprolactone and polyethylenimine as a gene carrier. Biomaterials 28:735–744
87. Lim YB, Kim SM, Suh H et al (2002) Biodegradable, endosome disruptive, and cationic network-type polymer as a highly efficient and nontoxic gene delivery carrier. Bioconjug Chem 13:952–957
88. Forrest ML, Koerber JT, Pack DW (2003) A degradable polyethylenimine derivative with low toxicity for highly efficient gene delivery. Bioconjug Chem 14:934–940
89. Ahn CH, Chae SY, Bae YH et al (2002) Biodegradable poly(ethylenimine) for plasmid DNA delivery 1. J Control Release 80:273–282
90. Shuai X, Merdan T, Unger F et al (2005) Supramolecular gene delivery vectors showing enhanced transgene expression and good biocompatibility. Bioconjug Chem 16:322–329
91. Shuai X, Merdan T, Unger F et al (2003) Novel biodegradable ternary copolymers hy-PEI-g-PCL-b-PEG: synthesis, characterization, and potential as efficient nonviral gene delivery vectors. Macromolecules 36:5751–5759
92. Russ V, Elfberg H, Thoma C et al (2008) Novel degradable oligoethylenimine acrylate ester-based pseudodendrimers for *in vitro* and *in vivo* gene transfer. Gene Ther 15:18–29
93. Anderson DG, Lynn DM, Langer R (2003) Semi-automated synthesis and screening of a large library of degradable cationic polymers for gene delivery. Angew Chem Int Ed Engl 42:3153–3158

94. Kloeckner J, Wagner E, Ogris M (2006) Degradable gene carriers based on oligomerized polyamines. Eur J Pharm Sci 29:414–425
95. Lynn DM, Anderson DG, Putnam D et al (2001) Accelerated discovery of synthetic transfection vectors: parallel synthesis and screening of a degradable polymer library. J Am Chem Soc 123:8155–8156
96. Kim TI, Seo HJ, Choi JS et al (2005) Synthesis of biodegradable cross-linked poly(beta-amino ester) for gene delivery and its modification, inducing enhanced transfection efficiency and stepwise degradation. Bioconjug Chem 16:1140–1148
97. Kim HJ, Kwon MS, Choi JS et al (2007) Synthesis and characterization of poly (amino ester) for slow biodegradable gene delivery vector. Bioorg Med Chem 15:1708–1715
98. Knorr V, Russ V, Allmendinger L et al (2008) Acetal linked oligoethylenimines for use as pH-sensitive gene carriers. Bioconjug Chem 19:1625–1634
99. Kim YH, Park JH, Lee M et al (2005) Polyethylenimine with acid-labile linkages as a biodegradable gene carrier. J Control Release 103:209–219
100. Shim MS, Kwon YJ (2009) Acid-responsive linear polyethylenimine for efficient, specific, and biocompatible siRNA delivery. Bioconjug Chem 20:488–499
101. Read ML, Bremner KH, Oupicky D et al (2003) Vectors based on reducible polycations facilitate intracellular release of nucleic acids. J Gene Med 5:232–245
102. Read ML, Singh S, Ahmed Z et al (2005) A versatile reducible polycation-based system for efficient delivery of a broad range of nucleic acids. Nucleic Acids Res 33:e86
103. Christensen LV, Chang CW, Kim WJ et al (2006) Reducible poly(amido ethylenimine) s designed for triggered intracellular gene delivery. Bioconjug Chem 17:1233–1240
104. Lin C, Zhong Z, Lok MC et al (2006) Linear poly(amido amine)s with secondary and tertiary amino groups and variable amounts of disulfide linkages: synthesis and *in vitro* gene transfer properties. J Control Release 116:130–137
105. Lin C, Zhong Z, Lok MC et al (2007) Novel bioreducible poly(amido amine)s for highly efficient gene delivery. Bioconjug Chem 18:138–145
106. Lin C, Zhong Z, Lok MC et al (2007) Random and block copolymers of bioreducible poly (amido amine)s with high- and low-basicity amino groups: study of DNA condensation and buffer capacity on gene transfection. J Control Release 123:67–75
107. Lin C, Blaauboer CJ, Timoneda MM et al (2008) Bioreducible poly(amido amine)s with-oligoamine side chains: synthesis, characterization, and structural effects on gene delivery. J Control Release 126:166–174
108. Zugates GT, Anderson DG, Little SR et al (2006) Synthesis of poly(beta-amino ester)s with thiol-reactive side chains for DNA delivery. J Am Chem Soc 128:12726–12734
109. Gosselin MA, Guo W, Lee RJ (2001) Efficient gene transfer using reversibly cross-linked low molecular weight polyethylenimine. Bioconjug Chem 12:989–994
110. Neu M, Germershaus O, Mao S et al (2007) Crosslinked nanocarriers based upon poly (ethylene imine) for systemic plasmid delivery: *in vitro* characterization and *in vivo* studies in mice. J Control Release 118:370–380
111. Peng Q, Hu C, Cheng J et al (2009) Influence of disulfide density and molecular weight on disulfide cross-linked polyethylenimine as gene vectors. Bioconjug Chem 20:340–346
112. Peng Q, Zhong Z, Zhuo R (2008) Disulfide cross-linked polyethylenimines (PEI) prepared via thiolation of low molecular weight PEI as highly efficient gene vectors. Bioconjug Chem 19:499–506
113. Kim WJ, Kim SW (2009) Efficient siRNA delivery with non-viral polymeric vehicles. Pharm Res 26:657–666
114. Breunig M, Hozsa C, Lungwitz U et al (2008) Mechanistic investigation of poly(ethylene imine)-based siRNA delivery: disulfide bonds boost intracellular release of the cargo. J Control Release 130:57–63
115. Jeong JH, Christensen LV, Yockman JW et al (2007) Reducible poly(amido ethylenimine) directed to enhance RNA interference. Biomaterials 28:1912–1917

116. Bolcato-Bellemin AL, Bonnet ME, Creusat G et al (2007) Sticky overhangs enhance siRNA-mediated gene silencing. Proc Natl Acad Sci USA 104:16050–16055
117. Meyer M, Dohmen C, Philipp A et al (2009) Synthesis and biological evaluation of a bioresponsive and endosomolytic siRNA-polymer conjugate. Mol Pharm 6:752–762
118. Tomalia DA, Baker H, Dewald J et al (1985) A new class of polymers: starburst-dendritic macromolecules. Polym J 17:117–132
119. Tomalia DA, Baker H, Dewald J et al (1986) Dendritic macromolecules: synthesis of starburst dendrimers. Macromolecules 19:2466–2468
120. Worner C, Mulhaupt R (1993) Polynitrile- and polyamine-functional poly(trimethylene imine) dendrimers. Angew Chem Int Ed Engl 32:1306–1311
121. Zinselmeyer BH, Mackay SP, Schatzlein AG et al (2002) The lower-generation polypropylenimine dendrimers are effective gene-transfer agents. Pharm Res 19:960–967
122. Schatzlein AG, Zinselmeyer BH, Elouzi A et al (2005) Preferential liver gene expression with polypropylenimine dendrimers. J Control Release 101:247–258
123. Harada A, Kawamura M, Matsuo T et al (2006) Synthesis and characterization of a head-tail type polycation block copolymer as a nonviral gene vector. Bioconjug Chem 17:3–5
124. Choi JS, Nam K, Park JY et al (2004) Enhanced transfection efficiency of PAMAM dendrimer by surface modification with L-arginine. J Control Release 99:445–456
125. Arima H, Kihara F, Hirayama F et al (2001) Enhancement of gene expression by polyamidoamine dendrimer conjugates with alpha-, beta-, and gamma-cyclodextrins. Bioconjug Chem 12:476–484
126. Wood KC, Azarin SM, Arap W et al (2008) Tumor-targeted gene delivery using molecularly engineered hybrid polymers functionalized with a tumor-homing peptide. Bioconjug Chem 19:403–405
127. Kim TI, Baek JU, Zhe BC et al (2007) Arginine-conjugated polypropylenimine dendrimer as a non-toxic and efficient gene delivery carrier. Biomaterials 28:2061–2067
128. Lee JW, Ko YH, Park SH et al (2001) Novel pseudorotaxane-terminated dendrimers: supramolecular modification of dendrimer periphery. Angew Chem Int Ed Engl 40:746–749
129. Lim YB, Kim T, Lee JW et al (2002) Self-assembled ternary complex of cationic dendrimer, cucurbituril, and DNA: noncovalent strategy in developing a gene delivery carrier. Bioconjug Chem 13:1181–1185
130. Kim TI, Baek JU, Zhe Bai C et al (2007) Arginine-conjugated polypropylenimine dendrimer as a non-toxic and efficient gene delivery carrier. Biomaterials 28:2061–2067
131. Taratula O, Garbuzenko OB, Kirkpatrick P et al (2009) Surface-engineered targeted PPI dendrimer for efficient intracellular and intratumoral siRNA delivery. J Control Release 140:284–293
132. Hartmann L, Krause E, Antonietti M et al (2006) Solid-phase supported polymer synthesis of sequence-defined, multifunctional poly(amidoamines). Biomacromolecules 7:1239–1244
133. Hartmann L, Hafele S, Peschka-Suss R et al (2008) Tailor-made poly(amidoamine)s for controlled complexation and condensation of DNA. Chemistry 14:2025–2033
134. Leng Q, Mixson AJ (2005) Small interfering RNA targeting Raf-1 inhibits tumor growth *in vitro* and *in vivo*. Cancer Gene Ther 12:682–690
135. Leng Q, Scaria P, Zhu J et al (2005) Highly branched HK peptides are effective carriers of siRNA. J Gene Med 7:977–986
136. Wang XL, Ramusovic S, Nguyen T et al (2007) Novel polymerizable surfactants with pH-sensitive amphiphilicity and cell membrane disruption for efficient siRNA delivery. Bioconjug Chem 18:2169–2177
137. Yu TL, Lu W-C, Liu W-H et al (2004) Solvents effect on the physical properties of semi-dilute poly(*N*-isopropyl acryl amide) solutions. Polymer 45:5579–5589
138. Liu RCW, Cantin S, Perrot F et al (2006) Effects of polymer architecture and composition on the interfacial properties of temperature-responsive hydrophobically-modified poly(*N*-isopropylacrylamides). Polym Adv Technol 17:798–803

139. CdLH A, Pennadam S, Alexander C (2005) Stimuli responsive polymers for biomedical applications. Chem Soc Rev 34:276–285
140. Griffiths PC, Alexander C, Nilmini R et al (2008) Physicochemical characterization of thermoresponsive poly(N-isopropylacrylamide)-poly(ethylene imine) graft copolymers. Biomacromolecules 9:1170–1178
141. Lavigne MD, Pennadam SS, Ellis J et al (2007) Enhanced gene expression through temperature profile-induced variations in molecular architecture of thermoresponsive polymer vectors. J Gene Med 9:44–54
142. Twaites BR, CdlH A, Cunliffe D et al (2004) Thermo and pH responsive polymers as gene delivery vectors: effect of polymer architecture on DNA complexation *in vitro*. J Control Release 97:551–566
143. Twaites BR, CdLH A, Lavigne M et al (2005) Thermoresponsive polymers as gene delivery vectors: cell viability, DNA transport and transfection studies. J Control Release 108:472–483
144. Zintchenko A, Ogris M, Wagner E (2006) Temperature dependent gene expression induced by PNIPAM-based copolymers: potential of hyperthermia in gene transfer. Bioconjug Chem 17:766–772
145. Türk M, Dinçer S, Pişkin E (2007) Smart and cationic poly(NIPA)/PEI block copolymers as non-viral vectors: *in vitro* and *in vivo* transfection studies. J Tissue Eng Regen Med 1:377–388
146. Sun T, Wang G, Feng L et al (2004) Reversible Switching between superhydrophilicity and superhydrophobicity. Angew Chem Int Ed 43:357–360
147. Roux E, Francis M, Winnik FM et al (2002) Polymer based pH-sensitive carriers as a means to improve the cytoplasmic delivery of drugs. Int J Pharm 242:25–36
148. Berg K, Selbo PK, Prasmickaite L et al (1999) Photochemical internalization: a novel technology for delivery of macromolecules into cytosol. Cancer Res 59:1180–1183
149. Hogset A, Prasmickaite L, Engesaeter BO et al (2003) Light directed gene transfer by photochemical internalisation. Curr Gene Ther 3:89–112
150. de Bruin KG, Fella C, Ogris M et al (2008) Dynamics of photoinduced endosomal release of polyplexes. J Control Release 130:175–182
151. Kloeckner J, Prasmickaite L, Hogset A et al (2004) Photochemically enhanced gene delivery of EGF receptor-targeted DNA polyplexes. J Drug Target 12:205–213
152. Bonsted A, Wagner E, Prasmickaite L et al (2008) Photochemical enhancement of DNA delivery by EGF receptor targeted polyplexes. Methods Mol Biol 434:171–181
153. Nishiyama N, Arnida JWD et al (2006) Photochemical enhancement of transgene expression by polymeric micelles incorporating plasmid DNA and dendrimer-based photosensitizer. J Drug Target 14:413–424
154. Nishiyama N, Iriyama A, Jang WD et al (2005) Light-induced gene transfer from packaged DNA enveloped in a dendrimeric photosensitizer. Nat Mater 4:934–941
155. Oliveira S, Fretz MM, Høgset A et al (2007) Photochemical internalization enhances silencing of epidermal growth factor receptor through improved endosomal escape of siRNA. Biochim Biophys Acta 1768:1211–1217
156. Wagner E (2008) Converging paths of viral and non-viral vector engineering. Mol Ther 16:1–2

Top Curr Chem (2010) 296: 251–281
DOI: 10.1007/128_2010_63

Published online: 2 June 2010

Photochemical Internalization: A New Tool for Gene and Oligonucleotide Delivery

Kristian Berg, Maria Berstad, Lina Prasmickaite, Anette Weyergang, Pål K. Selbo, Ida Hedfors, and Anders Høgset

Abstract Photochemical internalization (PCI) is a novel technology for release of endocytosed macromolecules into the cytosol. The technology is based on the use of photosensitizers located in endocytic vesicles. Upon activation by light such photosensitizers induce a release of macromolecules from their compartmentalization in endocytic vesicles. PCI has been shown to increase the biological activity of a large variety of macromolecules and other molecules that do not readily penetrate the plasma membrane, including type I ribosome-inactivating proteins, immunotoxins, plasmids, adenovirus, various oligonucleotides, dendrimer-based delivery of chemotherapeutica and unconjugated chemotherapeutica such as bleomycin and doxorubicin. This review will present the basis for the PCI concept and the most recent significant developments.

Keywords Drug delivery · Gene therapy · Macromolecule · Peptide nucleic acid · Photochemical internalization · Photodynamic · Photosensitizer · Protein toxin · siRNA

Contents

K. Berg (✉), M. Berstad, L. Prasmickaite, A. Weyergang, P.K. Selbo, and I. Hedfors
Department of Radiation Biology, The Norwegian Radium Hospital, Oslo University Hospital, Montebello, 0310 Oslo, Norway
e-mail: kristian.berg@rr-research.no
A. Høgset
PCI Biotech AS, Hoffsvn. 48, 0375 Oslo, Norway

1 Introduction

The outcome of treatment of diseases is dependent on the dose-limiting toxicity of the therapeutic regimen. Cancer treatment is still mainly based on the three cornerstones: surgery, ionizing radiation, and chemotherapy. Despite continuous improvements of clinical protocols the death rate of cancer is still very high. The low cure rates for many indications are not due to lack of efficiency of current treatment regimens, but to limited specificity resulting in dose-limiting toxicity and side effects (e.g., see [1]). This fact has paved the way for development of alternative treatment modalities which provide higher specificity for the target tissue, thus giving the opportunity for lower drug dosages and less side effects for the patient. One example is macromolecular-based therapies, which involves proteins (e.g., immununotoxins), DNA as in gene therapy (using viral and non-viral vectors and oligonucleotides), and polymers used for delivery of therapeutics. The utilization of macromolecules for treatment of cancer and other diseases is becoming increasingly relevant. Recent advances in molecular biology and biotechnology have made it possible to improve targeting and design of cytotoxic agents, DNA complexes, and other macromolecules for clinical applications. To achieve the expected biological effect of these macromolecules, internalization of the macromolecules to the cell cytosol is often crucial. At an intracellular level, the most fundamental obstacle for cytosolic release of the therapeutic molecule is the membrane-barrier of the endocytic vesicles[2–4]. This review will present photochemical internalization (PCI) as a technology to overcome this barrier with a particular focus on its utilization for delivery of genes and oligonucleotides.

2 Macromolecular Therapeutics: The Cellular Membrane as a Barrier to Therapeutic Effect

Macromolecules with therapeutic potential include proteins such as ribosome-inactivating protein toxins for treatment of cancer and other indications, antibodies and growth factors for cell surface targeting, peptides and mRNA for vaccination, DNA for gene therapy, and antisense oligonucleotides, ribozymes, peptide nucleic acids (PNAs) and siRNA for gene silencing [5]. A large number of macromolecules

are under development for use as medicines and several have already been approved[1]. There are many extra- and intracellular barriers for these molecules to overcome before they can arrive at the target cells, enter the cells, and reach intracellular therapeutic targets. Degradation by serum enzymes and elimination by cells of the reticulo-endothelial system, penetration into the target tissues through the endothelial lining, as well as transport limitations within the tissue are important hurdles to obtain sufficient biological effect of these macromolecules [6]. For molecules acting inside the cells the delivery system should also overcome the intracellular barriers, such as the plasma membrane, endocytic membranes and, in gene therapy, the nuclear membrane. Many of the delivery methods developed are based on improved endocytic uptake and release of the therapeutic molecule from the endocytic vesicles into the cytosol. However, a major limitation in the use of macromolecular therapy is still the low rate of penetration through the membranes of endocytic vesicles and degradation of the macromolecules by lysosomal enzymes [7]. In accordance with these delivery challenges, most approved macromolecular therapeutics exert their effects on cell surfaces, more frequently targeting hematological diseases than solid organs. In the case of intracellular targeting the active compound is a small molecule (e.g., the cytotoxic antitumor antibiotic calicheamicin, Mylotarg) which exerts an intrinsic ability to penetrate some cellular membranes (e.g., diphtheria toxin, Ontak). Thus, in order for macromolecular therapeutics with intracellular targets to become an important part of approved medicine, improved intracellular delivery technologies are needed.

3 Photodynamic Therapy

The use of photochemical treatment to stimulate translocation of endocytosed macromolecules into the cytosol is a novel technology to improve therapeutic efficacy. The technology as described in this review is derived from photodynamic therapy (PDT) and is named PCI. In both cases a photosensitizer is used in combination with light to exert the treatment effects. The basic mechanisms of the photosensitizers and their tissue interaction in combination with light will be described with emphasis on the properties of the photosensitizers used in PCI before describing the use of PCI for cytosolic delivery of macromolecules.

[1]E.g., a 28-base RNA aptamer (Pegaptanib), a p53 expressing adenovirus (Gendicine, approved in China), a replication-selective adenovirus (H101, approved in China), a CD33-targeted immunoconjugate (Mylotarg), an HER2-targeted antibody (Herceptin), EGFR-targeted antibodies (Cetuximab and Panitumumab), anti-CD20 antibodies (Rituximab, Ibritumomab tiuxetan, and Tositumomab-I^{131}), anti-VEGF antibody (Bevacizumab), anti-CD52 (Alemtuzumab), anti-TNFα antibody (Infliksimab), and recombinant IL-2 truncated diphtheria toxin fusion protein (Ontak), erythropoitin, interferons, and colony-stimulating factors.

3.1 Photosensitizers

A photosensitizer is defined as a chemical entity, which upon absorption of light induces a chemical or physical alteration of another chemical entity. Most photosensitizers and all clinically approved photosensitizers (with the exception of methylene blue) used in PDT are based on or related to the tetrapyrrole macrocycle [8]. Porphyrins are comprised of four pyrrole subunits linked together by four methane bridges as shown in Fig. 1. This tetrapyrrole ring structure is named porphin and derivatives of porphins are named porphyrins. Tetrapyrroles are naturally occurring pigments, which are used in many biological processes. These tetrapyrroles are unable to induce any photochemical or photophysical reactions in other compounds or are rapidly quenched in their normal surroundings, as in chlorophyll. In all these tetrapyrroles a metal ion is coordinated in the middle of the compounds. The presence of a coordinated metal ion and its electronic properties are of importance for the photocytotoxic potential of porphyrins as photosensitizers. By removal of the metal, tetrapyrroles become efficient photosensitizers as well as acquiring fluorescing properties. An example is removal of Fe^{2+} from heme to form protoporphyrin IX, a compound responsible for the light-sensitivity disease erythropoetic protoporphyria and the main photosensitizer in 5-aminolevulinic acid-based PDT [9, 10]. Most efficient porphyrin-based photosensitizers therefore lack coordinated metal ions. Coordinated metal ions increase the probability for non-radioactive decay of the triplet state (see below), paramagnetic metals like Fe^{3+} being much more efficient than diamagnetic metals like Al^{3+} and Mg^{2+}. Several metallophotosensitizers have however been developed for clinical purposes.

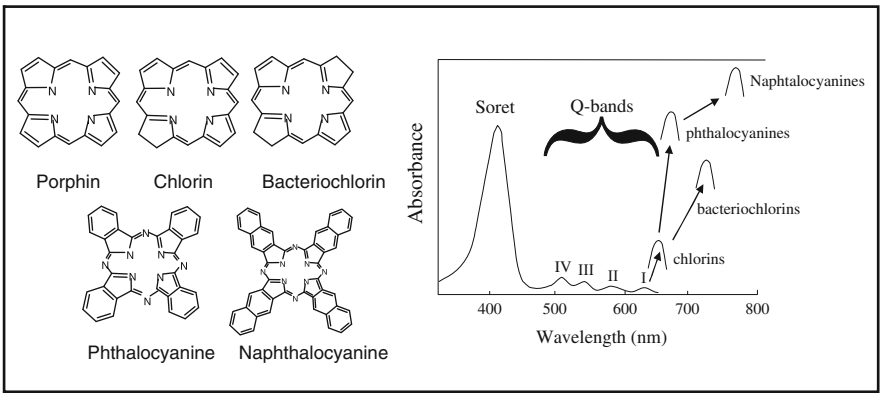

Fig. 1 Basic structure *(left side)* and the absorption spectra *(right side)* of some photosensitizers. The absorption spectra of porphyrins (derived from porphins) consists of a Soret band (around 400 nm) and four Q-bands. Upon reduction of one or two double-bonds of the tetra-pyrrole structure or by expanding the number of π-electrons (by expanding the ring structure), the outermost Q-band becomes bathochromically shifted and the absorption coefficient increased as indicated on the figure. As described in the text, such chemical modifications are important for improving the therapeutic effect in deeper tissue layers

Although in most cases they have lower quantum yields for cell inactivation, they have other properties like improved solubility and stability, which makes them interesting as therapeutic substances. The metals used at least in experimental PDT include Zn, Pd, Sn, Ru, Pt, Lu, Gd, and Al.

Porphyrins and porphyrin-related dyes (Fig. 1) used in PDT have substituents in the peripheral positions of the pyrrole rings, on the four methine carbons (meso-positions) and/or coordinated metals. These derivatives are synthesized to influence the photophysical properties, water/lipid solubility, amphiphilicity, pK_a, and stability of the compounds [11]. These parameters determine the biodistribution of the compounds, e.g., the intracellular localization, tissue distribution, and pharmacokinetics. Most photosensitizers used in PDT are relatively hydrophobic or amphiphilic compounds, including carboxyl-groups to provide sufficient solubility (Fig. 2). The pK-values of the carboxyl-groups are sufficiently high to allow penetration through cellular membranes via the protonated form accumulating in various organelles depending on the physico-chemical properties of the photosensitizer. An exception is PSs with a large number of carboxyl groups ($\sim\geq 4$, e.g., NPe6, coproporphyrin, and uroporphyrin) that accumulate in endocytic vesicles. In contrast, the pK-values of the sulfonate groups of the photosensitizers used in PCI ($TPPS_{2a}$ and $AlPcS_{2a}$) are too low to allow penetration through cellular membranes. The need for an

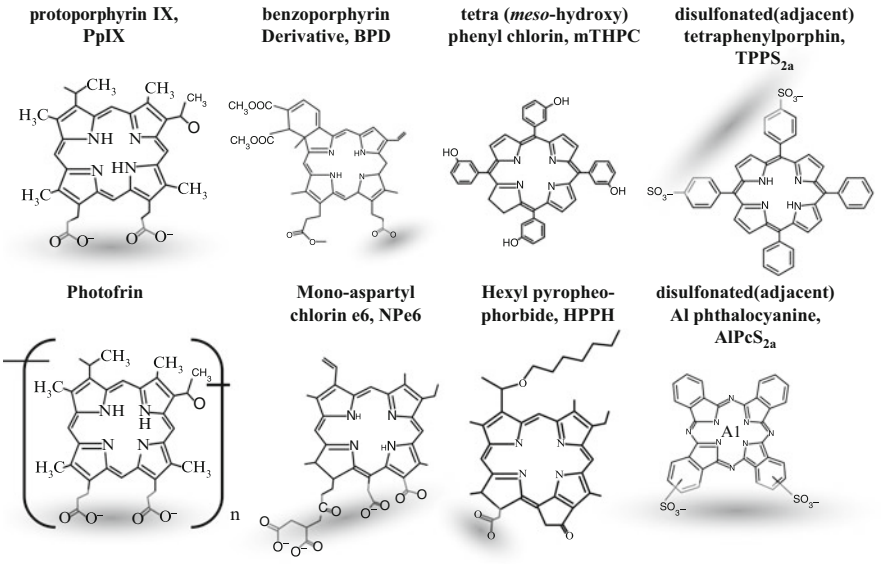

Fig. 2 Examples of photosensitizers presently approved for clinical applications or in clinical studies. mTHPC, tetra (*meso*-hydroxy) phenyl chlorin; BPD-MA, benzoporphyrin derivative; Photofrin is a mixture of several compounds where dimers or trimers of the indicated structure are assumed to be of major importance; PpIX, protoporphyrin IX – accumulating upon treatment with 5-aminolevulinic acid or its ester derivatives, NPe6, HPPH, Hexyl pyropheophorbide; $TPPS_{2a}$, disulfonated (adjacent) tetraphenylporphin; $AlPcS_{2a}$, disulfonated (adjacent) aluminum phthalocyanine. Areas with ionic side groups are indicated in *shadow*

amphiphilic character of the photosensitizers used in PDT is not fully revealed, but is due to the requirement for solubility combined with the need for membrane penetration [12].

3.2 Mechanisms of Action

The photodynamic reactions that are the basis for PCI and PDT require a combination of a photosensitizer, light, and oxygen to exert a therapeutic effect [8]. In the absence of one of these components, neither therapeutic nor side effects are induced. The photodynamic reactions are initiated by the excitation of the photosensitizer, followed by interaction with molecular oxygen and cascades of oxidation reactions and tissue damage. It should be emphasized that, for various reasons (high level of LDL-receptors, leaky vasculature, low lymphatic drainage, low interstitial pH), photosensitizers exert a preferential retention in tumor tissues [11, 13]. In combination with a localized light exposure PDT may be regarded as a relatively specific treatment modality with no systemic side effects, except skin photosensitivity that may last for days to some weeks.

3.2.1 Photophysical and Initial Photochemical Reactions

The photocytotoxic effects, which are utilized in PDT and PCI, are initiated by the absorption of light by the photosensitizer. A molecule that has absorbed a light quantum is excited to a short-lived excited state ($^1P^*$, Fig. 3). The absorbed energy can be released as heat, emitted as fluorescence (utilized for cancer diagnosis), or undergo intersystem crossing (ISC) to a long-lived triplet state ($^3P^*$). The extra energy in the triplet state may, as for the singlet state, be released as heat, as light (phosphorescence), or be used in photochemical or photophysical reactions to form reactive oxygen species (ROS). The triplet state may react in two ways, either by a type I mechanism involving electron or (less frequently) hydrogen atom transfer

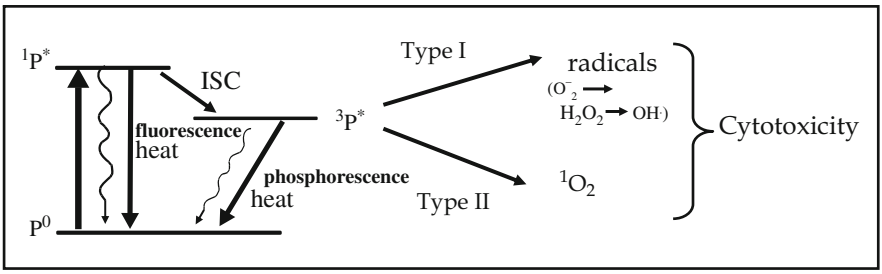

Fig. 3 Basic mechanisms in PDT and PCI. A simplified Jablonski diagram is shown where the vibrational levels are omitted. *P,* photosensitizer; *ISC*, intersystem crossing

between the photosensitizer and the target molecule or by a type II mechanism involving energy transfer to molecular oxygen (Fig. 3). In type I reactions free radicals are formed while in the type II reaction singlet oxygen ($^1O_2$) is formed. Singlet oxygen is an excited form of O_2, which is in the triplet form in its ground state, and is not a radical. Both mechanisms may occur during PDT and PCI and the relative importance depends on the surroundings and the nature of the substrate molecules. A significant amount of indirect evidence, i.e., by means of quenchers of $^1O_2$ and degradation of photosensitizers, and some direct evidence exists for the importance of $^1O_2$ in the photoinduced processes of PDT [14–16]. Singlet oxygen causes mainly membrane damage by oxidizing amino acids (tryptophan, cysteine, histidine, methionine, and phenylalanine), unsaturated fatty acids, and cholesterol. Additionally, guanine may also be oxidized by singlet oxygen. The lifetime of singlet oxygen is approximately ten times longer in organic than in aqueous solvents. Thus, the photodynamic reaction most efficiently targets cellular membranes and membrane-localized photosensitizers are therefore also regarded as the most efficient compounds for use in PDT.

3.2.2 Biological Targets

The therapeutic effect of PDT may be due to direct cell killing or vascular damage, and there are also indications of the importance of immune responses. The relative importance of these pathways to therapeutic effects depends on the photosensitizer and its formulation, the way of administration, and the time between administration of the photosensitizer and exposure to light.

Cells as Targets for PDT

The range of action of $^1O_2$ in cells is still not fully elucidated, but may be as short as 0.01–0.02 μm [17]. A short range of action of $^1O_2$ is indicated by the photochemically induced reduction of the enzymatic activity of monoamino oxidase and cytochrome c oxidase in the outer and inner mitochondrial membranes, respectively, but not of adenylate kinase [18]. Adenylate kinase is located between these two membranes which are separated by only 5–10 nm. Furthermore, lysosomal enzymes are less susceptible to photochemical inactivation by $TPPS_{2a}$ compared to $TPPS_4$ despite their similar localization [19]. $TPPS_4$ and $TPPS_{2a}$ are suggested to be located in the lysosomal matrix and the lysosomal membranes, respectively (Fig. 4a). Thus, $^1O_2$ formed in these cases diffuse substantially shorter than the size of the lysosomes (∼0.5 μm). Similarly, the membrane bound 3-THPP (tetra (3-hydroxyphenyl)porphin) damages selectively DNA close to the nuclear membrane, while the hydrophilic $TPPS_4$ induces random damage to DNA [20]. Therefore, the primary site of action of a photosensitizer seems to be highly restricted to its close vicinity, and studies of the cellular localization of photosensitizers may yield valuable information about the identity of the main primary targets in PDT.

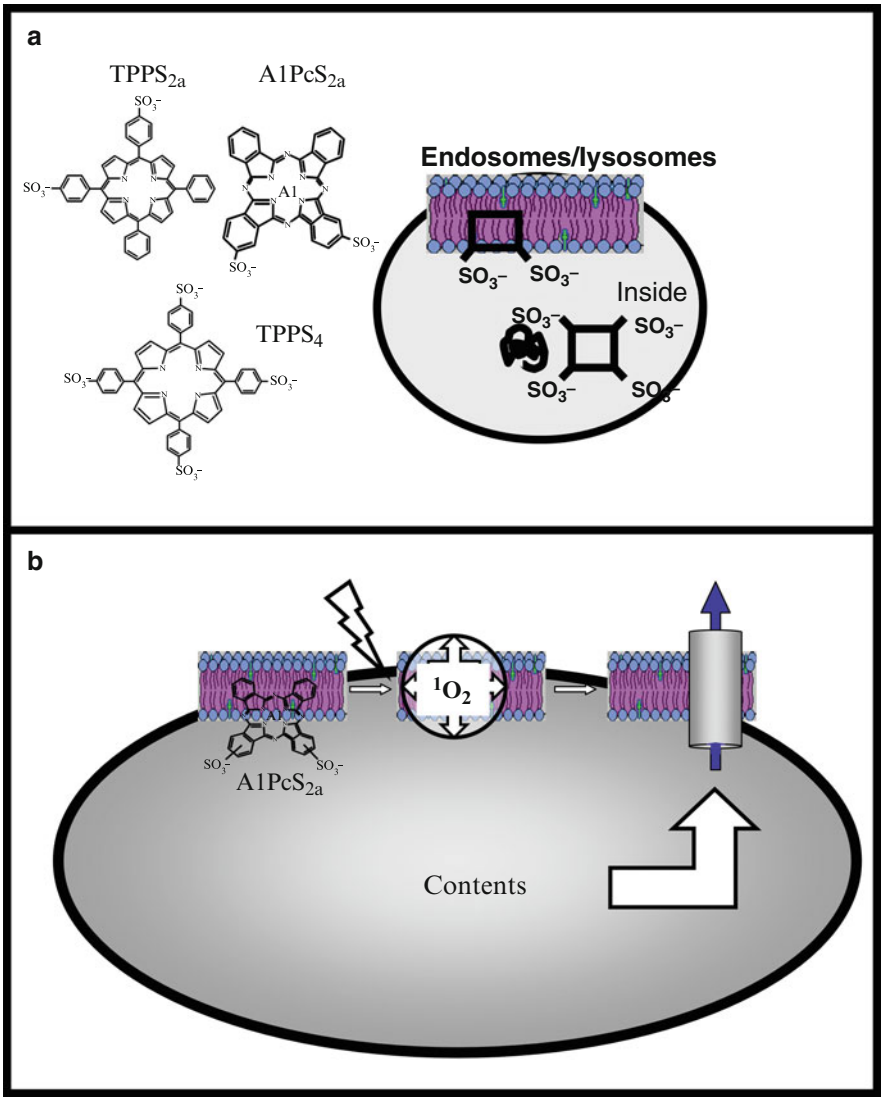

Fig. 4 (**a**) Proposed localization of sulfonated photosensitizers in endocytic vesicles. The figure shows a schematic drawing of an endocytic vesicle and drawings of the main location of a tetrasulfonated (tetra(4-sulfonatophenyl)porphine, TPPS4) and an amphiphilic disulfonated photosensitizer (tetraphenylporphine disulfonate ($TPPS_{2a}$) and aluminium phthalocyanine disulphonate ($AlPcS_{2a}$)) (not to scale). (**b**) Photochemical effect induced by a photosensitizer (AlPcS2a) located in the membrane of a vesicle. Upon illumination of the photosensitizer, reactive oxygen species, mainly singlet oxygen, are formed, constituents of the membranes are destroyed, and passage of the contents of the vesicle to the cytosol is allowed

However, the primary damage may only be the first step in a cascade of reactions leading to cell death. The importance of direct cell killing of a target tissue depends on the physico-chemical properties of the photosensitizer. While some photosensitizers mainly localize in the cells of a target tissue, others are located to a higher extent in the interstitial space of the tissue. This is shown by various *in vivo/in vitro* protocols [21, 22] and is in accordance with the intratumoral localization studies, e.g., showing the cellular locations of mono- and disulfonated aluminum phthalocyanines ($AlPcS_1$ and $AlPcS_2$) and the interstitial localization of the tri- and tetrasulfonated species $AlPcS_3$ and $AlPcS_4$ [23]. The direct photodamage to tumor or other target cells may also vary due to inhomogenous distribution of the photosensitizer. The amount of intravenously administered photosensitizers in tumor tissue as well as the cell killing may for some photosensitizers decrease with the distance from the vasculature [24].

Photoactivation of photosensitizers located in endocytic vesicles (endosomes and lysosomes) may damage the contents of these vesicles, resulting in rupture of the membranes of these vesicles and relocation of the contents including the photosensitizers to other intracellular compartments, depending on the physico-chemical properties of the photosensitizer. Hydrophilic photosensitizers, such as tetrasulfonated aluminum phthalocyanine and tetraphenylporphyrin ($AlPcS_4$ and $TPPS_4$), photoinactivate the contents of the endocytic vesicles (Fig. 4). In contrast, amphiphilic photosensitizers, such as $TPPS_{2a}$ and $AlPcS_{2a}$, damage to a much lower extent endocytic matrix components that are released into cytosol in a functionally intact form. As an example, 60% of endocytosed horseradish peroxidase and 40% of the lysosomal enzyme beta-*N*-acetyl-D-glucosaminidase activities were released into the cytosol at a light dose not inactivating the remaining enzyme activity [19, 25, 26].

PDT may be a strong inducer of apoptosis, depending again on the photosensitizer, the treatment conditions, and the cells. As for other inducers of apoptosis, PDT activates the caspase pathway leading to cleavage of several proteins and DNA fragmentations [27]. Cytochrome c is released from the mitochondria to bind to APAF-1 and procaspase 9. This stimulates cleavage of pro-caspase 9 to caspase 9 and initiates the caspase cascade leading to apoptotic fragmentation of the DNA. The release of cytochrome c from the mitochondria may be due to direct damage to the mitochondria, but indirect activation such as stimulation of the Fas death receptor on the plasma membrane followed by activation of caspase 8 and bid has been documented. Damage to lysosomes has been suggested to lead to release of lysosomally located cathepsins, which may activate caspase 3 directly. However, several studies indicate that catepsins instead cleave and thereby activate bid (a bcl-2 family protein) for binding to the mitochondria and release of cytochrome c (Fig. 5) [28, 29]. Bid has been shown to be activated by the lysosomally located NPe6 and light [29]. However, the impact of the cathepsin release–bid activation–caspase activation–apoptosis pathway for cell death by photoactivation of endocytically located photosensitizers has not been unequivocally documented. $TPPS_{2a}$-PDT has been shown to inactivate partly cathepsins and almost all cathepsin L + D activity released into cytosol is inactivated by cytosolic constituents, most likely stefins [19].

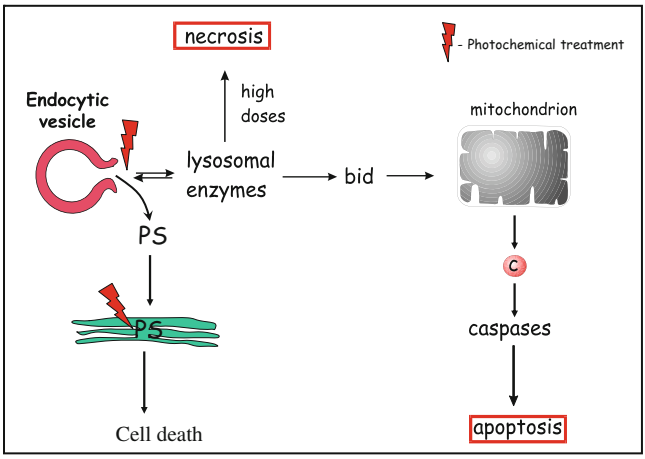

Fig. 5 Cell death induced by disruption of lysosomes. An endocytic vesicle is ruptured by the photochemical treatment and lysosomal enzymes and the photosensitizer is released into the cytosol. Large quantities of lysosomal enzymes will rapidly degrade vital proteins and cause necrosis, while lower quantities may cleave bid (to form truncated t-bid) and thereby induce apoptosis as indicated on the figure. The photosensitizer will relocate to other organelles during light exposure and induce photodamage to these organelles

In contrast, $TPPS_{2a}$-PDT inactivates the endoplasmic reticulum (ER) marker enzyme NADPH cytochrome c reductase, implying that $TPPS_{2a}$ is relocated during light exposure and thereby inducing cytotoxic effects through ER damage [30]. Thus, upon light exposure, endocytically located photosensitizers may induce cytotoxicity by release of cathepsins into the cytosol and/or induce damage to other organelles after relocation during light exposure.

Vascular Damage

PDT may induce vasoconstriction during or shortly after treatment while thrombus formation has been observed a few hours after treatment [31]. These effects will lead to vascular shutdown and tissue hypoxia and anoxia, causing delayed tumor growth. Targeting the vasculature is utilized in the treatment of age-related macular degeneration (AMD) where the photosensitizer is injected systemically shortly before light exposure of the macula [32]. The new vessels causing the reduced vision quality are in this way damaged, causing a slowing in the development of the disease. Several clinical protocols are now also initiated for treatment of cancers, such as prostate cancer, where a similar photosensitizer-light time interval as for AMD is performed in an attempt to shut down the tumor blood supply [33].

$AlPcS_{2a}$-based PDT has been shown *in vivo* to localize in the endothelial lining and to cause vascular shutdown in the central part of tumors, while the tumor periphery appears relatively resistant to PDT [34]. In contrast, PCI (of bleomycin,

see below) has been found to target more efficiently the tumor periphery and the deeper tumor layers and in this way induce a stronger tumor growth delay or cure [35]. These treatment responses must be taken into account when treatment protocols for PCI of macromolecular therapeutics are designed.

Immune Responses

In addition to the direct cytotoxic effect of PDT on the cells in the tissues and the vasculature targeting there are substantial documentation from *in vivo* models and some clinical documentation that immunological effects contribute to the therapeutic effect of PDT, in particular for cancer therapy [36–38]. Both attraction of inflammatory cells and other immune reactions have been observed after PDT, but this is beyond the scope of this review. However, the immune response and antitumor immunity induced by PDT as well as PCI of bleomycin has been described in several reviews [39, 40].

Light Penetration in Tissue

A potential limitation in the utilization of light for therapeutic purposes is the penetration of light through tissues. The penetration of light through tissues is limited mainly by heme, especially in hemoglobin, and melanin. Efficient penetration of light therefore requires wavelengths for photoactivation above about 600 nm where absorption of light by these chromophores is low [41]. An upper maximum wavelength for photoactivation is usually set by the energy required for excitation of O_2 to form singlet oxygen, i.e., 23 kcal/mol which is equivalent to the excess energy of the long lived form of singlet oxygen. This requires that the photosensitizer must be excited at wavelengths below about 850 nm. The therapeutic wavelength window is therefore usually defined as 600–800 nm, but shorter wavelengths may be used when thin lesions are to be treated. Thus, photosensitizers absorbing light in the 6–800 nm has been developed (Figs. 1 and 2). The treatment of internal organs is generally of no limitations any more due to the development of light sources and light applicators in PDT, which are used to treat hollow organs and other internal organs by interstitial fiber optics and surface exposure during surgical procedures. Therapeutic effect is regularly seen at 2–10 mm, depending on the photosensitizer, in tumor tissue exposed to light from an external light source. A large variety of light sources has been used for PDT [42]. In most cases lasers, especially diode lasers, are used for clinical applications due to their emission of monochromatic light, high power output, and easy delivery of the light to optical fibers. A large variety of non-laser light sources have also been used experimentally and clinically, especially for surface illumination. These light sources might be useful for irradiation of large surface areas such as several types of skin cancers as well as psoriasis. Recently light emitting diodes have been developed with sufficient power for surface irradiation.

4 The Principle of Photochemical Internalization

The invention of PCI as a technology for intracellular drug delivery is based upon the observed endosomal and lysosomal localization and relocalization of some photosensitizers and the observation that lysosomal enzymes were released into the cytosol in a functionally intact form after photochemical treatment with a subpopulation of the lysosomally located photosensitizers as described above. Accordingly, externally added and endocytosed proteins were found to be released from the endocytic vesicles to the cytosol upon photochemical treatment only with the same photosensitizers that did not inactivate the lysosomal enzymes. On this basis the treatment procedure developed for PCI is as described in Fig. 6. The introduction of molecules into the cytosol is achieved by first exposing the cells or tissues to a photosensitising dye and the molecule which one wants to deliver, both of which should preferentially localize in endosomes and/or lysosomes. Second, the cells or tissues are exposed to light of wavelengths inducing a photochemical reaction. This reaction will lead to disruption of lysosomal and/or endosomal membranes and the contents of the endocytic vesicles will be released into the cytosol. The photochemically induced relocation of macromolecules has been shown by fluorescently labeled gelonin, peptide, polyplex-complexed plasmid and dextran-particles [25, 43, 44]. Detailed descriptions of practical aspects of the technology have previously been published [45, 46].

In contrast to the original treatment procedure, it was later found that molecules to be translocated to the cytosol by PCI could be delivered to the cells after the photochemical treatment [43]. The treatment effect by this procedure has been found comparable to that of the original procedure in both *in vitro* and *in vivo* studies. However, the molecule to be translocated to cytosol has to be administrated shortly after the photochemical treatment and a few hours after the photochemical treatment there is no longer a detectable PCI effect. The mechanisms behind this effect is not fully revealed, but our working hypothesis is that the endocytic vesicles formed after the photochemical treatment and containing the macromolecules to be delivered fuse with the photochemically ruptured endocytic vesicles and thereby release the endocytosed material into the cytosol as described in Fig. 7. It has recently been found that by PCI of macromolecules containing a targeting moiety the cargo cannot be administrated after the photochemical treatment apparently due to photochemical damage to the corresponding receptor (Fig. 8) [47–49].

PCI has been shown to increase the biological activity of a large variety of macromolecules and other molecules that do not readily penetrate the plasma membrane (Table 1). PCI has also been shown to enhance the treatment effect of targeted therapeutic macromolecules. These results show that PCI can induce efficient light-directed delivery of macromolecules into the cytosol, indicating that PCI may have a variety of useful applications for site-specific drug delivery, e.g., in gene therapy, vaccination, and cancer treatment. PCI of BLM has recently been approved for a clinical Phase I trial, where several indications have been included. The first patients with head and neck cancer have recently been treated at

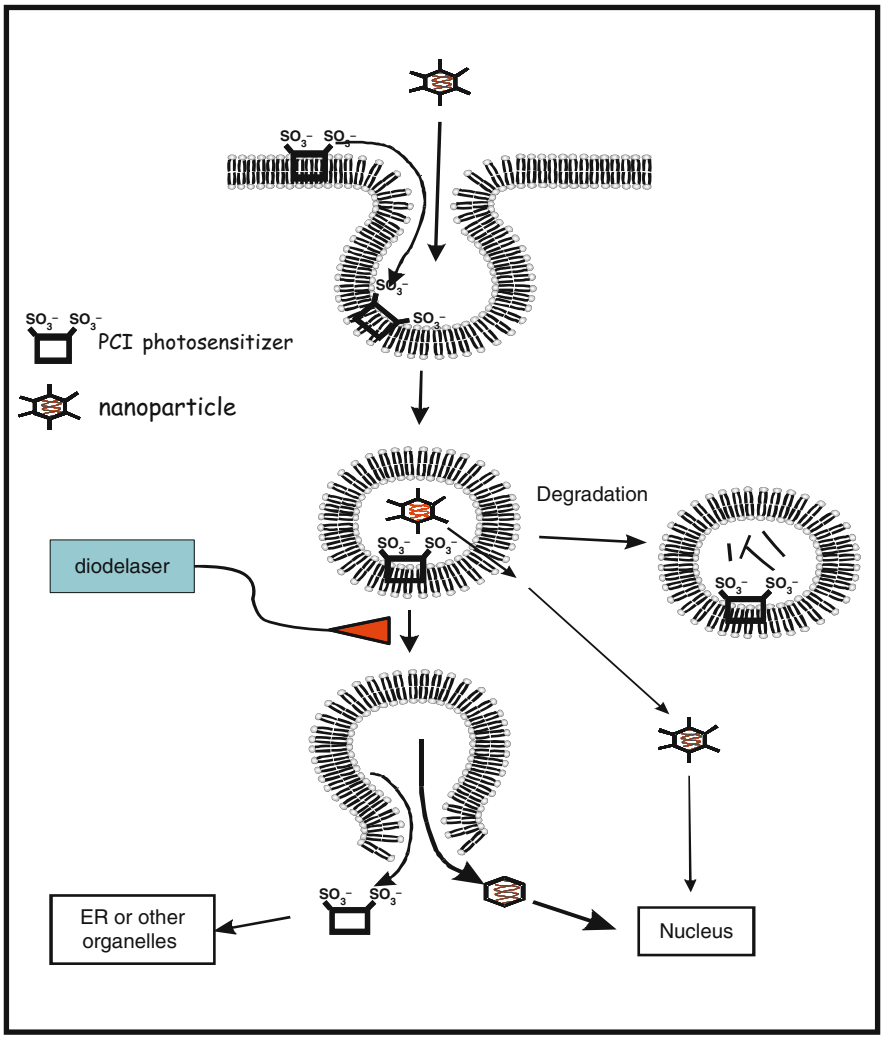

Fig. 6 Illustration of the PCI principle. The photosensitizer and the macromolecular therapeutics (here visualized by a nanoparticle for gene delivery) are endocytosed as indicated and accumulating in endocytic vesicles. The nanoparticle may be degraded by hydrolytic enzymes in late endosomes or lysosomes, translocated to the cytosol by intrinsic properties of the designed nanoparticle or released into the cytosol by a photochemically induced rupture of the endocytic vesicle as illustrated by the use of a diodelaser. The DNA may thereafter enter the nucleus for transgene expression

the University College London Hospital. The present status on the development of PCI for delivery of different classes of molecules will be described below with emphasis on delivery of genes and oligonucleotides. Additional information may also be found in previous reviews [50, 51].

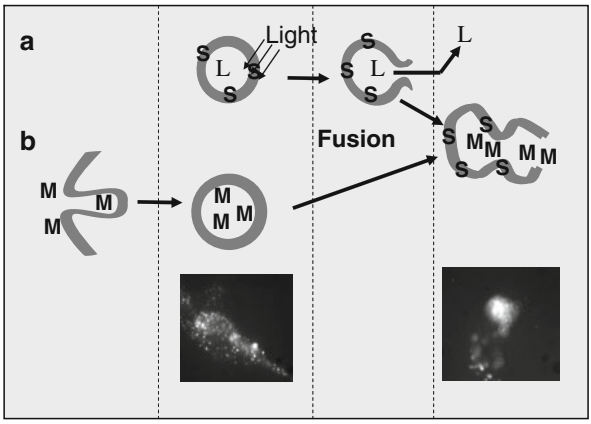

Fig. 7 An illustration of how molecules can enter cytosol after photochemical treatment (light first principle). (**a**) The photosensitizer (S) is endocytosed by the cells and when exposed to light the membranes of these vesicles will rupture and the contents (L) released into the cytosol. (**b**) Macromolecules that are administrated after the photochemical treatment will be endocytosed and end up in intact newly formed vesicles. These vesicles may then fuse with the photochemically damaged vesicles and the contents of the fused vesicles are released into the cytosol. The pictures at the *bottom* shows cells stained with fluorescently labelled dextran particles delivered before or after the photochemical treatment

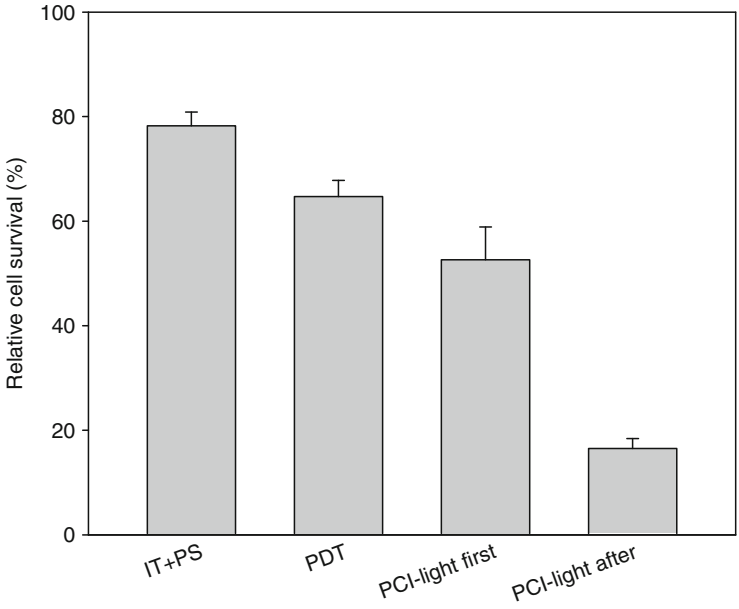

Fig. 8 PCI of trastuzumab-saporin. Zr-75-1 breast cancer cells were treated with $TPCS_{2a}$ (0.2 μg/mL) and light. The PCI-treated cells were treated with a trastuzumab-saporin conjugate for 18 h either before light ("light after regimen") or after ("light first regimen") light exposure according to previous protocols [49]. The cell survival was measure with the MTT-assay 2 days after light exposure. IT + PS, cells treated with trastuzumab-saporin and photosensitizer in the absence of light

Table 1 *In vitro* and *in vivo* experiments to demonstrate PCI

Macromolecules	Photo-sensitizer	Cell line	Potentiation with PCI	References
1. Proteins				
Gelonin	$TPPS_4$,	NHIK 3025, BL2-8G-E6	Yes	[25]
	$TPPS_{2a}$	NHIK 3025, BL2-8G-E6, WiDr, Km20L2, Col115, HCT116, T47D, THX, OHS, U87*, D54, EB, V79, COS-7, CME-1, SW 982, FLS, A-375, T24, A-431	Yes	[44, 75]
	$AlPCS_{2a}$	WiDr, KM20L2, HCT116, Malme-3, Malme-3 M, FM3, V79, BL2-8G-E6	Yes	[104]
	ZnPc, BPD	NHIK 3025	No	[25]
	3-THPP	NHIK 3025, WiDr	No	[104]
	Chlorine e6	D54	Yes	Unpublished
Saporin	$TPPS_{2a}$	NuTu-19, MDA MB 435, CHO*, WiDr	Yes	
Saporin (liposome-formulation)	$TPPS_{2a}$	OVCAR-3	Yes	[107]
Saporin (dendrimer-formulation)	$TPPS_{2a}$	CA9-22, KJ-1	Yes	[106]
Horseradish peroxidase	$TPPS_{2a}$	NHIK3025	Yes	[25]
Targeted proteins				
MOC-31-gelonin	$TPPS_{2a}$	WiDr, T47D, KM20L2, H-146	Yes	[104]
	$AlPcS_{2a}$	WiDr, KM20L2	Yes	[104]
	3-THPP	WiDr	No	[104]
	ALA-PPIX	WiDr	Yes	[115]
2. Genes (reporters and therapeutic-relevant)				
Virus mediated:				
AdCMV-lacZ	$TPPS_{2a}$	WiDr, FEMXIII, HeLa, HuFib, CME-1, SW 982, FLS, U87-Mg, GaMg, HCT116, Raji, THX, OHS, SaOs	Yes	[85, 86, 116, 117]
AdCMV-eGFP	$TPPS_{2a}$	WiDr, HCT116, THX	Yes	[85]
AdCMV-lacZ	$AlPcS_{2a}$	WiDr, HCT116	Yes	[118]
TRAIL	$TPPS_{2a}$	WiDr, HCT116,	Yes	[74]

(*continued*)

Table 1 (continued)

Macromolecules	Photo-sensitizer	Cell line	Potentiation with PCI	References
Glucosylated PEI with p53 gene	$TPPS_{2a}$	FaDu, PANC3	Yes	[72, 119]
PEI with PTEN gene	$TPPS_{2a}$	Ishikawa	Yes	[73]
Non-virus mediated:				
Poly-L-lysine (with reporter gene EGFP)	$TPPS_{2a}$, $TPPS_4$, $AlPcS_{2a}$	HCT116, THX, CME-1, SW 982, HUH7, CT26, DU145, MCF-7, HeLa, Cos-7	Yes	[112, 116, 120]
	3THPP	THX	No	[121]
PEG-PLL	PEG-PLL/dendrimer-phthalocyanine	HUH-7	Yes	[81]
PEG-aspartatamide	PEG-aspartatamide/ dendrimer-phthalocyanine	HUH-7	Yes	[82]
Polyethyleneimine (PEI) (with reporter genes eGFP, luciferase and therapeutic gene HSV-thymidine kinase)	$TPPS_{2a}$, $AlPcS_{2a}$	WiDr, HCT116, U87MG, HUH7, A431, HepG2	Yes	[70, 112] (unpublished)
Cationic lipids (with reporter eGFP)	$AlPcS_{2a}$	HCT116, BL2-G-E6	Yes	[25, 87]
	$AlPcS_{2a}$	THX	Yes	[112, 121]
Quadruplicated cationic peptide (NLS)	Dendrimer-phthalocyanine	HeLa	Yes	[80]
PAMAM-dendrimer	PAMAM-dendrimer-photosensitizer conjugate	HeLa	Yes	[83]
Targeted gene delivery:				
Epidermal growth factor (EGFR)-targeted PEI (with reporter genes eGFP, luciferase and therapeutic gene HSV-thymidinekinase	$TPPS_{2a}$, $AlPcS_{2a}$	HUH7, HepG2, A431	Yes	[75]
Transferrin-poly-L-lysine (with EGFP-reporter gene)	$AlPcS_{2a}$	HCT116	Yes	[112]
RGD-Adenovirus (w/GFP reporter gene)	$TPPS_{2a}$	WiDr	Yes	[85]
3. Oligonucleotides				
Peptide nucleic acids (PNA, hTERT)	$AlPcS_{2a}$, $TPPS_{2a}$	DU145	Yes	[65]
Tat-PNA (hTERT)	$TPPS_{2a}$	DU145	Yes	[122]

Peptide-PNA conjugates	$TPPS_{2a}$	OHS, HCT116, SW620	Yes	[67]
CPP-PNA	$AlPcS_{2a}$	HeLa	Yes	[66]
siRNA (Anti-EGFR) lipofectamine	$TPPS_{2a}$	A431	Yes	[56]
siRNA (S100A4) lipid carriers	$TPPS_{2a}$	HCT-116, SW620, OHS, RMS	Yes	[57]
siRNA (S100A4) polyethyleneamine	$TPPS_{2a}$	OHS	Yes	[58]
siRNA (anti-luciferase) dextran nanogels	$TPPS_{2a}$	HUH-7	Yes	[111]
4. Chemotherapeutics				
Bleomycin	$TPPS_{2a}$	V-79	Yes	[110]
	$AlPcS_{2a}$	WiDr	Yes	[110]
Camptothecin-loaded micelles	Dendrimer-phthalocyanine-loaded micelles	HeLa	Yes	[123]
5. *In vivo* experiments				
Gelonin	$AlPCS_{2a}$	TAX1, MFH,WiDr	Yes	[99, 124, 125]
Bleomycin	$AlPCS_{2a}$	WiDr, CT26Cl25, Tax-1, HT1080	Yes	[34, 35, 110, 126]
Quadruplicated cationic peptide (NLS)	Dendrimer-phthalocyanine	Conjunctiva	Yes	[80]
Glucosylated PEI with p53 gene	$AlPCS_{2a}$	HNSCC xenograft	Yes	[71]
siRNA (anti-EGFR)	$AlPcS_{2a}$	A431	Yes	[52]
Recombinant fusion protein scFvMEL/rGel	$AlPcS_{2a}$	A375	Yes	[105]

4.1 PCI-Based Oligonucleotide Delivery

Oligonucleotide-based gene therapy has attracted great attention due to the more simplified manufacturing process of oligonucleotids, their smaller size, and the localization of the target in the cytosol instead of the nucleus, although the nucleus may also be targeted. Several oligonucleotide structures have been developed, where presently siRNA seems most attractive. siRNA is double-stranded RNA containing sequences of 19–23 nucleotide that triggers the formation of a protein complex (RISC, RNA-induced silencing complex) inducing degradation of mRNA recognized by the specific siRNA sequence. siRNA is currently in clinical trials, but the most advanced trials all involve local administration as reviewed by Oliveira and co-workers [52].

Oligonucleotides, including siRNA, are exposed to similar challenges as all biomolecular therapeutics, e.g. degradation, transportation towards the target cells and into the cells as well as immunological responses. The sensitivity to enzymatic degradation, and the negative charge of most oligonucleotides and longer nucleotide sequences disfavouring association with the negative charge of the cell surface, have resulted in development of a large variety of cationic compounds, such as lipids and polymers, that strongly associate with nucleotides forming lipoplexes and polyplexes, respectively. These oligonucleotide complexes are endocytosed and released into the cytosol either by fusion with the endocytic membranes or by inducing swelling and rupture of the acidic endocytic vesicles through the "proton sponge" effect [53–55]. Several studies have shown that the ability of siRNA to exert gene silencing properties can be enhanced by PCI. PCI may enhance gene silencing of both siRNA lipoplexes and polyplexes, indicating that both lipoplexes and polyplexes are more efficient in facilitating cellular uptake into endocytic vesicles than in inducing translocation of the cargo into cytosol.

Oliveira and coworkers utilized the lipid vector Lipofectamine as vector for delivery of anti-EGFR siRNA and found that PCI could increase the treatment efficacy of the anti-EGFR siRNA tenfold by PCI in A431 head and neck squamous cell carcinoma cells in culture [56]. The same authors showed recently that PCI could also enhance the gene silencing *in vivo* by anti-EGFR siRNA/lipofectamine lipoplexes [52]. In contrast, Bøe et al. found no PCI effect of Lipofectamine-complexed siRNA targeting the pro-metastatic gene S100A4 in OHS osteosarcoma cells [57]. However, in this study Lipofectamine-complexed anti-S100A siRNA caused almost complete gene silencing alone and one may speculate that at lower suboptimal siRNA doses PCI might have contributed to enhancing gene silencing. Two other lipid vectors, jetSI and jetSI-ENDO, claimed to cause a proton sponge-based translocation of siRNA and were efficient in inducing S100A4 gene silencing only in combination with PCI. The PCI-enhanced delivery of siRNA does not seem to be restricted to lipoplexes since both various polyethyleneimine (PEI) formulations as well as siRNA-loaded dextran nanogel are potentiated by PCI [58]. Interestingly, PCI had no effect on the gene silencing effect of anti-S100A4 siRNA complexed to linear PEI, while the effect of several branched PEI-siRNA

complexes was improved by PCI. Branched PEI has been shown to cause stronger electrostatic interaction with pDNA than linear PEI, resulting in better compaction, higher zeta-potential, and smaller particle size. Accordingly, the strength of interaction between PEI and oligonuleotides has also been shown to influence the target mRNA downregulation [59].

In contrast to siRNA, peptide-nucleic acids (PNAs) do not induce any mRNA degradation, but instead cause a strong sense-antisense binding hindering gene expression. PNA belong to the third generation of antisense oligonucleotides in which the phosphate backbone is replaced by a pseudopeptide backbone composed of *N*-(2-aminoethyl) glycine units [60]. Due to the modified internucleotide linkage, PNAs are resistant to nucleases and peptidases and therefore are extremely stable in biological systems [61]. Despite the radical difference in the chemical composition of the backbone, PNA not only retains, but also improves the hybridization characteristics to DNA and RNA. PNAs seem to be non-toxic, as they are uncharged molecules with low affinity for proteins that normally bind nucleic acids [61]. As PNAs are neutral molecules, solubility and cellular uptake are serious problems that have to be overcome for PNAs to become useful tools in clinical settings. Several approaches have therefore been developed for the delivery of such molecules to intact cells based on electroporation, microinjection, or the generation of PNA/DNA complexes [61]. Improved intracellular delivery can also be obtained by coupling PNAs to lipids or peptides that are efficiently internalized by cells. Several efforts have been made to exploit the potential of "natural-occurring" peptides such as amphiphilic cationic/hydrophobic so-called cell-penetrating peptides (CPP), e.g., the peptide derived from Tat protein of HIV-1 virus [62]. Thus, CPPs are reported to have the capacity for transporting molecules such as oligonucleotides across biological membranes in a receptor-independent way. However, this concept has been questioned as based on an artefact caused by the fixation procedure [54, 63]. It has recently been found that cellular uptake of several cell penetrating peptide (CPP)-conjugates occurs predominantly via an endocytotic pathway and that endosomal escape is therefore one of the major rate-limiting steps of CPP-mediated cellular delivery due to trapping of the CPP conjugates in the endosomal/lysosomal compartment [63, 64].

Despite the low uptake of PNAs in living cells, it has been demonstrated that naked or chimeric PNAs enter some cells through a liquid-phase endocytosis and tend to accumulate in endocytic compartments [63]. The development of endosome-disruptive strategies is thus of great importance to allow PNAs to co-localize with their specific targets. For this purpose, PCI represents a new approach to achieve the photochemically inducible release in the cytoplasm of endocytosed PNA. PCI has been shown to induce cytosolic delivery of a 15-mer naked PNA directed against the hTERT mRNA (hTERT-PNA) [65]. PCI of hTERT-PNA was found to reduce significantly the catalytic activity of telomerase as well as the cell growth, which reflected the higher bioavailability of PNA at the level of the target. The treatment effect of PCI was compared to the antitelomerase activity of a chimeric PNA molecule, made by conjugating the hTERT-PNA to the HIV-Tat internalizing peptide (Tat-hTERT-PNA). The results of the TRAP (telomeric repeat amplification protocol)-assay indicated a very modest effect on telomerase activity

and significantly lower than that obtained with PCI of a comparable dose of hTERT-PNA. Such results demonstrate that the PCI approach represents a more efficient system for the delivery of PNAs than conjugation with CPP.

Chimeric PNA molecules with a specific or unspecific (e.g., cationic) targeting moiety enhance significantly the cellular uptake of PNA. Thus, the observation of PCI as an enhancer of the anti-telomerase effect of Tat-hTERT-PNA represent a major improvement in the development of PCI of PNA [65]. PCI was found to inhibit both telomerase activity and hTERT protein expression, resulting in induction of apoptosis. This is in accordance with findings demonstrating that the antisense effects of different PNA-conjugates (Tat, Arg_7, KLA) were significantly enhanced, both at cytosolic and nuclear level, in HeLa pLuc 705 and p53R cell systems as a consequence of the PCI approach [66]. Shiraishi and Nielsen [66] found PCI to enhance the antisense activity of all the cationic conjugates more than 10-fold while PCI of naked PNA was improved only 2.5-fold. The most efficient conjugate was with Tat where PCI enhanced the antisense effect by two orders of magnitude. Similar results were reported by Bøe and Hovig, who found PCI of two PNAs towards S100A4 linked to cationic peptides (5+) to inhibit S100A4 expression in a dose- and time-dependent manner [67]. Based on fluorescence microscopy of fluorescence labeled PNAs, charged as well as neutral PNAs were relocated to the nucleus after PCI although a higher extracellular concentration was needed for the neutral PNAs. PCI of PNA is clearly improved with respect to PNA targeting effects by conjugation to a cationic peptide, but the optimal peptide sequence cannot be deduced from these reports. The cellular uptake seems to be increased by increasing the peptide charge up to 5+, but the antisense effect of the PNA-peptide alone and in combination with PCI does not make a simple correlation with the charge of the peptide, e.g. PCI of PNA linked to the Tat-peptide (8+) and a KLA peptide (5+) induced similar antisense effects while various arg/lys sequences with charge in the same range were less efficient [66].

Overall, experimental evidence indicates that the PCI approach represents a new and more efficient system for the internalization of oligonucleotides and emphasizes the importance of the endosomal release to enhance the bioavailability, and thus the gene silencing activity, of oligonucleotides. As a consequence, PCI makes it possible to reduce the amount of oligonucleotides required to induce the specific biological effect compared to other delivery systems. Such a new delivery approach could be exploited for *in vivo* applications. In fact, the actual efficiency of oligonuleotides as gene silencing molecules has been demonstrated *in vivo* by PCI of anti-EGFR siRNA, encouraging further development towards clinical use [52]. However, it should be emphasized that in this study siRNA was injected intratumorally.

4.2 PCI-Based Gene Delivery

Gene therapy is a novel therapeutic modality receiving great attention and being generally recognized as having the potential to constitute treatment for a wide range

of diseases [68]. However, although there are some encouraging clinical trials, gene therapy have hitherto largely given quite disappointing conclusions [69]. Treatment of severe combined immunodeficiency is the most successful result of gene therapy, although it caused a lymphoproliferative disease in some of the patients. Thus, efficacy and safety are still main issues in gene therapy. An important reason for these challenges is that methods for efficient and specific delivery of therapeutic genes *in vivo* are lacking [68]. Delivery of genes to cells requires in most cases that the DNA is protected from degradation and that the cellular uptake is facilitated. The vehicles used for such purposes, named vectors, may be divided into chemical or non-viral and viral vectors. In addition, physical methods such as electroporation may be utilized.PCI, which can be combined with both non-viral and viral vectors, may be viewed as a physico-chemical vector.

With most gene delivery systems the therapeutic gene is taken into the cell by endocytosis. For many of these systems, especially non-viral-based, translocation of the gene out of the endocytic vesicles constitutes a major hindrance for realization of the full therapeutic potential of the gene. PCI is a method for overcoming this hindrance. Photochemical internalization has been studied as a gene delivery technology (reviewed in [50, 51]), both with several non-viral, adenoviral as well as adeno-associated viral vectors, mainly by utilizing reporter genes such as genes encoding EGFP (enhanced green fluorescent protein) or ß-galactosidase. However, PCI-mediated gene delivery has also been shown to induce the delivery of therapeutic genes, such as the genes encoding HSV-tk (Herpes Simplex Virus thymidine kinase) [70], p53 [71, 72], PTEN [73], TRAIL [74], and IL-12 (interleukin-12) (unpublished results).

4.2.1 Non-Viral Vectors

The non-viral vectors may be divided into polymers (polyplexes), and lipids (lipoplexes). These vectors are generally cationic in order to form complexes easily with negatively charged DNA and are added in sufficient amounts to generate positive charge ratios (N:P) in order to stimulate association with the cell surface. In general, the advantages of using non-viral vectors are low or no immunogenicity and relatively simple synthesis procedures, but they exert lower transfection efficacies than the viral vectors.

PCI has been found to enhance the transgene expression of both reporter and therapeutic genes incorporated into plasmids and delivered by various non-viral vectors (Table 1). In general, PCI enhances transgene expression from plasmids incorporated into polyplexes, while the PCI effect on lipoplexes is more dependent on the structure of the lipoplex and probably also on the cell line. The vectors protect the plasmid DNA from degradation by serum nucleases, enhance cellular endocytic uptake by establishing an overall positive complex charge, and stimulate endolysosomal release into the cytosol. Polyethyleneimine (PEI) is one of the most frequently used non-viral vectors both *in vitro* and *in vivo*. PEI stimulates endolysosomal release by the "proton sponge effect" [53], with an efficacy highly

dependent on its size and structure (linear or branched). The PCI-induced enhancement of transfection has mainly been evaluated using 22-kDa linear PEI, where expression of transgene luciferase was enhanced by up to 600-fold and expression of EGFP transgene more than 35-fold [70, 75]. Branched PEI exerts a stronger electrostatic interaction with plasmid DNA than linear PEI, resulting in more compact and smaller particles with higher zeta-potential. In a recent comparative study, branched PEI was found *in vitro* to lead to stronger luciferase activity than the linear PEI [76], while others have found the opposite [77]. We have found that PCI also enhances transfection by plasmids complexed with branched PEI (Fig. 9), but the optimal parameters for PEI-based PCI are still to be determined. PCI has also been shown to be efficient in enhancing transfection of poly-L-lysine polyplexes, which are highly inefficient alone since these polyplexes do not induce any proton sponge effect [51].

An *in vivo* study showed that treatment of head and neck squamous cell carcinomas deficient in active p53 with intratumoral injection of the photosensitizer $AlPcS_{2a}$ and a plasmid encoding p53 complexed to a glycosylated PEI caused dramatic tumor regression in all the transfected animals [71]. In contrast, similar PDT or PEI-p53 treatments did not delay tumor growth. In this study the tumors were relatively large at the time of the first treatment (500 mm^3) and the tumors were treated once a week for up to 7 weeks. These results thus indicate that repeated local treatments might be feasible to control bulky tumors. However, development of systemic administration of the polyplex for homogeneous and non-toxic transfection is a major goal for future gene therapy protocols. Polyethylene glycol

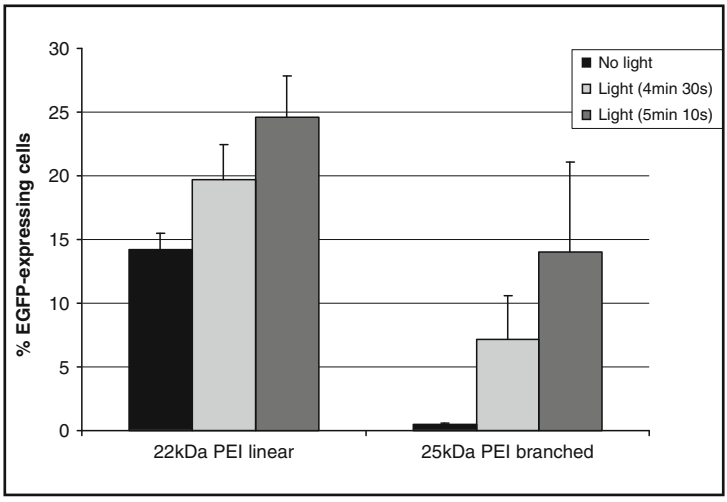

Fig. 9 PCI-induced transfection utilizing branched and linear PEI as vector. HT116 colon carcinoma cells were treated with $AlPcS_{2a}$ (20 μg/mL) for 18 h followed by a 4-h incubation with an plasmid encoding EGFP and complexed with 25 kDa branched or 22 kDa linear PEI at an N:P ratio of 4 before light exposure. EGFP expression was measure by flow cytometry 2 days later. The photochemical treatment caused 40–60% cytotoxicity

(PEG) is widely used for shielding biomolecular therapeutics and prolongs their circulating half-lives. PEGylation is also known to reduce transfection efficacy of non-viral vectors, an effect that may however be reversed by PCI [75]. PEG linked to a targeting ligand, such as EGF, transferrin or a mAb, and complexed with an optimal PEI compound should exert many of the requirements needed for *in vivo* evaluation of PCI-enhanced gene therapy.

Dendrimers have attracted great attention as polyplexes for delivery of plasmids as well as oligonucleotides although toxicity is also a matter of concern with dendrimers, assumed to be linked to their highly positive charge density [78, 79]. Kataoka and coworkers have designed dendrimer-based nanoparticles that have shown great promise both *in vitro* and *in vivo* [80]. Plasmids were complexed with positively charged NLS (nuclear-localizing sequence) peptide at an N:P ratio of 2 and thereafter covered by negatively charged dendrimers containing a centrally located phthalocyanine photosensitizer. The overall charge was negative, but with the negative charges based on carboxyl-groups the dendrimers became closer to neutral in the acidic environment of the endocytic vesicles. Thus, the photosensitizer-dendrimer conjugates were assumed to stick closer to the endocytic members, and thereby presumably more efficiently sensitize these membranes to photochemical rupture than more hydrophilic compounds. PCI utilizing these ternary nanoparticles enhanced transgene expression more than 100-fold with low photocytotoxicity and showed successful gene delivery *in vivo*. The photocytotoxicity of endocytically located photosensitizers is partly assumed to be due to relocation of the photosensitizer during light exposure to the membranes of other intracellular compartments. The photosensitizer-dendrimer conjugate may become more water-soluble when entering the cytosol (with its higher pH) and therefore less efficient in sensitizing cells to photoinactivation. However, the overall negative charge of this complex contradicts systemic *in vivo* delivery. The authors have therefore modified the complexes by designing two different nanoparticles, one with the photosensitizer-dendrimer conjugate and the other with a plasmid as a core, both covered with PEGylated polylysin [81]. The PEGylated polylysin was later replaced with PEGylated catiomer based on poly (β-benzyl-L-aspartate carrying ethylenediamines via an amide binding [82]. They all showed strong PCI-induced enhancement of transgene expression with little photocytotoxicity and may be appropriate for systemic *in vivo* PCI-mediated gene delivery. Recently, Shieh and coworkers showed similar properties, i.e., high PCI-mediated gene delivery and low photocytotoxicity, by utilizing a photosensitizer linked to a cationic polyamidoamine (PAMAM) dendrimer [83]. In cancer therapy, a low photocytotoxicity may be of lesser importance since the main goal is tumor eradication. However, one of the main side effects to be expected from the PCI treatment is skin photosensitivity as seen in PDT and may be avoided by the dendrimer-linked photosensitizers. PCI based on dendrimer-conjugated photosensitizers may also be utilized for treatment of non-cancerous diseases such as in gene-replacement therapy where photocytotoxicity must be avoided.

4.2.2 Adenoviral Vectors

Adenovirus vectors are known to be taken into cells by endocytosis and to be released from endosomes by a well regulated process, assumed to be highly efficient [84]. It is therefore somewhat surprising that PCI is able to increase the number of adenoviral transduced cells by up to 30-fold. Nevertheless, PCI with adenoviral vectors has been tested in several different cell lines, and in all cases improved transduction has been observed [85]. The adenovirus activated by means of PCI seems to follow the same cellular pathways as for conventional adenovirus infection, i.e., the fraction of transduced cells followed a linear relationship with the Coxsackie and Adenoviral Receptor (CAR) level of the cells and is integrin dependent. Furthermore, PCI increase the number of nuclearly located viral DNA molecules as measured by real-time PCR and fluorescence in situ hybridization (FISH) [86]. The results so far indicate that the main cause of the PCI effect on transduction with adenovirus is related to enhanced release of the viral particles from the endocytic vesicles into the cytosol. In accordance with what has been found for PCI of plasmids the adenovirus may be delivered after the photochemical treatment (unpublished results). However, adenovirus may be delivered up to 12 h after the photochemical treatment, which is longer than what is effective for PCI of plasmids [43, 87].

Immunological reactions and similar or lower levels of CAR in tumor tissue are major hurdles in clinical use of adenovirus as vectors in gene therapy [88, 89]. Thus, changing the Adv tropism and retargeting as well as shielding the virus from immune responses are crucial factors for efficient systemic gene therapy. In this respect PCI has been shown to potentiate efficiently transduction mediated with adenovirus complexed with polycations [90–92]. Further, adenovirus complexed with the cationic polymer metacrylate (pDMAEMA) conjugated to EGF and non-covalently PEGylated increased the fraction of transduced DU145 prostate cancer cells from 10% to 70% by means of PCI [91].

4.2.3 Adeno-Associated Viral Vector

Adeno-associated viruses (AAV) derived from endemic non-pathogenic parvo-viruses have several properties that make them attractive as vectors in gene therapy [93]. These properties include the absence of host inflammatory response, low cytotoxicity, a low cell-mediated immune response, the ability to transduce non-dividing cells, the induction of long-term gene expression, and a broad tropism. A major limitation is the packing constraint of about 5 kbs. PCI has been found to increase the transduction efficacy of a serotype 5 AAV in one of two glioblastoma cell lines tested. The non-responding cell line required a much lower number of viral particles to transduce the same number of cells and it was speculated that PCI might improve the transduction efficacy only in cells difficult to transduce by AAVs [94].

Overall, PCI has the potential to be a very useful technology for *in vitro* and *in vivo* gene delivery, both because it can improve the delivery of genes in general and because it is a light dependent process, rendering the therapeutic gene active only in illuminated sites of the body. The possibility of using photochemically activated promoters may further add to the specificity of such treatment [95–97]. Thus, by the employment of PCI, adverse effects due to gene expression in non-target areas of, for example, a gene encoding a cytotoxic protein could largely be avoided, making PCI especially attractive for gene therapy of cancer and localized diseases.

4.3 PCI of Other Therapeutics

As for gene delivery, a major obstacle for successful treatment using macromolecular-based therapeutics is endo-lysosomal sequestration of the drugs. Originally, PCI was developed as a drug delivery system where protein toxins were used as model macromolecular drugs.

4.3.1 Ribosome-Inactivation Protein Toxins

RIPs are plant protein toxins that are able to inhibit enzymatically ribosomal activity and are therefore highly cytotoxic [98]. RIPs are taken up in the cells by means of endocytosis, and only a small fraction (5% or less) are translocated to the cytosol where the toxins inhibit the protein synthesis and eventually kill the cell. PCI may be used to increase both the efficacy and specificity of these toxins. RIPs are divided into two groups, type I and type II. Type II RIPs, like ricin, consists of two polypeptide chains, one cytotoxic A-chain with *N*-glycosidase activity and one B-chain which binds to the cell surface. Type I RIPs, like gelonin, agrostin, and saporin, lack the B chain, which make them poorly transported over the cell- and intracellular membranes to the cell cytosol. Hence, the cytotoxic effect of these protein toxins is usually absent or very low. A considerable cytotoxic effect of type I RIPs has been shown in combination with PCI, both *in vitro* and *in vivo* [25, 99].

Targeted Delivery of Protein Toxins to Tumor Cells

The development of monoclonal antibodies (mAbs) has revolutionized cancer treatment, and several mAbs are today approved for clinical use. Treatment resistance is often a problem in mAbs-treatment where multiple treatment series are necessary [100]. Drug response can be increased by binding mAbs to cytotoxic compounds, such as protein toxins, forming immunotoxins (ITs) [101]. The historical problems with first and second generation ITs are largely solved by the use of recombinant DNA technology where chimeric proteins consisting of the Fv-fragment of an antibody and

a protein toxin are constructed [101]. Antibodies or antibody fragments can be replaced with other targeting molecules like cytokines or growth-factors (e.g., IL-2, EGF, and VEGF). One of the advantages of using RIP-based ITs in cancer treatment is that these molecules are highly toxic when they enter the cytosol of the cell. It is estimated that as few as 1–10 RIP molecules in the cytosol is sufficient to kill a cell [102]. However, there are some disadvantages of using protein toxins for the treatment of solid tumors, such as (1) limited penetration through the malignant tissue, (2) expression of neutralizing antibodies due to repeated injections of the IT, and (3) uptake of the IT in normal cells causing side effects such as vascular leak syndrome (VLS), hemolytic-uremic syndrome and damage to the liver and other organs which express the target-antigen on the cell surface [103]. Since type I RIPs are almost unable to penetrate the membranes of endocytic vesicles, targeted fusion toxins based on type I RIPs may induce less side effects than type II based ITs.

As a second enhancement of mAb-treatment, PCI can be used to activate locally type I RIP-based ITs by a photochemical release of the protein toxin into the cytosol of the target cell. This activity is induced only in the tissue that is exposed to light and, consequently, the dose limiting adverse effects of the IT should be highly reduced. Accordingly, PCI has been shown to increase the effect of gelonin based ITs by PCI targeting EpCAM [104]. Recently, PCI of the melanoma targeting fusion toxin MELscFv-rGel was demonstrated [105]. PCI strongly augmented the therapeutic effect of MELsvFc-rGel *in vitro* and synergistic effects were also achieved *in vivo*. This is the first *in vivo* study that documents therapeutic effects of PCI of a targeting macromolecule after systemic administration. Of particular interest, compared to other studies where ITs are injected multiple times, the IT was administered only once in this study and no adverse effects were observed.

In cancer therapy, the leaky vasculature and the reduced lymphatic drainage results in an enhanced permeation and retention (EPR) of nanoparticles. In accordance with PCI-mediated transfection using cationic dendrimers, a similar enhancement of cytotoxicity was observed with the cationic polyamidoamine (PAMAM) dendrimer conjugated to saporin [106]. These nanoparticles may utilize the EPR effect for increased tumor uptake and the positive charge of the dendrimer for electrostatic interaction with the negative cell surface charge to enhance the cellular uptake into endocytic vesicles, resulting in passive tumor targeting. PAMAM dendrimers may also be conjugated to targeting ligands for additional specificity. Similarly, liposomal delivery of saporin, protecting the cargo from lysosomal degradation, has been found efficient when combined with PCI for tumor cell eradication[107].

4.3.2 PCI of Bleomycin and Other Chemotherapeutics

A few chemotherapeutic agents accumulate in endocytic vesicles probably due to their size and/or charge. Bleomycin (BLM, MW ~1,400) is a chemotherapeutic drug approved for the treatment of many forms of cancer. The applicability of bleomycin is, however, limited by the adverse effects of the treatment, especially interstitial pneumonia causing irreversible lung fibrosis in 3% of the treated patients

[108]. The main reason for the limited therapeutic effect of BLM is its poor ability to penetrate the plasma membrane. It has been reported that 500 molecules of BLM is sufficient to kill a cancer cell [109]. This indicates that once translocated in the cell cytosol, BLM is a highly effective chemotherapeutic drug. PCI has been shown to improve its cytotoxic effect both *in vitro* and *in vivo*, indicating that not only large macromolecules like proteins and DNA may profit from a PCI-based treatment, but also smaller molecules with a low ability to penetrate biological membranes [110]. This may make it possible to reduce the administered dose of bleomycin, thereby reducing the side effects without losing clinical efficacy. In earlier *in vivo* studies subcutaneously growing xenografts have been utilized to document the PCI principle. More recently, PCI of bleomycin has been found to delay significantly growth of human invasive fibrosarcoma cells injected intramuscularly in athymic mice [34, 35]. PCI may also reverse resistance to weak base chemotherapeutics such as doxorubicin when resistance is caused by lowered pH in endocytic vesicles [106]. Other chemotherapeutic agents linked to polymers and nanoparticles may also exert a therapeutic benefit in combination with PCI [111].

5 Targeting and Specificity

In cancer therapy, as well as in the treatment of many other diseases, there is a need for improved specificity of the treatment. PCI relies on the use of photosensitizers, which accumulate preferentially in neoplastic lesions and induce a cytotoxic reaction only in the light-exposed areas. A further improved treatment specificity may however be established by cell specific targeting of the photosensitizer and/or the therapeutic macromolecule. Several targeting methods are under development, such as the use of antibodies and derivatives thereof, receptor ligands, peptides, tissue-specific promoters, and replication. Some targeting principles have been evaluated in combinations with PCI, such as immunotoxins [105], transferrin- and epidermal growth factor-conjugated vectors [45, 112], protein affinity-toxins [113], RGD sequences for integrin-targeting [85], and nanoparticles [83, 111, 114]. These results indicate that PCI can be used in combination with other targeting principles to improve therapeutic specificity further.

Acknowledgments This study has been financially supported by the Norwegian Radium Hospital Research Foundation and the Norwegian Cancer Society.

References

1. Hauer-Jensen M, Wang J, Boerma M, Fu Q, Denham JW (2007) Curr Opin Support Palliat Care 1:23
2. Christie RJ, Grainger DW (2003) Adv Drug Deliv Rev 55:421

3. Pack DW, Hoffman AS, Pun S, Stayton PS (2005) Nat Rev Drug Discov 4:581
4. Russ V, Wagner E (2007) Pharm Res 24:1047
5. Juliano RL, Astriab-Fisher A, Falke D (2001) Mol Interv 1:40
6. Jain RK (2001) Adv Drug Deliv Rev 46:149
7. Cho YW, Kim JD, Park K (2003) J Pharm Pharmacol 55:721
8. Brown SB, Brown EA, Walker I (2004) Lancet Oncol 5:497
9. Krammer B, Plaetzer K (2008) Photochem Photobiol Sci 7:283
10. Minder EI, Schneider-Yin X, Steurer J, Bachmann LM (2009) Cell Mol Biol (Noisy -le-grand) 55:84
11. MacDonald IJ, Dougherty T (2000) Basic principles of photodynamic therapy 5(2):105
12. Lavi A, Weitman H, Holmes RT, Smith KM, Ehrenberg B (2002) Biophys J 82:2101
13. Peng Q, Moan J (1995) Br J Cancer 72:565
14. Breitenbach T, Kuimova MK, Gbur P, Hatz S, Schack NB, Pedersen BW, Lambert JD, Poulsen L, Ogilby PR (2009) Photochem Photobiol Sci 8:442
15. Moan J, Pettersen EO, Christensen T (1979) Br J Cancer 39:398
16. Niedre MJ, Secord AJ, Patterson MS, Wilson BC (2003) Cancer Res 63:7986
17. Moan J, Berg K (1991) Photochem Photobiol 53:549
18. Murant RS, Gibson SL, Hilf R (1987) Cancer Res 47:4323
19. Berg K, Moan J (1994) Int J Cancer 59:814
20. Kvam E, Stokke T (1994) Photochem Photobiol 59:437
21. Chan WS, Brasseur N, La Madeleine C, Ouellet R, van Lier JE (1997) Eur J Cancer [A] 33A:1855
22. Henderson B, Dougherty TJ (1992) Photochem Photobiol 55:145
23. Peng Q, Moan J, Farrants G, Danielsen HE, Rimington C (1990) Cancer Lett 53:129
24. Korbelik M, Krosl G (1994) Br J Cancer 70:604
25. Berg K, Selbo PK, Prasmickaite L, Tjelle TE, Sandvig K, Moan D, Gaudernack G, Fodstad Ø, Kjolsrud, Anholt, Rodal G, Rodal S, Høgset (1999) Cancer Res 59:1180
26. Moan J, Berg K, Anholt H, Madslien K (1994) Int J Cancer 58:865
27. Oleinick NL, Morris RL, Belichenko I (2002) Photochem Photobiol Sci 1:1
28. Cirman T, Oresic K, Mazovec GD, Turk V, Reed JC, Myers RM, Salvesen GS, Turk B (2004) J Biol Chem 279:3578
29. Reiners JJ Jr, Caruso JA, Mathieu P, Chelladurai B, Yin XM, Kessel D (2002) Cell Death Differ 9:934
30. Rodal GH, Rodal SK, Moan J, Berg K (1998) J Photochem Photobiol B – Biol 45:150
31. Bhuvaneswari R, Gan YY, Soo KC, Olivo M (2009) Cell Mol Life Sci 66:2275
32. Shah GK, Sang DN, Hughes MS (2009) Retina 29:133
33. Marberger M, Carroll PR, Zelefsky MJ, Coleman JA, Hricak H, Scardino PT, Abenhaim LL (2008) Urology 72:S36
34. Norum OJ, Gaustad JV, Angell-Petersen E, Rofstad EK, Peng Q, Giercksky KE, Berg K (2009) Photochem Photobiol 85:740
35. Norum OJ, Giercksky KE, Berg K (2009) Photochem Photobiol Sci 8:758
36. Abdel-Hady ES, Martin-Hirsch P, Duggan-Keen M, Stern PL, Moore JV, Corbitt G, Kitchener HC, Hampson IN (2001) Cancer Res 61:192
37. Thong PS, Ong KW, Goh NS, Kho KW, Manivasager V, Bhuvaneswari R, Olivo M, Soo KC (2007) Lancet Oncol 8:950
38. Yanai H, Kuroiwa Y, Shimizu N, Matsubara Y, Okamoto T, Hirano A, Nakamura Y, Okita K, Sekine T (2002) Int J Gastrointest Cancer 32:139
39. Castano AP, Mroz P, Hamblin MR (2006) Nat Rev Cancer 6:535
40. Norum OJ, Selbo PK, Weyergang A, Giercksky KE, Berg K (2009) J Photochem Photobiol B 96:83
41. Konig K (2000) J Microsc 200:83
42. Brancaleon L, Moseley H (2002) Lasers Med Sci 17:173

43. Prasmickaite L, Hogset A, Selbo PK, Engesaeter BO, Hellum M, Berg K (2002) Br J Cancer 86:652
44. Selbo PK, Sandvig K, Kirveliene V, Berg K (2000) Biochim Biophys Acta 1475:307
45. Bonsted A, Wagner E, Prasmickaite L, Hogset A, Berg K (2008) Methods Mol Biol 434:171
46. Shiraishi T, Nielsen PE (2006) Nat Protoc 1:633
47. Weyergang A, Kaalhus O, Berg K (2008) Photochem Photobiol Sci 7:1032
48. Weyergang A, Selbo PK, Berg K (2007) Biochem Pharmacol 74:226
49. Yip WL, Weyergang A, Berg K, Tonnesen HH, Selbo PK (2007) Mol Pharm 4:241
50. Berg K, Folini M, Prasmickaite L, Selbo PK, Bonsted A, Engesaeter BO, Zaffaroni N, Weyergang A, Dietze A, Maelandsmo GM, Wagner E, Norum OJ, Hogset A (2007) Curr Pharm Biotechnol 8:362
51. Hogset A, Prasmickaite L, Selbo PK, Hellum M, Engesaeter BO, Bonsted A, Berg K (2004) Adv Drug Deliv Rev 56:95
52. Oliveira S, Hogset A, Storm G, Schiffelers RM (2008) Curr Pharm Des 14:3686
53. Boussif O, Lezoualc'h F, Zanta MA, Mergny MD, Scherman D, Demeneix B, Behr JP (1995) Proc Natl Acad Sci U S A 92:7297
54. Fretz MM, Mastrobattista E, Koning GA, Jiskoot W, Storm G (2005) Int J Pharm 298:305
55. Tseng YC, Mozumdar S, Huang L (2009) Adv Drug Deliv Rev 61:721
56. Oliveira S, Fretz MM, Hogset A, Storm G, Schiffelers RM (2007) Biochim Biophys Acta 1768:1211
57. Boe S, Longva AS, Hovig E (2007) Oligonucleotides 17:166
58. Boe S, Longva AS, Hovig E (2008) Oligonucleotides 18:123
59. Sundaram S, Lee LK, Roth CM (2007) Nucleic Acids Res 35:4396
60. Kurreck J (2003) Eur J Biochem 270:1628
61. Koppelhus U, Nielsen PE (2003) Adv Drug Deliv Rev 55:267
62. Brooks H, Lebleu B, Vives E (2005) Adv Drug Deliv Rev 57:559
63. Richard JP, Melikov K, Vives E, Ramos C, Verbeure B, Gait MJ, Chernomordik LV, Lebleu B (2003) J Biol Chem 278:585
64. Pujals S, Fernandez-Carneado J, Lopez-Iglesias C, Kogan MJ, Giralt E (2006) Biochim Biophys Acta 1758:264
65. Folini M, Berg K, Millo E, Villa R, Prasmickaite L, Daidone MG, Benatti U, Zaffaroni N (2003) Cancer Res 63:3490
66. Shiraishi T, Nielsen PE (2006) FEBS Lett 580:1451
67. Boe S, Hovig E (2006) Oligonucleotides 16:145
68. Cao S, Cripps A, Wei MQ (2010) Clin Exp Pharmacol Physiol 37:108
69. De Ravin SS, Malech HL (2009) Immunol Res 43:223
70. Prasmickaite L, Hogset A, Olsen VM, Kaalhus O, Mikalsen SO, Berg K (2004) Cancer Gene Ther 11:514
71. Ndoye A, Dolivet G, Hogset A, Leroux A, Fifre A, Erbacher P, Berg K, Behr JP, Guillemin F, Merlin JL (2006) Mol Ther 13:1156
72. Ndoye A, Merlin JL, Leroux A, Dolivet G, Erbacher P, Behr JP, Berg K, Guillemin F (2004) J Gene Med 6:884
73. Maurice-Duelli A, Ndoye A, Bouali S, Leroux A, Merlin JL (2004) Technol Cancer Res Treat 3:459
74. Engesaeter BO, Bonsted A, Lillehammer T, Engebraaten O, Berg K, Maelandsmo GM (2006) Cancer Biol Ther 5:1511
75. Kloeckner J, Prasmickaite L, Hogset A, Berg K, Wagner E (2004) J Drug Target 12:205
76. Intra J, Salem AK (2008) J Control Release 130:129
77. Hanzlikova M, Soininen P, Lampela P, Mannisto PT, Raasmaja A (2009) Plasmid 61:15
78. Aillon KL, Xie Y, El-Gendy N, Berkland CJ, Forrest ML (2009) Adv Drug Deliv Rev 61:457
79. Dufes C, Uchegbu IF, Schatzlein AG (2005) Adv Drug Deliv Rev 57:2177
80. Nishiyama N, Iriyama A, Jang WD, Miyata K, Itaka K, Inoue Y, Takahashi H, Yanagi Y, Tamaki Y, Koyama H, Kataoka K (2005) Nat Mater 4:934

81. Nishiyama N, Arnida A, Jang WD, Date K, Miyata K, Kataoka K (2006) J Drug Target 14:413
82. Arnida I, Nishiyama N, Kanayama N, Jang WD, Yamasaki Y, Kataoka K (2006) J Control Release 115:208
83. Shieh MJ, Peng CL, Lou PJ, Chiu CH, Tsai TY, Hsu CY, Yeh CY, Lai PS (2008) J Control Release 129:200
84. Greber UF, Willetts M, Webster P, Helenius A (1993) Cell 75:477
85. Engesaeter BO, Bonsted A, Berg K, Hogset A, Engebraten O, Fodstad O, Curiel DT, Maelandsmo GM (2005) Cancer Gene Ther 12:439
86. Engesaeter BO, Tveito S, Bonsted A, Engebraaten O, Berg K, Maelandsmo GM (2006) J Gene Med 8:707
87. Hellum M, Hogset A, Engesaeter BO, Prasmickaite L, Stokke T, Wheeler C, Berg K (2003) Photochem Photobiol Sci 2:407
88. Nandi S, Lesniak MS (2009) Expert Opin Biol Ther 9:737
89. Strauss R, Sova P, Liu Y, Li ZY, Tuve S, Pritchard D, Brinkkoetter P, Moller T, Wildner O, Pesonen S, Hemminki A, Urban N, Drescher C, Lieber A (2009) Cancer Res 69:5115
90. Bonsted A, Engesaeter BO, Hogset A, Berg K (2006) Photochem Photobiol Sci 5:411
91. Bonsted A, Engesaeter BO, Hogset A, Maelandsmo GM, Prasmickaite L, D'Oliveira C, Hennink WE, van Steenis JH, Berg K (2006) J Gene Med 8:286
92. Bonsted A, Engesaeter BO, Hogset A, Maelandsmo GM, Prasmickaite L, Kaalhus O, Berg K (2004) Gene Ther 11:152
93. Buning H, Ried MU, Perabo L, Gerner FM, Huttner NA, Enssle J, Hallek M (2003) Gene Ther 10:1142
94. Bonsted A, Hogset A, Hoover F, Berg K (2005) Anticancer Res 25:291
95. Luna MC, Chen X, Wong S, Tsui J, Rucker N, Lee AS, Gomer CJ (2002) Cancer Res 62:1458
96. Prasmickaite L, Cekaite L, Hellum M, Hovig E, Hogset A, Berg K (2006) FEBS Lett 580:5739
97. Prasmickaite L, Hellum M, Kaalhus O, Hogset A, Wagner E, Berg K (2006) Photochem Photobiol 82:809
98. Stirpe F, Battelli MG (2006) Cell Mol Life Sci 63:1850
99. Selbo PK, Sivam G, Fodstad O, Sandvig K, Berg K (2001) Int J Cancer 92:761
100. Bedard PL, de Azambuja E, Cardoso F (2009) Curr Cancer Drug Targets 9:148
101. Pastan I, Hassan R, FitzGerald DJ, Kreitman RJ (2006) Nat Rev Cancer 6:559
102. Eiklid K, Olsnes S, Pihl A (1980) Exp Cell Res 126:321
103. Imai K, Takaoka A (2006) Nat Rev Cancer 6:714
104. Selbo PK, Sivam G, Fodstad O, Sandvig K, Berg K (2000) Int J Cancer 87:853
105. Selbo PK, Rosenblum MG, Cheung LH, Zhang W, Berg K (2009) PLoS One 4(8):e6691
106. Lai PS, Pai CL, Peng CL, Shieh MJ, Berg K, Lou PJ (2008) J Biomed Mater Res A 87:147
107. Fretz MM, Hogset A, Koning GA, Jiskoot W, Storm G (2007) Pharm Res 24:2040
108. Azambuja E, Fleck JF, Batista RG, Menna Barreto SS (2005) Pulm Pharmacol Ther 18:363
109. Poddevin B, Orlowski S, Belehradek J Jr, Mir LM (1991) Biochem Pharmacol 42(Suppl): S67–S75
110. Berg K, Dietze A, Kaalhus O, Hogset A (2005) Clin Cancer Res 11:8476
111. Raemdonck K, Naeye B, Buyens K, Vandenbroucke RE, Høgset A, Demeester J, de Smedt S (2009) Biodegradable dextran nanogels for RNA interference: focusing on endosomal escape and intracellular siRNA delivery. Adv Funct Mater 19:1–10
112. Prasmickaite L, Hogset A, Tjelle TE, Olsen VM, Berg K (2000) J Gene Med 2:477
113. Weyergang A, Selbo PK, Berg K (2006) J Control Release 111:165
114. Nishiyama N, Morimoto Y, Jang WD, Kataoka K (2009) Adv Drug Deliv Rev 61:327
115. Selbo PK, Kaalhus O, Sivam G, Berg K (2001) Photochem Photobiol 74:303
116. Dietze A, Bonsted A, Hogset A, Berg K (2003) Photochem Photobiol 78:283
117. Dietze A, Engesaeter B, Berg K (2005) Photochem Photobiol Sci 4:341

118. Hogset A, Engesaeter BO, Prasmickaite L, Berg K, Fodstad O, Maelandsmo GM (2002) Cancer Gene Ther 9:365
119. Ndoye A, Bouali S, Dolivet G, Leroux A, Erbacher P, Behr JP, Berg K, Guillemin F, Merlin JL (2004) Int J Oncol 25:1575
120. Høgset A, Prasmickaite L, Tjelle TE, Berg K (2000) Hum Gene Ther 11:869
121. Prasmickaite L, Hogset A, Berg K (2001) Photochem Photobiol 73:388
122. Folini M, Bandiera R, Millo E, Gandellini P, Sozzi G, Gasparini P, Longoni N, Binda M, Daidone MG, Berg K, Zaffaroni N (2007) Cell Prolif 40:905
123. Cabral H, Nakanishi M, Kumagai M, Jang WD, Nishiyama N, Kataoka K (2009) Pharm Res 26:82
124. Berg K, Høgset A, Prasmickaite L, Weyergang A, Bonsted A, Dietze A, Lou PJ, Bown S, Norum OJ, Møllergård HM, Selbo PK (2006) Photochemical internalization (PCI): a novel technology for activation of endocytosed therapeutic agents. Med Laser Appl 21:239–250
125. Dietze A, Peng Q, Selbo PK, Kaalhus O, Muller C, Bown S, Berg K (2005) Br J Cancer 92:2004
126. Norum OJ, Bruland OS, Gorunova L, Berg K (2009) Int J Radiat Oncol Biol Phys 75(3):878

Top Curr Chem (2010) 296: 283–304
DOI: 10.1007/128_2010_66

Published online: 2 June 2010

Visualizing Uptake and Intracellular Trafficking of Gene Carriers by Single-Particle Tracking

N. Ruthardt and C. Bräuchle

Abstract Single-particle microscopy und live-cell single-particle tracking are powerful tools to follow the cellular internalization pathway of individual nanoparticles such as viruses and gene carriers and investigate their interaction with living cells. Those single-cell and single-particle methods can elucidate the "black box" between application of the gene carrier to the cell and the final gene expression and allow the essential bottlenecks to be identified in great detail on the cellular level. In this review we will give a short introduction into single-particle tracking microscopy and present an overview of the mechanisms of DNA delivery from attachment to the cell membrane over internalization towards nuclear entry unraveled by single-particle methods.

Keywords DNA/RNA transfection, Fluorescence wide-field microscopy, Gene carriers, Gene therapy, Single-particle tracking, Trajectory analysis

Contents

N. Ruthardt (✉), C. Bräuchle
Department of Chemistry and Biochemistry, Ludwig-Maximilians-Universität München, Butenandtstr. 5-13, 81377 München, Germany
e-mail: Nadia.Ruthardt@cup.uni-muenchen.de
Center for NanoScience (CeNS), Ludwig-Maximilians-Universität München, Butenandtstr. 5-13, 81377 München, Germany

Abbreviations

EGF	Epidermal growth factor
EGFP	Enhanced green fluorescent protein
NGF	Nerve growth factor
PEI	Polyethyleneimide
PLL	Poly-L-lysine

1 Introduction

The delivery of nucleic acids (DNA or RNA) into cells is of central interest for gene therapy in a variety of human diseases including cancer [1]. In order to be transcribed and to exert its intended action, the foreign DNA has ultimately to reach the nucleus of the target cell. In the case of RNA, transport into the nucleus is not necessary as the action of RNA occurs in the cytoplasm (e.g., siRNA). Tissues and cells do not possess special mechanisms for uptake of DNA and several barriers hamper the efficient delivery of the DNA into the nucleus. Those barriers include general obstacles in the body to reach the target tissue after systemic delivery as well as barriers on the cellular level [2]. In order to deliver the DNA, gene carriers (also referred to as gene vectors) have to be used to achieve packaging of the DNA, protection in the body against degradation and eventually specific targeting to the diseased tissue. Currently, two approaches for gene carriers are used: viral and non-viral gene carriers. Several excellent reviews exist for both approaches [3–11]. In this review, we will only discuss non-viral gene carriers. Those artificial carriers have the advantage of a chemically defined synthesis and strongly reduced immune response of the body compared to viral-vectors. However, all currently studied non-viral systems are far less efficient than viral systems based on viruses that have been optimized by natural selection over millions of years. Therefore, one approach to optimize non-viral vectors is to mimic the infection pathway of viruses. In order to do so, the infection pathway of viruses has to be resolved in great detail [12–15] as well as the single steps of the entry pathway of the "artificial viruses" in order to identify the barriers and bottlenecks for gene delivery as a basis for further optimizations [2, 16, 17]. Bulk measurements use the expression of a transgene

as read-out for transfection efficiency, leaving a "black box" for the events between application of the gene carrier to the cell and the final gene expression. Single cell and single-particle methods can elucidate the "black box" and resolve the individual steps of transfection in real time. Thereby, they allow the essential bottlenecks to be identified in great detail on the cellular level that have to be passed once a gene carrier has reached its target cell after systemic administration to the body. Live-cell fluorescence microscopy also has the advantage of including dynamic information on the transfection process as it contains temporal as well as spatial information with high resolution. In this review, we concentrate on single-particle tracking using highly sensitive fluorescence live-cell microscopy for investigation of the transfection pathway in real-time on a single cell level.

2 Investigating the Internalization of Gene Carriers into Cells

Most of the insights into internalization and efficiency of various gene carriers have been obtained by techniques such as flow cytometry and confocal microscopy. Whereas the first is a bulk measurement technique with ensemble averaging of up to several thousand cells and does not provide detailed information on the uptake process on a single cell level, the latter has been used with fixed cells to acquire snapshots of the transfection process on a single cell level. The main optical technique used to study the internalization pathway of gene carriers is multi-color live-cell fluorescence microscopy [18]. Compartments of the endocytic pathway in living cells can be visualized by fluorescently labeled markers (e.g., dye-coupled transferrin, cholera toxin B, or dextrans) or more specifically by cellular expression of marker proteins fused to fluorescent proteins (e.g., clathrin-GFP, caveolin-GFP) [19]. The entry of gene carriers labeled with a fluorescent dye can then be followed in the living cell and colocalization analysis with cellular compartments labeled with another fluorescent dye provides information about the route taken. This method can be extended by using chemical inhibitors or siRNA for specific entry pathways to test whether the internalization of gene carriers can successfully be blocked. However, the use of markers and inhibitors at the single cell level has some caveats [20]. Based on those techniques, it was revealed that all tested gene carriers enter cells by endocytosis [21–23], and also those connected to cell penetrating peptides [24–26]. However, there is no generalized internalization pathway for gene carriers. The exact endocytic pathway used by gene carriers is strongly dependent on the individual cell type and also the sort of gene carrier [21, 27]. Often, several endocytosis pathways are used simultaneously and inhibition of one pathway may increase the internalization by an alternative route. In addition, the pathway finally resulting in successful gene expression varies with cell line and also gene carrier type [27]. Therefore, the knowledge of the exact internalization pathway of a specific gene carrier is required to improve its efficiency. One approach to increase transfection efficiency is to predefine a pathway leading to successful gene expression by targeting to a specific receptor.

This can concomitantly be connected to cell specific targeting [28–31]. However, the exact entry pathway has to be defined for each target cell line and particle type individually. The possibilities of traditional confocal microscopy as described above to extract dynamic information are limited. A relatively new technique to investigate the dynamic process of transfection in detail is the tracking of single gene carriers in real-time in living cells to obtain spatial as well as temporal information with high resolution.

3 Single-Particle Tracking Microscopy

3.1 Microscope Set-Up

Single-particle techniques using highly sensitive fluorescence wide-field microscopy reveal the internalization process on short time scales and in great detail. This allows continuous observation of the internalization of single gene carriers, starting with their attachment to the cell membrane, followed by individual steps of the uptake process and intracellular trafficking. Imaging of single gene carriers eventually labeled with a few fluorophores at high temporal resolution over several minutes requires highly sensitive detection methods. Typically, these highly sensitive microscopes are custom-built and based on an inverted microscope (Fig. 1). Excitation is performed by laser light which provides the necessary excitation intensity required for strong photon emission by the fluorophores. Typical laser lines are 488, 532, 561, and 635 nm for excitation of common fluorophores. The availability of several laser lines allows simultaneous imaging of two to three fluorophores, depending on emission spectra of the labels and filters available. The aligned laser light is guided into the back of the objective by optics such as mirrors, dichroic mirrors, lenses, and optical fibers. Acousto-optical tunable filters (AOTFs) allow selecting the appropriate excitation laser without speed limitations or vibrational and mechanical constrains related to mechanical shutters or rotating wheels. In addition, they can easily accommodate several laser lines at different output wavelengths. The cells are kept at 37°C throughout the experiment by a temperature controlled stage (heating table). As oil immersion objectives are in direct contact with the cover glass surface where the cells are grown, they act as a strong heat sink for the cells. Hence, it is necessary to heat the objective to 39°C and an adjustable correction collar is needed to correct the optics for the higher temperature. There are also microscope stage incubator chambers available for adjusting the CO_2 level, but with the exception of long-time experiments, the use of CO_2-independent medium is sufficient. Focal instabilities in the microscope mechanics due to temperature changes in the surroundings after mounting the sample are major troubles for single-particle tracking. An auto-focus system is advantageous and keeps the sample at a constant z-position. The emission light is typically collected by 60× or 100× oil immersion objectives with high numerical

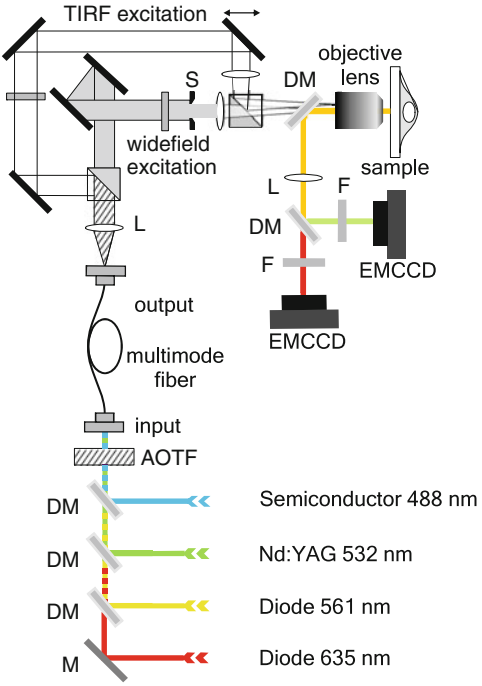

Fig. 1 Schematic drawing of a wide-field single-particle tracking fluorescence microscope equipped. Several lasers are used as excitation source for different fluorophores with fast selection by an acousto-optical tunable filter (AOTF). The collimated laser light is coupled into the objective such that only the observed area is illuminated. The emission light is separated from the excitation light by a dichroic mirror. In the case of multi-color imaging, the emission light is separated by a second dichroic mirror and the two emission channels are detected on EM CCD cameras. As an option, the excitation path can alternatively be switched by a beam splitter to total internal reflection illumination (TIRF) for imaging of processes close to the coverslip, e.g., the basal cellular plasma membrane. *DC* dichroic mirror, *M* mirror, *L* lens, *S* slit, *F* filter. Adapted with permission, courtesy of Dr. Sergey Ivanchenko

aperture up to 1.49 NA and separated from the excitation light by appropriate dichroic mirrors depending on the fluorophores used. The fluorescence emission is then directed to and detected by a highly sensitive and fast electron multiplied charge-coupled device (EM CCD) camera. For multi-color imaging, the use of two separate cameras for detection instead of simultaneous illumination of the two halves of a single camera chip increases the field of view and combinatorial possibilities of multiple fluorophores for labeling, but also increases the cost of the set-up substantially. The exact configuration of the set-up, mainly the choice of lasers, dichroic mirrors, and filters, depends on the combination of fluorophores used and may have to be adapted for the individual experiments by the user. Also accessory optics like total internal reflection fluorescence microscopy (TIRFM) illumination (see Fig. 1) or confocal detection can be added to increase the flexibility and variability of custom-built set-ups. TIRF illumination is especially interesting for fast tracking of cell surface associated events at the basal plasma membrane.

3.2 Trajectory Analysis and Mean-Square Displacement Plots

In the acquired image sequences, the fluorescent particles can be identified as bright spots on a dark background. Each frame in the movie is a representation of the position of the particles at a certain time point. By extraction of the x and y coordinates of the particles derived from the centroids of their diffraction limited spots in all frames of the movie, the trajectories of the particles can be obtained. This is typically performed by a particle-finding algorithm that first reduces background noise and then selects particles by setting an intensity threshold of the filtered image in the first round. In the second round, particles for tracking are selected based on their intensity and size. The x and y coordinates are obtained by fitting a 2D-Gaussian function to the particle's intensity profile (Fig. 2a). The particle coordinates are subsequently used for calculating the corresponding trajectories based on a nearest-neighbor algorithm [32, 33]. With this method, a positional accuracy well beyond the optical diffraction limit can be achieved. The centroid position of a sufficiently bright fluoropore can be determined with nanometer precision [34]. Thus, trajectories can be generated that are well below the resolution of light microscopes and impressively demonstrate the power of single-particle tracking.

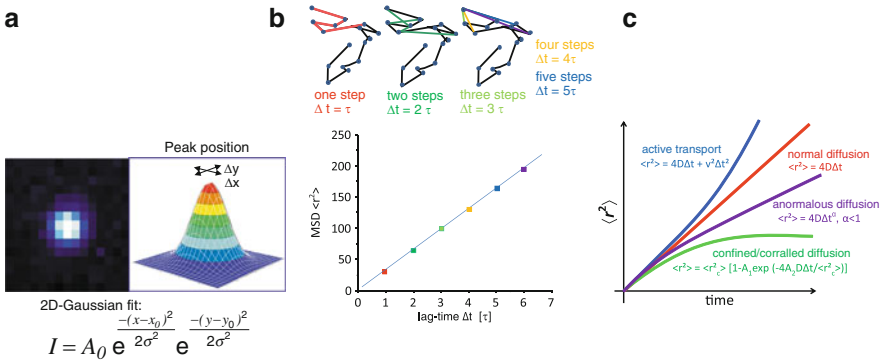

Fig. 2 Positional detection and mean-square displacement (MSD). (**a**) The x, y-coordinates of a particle at a certain time point are derived from its diffraction limited spot by fitting a 2D-Gaussian function to its intensity profile. In this way, a positional accuracy far below the optical resolution is obtained. (**b**) The figure depicts a simplified scheme for the analysis of a trajectory and the corresponding plot of the time dependency of the MSD. The average of all steps within the trajectory for each time-lag Δt, with $\Delta t = \tau, \Delta t = 2\tau, \ldots$ (where τ = acquisition time interval from frame to frame) gives a point in the plot of MSD = f(t). (**c**) The time dependence of the MSD allows the classification of several modes of motion by evaluating the best fit of the MSD plot to one of the four formulas. A linear plot indicates normal diffusion and can be described by $<r^2> = 4D\Delta t$ (D = diffusion coefficient). A quadratic dependence of $<r^2>$ on Δt indicates directed motion and can be fitted by $<r^2> = v^2\Delta t^2 + 4D\Delta t$ (v = mean velocity). An asymptotic behavior for larger Δt with $<r^2> = <r_c^2>\,[1 - A_1 \exp(-4A_2 D\Delta t/<r_c^2>)]$ indicates confined diffusion. Anomalous diffusion is indicated by a best fit with $<r^2> = 4D\Delta t^{\alpha}$ and $\alpha < 1$ (sub-diffusive)

The resulting trajectories are usually analyzed for the mode of motion executed by the particle as the motion provides information on the location and status of the particle as described in this review. The most common analysis starts with the calculation of the so-called mean-square displacement (MSD). Then, the time dependence of the MSD is plotted. This plot allows a mode of motion analysis [35]. A simplified way to calculate the MSD is depicted in Fig. 2b. The mean square displacement $<r^2>$ describes the average of the squared distances between a particle's start and end positions for all time-lags of certain length Δt within one trajectory.

With increasing time-lag, however, the uncertainty of the MSD values increases. When the calculated time-lag becomes a substantial fraction of the total points of the trajectory, there are not enough pairs of data points for an accurate calculation of the MSD as shown by the formulas for the standard deviation [36]. To account for this uncertainty, the MSD should always be calculated for time-lags corresponding to only about one quarter of the total number of points in the trajectory [35]. So, for example, in a trajectory with 800 data points, the MSD is calculated only for time-lags spanning a maximum of 200 points. As a consequence, the time-axis of an MSD plot can only represent a fraction of the time scale of the trajectory. From evaluation of the MSD plot, information about the mode of motion can be obtained (Fig. 2c). This mode of motion can then be interpreted in a biological context and conclusions on the location and environment of the tracked particle can be drawn.

Normal and anomalous diffusion is described by

$$\left\langle r^2 \right\rangle = 4D\Delta t^{\alpha}, \tag{1}$$

where D is the diffusion coefficient. The factor 4 is specific for diffusion in two dimensions. For normal diffusion (Brownian motion), $\alpha = 1$ and a linear dependence of $<r^2>$ on the time interval Δt is given. Anomalous diffusion is described by $\alpha < 1$ and is typically observed, when the diffusive particle is hindered by obstacles.

Confined or corralled diffusion is indicated by an asymptotic behavior of $<r^2>$ for large Δt and implies a confinement for the diffusive particle. The following formula describes the relation between $<r^2>$ and Δt:

$$\left\langle r^2 \right\rangle = \left\langle r_c^2 \right\rangle \left[1 - A_1 \exp\left(-4A_2 D\Delta t / \left\langle r_c^2 \right\rangle\right)\right]. \tag{2}$$

$<r_c{}^2>$ is an approximation of the size of the confinement and the constants A_1 and A_2 are determined by the confinement geometry. The asymptotic value of $<r^2>$ for large Δt, which is independent of the confinement geometry, can be taken for the calculation of the size of the confinement $<r_c{}^2>$. We note that confinement within a certain region can only be observed when the observation time is long compared to the time between successive contacts of the particle with the barrier. For short observation times, normal or anomalous diffusion within the confinement is observed.

Active transport is described by a quadratic dependence of the mean square displacement $<r^2>$ on Δt with

$$\left\langle r^2 \right\rangle = v^2 \Delta t^2 + 4D\Delta t. \tag{3}$$

v is the velocity of the directed motion which is also called drift. Superimposed on this motion is a normal diffusion with the diffusion coefficient D. The whole process can be described with the picture of a conveyor belt, where particles are transported but can also diffuse to both sides as well as along the belt. By fitting (3) to an MSD curve, the mean velocity v of the directed motion and the diffusion coefficient D are obtained.

MSD curves of diffusive motion can be very heterogeneous (Fig. 3) and it has to be tested which of the models for diffusion results in a higher correlation coefficient for the fitted plot.

4 Single-Particle Tracking of Gene Carrier Internalization

Combining sensitive fluorescence wide-field microscopy and single-particle tracking, de Bruin and coworkers followed the internalization process of single polymeric gene carriers (polyplexes) in real time in living cells with a temporal resolution of 300 ms [37]. In trajectories showing the full internalization process of epidermal growth factor receptor (EGFR)-targeted polyplexes starting with attachment to the cell membrane followed by uptake into the cell and finally active transport towards the nucleus, they typically found three phases of motion (Fig. 3, the video corresponding to the trajectory can be found in the supplemental material of [37]). Phase I showed slow directed motion, phase II consisted either of normal, anomalous, and confined diffusion or a combination of them, and finally phase III showed fast active transport in the cytoplasm. Shortly after attachment to the cell membrane, the polyplexes started a slow directed transport during phase I with velocities of typically 0.01 μm/s. This transport was attributed to the movement of the underlying actin cytoskeleton mediated by the EGF receptor and linker proteins as revealed by dual-color microscopy. The polyplexes were thus transported by the retrograde actin flow within the cell. A similar behavior was also observed for untargeted polyplexes by Bausinger et al. [38], where the cell-surface attached polyplexes colocalized with actin fibers of the underlying cortical actin network. In these experiments, single-particle tracking of the membrane bound polyplexes revealed a variety of motion behavior including 2D free diffusion, anomalous diffusion as well as complete immobilization. In addition, slow active transport around 0.01 μm/s typical for actin mediated transport was observed at later stages. For untargeted cationic gene carriers, cell-surface proteoglycans such as heparan sulfate proteoglycans (HSPGs) have been suggested as a kind of “unspecific receptor” with binding characteristics based on electrostatic interactions [23, 39].

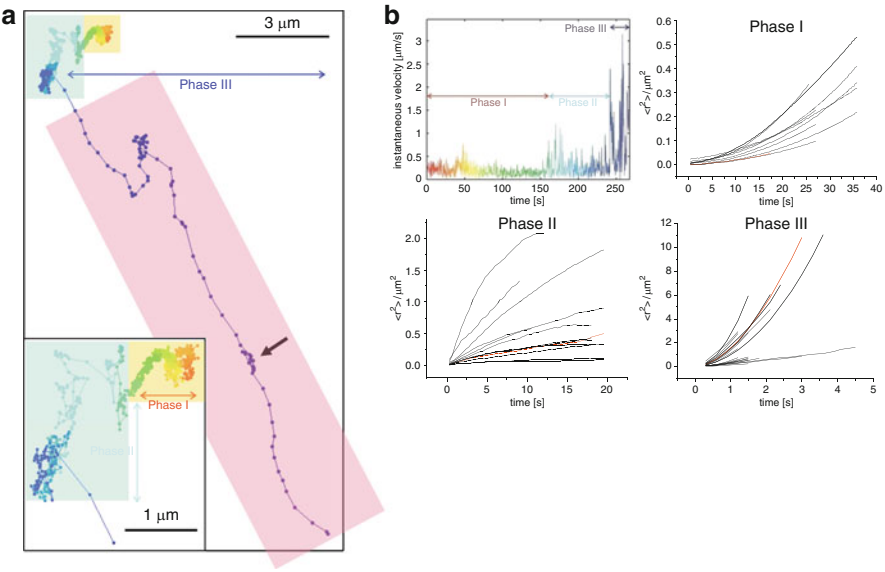

Fig. 3 Single-particle tracking of the internalization of an epidermal growth factor receptor (EGFR)-targeted polyplex. (**a**) Trajectory of a polyplex incubated on a HuH7 cell. The particle was tracked for 4 min and 30 s at a temporal resolution of 300 ms and the trajectory displays the three phases typically observed during internalization. The trajectory starts immediately after the polyplex attached to the cell membrane. The color of the trajectory is shown as changing from red to blue-violet with progressing time and matches the corresponding velocity plot in (**b**). The *arrow* indicates a spot of back-and-forward movement. The corresponding video is available as supplemental information in [37]. The *overlaying color boxes* mark the phases: *yellow*: phase I – slow active transport, *blue*: phase II – anomalous and confined diffusion, *purple*: phase III – active transport. (**b**) Instantaneous velocity plot of the trajectory shown in (**a**) and MSD plots of the three phases analyzed from several trajectories. The plots corresponding to the trajectory presented in panel (a) are drawn in *red*. Based on (1), the mean drift velocity for all plots in phase I was $v_I = 0.015$ μm/s and the corresponding diffusion coefficient $D_I = 4 \times 10^{-4}$ μm^2/s. For phase II, the plots could not be averaged due to heterogeneous appearance showing anomalous, normal and confined diffusion. In case of confined motion, the confinement diameters calculated from the information provided in (2) ranged from 0.3 to 2.0 μm. The values for α in anomalous diffusion ranged from 0.4 to 0.7. Phase III plots show a quadratic dependence of $<r^2>$ on Δt indicating directed motion. The mean velocity for the presented trajectories was calculated as $v_{III} = 0.7$ μm^2/s with a corresponding mean diffusion coefficient of $D_{III} = 0.1$ μm^2/s. Adapted with permission from the American Society of Gene Therapy [37]

The results of the single-particle tracking from Bausinger et al. support the model of receptor binding by the polyplexes and receptor clustering before endocytosis occurs. Recent experiments using colocalization with fluorescent markers, inhibitor, and siRNA treatment by Payne [40] provides strong evidence for proteoglycans as the unspecific receptors for polyplexes. Targeting gene carriers to specific cell surface receptors can influence the internalization behavior. De Bruin [37] and coworkers demonstrated in their study that targeting of polyplexes to the EGF receptor leads to increased and accelerated endocytosis of the polyplexes. Instead of

the unspecific proteoglycan mediated endocytosis, the polyplexes were quickly internalized by the specific EGF receptor mediated endocytosis. The fast endocytosis was represented in the trajectories by strongly shortened time spans of phase I motion.

The internalization event itself – namely the pinching off of an endocytic vesicle from the plasma membrane – cannot be resolved by light microscopy. However, by combining single-particle tracking with fluorescence quenching of extracellular polyplexes at different time points, de Bruin et al. [37] showed that the internalization into an endocytic vesicle occurs during phase I. More interestingly, some polyplexes defined as intracellular continued the slow directed movement characteristic for phase I for a certain time before entering the movement characteristic for intracellular particles. They suggested that the newly formed endocytic vesicles close to the membrane may be trapped in the cortical actin cytoskeleton and therefore show motion similar to the polyplexes bound to the membrane and connected to the actin cytoskeleton by transmembrane proteins.

5 Types of Intracellular Movement

After internalization in phase I, most polyplexes show anomalous or confined diffusion (phase II) followed by active transport (phase III) [37]. The anomalous diffusion and confinement displayed by the MSD analysis represent the local microenvironment of the particles in the cytoplasm where the cytoskeleton, organelles and large macromolecules are local obstacles for free diffusion. Suh et al. [41] tracked internalized polyplexes with a temporal resolution of 33 ms and found diffusive motion of polyplexes where the corresponding trajectories showed hop diffusion (Fig. 4). These hop diffusion patterns can be interpreted as the cages of the

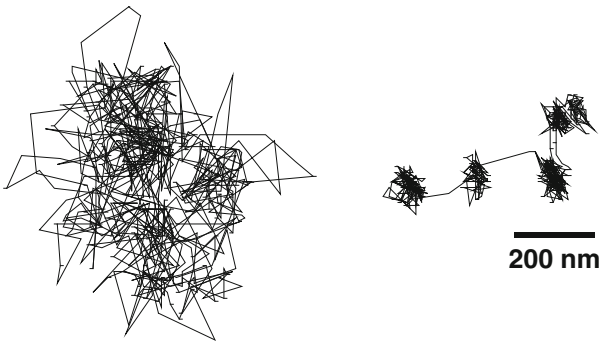

Fig. 4 Example trajectories of diffusive (*left*) and subdiffusive (*right*) gene carriers recorded with a temporal resolution of 33 ms. The subdiffusive trajectory is characterized by confined motion in the MSD plot. However, the hop diffusion pattern of the trajectory can only be detected by its morphological pattern and not by the shape of MSD plot. Adapted with permission from the American Chemical Society and American Institute of Chemical Engineers [41]

local microenvironment or may even represent the attachment of the vesicles to subcellular structures followed by detachment.

Long range active transport occurs with motor proteins (kinesins or dyneins) along microtubules with velocities up to 4 μm/s and is a feature of internalized particles. Typically, this long range active transport displays the so-called stop-and-go motion as a result from binding and unbinding of motor proteins to the microtubules [37, 41, 42]. Reversal of the transport direction can frequently be observed (see arrow in Fig. 3). In addition to active transport along microtubules, active transport in the cytosol can also occur by so-called actin comet tails. In contrast to active transport by motor proteins, this type of movement is generated by polymerization of actin behind the moved cargo without involvement of motor proteins [43]. The resulting force is used for example, by bacterial pathogens for movement in infected host cells as well as for transport of organelles within the cell. De Bruin et al. observed active transport of endosomes containing polyplexes by actin tails (see supplementary video in [37]). Merrifield et al. tracked endosomes moving by actin tails with a velocity of 0.24 ± 0.10 μm/s [44]. With single-particle tracking, it can be detected by dual-color microscopy with simultaneous imaging of fluorescently labeled actin in order to identify actin tails correlating with active movement.

It has to be noted that the detection of the various diffusive states as well as active transport depends on the time scale of observation. For short time scales, the short-range motion of tracked particles may seem similar and indicates the same local microenvironment for the particles as it is dominated by Brownian motion [37, 41]. Confined diffusion as well as active transport require a minimal duration for detection and appear at longer time scales (see MSD plot). To display confined diffusion, the particle has to experience the boundaries of confinement in its local microenvironment which restrict the free diffusion on longer time scales. Similarly, for active transport, the second part of (3) $4D\Delta t$ is predominant on short time scales. The active transport component $v^2\Delta t^2$ becomes dominant at longer observation periods.

In addition, to detect the various types of motion displayed by a moving particle within a trajectory, the MSD must be taken over subregions of the trajectory. Otherwise, the MSD over the full trajectory would result in an averaging effect over all modes of motion. The careful description of the various modes of motion within one trajectory requires the separation of the trajectory in several parts, e.g., manually according to morphological differences or by velocity thresholds [37, 41]. A careful trajectory analysis also includes a morphological analysis of the trajectory pattern and should include more information than the shape of the MSD or effective diffusion coefficient curves. Particles showing hop diffusion may fulfil all analysis criteria for "diffusive" motion whilst the hop diffusion pattern is only visible in the trajectory [41].

A more sophisticated method for automated trajectory analysis and mode of motion detection provides the use of a rolling-window algorithm. The algorithm described by Arcizet et al. [45, 46] reliably separates the active and passive states of particles and extracts the velocity during active states as well as the diffusion coefficients during passive states (Fig. 5). It takes into account that active transport by microtubules is characteristically directional over a certain time and measures

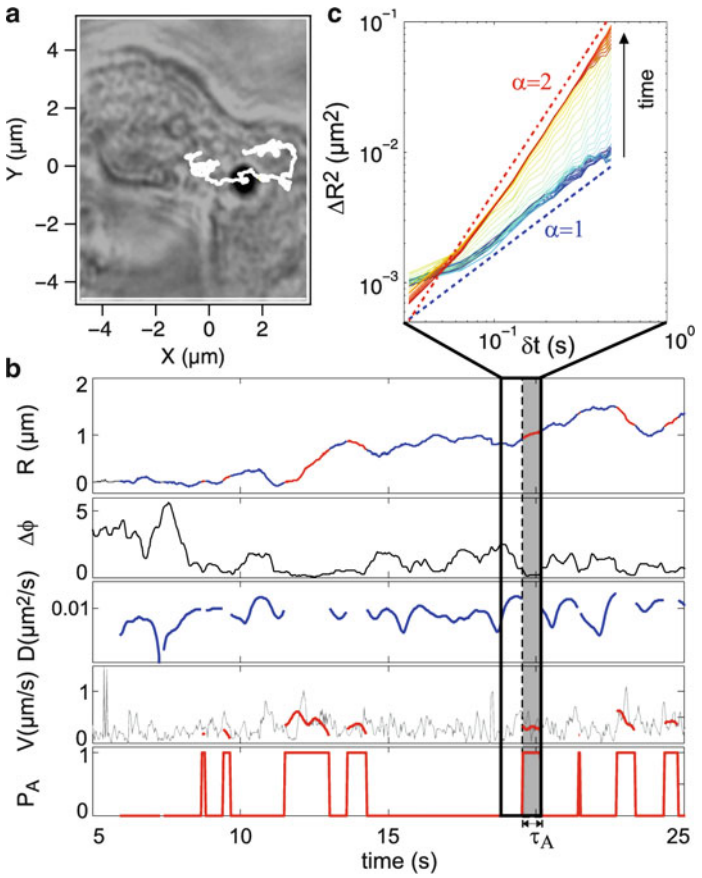

Fig. 5 Trajectory analysis with an automated rolling-window algorithm for detecting active transport and diffusive phases of motion. (**a**) Analyzed trajectory of an internalized microbead overlayed onto the transmission image of the cell. (**b**) The rolling-window algorithm analysis of the trajectory with, from the top to the bottom, displacement *R(t)* with diffusive (*blue*) and active (*red*) phases, standard deviation $\Delta\phi$ of the angle correlation function, diffusion coefficient *D(t)* retrieved during the diffusive states, instantaneous velocity (*light grey*) and algorithm-retrieved velocity during the active phases (*red*), and the binary state variable P_A for active motion probability. The *shaded* part of the frame highlights an active phase. (**c**) Examples of local MSD calculated with fits to (1) with trends for $\alpha = 1$ (normal diffusion, *blue dotted line*) and 2 (active transport, *red dotted line*). Reproduced with the permission from the American Physical Society [46]

the directional persistence of particle motion by the angular correlation of following steps by an angle correlation function [46] resulting in an estimate of the probability of the particle undergoing active motion within the analyzed subregion. Of course, the higher the temporal resolution and the more data points acquired, the better and more detailed the analysis can be. As a consequence, for very fast transport events, the temporal resolution has to be high enough to acquire sufficient data points for analysis and separation between modes of motion.

6 Defining the Endosomal Pathway by Its Motion Characteristics

As gene carriers are internalized by endocytosis, the motion characteristics inside the cell resembles the movement of the endosomal compartments within the cell and the formed vesicles are transported along the microtubule network [38]. Suh et al. [41] quantified the transport of individual internalized polyplexes by multiple-particle tracking and showed that the intracellular transport characteristics of polyplexes depend on spatial location and time posttransfection. Within 30 min, polyplexes accumulated around the nucleus. An average of the transport modes over a 22.5 h period after transfection showed that the largest fraction of polyplexes with active transport was found in the peripheral region of the cells whereas polyplexes close to the nucleus were largely diffusive and subdiffusive. Disruption of the microtubule network by nocodazole completely inhibits active transport and also the perinuclear accumulation of polyplexes [37, 40, 47].

Sauer et al. [48] investigated the internalization of magnetic polyplexes with single-particle tracking. Magnetic particles can be directed within the body to the diseased tissue by application of a magnetic field. On the single cell level, the three-phased internalization behavior was also observed for these particles and was found to be independent of the applied magnetic field. Therefore, the application of a magnetic field affected only extracellular magnetic polyplexes and concentrated these particles onto the plasma membrane whereas the cellular processes of uptake and trafficking were unaffected.

The three phases described by de Bruin et al. [37] for the internalization of polyplexes were also found in a study of endocytic trafficking of single receptors by Rajan et al. [49]. They took advantage of the extraordinary features of quantum dots (QDots) to follow the internalization of single nerve growth factor (NGF) receptors by single-particle tracking on the single protein level at 79 ms temporal and nanometer-scale spatial resolution. QDots are fluorescent semiconductor nanocrystals with tunable fluorescence emission dependent on their size. They are extremely bright with extraordinary photostability. The emission spectrum shows a characteristic narrow peak, making it favorable for multi-color applications. Common fluorescent dyes such as Alexa, Cyanine, or Atto dyes suffer from fast bleaching and limited signal-to-noise ratio against the autofluorescence background of living cells. This is especially critical in cases where labeling at single molecule ratio is required [15]. The photophysical properties of the labeling dyes are then critical for sufficiently long tracking to obtain meaningful trajectories. A drawback of QDots is their blinking behavior, which, on the other hand, can be used to discriminate between single QDots and aggregates. By tracking the endocytosis of single labeled receptors by QDot-NGF, Rajan et al. demonstrate that the distinct phases of motion reflect the underlying phases of endocytosis which are regulated with a high degree of uniformity. Once endocytosed, the receptor-QDot-NGF complexes did not show much variation and their dynamics are correlated with the type of the endosomal compartment. By tracking the internalization of QDot-NGF complexes in neurons

at 10 frames/s, Cui et al. investigated the long range motion characteristic of endosomes in axons [42]. Within the axons, single QD-NGF containing endosomes showed active transport along microtubules with typical stop-and-go motion towards the cell body. Interestingly, their study showed that the average speed of endosomal movement varied considerably between axons and suggests that the ability to support endosomal traffic may differ between individual axons. The superior optical properties of QDots compared to conventional organic fluorophores even allow the detection of individual microtubule motor steps in living cells. By tracking endocytosed QDots with an extremely short temporal resolution of 300 μs, Nan et al. [50] resolved individual 8 nm steps taken by endosomes traveling with a velocity of about 3 μm/s.

7 Endosomal Release of Gene Carriers

In order to reach the nucleus, DNA intended for transfection has to escape the endosome and be released from the carrier. Currently, this is a major bottleneck of non-viral gene carriers [22, 51]. To optimize the overall efficiency of transfection, the mechanism of endosomal release utilized by current gene carriers is being investigated but is not yet fully understood. For PEI – the polymer with the highest transfection efficiency – two hypotheses for its release are discussed: first, the proton-sponge effect and second the membrane destabilizing effect [52]. The first hypothesis is based on the high buffering capacity of PEI accompanied by an increased chloride accumulation resulting in osmotic swelling of the endosome [53], the second model by binding of PEI to the membrane [54]. An approach to increase endosomal escape is the use of membrane destabilizing peptides [55, 56]. Generally, the release of gene carriers may be a slow and transient process occurring at different times for each endosome. To image the endosomal escape and DNA release behavior of different polyplex compositions with varying polymers on a single vesicle level, de Bruin et al. took advantage of the possibility of inducing release of internalized double-labeled polyplexes photochemically using laser light [57]. In this technique, endosomal membranes were loaded with a photosensitizer that was activated by a 405 nm laser pulse to produce singlet oxygen resulting in the rupture of endosomal membranes and release of the endosomal content. By imaging the release process of single endosomes at high temporal resolution, they showed that the release of the DNA is dependent on the polymer used for complexation. After rupture of the endosomal membrane, escape of the content occurred on a millisecond time scale. In the case of polyplexes based on PEI and DNA, the fluorescence signal of the labeled PEI vanished in less than 1 s due to diffusion into the cytosol. The fluorescence signal of the labeled DNA, in contrast, remained at the location of the ruptured endosome (Fig. 6). As DNA molecules larger than ~1,000 bp cannot diffuse within the crowded cytoplasm [58], released plasmid DNA is basically immobile in contrast to the smaller sized polymer. However, the DNA was protected from degradation until endosomal rupture occurred and

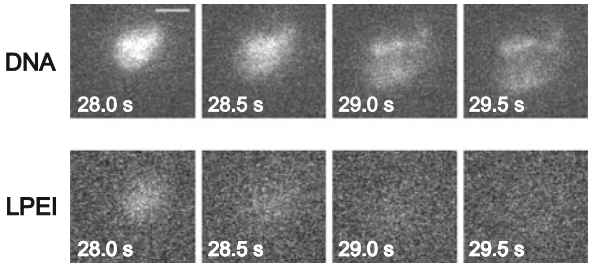

Fig. 6 Endosomal release of PEI/DNA polyplexes. Rupture of a single endosome filled with polyplexes consisting of DNA and PEI labeled by different fluorophores. The *upper panel* shows the DNA signal and reveals that the intact DNA remains in a confined area of the damaged endosome without diffusion in the cytosol. The *lower panel* shows the polymer signal whose fluorescence signal disappears due to diffusion into the cytosol. *Scale bar*: 2 μm. Reproduced with permission from Elsevier B.V. [57]

successfully released from the PEI. For polyplexes composed of PLL and DNA, the endosomal escape was different. The DNA remained either tightly bound to the polymer or vanished quickly by diffusion simultaneously with the polymer due to degradation within the endosome before its rupture. How the DNA molecules get into the nucleus after release is still unclear. There is evidence that plasmid DNA can be trafficked in the cytosol along microtubules. The DNA interacts with microtubules most likely through cytosolic adaptor proteins as demonstrated by Vaughan and Dean [59] using a microtubule spin-down assay. They also showed that microinjected plasmid DNA accumulates around the nucleus after 5 h over distances that are unlikely for free diffusion. However, active transport of free plasmid DNA in the cytoplasm has not been shown yet.

This is in contrast to viruses, where the virus particles also show active transport when present in the cytosol after fusion with the plasma membrane or endosomal membrane [60–62]. This is due to the ability of specific proteins of the virus particle to bind motor proteins. Single-particle tracking reveals that the quantitative intracellular transport properties of internalized non-viral gene vectors (e.g., polyplexes) are similar to that of viral vectors (e.g., adenovirus) [63]. Suk et al. showed that over 80% of polyplexes and adenoviruses in neurons are subdiffusive and 11–13% are actively transported. However, their trafficking pathways are substantially different. Polyplexes colocalized with endosomal compartments whereas adenovirus particles quickly escaped endosomes after endocytosis. Nevertheless, both exploit the intracellular transport machinery to be actively transported.

8 Nuclear Entry of Transgenes

The detection of gene carriers in the nucleus by optical methods is controversially reported. Some studies report the presence of gene carriers in the nucleus [64–66], in others the presence of gene carriers was not detected in the nucleus [22, 54, 67,

68]. It is also unclear whether complete particles can actually enter the nucleus. A possible scenario for polyplexes to enter the nucleus is during mitosis when the breakdown of the nuclear envelope occurs. Polyplexes have been shown to move along the astral microtubules of the mitotic spindle apparatus [38] and it was shown that mitosis increases the rate of successfully transfected cells [69–72]. In most studies the evidence for transgenic DNA in the nucleus is given indirectly by the expression of the transgene. One reason for the difficulty to detect transgenic DNA in the nucleus by optical methods is that the number of DNA molecules finally reaching the nucleus is very small compared to the amount of DNA added to the cells. By using quantitative PCR, Cohen et al. found 75 and 50,000 plasmids per nucleus for B16F10 cells and A549 cells (which scaled to only 1 and 5% of the applied dose). Interestingly, lipoplex-delivered plasmids were more efficiently expressed than polyplex-delivered plasmids, indicating that PEI may remain bound to the DNA and render it transcriptionally inactive. It also seems that there is an upper limit for gene expression as any increase above 3,000 plasmids per nucleus resulted only in marginal increase in expression of the transgene as demonstrated by Cohen et al. [73].

Whether the components of the gene carriers actually remain associated during import into the nucleus or enter individually cannot be answered by optical methods as their resolution is limited. A possible technique to study the complexation of DNA within cells is fluorescence correlation spectroscopy (FCS). Clamme et al. studied the intracellular fate of PEI after transfection with polyplexes by two-photon fluorescence FCS [54]. They showed that PEI binds to the inner membrane of endosomes and lysosomes and shows free diffusion in the cytosol as well as the nucleus. However, they did not detect any PEI/DNA complexes inside the nucleus.

Expression studies combined with mathematical modeling of transfection indicates that actively transcribed plasmids after poly- or lipoplex mediated transfection may be even as low as around three plasmids per nucleus [72]. As a consequence, tracking the entry of DNA which is finally transcribed into the nucleus in living cells with optical methods resembles the search for the needle-in-the-haystack. As described above, single-particle tracking certainly provides the possibilities to track a single labeled plasmid during the transfection cycle. However, as only a few percent of the plasmids actually reach the nucleus, the background of internalized labeled DNA may hinder the detection of the few plasmids actually entering the nucleus.

9 Future Techniques: Going to the Third Dimension

Most single-particle tracking studies are performed in x, y and therefore represent a 2D projection of the real movement. Particles apparently immobile in x, y can actually show movement along the z-axis and a 2D analysis would provide misleading results. Particles moving several microns along the z-axis will usually be completely lost during tracking as they move out of the focal area. Confocal

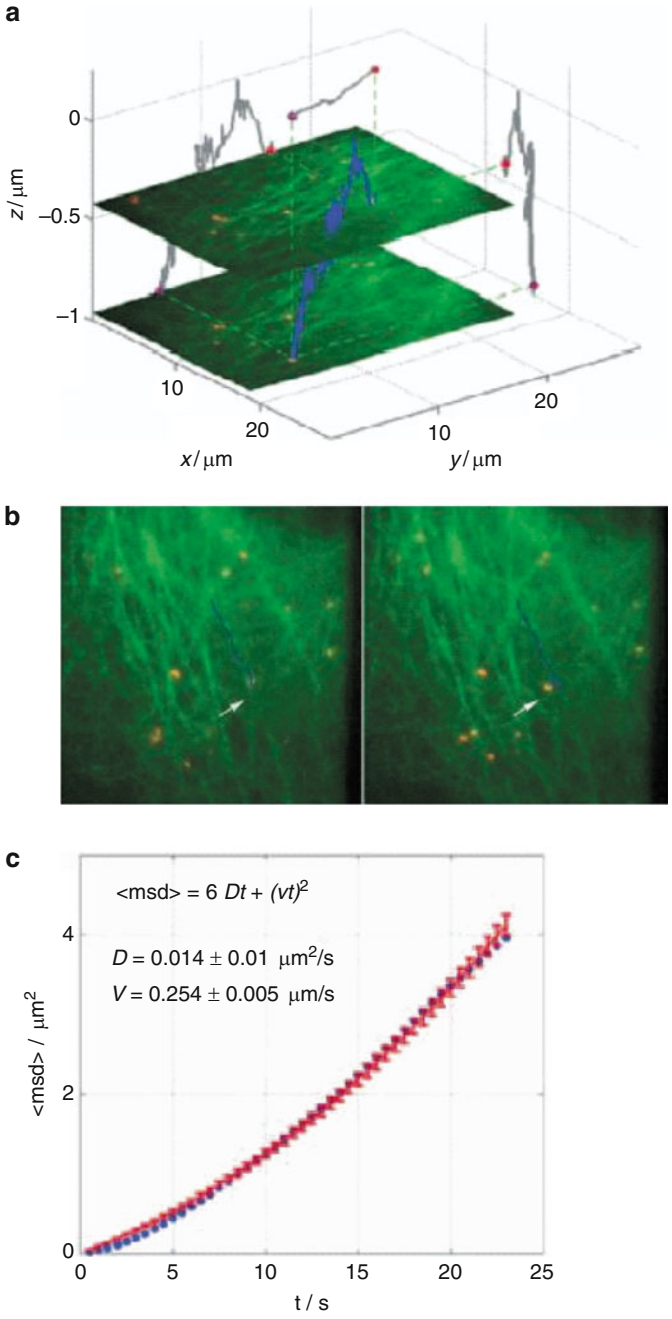

Fig. 7 3D orbital tracking of a polyplex inside a cell(**a**) The 3D trajectory (*blue*) of a polyplex was tracked in HuH7 cells with EGFP labeled tubulin (green structures in the image). Overlayed onto the 3D trajectory are two wide-field images taken at different z-positions during the measurement.

microscopes such as laser scanning or spinning disk microscopes also allow sampling of the z-axis. The acquisition of z-sections, however, is time consuming and usually results in a temporal resolution too slow for detection of fast movement. To extend the capabilities for 3D analysis with a conventional wide-field microscope, Holtzer et al. [74] introduced a cylindrical lens into the emission pathway to produce axial astigmatism. The resulting ellipticity was used to calculate the z-position of small objects with a positional accuracy of 40 nm lateral and 90 nm axial. With this set-up, they were able to track endocytosed QDots at an interval time of 50 ms in three dimensions. An alternative 3D single-particle tracking approach was developed by Katayama et al. [75]. They used a confocal orbital tracking approach with feedback loop for tracking in real time during recording. With this method, the orbiting laser beam is kept centered on the tracked particle. By using two planes for the confocal detection, one above the particle and one below, the z-position of the particle is detected. The orbit is centered on the particle by an online feedback algorithm. In addition, a concomitantly recorded wide-field image in a second channel shows the local environment. This technique allows fast tracking with a temporal resolution down to 16 ms and tracking accuracy of $\sim$20 nm in lateral and 60 nm in axial directions. Due to the simultaneous wide-field imaging, both methods can be used to determine the lateral position of the particle as the particle is kept in focus by the feedback algorithm. With this method, Katayama et al. tracked internalized polyplexes in enhanced green fluorescent protein (EGFP)-tubulin labeled cells (Fig. 7). They showed active transport along microtubules, which were detected in the wide-field channels, with considerable motion along the z-axis as revealed by the 3D trajectory recorded by the confocal channel. However, confocal 3D tracking is limited in terms of multiple-particle tracking.

10 Conclusion and Outlook

Single-particle tracking in real time is a powerful technique to follow the entry pathway of gene carriers as well as their intracellular fate in great detail. The development of nanoparticles as gene carriers will continue and further functionalities such as specific targeting, redox- or pH-sensitivity, etc., will be added. This will lead to even smarter carrier systems [76]. Such systems are constructed to

Fig. 7 (continued) 2D projections of the 3D trajectory are shown in *gray* on the respective axes. (**b**) Two frames of the wide-field movie that was concomitantly recorded during orbital tracking of a polyplex (*red dots*). The wide-field movie allows the correlation of motion events with cellular structures such as microtubules (*green*). (**c**) MSD plot (*blue curve*) of the blue trajectory presented in (**a**). The plot is fitted (*red curve*) with $<r^2> = v^2\Delta t^2 + 6D\Delta t$ in contrast to (3), as the factor 6 is specific for diffusion in three dimensions.Reproduced with permission from Wiley-VCH [75], courtesy of Prof. Don C. Lamb

follow a defined sequence of steps to exert special functions at specific locations in the cell. Single-particle microscopy offers the possibility to follow the action of those smart carrier systems in real time and visualize their correct or incorrect behavior on the cellular level. By combining single-cell single-particle techniques with imaging of the systemic pathway in the living animal [77], it will be possible to follow the full pathway of a single-particle from the point of application in the body throughout the whole animal to the target tissue and subcellular point of action. Thus, the combined possibilities of the various techniques will allow unraveling of the full picture of the "infection pathway" of gene carriers and detection of the critical steps for further optimization to the ultimate goal of a fully functional "artificial virus".

Acknowledgments This work was supported by the Nanosystems Initiative Munich (NIM) and the Center for Integrated Protein Science Munich (CiPSM) and the SFB 749.

References

1. Verma IM, Weitzman MD (2005) Gene therapy: twenty-first century medicine. Annu Rev Biochem 74:711–738
2. Read ML, Logan A, Seymour LW (2005) Barriers to gene delivery using synthetic vectors. Adv Genet 53PA:19–46
3. Burton EA, Fink DJ, Glorioso JC (2002) Gene delivery using herpes simplex virus vectors. DNA Cell Biol 21:915–936
4. Campbell EM, Hope TJ (2005) Gene therapy progress and prospects: viral trafficking during infection. Gene Ther 12:1353–1359
5. Carter PJ, Samulski RJ (2000) Adeno-associated viral vectors as gene delivery vehicles. Int J Mol Med 6:17–27
6. Duan Y, Zhang S, Wang B, Yang B, Zhi D (2009) The biological routes of gene delivery mediated by lipid-based non-viral vectors. Expert Opin Drug Deliv 6:1351–1361
7. Liu F, Huang L (2002) Development of non-viral vectors for systemic gene delivery. J Control Release 78:259–266
8. Niidome T, Huang L (2002) Gene therapy progress and prospects: nonviral vectors. Gene Ther 9:1647–1652
9. Park TG, Jeong JH, Kim SW (2006) Current status of polymeric gene delivery systems. Adv Drug Deliv Rev 58:467–486
10. Schaffert D, Wagner E (2008) Gene therapy progress and prospects: synthetic polymer-based systems. Gene Ther 15:1131–1138
11. Wagner E (2004) Strategies to improve DNA polyplexes for in vivo gene transfer: will "artificial viruses" be the answer? Pharm Res 21:8–14
12. Brandenburg B, Zhuang X (2007) Virus trafficking – learning from single-virus tracking. Nat Rev Microbiol 5:197–208
13. Lakadamyali M, Rust MJ, Babcock HP, Zhuang X (2003) Visualizing infection of individual influenza viruses. Proc Natl Acad Sci USA 100:9280–9285
14. Marsh M, Helenius A (2006) Virus entry: open sesame. Cell 124:729–740
15. Seisenberger G, Ried MU, Endress T, Buning H, Hallek M, Bräuchle C (2001) Real-time single-molecule imaging of the infection pathway of an adeno-associated virus. Science 294:1929–1932

16. Khalil IA, Kogure K, Akita H, Harashima H (2006) Uptake pathways and subsequent intracellular trafficking in nonviral gene delivery. Pharmacol Rev 58:32–45
17. Medina-Kauwe LK, Xie J, Hamm-Alvarez S (2005) Intracellular trafficking of nonviral vectors. Gene Ther 12:1734–1751
18. Payne CK (2007) Imaging gene delivery with fluorescence microscopy. Nanomed 2:847–860
19. Watson P, Jones AT, Stephens DJ (2005) Intracellular trafficking pathways and drug delivery: fluorescence imaging of living and fixed cells. Adv Drug Deliv Rev 57:43–61
20. Vercauteren D et al (2010) The use of inhibitors to study endocytic pathways of gene carriers: optimization and pitfalls. Mol Ther 18:561–569
21. Rejman J, Bragonzi A, Conese M (2005) Role of clathrin- and caveolae-mediated endocytosis in gene transfer mediated by lipo- and polyplexes. Mol Ther 12:468–474
22. Remy-Kristensen A, Clamme JP, Vuilleumier C, Kuhry JG, Mely Y (2001) Role of endocytosis in the transfection of L929 fibroblasts by polyethylenimine/DNA complexes. Biochim Biophys Acta 1514:21–32
23. Kopatz I, Remy JS, Behr JP (2004) A model for non-viral gene delivery: through syndecan adhesion molecules and powered by actin. J Gene Med 6:769–776
24. Lundin P, Johansson H, Guterstam P, Holm T, Hansen M, Langel U, EL Andaloussi S (2008) Distinct uptake routes of cell-penetrating peptide conjugates. Bioconjug Chem 19:2535–2542
25. Mae M, Andaloussi SE, Lehto T, Langel U (2009) Chemically modified cell-penetrating peptides for the delivery of nucleic acids. Expert Opin Drug Deliv 6:1195–1205
26. Rinne J, Albarran B, Jylhava J, Ihalainen TO, Kankaanpaa P, Hytonen VP, Stayton PS, Kulomaa MS, Vihinen-Ranta M (2007) Internalization of novel non-viral vector TAT-streptavidin into human cells. BMC Biotechnol 7:1
27. von Gersdorff K, Sanders NN, Vandenbroucke R, De Smedt SC, Wagner E, Ogris M (2006) The internalization route resulting in successful gene expression depends on both cell line and polyethylenimine polyplex type. Mol Ther 14:745–753
28. Benns JM, Kim SW (2000) Tailoring new gene delivery designs for specific targets. J Drug Target 8:1–12
29. Cheng H, Zhu JL, Zeng X, Jing Y, Zhang XZ, Zhuo RX (2009) Targeted gene delivery mediated by folate-polyethylenimine-block-poly(ethylene glycol) with receptor selectivity. Bioconjug Chem 20:481–487
30. Lu T, Sun J, Chen X, Zhang P, Jing X (2009) Folate-conjugated micelles and their folate-receptor-mediated endocytosis. Macromol Biosci 9:1059–1068
31. Frederiksen KS, Abrahamsen N, Cristiano RJ, Damstrup L, Poulsen HS (2000) Gene delivery by an epidermal growth factor/DNA polyplex to small cell lung cancer cell lines expressing low levels of epidermal growth factor receptor. Cancer Gene Ther 7:262–268
32. Godinez WJ, Lampe M, Worz S, Muller B, Eils R, Rohr K (2009) Deterministic and probabilistic approaches for tracking virus particles in time-lapse fluorescence microscopy image sequences. Med Image Anal 13:325–342
33. Sbalzarini IF, Koumoutsakos P (2005) Feature point tracking and trajectory analysis for video imaging in cell biology. J Struct Biol 151:182–195
34. Yildiz A, Forkey JN, McKinney SA, Ha T, Goldman YE, Selvin PR (2003) Myosin V walks hand-over-hand: single fluorophore imaging with 1.5-nm localization. Science 300:2061–2065
35. Saxton MJ, Jacobson K (1997) Single-particle tracking: applications to membrane dynamics. Annu Rev Biophys Biomol Struct 26:373–399
36. Qian H, Sheetz MP, Elson EL (1991) Single particle tracking. Analysis of diffusion and flow in two-dimensional systems. Biophys J 60:910–921
37. de Bruin K, Ruthardt N, von Gersdorff K, Bausinger R, Wagner E, Ogris M, Bräuchle C (2007) Cellular dynamics of EGF receptor-targeted synthetic viruses. Mol Ther 15:1297–1305
38. Bausinger R, von Gersdorff K, Braeckmans K, Ogris M, Wagner E, Bräuchle C, Zumbusch A (2006) The transport of nanosized gene carriers unraveled by live-cell imaging. Angew Chem Int Ed Engl 45:1568–1572

39. Mislick KA, Baldeschwieler JD (1996) Evidence for the role of proteoglycans in cation-mediated gene transfer. Proc Natl Acad Sci USA 93:12349–12354
40. Payne CK, Jones SA, Chen C, Zhuang X (2007) Internalization and trafficking of cell surface proteoglycans and proteoglycan-binding ligands. Traffic 8:389–401
41. Suh J, Wirtz D, Hanes J (2004) Real-time intracellular transport of gene nanocarriers studied by multiple particle tracking. Biotechnol Prog 20:598–602
42. Cui B, Wu C, Chen L, Ramirez A, Bearer EL, Li WP, Mobley WC, Chu S (2007) One at a time, live tracking of NGF axonal transport using quantum dots. Proc Natl Acad Sci USA 104:13666–13671
43. Fehrenbacher K, Huckaba T, Yang HC, Boldogh I, Pon L (2003) Actin comet tails, endosomes and endosymbionts. J Exp Biol 206:1977–1984
44. Merrifield CJ, Moss SE, Ballestrem C, Imhof BA, Giese G, Wunderlich I, Almers W (1999) Endocytic vesicles move at the tips of actin tails in cultured mast cells. Nat Cell Biol 1:72–74
45. Mahowald J, Arcizet D, Heinrich D (2009) Impact of external stimuli and cell micro-architecture on intracellular transport states. Chemphyschem 10:1559–1566
46. Arcizet D, Meier B, Sackmann E, Rädler JO, Heinrich D (2008) Temporal analysis of active and passive transport in living cells. Phys Rev Lett 101:248103
47. Suh J, Wirtz D, Hanes J (2003) Efficient active transport of gene nanocarriers to the cell nucleus. Proc Natl Acad Sci USA 100:3878–3882
48. Sauer AM, de Bruin KG, Ruthardt N, Mykhaylyk O, Plank C, Bräuchle C (2009) Dynamics of magnetic lipoplexes studied by single-particle tracking in living cells. J Control Release 137:136–145
49. Rajan SS, Liu HY, Vu TQ (2008) Ligand-bound quantum dot probes for studying the molecular scale dynamics of receptor endocytic trafficking in live cells. ACS Nano 2:1153–1166
50. Nan X, Sims PA, Chen P, Xie XS (2005) Observation of individual microtubule motor steps in living cells with endocytosed quantum dots. J Phys Chem B 109:24220–24224
51. Lechardeur D, Verkman AS, Lukacs GL (2005) Intracellular routing of plasmid DNA during non-viral gene transfer. Adv Drug Deliv Rev 57:755–767
52. Klemm AR, Young D, Lloyd JB (1998) Effects of polyethyleneimine on endocytosis and lysosome stability. Biochem Pharmacol 56:41–46
53. Sonawane ND, Szoka FC Jr, Verkman AS (2003) Chloride accumulation and swelling in endosomes enhances DNA transfer by polyamine-DNA polyplexes. J Biol Chem 278:44826–44831
54. Clamme JP, Krishnamoorthy G, Mely Y (2003) Intracellular dynamics of the gene delivery vehicle polyethylenimine during transfection: investigation by two-photon fluorescence correlation spectroscopy. Biochim Biophys Acta 1617:52–61
55. Boeckle S, Fahrmeir J, Roedl W, Ogris M, Wagner E (2006) Melittin analogs with high lytic activity at endosomal pH enhance transfection with purified targeted PEI polyplexes. J Control Release 112:240–248
56. Ogris M, Carlisle RC, Bettinger T, Seymour LW (2001) Melittin enables efficient vesicular escape and enhanced nuclear access of nonviral gene delivery vectors. J Biol Chem 276:47550–47555
57. de Bruin KG, Fella C, Ogris M, Wagner E, Ruthardt N, Bräuchle C (2008) Dynamics of photoinduced endosomal release of polyplexes. J Control Release 130:175–182
58. Lukacs GL, Haggie P, Seksek O, Lechardeur D, Freedman N, Verkman AS (2000) Size-dependent DNA mobility in cytoplasm and nucleus. J Biol Chem 275:1625–1629
59. Vaughan EE, Dean DA (2006) Intracellular trafficking of plasmids during transfection is mediated by microtubules. Mol Ther 13:422–428
60. Leopold PL, Kreitzer G, Miyazawa N, Rempel S, Pfister KK, Rodriguez-Boulan E, Crystal RG (2000) Dynein- and microtubule-mediated translocation of adenovirus serotype 5 occurs after endosomal lysis. Hum Gene Ther 11:151–165

61. Dohner K, Radtke K, Schmidt S, Sodeik B (2006) Eclipse phase of herpes simplex virus type 1 infection: efficient dynein-mediated capsid transport without the small capsid protein VP26. J Virol 80:8211–8224
62. Dohner K, Wolfstein A, Prank U, Echeverri C, Dujardin D, Vallee R, Sodeik B (2002) Function of dynein and dynactin in herpes simplex virus capsid transport. Mol Biol Cell 13:2795–2809
63. Suk JS, Suh J, Lai SK, Hanes J (2007) Quantifying the intracellular transport of viral and nonviral gene vectors in primary neurons. Exp Biol Med (Maywood) 232:461–469
64. Matsumoto Y, Itaka K, Yamasoba T, Kataoka K (2009) Intranuclear fluorescence resonance energy transfer analysis of plasmid DNA decondensation from nonviral gene carriers. J Gene Med 11:615–623
65. Godbey WT, Barry MA, Saggau P, Wu KK, Mikos AG (2000) Poly(ethylenimine)-mediated transfection: a new paradigm for gene delivery. J Biomed Mater Res 51:321–328
66. Godbey WT, Wu KK, Mikos AG (1999) Tracking the intracellular path of poly(ethylenimine)/DNA complexes for gene delivery. Proc Natl Acad Sci USA 96:5177–5181
67. Itaka K, Harada A, Yamasaki Y, Nakamura K, Kawaguchi H, Kataoka K (2004) In situ single cell observation by fluorescence resonance energy transfer reveals fast intra-cytoplasmic delivery and easy release of plasmid DNA complexed with linear polyethylenimine. J Gene Med 6:76–84
68. Bieber T, Meissner W, Kostin S, Niemann A, Elsasser HP (2002) Intracellular route and transcriptional competence of polyethylenimine-DNA complexes. J Control Release 82: 441–454
69. Brunner S, Sauer T, Carotta S, Cotten M, Saltik M, Wagner E (2000) Cell cycle dependence of gene transfer by lipoplex, polyplex and recombinant adenovirus. Gene Ther 7:401–407
70. Mortimer I, Tam P, MacLachlan I, Graham RW, Saravolac EG, Joshi PB (1999) Cationic lipid-mediated transfection of cells in culture requires mitotic activity. Gene Ther 6:403–411
71. Tseng WC, Haselton FR, Giorgio TD (1999) Mitosis enhances transgene expression of plasmid delivered by cationic liposomes. Biochim Biophys Acta 1445:53–64
72. Schwake G, Youssef S, Kuhr JT, Gude S, David MP, Mendoza E, Frey E, Rädler JO (2009) Predictive modeling of non-viral gene transfer. Biotechnol Bioeng 105:805–813
73. Cohen RN, van der Aa MA, Macaraeg N, Lee AP, Szoka FC Jr (2009) Quantification of plasmid DNA copies in the nucleus after lipoplex and polyplex transfection. J Control Release 135:166–174
74. Holtzer L, Meckel T, Schmidt T (2007) Nanometric three-dimensional tracking of individual quantum dots in cells. Appl Phys Lett 90:1–3
75. Katayama Y, Burkacky O, Meyer M, Bräuchle C, Gratton E, Lamb DC (2009) Real-time nanomicroscopy via three-dimensional single-particle tracking. Chemphyschem 10:2458–2464
76. Wagner E (2007) Programmed drug delivery: nanosystems for tumor targeting. Expert Opin Biol Ther 7:587–593
77. Zintchenko A, Susha AS, Concia M, Feldmann J, Wagner E, Rogach AL, Ogris M (2009) Drug nanocarriers labeled with near-infrared-emitting quantum dots (quantoplexes): imaging fast dynamics of distribution in living animals. Mol Ther 17:1849–1856

Index